ASSESSMENT OF A HYDRODYNAMIC WATER QUALITY MODEL, DUFLOW, FOR A WINTER RAINFALL RIVER

by

N. C. Nitsche

Study Leader: A. H. M. Görgens

Thesis presented in partial fulfilment of the requirements for the degree of Master of Engineering (Civil) at the University of Stellenbosch

Department of Civil Engineering

University of Stellenbosch

December 2000

DECLARATION

I the undersigned hereby declare that the work contained in this thesis is my own original work, and has not previously, in its entirety or in part, been submitted at any university for a degree.

Signature: Date:

SYNOPSIS

The Berg River is one of the largest rivers in the winter rainfall area of the Western Cape and is one of the most important water supply sources of the area. The Riviersonderend-Berg system needs to be expanded in order to meet increasing water demands of the Greater Cape Town (GCT) region. The implementation of future schemes will remove additional fresh water from the Berg River main stem, which will give rise to increased nutrient levels and higher salinity in the water. A water quality information system (WQIS) has been proposed to benefit the management of water resources, the flow quantity and the quality of the water. A part of this WQIS will be a water-quality simulation model that characterizes the water quality situation and is able to predict water quality responses to future implementations, as well as simulate different scenarios that can be used for management purposes.

The objective of this study is to represent the water quality situation of the Berg River in a simulation model by implementing, testing and verifying a water quality simulation model, and assembling a hydraulic and water quality database suitable to meet foregoing objectives.

This study firstly examined the water quality variables of concern: pH, Total Dissolved Salts (TDS) and phosphates to develop an understanding of the water quality responses and causes of the main stem of the Berg River system.

A thorough review of the available models has been undertaken in the light of certain selection criteria, before determining that DUFLOW would be an acceptable model for this study. The water quality variables that have been modelled are TDS, Phosphates as PO_4, Oxygen and Temperature. As no predefined module simulating temperature, TDS and COD was included; these algorithms, describing the processes of these water quality variables have been additionally coded. The coding was possible, as DUFLOW's water quality module consists of an open structure. The predefined water quality module was simplified to only include the water quality process algorithms, for water quality variables where data was available. Unfortunately, phosphates were mainly simulated on advection, and the influence of all the additional processes could not be assessed.

All data gathering and preparation for the model had to be completed before commencing the model

configuration. This included information on cross-sections, historical flow records, bridges and weirs for the hydraulic component of DUFLOW. For the water quality module, information on historical grab samples has been obtained and 'infilled' to provide daily time series.

To simulate the water quality in a river as accurately as possible, the flow simulation needs to be accurate. Ungauged subcatchment runoff was added to the simulation model to improve the correspondence between the simulated and the measured flow. Calibration of the water quality part of DUFLOW was completed by adjusting the different parameters after a sensitivity analysis. The model was verified by using a different time period than for the configuration, to ensure that an independent data set has been used.

After configuring, calibrating and verifying the model, the applicability of the model could be tested for different scenario runs. Three scenarios were chosen according to real situations:

- a short term effluent spill, with and without water releases from an upstream source (either Skuifraam Dam or Voëlvlei Dam);
- the impact on the flow and water quality situation of the river when an upstream dam is built;
- a long term management control scenario, that analyses load or concentration releases into the river according to limitations upstream and downstream of the discharge location.

The scenario analysis provides an opportunity to assess the applicability of DUFLOW to simulate real time management and operational issues in a river and to aid in management decisions.

SINOPSIS

Die Bergrivier is een van die grootste riviere in die winterreënvalgebied van die Weskaap en is een van die mees belangrike waterverskaffingsbronne in die area. Die Riviersonderend-Bergrivier-stelsel moet uitgebrei word om aan die groeiende waterbehoefte van die groter Kaapse Metropolitaanse Area te voldoen. Die implementering van toekomstige skemas sal addisionele vars water uit die hoof-loop van die Bergrivier onttrek, wat tot hoër voedingstof-vlakke en soutgehalte in die water sal lei. 'n Waterkwaliteitsinformasiestelsel (WQIS) sal van nut wees om die vloei-omvang en waterkwaliteit van waterbronne te bestuur. 'n Deel van die WQIS sal 'n waterkwaliteit-simulasiemodel wees, wat die waterkwaliteitsituasie sal kan ontleed, waterkwaliteit-reaksies op toekomstige implementerings kan voorspel, asook verskeie scenarios vir bestuursdoeleindes kan simuleer.

Hierdie studie behandel spesifiek die waterkwaliteitsveranderlikes pH, totale opgeloste soute, fosfate, temperatuur en suurstof om 'n begrip te ontwikkel van die waterkwaliteitsreaksies en oorsake van die hoof loop van die Bergriviersisteem. Die doelwit van hierdie studie is om die waterkwaliteitsituasie van die Bergrivier uit te beeld deur die implementering, toets en kalibrasie van 'n waterkwaliteit-simulasie model, asook die insameling van hidrouliese- en waterkwaliteitsdata om aan bogenoemde doelwitte te voldoen.

'n Reeks beskikbare modelle is deeglik ondersoek voordat besluit is dat die DUFLOW model 'n gepaste model vir hierdie spesifieke studie is. Die keuse was gebaseer op spesifieke vereistes wat as belangrik beskou is deur potensiële bestuursgeorienteerde gebruiksgroepe. Die waterkwaliteitsveranderlikes wat gemodelleer is, is totale opgeloste soute, fosfate as PO_4, suurstof en temperatuur. Omdat geen voorgegewe temperatuur-, TDS- en COD modules in die model ingesluit is nie, is die algoritmes wat die prosesse van hierdie waterkwaliteitsveranderlikes beskryf, addisioneel gekodeer. Die kodering is moontlik gemaak deur die oop struktuur van DUFLOW se waterkwaliteitsmodule. Die voorgegewe waterkwaliteitsmodule is vereenvoudig om alleenlik die waterkwaliteit proses-algoritmes in ag te neem wanneer data vir waterkwaliteitsveranderlikes beskikbaar was. Ongelukkig is die fosfate hoofsaaklik op beweging gesimuleer, en die invloed van alle addisionele prosesse kon nie getoets word nie.

Alle data-insameling en -voorbereidings vir die model moes voltooi word, voordat begin kon word met die opstel van die simulasie-model. Dit het inligting oor dwarssnitte, historiese vloeirekords, brûe en

keerwalle vir die hidrouliese komponent van DUFLOW ingesluit. Vir die waterkwaliteitsmodule is inligting van historiese bemonstering verkry en ingevul om 'n daaglikse tydreeks te verkry.

Om die water-kwaliteit van 'n rivier so akkuraat as moontlik te simuleer, moet die vloei-simulasie redelik akkuraat wees. Ongemete sub-opvanggebied afloop is bygetel om die korrelasie tussen die gesimuleerde en gemete vloei te verbeter. Kalibrasie van die waterkwaliteitmodule van DUFLOW is voltooi deur die verskillende parameters te verstel na 'n sensitiwiteits-analise. Die model is geverifieer deur 'n ander tydperiode as die vir die opstel te gebruik, om sodoende te verseker dat 'n onafhanklike data stel gebruik word.

Na die opstel, kalibrasie en verifiering van die model, kon dit toegepass word vir verskillende bestuurs-scenarios.

Drie scenarios is na aanleiding van werklike situasies gekies:

- 'n korttermyn uitvloeisel storting-situasie met en sonder loslatings van 'n stroomop bron (òf Skuifraamdam òf Voëlvleidam).
- die impak op die vloei- en waterkwaliteitsituasie van die rivier sou 'n dam stroomop gebou word.
- 'n langtermyn bestuurs-scenario waarin die lading en konsentrasies, veroorsaak deur die loslatings vanuit die dam na die rivier, ontleed word na aanleiding van beperkings stroomop en -af van die loslatingsplek.

Die analise van die scenarios verskaf 'n geleentheid om die toepaslikheid van DUFLOW te ondersoek om werklike operasionele aangeleenthede te simuleer en om sodoende bestuursbesluite te vergemaklik.

ACKNOWLEDGMENTS

I would like to thank the following people and organisations, without them this study would not have been possible:

- Prof Görgens for his guidance, knowledge and motivation throughout the study.
- The Water Research Commission for the opportunity and funding of this research.
- Delft University and Stowa for their dedicated assistance and help with the model configuration.
- Ninham Shand for providing the facilities to conduct this research, as well as their interest and encouragement.
- The Department of Water Affairs for providing plans of the weirs in the Berg River Catchment, daily flow and water quality data, as well as information on registered point sources.
- The municipality of Paarl for providing cross-sections along the river reach in Paarl, as well as abstraction data.
- All the irrigation boards abstracting water from the Berg River for their assistance in providing abstraction flow data.
- Elsenburg Agricultural College for supplying meteorological data.
- The Soils Science Department of the University of Stellenbosch in assisting in sampling water quality data of the Berg River.
- My family and friends for believing in me and supporting me to achieve my goals.

TABLE OF CONTENTS

LIST OF FIGURES

FIGURES **PAGE**

FIGURES **PAGE**

FIGURES **PAGE**

FIGURES **PAGE**

FIGURES **PAGE**

FIGURES **PAGE**

FIGURES **PAGE**

FIGURES **PAGE**

FIGURES **PAGE**

LIST OF TABLES

TABLE **PAGE**

TABLE PAGE

TABLE **PAGE**

CHAPTER 1

INTRODUCTION

1.1 Background

The Berg River is one of the largest rivers in the winter rainfall area of the Western Cape and is one of the most important water supply sources of the area.

The Riviersonderend-Berg system needs to be expanded to meet increasing water demands of the Greater Cape Town (GCT) region. The future schemes proposed to supply the demands are: the Skuifraam dam in the upper Berg region, Skuifraam Supplement Scheme downstream of Franschhoek and the Lorelei Diversion to an enlarged Voëlvlei Dam in the middle Berg region. The implementation of these schemes will remove additional fresh water from the Berg River main stem, which will lead to increased nutrient levels and higher salinity in the water. Concerns have been raised that the water would become unfit for use and ecological, and eutrophication and salinity problems will occur after implementing the above mentioned schemes.

In 1997 a Water Research Commission project was initiated to develop an integrated information system specifically for water quality (WQIS) to assist in Integrated Water Resource Management. The WQIS needs to be developed to provide a means of managing, planning and operating the Riviersonderend-Berg River system. The WQIS would include a water-quality simulation model that characterizes the water quality situation and can predict water quality responses to future implementations, and simulate different scenarios that can be used for management purposes.

The water quality processes that need to be included in the water simulation model are: salt transport, nutrient transport, eutrophication and temperature and oxygen variation, as these are the water quality variables that are of concern in the Berg River.

1.2 Objectives

The objectives of this study are:

- To develop an understanding of the water quality responses and causes of the main stem of the Berg River system.
- To represent the water quality situation of the Berg River in a simulation model by implementing, testing and verifying a water quality simulation model.
- To assemble a hydraulic and water quality database suitable to meet the foregoing objectives.

1.3 Methodology

The structure of this report is set out as follows:

Chapter 2:

This report begins with a literature review on the history and development of water quality simulation models. The different concepts used in water quality simulation models are clarified to the reader. The various models that are available, are reviewed and a model is chosen for this study following certain selection criterias.

Chapter 3:

The Berg River is chosen as a suitable river for this particular study. This chapter describes the Berg River catchment regarding current infrastructures, future developments, geography etc.

Chapter 4:

Before any modelling of the river could commence, the water quality situation of the river had to be analysed. A statistical analysis has been done for the water quality variables identified as variables of concern in the Berg River: pH, Total Dissolved Salts (TDS) and Phosphates as PO_4.

Chapter 5:

The software structure and the mathematical background of the water quality simulation model DUFLOW is described. The mathematics used for the hydraulic calculations is explained and the algorithms formulated for the water quality processes are discussed.

Chapter 6:

The data gathering and preparation for the model is first described in this chapter. The chapter is divided into a section describing all the hydraulic components and the configuration of the model; the second section follows to describe the data preparation and the configuration of the model for the water quality module.

Chapter 7:

After the configuration of the model, the model had to be calibrated to ensure that the simulated flow is similar to the measured flow. This chapter explains the approach taken to calibrate the flow module of the model.

Chapter 8:

This chapter describes the calibration and sensitivity analysis completed for the water quality module of the simulation model.

Chapter 9:

An important part of the model is to apply the model for different scenarios. This chapter outlines three different scenarios that can be applied to the model: a short term spill scenario, a simulation using a set of data simulated for a reservoir model and thirdly, a long term management scenario.

Chapter 10:

Conclusions are drawn and recommendations are made.

CHAPTER 2

CONCEPTUAL CONTEXT OF MODEL APPLICATION

2.1 INTRODUCTION

Modelling is a tool that is necessary in water quality management as it "*provides the link between the conceptual understanding of the physical catchment characteristics and the empirical quantification of the hydrological, water quality and ecological responses*" (Pegram et. al., 1997, pg17).

The above quotation summarizes the importance of modelling in water quality management, as it is able to describe the interaction between ecology, water quality, hydrology and hydraulics and, most important, allow for *what-if* scenarios which enable the users to attain a clearer understanding of the responses of the system as a whole.

The definition of a model is given by Carstensen et. al.(1997) as: *the abstract representation of a real system by the ideas and constituents and functional relationships.* The term *model* is used in many different ways to describe any representation of the *real system*, such as a laboratory model, computational model or conceptual model. The term *water quality model* or *simulation model* is used in this study to describe which computational hydraulic and water quality software is being used and either *submodels* or *algorithms,* describe the mathematical equations that represent the water quality processes.

The aim of hydrodynamic river water quality modelling is to describe and understand interactions between the hydraulics of the river and the chemical and biological water quality river constituents[1]. A model is very effective in assisting in water quality management decisions for different scenarios which would affect the river and the water users. As computers have been becoming more powerful, more complex systems and formulations of the interaction between the water quality variables have been able

[1] A water quality constituent (also called water quality variable) is defined as a biological or chemical (organic or inorganic) substance or physical characteristic that describes the quality of a water body. (DWAF(a), 1993).

to be modelled and understood.

The aim of this chapter is to provide the reader with the basic concepts of modelling and to clarify the terminology that will be used in this chapter. Additionally, a review has been carried out on some of the well-known water quality programs that are available and the findings summarized.

2.2 HISTORY OF RIVER WATER QUALITY MODELLING

The history of water quality modelling can be divided roughly into four periods:

- **1925-1960**

  The main water quality variables that were studied were Dissolved Oxygen(DO) and Biochemical Oxygen Demand (BOD). The algorithms concentrated on streams and estuaries. The goal was to manage effluent and understand its impact on the water body.

- **1960-1970**

  The first available computers made it possible to apply more complex mathematical formulations and thus the first computerized models were developed. One of the first computer models that was developed was for a study on the Delaware Estuary (Thomann, 1963, cited by Orlob, 1992), by using the Streeter and Phelps oxygen sag equation which was developed in 1925 for the Federal Water Pollution Control Administration (now called the US Environmental Protection Agency (EPA)). This model has been used and applied extensively. These first models that were developed concentrated on the temperature, dissolved oxygen and biochemical oxygen demand, as these were the major studies that were done in the beginning.

- **1970-1980**

  In the mid-70's a number of models were developed which also incorporated the various other water quality constituents, as knowledge on the eutrophication of water bodies improved with research. Well-known modellers such as Chen, Orlob, Di Toro and Thomann developed elaborate nutrient/food chain models. (Chapra, 1997). Non-point control of water quality

variables also became important during these years[2]. The increasing power of computers made it possible to study and model much more complex reaction processes of all the water quality constituents. Models were developed as decision tools for lakes, rivers and estuaries, some of which are DOSAG and QUAL1 which were developed by the Texas Water Development Board, and later extended to QUAL2E under the auspices of the EPA. (Orlob, 1992). QUAL2E is possibly the most used steady-state water quality model by practitioners in the English-party world.

- **1980-date**

  Since 1980 there has been growing emphasis on fully hydrodynamic modelling of rivers, reservoir and estuary processes, with closely-coupled water quality processes, as well as on the fate and transport of toxic substances. Also, the interactions of water quality constituents with the sediment are more widely researched and modelled (e.g. Chapra and Reckhow,1983). Some ecosystem models consider several classes of algae, zooplankton, invertebras, plants and fish. With the advancement in computer technology various models (i.e. reservoir, river and estuary) are incorporated together by interfaces and used as water quality management decision tools. Uncertainty analysis has also been added to water quality computer programs.

2.3 CONCEPTS IMPORTANT TO WATER QUALITY MODEL APPLICATIONS

Concepts important to water quality model applications include model constituents, attributes and concepts used in the actual model construction. There exists a wide range of terminology when describing the various aspects of models and model building, which according to Carstensen et al. (1997) is the result of the wide range of different scientific fields of researchers that work within the field of water quality management. Therefore, it is important to clarify the terms that will be used in this study.

[2] Non-point pollution sources are distributed or dispersed discharges of pollutants from surface run-off, infiltration or atmospheric sources. (DWAF, 1993)

2.3.1 Model elements

In water quality simulations there are normally two primary types of model elements: variables and parameters. The parameters are normally the kinetic coefficients of a chemical equation describing the response of a specific water body to outside or internal forces or stimuli (i.e. influenced by temperature, radiation, sediment, ratio of chemical mass etc.). The parameters are determined either through field studies or in the calibration process or "transferred" from other comparable applications. State variables are the water quality variables, such as concentration or loads of phosphates, chlorophyll-a, etc. that are of concern to the modeller.

2.3.2 Model attributes

Dimensions:

Models may be categorized as **zero dimensional, one dimensional, two dimensional** or **three dimensional**. Rivers are normally treated as one dimensional models, where the values of flow and quality only change in the longitudinal direction; one dimensional or two dimensional, where both longitudinal and depth-related dynamics are simulated, i.e. the lateral state is regarded as "average", reservoir models simulate the vertical changes. Zero dimensional models are normally only models that are used for reservoirs, these are also known as input-output models, here the assumption is made that the water is well mixed and only the input and output changes. Three dimensional models include the vertical, longitudinal and lateral changes.

Time:

The main distinction that is made among the various water quality models is between **steady state** and **dynamic** models. Steady state models assume that the variables do not change in time or in space, while dynamic models do take the variability of the variables in time and space into account and thus allow for modelling of non-point runoff and sudden increased effluent discharges. The output of the results is normally in the form of time-series.

Data:

Another division that can be made between the different water quality models is that of **deterministic**

and **stochastic** models. In deterministic models (also sometimes referred to mechanistic) a fixed relationship between input and output is assumed. This relationship may be empirical ("black box"), conceptual or mechanistic. Stochastic models allow for random variation in input parameters. The variations are described by statistical distributions. Observed streamflow and water quality data requirements for stochastic models are usually greater than for deterministic models to ensure reliable estimation of statistical parameters.

Purpose of Model:

Water quality models designed for computer solution are either **simulation** or **optimization** models. Simulation models calculate the concentration of the various variables based on the given river flow and the quantity and quality of the waste loading. Optimization models are effective in assisting management, as they include model management variables to test the impacts of certain management decisions.

Mathematical Computation:

The common basis for most water quality models is the principle of continuity or mass balance. The transport as well as the chemical and biological processes are calculated in many models. Transport processes that are usually included is advection, longitudinal and/or lateral dispersion, vertical convection (reservoirs) and eddy diffusion. A distinction in the equations is made between conservative and non-conservative variables. Conservative constituents undergo no chemical and biological changes and thus only the transport equations and geometrical characteristics of the river determine the concentration of the variable (i.e. TDS, Total Dissolved Solids). Non-conservative variables normally undergo biological and chemical changes and thus the water quality processes are more difficult to model.

Simulation models are normally solved either by formal integration of the basic differential equations or by numerical analysis techniques such as finite difference or finite element methods. Each of these approaches is based on a solution of simultaneous sets of linear and non-linear equations.

Input Data:

Another distinction is made between point sources and non-point sources. Point sources refer to the concentrated discharge of contaminants from a known source (i.e. effluent discharge from a sewage

treatment works). Non-point sources are spatially distributed or dispersed discharges and export of contaminants derived from the surface and subsurface drainage as well as from the atmosphere, they are often hydrometeorological driven. The characteristics of point sources are much easier understood as they are normally measurable. The difficulty in modelling non-point sources and point sources lies in the randomness with which they happen.

2.3.3 Model Building

The steps that are taken when developing a model are:

- Identification of the problem that needs to be studied
- Model Selection
- Configuration
- Sensitivity Analysis
- Model Calibration
- Model Verification
- Scenario Analysis

Identification of a problem:

The identification of the problem is a very important step in the model building process, as it will determine which model to use and the amount of data that is needed. The objectives of the study normally determine which water quality variables need to be studied, the resolution of the model and the data needs. In South Africa different requirements in a model are usually needed when compared to European models, as the focus tends to follow salinity and eutrophication and less on toxic substances modelling, which is presently the main concern.

Model Selection:

A choice of model is based on various criteria, of which the most commons are:

- *the ability of the model to describe the specific problem*

  A model should be selected based on its adequacy for the intended use, for the specific waterbody, and for the critical conditions occurring at that waterbody. An obvious consideration

for narrowing the selection of an appropriate model is based on the waterbody type (river, estuary, or lake) and the type of analysis wanted (salinity, nutrients etc.).

- *whether the assumptions made in the model are relevant to the specific study area (i.e. the equations used)*

  For some process algorithms, a number of assumptions have been made to decide on certain parameters and equations. Care needs to be taken that the algorithms are flexible enough to allow for alterations or are relevant to the study area, especially when models have been programmed for particular climatic circumstances, but then used in different circumstances.

- *degree of model complexity*[3] *and data availability*

  The extent of the data that is needed for the model is often dependent on the model complexity. One should consider the data requirements and whether the required historical data is available. The level of analysis has to be appropriate to the problem investigated, i.e. simple models[4] or complex models .

- *the resolution wanted for the specific problem (i.e. space and time step)*

  The model has to represent the specific problem studied, i.e. if eutrophication has to be modelled, normally daily time steps are used, although a smaller time step might be more appropriate to accommodate the photosynthesis of the algae which fluctuates during the day.

- *the availability, cost and support of the model*

  One should consider model familiarity, technical support and model availability, documentation quality, application ease, and professional recognition and acceptance of a model. There are a number of models available free of charge from the Internet (mainly EPA models such as WASP and Qual2E), while other models are very expensive for South Africa (e.g. Mike 11, ISIS; see

---

3 Complex is a relative attribute that assesses whether the model contains more than one state variable, parameter and type or there exist multiple solutions of the model equations. (Carstensen et. al., 1997)

4 A simple model is characterized by few parameters and equations. (Carstensen et. al. 1997)

section 2.5 for details).

For any specific water quality situation studied, the appropriate model depends largely on the problem investigated and the availability of the data required. Different models place emphasis on different water quality variables or just use different mathematical formulations which could be unsuitable for the specific river studied and the problem investigated. Most important, the model needs to be capable of configuration, calibration, verification and simulation within the limits of time and money. This is difficult to determine at the beginning, as the configuration time is very dependent on the specific study and the prior knowledge of the model.

Sensitivity Analysis:

A sensitivity analysis is important for the calibration process, as it determines which parameters have a significant impact on the model results. The term objective function is used for the statistical functions that are applied to determine the degree of influence the parameters have on the results. A list of objective functions and the approach that should be used in model calibration and sensitivity analysis is given by Görgens (1983) for hydrological modelling, but the same approach applies to calibrating water quality models.

Calibration:

The definition of a model calibration is given in Thomann and Mueller (1987) as: *the first stage testing or tuning of a model to a set of field data,..,such tuning to include a consistent and rational set of theoretically defensible parameters and input.* The value of the parameters can be deduced from field measurements, but normally adjustments are made to the default parameters in the model until an optimal fit is achieved between the simulated data set and the measured prototype data. The 'goodness-of-fit' is determined by curve-fitting and applying the objective functions to analyse the goodness-of-fit. Consideration should be given to the realistic range that the parameters can have in the specific model for the specific water body. The process of the calibration includes firstly ensuring the accurateness of the input data, boundary functions and the physical representation of the river and then secondly adjusting the parameters.

Verification:

The terms verification and validation are often both used to describe the confirmation of a model by using a set of data that is totally independent of the data set that has been used to calibrate the model. Carstensen et al.(1997), Chapra (1997)and Reckhow et al. (1990) discourage both terms and propose terms such as confirmation, robustness and corroboration for this model step, as *"...it is obvious that a model can never describe reality completely. Therefore, there will always exist experimental conditions for which the model is not valid. Hence, validation of a model is utopian!"* (Carstensen et al.1997, pg. 164). However, in this study the term *verification* will be used to describe the process of ensuring that the model applied to the specific river for a set of data can be applied to another situation and *validation* is the examination of the numerical models used to describe the water quality processes and the computer code to ascertain that there are no numerical problems with obtaining a solution. Validation is normally the concern of the algorithm and software developers and the assumption that the model is valid numerically is already made at the begin of the model building.

Scenario Analysis:

The verified model is then used for different scenario analysis. When using the verified model for different scenarios the uncertainty of the parameter estimation and data errors have to be kept in mind as different scenarios could affect the parameter that has been used to calibrate the model and increase the error. A scenario analysis is also sometimes termed a model postaudit (Thomann and Mueller, 1987; Chapra 1997).

2.4 DATA CONSIDERATIONS FOR MODEL USE

The resolution of data requirements is very dependent on the modelling method. The data requirements depend on the complexity of the model and the make-up of the overall uncertainties present:

"*The underlying uncertainty is due to inherent randomness of the natural phenomenon. However, uncertainty arises also from the inaccuracies in the estimation of the parameters and in the choice of distribution. Uncertainties associated with errors of parameter estimation can be reduced by increasing the amount of data, whereas the uncertainty associated with the inherent variability may remain*

unchanged or may even increase with additional data." (Ang and Tang, 1975)

As can be seen from the quotation, uncertainty in the data result mainly from:

- quality of data
- parameter estimation

Uncertainty of results can be divided into the uncertainty which arises from the deviation in measurements itself, as well as in uncertainty which arises due to errors in estimating the parameters:

Quality of data:

The errors that can occur can result from:

- different laboratory techniques and errors in laboratory measurements
- different sampling times (e.g. in case of constituents such as phytoplankton that is dependent on the light during that specific hour)
- different sampling position (e.g. samples taken in small pools might show higher concentration than in flowing water)
- precision of data needed for river schematization, i.e. river geometry, flow measurements and river bed roughness coefficient

Parameter Estimation:

The confidence of the value of parameters has normally been established in the calibration procedure. A sensitivity analysis should be used to indicate which parameter has a significant influence on the simulation results.

Objective Functions:

Statistical indicators that determine the goodness-of-fit between measured and simulated data are called objective functions. The statistical goodness of fit tests gives the modeller information on the degree of the error between observed and simulated values, as well as the degree of influence a certain parameter might have on the results. There are several different statistical tests that can be performed on the two sets of data and depending on the model, the objectives and the problem studied, appropriate objective

functions can be selected. Some statistical methods that can be used are described in Görgens (1983) and Reckhow et al. (1990). Görgens (1983) also describes the procedures one should follow when using objective functions in sensitivity analyses and calibration procedures. The statistical objective functions used in this study are explained in section 7.2.

2.5 REVIEW OF WATER QUALITY MODELS FOR RIVERS

Available models cover a range of purposes, such as combined river and reservoir models, runoff models, hydrology models, ground water models or only stream hydraulics models. The review of models below reviews hydrodynamic water quality models (except for Qual2E, which is steady state).

Below, a short description is given to various models that are currently available and Table 2.1 summarizes the main features.

2.5.1 American models:

WQRRS

(Hydrologic Engineering Center, 1978)

The WQRRS (Water Quality for River-Reservoir Systems) package includes SHP (Stream Hydraulics package), WQRRSQ (Stream Water Quality) and WQRRSR (Reservoir water quality model). The three components of the system may also be used independently. The hydraulic computations can be calculated either by hydrological routing, kinematic routing, steady flow equations or by the unsteady flow equations (using St Venant equations). The stream hydraulic module routes down the flow using several different methods (St. Venant equations, Kinematic Wave, Muskingum, Modified Puls) and is able to model both steady and unsteady flow regimes. The river quality module assumes, on the contrary steady flow conditions, and models aerobic degradation as well as simple diffusion of non reactive pollutants. The water quality models are able to calculate dissolved oxygen, total dissolved solids, the nutrients, alkalinity and carbon , two types of phytoplankton, benthic algae, zooplankton, benthic animals and three types of fish, organic sediment and coliform bacteria.

CE-QUAL-RIV1

(Environmental Laboratory, 1995)

This model is a fully dynamic one dimensional flow and water quality simulation model (US Army Corps of Engineers Waterways Experiment Station 1990). It was developed by the Ohio State University for the Environment Protection Agency (Bedford et al, 1983). This model is developed for highly unsteady flow conditions, and is able to handle various control structures as well as multiple control structures, such as dams and navigation locks. The model also includes two stand alone programs, that can be interfaced or used separately. RIV1H is the hydrodynamic model which uses a numerical solution to the St Venant flow equations, RIV1Q is the water quality program that simulates temperature, dissolved oxygen, biochemical oxygen demand and nutrients.

QUAL-2E

(Brown,L. And T.O. Barnwell, 1995)

QUAL2E has a long history with its first model being QUAL1 which was developed by the Texas Water Development Board (Orlob, 1992). The early and widespread use of QUAL2E makes it a standard against which other models are normally compared (Shanhan et al., 1998), but it also has a particular limitation in that it cannot simulate unsteady flow.

The Enhanced Stream Water Quality Model (QUAL2E) is applicable to well mixed, dendritic streams. It simulates the major processes of nutrient cycles, algae production, benthic and carbonaceous demand, atmospheric reaeration and their effects on the dissolved oxygen balance. It can predict up to 15 water quality constituent concentrations. It is intended as a water quality planning tool for developing total maximum daily loads (TMDLs) and can also be used in conjunction with field sampling for identifying the magnitude and quality characteristics of nonpoint sources. By operating the model dynamically, the user can study dissolved oxygen variations and algal growth. However, the effects of dynamic forcing functions, such as headwater flows or point source loads, cannot be modelled with QUAL2E. QUAL2EU allows users to perform three types of uncertainty analyses: sensitivity analysis, first order error analysis, and Monte Carlo simulation

WASP

(Ambrose et al., 1993)

The Water Quality Analysis Simulation Program (WASP) was developed and is maintained by the Environmental Protection Agency (EPA). It includes simulation for rivers, reservoirs and estuaries. It simulates time varying responses, the equations used are dispersion and advection. Point and non-point loading can be modelled and the water quality processes are modelled in special subroutines which allow the user to supply his own processes that are specific for the problem studied. It allows,by representing the water body as different segments, for one dimensional, two dimensional and three dimensional modelling. WASP consists of the hydrodynamic model DYNHYD and the water quality model WASP. WASP includes two different groups of water quality models, firstly EUTRO which is used to simulate dissolved oxygen, biochemical oxygen demand, nutrients and eutrophication., secondly TOXI, which simulates toxic pollution, comprising organic chemicals, metals and sediment. DYNHYD and WASP are able to stand alone, i.e. be used without the other model.

2.5.2 European Models:

DUFLOW

(STOWA/EDS, 1998)

DUFLOW (Dutch Flow)is the joint ownership of the Faculty of Civil Engineering at Delft University of Technology and the Public Works Department (Rijkswaterstaat), International Institute for Hydraulic and Environmental Engineering (IHE), the Delft University of Technology, the Agricultural University of Wageningen and STOWA. It includes three models, DUFLOW the hydrodynamic water quantity and water quality model, RAM, the precipitation runoff module and MODUFLOW, which incorporates Duflow with the ground water module MODFLOW. DUFLOW comes with two predefined water quality models, EUTROF1 and EUTROF2. Similar to WASP, the water quality processes can be modelled in special subroutines which allows the user to supply his own processes that are specific for the problem studied. The flow model is a one dimensional and uses the St Venant equations with numerical solution to calculate the flow. EUTROF1 includes the cycling of nitrogen, phosphorous and oxygen, as well as the growth of one phytoplankton species. In EUTROF2 the sediment water interaction is included as well as three algae species.

ISIS

(HR Wallingford, 1997)

ISIS contains various separate modules: the ISIS Flow, the ISIS Quality and ISIS Routing.

ISIS Flow is a full hydrodynamic simulator using 4 point implicit finite difference scheme as numerical solution for modelling flows and levels in open channels and estuaries. ISIS Flow is able to model complex looped and branched networks, and flood plain flows. ISIS Flow has options that include simple backwaters, flow routing and full unsteady simulation. Common types of bridges, culverts, sluices and weirs can be modelled.

ISIS Quality simulates water quality and includes advection / diffusion of conservative and non-conservative water quality variables, as well as water temperature, sediment transport, interaction of quality variables with sediments, phytoplankton and pH. The user is able to specify the processes included in the simulation.

MIKE-11

(DHI, 1992)

MIKE11 includes basic modules for rainfall-runoff, hydrodynamics, advection-dispersion and cohesive, as well as non-cohesive sediments and water quality simulations.

The hydrodynamic module an implicit, finite difference computation of unsteady flows in rivers and estuaries. Both subcritical and supercritical flow can be described by means of a numerical scheme which adapts according to the local flow conditions. The computational scheme is applicable to vertically homogeneous flow conditions ranging from steep river flows to tidally influenced estuaries. In addition to the fully dynamic description, a choice of other flow descriptions is available, such as diffusive wave, kinematic wave and quasi-steady state.

The water quality module requires output from the hydrodynamic module, in space and time, of discharge and water level, cross-sectional area and hydraulic radius. Conservative constituents can be modelled with the advection-dispersion module. For non-conservative constituents the user needs an additional module, the water quality module, which simulates degradation of organic matter, the

photosynthesis and respiration of plants, nitrification and the exchange of oxygen with the atmosphere. Two add-on modules are available for the Water Quality Module : the Water Quality Heavy Metals Module (WQHM) and the Eutrophication Module (EU).

Table 2.1 Comparison of model attributes

	CE-QUAL-RIV1	QUAL2E	WASP	WQRRS	DUFLOW	ISIS	MIKE-11
Distributers	US Army Corps of Engineers Waterways Experiment Station	EPA	EPA	US Army Corps of Engineers Hydrologic Engineering Center.	Delft, IHE, Agricultural University of Wageningen and STOWA	HR Wallingford	Danish Hydraulic Institute DHI
Dimensional Characteristics	one	one	one, two and three for quality module, one dim. for river module, 2,3 for lakes and estuary	one	one	one	one
Hydraulics	unsteady flow	steady flow	dynamic, unsteady flow	hydrological routing, kinematic routing, steady and unsteady flow	fully dynamic	kinematic routing, steady and fully dynamic	kinematic routing, diffusive wave approx. and fully dynamic
Equations used	St Venant	steady flow	St Venant	St Venant	St Venant	St Venant	St Venant
Numerical solution	finite difference, 4 point Preissmann scheme	N/A	finite difference	finite elements	finite difference, 4 point Preissmann scheme	finite difference, 4 point Preissmann scheme	finite difference, 6 point Abbot scheme
Water Quality Transport	advection, dispersion	advection/ dispersion	advection, dispersion	advection/dispersion	dispersion	advection/diffusion	advection/ diffusion
Water Quality Variables	temperature, DO, BOD and nutrients, Chl-1, algae	temperature, salinity, BOD-DO, Nitrogen, Phosphates, Chl-a, conservative and non-conservative variables	open structure, two predefined models : TOXI5 and EUTRO5	DO, BOD, nutrients, TDS, alkalinity, 2 types of phytoplankton, benthic algae + animals, zooplankton, 3 types of fish, organic sediment and chl-a	open structure, 2 predefined models EUTROF1 and EUTROF2	open structure, predefined quality model; conservative and non-conservative pollutants, water temperature, sediment transport	conservative and non-conservative; phosphates, eutrophication, heavy metals and sediments
Point/ Non-point sources	Point Sources	Point sources	point and diffuse mass loading	Point loading	point loading, diffuse loading only with prec., runoff module	point loading	point loading
Cost (at time of 1999)	Available from US Army Corps of Engineers Waterways Experiment Station	available from EPA through the internet, QUAL2E U$ 330	available from EPA through the internet, WASP5/ DYNHD5 U$ 330	available from US Army Corps of Engineers Hydrologic Engineering Center.	R 12 000 (DFL 4000)	R 50 000 (+ R10000 per module)	R 100 000+

2.6 DISCUSSION

In section 2.3.3 the selection criterias for choosing a suitable model have been discussed. In the case of the current Berg River study the following selection criteria have been declared important by the potential management-orientated user group (DWAF, pers. comm., 1999):

- user friendliness of model, availabilty and support of model
- cost of model
- ability to model water quality variables identified as variables of concern: salinity, oxygen, temperature and phosphates
- applicability, or ability to adjust to South African situation
- fine time resolution (daily)
- should be a hydrodynamic model for modelling flow variations during floods, low flows and in tributaries in time and space
- cost, availability and support in South Africa

With the introduction of the new Water Act in South Africa, water resource management and planning involves various users and goals. In order to be able to execute decisions the user does not want to rely on a complex model where extensive user expertise is necessary; but rather fast and reliable. If the model should be used as a management "tool", continuous support and availability is necessary. Due to South African conditions, it is desirable to have a model that is flexible and can be changed according to the specific problems studied and encountered. The model should be able to cope with different time steps and also with sudden and fast releases of the proposed dam or sudden spills that occur at a point source.

Using the selection criteria as a guide, it has been decided to use the DUFLOW model for this particular study. Although DUFLOW has the same limitations as say ISIS (no evaporation modelling), it is still much cheaper and comprises of an open water quality structure where the water quality processes can either be simplified or added/removed. The model allows the user to create a model in a user-friendly way through windows based interfaces and a graphical editor. As it is a hydrodynamic water quality model, the time and space steps can be entered as desired by the user; thus allowing fine time resolution. By inserting scenarios, the model could be used for management purposes.

2.7 REFERENCES

Ambrose, R.B, T.A. Wool, J.L Martin, 1993. *The water Quality Analysis Simulation Program WASP5. Part A: Model Documentation.* U.S. EPA, Athens, USA

Ang, A. H-S., W.H. Tang, 1975. *Probability Concepts in Engineering Planning and Design. Volume 1- Basic Principles*. Braun-Breumfield Inc.,Canada.

Brown, L and T.O. Barnwell, 1995. The Enhanced Stream Water Quality Models QUAL2E and QUAL2E-UNCAS: Documentation and User Manual. EPA report EPA/600/3-87/007. Athens.

Carstensen, J., P.A. Vanrolleghem, W. Rauch and P. Reichert, 1997. *Terminology and methodology in modelling for water quality management: a discussion starter.* Water Science and Technology, Vol (36) No 5, pg 157-168.

Chapra, S., 1997. Surface Water-Quality Modeling. McGraw-Hill Companies, USA

Chapra, S and Reckhow, K.H., 1983. *Engineering Approaches for lake management, Vol 2: mechanistic Modeling.* Butterworth Publishers. USA

DHI, 1992. *Mike 11 version 3.01, a microcomputer based modelling system for rivers and channels, Reference Manual,* Danish Hydraulic Institute Software.

DWAF, 1993. *South African Water Quality Guidelines, Volume 1: Domestic Use.* Department of Water Affairs and Forestry, Pretoria.

Environmental Laboratory, 1995. *CE-QUAL-RIV1 : A Dynamic One-Dimensional (Longitudinal) Water Quality Model for Streams. User Manual.* Instruction Report E-95, U.S. Army Engineer Waterways Experiment Station, Vicksburg, MS.

Görgens, AHM., 1983. *Conceptual Modelling on the Rainfall-Runoff Process in Semi-Arid Catchments*. Hydrological Research Unit, Rhodes University, Report No. 1/83, Grahamstown, South Africa.

Hydrologic Engineering Center, 1978. *WQRRS User's Manual.* CPD-8.Hydrologic Engineering Center.US Army Corps of Engineers , Davis, USA

HR Wallingford, 1997. *ISIS Flow, User Manual.* Halcrow/HR Wallingford, UK

Orlob, G.T., 1992. *Water-Quality Modeling for Decision Making.* ASCE Journal of Water Resources Planning and Management. Vol 118 (No 3) pg 295-307

Pegram, GC, AHM Görgens and AB Ottermann, 1997 . *A framework for addressing the information needs of catchment water quality management*, Water SA, Vol 23 No.1

Reckhow, K.H., J.T Clements and R.C. Dodd, 1990. *Statistical Evaluation of Mechanistic Water-Quality Models. ASCE Journal of Environmental Engineering,* Vol 116 No 2.

Sanders, T.G. , R.C. Ward, J.C. Loftis, T.D.Steele, D.D. Adrian and V. Yevjevich, 1983. *Design of Networks for Monitoring Water Quality*, Water Resources Publications, Littleton, Colorado

Shanahan, P, M.Henze, L. Koncsos, W.Rauch, P. Reichert, L. Somlyódy and P. Vanrolleghem, 1998. *River Water Quality Modelling: 2. Problems of the Art.* Water Science and Technology, Vol 38, No.11, pp. 245-252, IAWQ

STOWA/EDS, 1998. *Duflow for Windows . Version 3.0.* EDS, Leidschendam, The Netherlands.

Thomann, R.V., 1963. *Mathematical Model for Dissolved Oxygen*, Journal of Sanitary Engineering, ASCE, Vol 89, No. 5.

Thomann, R.V. and J.A. Mueller, 1987. *Principles of Surface Water Quality Modeling and Control.* Harper and Row, New York.

CHAPTER 3

DESCRIPTION OF THE BERG RIVER BASIN

3.1 GEOGRAPHY

The Berg River lies in the Western Cape and its catchment lies between latitude 23°45' and 33°50' south and longitude 18°15' and 18°55' east. The Berg River rises in the Jonkershoek and Franschhoek mountains and flows in a north westerly direction where it eventually discharges into the sea at Laaiplek. The major tributaries are the Franschhoek, Wemmers, Krom, Kompagnies, Klein Berg, Vier-en-Twintig Rivieren, Matjies, Platkloof, Boesmans and Sout Rivers. The river is about 270 km long and has a catchment of some 9000 km^2 (DWAF(c), 1993).

Figure 3.1 shows the gauging stations situated in the Berg River main stem, as well as the tributaries.

3.2 TOPOGRAPHY, GEOLOGY AND CLIMATE

The mainstem river is about 160 km long from the headwaters to the sea and its width varies from 1 to 5 km near its headwaters to between 30 to 40 km long at the coast. (Bath, 1989). The lower reach of the river is extremely flat so that sea water intrusion pushes up nearly 100 km from the river mouth under high tide conditions (Bath, 1989).

The Berg River is geologically an old river system. This can be seen firstly from the rapid fall in profile from headwaters and which then flattens out in the Paarl area, secondly from the degree of meandering of the main river channel and thirdly the existence of multiple channels separated by low lying islands in the lower reaches and the great width of the river valley (Bath, 1989).

The basin of the Berg River is bounded on the eastern side by a range of mountains (RL 1500m), on the western side the basin flattens out to a hilly plain. Downstream of Paarl/Wellington sandstone formations give way to Malmesbury shales, thereafter tributaries on the eastern bank of the Berg River drain areas

with Table Mountain Sandstone, while the western bank drains areas with the saline Malmesbury Shale as dominant geological formation (DWAF(c), 1993). Figure 3.2 shows the different geological formations found in the Berg River Catchment.

The Berg River catchment lies in the Winter rainfall area of the south-western Cape, about 80% of the rainfall falls in the months of April to September. Rainfall in the mountains is about 3000mm per year (Midgley et. al., 1994). The snow that falls on the peaks and upper slopes of the mountains during intermittent cold spells in the winter also contributes to the flows. In the adjoining valleys, rainfall varies from 900 to 1200 mm annually, but drops to between 400 and 500 mm in the hilly plain through which the river flows most of its length, and to even less when it approaches the sea (Midgley et. al., 1994). The tributaries are perennial on the eastern side and semi-perennial on the western side.

3.3 LAND COVER

Present land covers in the Berg River catchment fall primarily into three types: agricultural, forestry and urban. Agricultural land use is further divided into irrigated, and dry land farming activities. The latter of these make up the largest proportion of the catchment (DWAF(c), 1993).

There are 14 irrigation boards in the Berg River catchment area (Pers. Com., W. Enright, 2000). These are:

- La Motte
- Dal Josafat
- Palmiet River
- Kromme River
- Kleinberg River
- Twenty Four Rivers
- Berg River
- Simonsberg
- Suid-Agter-Paarl
- Noord-Agter-Paarl
- Perdeberg

- Riebeek Kasteel
- Riebeek Wes
- Lower Berg River

From the allocated amount of water, Upper Berg River Irrigation Board uses about 41%, the Twenty Four Rivers Irrigation Board and Klein Berg River area about 27% and 24% respectively, while the lower Berg River Irrigation Board uses only about 8% of the water used for irrigation (DWAF(c), 1993). A summary has been given in the Situation Analysis of the Berg River (DWAF(c), 1993) of the areas of the various crops under irrigation in the upper and middle reaches of the Berg River. The data was obtained from the irrigation boards in the Berg River catchment and from Burger et al., 1971. Although the data from Burger et. al., 1971, is old and possibly outdated, information from the irrigation boards still supported the recent data and the percentages of irrigation crops used has not changed much. Figure 3.3 shows the land use in the Berg River catchment, the lower reaches of the Berg River dry land farming is the predominant agricultural land use. Table 3.1. shows the percentage of crops irrigated in the upper and middle reaches (DWAF(c), 1993).

Table 3.1 Percentage of various crops under irrigation in the upper and middle reaches of the Berg River catchment. (DWAFc, 1993)

Crop	**% Area irrigated in the upper and middle Berg River reaches**
Soft Fruits (Apricots, Pears, Peaches etc.)	7.7
Sub Tropical Fruits (Oranges, lemon etc.)	3.2
Vineyards	51.6
Vegetables	1.7
Tobacco	0.5
Artificial pasture	10.6
Other (Almonds, Apples, Olives, Cherries etc.)	24.7

3.4 WATER INFRASTRUCTURE DEVELOPMENTS IN THE CATCHMENT

3.4.1 Voëlvlei Dam

The Voëlvlei Dam is an off channel storage dam, it was the first large water supply scheme that was developed in the Berg River catchment. The first Voëlvlei scheme was completed in 1953. The natural Vogelvlei lake was impounded by building a small wall structure. As the natural vlei had a catchment of only 40 km^2, additional water was diverted from the Klein Berg River, where a small weir was built, into a canal to the dam. In 1971 the dam was raised to its present full supply capacity of 172 Mm^3 (DWAF(d), 1994). The dam is currently supplied by diverted runoff from the Klein Berg River, and additionally Twenty-four Rivers and Leeu River catchments through canals. The dam supplies water to Cape Town, the Swartland Scheme and irrigation water for downstream users. The water for the Swartland Scheme supplies Riebeekkasteel, Riebeek Wes and Malmesbury, while the Voëlvlei water treatment works supplies Cape Town (DWAF(a), 1992). The irrigation water is released into the Berg River along with water for the Withoogte Scheme which is then abstracted from Misverstand Weir further downstream (DWAF(d), 1994).

3.4.2 Wemmershoek Dam

The Wemmers River was impounded in 1957 and supplies part of Cape Town's urban demand (DWAF(a), 1992). The Dam is owned by the City of Cape Town. The water from the Wemmershoek water treatment works supplies Cape Town, Paarl and Wellington (DWAF(a), 1992).The full supply capacity is 58.8 Mm^3 and a yield of 56 Mm^3 /a (DWAF(a), 1992). During low flow in the Berg River this scheme release compensation water to supply irrigation demands as far as the Voëlvlei canal. Since the completion of the Theewaterskloof-Riviersonderend (RSE) scheme the releases have been made from a tunnel into the upper Berg River at Robertsvlei.

3.4.3 Misverstand Dam

At Misverstand, in the lower Berg River, a weir was built across the river in 1975 to enable water to be abstracted (DWAF(d), 1994). The dam is linked to the Withoogte water treatment works via a 12.5 km pipeline, which supplies water to Moorreesburg, Vredenburg, Saldanha Bay and Langebaan. The capacity is about 6 Mm^3 (DWAF(d), 1994).

3.4.4 Theewaterskloof Dam

Although the Theewaterskloof Dam and the Riviersonderend scheme do not lie in the Berg River, it does supply water into the Berg River. The Theewaterskloof Dam has a capacity of about 480 Mm^3, and the system has a yield of 207 Mm^3 /a (DWAF(a), 1992).The dam was built in 1980 and is used to supply the Cape Town Municipality and irrigation in the Riviersonderend, Eerste and Berg River valleys (DWAF(e), 1994).

3.4.5 Future Developments

Due to mainly increasing population, a solution had to be found to meet Cape Towns increasing water demand. The following schemes are being investigated for imminent implementation in the Berg River: Skuifraam Dam in the Upper Berg, Skuifraam Supplement Pump Scheme downstream of Franschhoek and Lorelei Diversions to an enlarged Voëlvlei Dam in the Middle Berg (see Figure 3.4).

Skuifraam Dam:

Skuifraam Dam is proposed for the upper reaches of the upper Berg River just downstream of the confluence of the Berg and Wolwekloof Rivers. The dam would capture flood flows and transfer water to the Theewaterskloof Dam. The full supply capacity is supposed to be 168 Mm^3 and the naturalised inflow is estimated to be 115 Mm^3 (DWAF(f), 1994), the yield has been calculated to be 56 Mm^3/a. Detailed operation rules and use of the Skuifraam Scheme is described in the report *Development of the Upper Berg River (Skuifraam Scheme)* (DWAF(g), 1994).

Skuifraam Supplement Scheme:

The MAR between Skuifraam and Paarl increases by about 150 Mm^3/a (DWAF(f), 1994). Skuifraam Supplement Pumping Scheme has been proposed to abstract this potential water. The Skuifraam Supplement Scheme will have an off-channel balancing dam of about 4ha and the height of the diversion weir will be about 5m (DWAF(f), 1994). The water will be pumped at a capacity of $4m^3/s$ into the Skuifraam Dam. This scheme is presently in the planning stage.

Concerns have been raised that the salinity might increase after building the Skuifraam Dam, as the winter flow downstream of Skuifraam Dam would be reduced. A study done by Ninham Shand for the Western Cape System Analysis has however shown that this will have little effect on the salinity in the lower reaches (DWAF(b), 1993).

3.4.6 Operation of the Berg River-Theewaterskloof Link

The RSE scheme includes the Theewaterskloof dam on the Sonderend River, an underground tunnel goes through the Franschhoek mountains to the Blackheath water treatment works near Cape Town and an outlet in the upper Berg River which releases compensation water to supply irrigation demands in the Berg River, as well as an additional tunnel in the Upper Berg River that passes under the Klein Drakenstein Mountains to a balancing dam at Kleinplaas on the Jonkershoek tributary of the Eerste River; a third tunnel leads from the dam to an outlet near to Stellenbosch (DWAF(a), 1992). The three tunnels of the system are the Franschhoek/Jonkershoek Tunnel, the Dasbos and the Stellenboschberg Tunnels. The Franschhoek/Jonkershoek Tunnel is the main tunnel in the system and branches into the Dasbos and Stellenboschberg Tunnels, a pipeline connects the Franschhoek/Jonkershoek Tunnel to the Wemmershoek Dam, while another pipeline connects the Kleinplaas Dam, which is situated on the Eerste River, to the Stellenboschberg Tunnel. There are also minor pipelines from the Elandskloof Dam and also the Jonkershoek Weir to supply domestic demands. Diversion works on the Banhoek and Wolwekloof Rivers (tributaries of the Berg River), allow surplus winter flows to be diverted and conveyed through the tunnel system into Theewaterskloof Dam where the water is stored. In summer it can then be released back through the tunnel system to the various outlets (DWAF(e), 1992). The total releases into the Berg River are ranging from 15 to 35 Mm^3/a to supplement natural flow in the River.This quantity includes about 10 Mm^3/a which have been previously made by Wemmershoek Dam

(Pers. Com., W. Enright, 2000). The maximum capacity of the tunnel outlet is 6.6 m^3/s (DWAF(e), 1994).

The proposed Skuifraam Dam would transfer water to the Theewaterskloof Dam. The transfer will be achieved by pumping water through a pipeline into the Dasbos Tunnel and from there into the Franschhoek/Jonkershoek Tunnel, where water will be released into the Berg River for downstream irrigation demands and then the surplus water will be transferred into Theewaterskloof Dam. (DWAF(e), 1994)

3.5 REFERENCES

Bath, A.J., 1989. *Phosphate transport in the Berg River, Western Cape.* Technical report of the Department of Water Affairs and Forestry, Pretoria. TR 143.

Department of Water Affairs and Forestry, South Africa (a), 1992. *Description of existing urban water supply infrastructure.* Prepared by R Blackhurst and PR Little of Ninham Shand Inc. in association with BKS Inc. as part of the Western Cape System Analysis. DWAF Report No. P G000/00/1490. NSI Report No. 1752/5131.

Department of Water Affairs and Forestry, South Africa(b), 1993. *Hydro-salinity modelling of the Berg River Basin.* Report by Ninham Shand Inc. in association with BKS Inc. for the Department of Water Affairs.. DWAF report no. P G000/00/3392

Department of Water Affairs and Forestry, South Africa (c), 1993. G Quibell. *Water Quality in the Berg River: A Situation Analysis.* Department of Water Affairs and Forestry.

Department of Water Affairs and Forestry, South Africa (d), 1994. *Berg River Sub-system Analysis.* Prepared by R R Berg and M Thompson of Ninham Shand Inc. in association with BKS Inc. as part of the Western Cape System Analysis. DWAF Report No. P G000/00/4493. NSI Report No. 2030/5131.

Department of Water Affairs and Forestry, South Africa (e), 1994. *The Riviersonderend-Berg Sub-system Analysis.* Prepared by P Dunn and PR Little of Ninham Shand Inc. in association with BKS Inc. as part of the Western Cape System Analysis. DWAF Report No. P G000/00/4093. NSI Report No. 2048/5131.

Department of Water Affairs and Forestry, South Africa (f), 1994. *Options for the Supply of Water in the Western Cape.* Prepared by C A Carter and P R Little of Ninham Shand Inc. in association with BKS Inc. as part of the Western Cape System Analysis. DWAF Report No. P G000/00/4893. NSI Report No. 2094/5131.

Department of Water Affairs and Forestry, South Africa (g), 1994. *Development of the Upper Berg River (Skuifraam Scheme)*. Prepared by C A Carter of Ninham Shand Inc. in association with BKS Inc. as part of the Western Cape System Analysis. DWAF Report No. P G000/00/5793. NSI Report No. 2105/5131.

Enright, W., Personal Communication, Department of Water Affairs and Forestry, 2000.

Midgley,D.C. ; W.V. Pitman and B. J. Middleton, 1994. *Surface Water Resources of Southern Africa 1990: Volume 4* WRC report 298/4.1/94 (Appendices) and 298/4.2/94 (Book of maps)

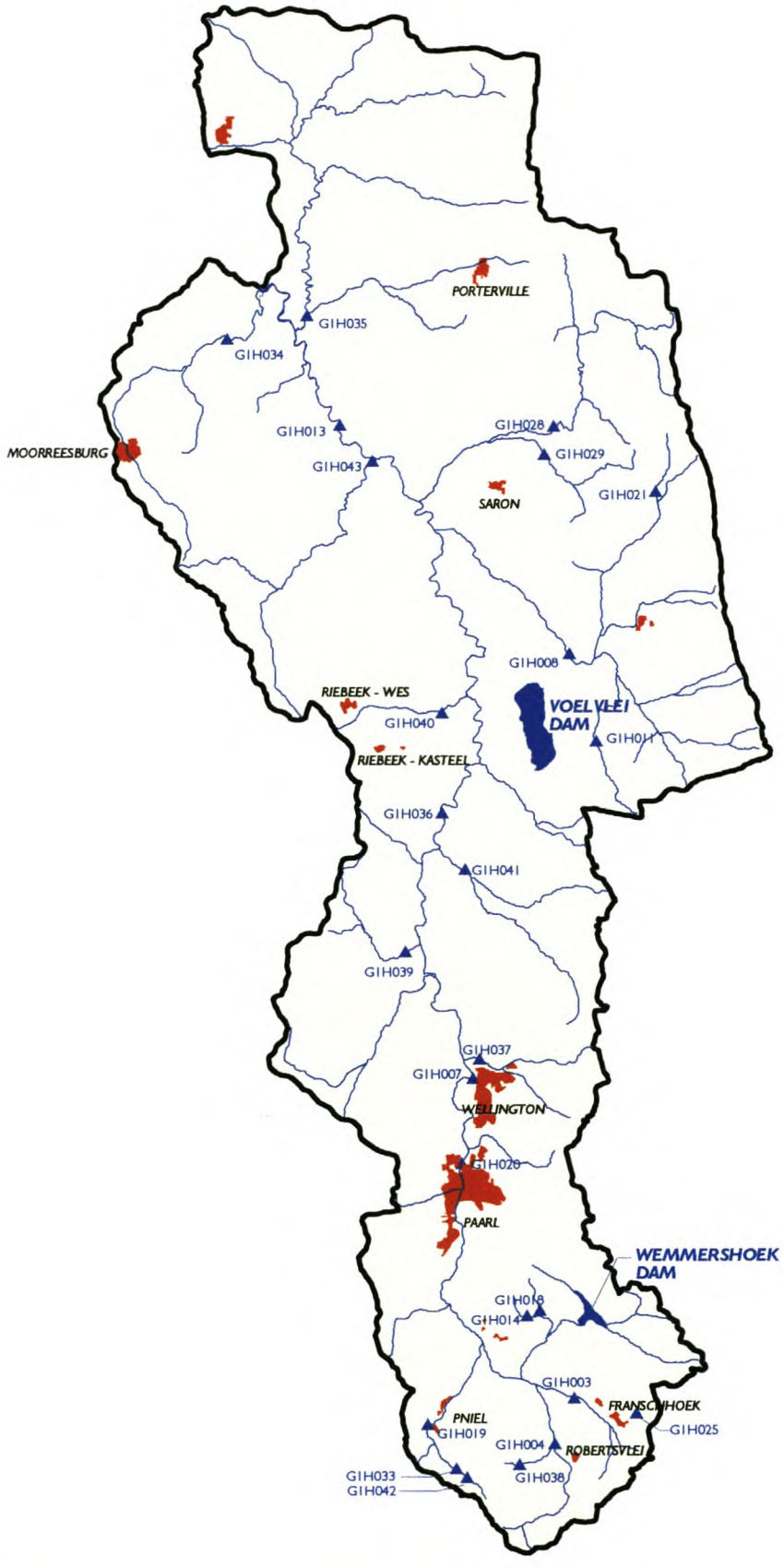

N

SCALE - 1: 600 000

0 5 10 15km

LEGEND :

Study Area | Dam

Town | River | Flow Gauge

ASSESSMENT OF A HYDRODYNAMIC WATER QUALITY MODEL, DUFLOW, FOR A WINTER RAINFALL RIVER

DATE : JULY 2000

Gauging Stations in the Berg River Region

FIGURE No. : **3.1**

P:\8276\ARCVIEW\PROJECTS\INITSCHEA.APR

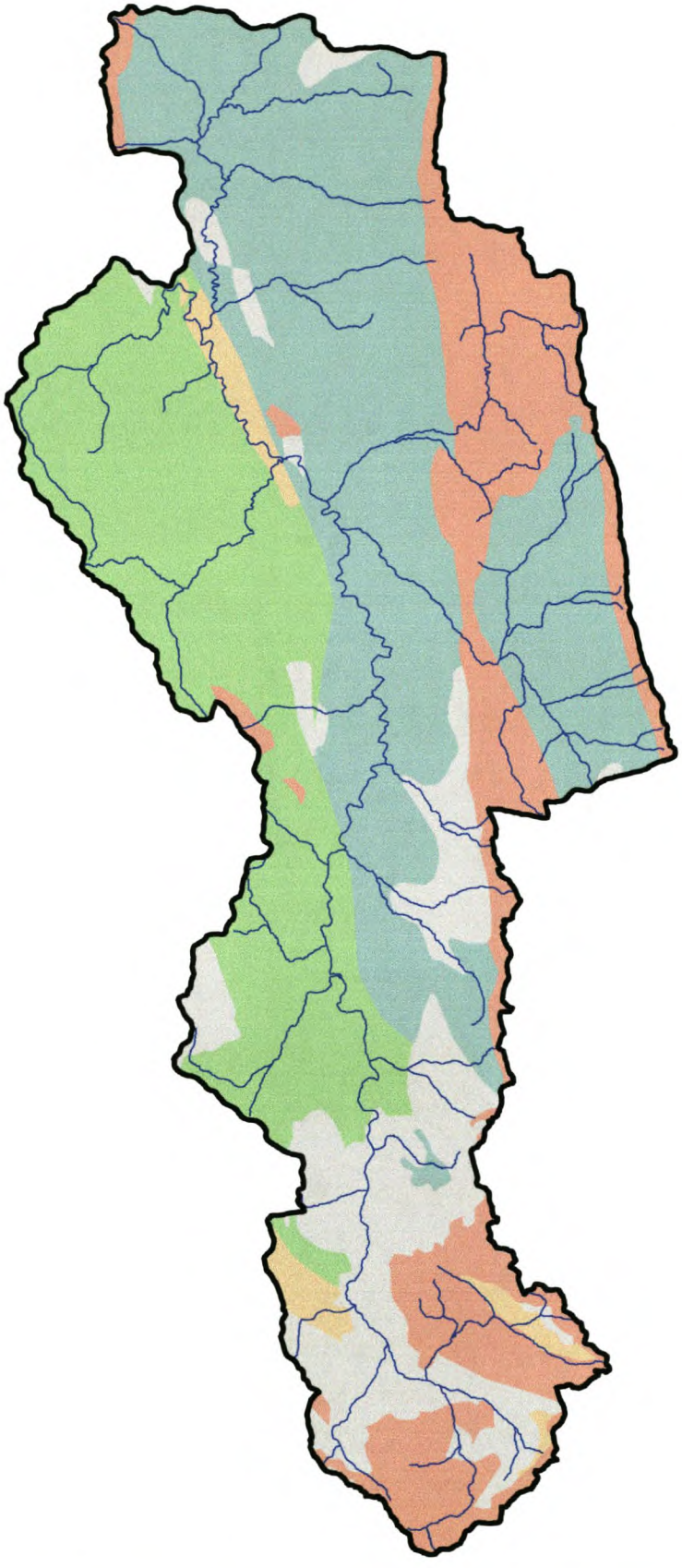

N

SCALE - 1: 600 000

0 5 10 15km

LEGEND :

Geological Classification

Study Area

River

Boland

Malmesbury

Swartland

Table Mountain

ASSESSMENT OF A HYDRODYNAMIC WATER QUALITY MODEL, DUFLOW, FOR A WINTER RAINFALL RIVER

DATE : JULY 2000

Geology in the Berg River Catchment

FIGURE No. : **3.2**

P:\8276\ARCVIEW\PROJECTS\INITSCHEAPR

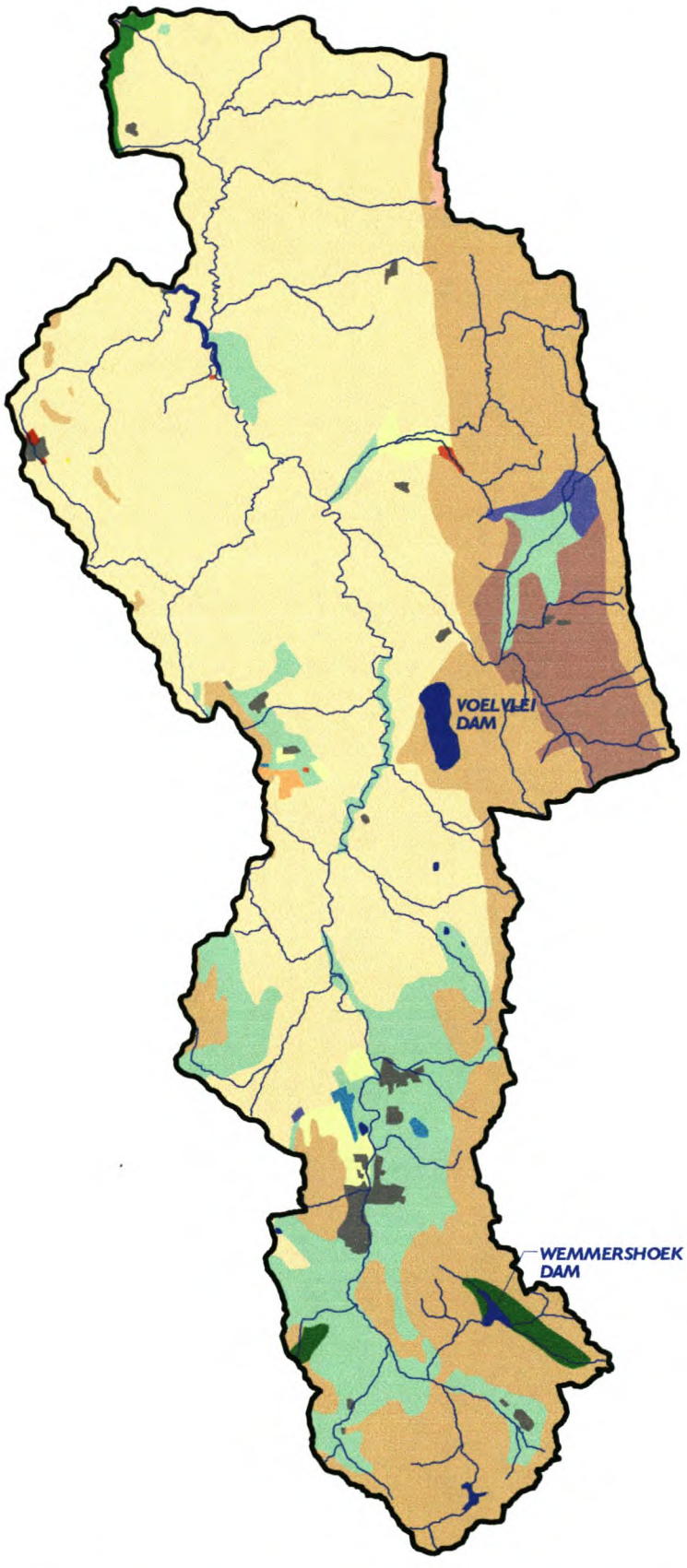

N

SCALE - 1: 600 000

0 5 10 15km

LEGEND :

Study Area

River

LANDUSE CLASSIFICATION

- Annual small grain
- Annual small grain/Natural grazing
- Small holdings
- Stone fruit
- Wine grapes/Table grapes
- Citrus
- Dams
- Stone fruit/Pome fruit
- Table grapes
- Wine grapes
- Natural grazing
- Other crops
- Unclassified
- Urban areas
- Pans
- Forestry
- Mining
- Reserves and Mountain veld
- Vegetables

ASSESSMENT OF A HYDRODYNAMIC WATER QUALITY MODEL, DUFLOW, FOR A WINTER RAINFALL RIVER

DATE : JULY 2000

Landuse in the Berg River Catchment

FIGURE No. : **3.3**

P:\8276\ARCVIEW\PROJECTS\INITSCHE.APR

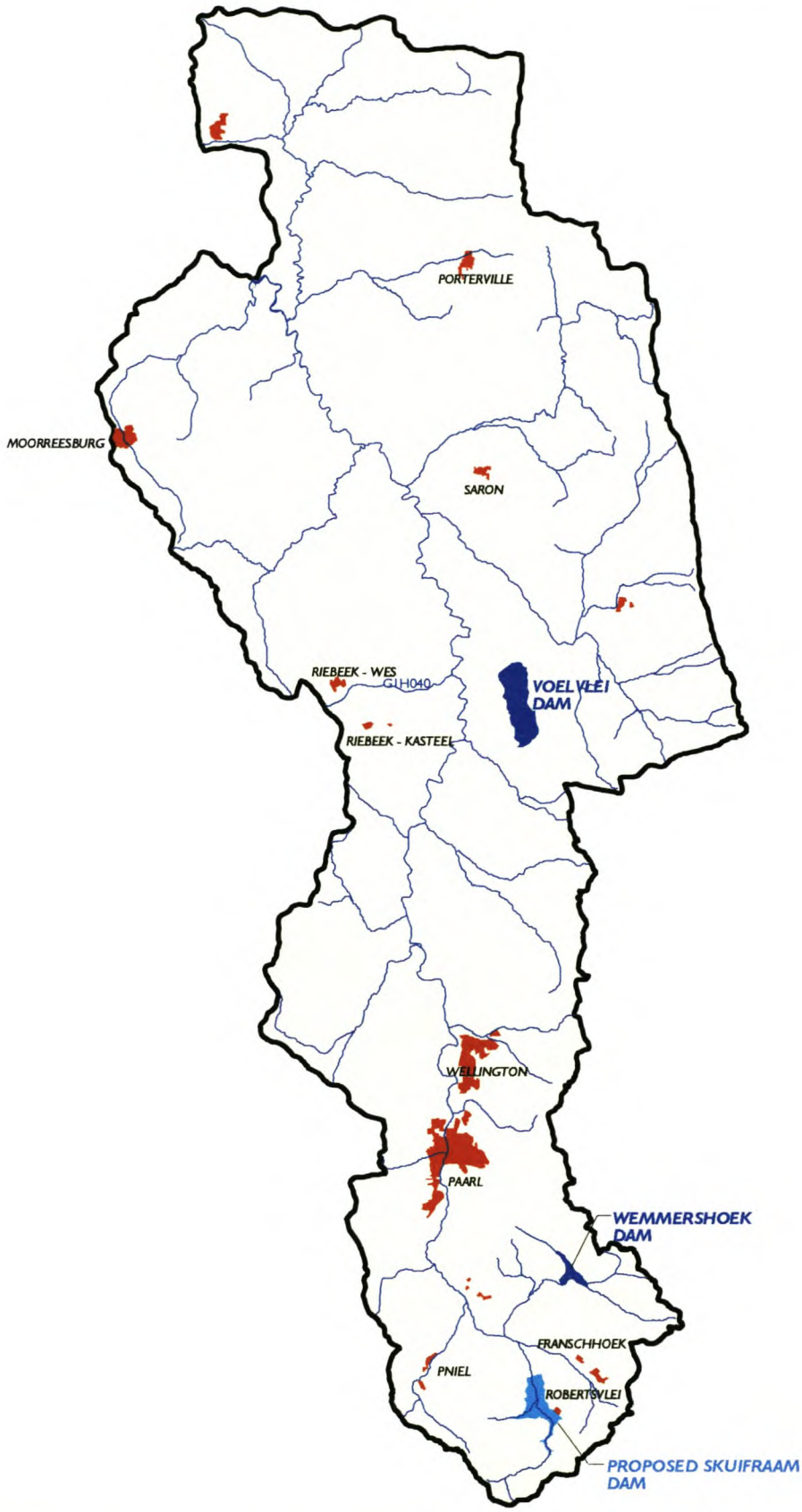

N

SCALE - 1: 600 000

0 5 10 15km

LEGEND :

Study Area | Dam | River

Town | Proposed Dam

ASSESSMENT OF A HYDRODYNAMIC WATER QUALITY MODEL, DUFLOW, FOR A WINTER RAINFALL RIVER

DATE : JULY 2000

Future Developments in the Berg River Catchment

FIGURE No. : **3.4**

P:\827\6\ARCVIEW\PROJECTS\NITSCHE.APR

CHAPTER 4

REVIEW OF WATER QUALITY STATUS OF BERG RIVER MAIN STEM

4.1 INTRODUCTION

To provide insight into the role a hydrodynamic model can play in the Berg River systems operations, it is necessary to assess the water quality status of the main stem of the Berg River and how it has changed through time.

To give a brief background to the studies that have been done in the past of the water quality situation in the Berg River, the most important findings are summarized in the first section of this chapter. These studies have been initiated due to concerns that water users have expressed about certain water quality variables.

From these studies, a minimum group of water quality variables of concern was identified, the relevant data assembled for the period of best availability; October 1992 to September 1998, and analysed for trends in comparison with the most recent source of information, i.e. the report '*Water Quality in the Berg River: A Situation Analysis' (DWAF(a), 1993)* which analysed samples taken until end of 1991. These results are discussed below in detail, showing the results in table format.

The study area was divided into four reaches and the data of the gauging station in the particular reach has been analysed and treated as "typical" values for the specific reach. Additionally, results are shown of gauging stations representing tributaries draining Table Mountain Sandstone , and a tributary draining saline Malmesbury shales as dominant geological formation. The quality of the water was also analysed by dividing the quality criterias into municipal and raw water users.

4.2 STUDIES DONE ON THE WATER QUALITY OF THE BERG RIVER

Concerns of salinity increase in the Berg River main stem and eutrophication at the Misverstand weir has led to various research investigations in the past.

One of the first studies was in the 1950s by Harrison and Elsworth (DWAF(a), 1993). This study was initiated to determine the degree of pollution of the river. Fourie and Steer (as cited by DWAF(a), 1993) and Fourie and Görgens (1977) investigated the mineralisation of the river. It was found that the salinity increases of the river could be the result of increasing irrigation along the river.

Bath (1989) studied the phosphate transport of the river and concluded that 80% of the annual phosphorous was contributed by diffuse sources. The implementation of the 1 mg/l special standard for phosphate was postponed, as it was shown that it would have an minimal effect on the phosphorous loading in the river (DWAF(a), 1993). A phosphorous transport module was developed which should assess the fate and transport of phosphorous along the river in order to be able to control it (Bath and Marais, 1991).

Due to concerns that the salinity in the Berg river would increase if Skuifraam Dam would be built in the upper reaches where the good quality water would be impounded, a salinity modelling study was undertaken by Ninham Shand. (DWAF(c), 1993). This study showed that the Skuifraam Dam would have relatively small effects on the salinity of the lower reaches in the river.

4.3 VARIABLES OF CONCERN

In line with the Situation Analysis by DWAF, which identified 12 variables of concern, the following variables of concern were considered:

- pH
- Salinity : Total Dissolved Salts (TDS) and EC
- Phosphate
- Temperature
- Oxygen

These variables of concern were chosen due to the availability of data. Although for oxygen no data is available, it is temperature dependent, and the concentrations can therefore be approximated (refer to section 6.3.3.2). Nitrates as NO_2 and NO_3 are also of major concern, but as nitrates are dependent on many chemical and biological factors and should not be modelled only by advection and dispersion, it has been decided to concentrate on the phosphate concentration in the river as an indication of the nutrient level in the river.

4.4 DELINEATION OF STUDY AREA

For ease of comparison we used the same division of the Berg River System as DWAF used in the Situation Analysis (DWAF(a), 1993). Water quality variables have been analysed and seperated according to the river reach, one gauging station per reach representing the average expected water quality values. Additionally, the water quality data of gauging stations representing a tributary draining the Table Mountain Sandstone, and a tributary draining the Malmesbury Shales as dominant geological formation, have been analysed evaluated. Figure 3.1 already showed the gauging stations in the Berg River Catchment.

The river reaches have been divided into:

River Reach 1

The river reach 1 includes the Berg River and all the tributaries upstream of Paarl (G1H020). No large urban or industrial sites occur in this region. The river and tributaries drain areas with Table Mountain Sandstone as dominant geological formation. The water quality data of G1H004 illustrates the quality of the water one can expect in the Upper Berg River.

River Reach 2

This reach covers the part of the catchment from Dal Josafat (G1H020) to Hermon (G1H036). Paarl and Wellington lie along this reach. Tributaries on the eastern bank of the Berg River drain areas with Table Mountain Sandstone, while the western bank drains areas with the saline Malmesbury Shale as dominant geological formation (DWAF(a), 1993). The reach stops just before the Voëlvlei canal where better quality water is released to supply downstream users. Summer irrigation demands are supplied by releases from the Theewaterskloof tunnel.

River Reach 3

This reach lies from G1H036 to the old Berg River pumpstation (G1H023). Only Klein Berg River and Twenty-Four Rivers drain the Table Mountain Sandstone. The water quality is improved by the releases of the Voëlvlei Dam to supply summer irrigation demands. This reach includes the impoundment at Misverstand from where the Withoogte WTW abstracts water.

River Reach 4

This reach marks the section that is influenced by the tidal effects and is consequently characterised by higher salinity. The water quality data of G1H023 is indicative of the water quality in this reach.

4.5 WATER USERS

In the comparison of trends that follow below the division of users into municipal and raw water users in the Situation Analysis (DWAF(a),1993) was accepted for this study.

4.6 ASSESSMENT OF PH

4.6.1 Introduction

The pH of water is determined by the concentration of the hydrogen ion (H+). A pH below 7 indicates that the water is acidic in nature, while above 7 it is alkaline. Most fresh waters are more or less neutral with pH ranges around 6-8 (Dallas, Day, 1993). The pH of natural waters influences physical, chemical and biological processes in the system. The surface waters in the upper Berg River Catchment tend to be acidic.

N.B.: In all the samples taken one can see a step of about +1 pH after 1989/1990. It should be noted that in 1989 DWAF improved the preservation of samples through a more efficient preservation method, as well as improving laboratory procedures, that prevented microbiological acidification in the sample (Dr P. Kempster, IWQS: pers.comm., 1998).

4.6.2 Main Stem Sampling Stations

Spatial Pattern

It can be seen from Table 4.10 that the tributaries on the eastern bank of the river tend to be more acidic than the waters of the western bank tributaries. This is because the tributaries on the eastern bank drain areas with Table Mountain Sandstone as main geological formation, which weather to acidic soils and are also low in salts. The water of the Berg River becomes more alkaline downstream with the more acidic water at the origin of the river. Refer to Table 4.2 for intervals of pH that were used by DWAF to analyse the quality of the water.

Temporal Pattern

Findings in '*Water Quality in the Berg River: A Situation Analysis*'(DWAF (a), 1993)	**Trends during 1992-1998**
The pH does not seem to indicate a seasonal trend, although unusual long-term changes were observed at river reach 3. In the early 1970's the pH varied between 7 and 8 while in the term 1970 to 1980 the pH declined and ranged from 5.5 to 7 in 1980. The pH increased again, especially in 1989, 1990 and reached values ranging from 7 and 8 in 1991.	The means of the different sampling stations seem to stay constant after the increase in pH in 1989/90. Only few samples fall above a pH 8.5 and thus no actual problems should be encountered with irrigation (refer to Table 4.2 and 4.3). At all the sampling stations (Figures 4.1 to 4.10, also Table 4.3 and Table 4.10) the range of the pH's seems to deviate less from the median than was the case in the previous years and the values are concentrated more around the median.

4.6.3 Municipal Supply

Many of the problems that are encountered by the municipal supplies occur due to the acidic nature of the water of the upper Berg River Catchment. The raw water tends to dissolve the cement lining of the water distribution networks (aggression) and thus the water needs to be treated in order to raise the pH. This increases the cost of the water treatment. The pH also influences the solubility of iron and aluminium. The concentration of these elements is quite high in waters with low pH, but as aluminium and iron are removed in the treatment process, problems would not be expected of the treated water. (DWAF(b), 1993). The intervals that were used by DWAF to assess the pH of the water can be seen in Table 4.4.

Sampling Station	*Findings in 'Water Quality in the Berg River: A Situation Analysis' (DWAF(a), 1993)*	***Trends during 1992-1998***
Wemmershoek water treatment works G1R002	At Wemmershoek water treatment works the pH lies mostly below the value of 6.5. This means that 'for most of the time the water is potentially aggressive to cement structures, and that the water would require a high lime dosage to condition the final water to pH 9'. It has been observed that the alkalinity of the water is mostly low (<5mg/l as $CaCO_3$) and will thus react readily to lime addition. The pH of the water is nevertheless not considered to be a problem within the treatment works. pH does not seem to be seasonal.	Only 46 samples were taken during the period 1991 to 1998, with only 3 samples during 1993.The pH values seem to stay constant since the increase in 1989. The majority of the pH values of the samples lie between 6 and 7 (refer to Tables 4.5 and 4.13 and Figures 4.9).
Swartland water treatment works G1R001	For 35% of the time the pH of the water is below 6.5, when excess lime needs to be used. The alkalinity is low and pH conditioning should not be a problem. The pH varies from 8.9 to 4.2 with a median of about 6.7.	The pH values deviate less from their mean in the years 1993 to 1998. From 1989 to 1993 more occasional high pH values (over pH 8.5) were measured. Most values are between 6.5 and 8.5 (refer to Tables 4.5 and 4.13 and Figure 4.8).
Withoogte water treatment works G1R003	The pH seems to be seasonal, peaking in the summer months. The pH also seems to have increased over the years. The range, including the increase from 1989 to 1990, is from 5.3 to 8.8 with a median of 6.9. As most of the values lie between 6.5 and 8.5, there should not be any problems for municipal supplies.	The pH values lie mainly between pH 7 and 8. No values over pH 8.5 were observed. In the summer of 1992 some values were very low at pH 4 to 5, but thereafter the values were all above pH 6 again. The pH values seem to be seasonal but the seasonality seems not apparent in the years 1996, 1997. Here also, the deviation from the mean seems to be less than in the previous years (refer to Tables 4.5 and 4.13 and Figure 4.10).

4.7 ASSESSMENT OF EC AND TDS

4.7.1 Introduction

Electrical Conductivity represents the ability of the water to conduct an electrical current. It is a measure of the concentration of dissolved salts and hence the salinity and total dissolved salts (TDS) contents of the water. Taste, hardness and corrosion are affected by the components of TDS, including chlorides, sulphates, magnesium, calcium and carbonates.

The South African Water Quality Guidelines expresses the target range in conductivity (mS/m) and lists the corresponding value for total dissolved solids in milligrams per litre (mg/l). Since the majority of material dissolved in most water is ionic, TDS and conductivity usually correlate closely for a particular type of water. (Dallas, Day, 1993) In the South African Guidelines the relationship between Total Dissolved Salts (TDS) and Electrical Conductivity (EC) is specified as:
EC (mS/m) * 6.5 = TDS (mg/l),
but in reality it varies, depending on the nature and concentration of the solutes present, their degree of dissociation into ions, the amount of electrical charge on each ion, the mobility of the ions and the temperature of the solution (DWAF (b), 1993).

To be able to compare the samples of the period 1980-1990 that were analysed for the Situation Analysis (DWAF(a), 1993) with the samples of 1991-1998, EC was taken as the measure of salinity.

4.7.2 Main Stem Sampling Stations

Spatial Pattern

High salinity occurs in the rivers draining the Malmesbury Shales (Doring, Fish, Sand, Matjies, Sout and Morreesburg Rivers). This makes the water of these rivers highly unsuitable for irrigation and yield losses should be expected. The tributaries draining the Table Mountain series as dominant geological formation show a low TDS concentration.

The water of the Berg River becomes more saline further downstream due to the runoff from the Malmesbury Shales.

Temporal Pattern

Refer to Table 4.6 for intervals of EC that were used by DWAF to assess the quality of the water for irrigation.

Findings in 'Water Quality in the Berg River: A Situation Analysis'(DWAF(a), 1993)	***Trends during 1992-1998***
It was detected in the analysis by DWAF that positive trends exist in the years 1980 to 1992 at all the points analysed for EC. It was implied that this increase in salinity is because of increases predominantly in the sodium and chloride concentrations.	Comparing the percentage of values falling in a certain range (see Table 4.7) one could say that the salinity has increased slightly over the years in the lower reaches, although this increase is not very high. From the Figures 4.11-4.16 one can see clearly that the EC has a seasonal pattern. The seasonal variation in conductivity for G1H020 (Figure 4.12) and G1H036 (Figure 4.13) is probably caused by saline irrigation return flow entering the river during the low flow summer months. (DWAF (d), 1993). Refer to Table 4.7 and Table 4.11 for statistics of salinity and percentages falling into th intervals specified.

4.7.3 Municipal Supply

The intervals that were used by DWAF to assess the quality of the water with respect to salinity can be seen in Table 4.8.

Sampling Station	*Findings in 'Water Quality in the Berg River: A Situation Analysis' (DWAF(a), 1993)*	*Trends during 1992-1998*
Wemmershoek water treatment works G1R002	The EC of the water supplied to Wemmershoek water treatment works remains steadily below 4 mS/m, except for an outlier on the 7th August 1986: EC = 88mS/m, TDS value is 595 mg/l.	There does not seem to be an increase in EC values. Most of the samples taken fall below 5 mS/m. (refer to Table 4.9 and 4.14 and Figure 4.19)
Swartland water treatment works G1R001	The EC of the water ranges from 8 to 14 mS/m and problems should not be encountered.	All samples taken are below 25mS/m. There seemed to be an increase in salinity from the years 1992 to 1994, but thereafter it seems to decrease again and most samples are just above 11 mS/m. (refer to Table 4.9 and 4.14 and Figure 4.18)
Withoogte water treatment works G1R003	At Misverstand Weir the EC does not seem to be seasonal, but it has been perceived that the EC is higher in the wetter months in the year. It has been suggested that rainfall washoff is responsible for the higher salt concentrations and that long term trends in the salinity are likely to follow the trends of the rainfall cycles. The range is from 13 to 95 mS/m with a median at about 37.2 mS/m.	There does not seem to be an increase in EC values at Misverstand weir. (refer to Table 4.9 and 4.14 and Figure 4.20)

4.8 ASSESSMENT OF PHOSPHATES

4.8.1 Introduction

Eutrophication refers to water, particularly in lakes and reservoirs, which is high in nutrients and hence has excessive plant and algae growth, rendering the water less fit for use.

DWAF assessed the trophic status of the Berg River by examining the chlorophyll a concentration. For economy of efficiency it was decided to focus in this study on phosphates as indicator of the nutrient status.

4.8.2 Main Stem Sampling Stations

Findings in 'Water Quality in the Berg River: A Situation Analysis'(DWAF(a), 1993)	***Trends during 1992-1998***
It has been observed by studying the chlorophyll a concentrations that the concentrations still fall within the South African target guideline range. It has been concluded that chlorophyll-a related problems for recreation or irrigation is unlikely.	An increase in phosphate concentrations at all stations (refer to Figures 4.31 to 4.37 and Table 4.12) can be clearly seen. In the years 1980-1990 there seems to be more occasional outliers in the concentrations.

4.8.3 Municipal Supply

Sampling Station	*Findings in 'Water Quality in the Berg River: A Situation Analysis' (DWAF(a), 1993)*	*Trends during 1992-1998*
Wemmershoek water treatment works G1R002	From the analysis of the chlorophyll-a concentrations it was suggested that at Wemmershoek WTW, Voëlvlei and Swartland WTWs no serious problems are expected with regard to the chlorophyll a concentrations.	At Wemmershoek water treatment works (G1R002) only few samples were taken and it is difficult to see any pattern to be able to compare it to the previous years. The samples taken show still a low phosphate concentration and thus there should be minimum algal growth.(see also Figure 4.39 and Table 4.15)
Swartland water treatment works G1R001	From the analysis of the chlorophyll-a concentrations it was suggested that at Wemmershoek WTW, Voëlvlei and Swartland WTWs no serious problems are expected with regard to the chlorophyll a concentrations.	At the Swartland water treatment works the range of phosphorus lies between 0 to 0.04 with most values between 0.01 and 0.03, where previously the values mostly fell below 0.02 mg/l. Here also the concentration of phosphate is still relatively low. (see Figure 4.38 and Table 4.15)
Withoogte water treatment works G1R003	"Nutrient concentrations in Misverstand weir are more than sufficient to sustain a large algae population, but the number of algae in this water body are held in check by the high turbidity of the system. Elevated turbidity reduces the amount of light available to the algae and hence inhibits their growth. However in the Misverstand weir the physical and chemical conditions are such that they promote the development of a type of algae which creates taste and odour problems at very low concentrations." (*DWAF(a), 1993*). At Misverstand weir the chlorophyll-a concentrations are much higher and the water needs to be treated accordingly. The chlorophyll a concentrations seem strongly seasonal with peak concentrations in summer.	From the graphs of Withoogte (Misverstand weir) and at Swartland water treatment works one can very clearly see that the phosphate concentrations have increased from 1991 onwards. The phosphate concentration ranges from 0.01 to 0.06 with most values at 0.025 mg/l as PO_4 (refer to Figure 4.40 and Table 4.15).

4.9 ADDITIONAL WATER QUALITY SAMPLES TAKEN IN THE BERG RIVER MAIN STEM

Additional water quality samples have been taken in the Berg River main stem weekly over a two month period. The water quality variables sampled were EC, pH, Oxygen and Temperature. The location the samples were taken are at:

- Bien Donne : lies upstream of Paarl, wine and fruit farm
- Picardi: lies in Paarl just upstream of railway bridge, samples were taken at the effluent discharge and just downstream of effluent discharge
- Wellington: samples were taken downstream of Krom River confluence at Sanddrift downstream of Leather factory in Wellington

Table 4.1: Summary of water quality samples taken in the Berg River

	pH	EC (mS/m)	O_2 (mg/l)	Temp (°C)
Bien Donne	6.7	7.2	9.6	19.3
Picardi (ds of effl.)	6.8	8.4	/	/
Picardi (at effl.)	6.7	24.4	/	/
Wellington	6.9	17.2	7.7	18.4

Comparing the EC results (Table 4.1)with Table 4.11, it can be seen that the EC values measured upstream of Dal Josafat (G1H020) are below the mean of 10.6 mS/m at G1H020. At Wellington the EC value measured is 6.6 mS/m higher than the mean measured at G1H020. These measured values indicate that the EC in the river increases rapidly downstream of Paarl, which could be the result of the industrial effluent discharging into the river.

Comparing the pH results with Table 4.10, it can be seen that the pH samples measured just upstream of G1H020 (Bien Donne and Picardi) are below the average pH of 7.3 calculated for the historical grab

samples taken at G1H020. The pH measurements taken at Wellington are also below the average at G1H020.

As no other oxygen samples have been taken in the Berg River no comparison to other samples can be made.

The temperature samples lie below 20°C. The samples have been taken between March and end of May, and comparing the results to Table 6.15 of section 6.3.1, these averages are to be expected.

4.10 CONCLUSIONS

- **Assessment of pH**

After the change in preservation of samples (1989,1990) the pH concentration seems to be more consistent and deviates less around the mean. Problems that could occur for the municipal water users stem from the low pH of the upper Berg river and the acidic runoff from the Table Mountain Sandstone areas.

- **Assessment of salinity**

No significant increase in salinity during the period 1992-1998 is evident and should therefore at this time not be necessarily a cause of concern. The lower part of the Berg River is much more saline than the upper reaches (which could create problems for the municipal supply and irrigation) and care should be taken that these reaches do not increase in salinity over the years.

- **Assessment of phosphate**

At all stations an increase in phosphates over the years can be seen.

4.11 REFERENCES

Bath, A.J., 1989. *Phosphate transport in the Berg River, Western Cape.* Technical report of the Deopartment of Water Affairs and Forestry, Pretoria. TR 143.

Bath, A.J. and G.v.R. Marais, 1991. *Application of a Phosphate Transport Model for the Management of the upper Berg River Basin.* Paper presented at the 5th South African National Hydrological Symposium. Stellenbosch, 3A-4-1 to 3A-4-10.

Dallas,H.F; J. A. Day, 1993. *The Effect of Water Quality Variables on Riverine Ecosystems: A Review.* Freshwater Research Unit, UCT prepared for WRC.

DWAF(a), 1993. G Quibell. *Water Quality in the Berg River: A Situation Analysis.* Department of Water Affairs and Forestry.

DWAF(b), 1993. *South African Water Quality Guidelines, Volume 2 Domestic Water.* Department of Water Affairs and Forestry, Pretoria.

DWAF(b), 1993. *South African Water Quality Guidelines, Volume 5 Industrial Water Use.* Department of Water Affairs and Forestry, Pretoria.

DWAF(b), 1993.*South African Water Quality Guidelines,Agricultural Water Use.* Department of Water Affairs and Forestry, Pretoria.

DWAF(c), 1993. *Hydro-salinity modelling of the Berg River Basin.* Report by Ninham Shand Inc. in association with BKS Inc. for the Department of Water Affairs.. DWAF report no. P G000/00/3392

DWAF(d), 1993. *Western Cape System Analysis: Water Quality Volume 1: General.* Report by Ninham Shand Inc. in association with BKS Inc. for the Department of Water Affairs. DWAF report no. P G000/00/2891

Fourier, J.M and Steer, A.G., 1971. *A survey of water quality of the Great Berg River (1963 to 1970)* Research Report of the National Institute for Water Research. CSIR, Cape Town. As cited by DWAF(a) 1993.

Fourier, J.M. and Görgens, AHM., 1977. *Mineralisation studies of the Berg River. (1974 to 1976).* Research Report of the National Institute for Water research, CSIR, Research Report No 334

Table 4.2 Intervals of pH values used in the Situation Analysis (DWAF(a), 1993) to assess the quality of the water for irrigation usage

pH	Impact
<7	Possible problems when used on acidic soils, the water is corrosive, and may cause eye irritation in swimmers.
>= 6.5 < 8.5	No significant problems identified.
>= 8.5	Possible problems when irrigated on alkaline soils, restrictions on drip irrigation.

Table 4.3 Percentage of pH values falling below pH 7 for raw water users

Station		Prior 1991 DWAF Situation Analysis (data from 1980 where available)	Jan 1991 to May 1998
River Reach 1			
G1H004 (Upper Berg River)	pH < 7 pH > 7	90% 10%	58% 42%
G1H020 (Paarl)	pH < 7 pH > 7	82% 18%	17% 83%
River Reach 2			
G1H036	pH < 7 pH > 7	63% 37%	4% 96%
G1H037 (Krom River)	pH < 7 pH > 7	74% 26%	3% 97%
G1H041 (Kompanjies River)	pH < 7 pH > 7	65% 35%	3% 97%
River Reach 3			
G1H008 (Little Berg River)	pH < 7 pH > 7	83% 17%	4% 96%
G1H013 (Drie Heuwels)	pH < 7 pH > 7	65% 35%	3% 97%
River Reach 4			
G1H023 (Old Pumping Station)	pH < 7 pH > 7	12% 88%	1% 99%

Table 4.4 Intervals of pH values used in the Situation Analysis (DWAF(a), 1993) to assess the quality of the water with respect to raw water supplied to water treatment works

pH	Impact
<6.5	The water is aggressive to cement, and requires increased lime dosage.
>= 6.5 < 8.5	The water can be treated without significant problems.
>= 8.5	The water cannot be effectively disinfected.

Table 4.5 Percentage of pH values falling below pH 7 for municipal supply

Station		Prior 1991 DWAF Situation Analysis (data from 1980 where available)	Jan 1991 to May 1998
G1R002 Wemmershoek Water Treatment Works	pH < 6.5 pH >6.5 <8.5 pH >8.5	70% 30%	63% 37%
G1R001 Swartland Water Treatment Works	pH < 6.5 pH >6.5 <8.5 pH >8.5	35% 62% 3%	1% 98% 1%
G1R003 Withoogte Water Treatment Works	pH < 6.5 pH >6.5 <8.5 pH >8.5	19% 80% 1%	2% 98%

Table 4.6 Intervals of EC values used in the Situation Analysis (DWAF(a), 1993) to assess the quality of the water for irrigation usuage

EC (mS/m)	Impact
<40	SA target guideline range. 100% yield on all crops.
>= 40 < 90	95% yield for moderately sensitive crops for surface irrigation.
>= 90 < 270	90% yield for all moderately tolerant crops.
>= 270 < 430	80% yield for all moderately tolerant crops.
>= 430	Not recommended for irrigation on any crops.

Table 4.7 Percentage of EC values for irrigation

Station		Prior 1991 DWAF Situation Analysis (data from 1980 where available)	Jan 1991 to May 1998
River Reach 1			
G1H004 (Upper Berg River)	EC < 40	100%	100%
G1H020 (Paarl)	EC < 40	100%	100%
River Reach 2			
G1H036	EC < 40 EC >= 40 < 90	97.5% 2.5%	99.2% 0.8%
G1H037 (Krom River)	EC < 40 EC >= 40 < 90	99.8% 0.2%	100% 0%
G1H041 (Kompanjies River)	EC < 40 EC >= 40 < 90 EC>= 90 < 270	84% 15% 1%	82.3% 17% 0.7%
River Reach 3			
G1H008 (Little Berg River)	EC < 40 EC >= 40 < 90	100% 0%	98% 2%
G1H013 (Drie Heuwels)	EC < 40 EC >= 40 < 90	99% 1%	98% 2%
River Reach 4			
G1H023 (Old Pumping Station)	EC < 40 EC >= 40 < 90 EC>= 90 < 270 EC>= 270 < 430 EC>= 430	9% 30% 53% 7% 1%	6.5% 48% 40.3% 2.6% 2.6%

Table 4.8 Intervals of EC values used in the Situation Analysis (DWAF(a), 1993) to assess the quality of the water with respect to raw water supplied to water treatment works

EC (mS/m)	Impact
<70	Below the drinking water criteria, but some sensitive industries may experience problems. The SA target guideline range for the leather industry.
>= 70 < 150	Exceeds the recommended limit for SA drinking water, and the US EPA limit (above 77 mS/m). Moderate increases in water costs for the leather industry.
>= 150 <300	Possible palatability problems. Problematic for most industries. Corrosion for scale forming properties evident. Substantial increase in water costs for the leather industry.
>=300	Laxative effects in humans. Exceeds the maximum permissible limit for EC in SA drinking water. Unsuitable for most industries.

Table 4.9 Percentage of EC values falling in the indicated intervals for municipal users

Station		Prior 1991 DWAF Situation Analysis (data from 1980 where available)	Jan 1991 to May 1998
G1R002 **Wemmershoek Water Treatment Works**	**EC <70**	**100%**	**100%**
G1R001 **Swartland Water Treatment Works**	**EC <70**	**100%**	**100%**
G1R003 **Withoogte Water Treatment Works**	**EC <70** **EC 70-150**	**97%** **3%**	**98%** **2%**

Table 4.10 Statistics of pH at River Gauging Stations

Station		Prior 1991 DWAF Situation Analysis (data from 1980 where available)	Jan 1991 to May 1998
River Reach 1			
G1H004 (Upper Berg River)	Mean	5.62	6.61
	Standard Deviation	0.977	0.65
	Minimum Value	3.76	4.83
	Maximum Value	7.89	8.49
	Number of samples	95	226
G1H020 (Paarl)	Mean	6.205	7.29
	Standard Deviation	0.765	0.316
	Minimum Value	3.26	6.4
	Maximum Value	8.45	8.91
	Number of samples	601	308
River Reach 2			
G1H036	Mean	6.96	7.55
	Standard Deviation	0.65	0.504
	Minimum Value	4.1	0.01
	Maximum Value	8.63	8.49
	Number of samples	341	311
G1H041 (Kompanjies River)	Mean	6.74	7.59
	Standard Deviation	0.876	0.3
	Minimum Value	2.07	6.57
	Maximum Value	9.9	8.45
	Number of samples	502	226
River Reach 3			
G1H008 (Little Berg River)	Mean	6.71	7.53
	Standard Deviation	0.676	0.261
	Minimum Value	4.6	6.77
	Maximum Value	8.58	8.45
	Number of samples	444	297
G1H013 (Drie Heuwels)	Mean	6.73	7.589
	Standard Deviation	0.67	0.379
	Minimum Value	3.48	4.25
	Maximum Value	9.4	8.48
	Number of samples	598	313
River Reach 4			
G1H023 (Old Pumping Station)	Mean	7.08	7.67
	Standard Deviation	0.478	0.245
	Minimum Value	5.9	7
	Maximum Value	8.14	8.2
	Number of samples	95	68

Table 4.11 Statistics of Electrical Conductivity at River Gauging Stations

Station		Prior 1991 DWAF Situation Analysis (data from 1980 where available)	Jan 1991 to May 1998
River Reach 1			
G1H004 (Upper Berg River)	Mean	5.67	5.59
	Standard Deviation	2.9	1.17
	Minimum Value	2.4	2.9
	Maximum Value	19.5	11.2
	Number of samples	344	238
G1H020 (Paarl)	Mean	11	10.56
	Standard Deviation	3.15	3
	Minimum Value	3.3	5.8
	Maximum Value	42.6	41.9
	Number of samples	603	308
River Reach 2			
G1H036	Mean	22.35	21.67
	Standard Deviation	8.38	6.34
	Minimum Value	6.5	7.8
	Maximum Value	111.8	69.5
	Number of samples	413	311
G1H041 (Kompanjies River)	Mean	29.68	31
	Standard Deviation	40.74	15
	Minimum Value	7.3	10.6
	Maximum Value	865	95
	Number of samples	502	226
River Reach 3			
G1H008 (Little Berg River)	Mean	17.58	20.73
	Standard Deviation	5.62	6
	Minimum Value	3.1	5.2
	Maximum Value	51.2	50.9
	Number of samples	444	297
G1H013 (Drie Heuwels)	Mean	26.11	26.26
	Standard Deviation	9.88	8.79
	Minimum Value	3.5	7.4
	Maximum Value	69.5	63
	Number of samples	548	364
River Reach 4			
G1H023 (Old Pumping Station)	Mean	119.24	111.1
	Standard Deviation	73.96	109.65
	Minimum Value	21.8	23.9
	Maximum Value	437.7	737
	Number of samples	95	68

Table 4.12 Statistics of Phosphate Values at River Gauging Stations

Station		Prior 1991 DWAF Situation Analysis (data from 1980 where available)	Jan 1991 to May 1998
River Reach 1			
G1H004 (Upper Berg River)	Mean Standard Deviation Minimum Value Maximum Value Number of samples	0.0155 0.014 0 0.073 95	0.022 0.0295 0 0.416
G1H020 (Paarl)	Mean Standard Deviation Minimum Value Maximum Value Number of samples	0.0371 0.2188 0 3.344 553	0.0309 0.048 0 0.78 294
River Reach 2			
G1H036	Mean Standard Deviation Minimum Value Maximum Value Number of samples	0.0577 0.074 0 0.989 319	0.0759 0.0557 0.001 0.384 300
G1H041 (Kompanjies River)	Mean Standard Deviation Minimum Value Maximum Value Number of samples	0.0309 0.065 0 0.853 464	0.0255 0.024 0 0.223 213
River Reach 3			
G1H008 (Little Berg River)	Mean Standard Deviation Minimum Value Maximum Value Number of samples	0.0132 0.0593 0 1.09 411	0.0203 0.0132 0 0.121 289
G1H013 (Drie Heuwels)	Mean Standard Deviation Minimum Value Maximum Value Number of samples	0.0209 0.025 0 0.214 587	0.0318 0.0335 0 0.63 313
River Reach 4			
G1H023 (Old Pumping Station)	Mean Standard Deviation Minimum Value Maximum Value Number of samples	0.0142 0.0124 0 0.067 95	0.0316 0.0239 0.002 0.12 68

Table 4. 13 Statistics of pH for Water Treatment Works

Station		Prior 1991 DWAF Situation Analysis (data from 1980 where available)	Jan 1991 to May 1998
G1R002			
Wemmershoek Water Treatment Works	Mean	5.25	6.453
	Standard Deviation	0.816	0.528
	Minimum Value	4	5.11
	Maximum Value	7.42	8.04
	Number of Samples	132	33
G1R001			
Swartland Water Treatment Works	Mean	6.89	7.465
	Standard Deviation	0.704	0.358
	Minimum Value	4.24	4.46
	Maximum Value	9.26	8.82
	Number of Samples	494	431
G1R003			
Withoogte Water Treatment Works	Mean	7.02	7.597
	Standard Deviation	0.535	0.528
	Minimum Value	5.34	4.35
	Maximum Value	8.81	8.39
	Number of Samples	486	308

Table 4.14 Statistics of Electrical Conductivity for Water Treatment Works

Station		Prior 1991 DWAF Situation Analysis (data from 1980 where available)	Jan 1991 to May 1998
G1R002			
	Mean	5.135	4.436
Wemmershoek	Standard Deviation	7.341	2.977
Water Treatment	Minimum Value	3.1	3.2
Works	Maximum Value	88	20.7
	Number of Samples	132	33
G1R001			
	Mean	12.05	11.95
Swartland Water	Standard Deviation	1.4	1.82
Treatment Works	Minimum Value	2.8	8.8
	Maximum Value	17.5	27.5
	Number of Samples	494	431
G1R003			
	Mean	39.3	36.12
Withoogte Water	Standard Deviation	13.54	13.82
Treatment Works	Minimum Value	8.6	3.5
	Maximum Value	108.2	110.1
	Number of Samples	486	308

Table 4.15 Statistics of Phosphate Values for Water Treatment Works

Station		Prior 1991 DWAF Situation Analysis (data from 1980 where available)	Jan 1991 to May 1998
G1R002			
	Mean	0.005	0.01
Wemmershoek	Standard Deviation	0.006	0.006
Water Treatment	Minimum Value	0	0
Works	Maximum Value	0.037	0.03
	Number of Samples	132	33
G1R001			
	Mean	0.0057	0.016
Swartland Water	Standard Deviation	0.0064	0.0078
Treatment Works	Minimum Value	0	0
	Maximum Value	0.046	0.067
	Number of Samples	483	431
G1R003			
	Mean	0.0199	0.0306
Withoogte Water	Standard Deviation	0.0208	0.0251
Treatment Works	Minimum Value	0	0.004
	Maximum Value	0.293	0.299
	Number of Samples	485	308

Fig 4.1 pH at G1H004

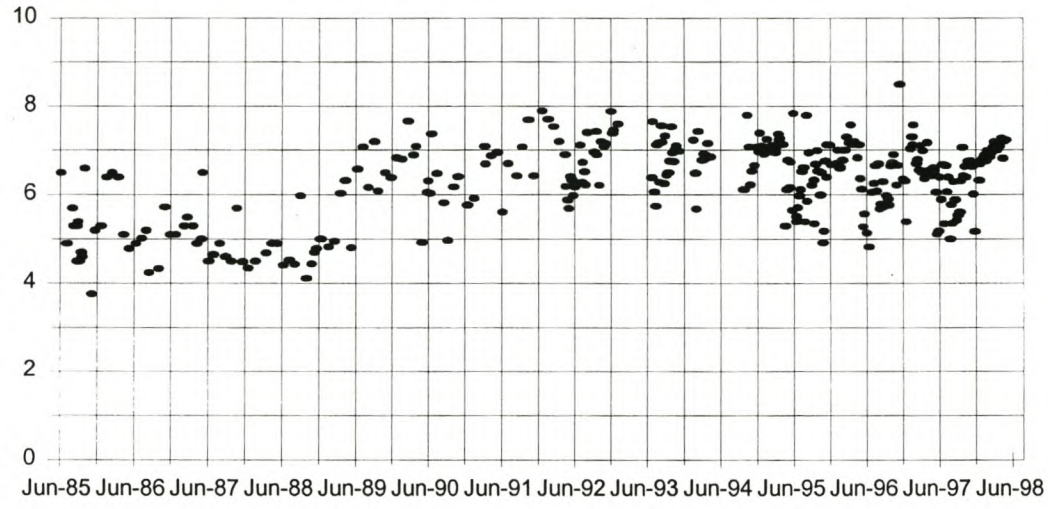

Fig 4.2 pH at G1H020

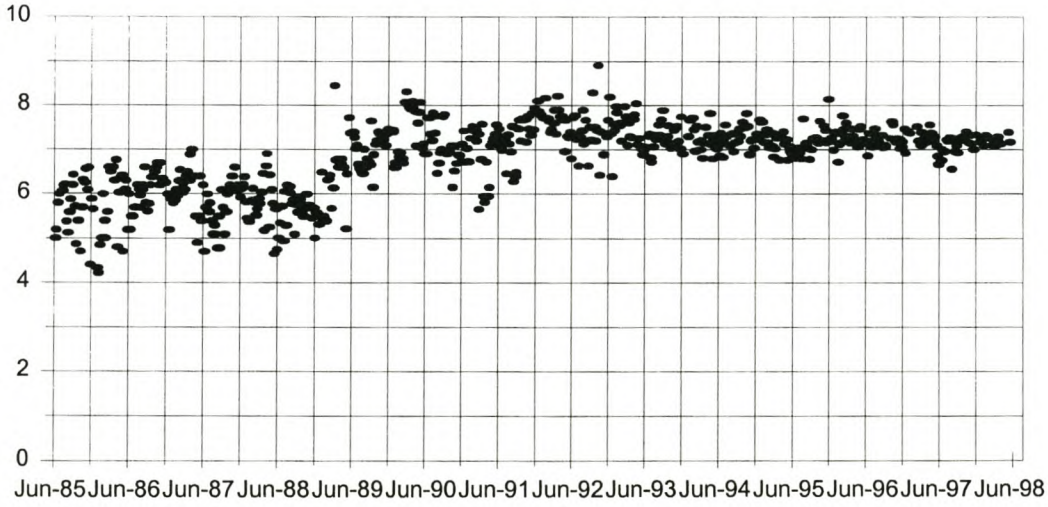

Fig 4.3 pH at G1H036

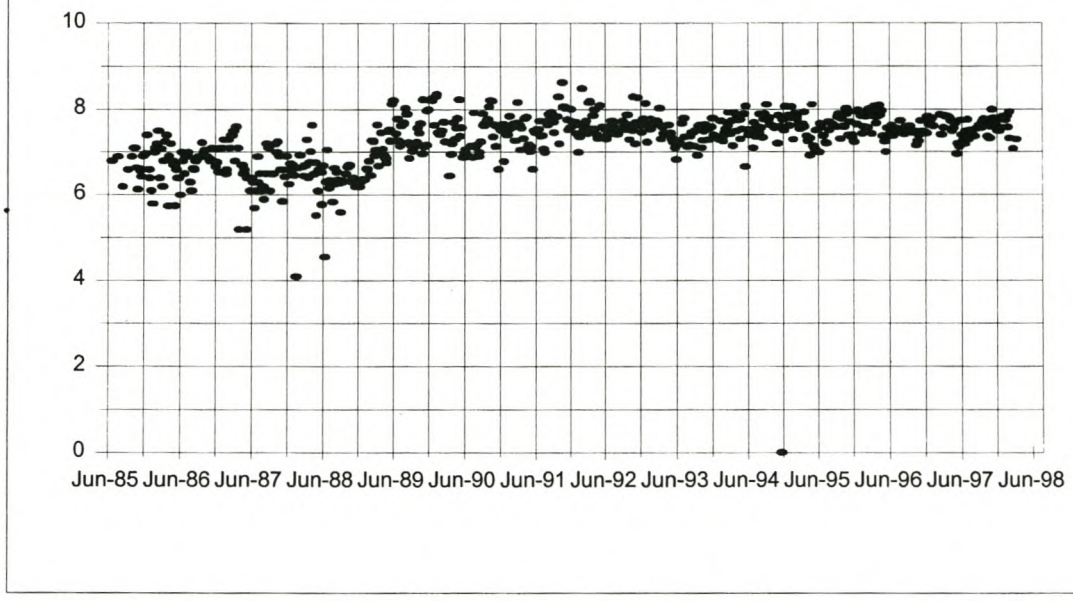

Fig 4.4 pH at G1H041

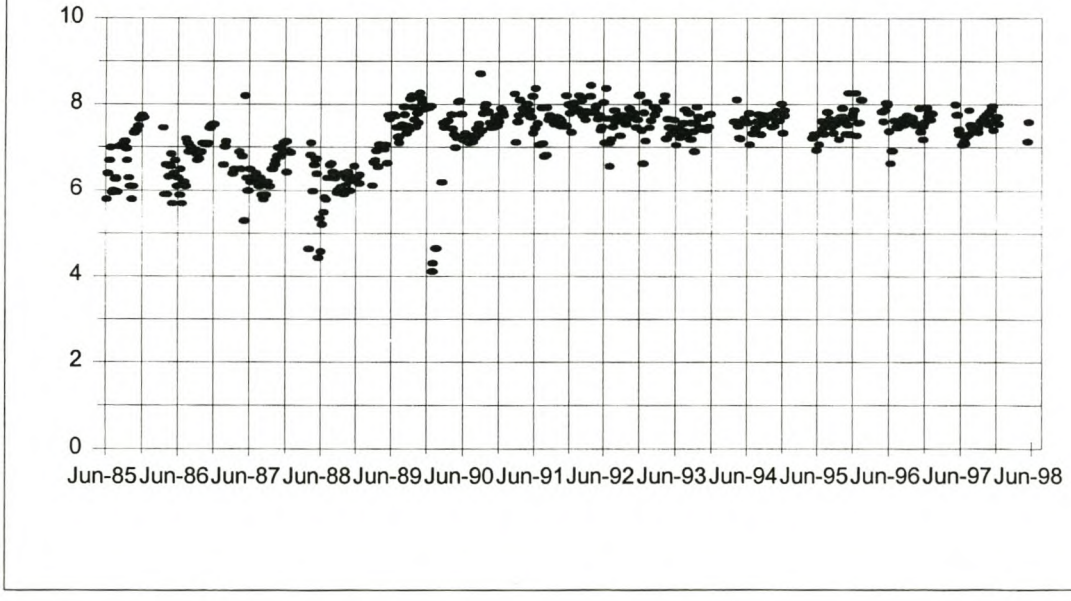

Fig 4.5 pH at G1H008

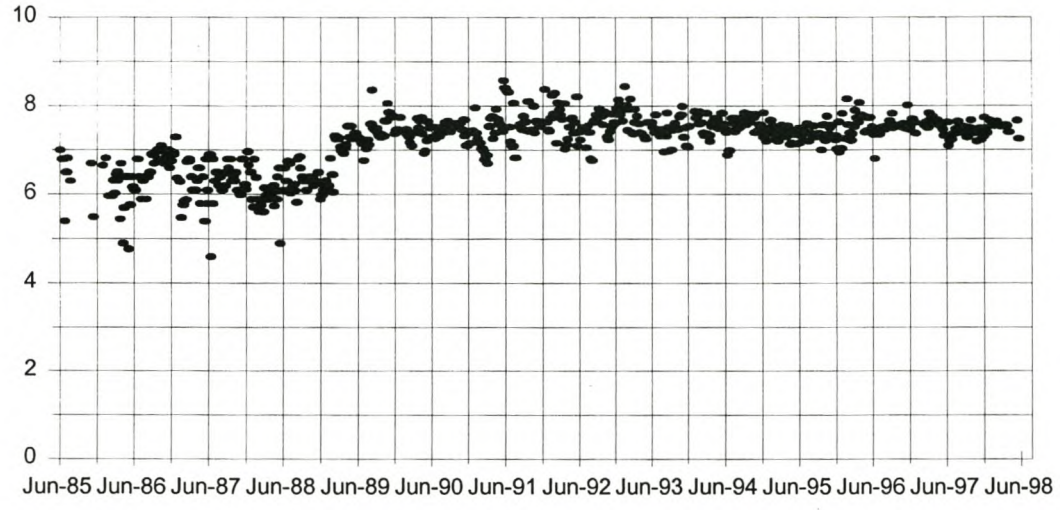

Fig 4.6 pH at G1H013

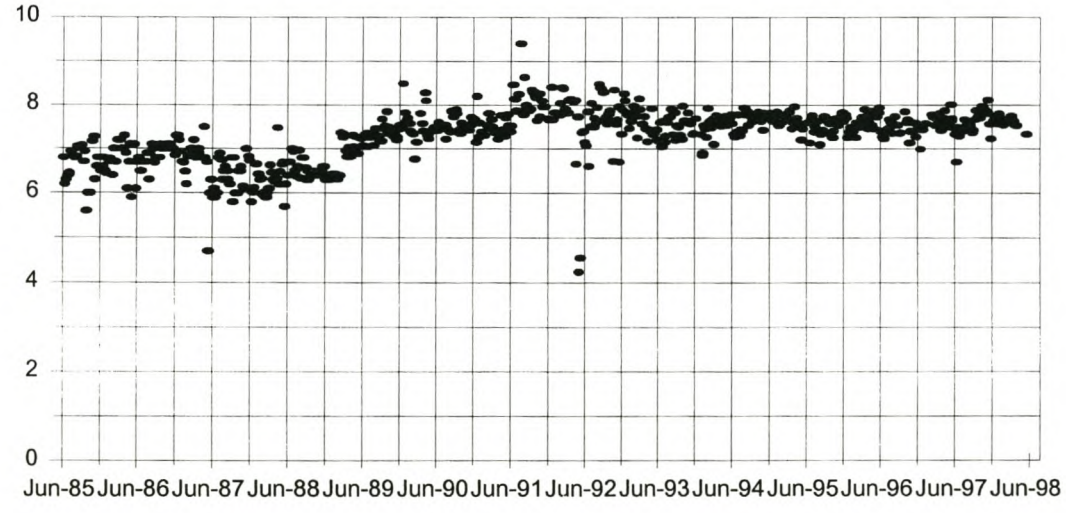

Fig 4.7 pH at G1H023

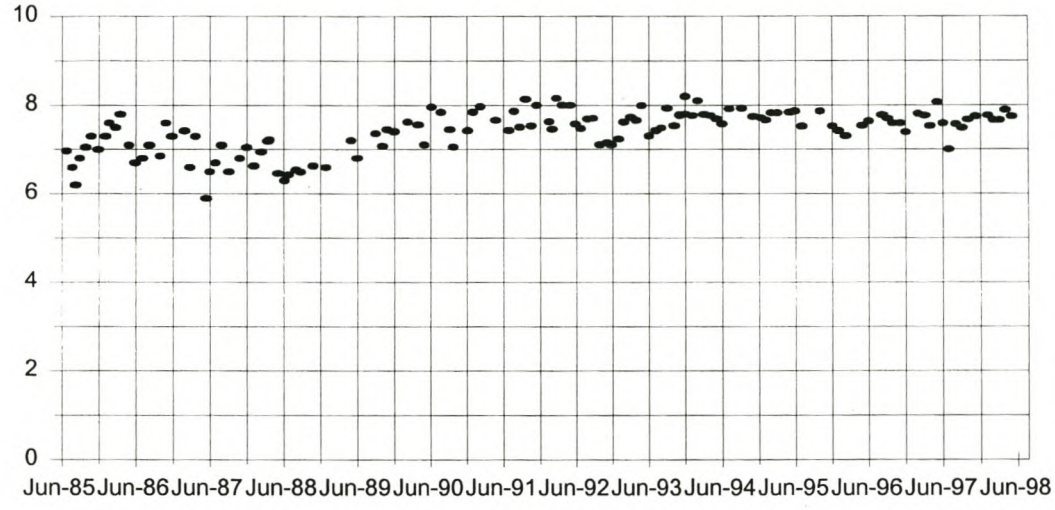

Fig 4.8 pH at G1R001

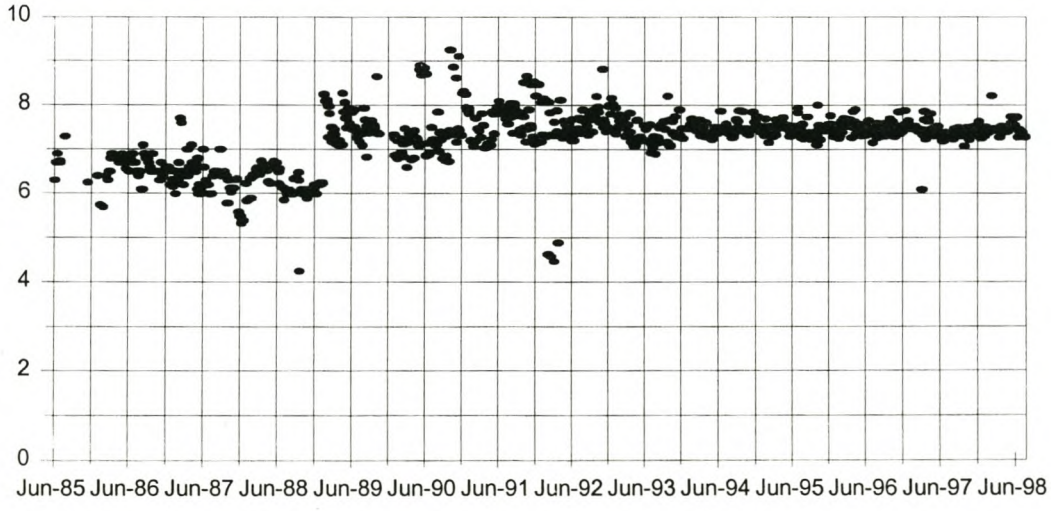

Fig. 4.9 pH at G1R002

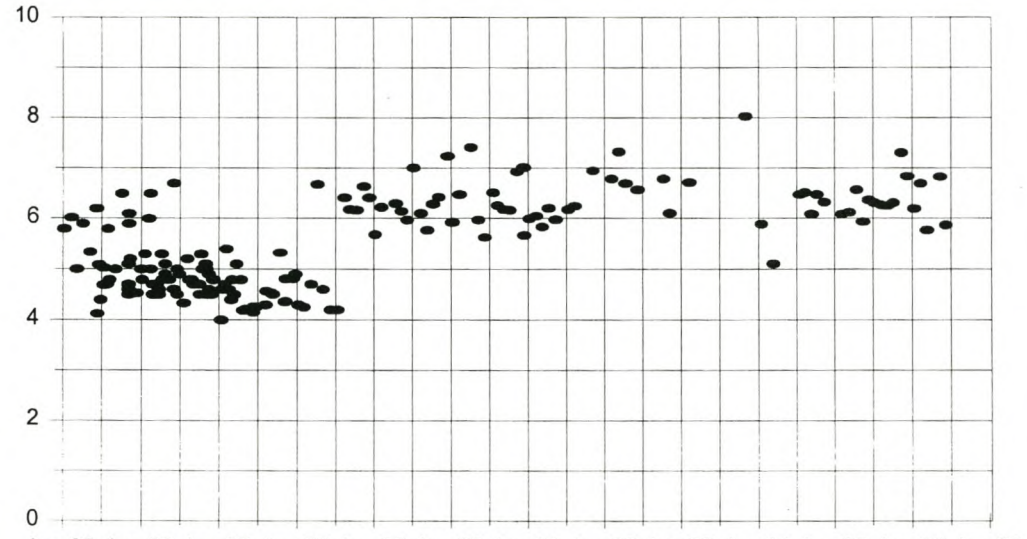

Fig 4.10 pH at G1R003

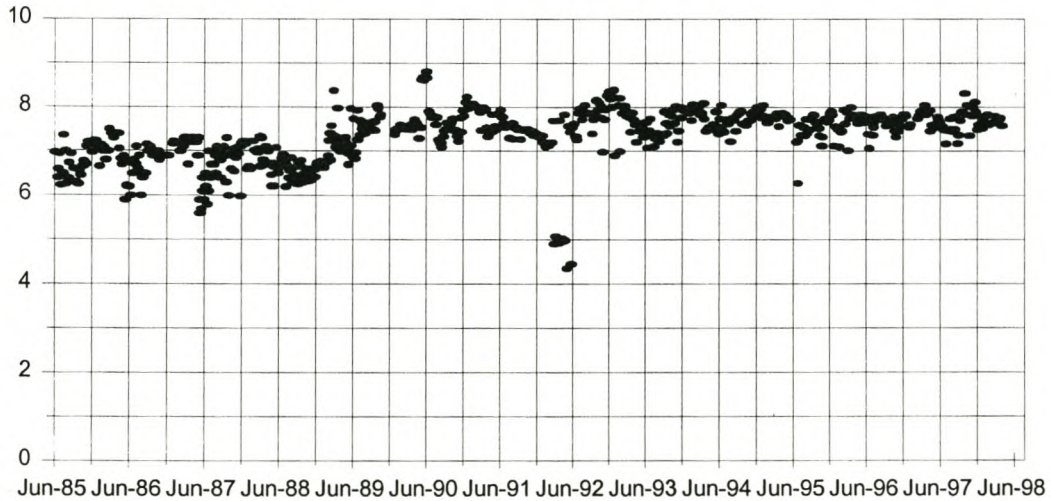

Fig 4.11 EC (mS/m) at G1H004

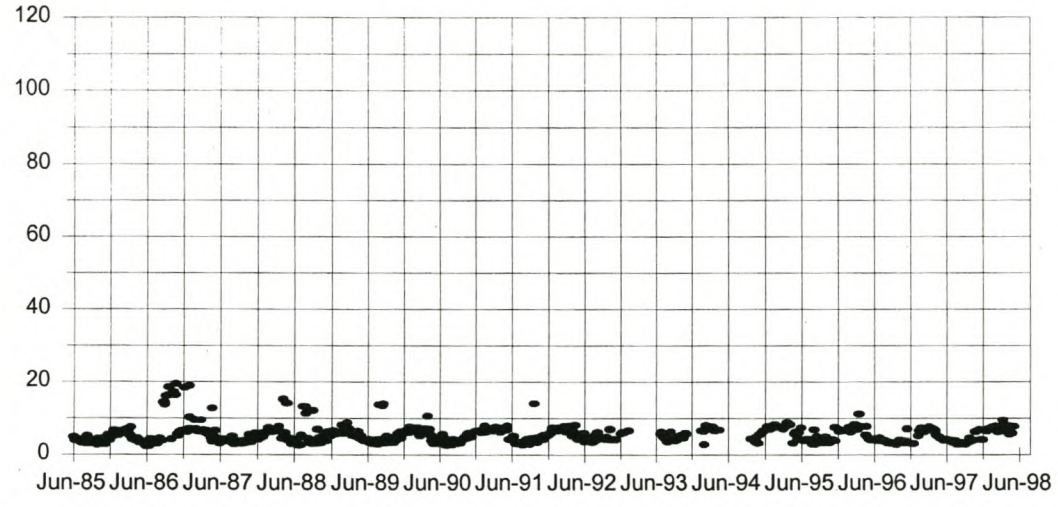

Fig 4.12 EC (mS/m) at G1H020

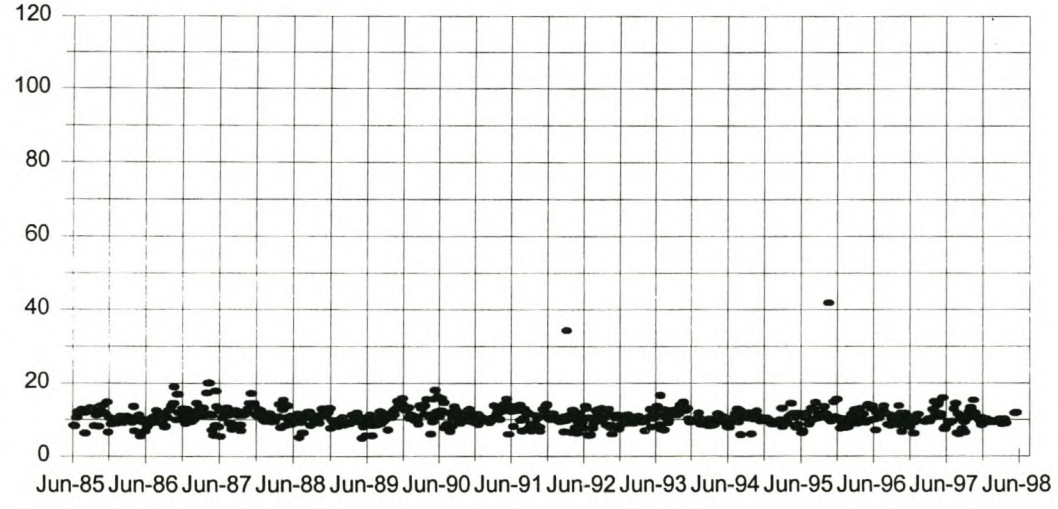

Fig 4.13 EC (mS/m) at G1H036

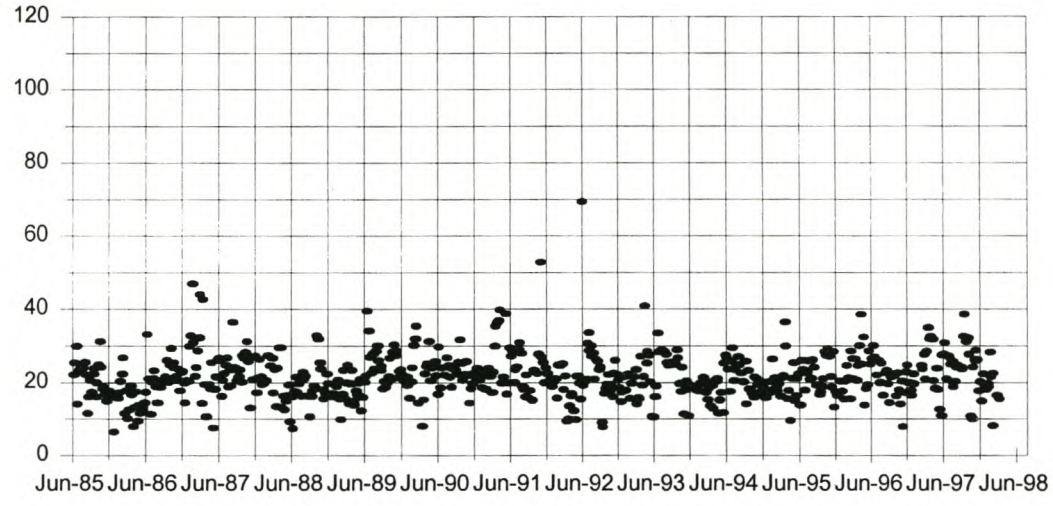

Fig 4.14 EC (mS/m) at G1H041

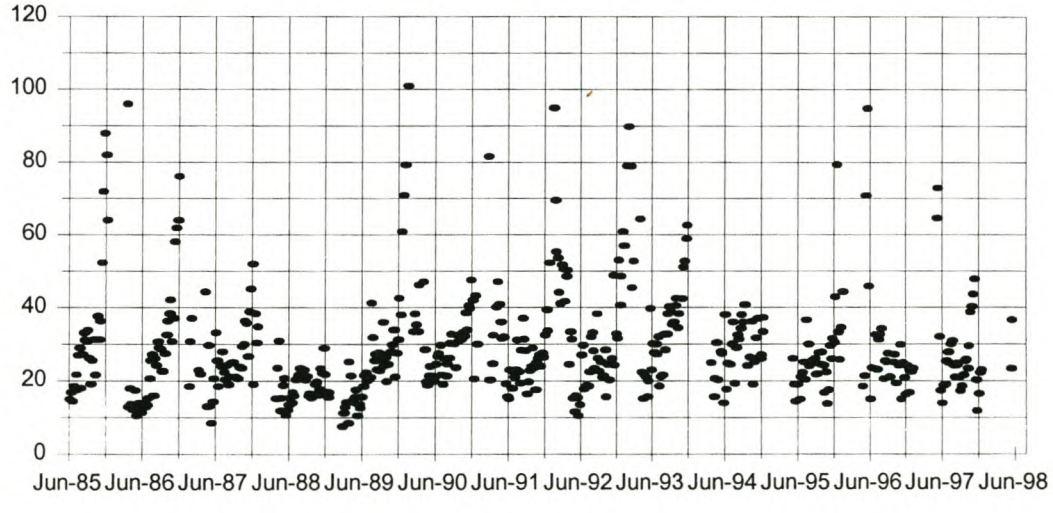

Fig 4.15 EC (mS/m) at G1H008

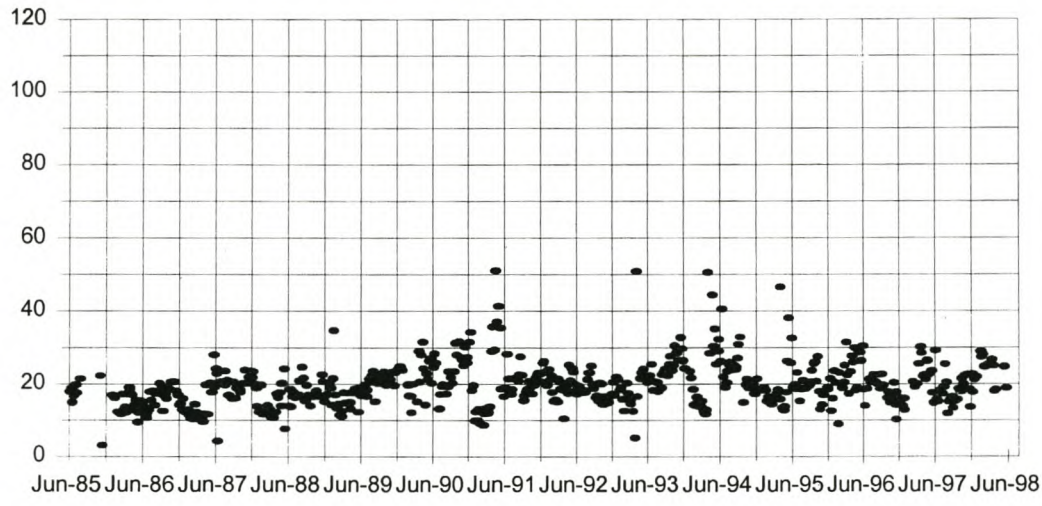

Fig 4.16 EC (mS/m) at G1H013

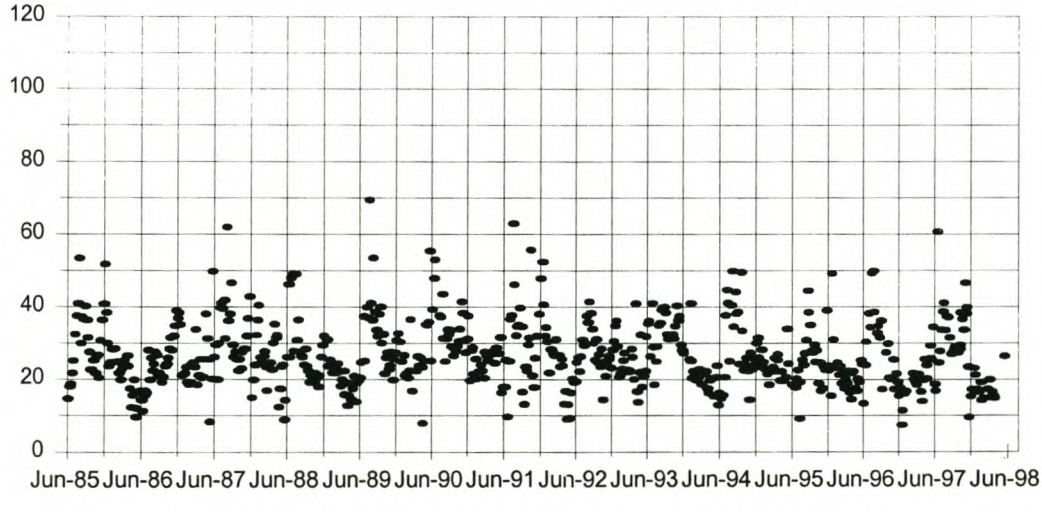

Fig 4.17 EC (mS/m) at G1H023

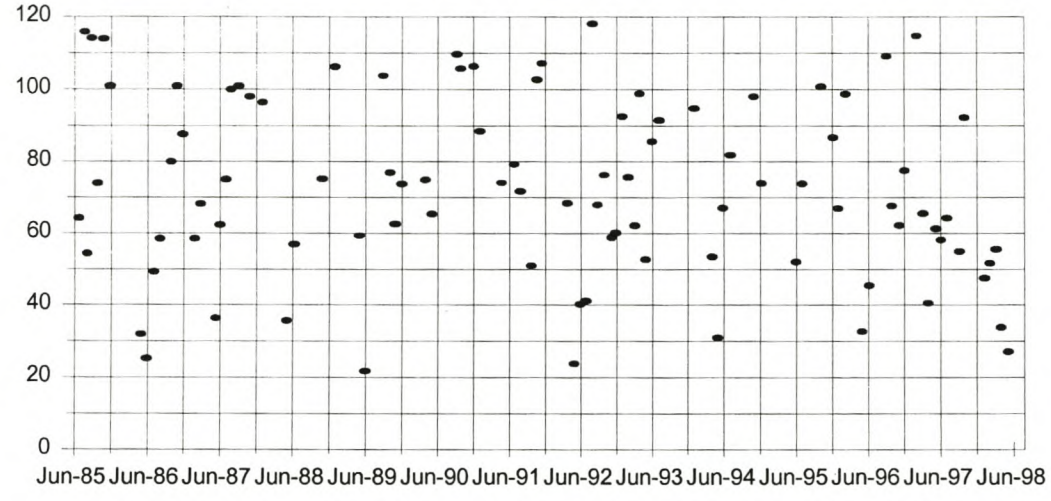

Fig 4.18 EC (mS/m) at G1R001

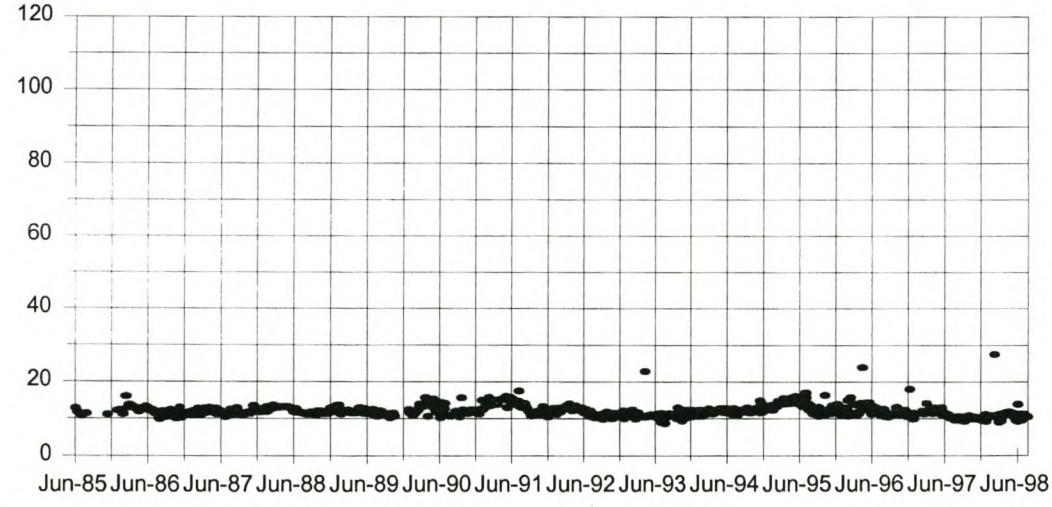

Fig. 4.19 EC (mS/m) at G1R002

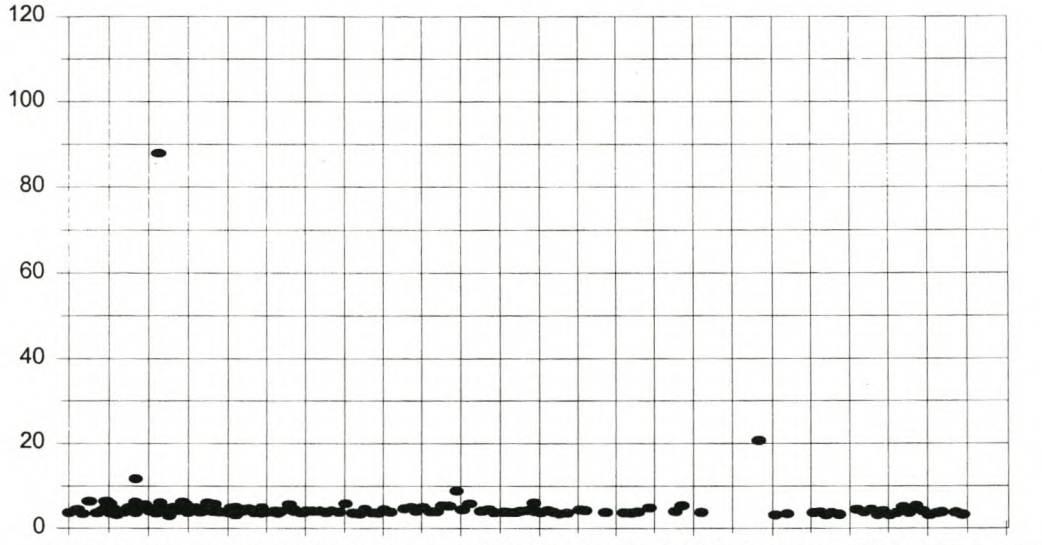

Fig 4.20 EC (mS/m) at G1R003

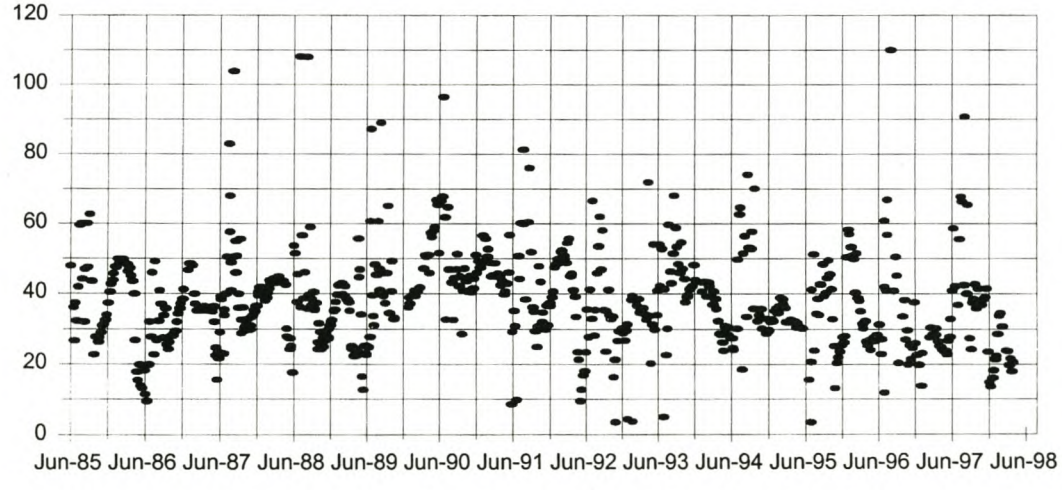

Fig 4.21 TDS (mg/l) at G1H004

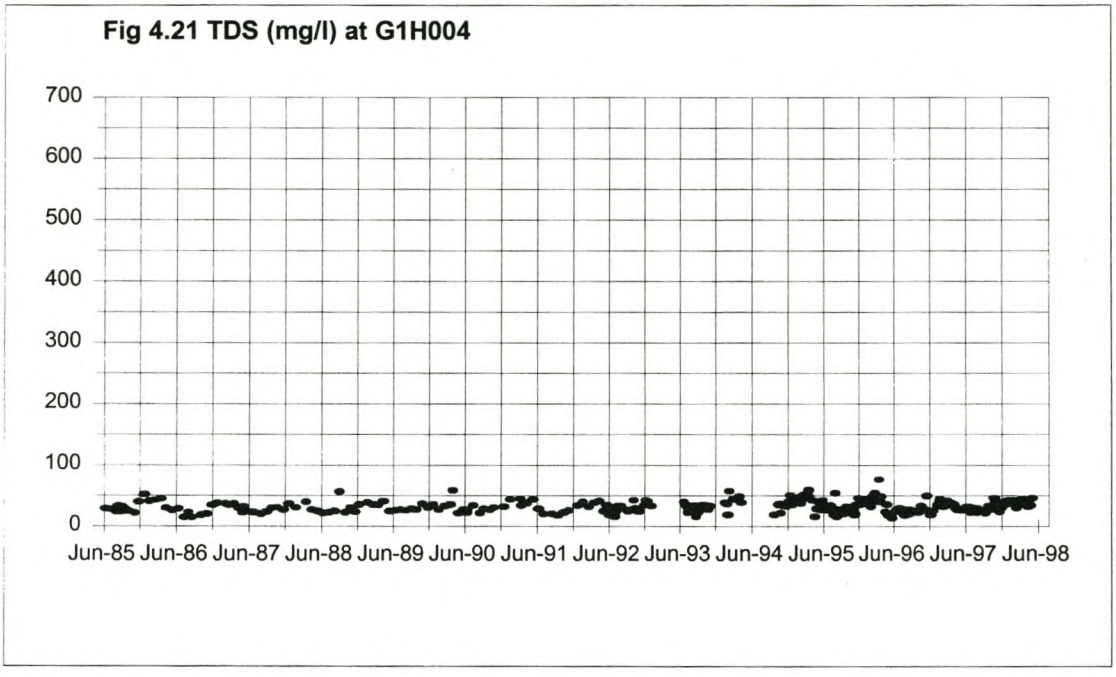

Fig 4.22 TDS (mg/l) at G1H020

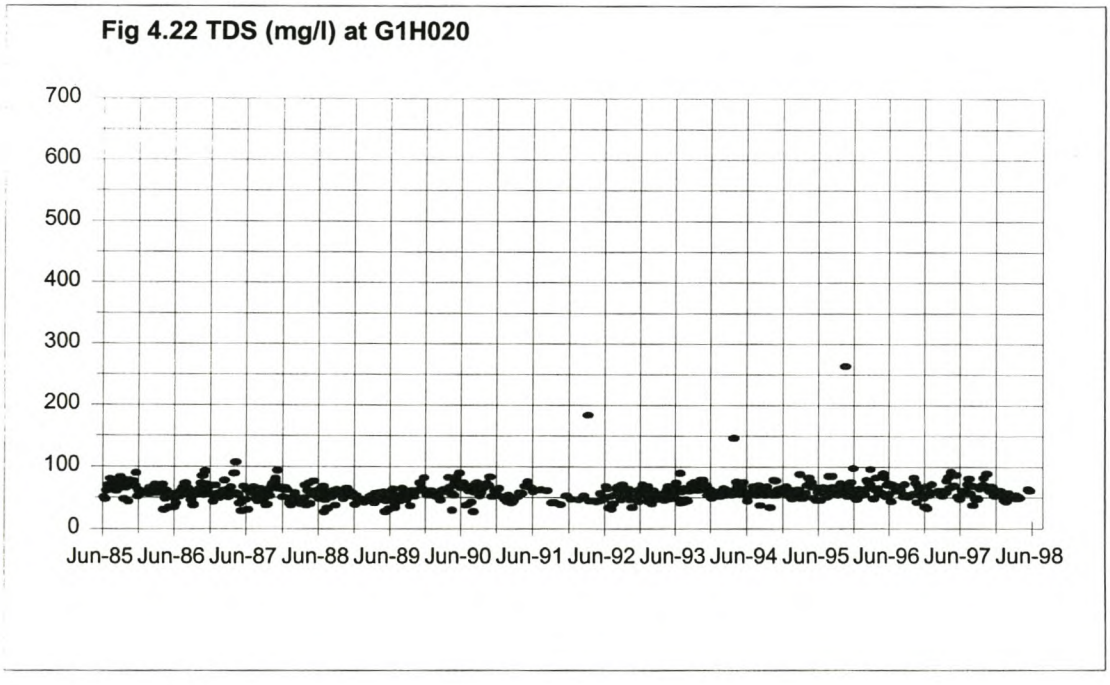

Fig 4.23 TDS (mg/l) at G1H036

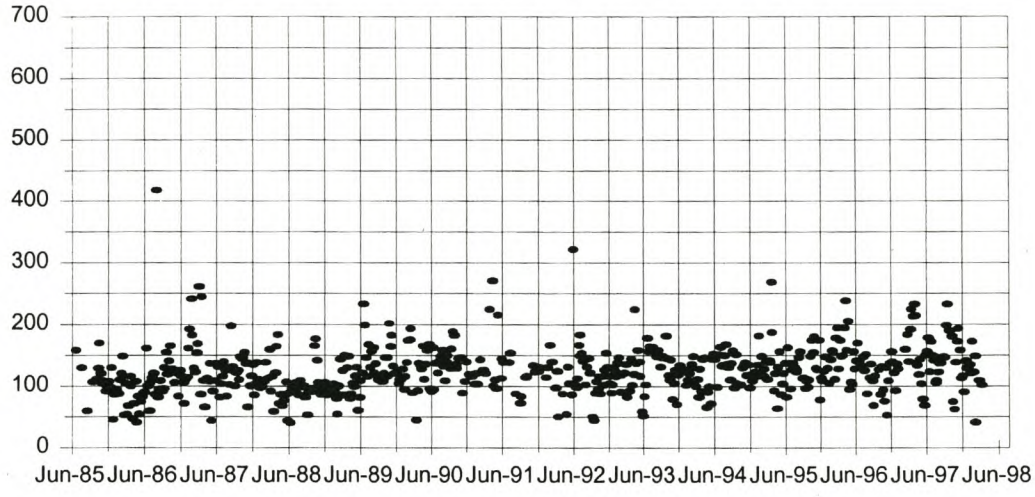

Fig 4.24 TDS (mg/l) at G1H041

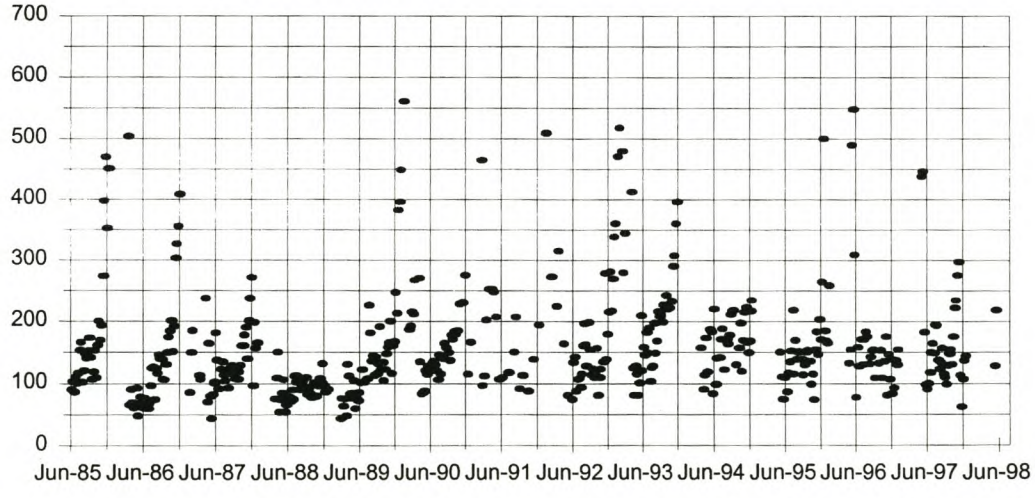

Fig 4.25 TDS (mg/l) at G1H008

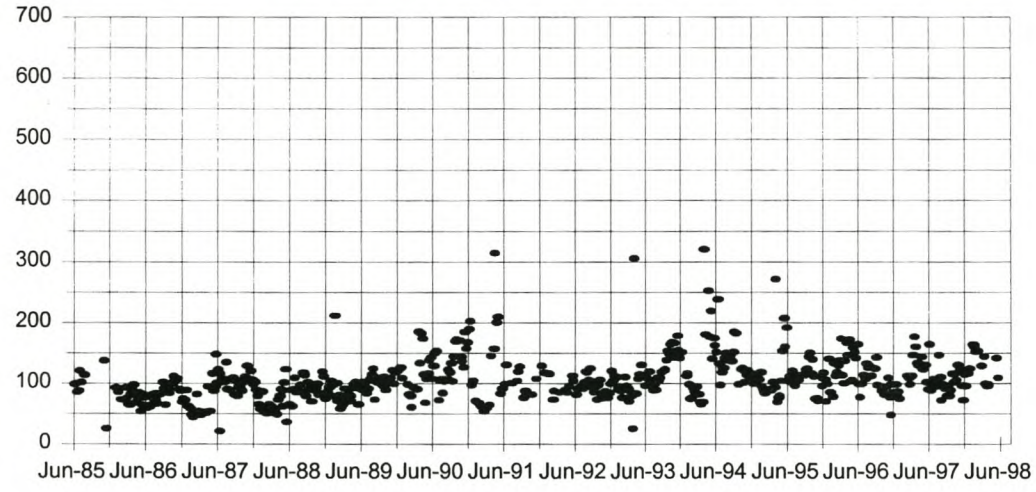

Fig 4.26 TDS (mg/l) at G1H013

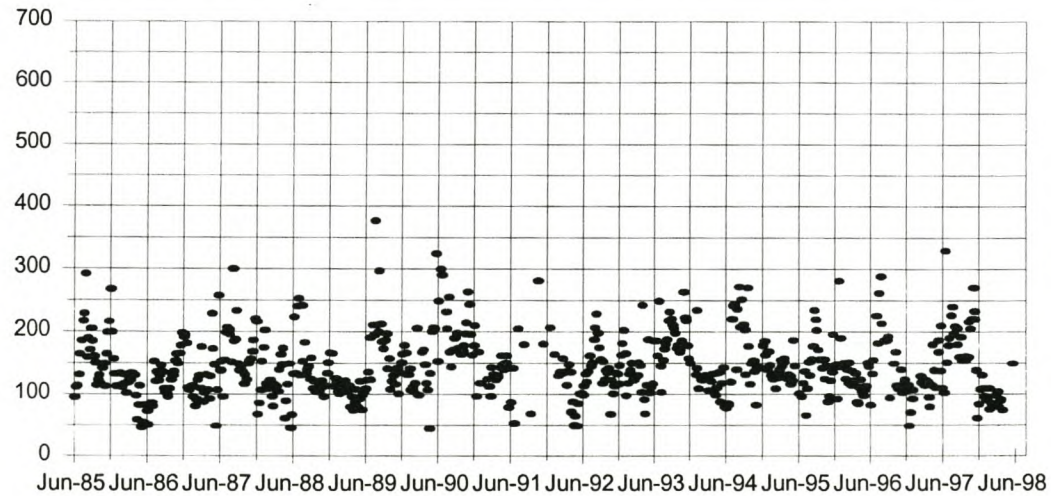

Fig 4.27 TDS (mg/l) at G1H023

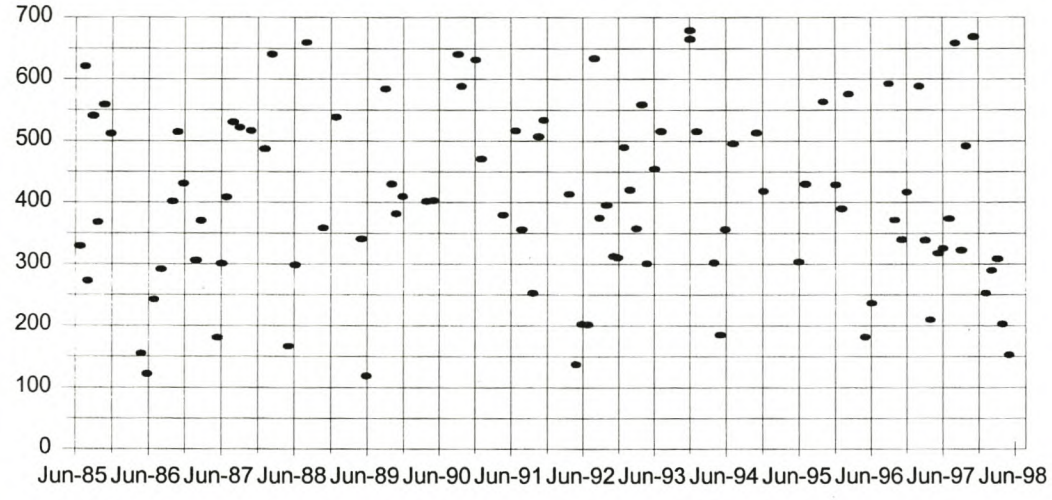

Fig 4.28 TDS (mg/l) at G1R001

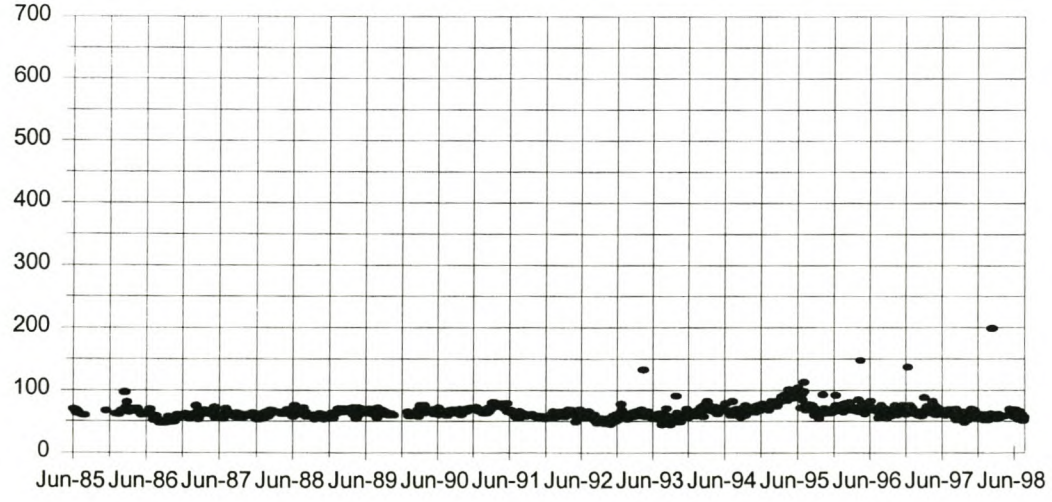

Fig. 4.29 TDS (mg/l) at G1R002

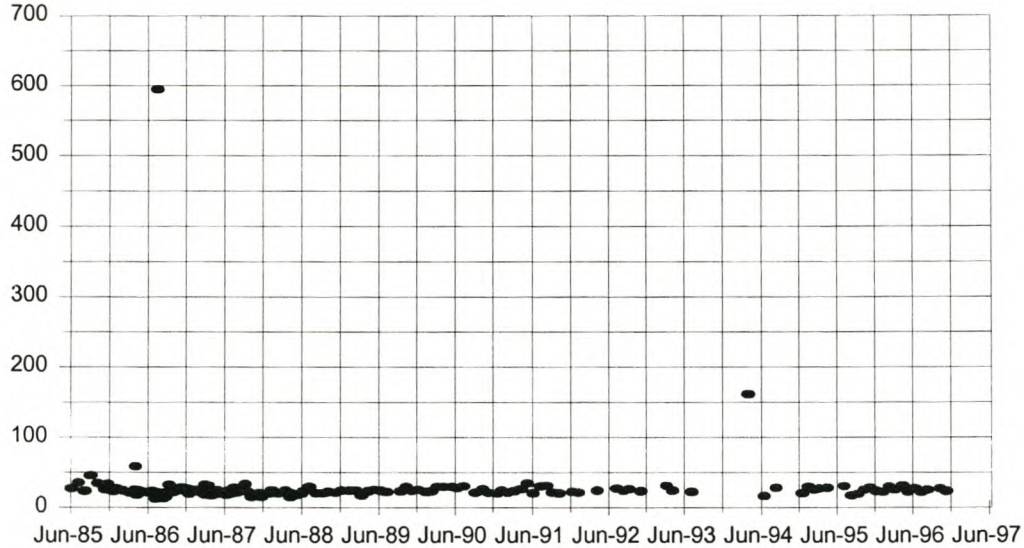

Fig 4.30 TDS (mg/l) at G1R003

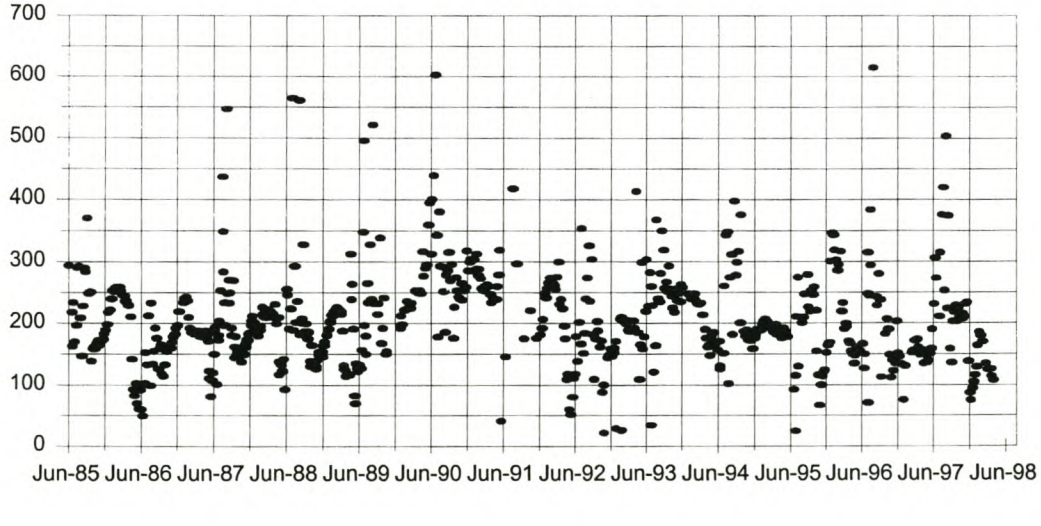

Fig 4.31 Phosphates (mg/l PO4 as P)
at G1H004

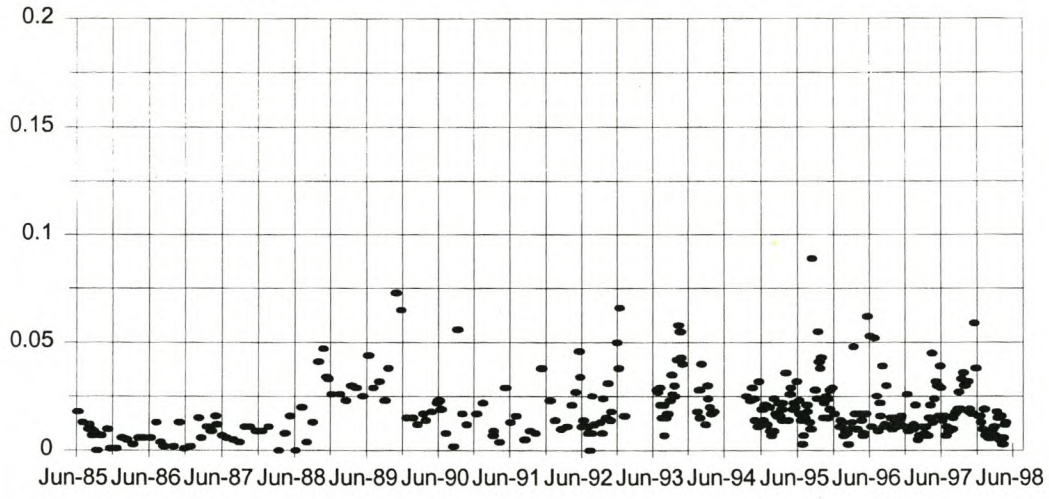

Fig 4.32 Phosphates (mg/l PO4 as P)
at G1H020

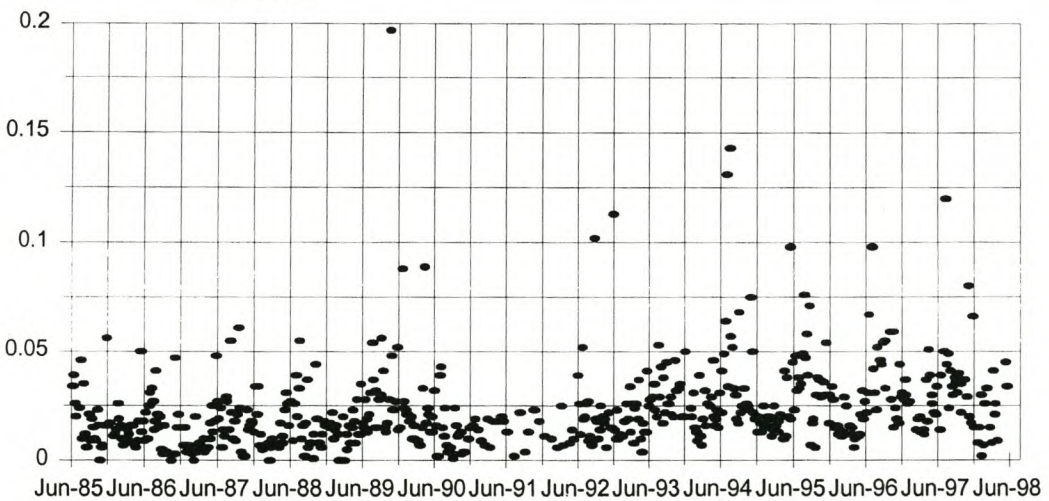

Fig 4.33 Phosphates (mg/l PO4 as P)
at G1H036

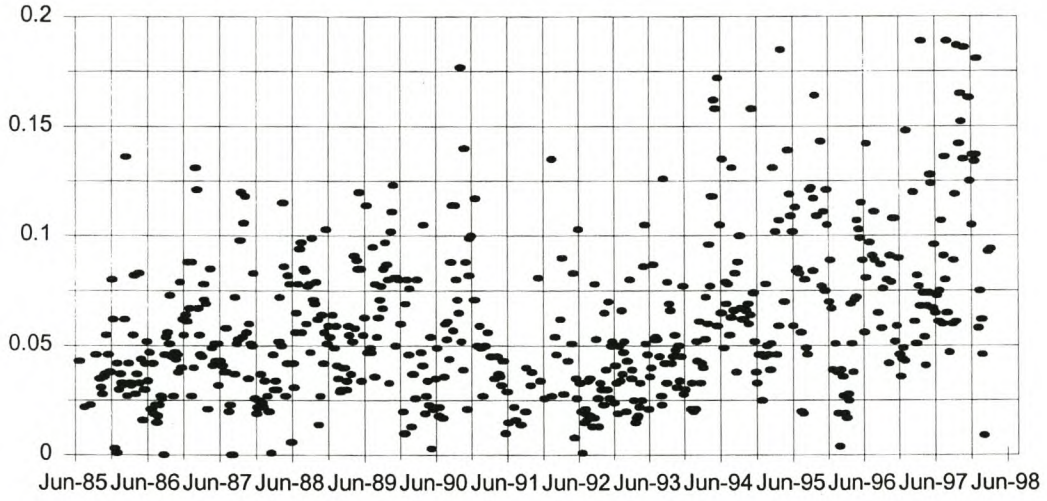

Fig 4.34 Phosphates (mg/l PO4 as P)
at G1H041

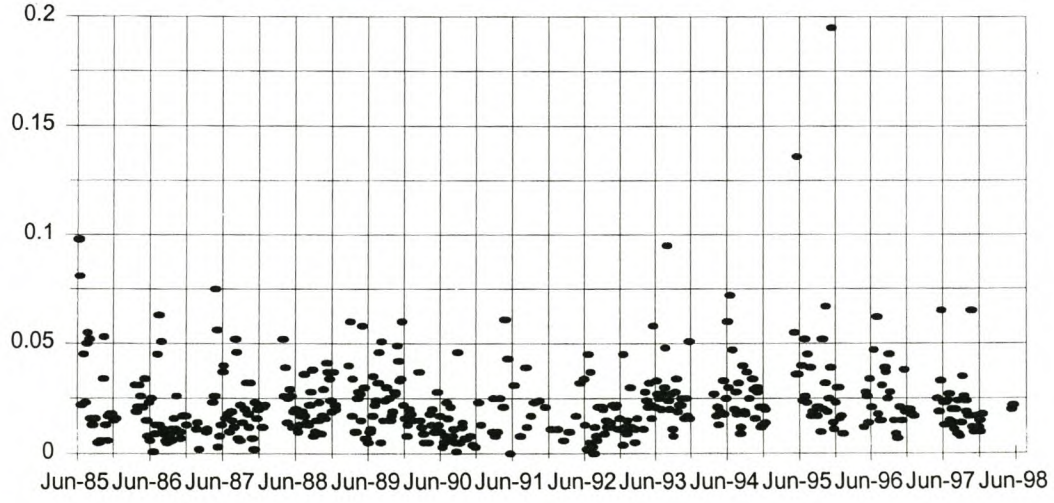

Fig 4.35 Phosphates (mg/l PO4 as P)
at G1H008

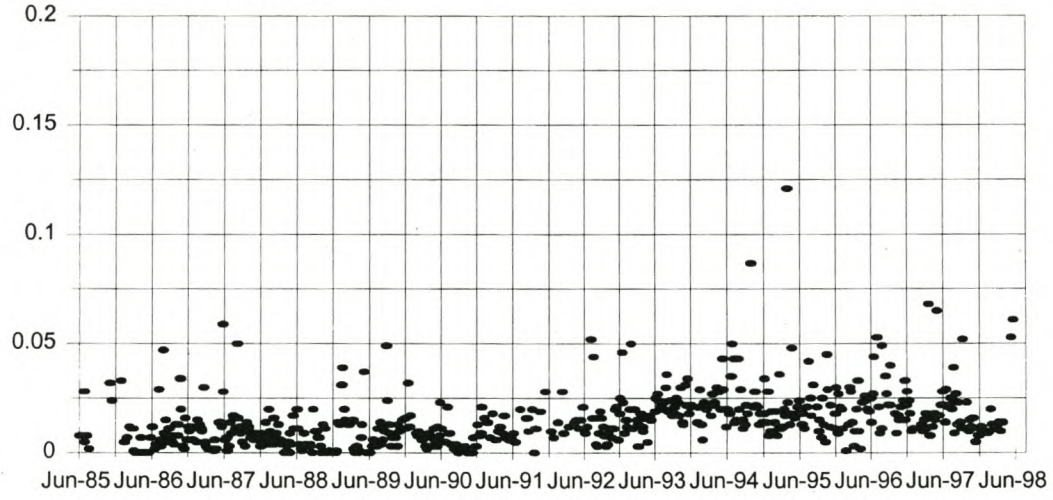

Fig 4.36 Phosphates (mg/l PO4 as P)
at G1H013

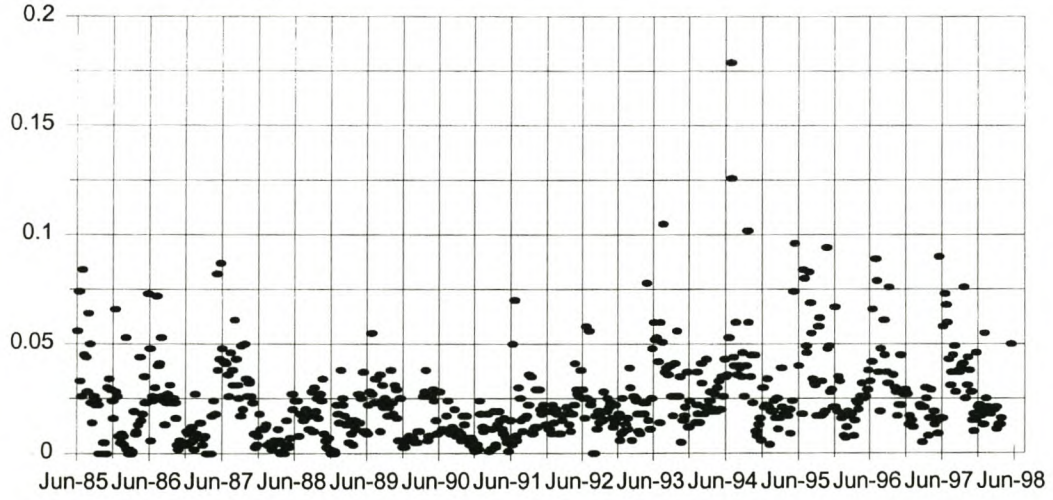

Fig 4.37 Phosphates (mg/l PO4 as P)
at G1H023

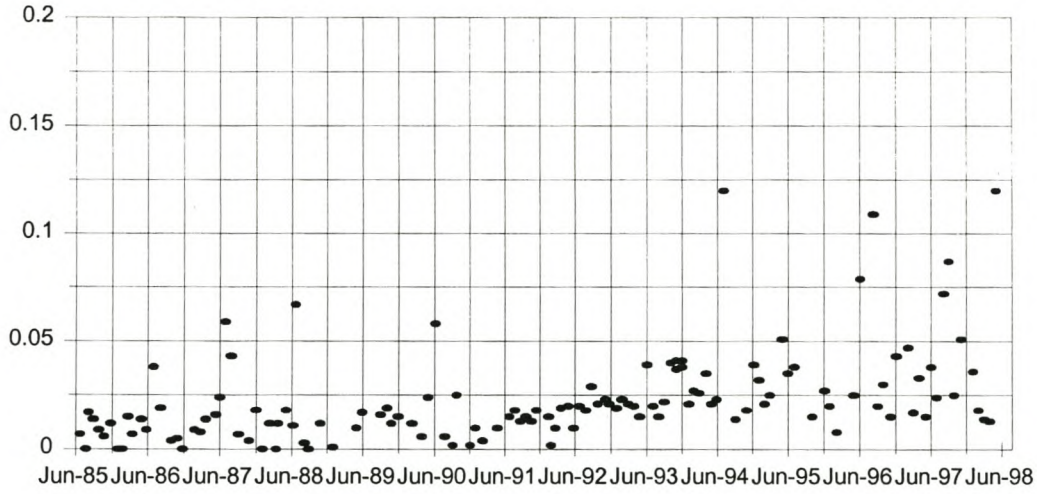

Fig 4.38 Phosphates (mg/l PO4 as P)
at G1R001

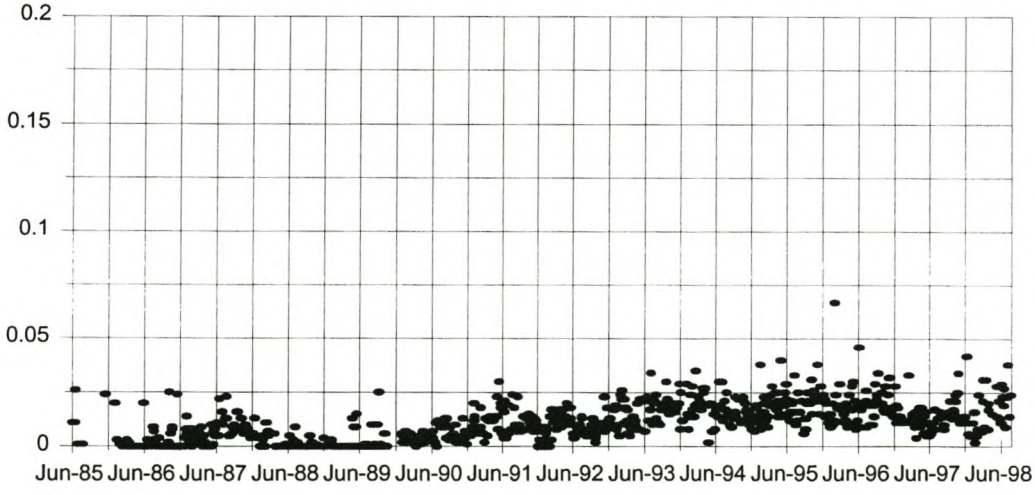

Fig 4.39 Phosphates (mg/l PO4 as P)
at G1R002

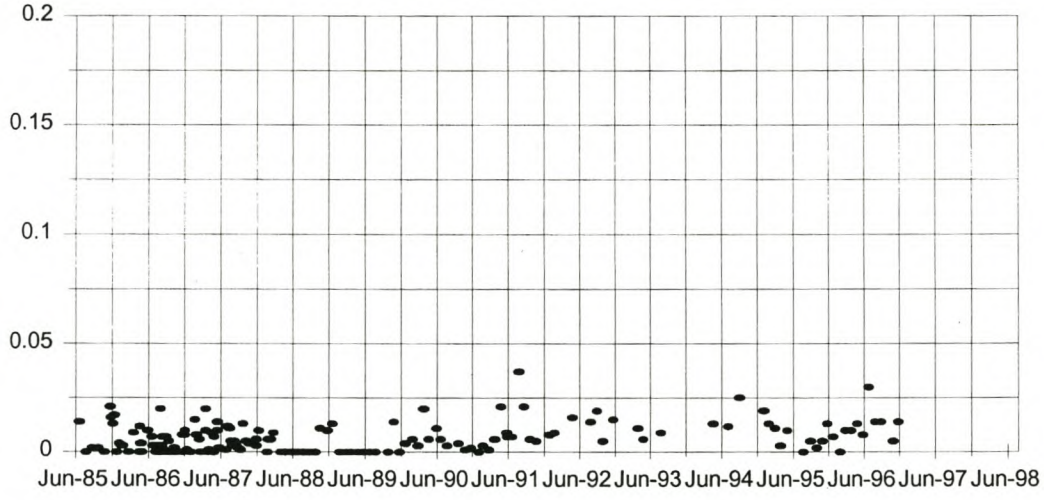

Fig 4.40 Phosphates (mg/l PO4 as P)
at G1R003

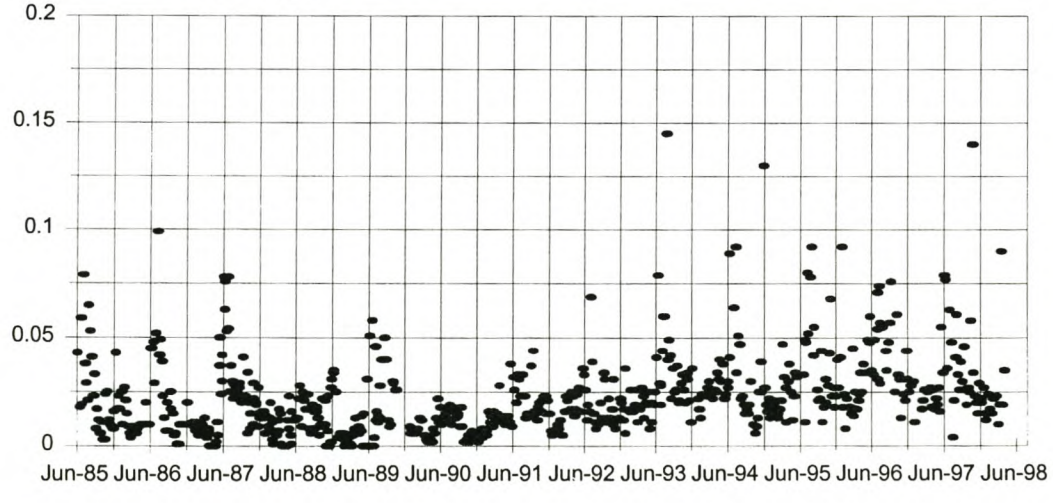

CHAPTER 5

SOFTWARE STRUCTURE AND MATHEMATICAL BACKGROUND TO DUFLOW WATER QUALITY MODEL

5.1 INTRODUCTION

On the basis of the review of available water quality models presented in Chapter 2, it was decided to use DUFLOW to model the Berg River because of the appropriateness of its scientific content, its user friendliness, the graphical interface and inexpensiveness compared to the various other packages that are on the market.

DUFLOW is the joint ownership of the Faculty of Civil Engineering at Delft University of Technology and the Public Works Department (Rijkswaterstaat), International Institute for Hydraulic and Environmental Engineering (IHE), the Agricultural University of Wageningen and STOWA.

For academic use, the cost for DUFLOW for Windows (version 3.0) and RAM (Precipitation runoff module) was 1000 Dutch Gulden. An additional 900 Dutch Gulden was paid for maintenance and service for a year. The delivery cost by DHL was an additional R 92-00.

PC system requirements for using the DUFLOW Modelling Studio are:

- minimal 486, suggested is a Pentium
- minimal 16 Mb internal memory, a minimum of 24 Mb is recommended
- minimal 50Mb external memory

Operating system requirements for running the DUFLOW Modelling Studio is:

- Windows95 or WindowsNT (4.00 or higher)

The DUFLOW package that was received late in October 1998 comprised an installation CD-ROM with a User's Guide and Reference Manual. For installing a component of the DUFLOW Modelling Studio

(DUFLOW, RAM or Moduflow) a password is needed.

In this Chapter a short description is given of the software structure of DUFLOW.

Additionally an outline is given, firstly, to the basic hydrodynamic equations and, secondly, to the water quality processes, as well as the numerical method that DUFLOW uses to solve these equations. A numerical method which is used to determine the solution of complex equations is defined as mathematical expressions quantifying fundamental physical principles (Koutitas, 1983).

In this chapter emphasis is placed on the approach DUFLOW uses to quantify unsteady flow and to describe water quality processes. These approaches are common to most one dimensional hydrodynamic water quality models that use some form of an implicit scheme as numerical solution.

5.2 DESCRIPTION OF THE DUFLOW MODEL SOFTWARE STRUCTURE

5.2.1 Features of the Interface

The user interface consists of the following components:

- Menus
- Toolbars
- Status Bar
- Scenario Manager window
- Working space with the Network window and Results windows
- Output windows

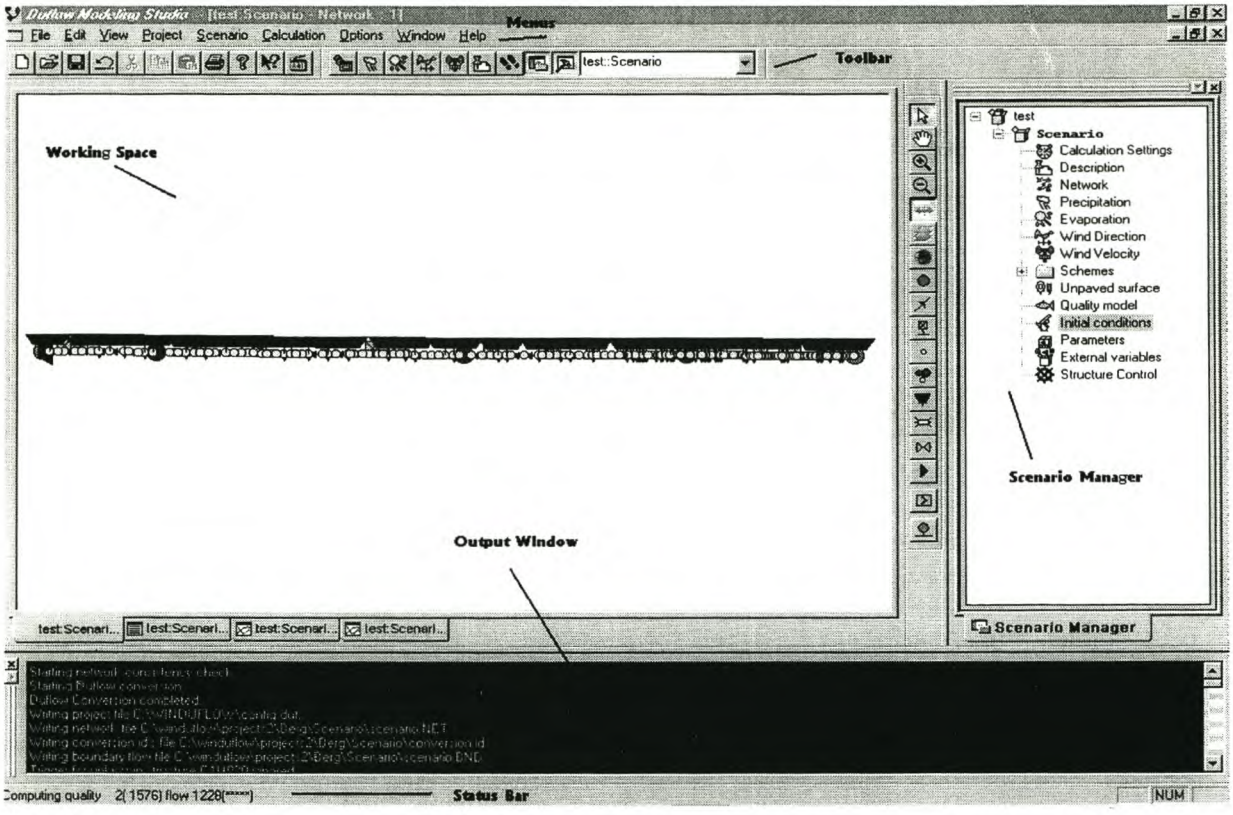

Figure 5.1: User interface components

The Network editor is a graphical editor that enables the user to draw the network schematization in a very user-friendly way. The mouse is used to place selected objects, such as nodes, sections and structures in the network window.

- *Nodes* are points at which one or more sections arise or end.
- A *section* connects two nodes.
- *Objects* that can be defined on sections are: structures, cross-sections, discharge points etc.

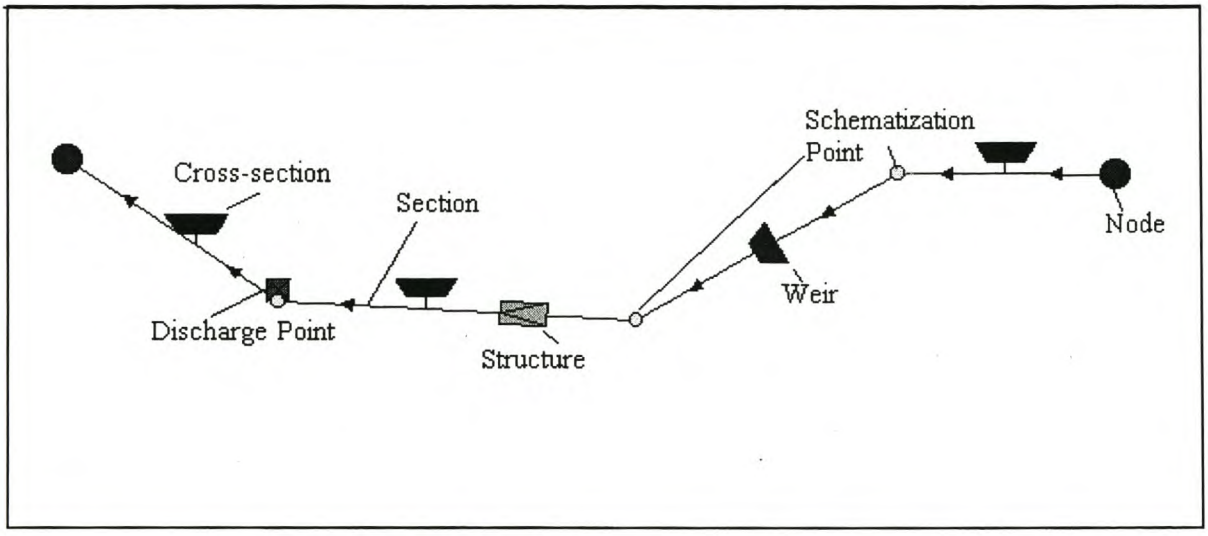

Figure 5.2: Network Schematization Objects

The properties of these objects can be modified in their property boxes. Cross-sections can be applied on miscellaneous places on the section. The cross-sectional profile over the entire section is interpolated between the different cross-sections given by the user.

5.2.2 Calculation options

Type of calculations possible:

- *Flow* : only flow can be calculated
- *Flow and Quality:* Flow and quality are calculated simultaneously
- *Quality* : (This option can only be used if an intermediate flow result file was generated in a flow calculation. In this case the necessary flow information for the mass transport is read from the intermediate flow result file.)
- *Box* : The use of this option enables the examination of the relative importance of the transport processes in comparison with the chemical and biological processes involved. Transport is not calculated, i.e. a steady flow is used where the parameters have been defined in the quality file. The calculations for the water quality thus only takes the processes into consideration (i.e. only the sinks and sources of the quality variable, the equations/processes are described in section 5.4.5)

5.2.3 Import and Export of Data

Time Series that are used as boundary conditions and discharge points can be imported from and exported to external files in ASCII format. Results in text form can also be exported in the text form to be used in spreadsheets for statistical analyses.

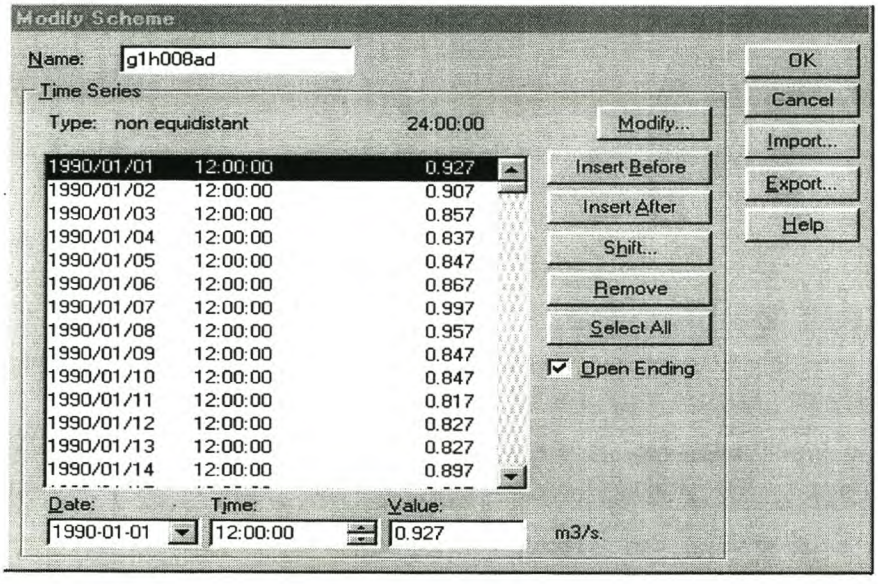

Figure 5.3: Time Series Property Box

5.2.4 Presentation of Results

The results of a calculation can be displayed in three different ways:

- A Time Related Graph,
- A Space Related Graph (the user can define the route that should be plotted)
- Results as Text in a table as a function of time (makes it possible to export the results into spreadsheets).

Both text and graphs are displayed in windows. These windows appear in the working space. A result window can contain the output of more than one variable or the output from different scenarios.

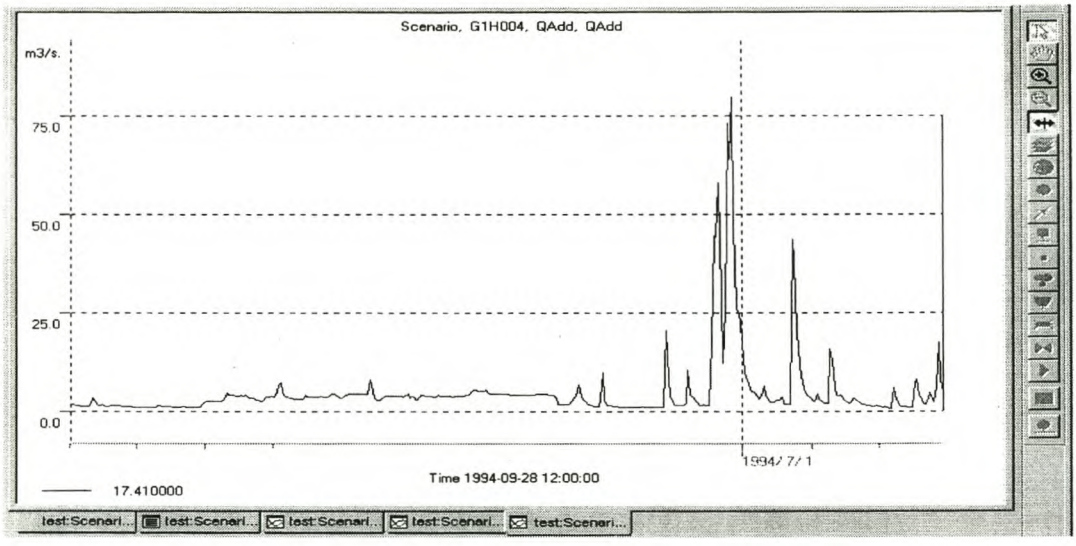

Figure 5.4: Time Related Graph

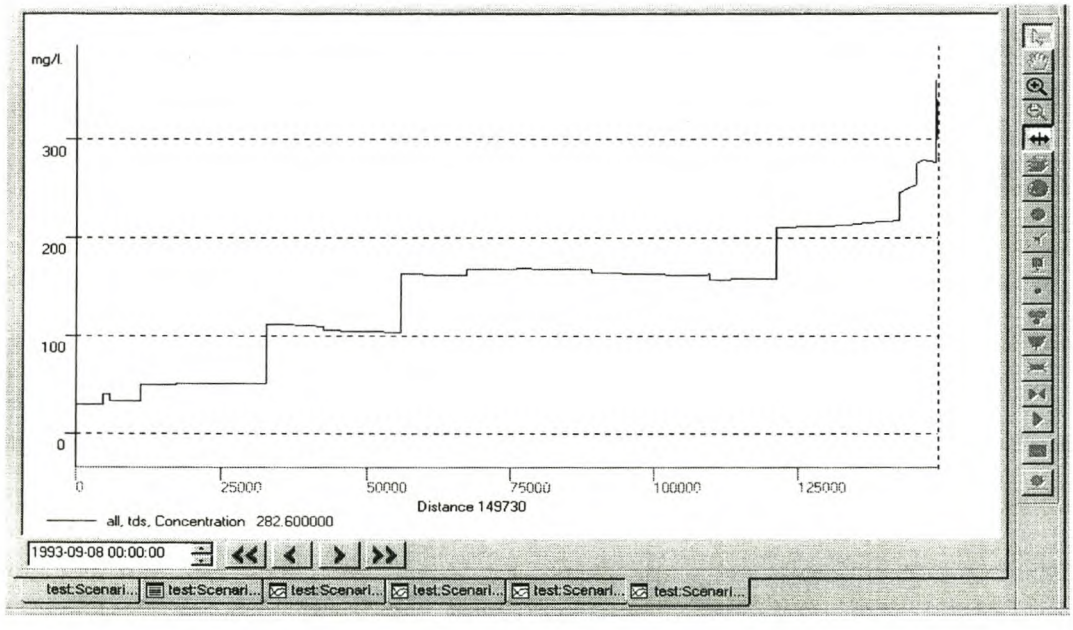

Figure 5.5: Space Related Graph

5.2.5 Configuration of the model

Network Schematization

The configuration of the model occurs through the network window. One can create the model easily by dragging and dropping elements (such as nodes, sections, weirs etc.) from the Network Palette into the Network window by using the mouse, one can also easily modify the schematization with schematization or bending points.

Cross-sections are also first added by using a toolbutton from the palette. Cross-sections are defined by schemes and at every cross-section a scheme has to be connected to the cross-section. A scheme is created in a cross-section dialog box and the data is entered here for the cross-section. The same scheme could be added for every cross-section.

To add a structure such as a weir, the same procedure is followed. First, the user can click the weir toolbar from the palette and drag it into the network window. The position of the weir can be changed in the Object Properties box by changing the distance from the last node. The needed data for the weir needs to be entered into this box.

Discharge points are added at schematization points and here the user can define a time series of discharged water, wasted load or concentration.

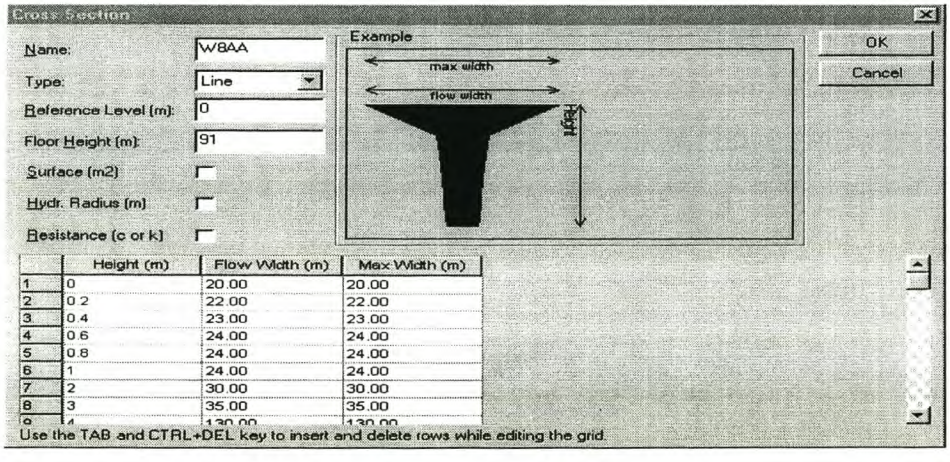

Figure 5.6: Cross-section Property Box

Calculation Settings

In the calculation settings dialog box the start calculation time and time step need to be selected. The type of calculation also needs to be specified. When the flow calculation is verified, a quality model can be added.

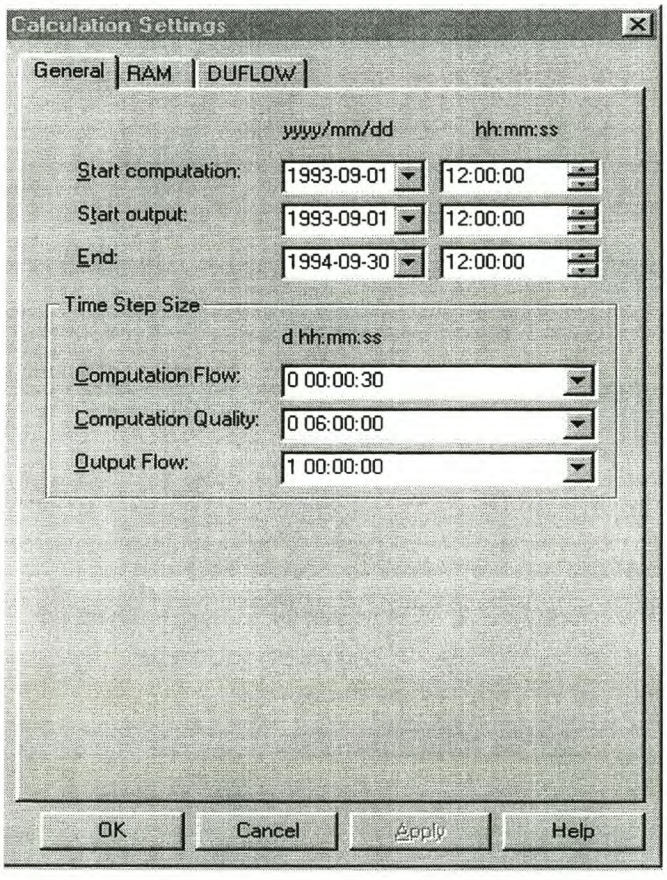

Figure 5.7: Calculation Settings Dialog Box

Scenarios

The programme consists of a Scenario Manager with which the user can define several different scenarios, without changing the base scenario. This gives the user the ability to see the result of different scenarios, such as pollution spills or sudden rainfall storms.

5.3 HYDRODYNAMIC MATHEMATICAL BACKGROUND

5.3.1 Introduction

DUFLOW can represent riverflow as non-uniform and unsteady. This is the most complex flow type as it requires the solution of the St. Venant equations through time and distance. A short description is given below to the mathematical approach to calculate unsteady non uniform flow.

5.3.2 Unsteady Flow Equations

The equations used to analyse unsteady flow in an open channel are the continuity equation and the momentum equation, known as the St. Venant equations. The assumptions made in order to be able to apply the St. Venant equations are, firstly, that the density of the water does not vary (incompressible), secondly, the slope of the river bed is small and thirdly, that wave lengths are large compared to the water depth and thus vertical accelerations can be neglected.

- The continuity equation

$$\frac{\delta Q}{\delta x}+\frac{\delta B}{\delta t}=0 \qquad 5.1$$

- The momentum equation

The second equation is the momentum equation. If the flow is assumed to be one dimensional, i.e. no acceleration in the vertical or lateral directions and the velocity is assumed to be constant over the section, then

$$\frac{\delta H}{\delta x}+\frac{v}{g}\frac{\delta v}{\delta x}+\frac{\delta v}{g\delta t}=s_0-s_e \qquad 5.2$$

Equation 5.2 can be written as:

$$\frac{\delta Q}{\delta t} + gA\frac{\delta H}{\delta x} + \frac{\delta(\alpha Q v)}{\delta x} + \frac{g|Q|Q}{C^2 AR} = 0 \qquad 5.3$$

(1) (2) (3) (4)

where

t	time (s)
x	distance (m)
H(x,t)	water level (m)
v (x,t)	mean velocity (m/s)
Q(x,t)	discharge at location x and time t (m^3/s)
R(x,H)	hydraulic radius of cross section (m)
A(x,H)	cross-sectional flow area (m^2)
b (x,H)	cross sectional storage width (m)
B(x,H)	cross sectional storage Area (m^2)
g	gravitational acceleration (m/s^2)
C(x,H)	Coefficient of de Chezy (m^2/s)
α	correction factor for non-uniformity of the velocity distribution in the advection term.
s_0	bed slope
s_e	friction slope

Term (1) of equation 5.3 is called the local acceleration term or rate of change in velocity with time. Term (2) is due to the effect of gravity on the water's surface slope. Term (3) is the convective acceleration term (change in velocity with distance) and term (4) is due to the effects of frictional resistance.

Resistance:

The channel friction can be calculated using:

- the formula of **De Chézy.**
  The "resistance" coefficient C in the definition of the sections is from the basic formula: $v=C\ (R \cdot s_0)^{1/2}$ (s_0 = bed slope)
- the formula of **Manning.**
  The "resistance" is the Manning coefficient k (1/n) from the basic formula $v=k \cdot R^{2/3} \cdot s_0^{1/2}$.

In the actual calculation $C=k \cdot R^{1/6}$ is substituted in the formula of De Chézy.The value of C is calculated for each time step during the simulation. Default in DUFLOW is the De Chézy coefficient.

Velocity Correction Factor:

The correction factor for non-uniformity of the velocity distribution in the advection term, which is defined as:

$$\alpha = \frac{A}{Q^2} \int v(y,z)^2 dydz \qquad 5.4$$

where the integral is taken over the cross section A.

In the case of complex cross sections, such as cross sections including floodplains, $\alpha=1.05$ with v the velocity in the main stream. The value may be indicated as greater, but the v is then defined as the average velocity for the total section (Rooseboom et. al., 1986).

Advection Term:

The advection term in the momentum equation

$$\frac{\delta(\alpha Q v)}{\delta x} \qquad 5.5$$

can be broken into

$$\alpha(2\frac{Q}{A}\frac{\delta Q}{\delta x}-\frac{Q^2}{A^2}\frac{\delta A}{\delta x}) \qquad 5.6$$

The first term in equation 5.6 represents the impact of change in discharge, while the second term expresses the effect of change in the cross-sectional flow area and is called the Froude term. In cases of abrupt changes in cross-section this Froude term may lead to computational instabilities. DUFLOW allows the user in the calculation settings to choose between 3 ways of calculating the advection term (STOWA, 1998):

a) Total Froude	:	includes the Froude term
b) Damped Froude	:	the absolute value of the Froude term will not exceed the friction term
c) Neglected Froude	:	the entire Froude term is neglected.

The solution to the St. Venant equations are complex and therefore a number of numerical methods have been developed to get a solution to the equations. It has to be recognized that although the St. Venant equations are capable of calculating supercritical flow, the numerical solution is not able to do so. Therefore, DUFLOW is unable to calculate supercritical flow.

5.3.3 Numerical Solutions to Unsteady Flow

There are three principal types of numerical methods used to calculate open channel flow: method of characteristics, finite differences and finite elements.

Method of Characteristics:

This method solves the unsteady flow equations by transforming the partial differential equations into normal differential equations and then solving them by numerical techniques. There are then two compatibility equations that are valid along two sets of characteristic lines. These methods can be divided into the way they are discretisized (i.e. grid or rectangular methods). (Some of the researchers that have investigated this numerical scheme are: Lai, 1976; Ghidaoui and Karney, 1994).

Finite Element Methods:

Finite element methods assume that the solution has a simple form over small elements. This leads to a system of simultaneous equations in matrices for each element, the equation is then solved inside each element by using the method of weighted residuals. This method is normally used in multi-dimensional modelling (Katopodes, 1984; Koutitas, 1983).

Finite Difference Methods:

The finite difference methods, which are more commonly used than finite element methods, can be further classified as implicit and explicit methods. Explicit schemes provide the solution for Q and H at every next time step for each point on the distance grid, while implicit schemes provide the solution for Q and H at the next time step for all the points on the grid simultaneously, which makes it more complex, as it requires the solution of a number of simultaneous equations. Explicit schemes are easier to use but must conform to the Courant stability criteria in order to be stable ($c\Delta t/\Delta x<1$, where c is the wave speed)(Koutitas, 1983),where as the implicit scheme are conditionally stable for all time steps; this is the main difference between the implicit and explicit scheme. The implicit method is said to be more efficient than the explicit method as computation time is much less; larger time steps can be used without influencing the stability of the equations, nor the acceptable accuracy of the solution.

Table 5.1: Comparison of finite difference schemes

Scheme	Description	References
Explicit finite difference schemes	These schemes were the first to be applied to the St. Venant equations and were widely used because of their simplicity in programming and execution. (Dooge, 1989).Explicit finite difference approximations that have been applied to flood routing include : The simple explicit scheme The diffusive scheme The leapfrog scheme The Lax-Wendroff scheme.	Dooge (1989) Grijsen (1986)
Implicit finite difference scheme	In implicit methods the solution is obtained by applying the implicit scheme at each of the nodes along the channel simultaneously, combining the difference equations obtained in this way with the boundary conditions at each end and solving the whole set of equations simultaneously. Some of the implicit schemes are: 4 point Preissmann scheme Crank Nicholson scheme Linear implicit schemes	Amein (1968) Amein and Fang (1970) Fread (1973) Amein and Chu (1975)

The 4 Point Implicit Preissmann Scheme:

DUFLOW discretises the St Venant equations by using the four-point implicit Preissmann scheme, which is discussed below.

Preissman proposed a general four point implicit scheme with a weighting of θ in 1960 (Grijsen, 1986). The discretization is done in space and time, i.e. in a two dimensional grid (see Figure 5.8). The

weighting $\theta = dt'/dt$ (refer to Figure 5.8). Therefore, the four point implicit schemes are unconditionally stable at $\theta = 0.5$ as the point P, which lies between the time lines and space lines in Figure 5.8 , lies exactly halfway between the time line n and (n+1). For $\theta=1$ the solution scheme becomes fully implicit, as the point P is exactly on the time line (n+1), while for a weighting of 0 the point P will lie on the current time line n and the scheme is then fully explicit (refer also to previous definitions of explicit and implicit schemes).

The water level H can be expressed as:

$$H_i^{n+\theta} = (1-\theta)H_i^n + \theta H_i^{n+1} \qquad 5.7$$

where a section Δx_i is defined from node x_i to node x_{i+1} and a time interval Δt from $t = t_n$ to time $t = t_{n+1}$, i is the number of the node (refer to Figure 5.8). In a similar way other dependent variables are approached. The transformed partial differential equations are written then as a set of algebraic equations by replacing the derivatives by finite difference equations.

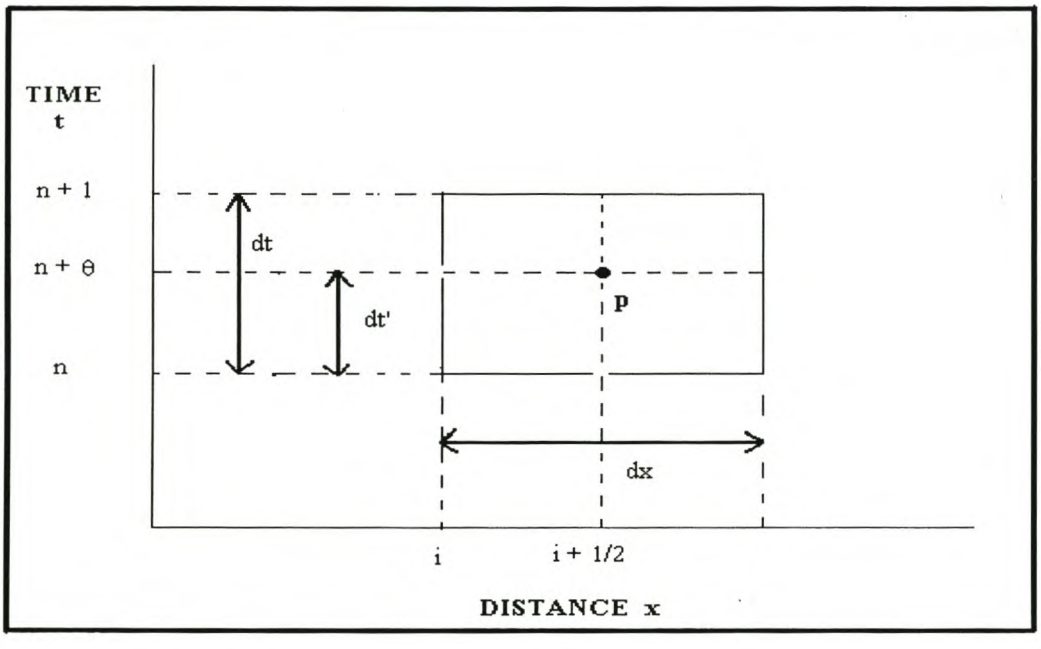

Figure 5.8: Four-point Preissmann scheme

With initially

$$H^{\upsilon}_{i+1/2} = H^{n}_{i+1/2}$$

$$B^{n}_{i+1/2} = B_{i+1/2}(H^{n}_{i+1/2})$$

$$b^{n}_{i+1/2} = b_{i+1/2}(H^{n}_{i+1/2})$$

$$B^{n,*}_{i+1/2} = B_{i+1/2} - b^{n}_{i+1/2}(H^{n}_{i+1/2})$$

The continuity equation 5.1 can be transformed to

$$\frac{B^{*,n+1}_{i+1/2} + b^{n+1}_{i+1/2} H^{n+1}_{i+1/2} - B^{n}_{i+1/2}}{\Delta t} + \frac{Q^{n+\theta}_{i+1} - Q^{n+\theta}_{i}}{\Delta x_i} = 0 \qquad 5.8$$

and the momentum equation 5.2 to

$$\frac{Q^{n+1}_{i+1/2} - Q^{n}_{i+1/2}}{\Delta t} + \frac{g A^{*}_{i+1/2}(H^{n+\theta}_{i+1} - H^{n+\theta}_{i})}{\Delta x_i} + \frac{\alpha\left(\frac{Q^{n}_{i+1}}{A^{*}_{i+1}} Q^{n+1}_{i+1} - \frac{Q^{n}_{i}}{A^{*}_{i}} Q^{n+1}_{i}\right)}{\Delta x_i} + \frac{g(Q^{n+1}_{i+1/2}|Q^{n+1}_{i+1/2}|)}{(C^2 A R)^{*}_{i+1/2}} = 0 \qquad 5.9$$

The * (like in A*) expresses that these values are approximated at time $t_{n+\theta}$. These * values are improved using an iterative process, the first approximation is adjusted in subsequent iteration steps.

Finally, all channel sections have two equations where Q and H are the unknowns at the new time level.

$$Q^{n+1}_{i} = N_{11} H^{n+1}_{i} + N_{12} H^{n+1}_{i+1} + N_{13} \qquad 5.10$$

$$Q^{n+1}_{i+1} = N_{21} H^{n+1}_{i} + N_{22} H^{n+1}_{i+1} + N_{23} \qquad 5.11$$

Solving the set of equations:

The number of unknowns is equal to 2(J+I) where J is the number of sections and I is the number of nodes; in each branch the unknowns are the flows at both ends and at each node the water level. The number of equations is also 2(J+I); for each channel section J two equations are derived (equations 5.10 and 5.11). A set of linear equations is solved at each time step.

The linear equations result in:

$$\sum M_{ij} H_j = R_i \qquad 5.12$$

The coefficients N_{11} , N_{12} , N_{21} and N_{22} of equations 5.10 and 5.11 contribute to a matrix as coefficients M_{ii} , M_{ij} , M_{ji} and M_{jj} respectively. N_{13} and N_{23} can be found in the matrix R. The structure of the set of equations is then:

$$\begin{matrix} & ij \\ i \\ j \end{matrix}\begin{bmatrix} * & * \\ * & * \end{bmatrix} * \begin{bmatrix} * \\ * \end{bmatrix} = \begin{bmatrix} * \\ * \end{bmatrix} \qquad 5.13$$

M * H = R

This matrix is then solved by the LUD decomposition. With the LUD decomposition the matrix is 'factorised' to a final matrix that has an lower triangular form that facilitates a backsubstitution process, and the solutions to the matrix can be found.

5.3.4 Boundary and Initial Conditions

A unique solution to the St. Venant equations requires two initial and two boundary conditions.

In DUFLOW the boundary conditions are user defined and may be specified as levels, discharges or a relation between the two. The best choice of what type of boundary to use, is the quantity or relation that is the least sensitive to the state of the model itself. Therefore, the upstream boundary condition in a river is preferably a discharge whereas the downstream boundary condition should be a water level, if the river flows into a lake or sea, or a level-discharge relation based on uniform flow, if the downstream boundary

is somewhere along the river (STOWA, 1998).The accuracy of the boundary condition's readings are of great importance as they determine a realistic solution to the calculations.

The initial conditions are specified at every node and schematization point as flow conditions at the initial time step. In DUFLOW the initial conditions are defined as a discharge and a water level. Care needs to be taken at very low flow (i.e. discharge and depth near to a value of 0), as the numerical calculations could become unstable. Any inaccuracies in the initial conditions are cancelled out after a reasonable number of time steps.

5.3.5 Cross-sections

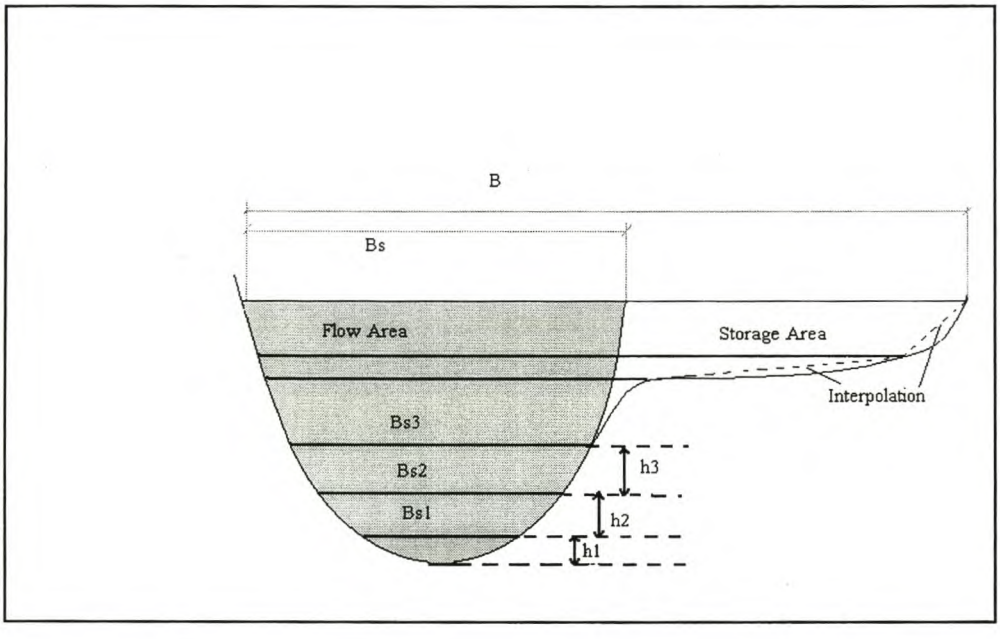

Figure 5.9: Schematization of cross-sections

Information about the the geometry of the river is needed for solving the set of equations. Information of the cross-sectional shape can be found from topographical maps or from surveys conducted in the area. For modelling purposes, cross-sections are often assumed trapezoidal, rectangular or of parabolic shape. DUFLOW gives the option to enter the cross-section as any of the three. The cross-section is entered as a function of depth, as can be seen in Figure 5.9. Therefore, storage areas and flow areas can

be entered at different depths. When including the floodplain, a decision needs to be made whether to model the cross-section as a complex cross-section, or a number of parallel branches with the different schematisations, introducing the flow from the floodplain as lateral flows into and from the main channel, as in Figure 5.10 .

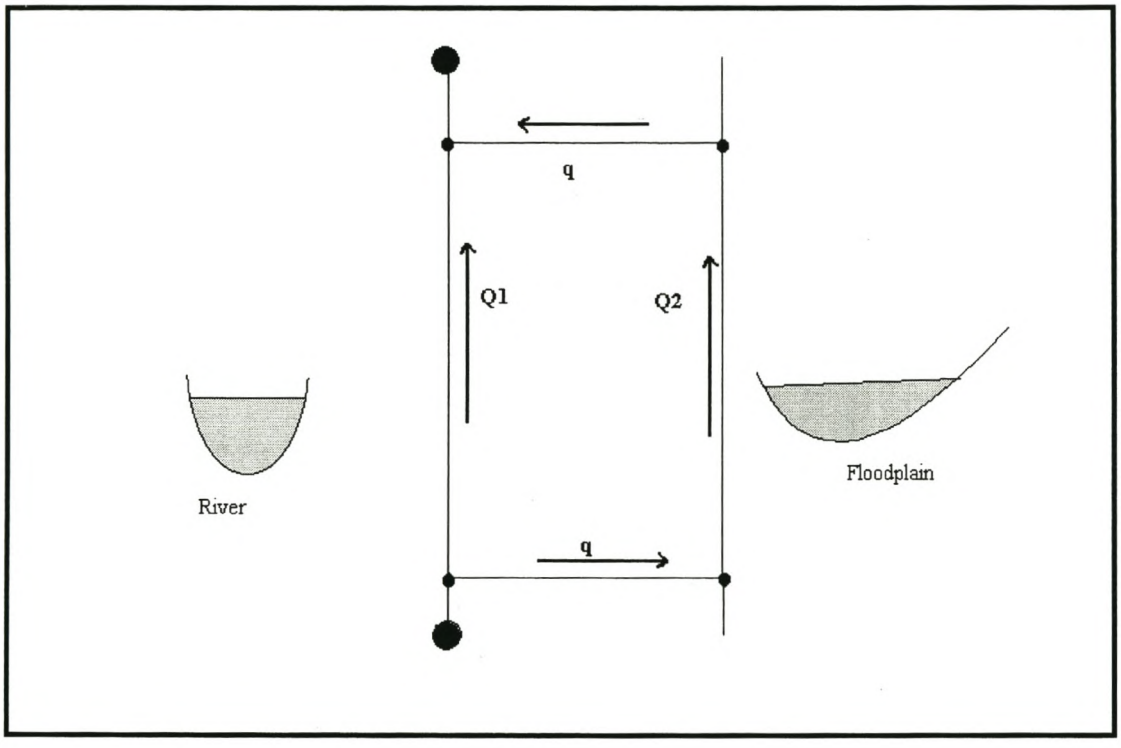

Figure 5.10: Schematisation of floodplain using lateral flows

5.3.6 Structures

Various types of control structures can be defined in DUFLOW such as weirs, culverts, pumps and syphons. Below is a description about general structures and weirs that were used in modelling the bridges and weirs in the Berg River. For a description on pumping systems, syphons and culverts the reader is referred to the DUFLOW manual (STOWA,1998). At weirs and other structures, discharges and levels can be modified and controlled by so-called trigger conditions: depending on flow conditions at specified locations in the network, parameters such as the width of a weir, the level of the sill, etc. can be adjusted during the computation to reflect for instance structural modifications during this period.

Weirs:

The discharge over a weir depends on the water level on both sides, the level of the sill, type of structures and the flow conditions (free surface flow or submerged conditions). A structure is defined between two nodes i and j and the discharge in the structure is denoted as Q. Figure 5.11 shows the flow conditions that can occur over a weir, where it is assumed that $H_i > H_j$. Under submerged conditions, if $H_i < H_j$, the conditions of flow are symmetrical with Figure 5.11 except for the loss coefficient. Table 5.2 should be read in conjucntion with Figure 5.11.

The general equation for the discharge over a weir is

$$Q_{n+1} = \mu B H \sqrt{2g\Delta H} \qquad 5.14$$

where:

B width of the weir, multiple notch handled by so-called trigger functions (refer to definition at end of this section)

μ the loss coefficient

H depth over the sill

ΔH difference in head between upstream and downstream head

Table 5.2: The quantities that are used for different flow conditions. (STOWA, 1998).

Flow Condition	**DMS-object**	**μ**	**H**	**ΔH**	**Description**
I	General Structure	μ_0	HO	$H_i^{n+1} - HO$	Vertical Gate
II	General Structure	μ_t	$\frac{2}{3} H_i^{n+1}$	$\frac{1}{3} H_i^n$	Vertical Gate
III	Weir	μ_v	$\frac{2}{3} H_i^{n+1}$	$\frac{1}{3} H_i^n$	Flow over weir
IV	Weir	μ_v	H_i^n	$H_i^{n+1} - H_j^{n+1}$	Flow over weir
V	General Structure	μ_t	H_i^n	$H_i^{n+1} - H_j^{n+1}$	Vertical Gate
VI	General Structure	μ_t	HO	$H_i^{n+1} - H_j^{n+1}$	Submerged flow through underflow sluice gate
VII	General Structure	μ_0	HO	$H_i^{n+1} - H_j^{n+1}$	Submerged flow through underflow sluice gate

The parameters are defined as:

H_i, H_j water depth over the sill respectively at the beginning and at the end of the section

HO height of opening

μ_0 loss coefficient, gate flow

μ_v loss coefficient, free surface flow

μ_t loss coefficient, transition between μ_0 and μ_v

$$\mu_t = \mu_v + 2\left(\frac{H_i}{HO} - 1\right)(\mu_0 - \mu_v) \qquad 5.15$$

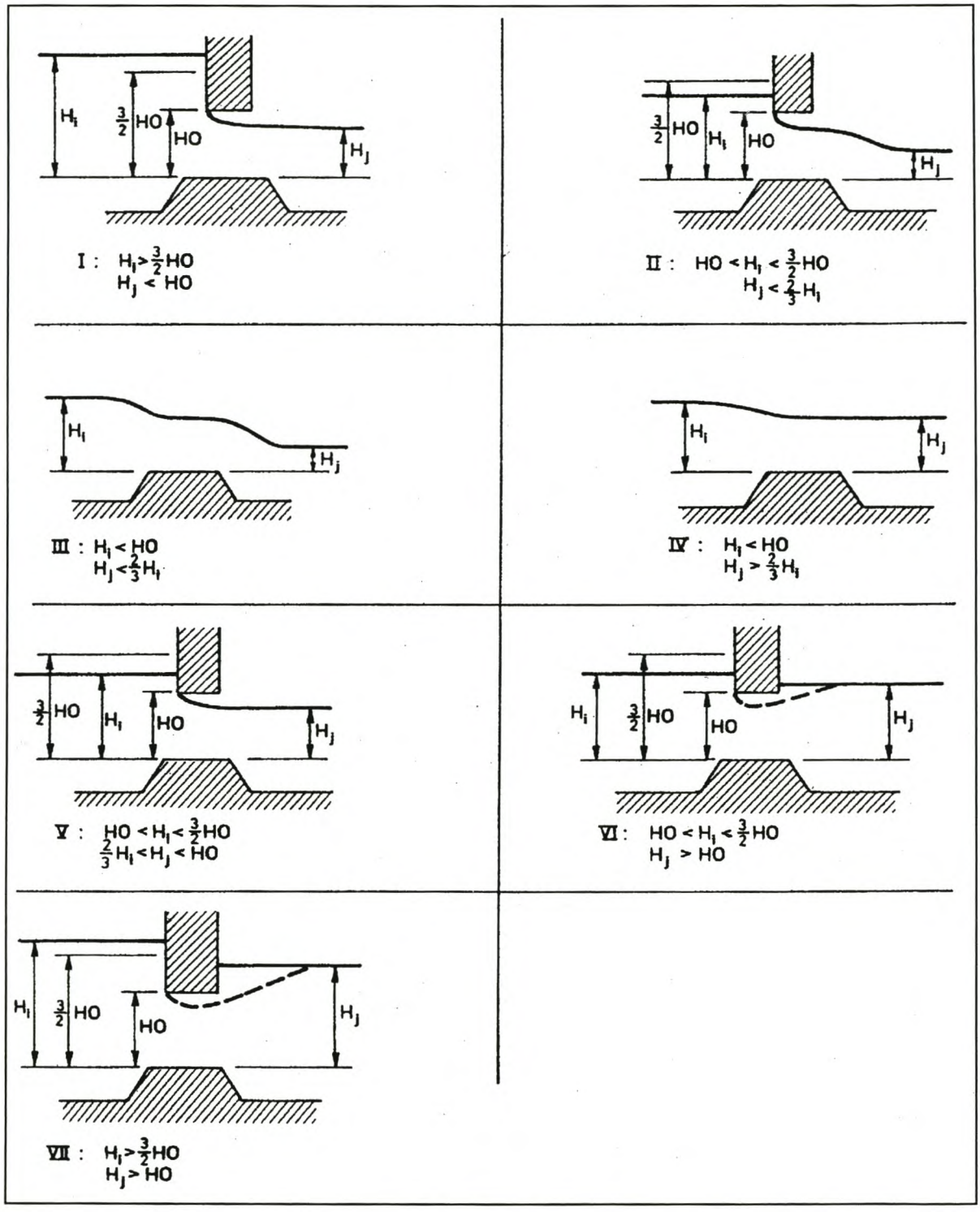

Figure 5.11: Structure Flow Conditions, covered by DUFLOW

Bridges:

Bridges are defined as General Structures. Required Data for the structures are the width of the flow opening of the structure, the height of the flow opening of the structure and the level of the upper side of the flow opening above the reference level.

Trigger Functions:

If a parameter of the structure varies according to hydraulic conditions (i.e. multiple notch of weir, or raising of gates at certain water levels), the specifications for the control of these structures can be defined in DUFLOW as *trigger series*. The operational parameter is defined, as well as which type of trigger (i.e. H node> H trigger, H>H+dH, etc), the operational parameter (sill level, gate level etc.) will change according to the entered conditions.

5.4 WATER QUALITY

5.4.1 Introduction

Water quality models predict changes in water quality variables due to loading, transport and reactions within the water body. The basic theory describing these changes is the conservation of mass. The water quality mass balance in a volume of water can be expressed as:

accumulation = loadings +- transport +- reactions

(Chapra and Reckhow, 1983)

where:

loadings	-	external loadings added to substances, mass of a material discharged per unit time into a volume of water
transport	-	the movement of matter through a volume
reactions	-	mass is gained or lost by chemical or biological reactions in the water body
accumulation	-	either positive (mass increases, as sources are greater than sinks) or negative (mass decreases, sinks are greater than sources)

If a water quality variable changes its mass due to chemical or biochemical reactions it is called a *non-conservative* constituent, while where a variable is just dependent on the transport it is a *conservative* constituent. *Sources* specify all the chemical reactions that contribute to an increase of mass of the constituent, while the *sinks* are responsible for the decrease of mass.

In the next sections, the terms will be explained and formulated mathematically, with emphasis on the approach DUFLOW takes to formulate the mass balance in acertain water volume.

5.4.2 Transport

Transport is the movement of matter through a certain volume along with water flow. The mathematical equation describing the transport of a variable in a one dimensional system is the advection-dispersion equation:

$$\frac{\delta(BC)}{\delta t} = -\frac{\delta(QC)}{\delta x} + \frac{\delta}{\delta x}(AD\frac{\delta C}{\delta x}) + P \qquad 5.16$$

(1) (2) (3) (4)

where:

C	constituent concentration(g/m^3)
Q	flow (m^3/s)
A	cross-sectional flow area (m^2)
D	dispersion coefficient (m^2/s)
B	cross-sectional storage area (m^2)
x	x co-ordinate
t	time (s)
P	production of the constituent per unit length (g/m.s)

Term (1) and (2)of the equation represents both the advection processes, while term (3) represents the longitudinal mixing in a water body, which is known as diffusion. With the advection, the particle is

swept along (advected) with a velocity comparable to that of a flow as well as molecular diffusion. Diffusion and advection are not always independent and mixing in a water body can occur as a result of both, the combination of advection and diffusion is therefore termed dispersion (Chadwick and Morfett, 1993).

The term (4) of equation 5.16 is called the production term P and it includes all physical, chemical and biological processes to which a specific constituent is subject to and will be described in section 5.4.5. A differentiation needs to be made between a conservative and a non-conservative constituent, a non-conservative quantity has a continuously decaying mass due to the biological or chemical reactions, even if no transport or diffusion takes place. A conservative constituent does not undergo any changing processes except for being transported and diffused. Therefore, the production term P would only apply to non-conservative variables.

The mass transport equation 5.16 is simplified to:

$$\frac{\delta S}{\delta x}+\frac{\delta(BC)}{\delta t}-P=0 \qquad 5.17$$

in which S is the transport (quantity passing a cross-section per unit time). This equation is the mass balance equation, which states that the accumulation of a water quality variable is equal to the production rate minus the transport gradient.

The transport by advection and dispersion is described as:

$$S=QC-AD\frac{\delta C}{\delta x} \qquad 5.18$$

The relation between the advective and diffusive transport is expressed by the Peclet number (Koutitas,1983). The Peclet number is defined as:

$$Pe=v\frac{\Delta x}{D} \qquad 5.19$$

High Peclet numbers show that the advective transport prevails over the diffusive one. Small numbers

mean that the diffusion predominates. Instabilty of equations can occur if the Peclet number becomes too large (Pe>2), and could be controlled by increasing the dispersion in the calibration procedure.

One Dimensional Dispersion :

The value of D (longitudinal dispersion coefficient) will vary along the channel, depending on the geometry of the channel.

The dispersion coefficient can be determined by either performing tracer studies in the river, or by estimating the dispersion from equations that have been developed which relate dispersion to the shear stress. Much research has been done on the dispersion coefficient and equations have been developed. Various approximations of determining the dispersion coefficient have evolved. The equations are normally based on Fischer's one-dimensional approximation flow (assuming that the flow is fully mixed) and Taylor's prediction of dispersion in a fully developed pipe (Fischer, 1968; Taylor, 1957).

A number of studies have shown that one-dimensional theory does not adequately describe longitudinal dispersion in many rivers, especially at low flow (Seo, 1990). Typically the time series of the measured concentration are positively skewed when compared to the actual calculated time series using the one-dimensional equation (i.e. the concentration time series calculated increases faster than the measured tracer time series). This could be due to temporary storage in 'dead zones' (slowly moving parts of the flow along the channel beds and banks) (Day, 1975; Nordin and Troutman, 1980; Valentine and Wood, 1977; Seo, 1990). Equations have been formulated to adapt the one dimensional equation to data from tracer studies by various methods. Some of the methods to determine the dispersion coefficient are summarized in Table 5.3.

Table 5.3: Dispersion Calculation Methods

Method	Author
Method of moments to estimate the skewness coefficient	Nordin and Troutman (1980)
Numerical Routing to estimate the longitudinal coefficient	Jobson (1987)
Differential equations incl. longitudinal advection in mainstream, regions of vortex in storage zones with mass interchange at the interface.	Il Won Seo (1990)
Taking the natural log from concentrations between two points and solving as a log-linear relationship.The dispersion coefficient can be estimated from the slope of the linear regression and the mean velocity.	Thomann and Mueller (1987)

DUFLOW gives the option to "Decouple"; i.e. only dispersion in forward direction is taken into account. Decoupling only takes place at those nodes where a discharge is located. Otherwise the dispersion is considered on both sides of a node. A dispersion coefficient needs to be specified at every node and discharge point, this allows the user to model the influence of different coefficients, as the dispersion coefficient varies along the river stretch.

The dispersion coefficient can range from $150*10^5$ cm ^{2} sec $^{-1}$ (Missouri River) to only 0.96 cm ^{2} sec $^{-1}$ (Coachelle Canal in California), depending on the river (Chapra, 1997).

5.4.3 Discretization of Mass Transport Equations

In the flow calculations the discharges were expressed as a set of linear equations as functions of water levels. For the water quality the transport (S) is expressed as functions of concentration(c). The Galerkin method is applied to obtain these expressions:

The mass conservation equation is integrated over a section and multiplied with a weighting function ψ:

$$\int_0^{\Delta x} \psi_i \left[\frac{\partial S_i}{\partial x} + \frac{\partial (B_i C)}{\partial t} - P_i \right] dx = 0 \qquad 5.20$$

This results in:

$$\psi_i S_i \Big|_0^{\Delta x} + \int_0^{\Delta x} \left[\psi_i \frac{\partial (B_i C)}{\partial t} - \frac{\partial \psi_i}{\partial x} \left(QC - A_i D \frac{\partial C}{\partial x} \right) - \psi_i P_i \right] dx = 0 \qquad 5.21$$

Two weighting functions are distinguished for every section:

$$\psi_1 = 1 - \frac{x}{\Delta x} \qquad 5.22$$

$$\psi_2 = \frac{x}{\Delta x} \qquad 5.23$$

C is assumed to vary linearly with each section, i.e.

$$C = \psi_1 c_1 + \psi_2 c_2 \qquad 5.24$$

in which c_1 and c_2 are the concentrations at the beginning and at the end of each section.

The solution then becomes:

For the beginning of the section:

$$-S_1 + \frac{\Delta x}{3} \frac{\partial B_1 c_1}{\partial t} + \frac{\Delta x}{6} \frac{\partial B_2 c_2}{\partial t} + \frac{Q_1 c_1 + Q_2 c_2}{2} - A_1 D \frac{c_2 - c_1}{\Delta x} - \frac{\Delta x}{3} P_1 - \frac{\Delta x}{6} P_2 = 0 \qquad 5.25$$

and at the end of the specific section:

$$S_2 + \frac{\Delta x}{6}\frac{\partial B_1 c_1}{\partial t} + \frac{\Delta x}{3}\frac{\partial B_2 c_2}{\partial t} - \frac{Q_1 c_1 + Q_2 c_2}{2} + A_2 D\frac{c_2 - c_1}{\Delta x} - \frac{\Delta x}{6}P_1 - \frac{\Delta x}{3}P_2 = 0 \qquad 5.26$$

These equations are also discretised with respect of time and give:

$$S_2^+ = -\frac{(1-\theta)}{\theta}S_2^- + \frac{\Delta x}{6\theta}\left(\frac{B_1^+ c_1^+ - B_1^- c_1^-}{\Delta t}\right) + \frac{\Delta x}{3\theta}\left(\frac{B_2^+ c_2^+ - B_2^- c_2^-}{\Delta t}\right) + \frac{\theta Q_1^+ c_1^+ + \theta Q_2^+ c_2^+ + (1-\theta)Q_1^- c_1^- + (1-\theta)Q_2^- c_2^-}{2\theta} - A_2 D\frac{\theta c_2^+ - \theta c_1^+ + (1-\theta)c_2^- - (1-\theta)c_1^-}{\Delta x\theta} + \frac{\Delta x}{6\theta}P_1 + \frac{\Delta x}{3\theta}P_2 = 0 \qquad 5.27$$

$$S_1^+ = -\frac{(1-\theta)}{\theta}S_1^- + \frac{\Delta x}{3\theta}\left(\frac{B_1^+ c_1^+ - B_1^- c_1^-}{\Delta t}\right) + \frac{\Delta x}{6\theta}\left(\frac{B_2^+ c_2^+ - B_2^- c_2^-}{\Delta t}\right) + \frac{\theta Q_1^+ c_1^+ + \theta Q_2^+ c_2^+ + (1-\theta)Q_1^- c_1^- + (1-\theta)Q_2^- c_2^-}{2\theta} - A_1 D\frac{\theta c_2^+ - \theta c_1^+ + (1-\theta)c_2^- - (1-\theta)c_1^-}{\Delta x\theta} - \frac{\Delta x}{3\theta}P_1 - \frac{\Delta x}{6\theta}P_2 = 0 \qquad 5.28$$

The indices + and - refer to present and last time step respectively. The weighting factor with respect to time is θ. Using a value θ=1 results into a fully implicit method (refer also to section 5.3.3). Unknowns are c_1, c_2, S_1 and S_2.

Using these equations together with the mass balance over the nodes, a set of linear equations is set up. With a system of matrix, as in the flow equations (equation 5.18), the solution to the various unknowns can be found by using the LUD decomposition.

5.4.4 Initial and Boundary Conditions

When simulating quality, if a flow boundary is defined at the upstream boundary of the network, a concentration boundary condition has to be defined as well. At the downstream boundary a concentration boundary condition is not necessary. The user has the option of entering the water quality data as loads or as concentration. If evaporation is modelled, the concentration will then not be defined, and it is treated as 0. At the physical boundaries, a concentration boundary for every defined dissolved substance is compulsary.

5.4.5 Water Quality Processes

As explained in section 5.4.2, the mass of water quality variables can be changed by a variety of chemical and biochemical reactions.

In DUFLOW the mathematical formulations describing the processes can be supplied by the user. These are supplied in a file which can be created or modified by using the user interface. A special description language DUPROL has been developed to allow this. DUFLOW comes with EUTROF1 and EUTROF2, which are two predefined eutrophication models. EUTROF1 includes the cycling of nitrogen, phosphorous and oxygen. The growth of one phytoplankton, chlorophyll-a, is simulated. EUTROF 2 describes the same as EUTROF1 but allows for the water-sediment exchange and has 3 different phytoplankton species which can be studied. EUTROF1 was used in the Berg River study; as it contains simpler algorithms describing the water quality processes, therefore less data and parameter intensive than EUTROF2. For this study alterations have been made to the model to allow additional modelling of TDS and temperature, as these variables are of great concern in the Berg river study (refer to section 5.4.5.1 for a description on the addition of the temperature processes; as well as section 5.4.5.3 for a description of the addition of COD in the oxygen algorithms).

In the computational part the process descriptions are combined with the transport equations. The lumped variable P (refer to equation 5.17) contains the certain processes of each water quality constituent.

The differential equations for the variables have normally the following form:

$$\frac{\delta C}{\delta t} = k_1 C + k_0 \qquad 5.29$$

the kinetic coefficients k_1 and k_0 are then written in the DUPROL interface, separately for each variable. If the kinetic coefficients are not defined, they are automatically set to zero.

In the following section certain processes are described for each of the constituents that are studied in the Berg River, which are TDS, Dissolved Oxygen, Nutrients (in the form of Phosphates) and Temperature.

5.4.5.1 Temperature:

The temperature of a water body is of particular significance as:

(a) temperature influences all biological and most chemical reactions,
(b) the discharge of municipal or industrial effluent may affect the aquatic ecosystem due to different temperatures than the receiving water, and
(c) variations in temperature affect the density of water and hence the transport of water (the transport algorithm assumes density to be constant).

In the following section, the mathematical equation of the influence of temperature on the chemical and biological reactions is considered. The mathematical model of the heat balance of a water body, with sinks and sources, is also described.

- *Temperature Dependence of Chemical Reactions:*

  The mass of a water quality constituent is influenced by a variety of chemical reactions. The rates of most reactions increase when the water temperature increases. As kinetic description of most biological reactions are based on a standard temperature of 20 degree Celsius, the reaction rates needs to be adjusted according to the surrounding water temperature.

To compute the reaction rate at another temperature, the following equation is used:

$$k_T = k_{20°C}\theta^{T-20°C} \qquad 5.30$$

where:

T	-	temperature in degree Celsius
k	-	reaction rate at 20 degree Celsius
θ	-	constant

this has been derived from the van't Hoff-Arrhenius equation, for more information on the derivation the reader is referred to Chapra and Reckhow (1983).

This equation is commonly used to depict the change in reaction rate due to the change in temperature. In DUFLOW the temperature coefficients for algal growth, mineralisation, nitrification, respiration and reaeration, as well as oxidation do need to be supplied by the user.

Temperature Model developed for this study:

The temperature of a given water body depends on the sources and losses of heat in a water body. These have to be therefore estimated as accurately as possible in order to assess the heat balance. Thomann and Mueller (1987) summarize the sources and sinks as follows:

Sources:

- Shortwave solar radiation
- Longwave atmospheric radiation
- Conduction of heat from atmosphere to water
- Direct heat inputs from municipal and industrial activities.

Sinks (losses):

- Longwave radiation emitted by water.
- Evaporation
- Conduction from water to atmosphere.

The heat balance in a small volume of the river will be:

Rate of change of temperature = heat in - heat out -+ net heat exchange

The EUTROF1 and the EUTROF2 model do not allow the user to model the temperature in the particular water body, but only take the effect of temperature on the kinetic reactions into account. Thus, for this study, a temperature submodel has been developed and incorporated into the EUTROF1 model by using the Compiler.

The components of the net heat exchange are (refer also to Figure 5.12):

$$J = Js + Ja - (Jb + Jc + Je) \qquad 5.31$$

where

J	=	total surface heat flux
Js	=	net solar shortwave radiation
Ja	=	atmospheric longwave radiation
Jb	=	longwave back radiation from the water
Jc	=	conduction
Je	=	evaporation

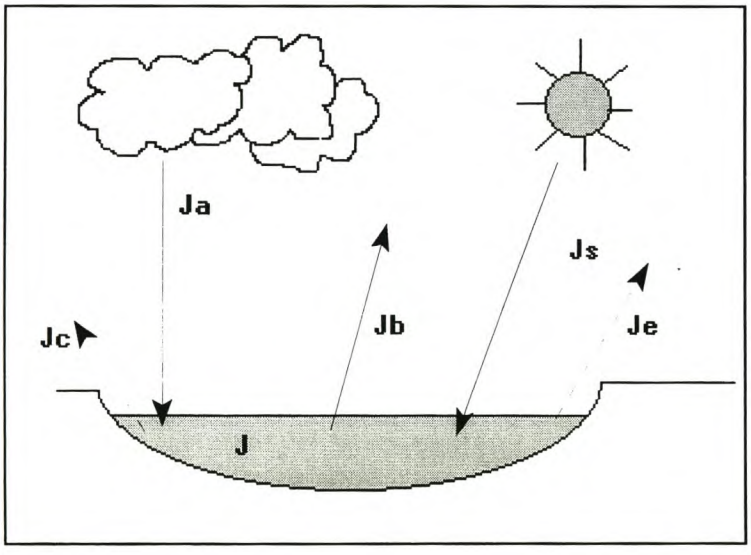

Figure 5.12: Sinks and Sources of Temperature Model

Net solar shortwave radiation (Js):

Solar radiation is dependent on various factors such as the solar altitude (depending on date, time of day, location), scattering of radiation by clouds and adsorption by atmospheric gases, reflection (dependent on condition of sky and water surface), as well as shading of the streams. Many algorithms have been developed to calculate the solar radiation and some water quality models allow the user to use these algorithms (CE-QUALl, RIV1 etc.). The reader is referred to Schulze (1995) for detailed explanations on developments of these algorithms especially with regard to South African conditions. These equations determining the solar radiation in Southern Africa have been developed by Drummond and Vonwinckel in 1957, Schulze and Mcgee in 1978 and Reid in 1981(Schulze, 1995). The Southern African Atlas of Agrohydrology and -Climatology (Schulze et al., 1997) uses an equation developed by Clemence in 1992 for mapping the solar radiation for different months in the whole of the country. Solar radiation is often measured by meteorological stations around the country and these measurements can be used directly in the equation. As radiation data is available at different stations near to the Berg River, these algorithms have not been used to calculate the solar radiation, but rather the actual measurements have been taken as input data.

Atmospheric longwave radiation (Ja):

Atmospheric longwave radiation is normally expressed as:

$$J_a = \sigma(T_{air}+273)^4 * (A + 0.031\sqrt{e_{air}})(1 - R_L) \qquad 5.32$$

(1) (2) (3)

where

Ja	=	Atmospheric Longwave Radiation (J/(m^{2}day))
σ	=	Stefan Boltzmann constant (4.9 * 10^{-3} J/(m^{2}day.K^4))
T_{air}	=	air temperature (°C)
A	=	a coefficient (0.5 to 0.7 (Chapra, 1997), or Schulze (1995) defines it as 0.56)
e_{air}	=	air vapour pressure (Pa)
R_L	=	reflection coefficient (generally small, about 0.03 (Chapra, 1997))

The first term takes the Stefann Boltzmann law into account, the second term calculates the atmospheric attenuation which represents the difference between the emittance value for the earth's surface and the effective emittance for the atmosphere, and the third term represents the reflection of the water body. These terms are explained below:

Stefan Boltzmann Law:

The Stefan Boltzmann law states that, the higher the temperature of an object, the shorter is the wavelength of its emission and the greater the quantity of energy emitted per unit of surface area.

This is expressed as :

$$J_{rad} = \epsilon \sigma T_a^4 \qquad 5.32$$

where

J_{rad} = Radiation (J/m^2day)

T_a = absolute temperature (K)

σ = Stefan Boltzmann constant ($J/(m^2dayK^4)$)

ϵ = emissivity of a body

The emissivity is a correction factor which takes into account that a body is not a perfect radiation emitter (Chapra, 1997).

Atmospheric Attenuation:

The air vapour pressure can be calculated, using:

$$e_{air} = 4.596 e^{\frac{17.27 T_{aveair}}{273.3 + T_{aveair}}} \qquad 5.33$$

where

e_{air} = air vapour pressure (Pa)

The assumptions are made that :

- air temperature cools down to dew temperature at night
- the variation of actual vapour density is small

(Schulze et al., 1997)

Reflection:

R_L is a coefficient that takes into account the back scattering of radiation by the cloud cover. Schulze (1995) calculates the effect of cloud cover by also taking the ratio of actual sunshine hours to maximum possible sunshine hours into account which will depend on latitude and time. As no data is available on the sunshine hours, this has not been modelled, but just kept as a parameter.

Back Radiation of water (Jb):

The back radiation (J/m^2day) from the water surface can also be represented by the Stefann Boltzmann law: T_s is the surface water temperature(°C); the other terms, emissivity and the Stefann Boltzmann constant have already been explained above.

$$J_b = \epsilon\sigma(T_s+273)^4 \qquad 5.34$$

Conduction (Jc):

With conduction the heat transfer is dependent on the water, as the heat is transferred from one molecule to another when the molecules of different temperatures come into contact. This occurs normally at the air-water interface. Conduction plays a more substantial role in the heat transfer in lakes than rivers as the air-water interface is larger. The algorithm representing conduction is dependent on the wind velocity and the difference between the temperatures of the water body and the air.

$$J_c = c_1 f(U_w)(T_s - T_{air}) \qquad 5.35$$

where

Jc	=	heat transfer due to conduction (J/m²day)
c_1	=	Bowen's coefficient (about 0.47 mmHg/°C)
T_s	=	water temperature
T_{air}	=	air temperature
$f(U_w)$	=	dependence of the transfer on wind velocity. Chapra (1997) recommends a relationship proposed by Brady, Graves and Geyer in 1969:

$$f(U_w)=19+0.95U_w^2 \qquad 5.36$$

where U_w is the wind speed measured in m/s at 4 metres above water surface.

Evaporation (Je):

The heat lost due to evaporation is determined by the rate of mass transfer from the water to the atmosphere times the latent heat of vaporization.

This is then:

$$J_e=\rho_w LE \qquad 5.37$$

where

J_e	=	heat transfer due to evaporation (J/m²day)
ρ_w	=	density of water (998.2 kg/m³)
L	=	latent heat (J/kg)
E	=	evaporation in m/day

The latent heat is calculated as:

$(5971.1-0.57\ T_s)*(4.1868*10^{-3})$ (Jørgensen and Gromiec, 1989) 5.38

the second term converts cal/g to J/kg.

All terms :

All above terms (equations 5.32 to 5.38) describe the change of heat in a water body. All the terms have been adjusted to give the units of J/(m^{2}d) and can then be inserted into equation 5.31. To convert change of heat (J/m^{2}day) to change in temperature (°C/day) following conversion is made:

$$\Delta T = \frac{J}{\rho_w C_p z} \qquad 5.39$$

where

ΔT = rate of change in temperature (°C/time)

ρ_w = density of water (998.2 kg/m^3)

C_p = specific heat of water (4182 J/(kg °C))

z = depth of water (m)

J = heat (J/m^2 time)

This conversion is based on the relationship of concentration to mass: c = mass/volume. This allows us to model temperature as a concentration and to use the equation 5.19 that is used for the transport of a concentration. Similar conversion equations are used by Qual-2E and CE-QUAL-RIV1.

5.4.5.2 Nutrients as Phosphorous

The major nutrients that contribute to eutrophication are phosphorus as phosphate ions (PO_4^{3-}) and nitrogen as nitrate (NO_3^-), nitrite (NO_2^-) and ammonium (NH_4^+) ions. Plants normally use the nutrients in inorganic form. The reduction of algal growth rate depends on the most limiting factor, which means that the growth of a phytoplankton is limited by the nutrient that is available in low levels in the water body. Several studies show that phosphorus is often the limiting nutrient to phytoplankton growth in rivers (Chapra, 1997).

Although DUFLOW models nitrates, ammonia and phosphates, only the impact of phosphates will be modelled in the Berg River.

Chapra (1997) attributes the scarcity of phosphorous to following reasons:

- Phosphorous is not very abundant in the earth's crust
- Phosphate minerals are not very soluble
- It does not exist in gaseous form
- Phosphate adsorbs strongly to fine-grained particles. Settling and sedimentation serves to remove phosphate from the water to the bottom sediments.

The main sources of phosphate are human activities, in the form of non-point sources from agricultural and urban land and point sources as waste water effluents. There are many ways to characterise phosphates. Two forms are used in DUFLOW to characterise phosphorus: organic and inorganic phosphorous.

- *Soluble reactive phosphorous* ($H_2PO_4^-$,HPO_4^{2-}, PO_4^{3-})
  This form of phosphorous is available for plants. It is also called orthophosphates.

- *Particulate organic phosphorous*
  This form consists of living plants, bacteria as well as organic detritus.

- *Nonparticulate organic phosphorous*
  Dissolved or colloidal organic compounds containing phosphorous. primary origin is decomposition of particulate organic P.

- *Particulate inorganic phosphorous*
  These are the phosphate minerals sorbed onto sediment such as clays or complexed with solid matter (eg .calcium carbonates or iron hydroxydes).

- *Nonparticulate inorganic phosphorous*
  These are condensed phosphates.

Chapra(1997) summarized these forms of phosphate found in a body of water as follows:

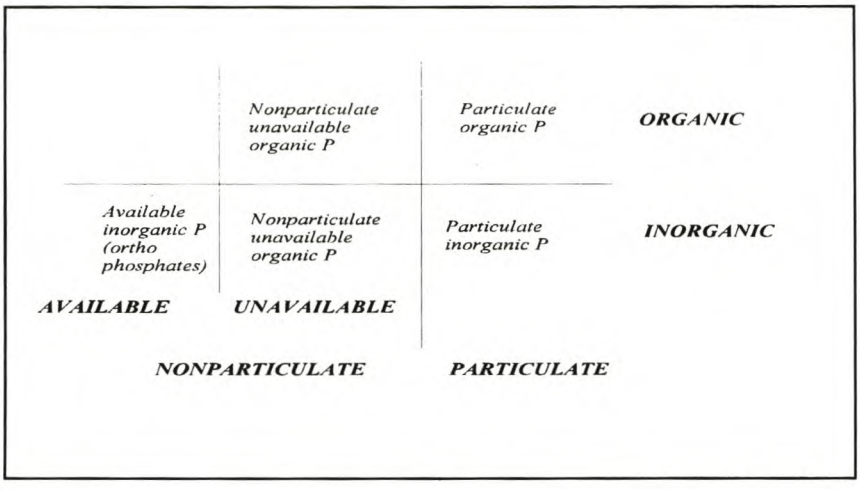

Figure 5.13: Diagram of Phosphate Constituents

The differentation into particulate and non-particulate is classified for measurement purposes. The *particulate is removed by settlement and can then be measured. The division into available* phosphorous is created especially for modelling purposes as this is the only form of phosphorus that is available for phytoplankton growth. The inorganic and organic form is often not mentioned in the literature or in water quality models but rather lumped into particulate and nonparticulate unavailable phosphates. In DUFLOW a distinction is only made between organic phosphorous and inorganic phosphorous, the organic particulate phosphates are modelled separately as the phytoplankton group.

The inorganic dissolved phosphorous (orthophosphate) is only available for algae growth and thus normally of interest. To calculate for the orthophosphates in the waterbody, DUFLOW calculates the amount by multiplying it by a factor which allows for the fraction of inorganic phosphates that have been sorbed onto sediments.

$$P_{ortho} = f_{dpano} * P_{inorg} \qquad 5.40$$

The dissolved fraction is calculated as:

$$f_{dpano} = \frac{1}{1 + K_{pip} SS} \qquad 5.41$$

K_{pip}	-	Partition constant phosphorous (about 0.01 l/mgSS)
SS	-	Suspended Solids Concentration
P_{inorg}	-	Inorganic Phosphate Concentration
P_{ortho}	-	Orthophosphate Concentration

No suspended solids data was available for the years that have been studied, thus the assumption has been made that SS=0. This means, that all the inorganic phosphate is measurable as orthophosphates.

DUFLOW models the organic and inorganic phosphate as:

Organic Phosphorous:

$$\frac{dP_{org}}{dt} = -k_{\min} \theta_{\min}^{(T-20)} P_{org} - \frac{v_{so}}{z}(1 - f_{dporg}) P_{org} + f_{porg}[k_{res} \theta_{ra}^{(T-20)} - k_{die}] a_{pc} A \qquad 5.42$$

Inorganic Phosphorous:

$$\frac{dP_{inorg}}{dt} = -\frac{v_{ss}}{z}(1 - f_{dpano}) + k_{\min} \theta_{\min}^{(T-20)} P_{org} - \mu_{\max} F_T F_N F_l a_{pc} A + (1 - f_{porg})[k_{res} \theta_{ra}^{(T-20)} + k_{die}] a_{pc} A + \frac{P_{flw}}{z} \qquad 5.43$$

where:

P_{org}	-	organic Phosphate Concentration
P_{inorg}	-	inorganic Phosphate Concentration
k_{min}	-	Mineralisation rate constant (l/day)
k_{res}	-	Respiration rate constant (l/day)
k_{die}	-	Die rate constant (l/day)
θ_{min}	-	Temperature coefficient for mineralisation
θ_{ra}	-	Temperature coefficient reaeration

T	-	Temperature (°C)
v_{so}	-	Nett settling velocity organic matter (m/day)
v_{ss}	-	Settling velocity suspended solids (m/day)
f_{dporg}	-	Fraction dissolved organic phosphorous
f_{porg}	-	Fraction algal phosphorous released as organic phosphorous
f_{dpano}	-	Fraction dissolved inorganic phosphorous
a_{pc}	-	Phosphorous to carbon ratio
A	-	Algal Biomass (mg C/l)
z	-	water depth (m)
F_T	-	Temperature dependency of algal growth rate
F_N	-	Nutrient limitation of algal growth rate
F_I	-	Light limitation of algal growth rate
μ_{max}	-	maximum specific growth rate algae

Equations 5.42 and 5.43 take into account the

- gain of organic P due to die-off of phytoplankton
- gain of inorganic P due to die-off of phytoplankton
- mineralisation of organic P to inorganic P (temperature dependent)
- settling of P
- release of inorganic P due to algal respiration
- adsorption of P to suspended solids

For more detail, the reader is referred to Thomann and Mueller (1987). As no algae, sediment or total phosphate data is available for the Berg river, equation 5.43 only remains with :

$$\frac{dPinorg}{dt} = k_{\min}\theta_{\min}^{(T-20)}P_{org}$$

The transport of the inorganic phosphate concentration (P_{inorg}) is the main influence on the simulation of the concentration, and not the process calculations.

5.4.5.3 Dissolved Oxygen (DO):

Dissolved Oxygen in the water body shows clearly the impact effluent has on the water and thus is ecologically of much interest. In a unpolluted river, the oxygen level will normally be near to the saturation level. The dissolved oxygen becomes depleted when effluents enter the river, because heterotrophic organisms (organisms that live on organic matter) deplete the oxygen in the process of breaking down the organic matter.

As the dissolved oxygen drops, reaeration from the temperature will become higher in order to reach the saturation concentration again. Reaeration is the process of oxygen adsorption from atmosphere to water. A critical level of oxygen is reached when the reaeration rate is equal to the depletion. Reaeration dominates over the decomposition after this critical point. The time series describing this process shows a 'sag' in the series before oxygen is recovered to its initial value. The equation formulated to describe the process leading to this critical oxygen value is therefore known as the dissolved oxygen "sag" equation of Streeter and Phelps (Thomann and Mueller, 1987).

In the water body, the sources of oxygen are:

- Reaeration from the atmosphere
- Photosynthetic oxygen production
- DO in incoming tributaries or effluents.

The sinks of DO are

- Oxidation of carbonaceous waste material.
- Oxidation of nitrogeneous waste material
- Oxygen demands of sediments.
- Use of oxygen for respiration for aquatic plants.

Oxygen in DUFLOW is modelled as:

$$\frac{dO_2}{dt} = k_{re}\theta_{re}^{(T-20)}(c_s - O_2) \qquad 5.44$$

where:

O_2	-	dissolved oxygen concentration (mg/l)
k_{re}	-	reaeration rate constant
θ_{re}	-	temperature coefficient reaeration
T	-	Temperature (°C)
c_s	-	saturation oxygen concentration (mg/l)

Equation 5.44 only models the reaeration.

Additional terms are included in DUFLOW in the equation describing oxygen, but have been omitted here as they will not be modelled in this particular study. The additional terms in the algorithm are:

- oxidation of carbon BOD,
- sediment oxygen demand
- Algal respiration.
- Nitrification.

Oxygen saturation concentration:

The oxygen saturation concentration is a fixed level of oxygen that is reached in the water body for a given temperature (Thomann and Mueller, 1987).

The oxygen saturation concentration is calculated using the following formulation (Hua, 1990):

$$C_s = 14.562 - 0.41022T + 0.0079910T^2 - 0.000077774T^3 \qquad 5.45$$

This oxygen saturation level is dependent on the temperature, salinity and pressure due to elevation. The above formulation makes no provision for the effects of salinity and pressure. If rivers are modelled to the estuary mouth or at high altitudes, these effects should be taken into consideration.

Formulations of the saturated oxygen concentration taking altitude and pressure into account can be read in Chapra (1997), Thomann and Mueller (1987).

Disolved oxygen deficit:

$$k_{re}\theta_{re}^{(T-20)}(c_s - O_2) \qquad 5.46$$

The DO deficit is introduced as the difference between oxygen saturation concentration (C_s) and oxygen. The reaeration coeffcient k_{re} determines the time it takes for the DO in the water body to recover to the equilibrium value. A high reaeration coefficient indicates rapid recovery, and lower reaeration coefficients slower recovery of the DO levels. The coeffcient is influenced by internal mixing and turbulence due to velocity gradients and fluctuations and by temperature.

Reaeration Rate:

Reaeration is the process of oxygen absorption from the atmosphere to the water. This is one of the main sources of oxygen in water. Much research has been performed on stream reaeration. The most commonly used formulations are summarized in Chapra(1997) and Thomann and Mueller(1987):

Table 5.4: Mathematical Models describing reaeration coefficients

Name	Year	Mathematical Model	Velocity used to develop equation (m/s)	Depth used to develop equation (m)	Comment
O'Connor-Dobbins	1956	$k_{re} = 3.93\ U^{0.5}\ H^{-1.5}$	0.15-0.49	1-30	can be applied to moderate to deep streams with moderate to low velocities (Chapra, 1997). The range of values obtained from measurements were 0.05/day to 12.2/day (Thomann and Mueller, 1987)
Churchill	1962	$k_{re} = 5.026\ U\ H^{-1.67}$	0.55-1.52	2-11	this formula applies to faster streams.
Owens and Gibbs	1964	$k_{re} = 5.32\ U^{0.67}\ H^{-1.85}$	0.03-0.55	0.4-2.4	used for shallower and fast moving streams

The O'Connor formulation is normally used in practice, but it can underestimate the reaeration coefficient for small streams. The mass transfer coefficient for oxygen (m/day) is calculated in DUFLOW using the O'Connor equation. As the depth increases, the reaeration coefficient approaches zero in the algorithm; this is in reality not the case and therefore an additional minimum value of oxygen transfer coefficient is introduced. This minimum value is normally in the range of 0.6-1 m/day. DUFLOW takes this minimum coefficient in consideration by introducing a minimum oxygen transfer coefficient (equations 5.47 and 5.48).

$$k_{re} = \frac{k_{mas}}{H} \qquad 5.47$$

$$k_{mas} = 3.93 U^{0.5} H^{-1.5} \qquad 5.48$$

or if $k_{mas} < k_{rmin}$: $k_{mas} = k_{rmin}$.

k_{rmin} is the minimum oxygen transfer coefficient (m/d) which is defined by the user.

COD:

At most South African waste water treatment plants the effluent will be tested for the Chemical Oxygen Demand (COD) rather than that the Bio-chemical Oxygen Demand (BOD) as in Europe. As DUFLOW only measures BOD_5 (5 day carbon BOD), another adjustment had to be made to allow the user to enter the COD data obtained and then converting it to oxygen. In the COD test the electron donor capacity of carbonaceous material is measured by oxidising the material by a strong oxidant in which the electron acceptor is oxygen. It is stoichiometrically known that when the equivalent of 1 g O_2 is used in the COD test, then the mass of COD oxidised is also 1g.

1g COD = 1g O_2 (UCT, 1984)

Thus, the COD value indicates how much oxygen is being used in the effluent. The term that has been introduced additionally to the oxygen algorithm is :

$$DO = DO - COD \qquad 5.49$$

If the effluent has a higher COD value than oxygen in the receiving water, it has been coded that a zero oxygen concentration will show instead of negative oxygen levels.

5.4.5.4 Total Dissolved Salts

EUTROF1 models no conservative substances, thus as with the additional coding of temperature and COD, TDS has been included as an additional variable. TDS is only dependent on the mass transport in the river and thus the term P of equation 5.17 is treated as 0. In the quality model k_0 and k_1 for the TDS are thus included as 0 (refer to equation 5.30), and only the transport is calculated.

5.4.5.5 Parameters used in water quality reactions

The parameters used in the reaction processes are the parameters that can also be adjusted by calibration. Table 6.21 in the next chapter represents the default values that DUFLOW uses.

5.5 ACCURACY AND STABILITY OF NUMERICAL MODELS

An accumulation of errors in the finite difference scheme is called *instability* (Grijsen, 1986). An implicit scheme is much more stable than an explicit scheme, because all the equations occur simultaneously and errors are not brought forward from one point to the following and then accumulate, such as is the case in an explicit scheme. Grijsen et. al. (1976, 1986) gives a comprehensive analysis of numerical errors resulting from explicit and implicit schemes and summarizes them for dynamic waves in 1986 .

The *accuracy* of the finite difference solution depends on the differential equation. *Accuracy* refers to the difference between the exact solution to the algorithms and the finite difference solution.

The stability and accuracy in implicit schemes depend largely on the implicity factor θ (refer to section 5.3.3), the time step Δt and section width Δx.

If a finite difference solution approaches the exact solution as the finite difference increment Δx approaches zero, the method is said to be *convergent* (Grijsen et. al., 1976).
Instabilities that do occur when calculating the flow and water quality can result from:

- Large differences in boundary values during the computational time step
- Errors in the initial conditions
- Large differences in the channel discretization

These instabilities can be controlled by changing the time or distance steps, or "smoothing" differences in the boundary values and cross sectional schematization.

5.6 TIME AND SPACE STEP

The space step can be defined by the user as a maximum length. The section between two nodes will then automatically be subdivided into equal space steps which are just smaller or equal than the maximum length specified by the user. The hydraulic characteristics between the space steps are interpolated. The time step is also defined by the user. It is not necessary to use the same time step for the hydrodynamic calculations as for the water quality concentrations. The results can be written at a higher time step than those specified for the calculation process. As mentioned in section 5.5, if instabilities do occur in the calculations they can be altered by changing the space and time steps. Normally, smaller values are used as the solution then becomes more accurate.

The selection of space and time step also influences the numerical dispersion and hence the stability in the computation. The numerical dispersion is introduced by discretization of the mass transport equation in the water quality calculations is expressed by (STOWA, 1998):

$$E_{num} = \frac{u}{2}(1-2\theta)u\Delta t \qquad 5.50$$

where

E_{num}	-	numerical dispersion
u	-	velocity (m/s)
Δt	-	time step (s)
θ	-	weighting used in 4 point Preissmann scheme (refer to section 5.3.3)

5.7 CONCLUSION

Hydrodynamic Model:

It has to be remembered that DUFLOW is unable to calculate supercritical flow, although the St Venant equations are able to do so. The implicit scheme shows some advantages to the explicit scheme especially with regard to schematization and calculation time. The implicit scheme is advantageous for this particular study, as it is unconditionally stable. This was of value when configuring the upper Berg River (as is explained in Chapter 6), where the slope of the river is very steep and small calculation steps are necessary.

Water Quality Model:

A limitation to the predefined eutrophication model EUTROF1 is, that no temperature, nor conservative variables such as TDS are modelled. Nevertheless, DUFLOW allows (by having an open structure) that the user can adjust the water quality model corresponding to the particular problem that needs to be studied. The water quality model should be altered to adjust the various algorithms for South African situations.

Time and Space:

As the hydrodynamic and water quality model do not necessarily need to have the same time step, the computation time can be greatly reduced by allowing the water quality time step to be higher than the hydrodynamic model. The benefit of allowing the user to define a time step is to analyse the water quality variables in the required time the chemical and biochemical processes take place . If at a later stage more data should become available, the model could run at an even finer resolution. As the numerical scheme is implicit it has major advantages regarding the space step. The user can define unequal space steps according to the problem and the output required. Also, the stability of the calculations are improved by using an implicit scheme.

5.8 REFERENCES

Amein, M., 1968. *An Implicit Method for Numerical Flood Routing.* Water Resources Research, Vol 4 No 4 pg 711-727.

Amein, M. and C.S. Fang, 1970. *Implicit Flood Routing on natural channels.* Journal of Hydraulic Engineering, ASCE. 12. pg 2481-2500.

Amein, M. and H. L. Chu,1975. *Implicit Numerical Modeling of Unsteady Flows.* Journal of Hydraulic Engineering, ASCE. Vol 101 No6. pg 717-731.

Chadwick, A. and John Morfett, 1993. *Hydraulics in Civil and Environmental Engineering.* Chapman & Hall.London. U.K.

Chapra, S. and K.H. Reckhow, 1983. *Engineering Approaches For Lake Management. Volume 2: Mechanistic Modeling.* Butterworth Publishers, U.S.

Chapra, S., 1997. *Surface Water-Quality Modeling.* Mc Graw-Hill. USA.

Day, T. J., 1975. Longitudinal Dispersion in Natural Channels. Water Resources Research 11(6):909-918.

Fischer, H.B., 1968. *Dispersion predictions in natural streams.* Journal of Sanitary Division. ASCE Vol 94 No 5. pg 927.

Fread, D.L., 1973. *Technique for Implicit Dynamic Routing in Rivers with Tributaries.* Water Resources Research. Vol 9 No 4 pg 918-927.

Ghidaoui, M.S. and B.W. Karney, 1994. *Equivalent Differential Equations in Fixed-Grid Characteristics Method.* Journal of Hydraulic Engineering. ASCE Vol 120 No 10, pg 1159-1175.

Grijsen, J.G. and C.B. Vreugdenhil, 1976. *Numerical Representation of Flood Waves in Rivers*. in Proceedings of the International Symposium on Unsteady Flow in Open Channels (ed H.S. Stephens and S.K. Hemmings)

Grijsen, J.G., 1986. Chapter 9 in *River Flow Simulation* in River Flow Modelling and Forecasting (ed D.A. Kraijenhoff and J.R. Moll). 241-272

Hesong, Hua, 1990. *Accurate Method for Calculation of Saturation DO.* Journal of Environmental Engineering. ASCE Vol 116 No 5, pg 988-990.

Jobson, H.E., 1987. *Estimation of Dispersion and First-Order Rate Coefficients by Numerical Routing*. Water Resources Research 23(1):169-180.

Jørgensen, S.E. and M.J. Gromiec, 1989. *Mathematical Submodels in Water Quality Systems. Elsevier Science Publishers*. Amsterdam. Netherland.

Katopedes, N.D., 1984. *A dissipative Galerkin scheme for open-channel flow.* Journal of Hydraulic Engineering, ASCE 110 (HY4) pg450-466

Koutitas, C.G., 1983 *Elements of Computational Hydraulics.* Pentech Press, London.

Kraijenhoff, D.A. and J.R. Moll (eds.), 1986. *River Flow Modelling and Forecasting*. D. Reidel Publishing Company.

Lai, C., 1976. *Some computational aspects of one- and two- dimensional unsteady flow simulation by the method of characteristrics.* Paper (D1-1) in Proceedings of the International Symposium on Unsteady Flow in Open Channels (ed H.S. Stephens and S.K. Hemmings)

Nordin, C.F. and B.M. Troutman, 1980. *Longitudinal Dispersion in Rivers: The Persistence of Skewness in Observed Data.* Water Resources Research, 16(1):123-128.

Rooseboom, A.; M.S. Basson; C.H. Loots; J.H. Wiggett and J. Bosman, 1986. *Road Drainage Manual.* National Transport Commission, South Africa.

Schulze, R.E., M Maharaj, SD Lynch, BJ Howe and B Melvil-Thomson, 1997. *South African Atlas of Agrohydrology and -Climatology.* Water Research Commission report TT82/96, Pretoria.

Schulze,R.E., 1995. *Hydrology and Agrohydrology : A Text to Accompany the ACRU 3.00 Agrohydrological Modelling System.* Water Research Commission, Pretoria, Report TT69/95.

Seo, I. W., 1990. *Laboratory and Numerical Investigation of Longitudinal Dispersion in Open Channels*. Water Resources Bulletin 26(5):811-822.

Stephens, H.S. and S.K. Hemmings (eds), 1976. *Proceedings of the International Symposium on Unsteady Flow in Open Channels.* BHRA. Newcastle upon Tyne, UK.

STOWA/EDS, 1998. *Duflow for Windows . Version 3.0.* EDS, Leidschendam, The Netherlands.

Taylor, 1953. *Dispersion of soluble matter in solvent flowing slowly through a tube*. Proceedings Royal Society, London Ser. A., 219

Thomann, R.V. and J.A. Mueller, 1987. *Principles of Surface Water Quality Modeling and Control.* Harper and Row, New York.

University of Cape Town, City Council of Johannesburg and National Institute for Water Research of the CSIR, 1984. *Theory, Design and Operation of Nutrient Removal Activated Sludge Processes.* prepared for Water Research Commission, Pretoria .

Valentine, E.M. and I.R. Wood,1977. *Longitudinal Dispersion with Dead Zones.* Journal of Hydraulics Division, ASCE. 103. HY9. pg 975-1990

CHAPTER 6

DATA PREPARATION AND CONFIGURATION OF THE MODEL

6.1 INTRODUCTION

This chapter presents the preparation of data and the configuration of the Berg River in the DUFLOW Modelling System (DMS). Referring to section 2.3.3 the configuration of the model is dependent on the complexity and the degree of resolution as well as accuracy required.

The first stage of developing the model was the data gathering and the preparation of the data according to the format that DUFLOW requires, these include the geometrical profile of the river, the boundary conditions (i.e. the flow hydrographs), the data for the various structures and also the water quality data that will be used in the model.

The chapter is divided into two main sections, the first section describing the configuration and data preparation for the hydraulic calculations, while the second section reports on the water quality data preparation and configuration.

6.2 HYDRODYNAMIC SCHEMATIZATION

6.2.1 Flow Data Preparation

The daily flow data was obtained from DWAF and modified into a format which is required by DUFLOW. Only the recent flow data was considered, i.e. measurements made from 1990 to 1998. Additional years could be added to the files, but the recent flow data set can be regarded as very representative. This would also slow down the model, due to extensive data output files. For more information on flow data prior to this period, an extensive review can be found in the Western Cape System Analysis (WCSA) report on the hydrology of the Berg River (DWAF(a), 1992).

Figures 6.1 and 6.2 show the inflow hydrographs of the major flow-contributing tributaries, for low flow period and also for the high flow period of the configuration years. Figure 3.1 already represented the gauging stations in the Berg River catchment.

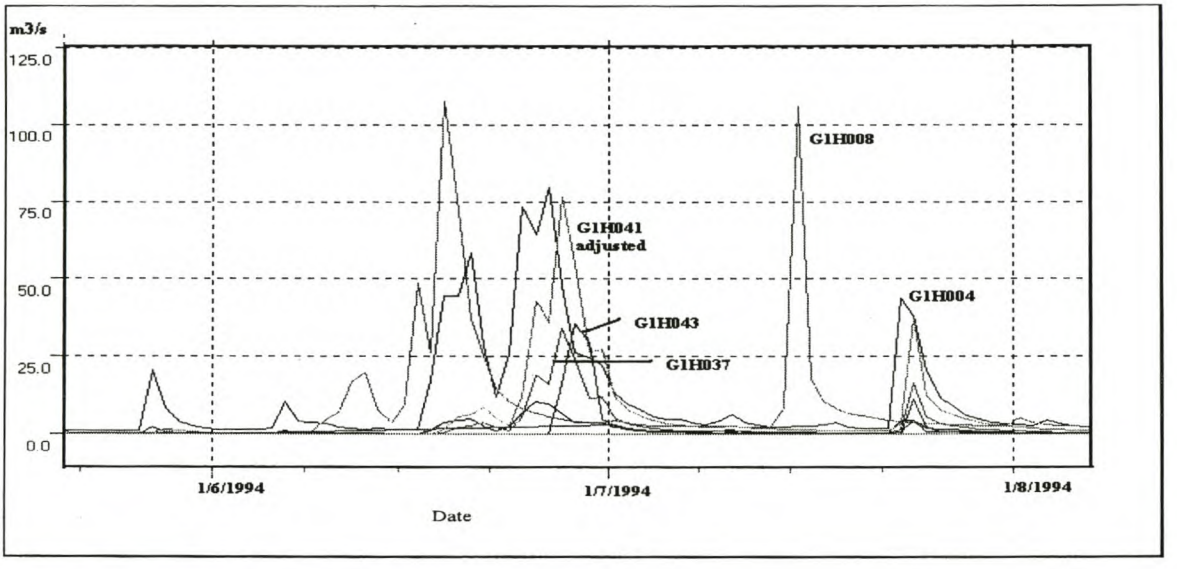

Figure 6.1: Incoming high-flow from tributaries

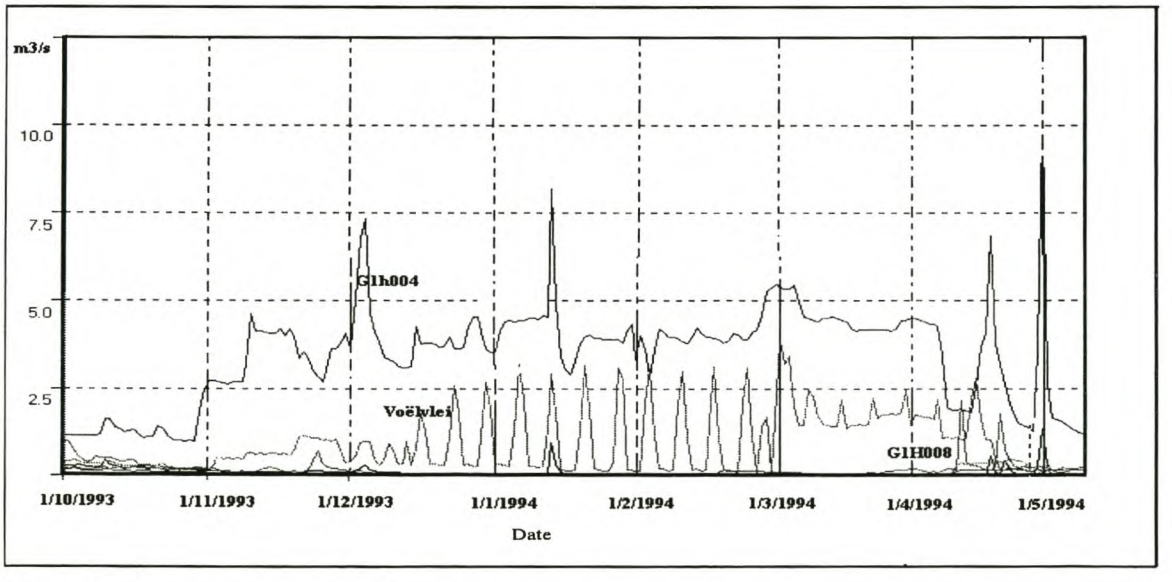

Figure 6.2: Incoming low-flow from tributaries

6.2.2 Nodes and Boundary Conditions

The two external nodes are upstream at upper Berg (G1H004) and downstream at Misverstand Dam (G1R003). Three internal nodes were also included in the schematization at the gauging stations G1H020 (Dal Josafat), G1H036 (Hermon) and G1H013 (Drie Heuwels). The total length of the river is approximately 149 km. The river length between the two external boundaries was divided into four reaches, which can be seen in Table 6.1.

Table 6.1 Reaches of the main stem Berg River

Reach	Beginning node	End node	Length (km)	Average Slope (%)
1	G1H004	G1H020	31	0.35
2	G1H020	G1H036	41	0.095
3	G1H036	G1H013	57	0.055
4	G1H013	G1R003	20.5	0.05

One boundary condition is needed at each end point of the network schematization (refer to section 5.3.4). The upstream boundary condition at G1H004 is the inflow hydrograph (see Figure 6.3), while at G1R003 a stage-discharge rating curve has been specified as the end boundary condition (see Figure 6.4). The rating curves for all the weirs were obtained from DWAF.

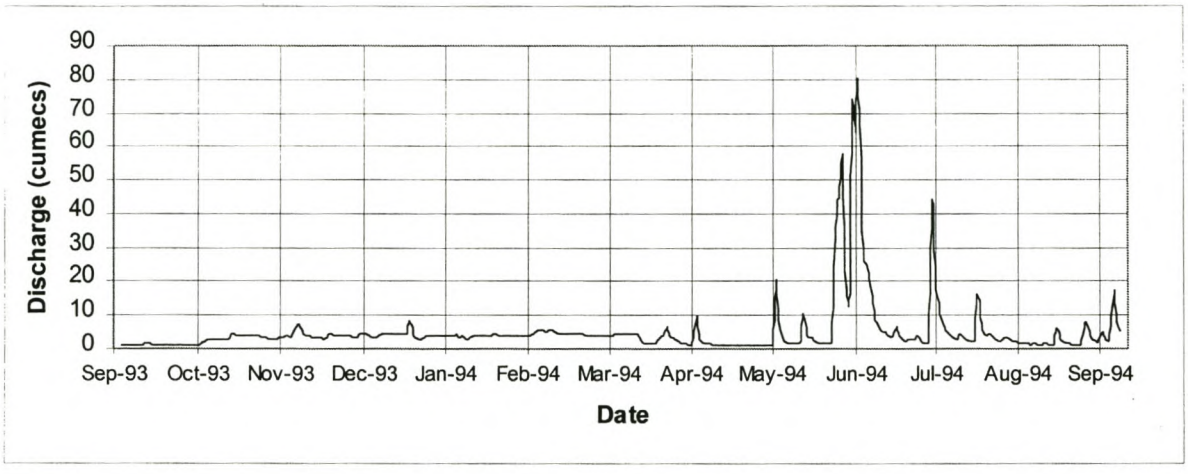

Figure 6.3: Inflow Hydrograph at G1H004

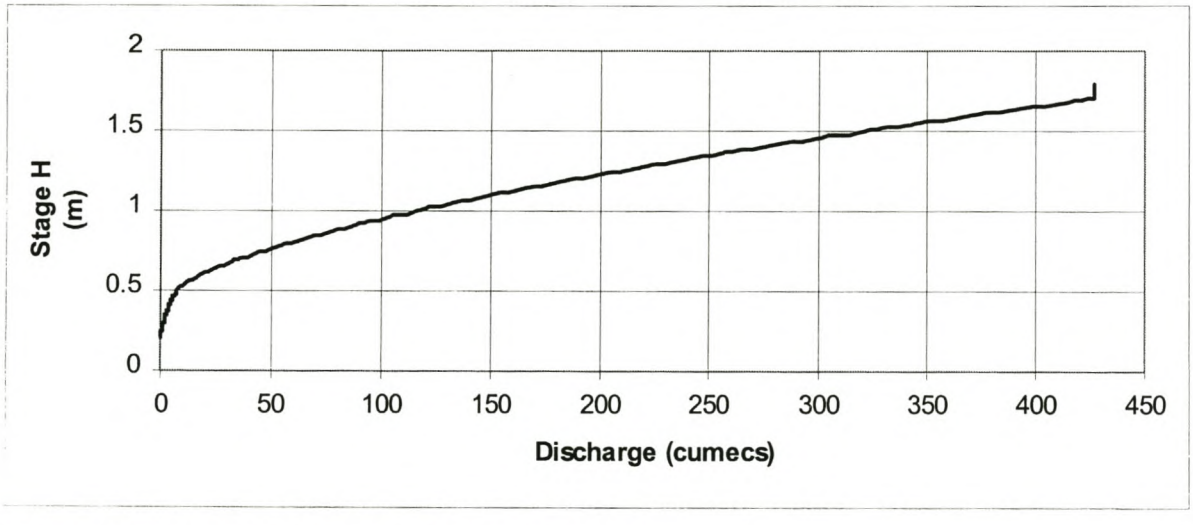

Figure 6.4: Stage-Discharge Relationship at G1R003

6.2.3 Cross-sections

The sources in Table 6.2 were able to provide detailed cross-sections for the Berg River.

Table 6.2: Sources of cross-sections provided in the Berg River

		Source	Comments
1	Skuifraam Dam Tailwater Cross–sections	DWAF	17 sections at 300m interval
2	Skuifraam Dam Supplement Scheme	Ninham Shand	1:2000m coverage
3	Paarl Cross-sections	Paarl Municipality	23 cross sections taken through Paarl
4	1:50 year Wellington Flood Study	Ninham Shand	1:2000m coverage
5	detailed Surveys	Robin Pharaoh and Associates/Satmap Solutions CC	26 detailed surveys from G1H004 to Misverstand at selected sites
6	Photosurveys	Photosurveys	67 photosurveys from G1H004 to Misverstand at selected sites
7	Main River Gauging Stations	DWAF	Local datum

A total of 108 cross-sections were used for configuration of the model. Some of the cross-sections were not surveyed beyond the banks and information on the characteristics of the flood plain were obtained from orthophotos (1:10 000).

The cross-sections were represented in DUFLOW with the width as a function of height (see section 5.3.5). Enough points had to be defined in order to represent the cross section as accurately as possible. The cross-sections are entered as symmetrical sections, but it appears that making non-symmetrical

profiles symmetric only causes a small error in the calculations (Grijsen, 1986). Most of the parameters used in the calculation of the water surface is dependent on the geometric parameters (surface area, roughness, width) etc. Therefore, it should be important to define the cross-sections with sufficient accuracy, and thus the widths were entered at height differences of 0.2m.

A minimum of one cross-section has to be defined per reach and an unlimited number of cross-sections may be inserted between two nodes. If the space step defined is smaller than the distance between two cross -sections then the hydraulic parameters, i.e. hydraulic radius, surface area which are calculated from the cross-sections, are interpolated linearly at the various points defined by the space step. Traver and Miller (1994) reviewed the effect interpolation has on the calculated water surface profile, as it is the most common practice in computer models, and concluded that the error introduced when interpolating the hydraulic parameters is insignificant compared with errors introduced from surveys.

Information of the cross-sections had to be provided manually, unfortunately there was no option to import or export the data as text files.

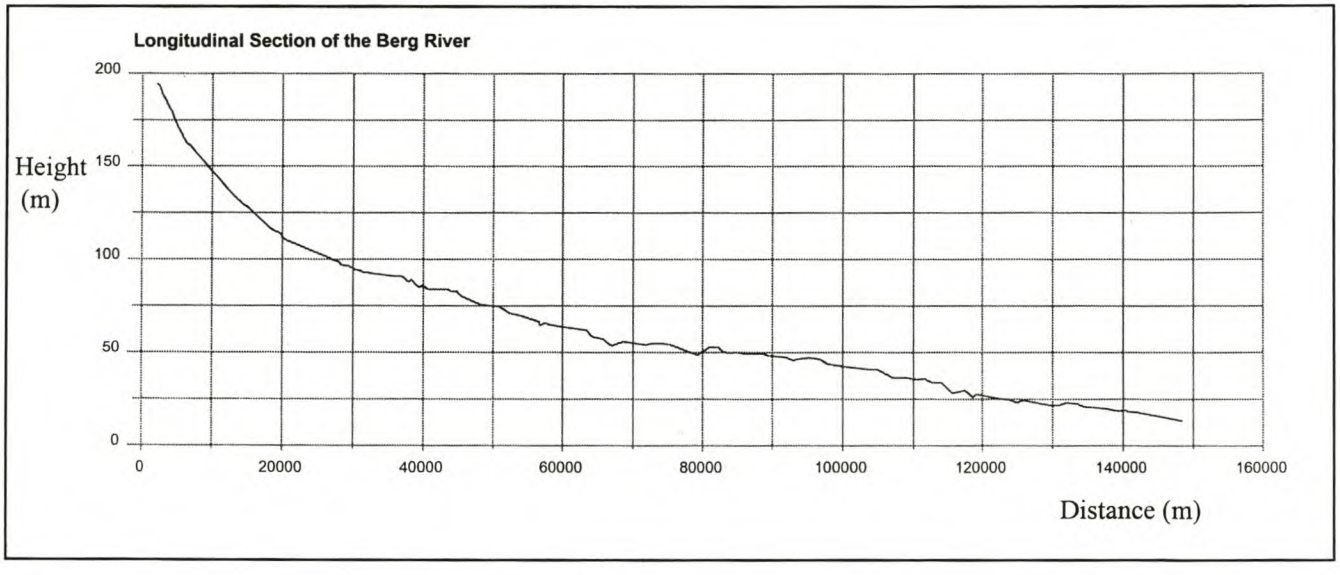

Figure 6.5: Longitudinal profile from G1H004 to Misverstand.

6.2.4 Structures

6.2.4.1 Weirs

Details for the weirs were obtained from plans which were made available by DWAF (Western Cape Regional Office). The height and the width of the weir were entered into the weir dialog box of DUFLOW. Trigger Levels have been specified for the different weirs, to take the multiple notches with increasing level into account (refer to 5.3.6 for details about trigger levels).

Table 6.3: Details of weirs

Gauging Station No	Weir Name	Latitude	Longitude	Description
G1H004	Driefontein	33°55' 36"	19°03' 41"	Crump weir was constructed 1980 (DWAF(c),1994); was originally a sharp crested weir.
G1H020	Noorder Paarl	33°42' 29"	18°56' 29"	The weir is situated just upstream of the Dal Josafat Bridge in Paarl. G1H020 consists of two sharp crested weirs and a hydro flume.
G1H036	Vleesbank	33°26' 06"	18°57' 25"	G1H036 has been built below Hermon Bridge, it consists of stepped crump weirs.
G1H013	Drieheuwels	33°07' 57"	18°51' 45"	Stepped crump weirs with a hydro flume.

6.2.4.2 Bridges

A total of 13 bridges were identified along the main stem of the Berg River for the river reach modelled. The information on the various bridges was available from Road Transport and Paarl Municipality. Table 6.4 describes the details of the bridges modelled. Information about the bridges needed for DUFLOW are: width of the bridge, the vertical clearance and the reduced level of the *top* of the bridge. For more complex cross-sections at the bridges, the structure control was used (section 5.3.6), by changing the width for various trigger levels. The information was entered into the DUFLOW dialog box manually.

From the 13 bridges identified, only 7 were modelled. For some of the bridges no information was available, while for Dal Josafat, Hermon and Jim Fouche Bridge the following reasons applied:

- the numerical scheme becomes easily unstable when the distance between two structures is too small. This was the case for Dal Josafat and G1H020 weir. Similarly, for Hermon Bridge the decision had to be made to either model the weir G1H036 or the bridge as the model becomes unstable when calculating for both structures simultaneously.
- In the upper reaches the slope is quite steep (approximately 0.35%) and Jim Fouche Bridge lies exactly between two incoming tributaries, Franschhoek River and Wemmers River, which lie only about 800 m from each other. The model experienced problems when this bridge was configured. In other circumstances this should not have been a problem (i.e. much shorter reach where even smaller space steps could be defined).

Where a structure is not modelled for practical reasons, its effect can be approximately retained by increasing the roughness coefficient in the specific reach.

Table 6.4: Details of Bridges

Name	Nr	Approximate Distance from G1H004 (km)
Jim Fouche Bridge	B5919, MR 191	6.5
N1	B4334	24.0
Market Street Bridge	B2994	26.9
Lady Grey Street Bridge	B0981	27.8
Rembrandt Bridge	N/A	28.0
Osbosch Street Bridge	N/A	29.6
Dal Josafat	N/A	30.5
Oudebrug	B4902, MR 27	38.1
Lady Loch Bridge	B3007, MR 222	41.7
Vogelgesang	N/A	48.2
Vleesbank	B4545A	72.0
Sonkwasdrift	B5792, DR 1154	92.2
Skoenmakersfontein	B5730, DR1161	107.3

6.2.5 Tributaries

The tributaries were entered at schematization points (see section 5.2.1 for definition on schematization points) that allow the user to insert the hydrographs as time series. The inflowing hydrographs were depicted in Figures 6.1 and 6.2, while Figure 3.1 showed the gauging stations in the Berg River catchment.

Table 6.5: Major Tributaries in the Berg River Catchment

Flow Gauge	River	Place name
G1H003	Franschhoek	La Provence
G1H019	Banhoek	Bosmanshoek
G1R002	Wemmers	Wemmershoek
G1H041	Kompagnjies	De Eikeboomen
G1H039	Doring	/
G1H043	Sandspruit	Vrisgewaagd
G1H008	Klein Berg	Mountain View
G1H035	Matjies	/
G1H034	Holle	/

6.2.6 Roughness Coefficient

The roughness can be expressed as the inverse of the Manning roughness coefficient n or by the Chezy coefficient C. DUFLOW gives the user the option to change the roughness at every cross-section and also at every point defined in the cross-section at the relevant sides of the section. This allows the section to have a different roughness at 0.5 m depth than the roughness at 1m. The sensitivity of the roughness coefficient has been investigated for calibration purposes; this is discussed in section 7.7. The initial roughness coefficients were based on Figure 3.8 in the NTC Road Drainage Manual (Rooseboom et. al., 1983).

6.2.7. Abstractions and Return Flows

6.2.7.1 Paarl Abstractions:

The municipality of Paarl receives water mainly from the Wemmershoek Dam, but additional water is abstracted from the river as the water from Wemmershoek Dam is costly (Pers. Com. A. Kowalewski, Paarl Municipality).

The abstraction data were made available as monthly average flows. Table 6.6 indicates that there is a 100% decrease in the winter months from the period before 1990 to 1999, while abstractions in the summer months has increased (310% in November). It has been assumed that the abstractions have increased linearly in the years and the calculated figures for 1993/1994 have been inserted into the model.

Table 6.6: Abstraction data of Paarl Municipality

	1980 to 1988 (DWAF(a), 1992)	Recent 1998/1999	% increase
	Monthly Average (Mm^3)	Monthly Average (Mm^3)	
October	0.04	0.088	120
November	0.03	0.096	310
December	0.04	0.11	175
January	0.07	0.086	23
February	0.06	0.164	173
March	0.07	0.19	171
April	0.07	0.13	86
May	0.04	0.017	-57
June	0.06	0	-100
July	0.05	0	-100
August	0.06	0.034	-43
September	0.06	0.125	108
Total	**0.6**	**1.04**	**73**

6.2.7.2 Other Industrial Abstractions:

'*Water Quality in the Berg River: A Situation Analysis*' (DWAF(b), 1993) describes industries which utilise water from the Berg River with little or no pretreatment. None of these industries reported, occur in the reach considered for this study and therefore the industrial abstractions have no effect on the flow modelled. The industries mentioned are : PPC De Hoek factory, which abstracts just below Misverstand weir; the Chempos factory, which abstracts water at the Old Berg River pumping station (G1H023) and the Dewdale trout farm which abstracts just upstream of G1H004 (approximately 2.5 km).

6.2.7.3 Irrigation:

There are 14 irrigation boards in the Berg River catchment area (Pers. Com., W. Enright, 2000). These are:

- La Motte
- Dal Josafat
- Palmiet River
- Kromme River
- Kleinberg River
- Twenty Four Rivers
- Berg River
- Simonsberg
- Suid-Agter-Paarl
- Noord-Agter-Paarl
- Perdeberg
- Riebeek Kasteel
- Riebeek Wes
- Lower Berg River

Information was made available by some of the irrigation boards for 1999. This information on abstractions was:

- West Coast District Council - 10 Mm^3/annum
- Perdeberg Irrigation Board - 6.25 Mm^3/annum
- Simondium Irrigation Board - 1.04 Mm^3/annum
- Simonsberg Irrigation Board - only after 1997

West Coast District Council is not an irrigation board, but uses the water for urban use. The West Coast District Council abstracts water at two places: at Voëlvlei Dam and at Misverstand Dam.

For the irrigation boards where no information was available, a rate of 7500m^3/ha/annum was applied to the scheduled areas. The monthly distribution of water abstracted was adjusted by following the seasonal distribution of the evaporation rate.
The irrigation demand was calculated as follows:

monthly crop factor * mean monthly A-Pan evaporation - effective rain/total rain ratio (0.7) * mean monthly precipitation

Following above mentioned calculation procedure, the water demands calculated for the irrigation boards are :

- Riebeek Kasteel - 1.1 Mm^3/annum
- Suid Agter Paarl - 2.7 Mm^3/annum
- Noord Agter Paarl - 2.0 Mm^3/annum

The total volume of abstractions was calculated to be 42 Mm^3/a for 1999. This present figure shows a rising trend when compared to the abstraction value of 35 Mm^3/a calculated for the WCSA in 1995 (DWAF(d), 1995). This rising trend is further illustrated by the '*Water Quality in the Berg River: A Situation Analysis*' (DWAF(b), 1993) that calculated abstractions to be 21.7 Mm^3/a from G1H004 to Sonkwasdrift.

Table 6.7: Abstractions in the Berg River for 1993/1994 (Mm^3)

	Oct	**Nov**	**Dec**	**Jan**	**Feb**	**Mar**	**Apr**	**May**	**June**	**July**	**Aug**	**Sept**
Mm^3	0.94	4.64	8.3	8.6	7.6	6.4	2.5	0.8	0.65	0.45	0.64	0.62

6.2.7.4 Return Flows:

Sewage Return Flows from Paarl are monitored by the Paarl municipality. The Paarl Sewage Treatment Works (STW) is the most significant effluent producer in the whole of the Berg River catchment. Table 6.8 shows a comparison of the volume discharged into the river at the time of the WCSA (DWAF(a), 1992) and the most recent discharges which have been made available by Paarl Municipality.

Table 6.8: Comparison of Return Flows in years at Paarl STW

	WCSA (DWAF(a), 1992)	**Recent 1997/1998**	**% increase**
	Ave (Mm^3)	**Ave (Mm^3)**	
October	0.6	0.885	47.5
November	0.5	0.897	79.4
December	0.5	0.695	39
January	0.5	0.751	50
February	0.5	0.62	24
March	0.6	0.739	23
April	0.5	0.795	59
May	0.6	0.974	62
June	0.7	1.03	43
July	0.8	1.4	75
August	0.8	1.15	44
September	0.7	0.9	28.6
Total	**7.3**	**10.84**	**48.5**

Sewage return flows from Wellington are not monitored, as the water is discharged into evaporation pans.

6.2.8 Evaporation Losses

Records of average daily evaporation was made available by Western Cape Department of Agriculture, Elsenburg.

As no function is incorporated in the DUFLOW model to calculate the evaporation loss rate relative to the function of surface area at the instant of time, the average evaporation loss was modelled as abstraction points.

The loss rate was calculated as:

Loss (m^3/s) = average width(m) * length between sections (m) * evaporation loss rate (m/s)

The evaporation rate was divided into several abstraction points in relative proportion to the surface areas that each abstraction/schematization point represented, in order to achieve even distribution of the evaporation along the river. This also ensured that a smoother concentration profile was calculated; thus the impact of the evaporation on the water quality was shown fairly realistically. This approach to the calculation of evaporation losses is simplistic, but for purposes of assessing the simulation model it is adequate. Studies on evaporation losses have been done on the Orange River, and the reader is referred to McKenzie and Craig (1997) for different methods of estimating potential evaporation from a water surface.

The evaporation rates of four meteorological stations have been applied to the Berg River model. Table 6.9 indicates average evaporation losses in mm/month for Bien Donne, while the average evaporation rates are summarized for the different meteorological stations in Table 6.20 of section 6.3.4.

Table 6.9: Evaporation Losses (mm/month) at Bien Donne for the year 1993/1994

	Oct	Nov	Dec	Jan	Feb	Mar	Apr	May	June	July	Aug	Sept
Mm^3	193	250	300	327	286	207	142	56	32	47	83	101

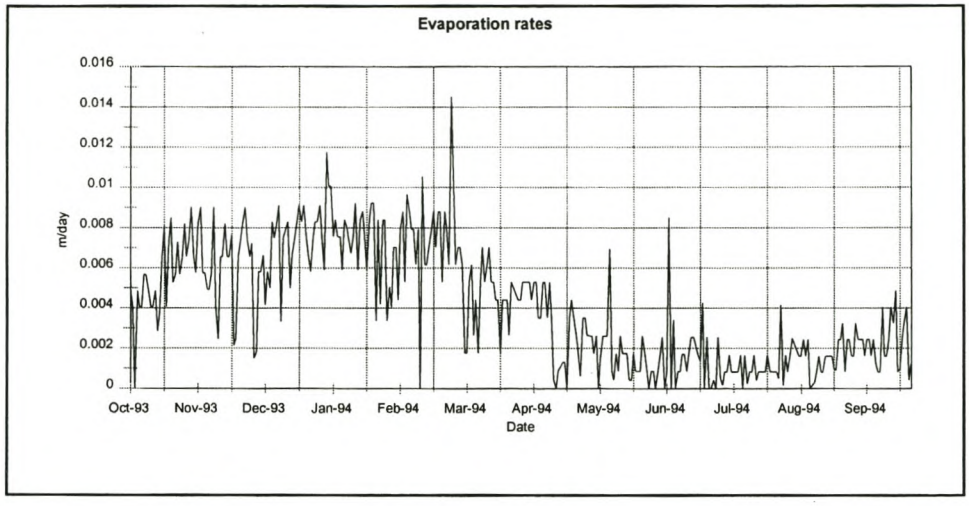

Figure 6.6: Graphical Representation of Evaporation Rates at Bien Donne

6.2.9 Other Losses

Other losses that have not been included in this study are the losses due to invading alien vegetation along the banks of the river. The impact of these losses needs to be studied and included in the model should the model be used as an operational tool. For more information the reader is referred to LeMaitre et. al. (2000) and Versfeld et. al. (1998).

6.3 WATER QUALITY CONFIGURATION

6.3.1 Water Quality Data Preparation

For the water quality program daily concentrations for the variables of concern are needed in the form of continuous time series. As the water quality data obtained by DWAF is measured mostly on a two weekly basis, the daily sequences have to be developed by 'infilling'. Table 6.10 shows the infilling techniques that have finally been used to infill the water quality time series.

Table 6.10: Infilling of water quality variables

Parameter with missing data	Parameter used for infilling	Infilling technique
Log TDS	Log Flow	Moving-Regression
Log PO_4	Log Flow	Moving-Regression
Water Temperature	Date	Harmonic Function

6.3.1.1 TDS and PO_4 Infilling

Two methods were investigated for this study, before deciding on a certain infilling method:

- The program **FLUX** (Walker, 1987)
- A **moving-regression** method (DWAF(e), 1998)

These two methods are described in this section along with the results obtained from the infilling method.

Flux:

Description:

Flux interprets water quality information and flow information from grab samples over the complete

flow record between two dates.

There are five different equations that can be used to calculate the concentrations (refer to Table 6.11). Flux has an option to divide the flow and concentration data into different data groups (stratification) and calculate loadings for the different groups using the calculation method chosen. The groups can be defined based upon flow, time or any other variable that seems to influence the load dynamics.

Discussion:

Flux seemed suitable for calculating monthly and yearly loads. For filling in daily concentration values the model-selected two regression functions were used (refer to Table 6.11). The results were not satisfactory as the daily concentrations would remain consistent over a certain period, as it is stratified according to flow. The method seemed to calculate a single concentration for the range of flows entered and thus the concentrations do not differ for every single value of flow, but rather displayed 5 different concentration values for the 5 ranges of flow stratified. The method could work well if very short periods of samples are entered and the flow does not vary as much.

Table 6.11: Calculation Methods for Flux

METHOD	DESCRIPTION	EQUATION
Direct Loading	The loading does not vary with flow, as the flux is only dependent on the mean of the grab samples. This method is suitable if the concentration tends to be inversely related to the flow.	W1=Mean(w)
Flow Weighted Concentration (Ratio Estimate)	The loading is estimated on the flow weighted average concentration times the mean flow over the averaging period. This method performs best when flow and concentration are unrelated.	$W2=\frac{Mean(w)Mean(Q)}{Mean(q)}$
Modified Ratio Estimate	Multiplying it by a factor to adjust to situations where concentration does vary with flow modifies the flow-weighted concentration.	$W3=W2\ \frac{(1+F_{wq}/n)}{(1+F_q/n)}$
Regression, First Order	The regression works well for log(c) versus log (q) slopes. The relationship between flow and concentration should be linear.	$W4=Mean(w)\ [\ Mean(Q)/Mean(q)]^{b+1}$
Regression, Second Order	The regression of first order is modified by a factor that is designed to account for differences in variance between the sampled and the total flow distributions.	$W5=W4\ \frac{(1+r\,F_Q)}{(1+r\,F_q)}$

Where

c_i	=	measured concentration in sample i (mg/m^3)
q_i	=	measured flow during sample i (hm^3/yr)
b	=	slope of log (c) versus log (q) regression
w_i	=	measured flux during sample i = qi ci (kg/yr)
w_{qi}	=	product of flux and flow for sample i (kg * hm^3/yr^2)
F_{wq}	=	Var(wq)/[Mean(w)Mean(q)]
F_q	=	Var(q)/[Mean(q) Mean(q)]
F_Q	=	Var(Q)/[Mean(Q)Mean(Q)]
Q_j	=	mean flow on day j (hm^3/yr)
n	=	number of samples (i)
N	=	number of daily flows (j)
W_m	=	estimated mean flux over N days, method m (kg/yr)
V_m	=	variance of estimated mean flux, method m $(kg/yr)^2$
r	=	0.5 b(b+1)
Mean(x)	=	mean of vector x
Var(x)	=	variance of vector x

(Walker, 1987)

Moving-Regression

Description:

The relationship between concentration and flow can be described as:

$C = aQ^b$

$\text{Log } C = \log a + b \log Q$

where

C	concentration of the water quality variable
Q	daily flow
a,b	regression coefficients

Studies of the relationship between flow and the concentration constituent have revealed that a single prescribed value for each of the regression coefficients a and b does not adequately describe the relationship between concentration and flow over the full range of most flow regimes in South Africa (DWAF(e), 1998). The regression coefficients vary because of different factors that influence the relationship between flow and the concentration such as variable loadings from point sources, or whether the sample has been taken during a rising (more surface runoff) or a falling hydrograph (more groundwater). A moving regression method was developed for the Amatole Water Resource System Analysis (DWAF(e), 1998), which takes these variations into account. The method looks at 5 to 9 sequential concentration values at a time (set by the user), calculates the corresponding regression coefficient a and b, predicts the intermediate values, and then takes the next block of values by moving one sample forward; thus allowing the variation in flow conditions to change the regression coefficients at every single value. It has been found that for most variables about 8 values at a time are adequate to describe the relationship between flow and the concentration. This represents about two months of weekly grab-samples. By increasing the number of values the calculated values show a more average trend and do not take sudden changes accurately into account. Less than six values are too few to provide an adequate regression fit. The numbers of variables were adjusted for the various stations to obtain the best correlation possible.

Discussion:

When the intervals between observed values are long (>14 days), the regression does not show satisfactory results. This is due to the strong seasonality of the concentration variables. The various results of this method for total dissolved salts (TDS) and phosphates are described in the next section. These water quality variables were infilled for all the catchments where flow and water quality data was available. Complications were experienced at following stations:

- G1R002 Wemmershoek Dam subcatchment

  The water quality grab samples are taken at the dam wall, and are therefore affected by the storage in the Wemmershoek Dam. The observed flow, used for the regression infilling method, is measured at the inflow into the dam. As there is no water quality data taken at the same location as the flow is measured, the water quality grab samples taken in the dam are the only indication of the expected water quality.

- G1H028/G1H029

Only intermittent flow data was available, as portions of the flows are diverted to Voëlvlei Dam.

Results of Infilling Method

TDS

The moving regression works well for the TDS infilling as can be seen from the figures at the end of this chapter (Figures 6.8 to 6.19). For zero flows the regression is interrupted and produces zero concentrations. From the statistics (refer to Table 6.12) it is illustrated that the difference in means of the observed and calculated values are low (all below 10%).

Phosphate as PO_4

One can see that a similar pattern occurs at low flow as for TDS infilling. Some stations show a better relationship between flow and phosphates (refer to Table 6.13 and Figures 6.20-6.31 at the end of this chapter). The errors between the measured and calculated values are very varied but after 1990 it seems that the differences are all below 20%, except for G1H003.

It has to be borne in mind that only about 8 grab samples values are taken at a time. If the variance is higher between the grab samples, the difference between the estimated values and the grab sample will be greater. As the method is based on a regression equation, the concentration maxima and minima may be over or underestimated. This is illustrated in Table 6.12 and 6.13, where the percentage difference in means show systematically negative values for all stations. Referring to the Figures (e.g. Figure 6.17) it is further illustrated that the infilling method is unable to reproduce the lower and upper extreme water quality values that have been sampled.

NOTE: *Certain statistical equations have been used to determine the accuracy of fit between the infilled and the measured data. These equations are described along with the calibration description in section 7.1, as the statistical equations (also known as objective functions) are used extensively in the calibration process.*

Table 6.12: Statistics of TDS Infilling

Gauging Station	No of Samples	Mean Concentration (infilled)	Mean Concentration (Grab Samples)	% error in mean	Std. Dev (infilled)	Std. Dev (grab samples)	% differ. in std deviation	R^2 (Loads)
Main Stream:								
G1H004	174	32	33	-2.8	6.9	10.3	-33	0.93
G1H020	303	59	61	-4	9.54	18.6	-49	0.98
G1H036	251	127	128	-1.1	23.4	35	-33	0.87
G1H013	271	151	153	-1	34.7	48.5	-28	0.89
G1R003	333	211	217	-2.8	65.2	78.5	-17	0.93
Tributaries:								
G1H003	163	82	83	-1	24.9	28.54	-13	0.98
G1R002	34	25	25	-1.4	1.59	4.14	-62	0.99
G1H019	277	39	40	-2.3	7.8	10.5	-26	0.93
G1H037	65	95	101	-5.5	26.4	31.4	-16	0.95
G1H039	130	2648	2712	-2.4	735	897.5	-18	0.97
G1H041	234	160	175	-8.5	51.5	88	-41	0.97
G1H008	300	113	118	-4	29.4	40.4	-27	0.99
G1H065	491	67	67	-0.2	8.4	10.2	-18	0.99
G1H043	106	4639	4665	-0.57	1263	1341	-6	0.99
G1H035	168	1637	1681	-2.6	648.7	840.5	-23	0.91
G1H034	315	6310	6253	0.9	2220	2297	-3	0.91

Table 6.13: Statistics of Phosphate as PO_4 Infilling

Gauging Station	No of Samples	Mean Concentration (infilled)	Mean Concentration (Grab Samples)	% error in mean	Std. Dev (infilled)	Std. Dev (grab samples)	% differ. in std deviation	R^2 (Loads)
Main Stream:								
G1H004	174	0.019	0.02	-9	0.0077	0.012	-35.8	0.80
G1H020	302	0.023	0.027	-16	0.013	0.047	-72.3	0.84
G1H036	252	0.053	0.059	-10	0.03	0.049	-38.8	0.88
G1H013	297	0.023	0.025	-7	0.016	0.021	-23.8	0.89
G1R003	354	0.024	0.025	-5.5	0.012	0.017	-29.4	0.92
Tributaries:								
G1H003	160	0.025	0.034	-25	0.0164	0.071	-77.0	0.79
G1R002	34	0.009	0.01	-10.8	0.003	0.008	-62.5	0.97
G1H019	267	0.012	0.013	-8.3	0.005	0.008	-37.5	0.9
G1H037	72	0.027	0.0277	-3.5	0.01	0.015	-33.3	0.87
G1H039	128	0.3	0.33	-9.7	0.16	0.212	-24.5	0.96
G1H041	234	0.02	0.024	-15	0.0099	0.023	-56.9	0.91
G1H008	294	0.016	0.017	-6.8	0.0087	0.011	-20.9	0.96
G1H065	506	0.013	0.014	-5.4	0.0057	0.0078	-26.9	0.86
G1H043	101	0.033	0.036	-7.8	0.012	0.019	-36.8	0.84
G1H035	164	0.038	0.046	-17	0.026	0.043	-39.5	0.95
G1H034	317	0.147	0.176	-16.5	0.15	0.18	-16.6	0.62

6.3.1.2 Temperature Infilling

Temperature was also measured on a two weekly basis. The air temperature was made available by Western Cape Department of Agriculture, Elsenburg; while the water temperature data was available from DWAF. Some stations (e.g. G1H004, G1H003 and G1H019) have only temperature measurements up to 1990, it was assumed that the missing temperature will follow the same function as in the years prior 1990.

Three methods were examined in order to determine the best suited function for the infilling of temperature:

1) Regression with the Air Temperature

Air Temperature Data was obtained by Western Cape Department of Agriculture, Elsenburg. The air temperature measurements of the catchment at stations near to the gauging stations of the river were compared to the water temperature and both follow similar harmonic functions. However, at most of the stations the measurements of the two temperature stations did not correspond in years, and therefore a regression between the air temperature and water temperature could not be performed for the majority of the stations.

For station G1H020 and Nederburg the sampling years coincided and a regression of grab sample values was attempted. A correlation coefficient of 0.81 was achieved.

2) Fourier Series

Forecasting and prediction of water temperature is often completed by approximating the daily average water temperature using a regression fit based on the Fourier series approximation (Long, 1976; Thomann 1967).

The regression analysis uses observation of a time series $X(t_i)$, i= 1,2,...n and assumes

$$F(t_i)=A_0+2\sum_{M}^{k=1} C_k \sin(2\pi k t_i+\Phi_k)$$

where

$$C_k=(A_k^2+B_k^2)^{1/2}$$

and

$$\Phi_k=\arctan\frac{A_k}{B_k}$$

and the Fourier coefficients A_k and B_k are obtained by a least squares fit of the data to the kth harmonic component (which in our case is 0.5 to obtain the annual cycle of temperature variations):

$$A_0=1/n\sum_{n}^{i=1} X(t_i)$$

$$A_k=1/n\sum_{n}^{i=1} X(t_i)\cos(2\pi k t_i)$$

and

$$B_k=1/n\sum_{n}^{i=1} X(t_i)\sin(2\pi k t_i)$$

3) Simple Harmonic Function

For most practical purposes a simple harmonic function is sufficient to describe the seasonal variation for temperature (Sanders et al., 1980). The function applied is:

$$y_t=A(\cos\omega t+B)$$

yt	=	value of function at time t
ω	=	360 degree/nr of samples per year
A,B	=	least squares fitted constants (see above)

Figures 6.32 to 6.42 at the end of this chapter displays the comparison of infilled and measured temperature values. This prediction of temperatures is a simplification of the above mentioned Fourier series, yet it seems to be sufficient to predict the temperatures reasonably accurately. Table 6.15 summarizes the coefficient of determination (R^2) and the errors for every year infilled for the various stations.

Table 6.14: Details of Temperature Infilling

Station	Years of Data	Nr of Samples	Function
G1H004	1987-1990	167	6.2 cos (x-31450) + 16.5
G1H003	1985-1990	167	6.25 cos (x-31450) + 18.3
G1H019	1980-1990	315	4.15 cos (x-31428) + 15
G1H036	1983-1998	570	6.5 cos (x-32897) + 18.8
G1H008	1993-1997	173	7 cos (x-32890) + 18
G1H039	1983-1997	274	7 cos (x-32175) + 18.8
G1H041	1980-1994	350	7 cos (x-32890) + 18
G1H013	1980-1997	627	7.5 cos (x-31450) + 19.3

Table 6.15: Statistics of Temperature Infilling

Station	Summer Mean Infilled (Oct-March)	Winter Mean Infilled (Apr-Sept)	Summer Mean Measured (Oct-March)	Winter Mean Measured (Apr-Sept)	Summer Mean Error	Winter Mean Error	(R^2)
G1H004	20.19	12.87	20.23	13.33	-0.19	-3.45	0.75
G1H003	21.67	14.52	20.58	14.1	5.3	2.98	0.67
G1H019	17.21	14.17	17.17	14.24	0.2	-0.5	0.7
G1H036	23.31	13.66	22.48	14.55	3.7	-6.1	0.63
G1H008	21.13	12.78	20.57	13.77	2.7	-7.2	0.00
G1H039	22.3	15.17	23.04	15.24	-3.2	-0.5	0.75
G1H041	22.23	14.15	21.69	14.44	2.5	-2	0.75
G1H013	23.4	15.3	23.6	14.6	-0.85	4.8	0.72

6.3.1.3 Oxygen Infilling

No oxygen data is available for the Berg River, but as oxygen is also temperature dependent, the saturated oxygen concentration may be used as upper limit reference values, assuming that no oxygen has been lost for any chemical process yet. The oxygen concentration was approximated by the following equation (Hua, 1990):

$$DO = 14.562 - 0.41022T_s + 0.0079910T_s^2 - 0.000077774T_s^3$$

where DO = saturated dissolved oxygen concentration (mg/l)

T_s = surface water temperature (°C)

6.3.1.4 Incorporation of observed grab samples in infilled time series

As one can see from Figures 6.8 to 6.31, the measured grab samples are not included in the generated time series. The infilled time series has been used initially in the configuration, as it follows a "smoother" trend without the measured data. In section 8.6.5, however, a sensitivity analysis has been completed with and without the grab samples incorporated into the infilled time series. The grab sample has been included in the time series by interpolating the two values before and after the grab sample in order to smoothen the impact it might have on the time series.

6.3.2 Water Quality Variables

The state variables that are not modelled (e.g. chl-a) for this study, but specified in the predefined water quality model, EUTROF1, have been assigned a zero value. The water quality concentrations of interest have been entered as non-uniform time series, which has been infilled according to section 6.3.1.

6.3.3 Abstractions

There are two possibilities for DUFLOW to calculate outflowing water quality loads at points where the water flows out of the system.

- If no water quality boundary condition is specified at a point, the concentration of the outflowing water volume will be treated as zero concentration. This option has been used at the evaporation points.

- At irrigation and water abstraction points, a water quality boundary condition had to be defined. The outflowing concentration is then calculated relative to the volume of the outflowing water.

6.3.4 External Variables

External variables, such as solar radiation, evaporation rates and air temperature have been imported into the DUFLOW dialog box as time series. External variables are required for the process calculations, refer to section 5.4.5 for a description of the various water quality processes. The meteorological information was obtained from the Department of Agriculture, Elsenburg and the Weather Bureau.

External parameters can be defined at every schematization point or node. This allows for more flexibility, as the external variables can be adjusted corresponding to their location. A limitation of DUFLOW is, that the time series at every schematization point are written to file and therefore the size of the external variables is quite high (51Mb).

Table 6.16 summarizes the meterological stations which have been used for predicting the influence of the meteorological input data required by DUFLOW, and the corresponding water gauging stations. Unfortunately, not all stations have measurements during the calibration period 1993-1994. The most complete data set for the whole range of years was for Bien Donne. For all stations downstream of G1H037 insufficient information was available for the meteorological stations situated in this area and data of Landau had to be used.

Table 6.16: Meteorological stations used and corresponding water gauging stations

Meteorological Station	Latitude	Longitude	Water Gauging Station	Latitude	Longitude
La Motte	33° 53'	19° 05'	G1H004	33° 55' 36	19° 03' 41
Bien Donne	33° 50'	18° 59'	G1H019	33° 54' 44	18° 56' 36
Nederburg	33° 43'	19° 01'	G1H020	33° 42' 29	18° 56' 29
Landau	33° 36'	18° 58'	G1H037	33° 37' 39	18° 59' 29

6.3.4.1 Air Temperature

Table 6.17 lists the average air temperature for the different stations. It can be observed from the table, that the difference in temperature between the different stations is minimal. La Motte experiences the highest summer temperatures.

Table 6.17: Average monthly air temperature measured at meteorological stations

	Oct	Nov	Dec	Jan	Feb	Mar	Apr	May	June	Jul	Aug	Sep
La Motte	25.1	25	28.2	23.7	23.8	21.7	20.1	14.4	12.2	11.8	13.4	15.5
Bien Donne	18.1	20.9	22.1	23.7	23.8	22	20	13.5	11.9	11.3	12.8	15.2
Nederburg	20.3	22.4	23.4	25.3	25.9	23.6	21.3	15.1	12.5	12.3	13.7	16.1
Landau	19.8	22.5	23.3	25.5	26.1	23.6	21.6	15	12.5	11.8	13.4	15.9

6.3.4.2 Solar radiation

Solar radiation was provided by the Department of Agriculture, Elsenburg at various weather stations along the river. Similar to the meteorological stations, most of the weather stations do not consist of uninterrupted periods of measurements, except for Bien Donne. It was therefore decided to use the radiation data of this station for the whole catchment. Radiation is required for the calculation of the temperature in the river (refer to section 5.4.5.1). Referring to Figure 6.8, a slight change in phase is perceived. The lowest recorded measurements are generally equal; while the December/January values are at a maximum in 1990 and 1996. Table 6.18 tabulates the monthly averages (MJ) at Bien Donne for the configuration period.

Table 6.18: Monthly Radiation Averages (MJ/day) at Bien Donne for 1993/1994

	Oct	Nov	Dec	Jan	Feb	Mar	Apr	May	June	Jul	Aug	Sep
Bien Donne	17.9	24.4	24.5	26.3	23.5	19.5	14.3	9.9	6.9	9.4	10.3	12.2

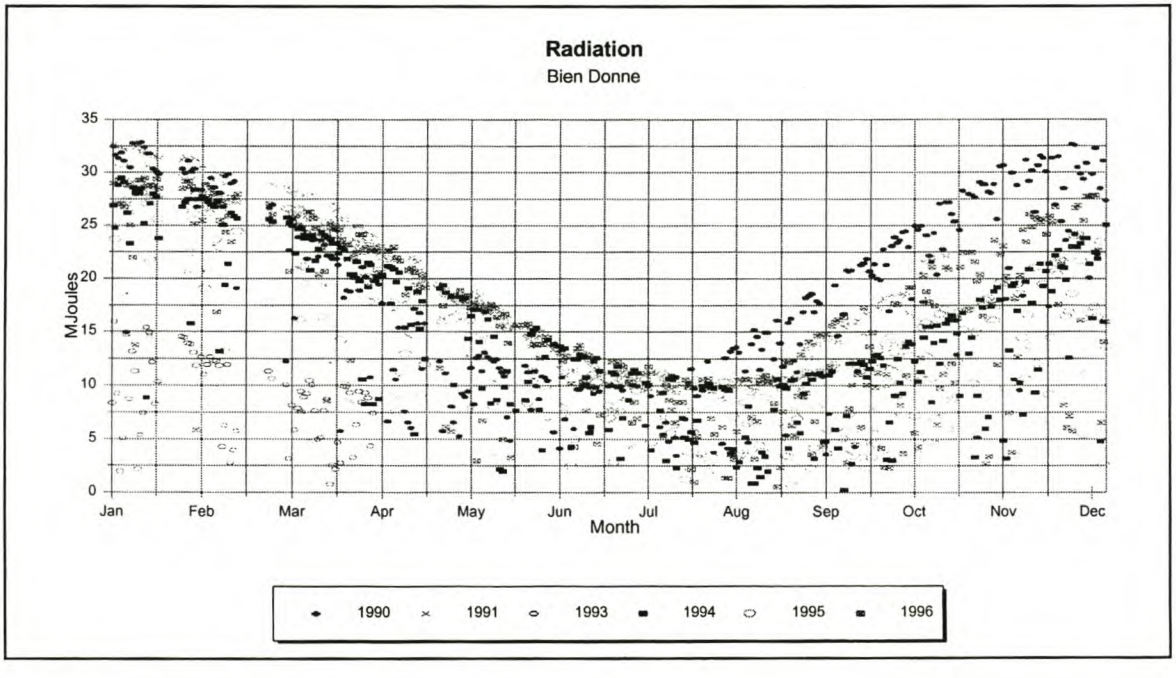

Figure 6.7: Radiation (MJ) at Bien Donne

6.3.4.3 Wind data

The wind data is a meteorological variable that is required for the water temperature computations (refer to section 5.4.5.1). Table 6.19 summarizes the monthly wind speed at the specific stations. Bien Donne experiences the highest wind nearly all year. The wind data was converted to m/s for the process calculations.

Table 6.19: Monthly wind speed (km/month) for 1993/1994

	Oct	Nov	Dec	Jan	Feb	Mar	Apr	May	June	Jul	Aug	Sep
La Motte	114.1	130.9	124.6	125.1	132.5	86.9	86.1	56	124.2	74.3	62.5	115.1
Bien Donne	207.9	237.4	274.1	271.3	284.9	208.7	154.4	66.2	155.2	89.6	153.8	184.4
Nederburg	196.8	224.1	254.1	240.3	279.7	194.2	165.5	87.3	156.1	92.1	146.1	169.1
Landau	113.8	114.6	127.5	129.3	120.7	94	82	61.6	91.1	69.5	84.8	96.4

6.3.4.4 Evaporation Rates

Evaporation rates are needed for the temperature process calculations (refer to section 5.4.5.1 for the process calculations and their specific algorithms). It can be observed from Table 6.20 that the highest evaporation rate is experienced in January. It is interesting to note that although Landau lies downstream of Nederburg, it experiences higher evaporation rates.

Table 6.20: Evaporation Rate (average mm/day) for the various meteorological stations

	Oct	Nov	Dec	Jan	Feb	Mar	Apr	May	June	Jul	Aug	Sep
La Motte	6.3	7.9	8.2	9	8.4	5.4	3.7	1.8	1.8	1.4	2.1	3.1
Bien Donne	6.2	8.3	9.7	10.6	10.2	6.7	4.9	1.8	1.3	1.5	2.7	3.4
Nederburg	8.3	10.4	11.5	12.1	12.8	8.5	6.1	2.4	1.1	1.6	3.2	4.2
Landau	6.4	8.3	8.6	9.6	9.5	5.9	3.8	1.9	1.1	1.1	2.2	3.1

6.3.5 Parameters

Default values for the parameters are used in the first simulation runs and are then adjusted at the calibration (refer to section 8.6 for a description of the sensitivity of the parameters). Table 6.21 lists the parameters that are used in the process calculations. All the other parameters that are predefined in the EUTROF1 model have been set to zero.

Table 6.21: Parameters used in DUFLOW

Parameter	Default Value	Description
A	0.56	Coefficient used in atmospheric longwave radiation (0.5-0.7)
ϵ	0.97	emissivity of a body
kr_{min}	0.1	Minimum oxygen transfer coefficient
rl	0.03	Reflection coefficient, usually small
t_{min}	1.047	minimum temperature reaction rate for PO_4
t_{rea}	1.024	reaction rate for PO_4

6.4 PROBLEMS ENCOUNTERED

The accuracy and stability of the calculations depend on the implicity factor θ, as well as the time step and the space step (refer to section 5.6). Most of the problems encountered during the test runs were due to these factors, especially in the upper reach as the slope is very steep (0.35%) and negative water depths were encountered at some sections. It took great effort to achieve a fairly stable flow condition which would be stable for calculating the correct water quality concentrations.

- The difficulties were experienced especially in the first reach from G1H004 to G1H020. Downstream of G1H020, the flow calculations were fairly stable. This is because the slope of the river is quite steep in the first reach and DUFLOW is not suitable for supercritical flow or near supercritical flow.
- Negative water depths were calculated at some sections in the river. The water quality

calculations were unable to calculate any concentration values because of these negative water depths, as the process descriptions occasionally need to take the square root of the water depth.

- In a longitudinal graph the concentrations would be shown as very strong " toothed " graphs. This is due to instability in the transport, which occurs when the Peclet number becomes too high (Pe>2) (see equation 5.19 for definition of the Peclet number).

- As initial conditions are user defined, a constant flow corresponding to the first date of simulation was taken as the upstream boundary value. The simulation was run until the longitudinal graph as well as the time series showed a stable calculation. The levels and the discharge calculated were then used as the initial value. Normally, the initial values should not create any problems as any error would cancel out after a few time steps, but as the calculations start at a very steep slope (average slope of 0.35% in reach 1, G1H004 to G1H020), it tends to calculate negative water depths from the very beginning and the errors then accumulate. The schematization points inserted forced the calculations to begin with positive water depths and also minimal space steps and therefore the calculations would not become unstable right at the start of the calculations.

All the above problems mentioned have been overcome by implementing very small space steps by adding schematization points (points where a level and discharge can be defined as initial values (refer also to Figure 5.2)) at very small distances. These distances depend on the problem area, for the first reach the schematization points were spaced at about 100m, while further downstream, where the slope is milder, the space steps were increased to about 2 km. This lets the computation proceed, but still not changes the fact that the configuration is very unstable and any change like an additional discharge point or cross-section will affect the stability. Also, because of the very small space steps, the time taken for the simulation increases and the output file for a year is about 12 Mb for the flow and about 50 Mb for the quality constituents.

6.5 REFERENCES

DWAF(a), 1992. *The hydrology of the Berg River Basin.* Internal report prepared by R R Berg of Ninham Shand Inc. in association with BKS Inc. as part of the Western Cape System Analysis. DWAF Report No. P G000/00/2391.

DWAF(b), 1993. G Quibell. *Water Quality in the Berg River: A Situation Analysis*. Department of Water Affairs and Forestry.

DWAF(c), 1994. *Flow Gauging Stations*: *Calibration and Evaluation, Volume III*: *Particulars of Gauging Stations*. Prepared by A Rooseboom and G R Basson of Ninham Shand Inc. in association with BKS Inc. as part of the Western cape System Analysis. DWAF report no. P G000/00/1090.

DWAF(d), 1995. *In-stream Flow Requirements, Volume 1: Proceedings of Skuifraam Dam Worksessions*. Prepared by P Dunn and J Larsen of Ninham Shand Inc. in association with BKS Inc. as part of the Western cape System Analysis. DWAF report no. P G000/00/4793.

DWAF(e), 1998. *Amatole Water Resource System Analysis. Water Quality Modelling.* Prepared in association with Gibb Africa. DWAF Report No. Pr 000/00/0295.

Enright, W., Personal Communication, Department of Water Affairs and Forestry, 2000.

Grijsen, J.G. 1986. *River Flow Simulation* in River Flow Modelling and Forecasting (edited by D.A. Kraijenhoff and J.R. Moll). Pg 241-272.

Hesong Hua, 1990. *Accurate Method for Calculation of Saturation DO.* ASCE Journal of Environmental Engineering. Vol 116, No 5, Pg. 988-990.

Kraijenhoff, D.A. and J.R. Moll (eds.), 1986. *River Flow Modelling and Forecasting*. D. Reidel Publishing Company.

Le Maitre, D.C., D.B. Versfeld and R.A. Chapman, 2000. *The impact of invading alien plants on surface water resources in South Africa: A preliminary assessment.* Water SA, Volume 26 No 3, p.397.

Long, Leland, 1976. *Water Temperature Forecasting and Estimation Using Fourier Series and Communication Theory Techniques.* Water Resources Research, Vol 12 No 5 October 1976, pg 881-887

McKenzie, R.S. and A.R. Craig, 1997. *Evaporation Losses from South African Rivers*, Sanciahs Conference. Pretoria. South Africa.

Rooseboom, A., M. Basson, C.H. Loots, J.H. Wiggett, J. Bosman, 1983. *Manual on Road Drainage: RSA.* National Road Transport Commission. Directorate of Land Transport. Pretoria.

Sanders, T.G, R.C. Ward, J.C. Loftis, T.D. Steele, D.D. Adrian, 1980. *Principles of Network Design for Water Quality Monitoring.*

Thomann, R.V, 1967. *Time-Series Analyses of Water-Quality Data.* Journal of the Sanitary Division. ASCE Vol 93 No SA1. Pp1-23.

Traver, Robert and Arthur C. Miller, 1993. *Open Channel Interpolation of Cross-sectional Properties.*Water Resources Bulletin. Pg 767-776.

Versfeld, D.B., Le Maitre, D.C. and R.A. Chapman, 1998. *Alien invading plants and water resources in South Africa: A preliminary assessment.* TT 99/98, WRC. Pretoria, South Africa.

Walker, W.W., 1987. *Emperical Methods for Predicting Eutrophication in impoundments, Report 4, Phase III: Application Manual.* Technical Report e-87-9. U.S. Army Corps of Engineers, Washington DC.

Figure 6.8:

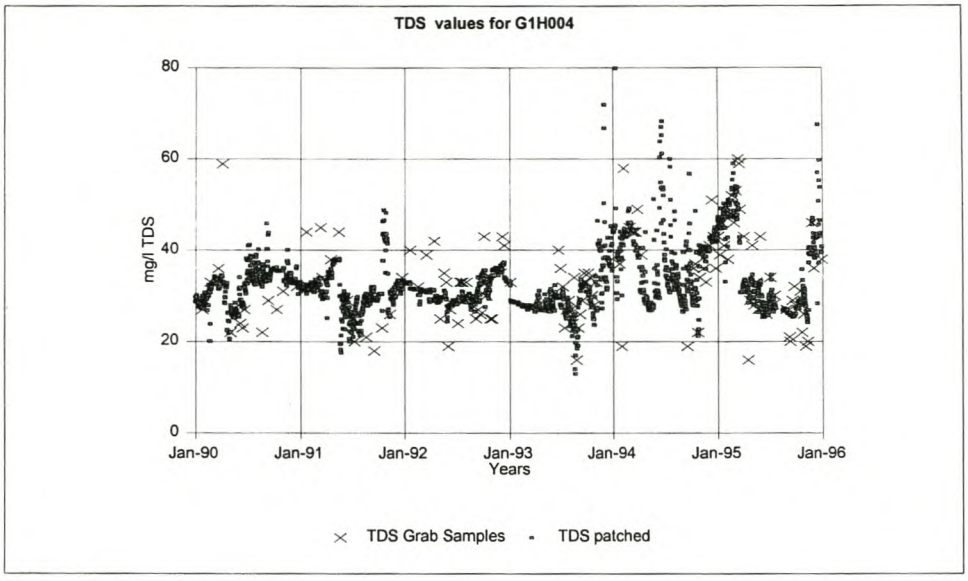

Figure 6.9:

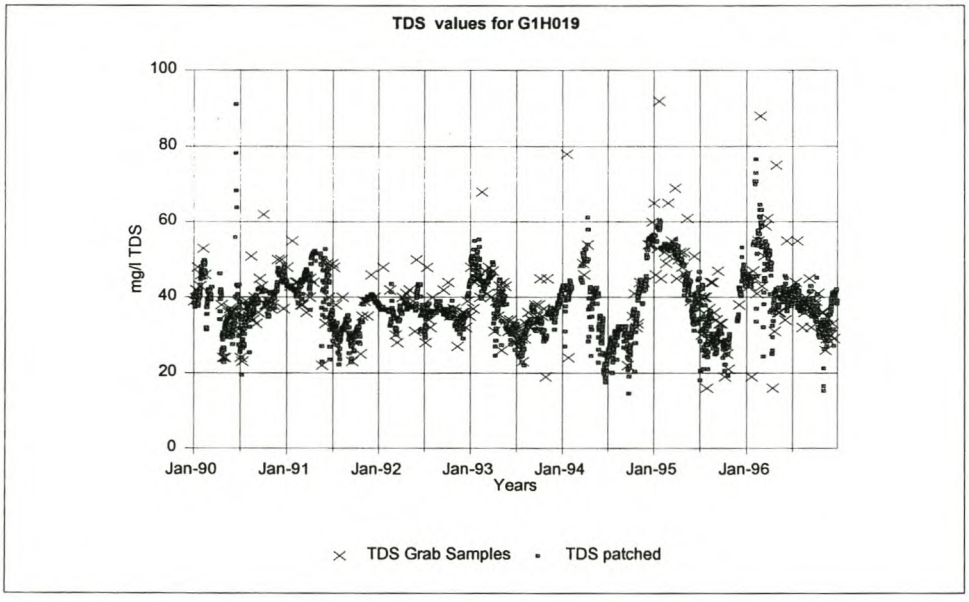

Figure 6.10:

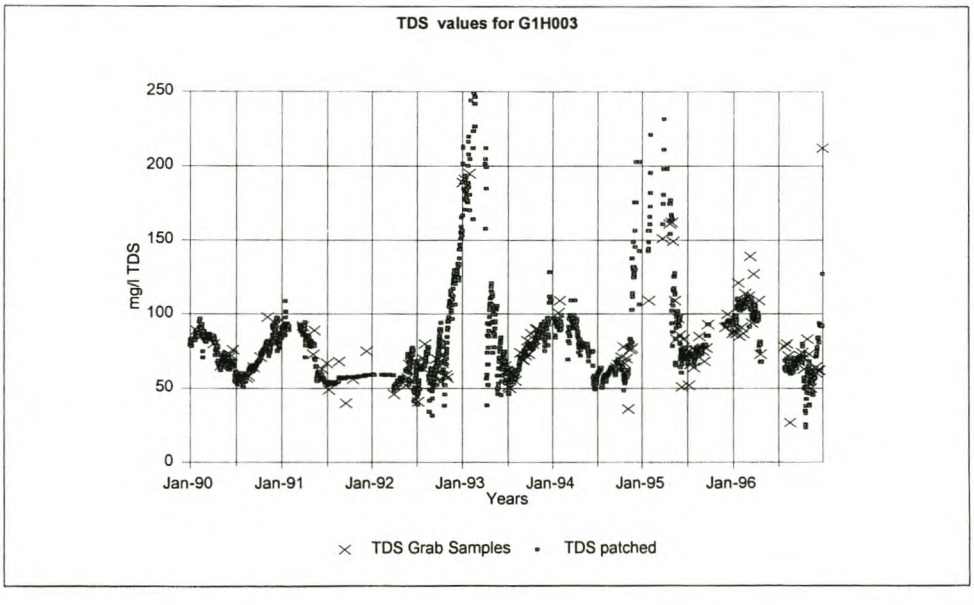

Figure 6.11:

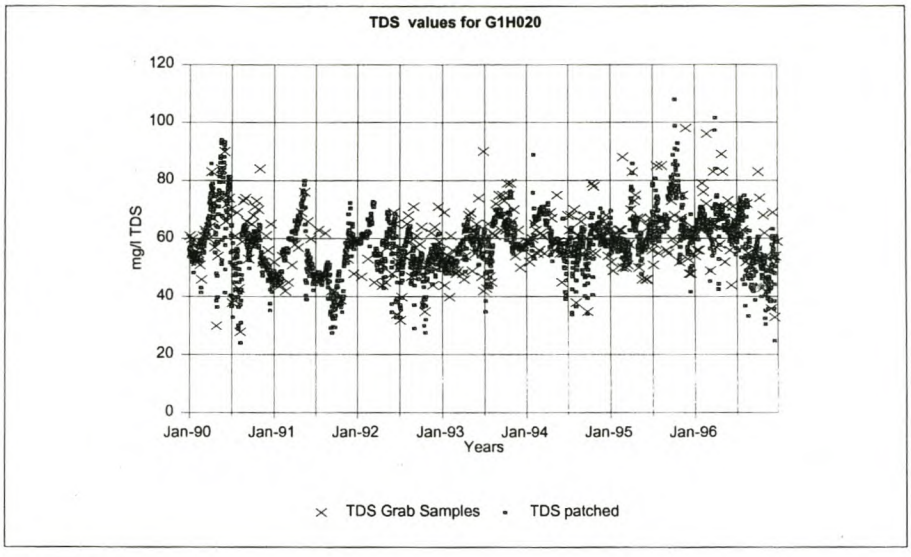

Figure 6.12:

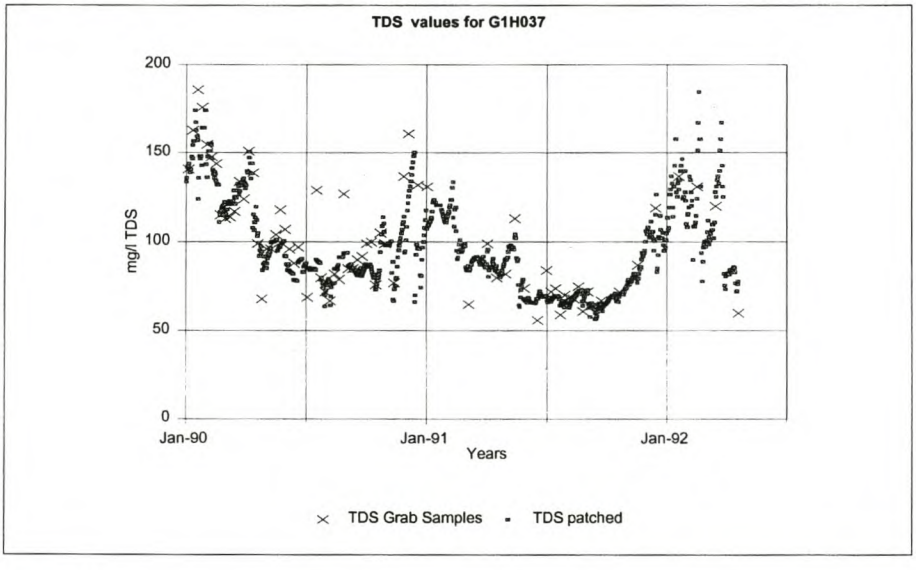

Figure 6.13:

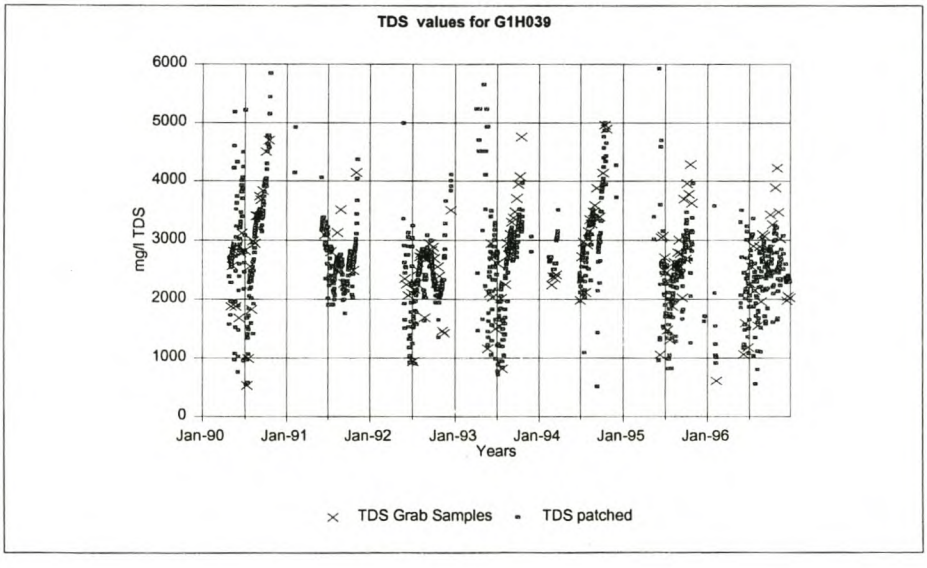

Figure 6.14:

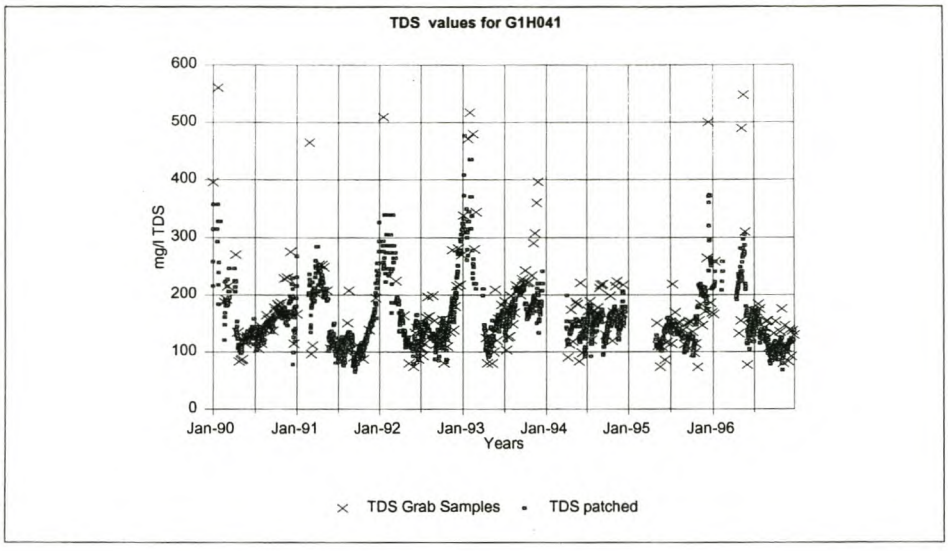

Figure 6.15:

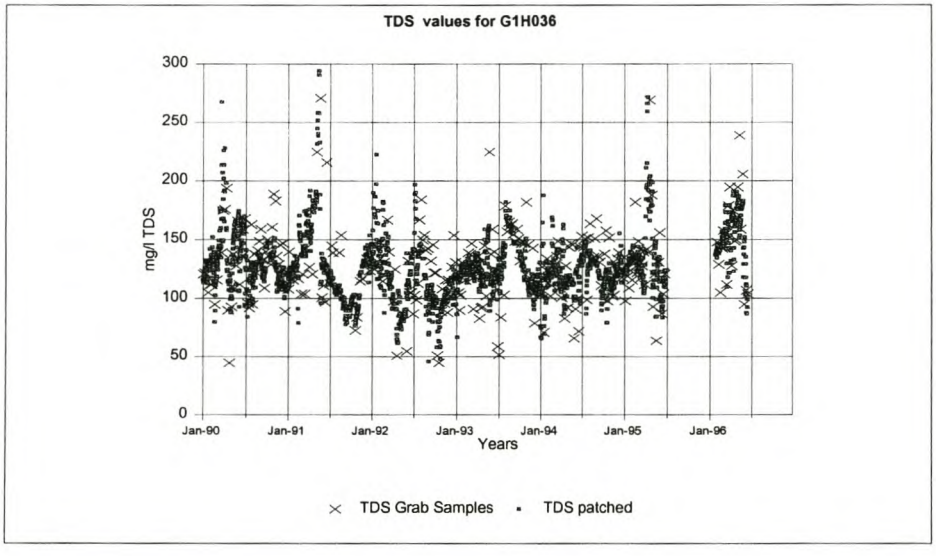

Figure 6.16:

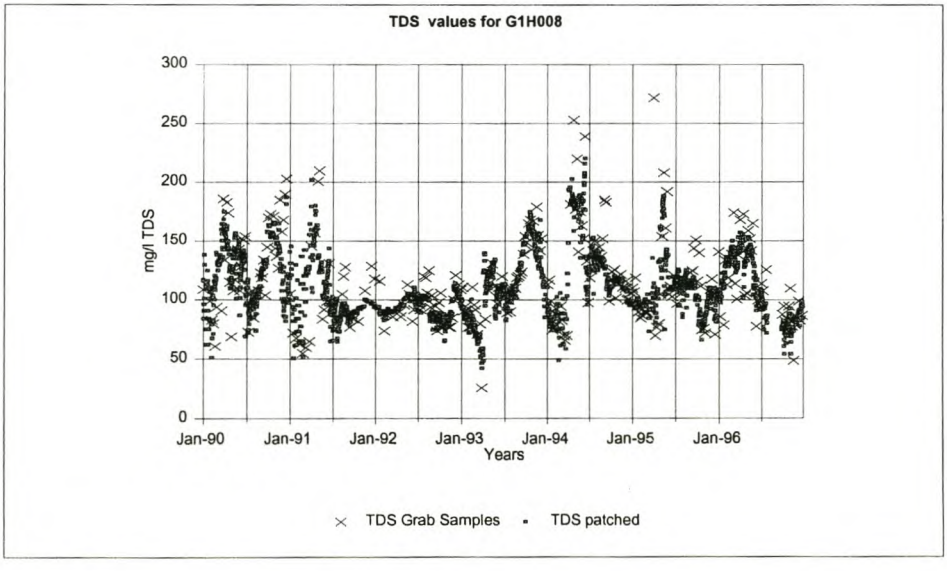

Figure 6.17:

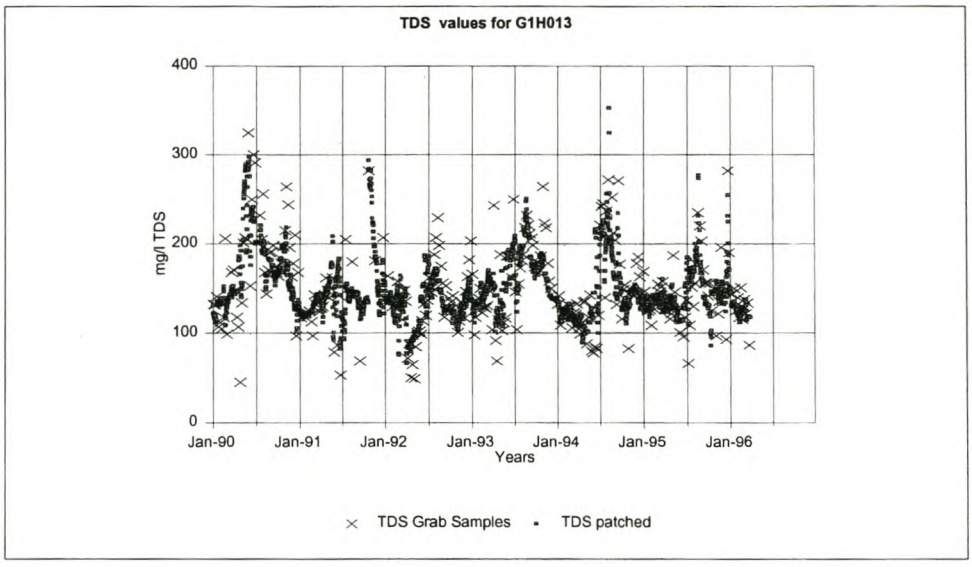

Figure 6.18:

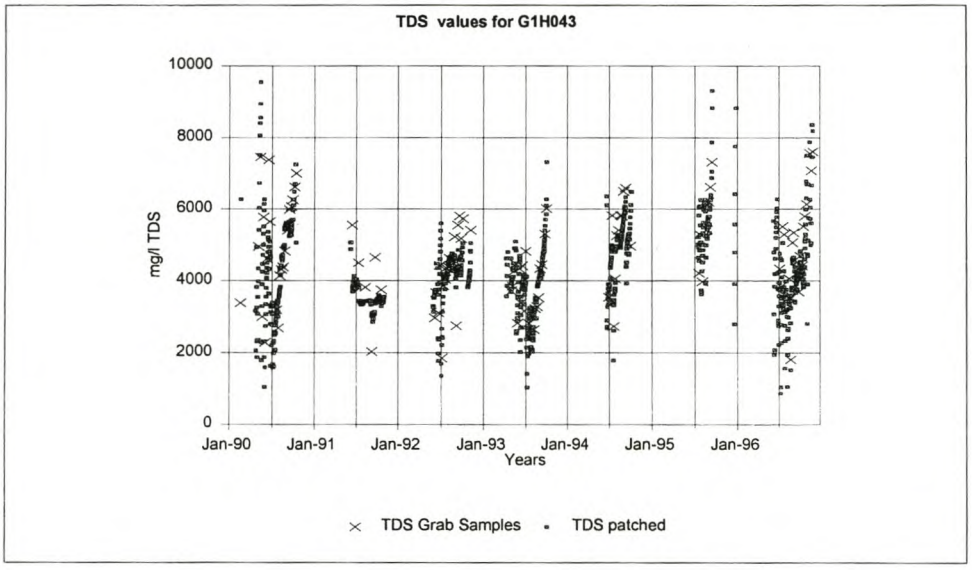

Figure 6.19:

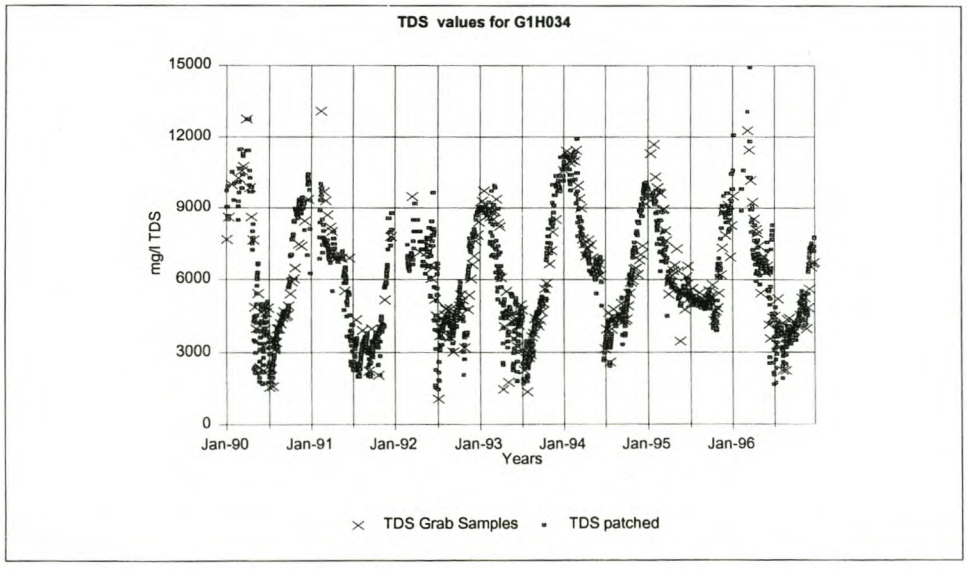

Figure 6.20:

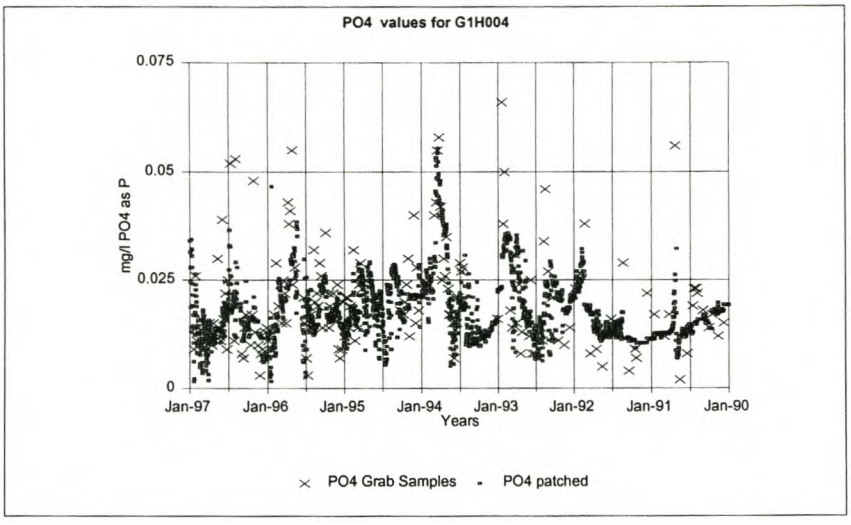

Figure 6.21:

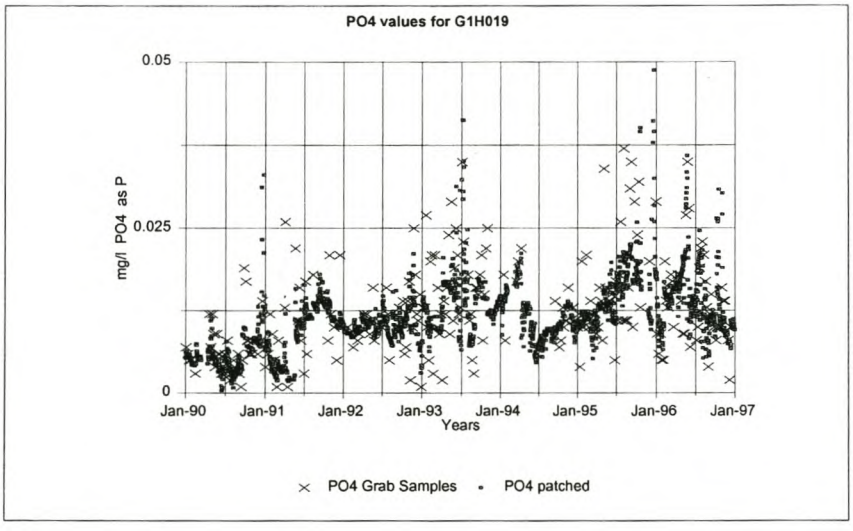

Figure 6.22:

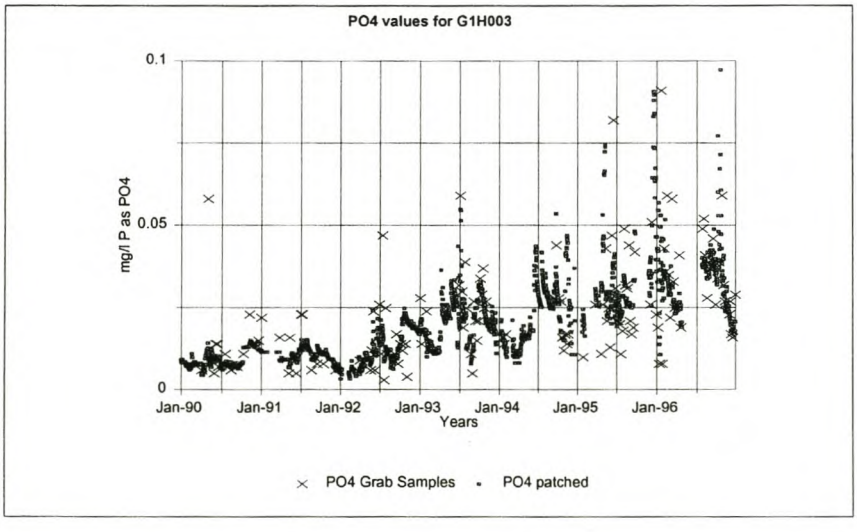

Figure 6.23:

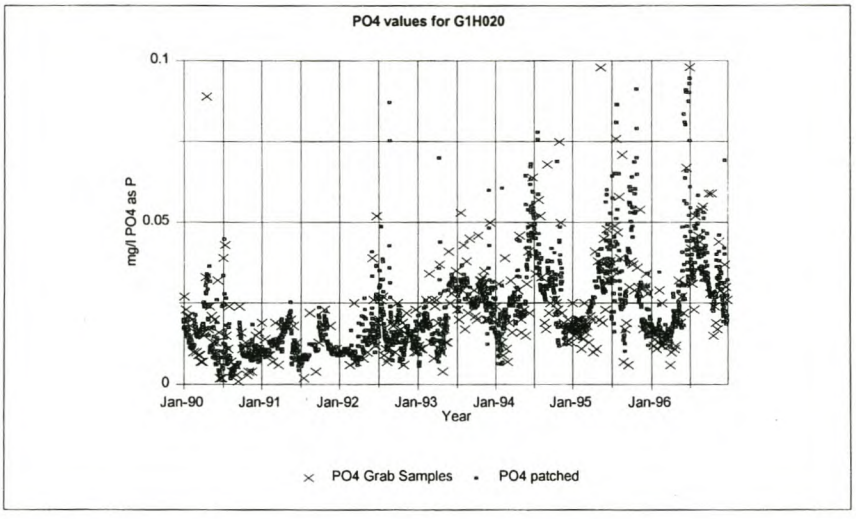

Figure 6.24:

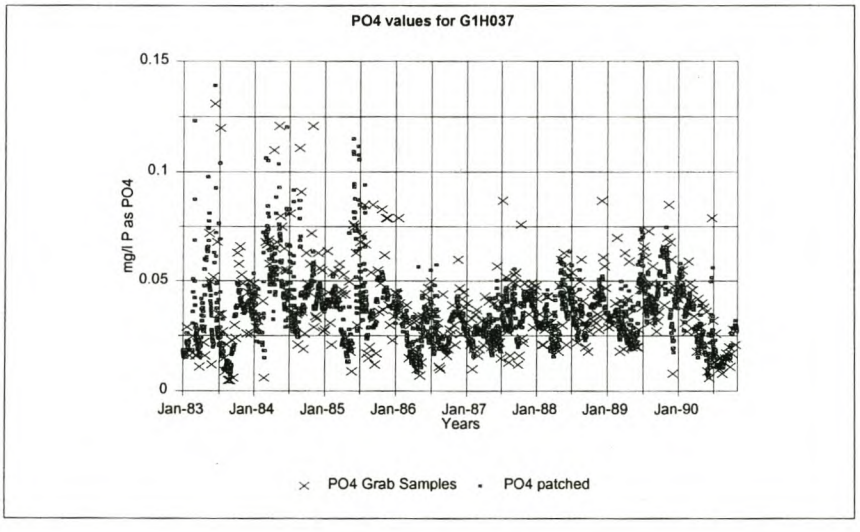

Figure 6.25:

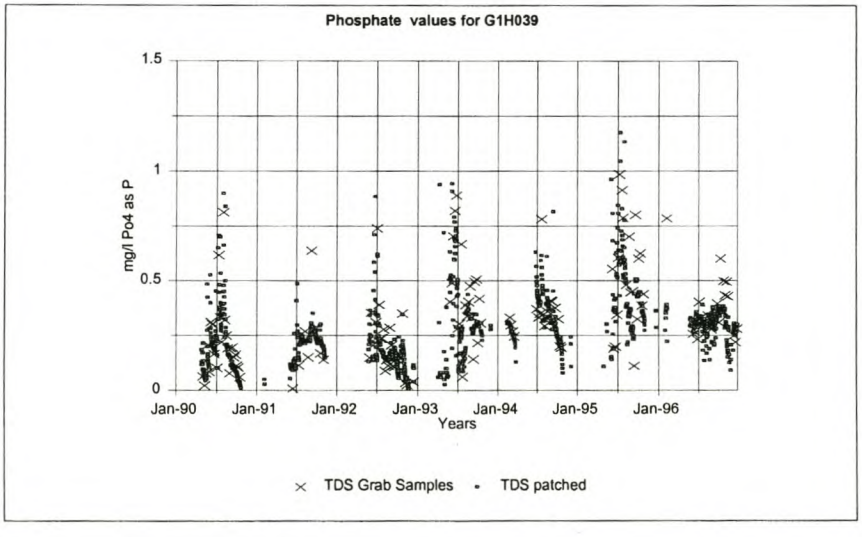

Figure 6.26:

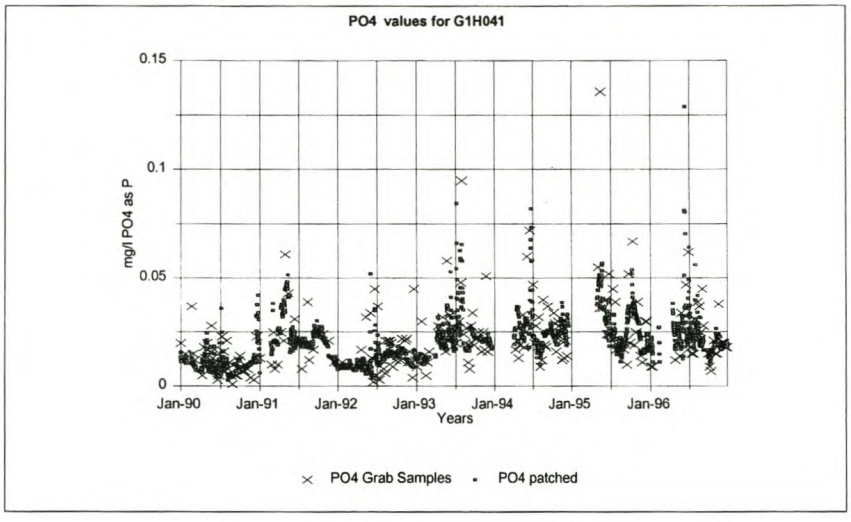

Figure 6.27:

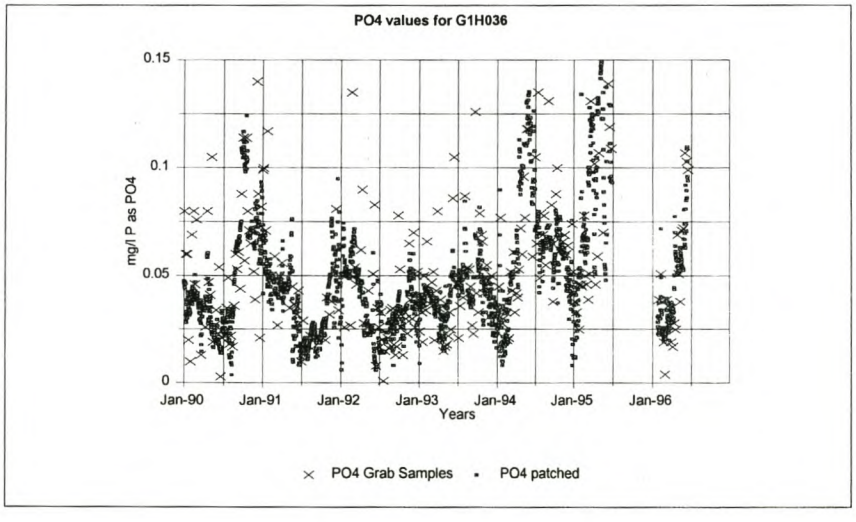

Figure 6.28:

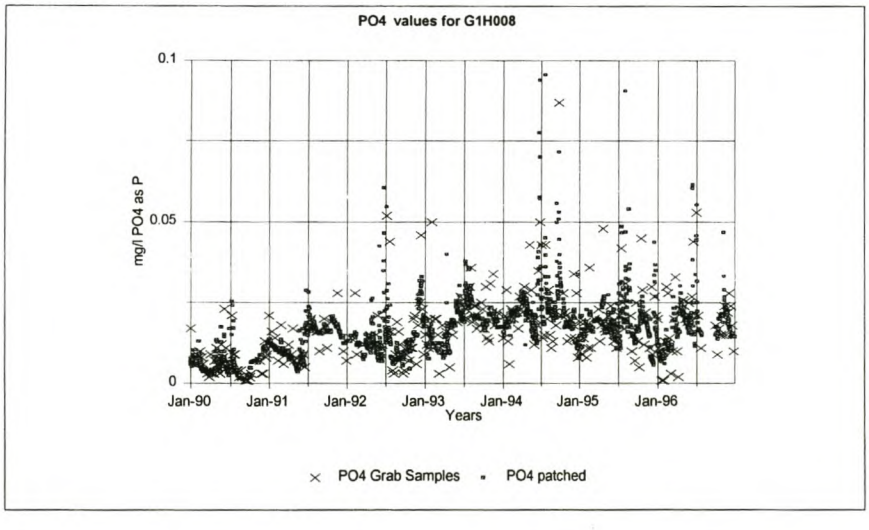

Figure 6.29:

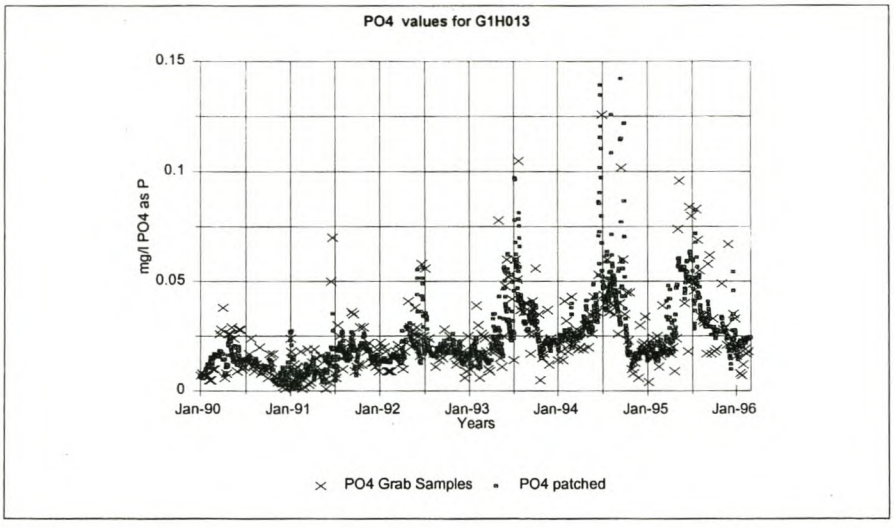

Figure 6.30:

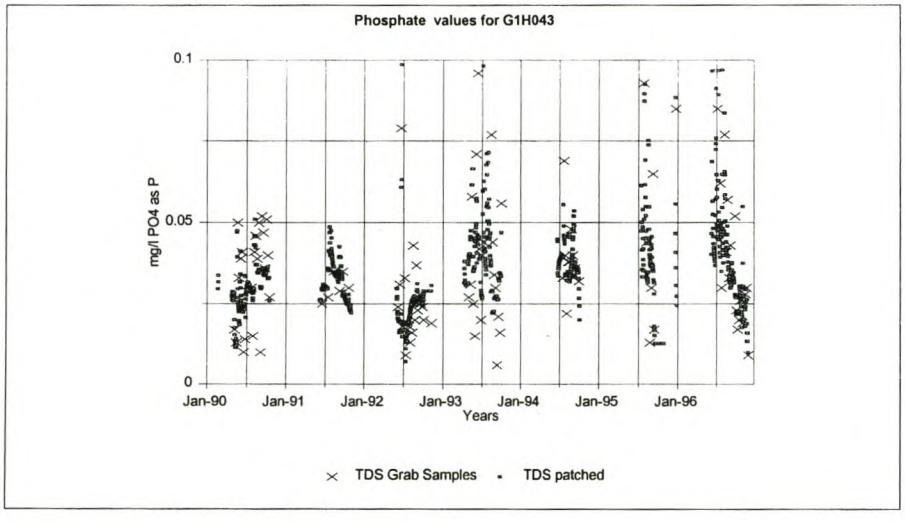

Figure 6.31:

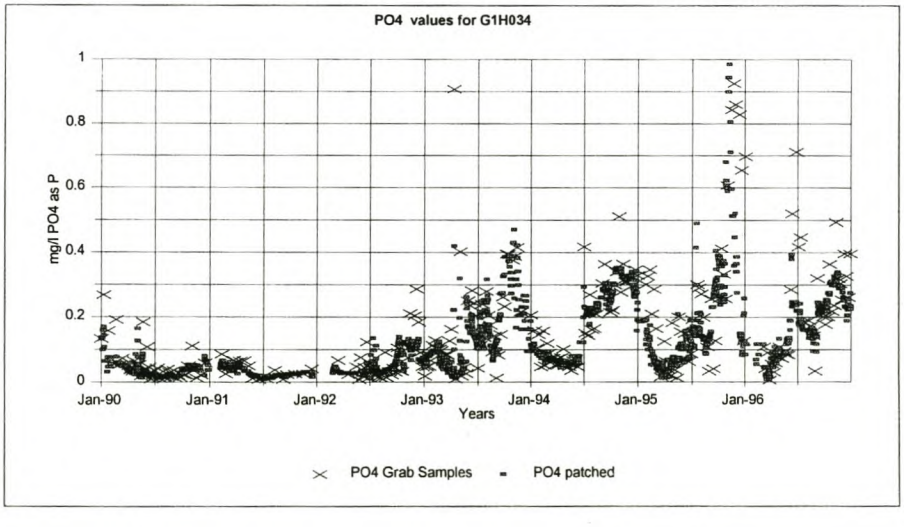

Figure 6.32:

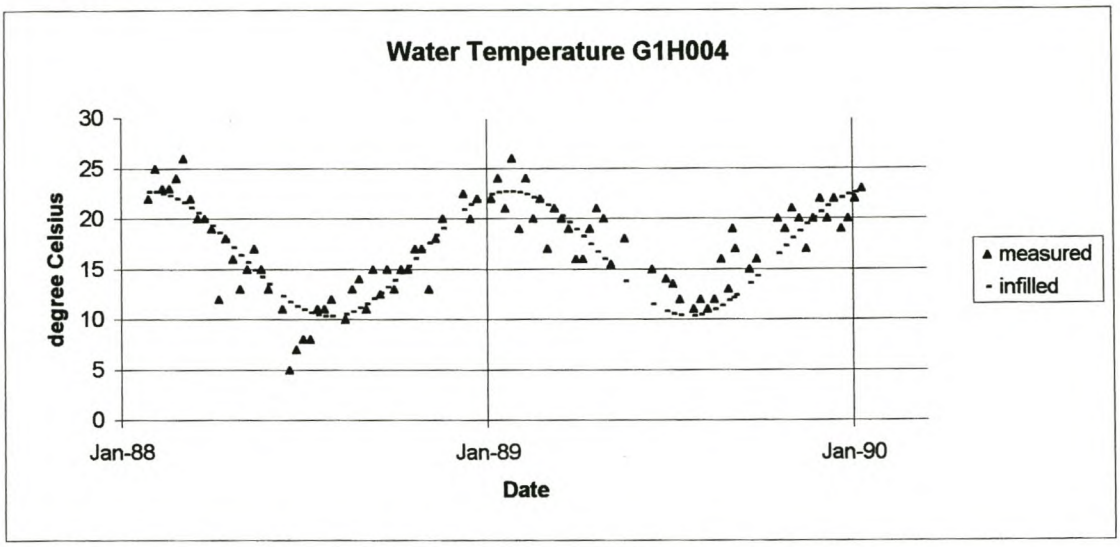

Figure 6.33:

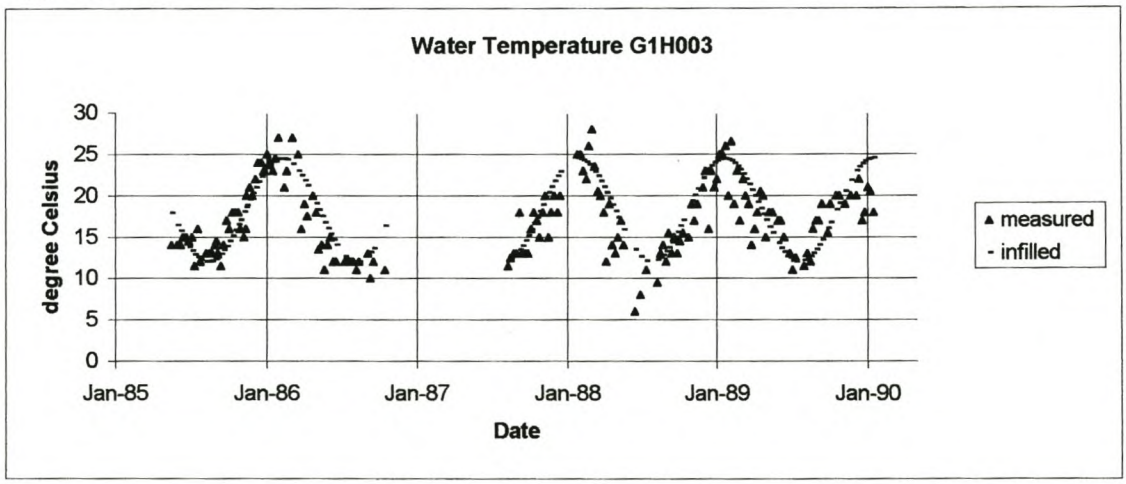

Figure 6.34:

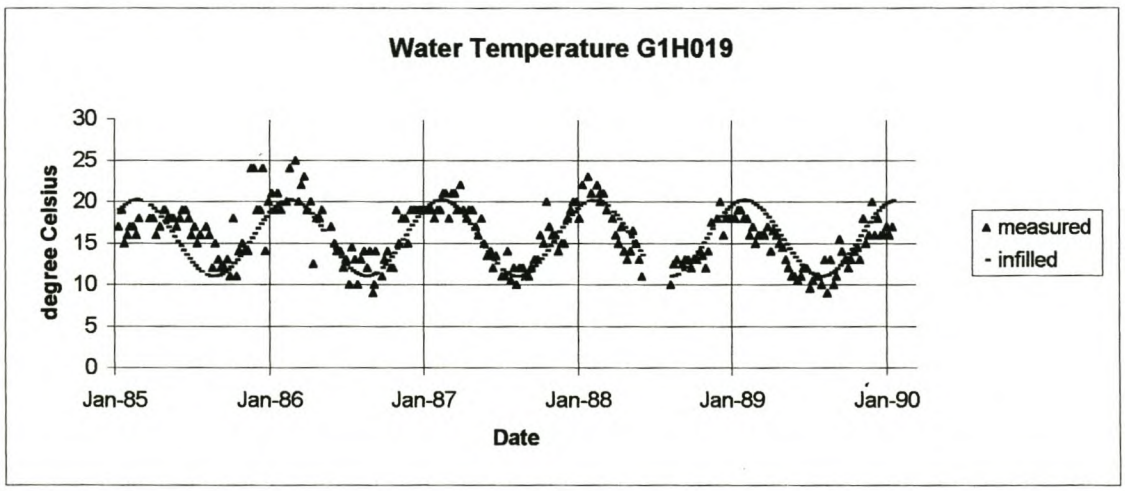

Figure 6.35:

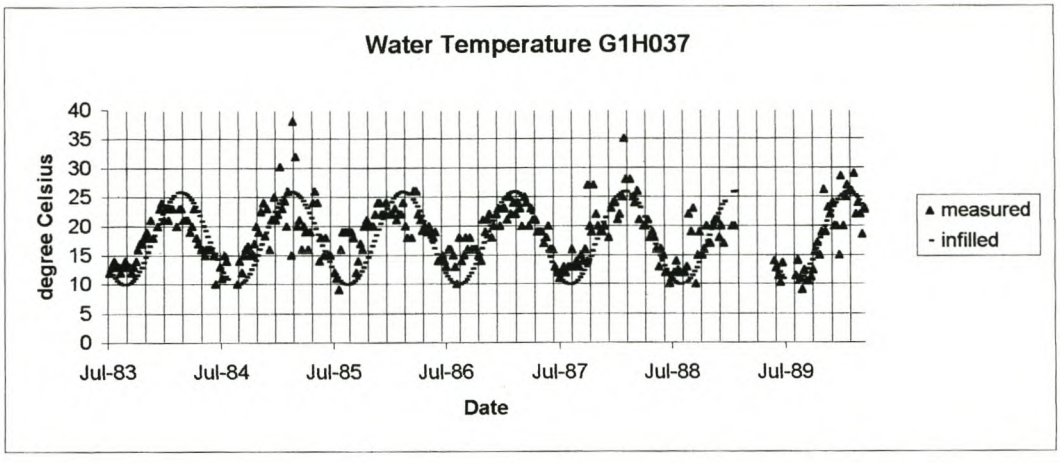

Figure 6.36:

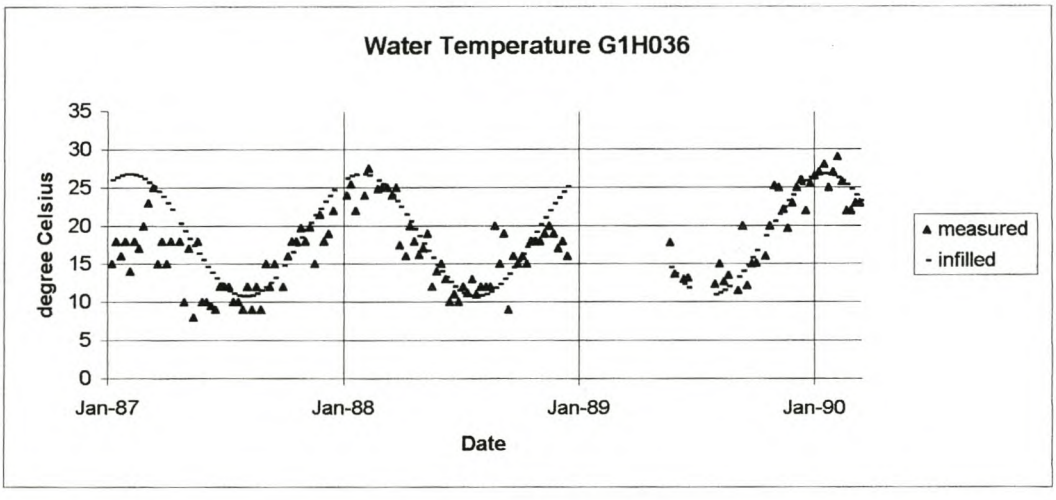

Figure 6.37:

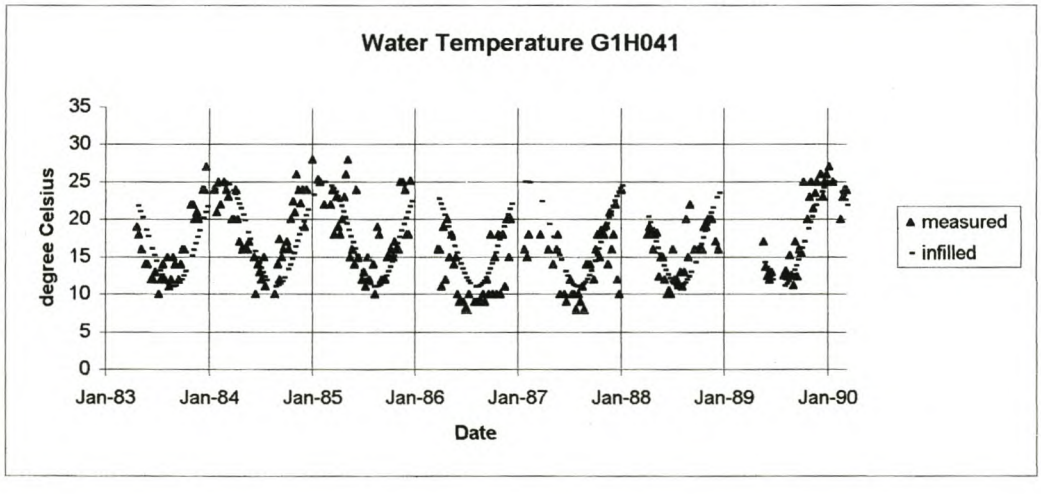

Figure 6.38:

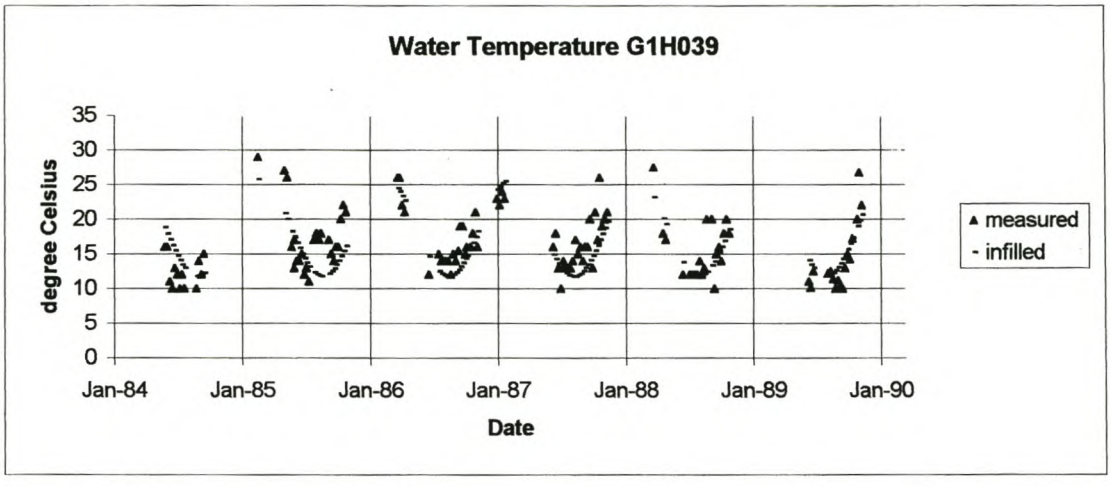

Figure 6.39:

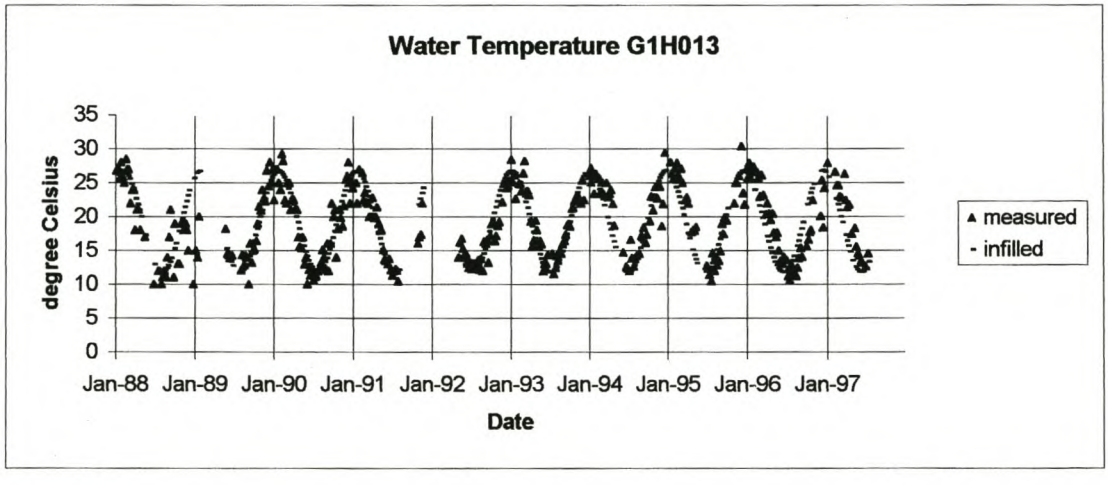

Figure 6.40:

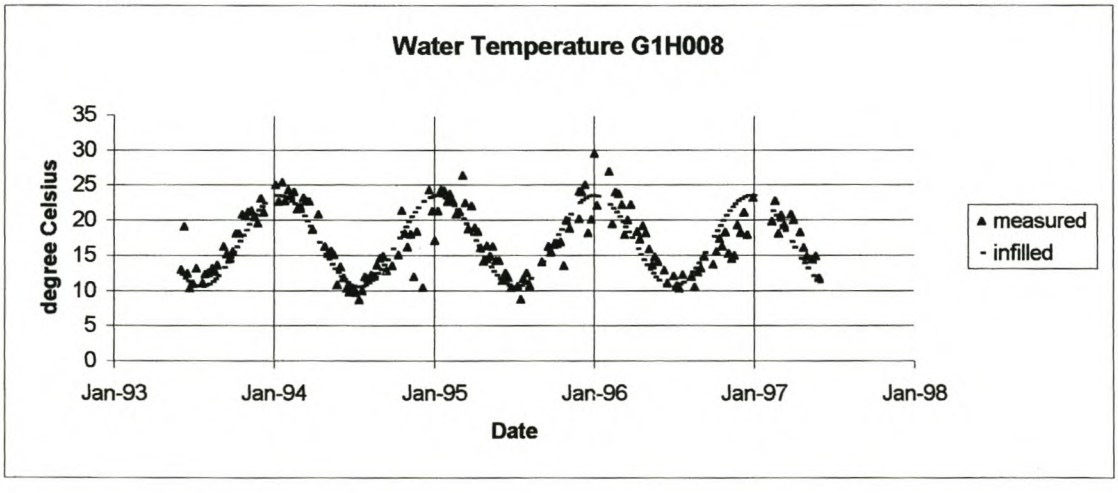

CHAPTER 7

FLOW MODEL SENSITIVITY, CALIBRATION AND VERIFICATION

7.1 INTRODUCTION

As explained in section 2.3.3, important steps in modelling (following the configuration of the model with a specific data set) are: *calibration, sensitivity analysis* and *verification*. These steps have also been taken for the Berg River model. As the water quality part of the model is dependent on the calibrated hydraulic component, and every error introduced in the flow module will influence the water quality calculations, it has been decided to separate the calibration and verification of the hydraulic and water quality module into two Chapters. This chapter deals therefore with the calibration and verification of the hydraulic component of the model, while Chapter 8 follows with the calibration and verification of the water quality module.

The 'goodness-of-fit' between the simulated values and the measured data set is determined by *objective functions*. The first section of this chapter describes the objective functions used in the following two chapters to analyse the results of the simulation.

The process of adjusting parameters by running the model at different parameter values until a satisfactory result is obtained is called *calibration* (Grijsen, 1986). A close correspondence between observed data and simulated data is required, as the model is supposed to represent the situation in reality. A *sensitivity analysis* is therefore important for the calibration process, as it determines which parameters have a significant impact on the model results. In the second section of this chapter the calibration of the flow simulation, by introducing ungauged runoff, and the sensitivity and adjustment of Manning's roughness value are discussed.

Lastly, the results of the model verification are presented. The term *verification* will be used to describe the process of ensuring that the model applied to the specific river for a set of data can be applied to another situation. The model was first verified in space, by using measured downstream hydrographs

(G1H020 and G1H036) as boundary inflow hydrographs, to determine the errors introduced in the model during the different reaches. Finally, the model was verified for a time period not used during the calibration.

7.2 OBJECTIVE FUNCTIONS

"The term objective function is now widely used to describe any specific fitting criterion employed in the parameter estimation process." (Görgens, 1983, pg 141). Therefore, the term **objective function** is used to describe the correspondence of simulated and observed values by several specific statistical procedures (goodness-of-fit criteria).These statistical tests are used to quantify the agreement between predictions and observations. The mathematical description of the objective functions needs to be introduced before progressing to the actual calibration procedure and sensitivity analysis description. It was decided to divide the results into three categories to analyse how the goodness-of-fit changes seasonally:

- overall yearly values
- low-flow period (October to April)
- high-flow period (May to September)

The objective functions used are:

- <u>% error in mean</u>

$$\%_e = 100 * \frac{(X_{si}(mean) - X_{ob}(mean))}{X_{ob}(mean)} \qquad 7.1$$

- <u>% error in volume or load</u>

$$\%_e = 100 * \frac{(X_{si}(vol) - X_{ob}(vol))}{X_{ob}(vol)} \qquad 7.2$$

- % error in std deviation

$$\%e = 100 * \frac{(X_{si}(sta) - X_{ob}(sta))}{X_{ob}(std)} \qquad 7.3$$

- Coefficient of determination (correlation coefficient)^2

$$correlationcoefficient = \frac{(n(\sum X_{si} * X_{ob}))}{\sqrt{((n * \sum X_{si}^2 - (\sum X_{si})^2) * (n * \sum X_{ob}^2 - (\sum X_{ob})^2))}} \qquad 7.4$$

- Coefficient of efficiency

$$= 1 - \frac{\sum^{n} (X_{si} * X_{ob})^2}{\sum^{n} (X_{ob} - X_{ob}(mean))^2} \qquad 7.5$$

The *percentage error* in mean, volume and standard deviation (eqn. 7.1-7.3) represents the difference between the predicted and the observed values. This measure is a good indication of the under- or oversimulation, it can however counterbalance discrepancies in the values. Therefore, additional functions are needed to assess the accuracy of the simulated values. The *coefficient of determination* (eqn. 7.4) indicates the degree of correlation between observed and simulated values. It approaches 1 when a high degree of correlation between the two values exists. The *coefficient of efficiency* (eqn. 7.5) is also a dimensionless measure of the correlation of the two values, it is however sensitive to systematic errors. Therefore, the difference between the coefficient of determination and the coefficient of efficiency is a function of the systematic error in the model simulation.

The reader is referred to Görgens (1983) for various other valuable objective functions and a step by step approach leading to objective function selection. Reckhow et. al. (1990) also describes useful statistical functions that can be used in the analysis.

7.3 MODEL CALIBRATION AND SENSITIVITY PROCEDURE

The process of adjusting parameters by running the model at different parameter values until a satisfactory result is obtained, is called *calibration* (Grijsen, 1986). A close correspondence between observed data and simulated data is required. Calibration and the sensitivity analysis of the Manning's resistance coefficient were completed simultaneously, as the sensitivity of the Manning's resistance coefficient indicates the degree of adjustment necessary for the parameter. The *sensitivity* of parameters means the relative significance of each parameter in the performance of the whole model (Görgens,1983; pg. 194).

The calibration procedure consisted of following steps:

- Determination of reliable calibration period
- Determining accuracy of boundary conditions
- Introducing flows of ungauged tributaries
- Calibrating flow by adjusting the resistance

7.4 CALIBRATION PERIOD

The calibration period October 1993 to October 1994 was chosen, for the following reasons:

Firstly, this period is a whole annual cycle and thus includes low as well as high flow. Wemmershoek inflow information was readily available from July 1993 onwards and in the interest of economy of time to it was decided to calibrate from this year onwards. There is adequate daily flow information for most of the gauging stations compared to other years.

Secondly, the daily flows at station G1H037 (Krom River tributary) were not measured anymore from 1993 onwards. To be able to use the model in the time period when Skuifraam Dam would have been built, this influence on the mass balance of the flows needs to be taken into consideration and thus it is treated as a ungauged tributary.

Also, this year chosen is after the change of preservation of water quality samples which has taken place in 1989 (see section 4.6.1).

7.5 BOUNDARY CONDITIONS AND INITIAL CONDITIONS

The accuracy of the inflow hydrograph and the downstream rating curve is important when considering calibration, especially for the numerical accuracy of the model. Accuracy ratings of the gauging stations were given at a re-rating survey (DWAF, 1994), rating curves were also established by taking the various conditions at the weirs into account (e.g. sedimentation). The accuracy ratings of these stations (0=lowest and 5= highest) are listed in Table 7.1.

The inflow hydrograph at G1H004 has a high rating and therefore it can be expected to be about 80% accurate. G1H003, G1H039 and G1H035 have a very low accuracy rating and this needs to be remembered when analysing the results of the model.

An error in the initial values does have an effect on the calculations, but any errors resulting from inaccuracies of the initial values are soon cancelled out after a few time steps. Therefore, enough "warm up" time has been allowed for in the simulation run for the flow to stabilise before any results are written to a file.

Table 7.1 Accuracy Rating of Gauging Stations

Station Number	River Name	Accuracy Rating
G1H004	Berg	4
G1H003	Franschhoek	1
G1H019	Banhoek	4
G1H020	Berg	4
G1H039	Doring	0
G1H041	Kompagnjies	5
G1H036	Berg	4
G1H008	Klein Berg	4
G1H043	Holle	3
G1H013	Berg	4
G1H035	Matjies	poor
G1H034	Sandspruit	3

7.6 ADDITION OF UNGAUGED SUBCATCHMENTS

The lack of data for certain tributaries produces difficulties in the comparison between measured data and simulated data. The winter flow is underestimated due to ungauged inflow, which then has an impact on the simulated water quality loads. The ungauged flow runoff therefore had to be estimated as follows:

The Berg River catchment was subdivided into subcatchments according to the MAP and also west and east, as the tributaries are perennial on the eastern side and semi-perennial on the western side and runoff from the Malmesbury shales is much higher in TDS than the Table Mountain sandstone runoff. The ungauged areas in the Berg River catchment have been marked out on topographical maps and the area sizes were determined. The ungauged hydrographs for the river were then estimated by multiplying the gauged daily hydrograph by the ratio of the ungauged runoff area to the gauged area. Additionally, a MAP-MAR (mean annual precipitation-mean annual runoff) weighting derived from the *Surface Water*

Resources of South Africa, 1990 (Midgley et. al., 1994) was applied. Table 7.2 summarizes the various correction factors which have been applied to correct for the ungauged inflow and the catchment area as well as the MAP of the gauged areas. The location of the corresponding areas are illustrated in Figure 7.1.

Table 7.2 Description of Gauged Tributaries

Catchment Number (Figure 7.1)	Flow Gauge	River	Description	Catchment Area	MAP
				km^2	mm
A	G1H004	Berg	Driefontein	72	2600
B	G1H019	Banhoek	Bosmanshoek	22	1804
C	G1H003	Franschhoek	La Provence	46	1005
D	G1R002	Wemmers	Wemmershoek	88	1302
E	G1H041	Kompagnjies	De Eikeboomen	122	707
F	G1H039	Doring	Grensplaas	42	433
G	G1H043	Sandspruit	Vrisgewaagd	150	437
H	G1H034	Holle	Moorreesburgspruit	160	410
I	G1H008	Klein Berg	Mountain View	615	624
J	G1H035	Matjies	Matjiesfontein	671	410

Table 7.3 Areas and Correction factors of Ungauged Tributaries

Catchment Number (Figure 7.1)	Ungauged Area	Area	MAP	MAP/MAR Factor (WR90)	Ungauged Area/ Gauged Area	Flow	Comments
		km^2	mm			m^3/s	
1	west area upstream of G1H020	222	978	0.56	222 / 22	5.65*G1H019	
2	east area upstream of G1H020	188.5	900	0.58	188.5 / 88	1.2*G1R002	
3	G1H037	130	939	1.8	130 / 122	1.9*G1H041	No data available from 1993 onwards
4	area at G1H041	164	574	0.64	164 / 122	0.86*G1H041	
5	area surrounding G1H039	225	574	0.5	225 / 42	2.7*G1H039	
6	G1H040 and surrounding area	260	547	2.5	260 / 150	4.3*G1H043	No data available for G1H040
7 and 9	G1H034 and surrounding area	170	400	0.63	170 / 160	0.64*G1H034	
8	G1H008 surrounding area	400	450	0.18	400 / 615	0.12*G1H008	

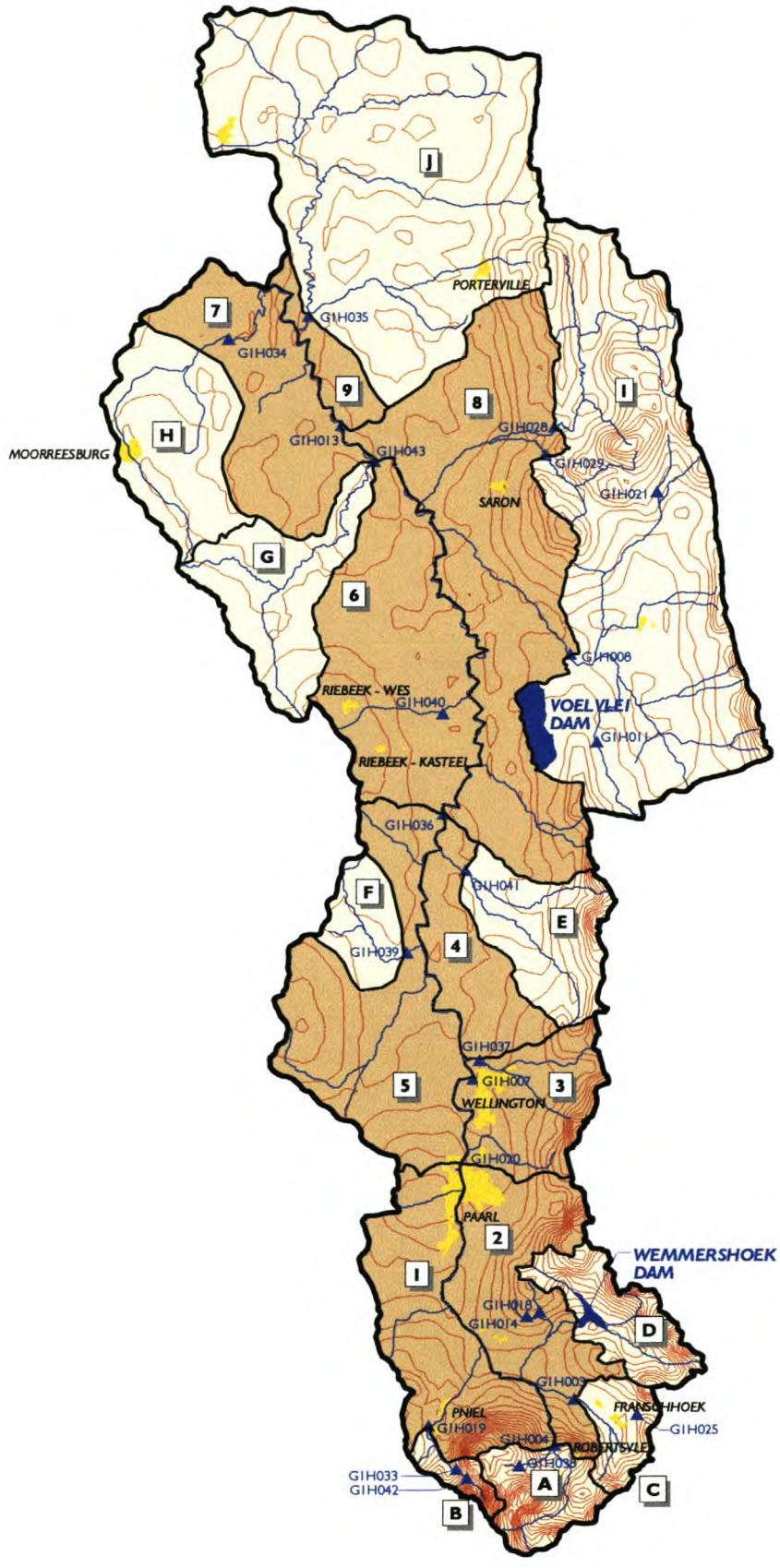

N

SCALE - 1: 600 000

0 5 10 15km

LEGEND :

Study Area | Gauged Sub-Catchment | Dam | Rainfall Isohyet

Town | Ungauged Sub-Catchment | River | Flow Gauge

ASSESSMENT OF A HYDRODYNAMIC WATER QUALITY MODEL, DUFLOW, FOR A WINTER RAINFALL RIVER

DATE : JULY 2000

Isohyetal Map Showing Gauged and Ungauged Sub-Catchments in the Berg River Region

FIGURE No. : **7.1**

P:\8276\ARCVIEW\PROJECTS\INITSCHEAPR

Discussion:

The subcatchment of G1H039 is used as gauged subcatchment although it has an accuracy rating of 0 (refer to Table 7.1); the addition of this subcatchment is still necessary as there is no other gauged subcatchment on the western side of the Berg River downstream of G1H020 and thus had to be used as an estimate of the runoff from the western tributaries into the main stem of the river.

Prior to the addition of the ungauged subcatchments, a mass balance of all the incoming flow, gauged and ungauged, was completed. Table 7.4 displays the results of the difference between the mass balance and the measured values at the gauging stations before and after the addition of the subcatchments. Flow volume which is still lacking between the measured and the flow added in the mass balance, could possibly be due to:

- higher ungauged runoff than estimated
- inaccuracy in the high flow measurements at the various gauging stations.

Most of the ungauged flow occurs in the reach between G1H036 and G1H013 (Table 7.4). G1H020 and G1H036 are slightly overestimated after addition of the ungauged inflow.

Table 7.4 Massbalance of flow corrected and measured for 1993/1994

		G1H020	G1H036	G1H013	G1R003
Difference in Volume (Mm^3) **before** addition of ungauged subcatchments	**low flow period** (Oct-Mar)	24	15	-13	19
	high flow (April-Sept)	-65	-36	-130	91
Difference in Volume (Mm^3) **after** addition of ungauged subcatchments	**low flow period** (Oct-Mar)	32	17	-12	18.7
	high flow (April-Sept)	11	9	-88	92

7.7 SENSITIVITY OF FLOW RESISTANCE

The hydrodynamic model was calibrated with the observed daily flow data for G1H020, G1H036, G1H013 and G1R003. Calibration was achieved by adapting the Manning's roughness coefficient until a satisfactory fit was achieved between the observed daily flow values and the model results.

Table 7.6 shows the sensitivity of the Manning's n value with respect to the mean and the standard deviation calculated. A run with n=0.06 was completed, followed by two runs with n=0.04 and n= 0.08, and compared with the n=0.06 simulation, which was treated as "*observed*" data. The % difference was calculated by:

$$\%diff = (sim_{ni} - sim_{n\,obs})/(sim_{n\,obs}) * 100\%$$

Change in mean:

It can be seen from the results (Table 7.6) that by increasing the Manning's value by an amount of 0.02 the change in mean is more significant than decreasing the Manning's resistance. The difference in Manning's roughness coefficient has the most effect at stations G1H020 and G1R003. For G1H020 and G1H036 a higher mean is simulated for both a negative and a positive change in the Manning's resistance coefficient. At station G1H013 a lower resistance coefficient simulates a lower mean, while for station G1R003 the mean is simulated lower for higher and lower resistances. The percentage changes are however very low (mostly below 1%), which indicates that the flow simulation is influenced minimal by the resistance. The coefficient of determination (R^2) shows a minimal degree of correlation between the 'observed' and the simulated discharges for an increased mannings n roughness, especially for the low flow period. Figure 7.2 illustrates the sensitivity of the resistance.

Table 7.5 : Sensitivity of Flow Resistance

	Diff. in mean (m^3/s) n=-0.02	Diff. in mean (m^3/s) n=0.02	Diff. in std deviation (m^3/s) n=-0.02	Diff. in std deviation (m^3/s) n=0.02	Diff. in R^2 n=-0.02	Diff. in R^2 n=0.02
Low flow period						
G1H020	0.1	0.13	0.97	1.46	-0.25	-2.39
G1H036	0.04	0.1	2.34	-0.78	-1.48	-1.67
G1H013	-0.02	0.07	1.38	2.76	0.08	-4.97
G1R003	-0.18	-0.13	1	0.67	-1.96	-5.76
High flow period						
G1H020	0.08	0.1	0.31	1.23	-0.07	-0.45
G1H036	-0.24	0.44	-0.46	-0.19	-0.32	-1.4
G1H013	0.03	0.37	0.16	1.04	-0.55	-1.3
G1R003	0.1	0.51	-9.04	0.38	-0.09	-1.51

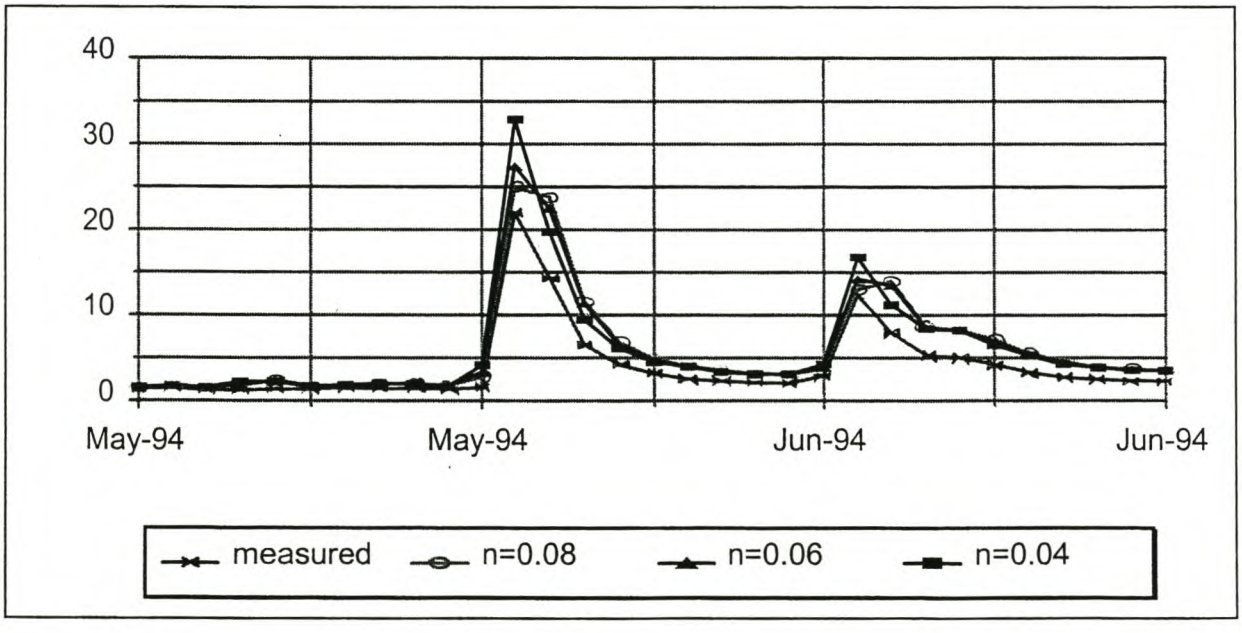

Figure 7.2: Sensitivity of Mannings Roughness Value

7.8 RESULTS OF FLOW MODEL CALIBRATION

For the final model a Manning's value of 0.06 was obtained by a trial and error approach as described in section 7.7. This value reproduced the observed values fairly accurately. The % error between the resistance factors is relatively small when compared to the error introduced by the missing flow in the peaks from the inflowing hydrographs, and the missing abstractions in the low flow period.

Low Flow:

It is evident from the large positive error in the low flow period (summer), that more abstractions take place than those registered/permitted. The result of the effect of alien invasive trees on the river flow, as well as the simplistic calculation of evaporation losses also contribute to the large positive error in the discharges. For calibration purposes an additional "lump" value could be added as additional unaccounted abstractions. It was however decided against it, as in certain time periods the low flow is very near to the measured data and additional abstractions could result in negative depths, which create instabilities when calculating the water quality (refer for example to Figure 7.8, where the simulated low flow follows the measured data quite comparably). The hydrograph of G1R003 (Figure 7.10) shows well defined short-lived increases in the simulated low flow, which is only slightly apparent in the measured data. These are due to the irrigation releases made by Voëlvlei Dam (refer also to Figure 6.2, where the inflow hydrograph of Voëlvlei releases can be seen). For G1H020 and G1H036 (Figures 7.4 and 7.6 respectively) the low flow pattern does not follow the measured data as consistently as for G1H013 (Figure 7.8) and the correlation coefficient is very low. For all gauging stations, March, April, October and November are clearly oversimulated. Refer to Figures 7.4, 7.6, 7.8 and 7.10 for the graphical representation of the results for the simulated low flow. Table 7.6 shows the statistical results of the comparison between the measured data and the simulated flow.

High Flow:

The simulated high flow follows the pattern of the measured high flow hydrograph for all stations, although the peaks are underestimated at especially G1H013 (Figure 7.7) and G1R003 (Figure 7.9) . G1H013 and G1R003 have an additional simulated peak in July, which is the result of the inflowing hydrograph of G1H008 (refer also to Figure 6.1), and the additional runoff from the ungauged subcatchment 8 that has been corrected with the flows of G1H008. The correctness of this adjustment may be suspect. The undersimulated flood peaks could be the result of errors in the correction of

ungauged subcatchments or errors in the measurement of the water level at tributary gauging stations, when flooded. The correlation coefficient at all stations for the high flow is acceptable. The volume and the mean are oversimulated although the actual peaks are undersimulated. This is due to the short period where the actual peak occurs, and the volume during the *"high flow"* winter months for the lower discharges is oversimulated.

Refer to Figures 7.3, 7.5, 7.7 and 7.9 for the graphical representation of the results for the simulated low flow. Table 7.6 shows the statistical results of the comparison between the measured data and the simulated flow.

Table 7.6 : Results of model calibration

	G1H020	G1H036	G1H013	G1R003
% diff in mean				
Total	5.6	17.6	-8	10
Summer	13.4	54	26	88
Winter	4.5	14.8	-10	6
R^2				
Total	0.98	0.98	0.92	0.94
Summer	0.83	0.71	0.73	0.64
Winter	0.97	0.98	0.92	0.93
MCE				
Total	0.95	0.95	0.81	0.87
Summer	0.41	0.54	0.47	0.22
Winter	0.94	0.96	0.82	0.88
% diff in std deviation				
Total	-2.4	9.6	-29	-13.7
Summer	18.8	-5.7	-12	1.47
Winter	-3.5	9.5	-30	-15

7.9 MODEL VERIFICATION

The term *verification* will be used to describe the process of ensuring that the model applied to the specific river for a particular set of calibration data can be applied to another period of data; this is to ensure that the errors in the simulated values are acceptable. The configured model was verified in space and time. Verification in time shows whether the errors are consistent for a total independent set of data in time; and whether the correction factors of the addition of ungauged runoff are acceptable. Verification in space indicates the degree of accumulation of errors along the four river reaches and whether the correction of the ungauged runoff is acceptable.

7.9.1 Verification in space

To verify the model in space, the measured flows at G1H020 was used as inflow hydrograph at G1H020 instead of the simulated values, and G1H036 was used as inflow hydrograph at G1H036. This was done to ensure that the errors are similar of the verification and configured model.

G1H020 and G1H036 as Inflow Hydrograph

It was clear after a verification run, using the G1H020 hydrograph as input at G1H020, that most of the errors downstream of this gauging stations occurred due to addition of ungauged inflow in this reach. Table 7.7 summarizes the result between the verification model, the measured data and the original model. From the results of G1H020 it can be perceived that the configured model represents the verification model, although the summer flows are still oversimulated at the downstream stations. The correlation coefficient of the verification run is higher than the configured model and this could be due to the simulated peaks that are measured in the low flow period. The systematic error is much less than in the configured model. Most of the errors that take place at G1R003 could be the result of incorrect addition of flow from the ungauged catchments between G1H020 and G1H036. This is portrayed by the improvements in the errors when using G1H036 as inflow hydrograph. Additional abstractions may occur in this reach.

Table 7.7 Results of Verification Run using G1H020 as Inflow Hydrograph

		G1H036	G1H013	G1R003
% diff in mean				
original model run	Summer	54	26	88
	Winter	14.8	-10	6
verification run	Summer	37	16	68
	Winter	7	-15	0.5
R^2				
original model run	Summer	0.71	0.73	0.64
	Winter	0.98	0.92	0.93
verification run	Summer	0.96	0.85	0.77
	Winter	0.97	0.91	0.93
MCE				
original model run	Summer	0.54	0.70	0.22
	Winter	0.96	0.82	0.88
verification run	Summer	0.64	0.65	0.08
	Winter	0.93	0.79	0.86

Table 7.8 Results of Verification Run using G1H036 as Inflow Hydrograph

		G1H013	G1R003
% diff in mean			
original model run	Summer	26	88
	Winter	-10	6
verification run	Summer	-7	27
	Winter	-20.5	-5
R^2			
original model run	Summer	0.73	0.64
	Winter	0.92	0.93
verification run	Summer	0.94	0.85
	Winter	0.94	0.95
MCE			
original model run	Summer	0.77	0.22
	Winter	0.82	0.88
verification run	Summer	0.87	0.71
	Winter	0.77	0.87

7.9.2 Verification in time

Verification in time was completed by using a totally independent set of data and comparing the errors to the errors resulting from the configuration model. The year 1994/1995 was chosen for verification in time, as 1996 and 1997 comprises of gaps in flow measurement at G1H036 and G1H013, and not all flow measurements are recorded yet for 1998/1999. Unfortunately, for the station G1H036 the flow measurements are also incomplete from the 3rd of July onwards. It therefore should be noted that the statistical comparison for the high flows have only been included up to that date and are thus not a complete reflection on the correlation to the measured data. The other stations reflect the differences between the measured and the calculated data. This year has experienced much higher flows and also more defined high peaks (3 larger peaks and smaller peaks before July) than the configuration data (one

defined peak). Figures 7.11 to 7.18 show the verification simulated values graphically.

Comparing Tables 7.9 and 7.6, it can be seen that the errors simulated for the verification data are less than for the calibration data. This indicates that the correction factors applied to the ungauged runoff are acceptable. G1R003 is again oversimulated by a high percentage for the summer period. This would be the result of unknown abstractions, as the contribution of flow from the corrected ungauged areas 7,9 (refer to Figure 7.1) is minimal in this period, as the tributary G1H034 is semi-perennial. The simulated low flow displays a better degree of correspondence than the configured data (refer to Table 7.7), and all coefficients of determinations are above 0.8. Again it can be perceived that the correction factors applied to the ungauged runoff and the information obtained about the abstractions prove to be satisfactory for the low flow, except for the reach G1H013 to G1R003

Table 7.9: Verification in time (1994/1995)

	G1H020	**G1H036**	**G1H013**	**G1R003**
% diff in mean				
Total	-27	12	-30	-8
Summer	5.8	31.3	15.1	72
Winter	-34.6	-0.4	-36	-16.7
R^2				
Total	0.91	0.86	0.82	0.88
Summer	0.80	0.82	0.86	0.81
Winter	0.90	0.86	0.80	0.87
MCE				
Total	0.63	0.72	0.50	0.76
Summer	0.91	0.78	0.82	0.60
Winter	0.69	0.79	0.57	0.80
% diff in std deviation				
Total	-51	0.3	-55	-28.2
Summer	-7.5	-11	14	9.8
Winter	-52	3.8	-58	-29

7.10 DISCUSSION OF FINAL MODEL RESULTS

The objective in this chapter was to develop a flow model capable of predicting the hydrograph at any point in the main river channel. It can be concluded from the statistics mentioned for the various calibration and verification runs, that the model has the ability to predict, with sufficient accuracy, the hydrograph at any downstream section in the river. The accuracy is mainly dependent on the accuracy of the inflowing measured hydrographs and also the estimated runoff of ungauged subcatchments. Other factors such as the accuracy of the boundary conditions also contribute to the errors.

The model accurately predicts the mass balance in the system, but knowledge of flow discharging into the river is insufficient to accurately add missing peak flow in order to be able to predict the hydrograph exactly as was measured. The errors resulting for underestimation of the high flow peaks and overestimation of the low flow, are mainly the result of inaccurate estimation of the ungauged flow. This can be seen from the verification simulation in space (section 7.9). To be able to predict a flow hydrograph accurately, the input data and all the information about abstractions and return flows need to be known. Unfortunately, for most situations, this information is either inaccurate, incomplete or non-existent.

The verification in time proved that the correction factors applied to the low flow are satisfactory. The results of the verification in time proved to be better than the configured data results. The correction factors for the high flow are however not acceptable, as the peak flows which are higher than the configured peaks are about 125 m^3/s less. Either the actual peak flows measured at the gauging stations are unacceptable or additional correction factors should be applied to the ungauged runoff, although this should have been covered by the MAP/MAR correction factor.

7.11 REFERENCES

DWAF, 1994. *Flow Gauging Stations*: *Calibration and Evaluation, Volume I to VI*: *Particulars of Gauging Stations*. Prepared by A Rooseboom and G R Basson of Ninham Shand Inc. in association with BKS Inc. As part of the Western cape System Analysis. DWAF report no. P G000/00/1090

Görgens, A.H.M., 1983. *Conceptual Modelling of the Rainfall-Runoff Process in Semi-Arid Catchments*. Hydrological Research Unit, Rhodes University, Report No. 1/83, Grahamstown, South Africa.

Grijsen, J.G., 1986. *River Flow Simulation* in River Flow Modelling and Forecasting (ed D.A. Kraijenhoff and J.R. Moll). 241-272

Kraijenhoff, D.A. and J.R. Moll (eds.), 1986. *River Flow Modelling and Forecasting*. D. Reidel Publishing Company.

Midgley, D.C., W.V. Pitman and B.J. Middleton, 1994. *Surface Water Resources of Southern Africa 1990: Volume 4.* WRC Report 298/4.1/94 (Appendices) and 298/4.2/94 (Book of maps).

Reckhow, K. H., Clements, J. T. And R.C. Dodd, 1990. *Statistical Evaluation of Mechanistic Water-Quality Models.* ASCE Journal of Env. Eng. Vol 116 No 2, pg 250-268.

Figure 7.3: Discharge at G1H020 for high flows (calibration simulation)

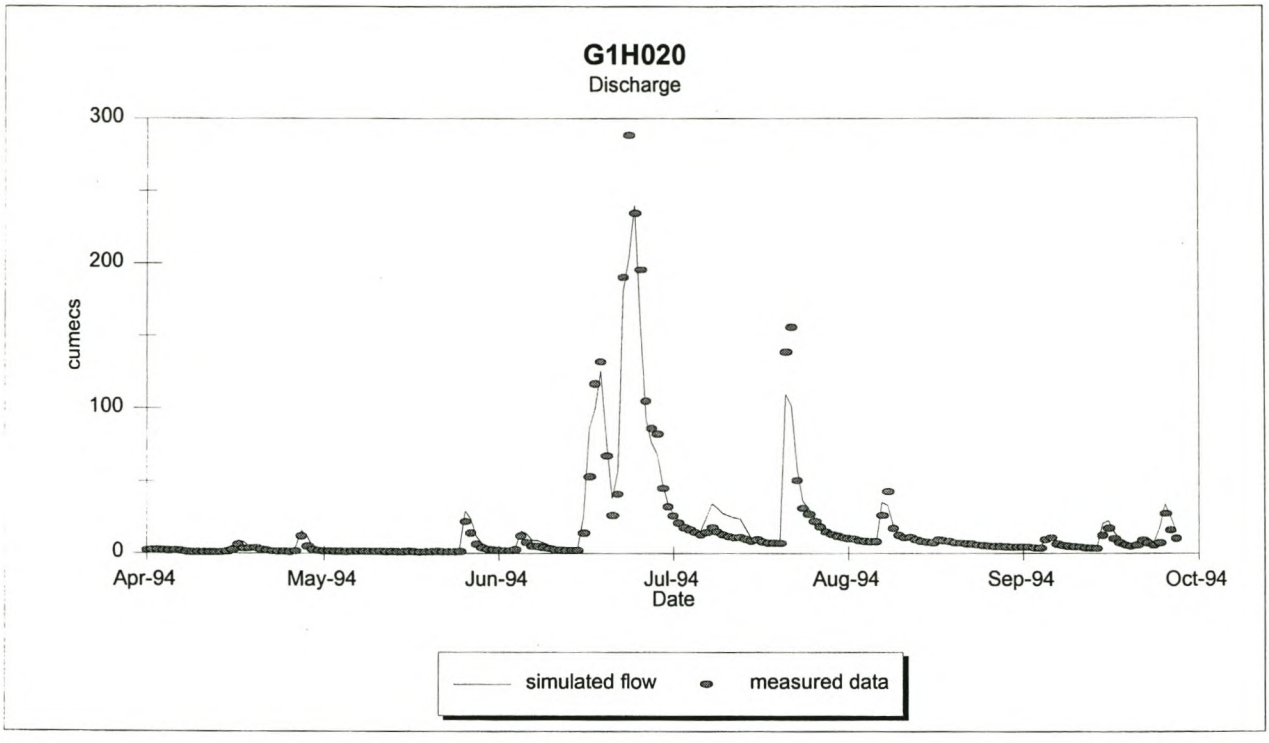

Figure 7.4: Discharge at G1H020 for low flows (calibration simulation)

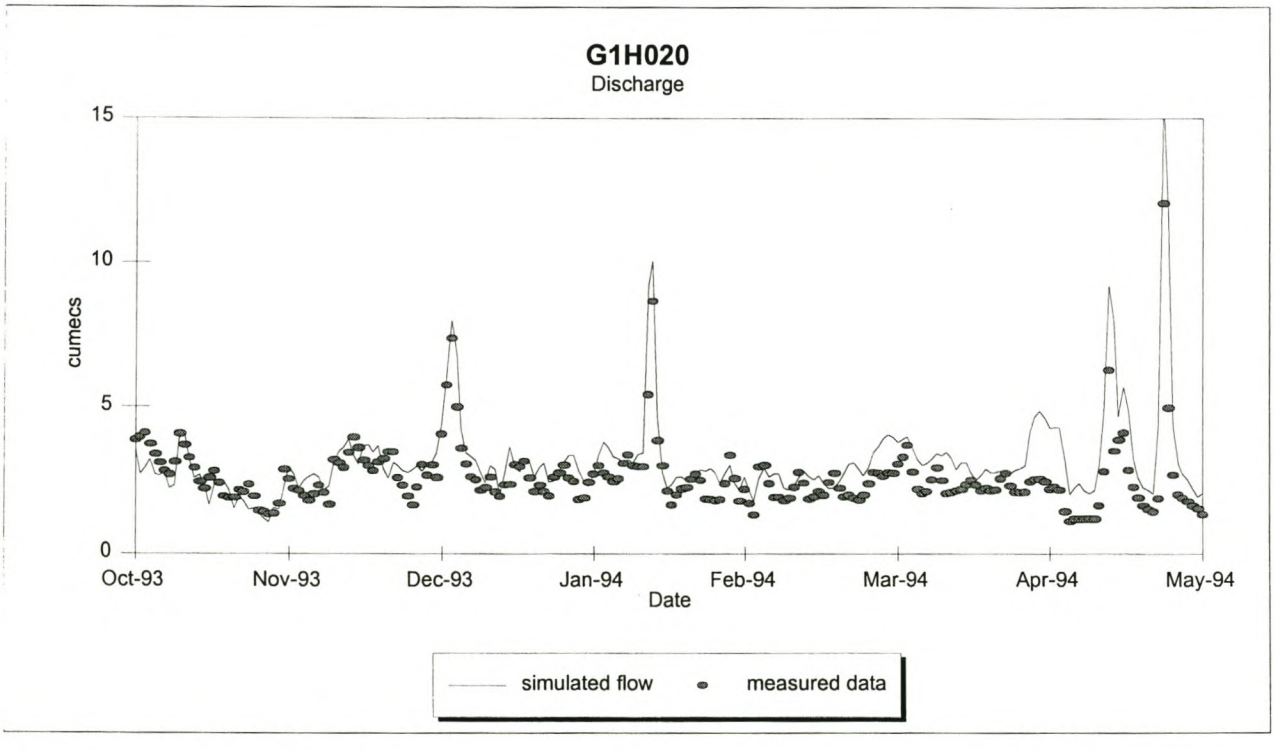

Figure 7.5: Discharge at G1H036 for high flows (calibration simulation)

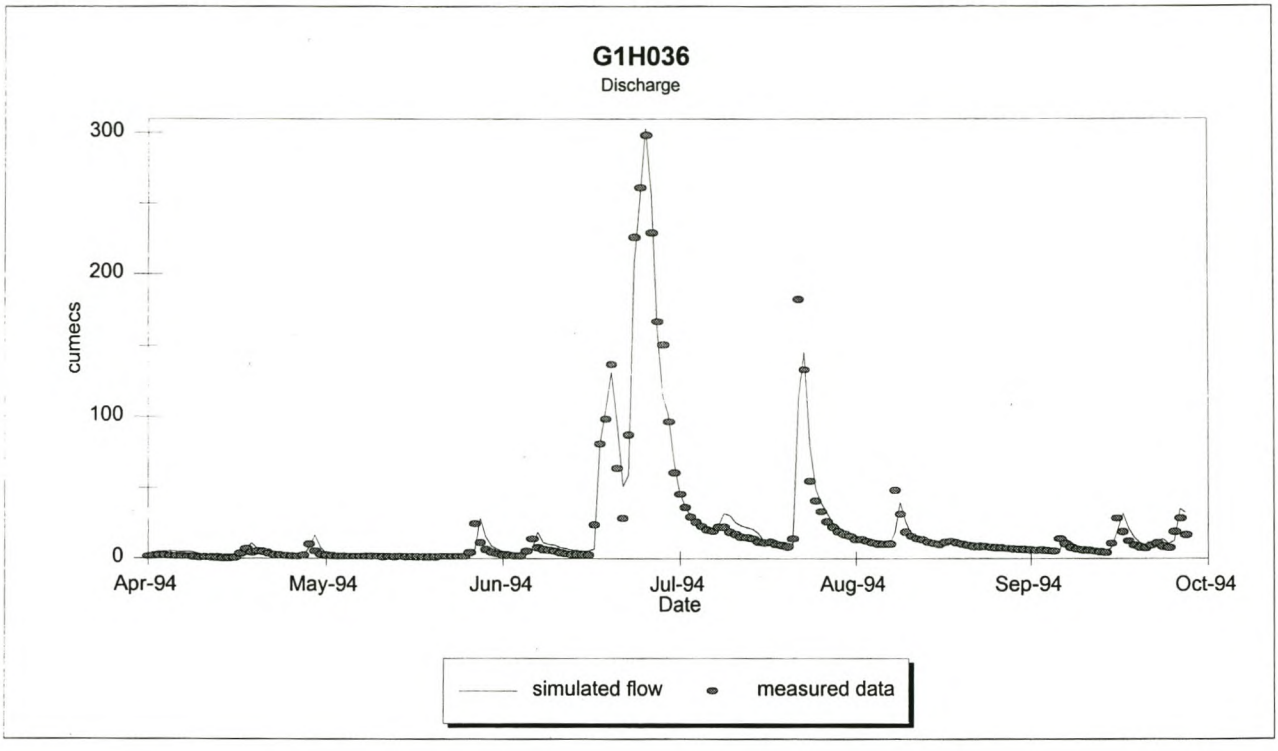

Figure 7.6: Discharge at G1H036 for low flows (calibration simulation)

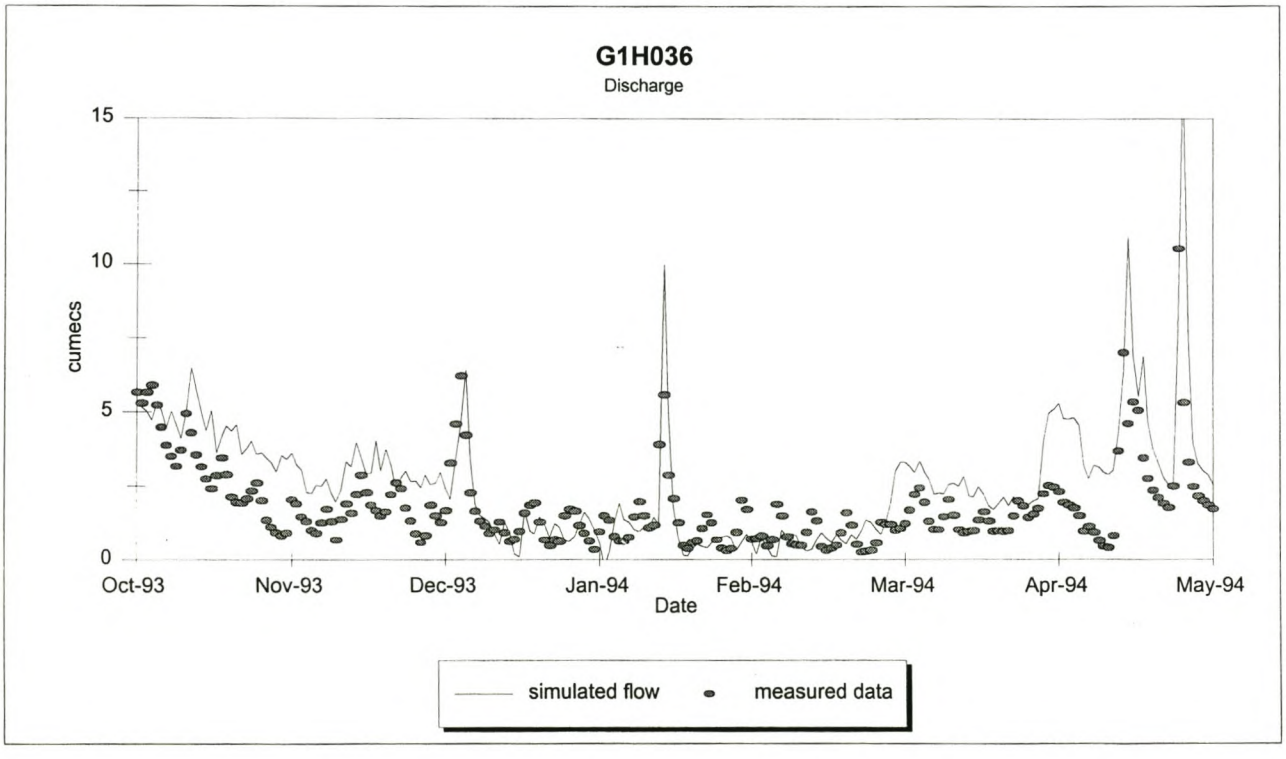

Figure 7.7: Discharge at G1H013 for high flows (calibration simulation)

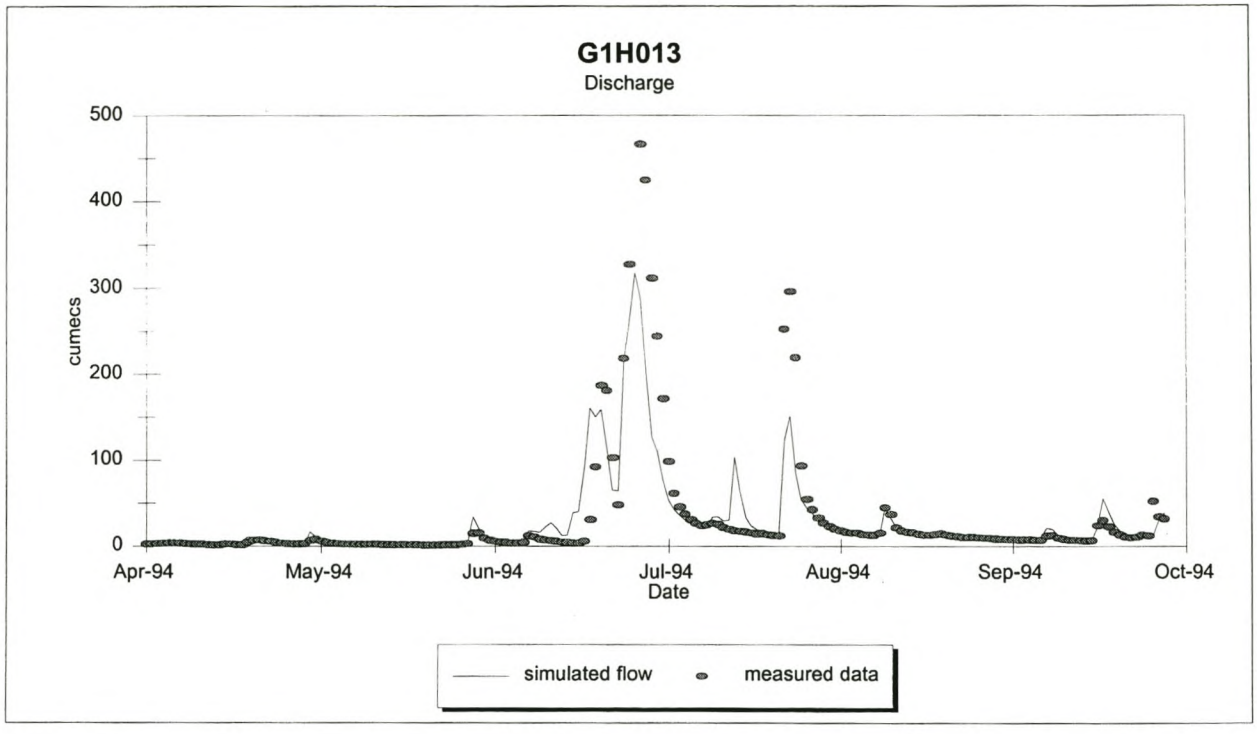

Figure 7.8: Discharge at G1H013 for low flows (calibration simulation)

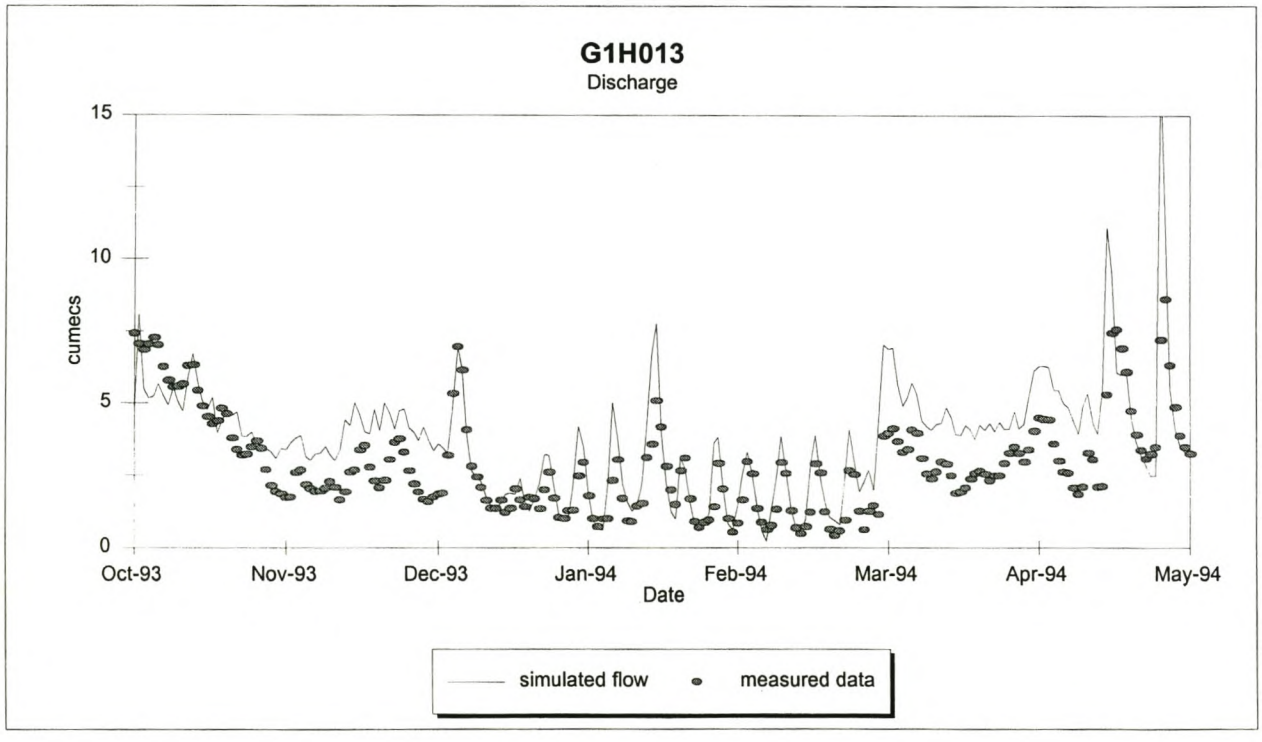

Figure 7.9: Discharge at G1R003 for high flows (calibration simulation)

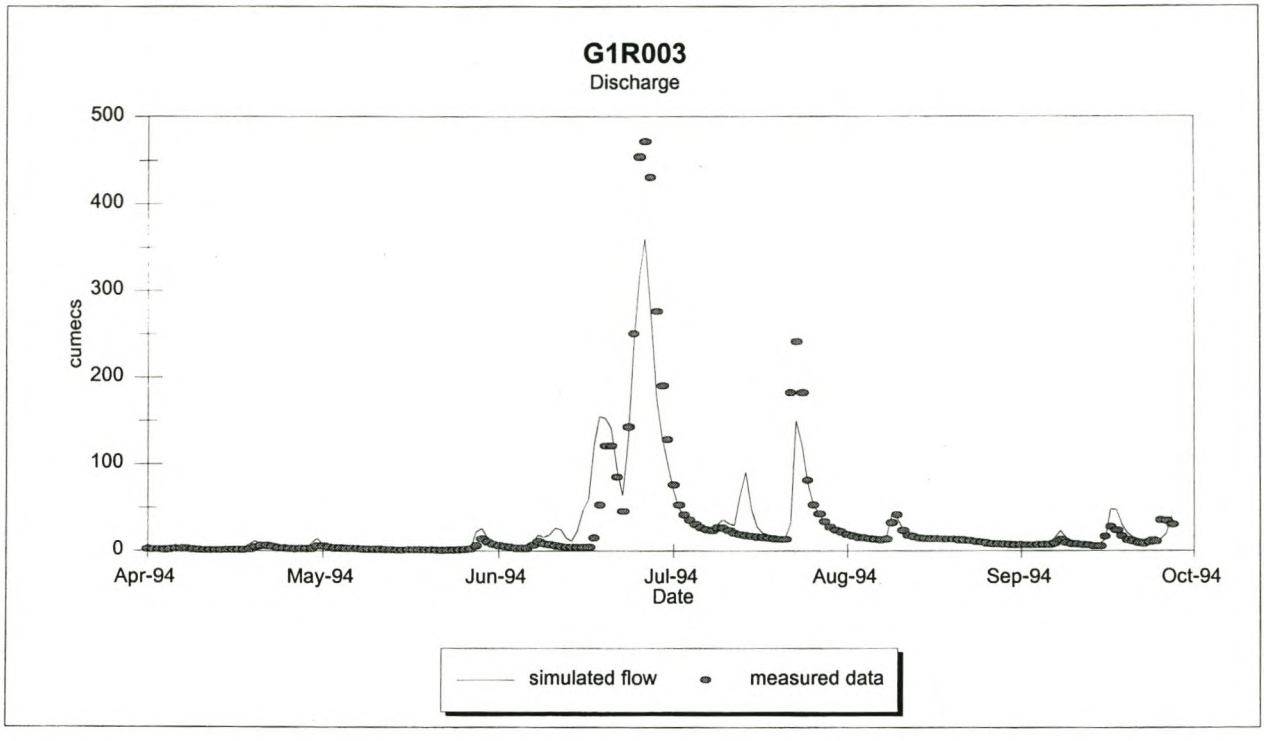

Figure 7.10: Discharge at G1R003 for low flows (calibration simulation)

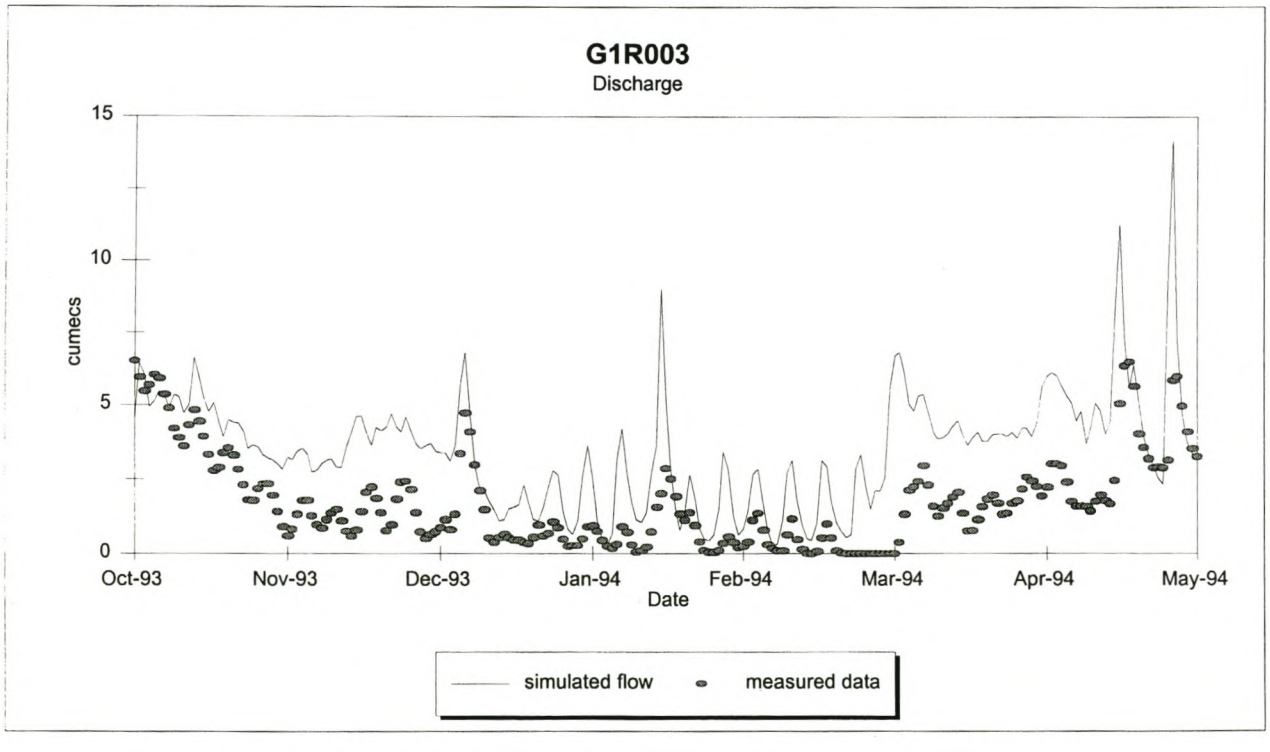

Figure 7.11: Discharge at G1H020 for high flows (verification simulation)

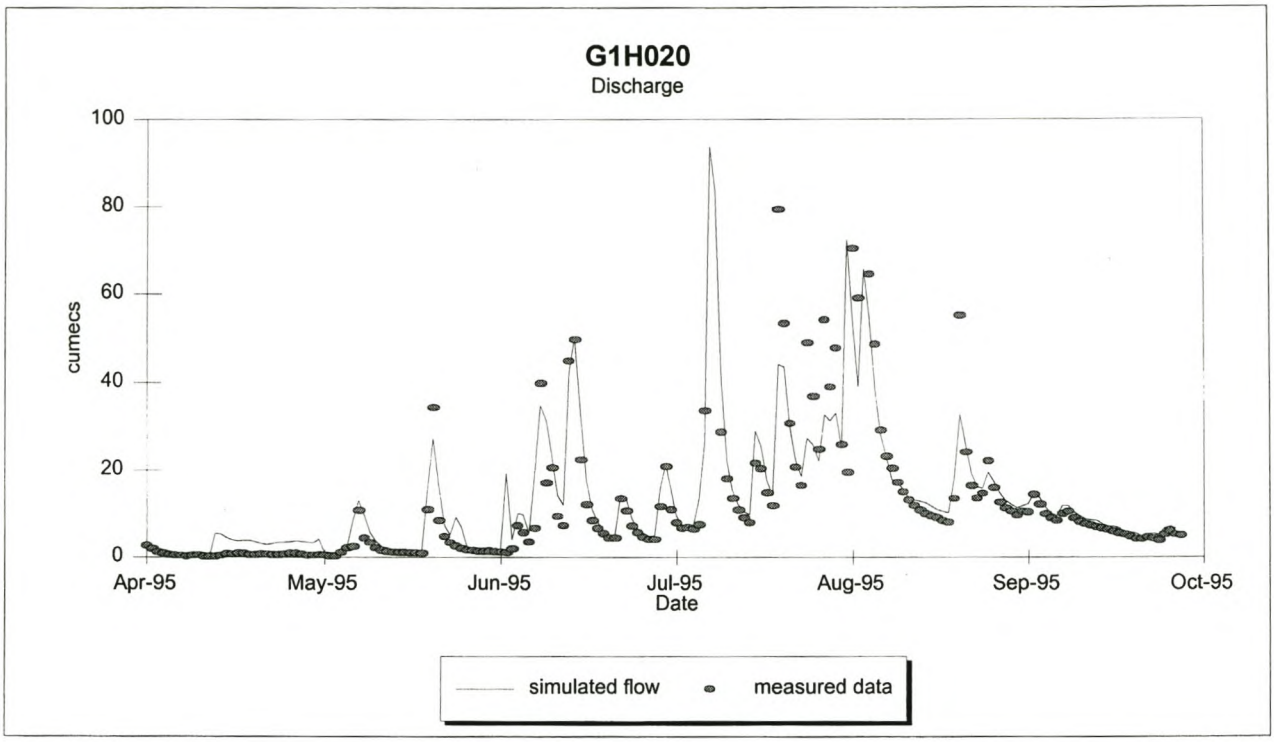

Figure 7.12: Discharge at G1H020 for low flows (verification simulation)

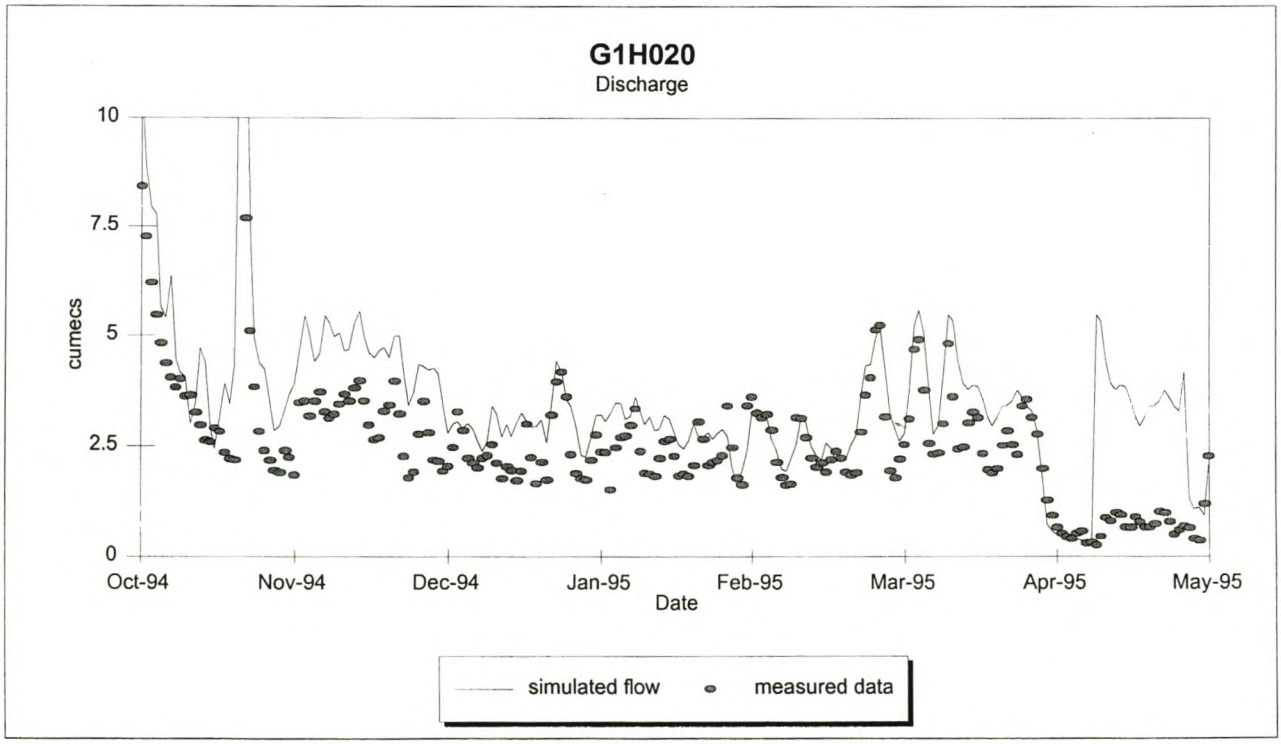

Figure 7.13: Discharge at G1H036 for high flows (verification simulation)

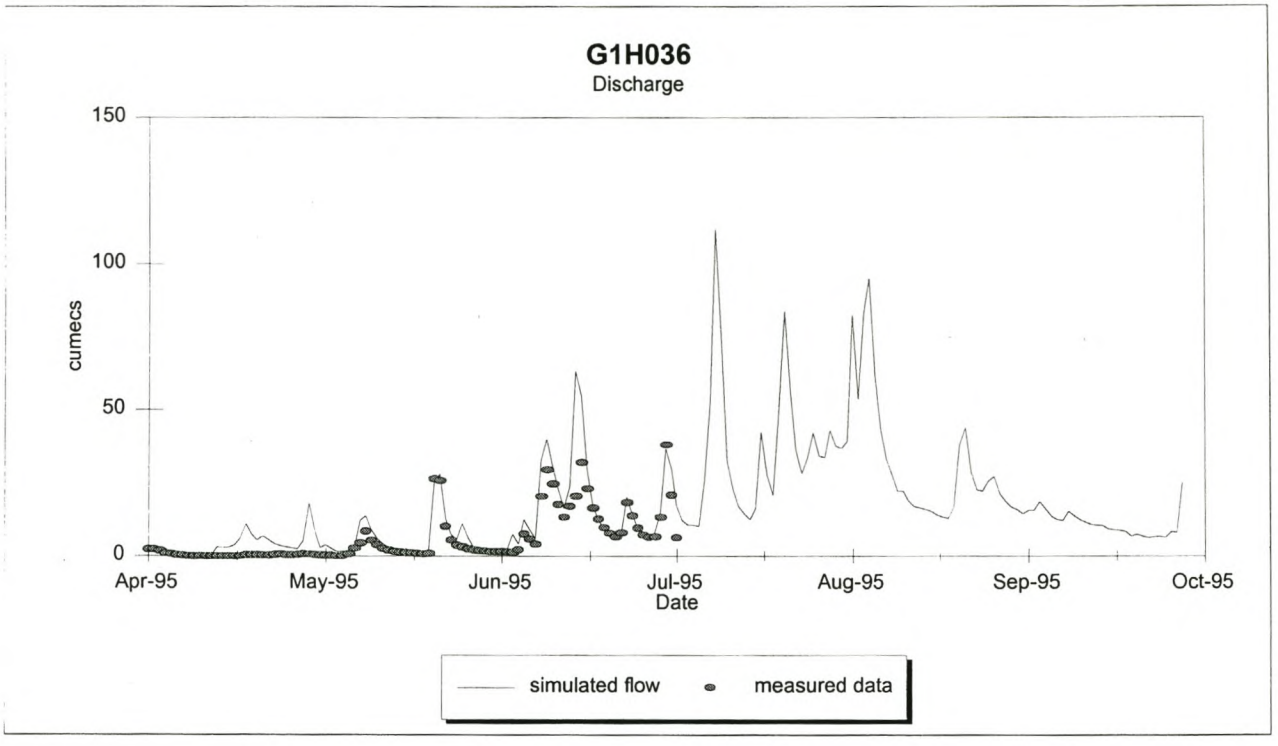

Figure 7.14: Discharge at G1H036 for low flows (verification simulation)

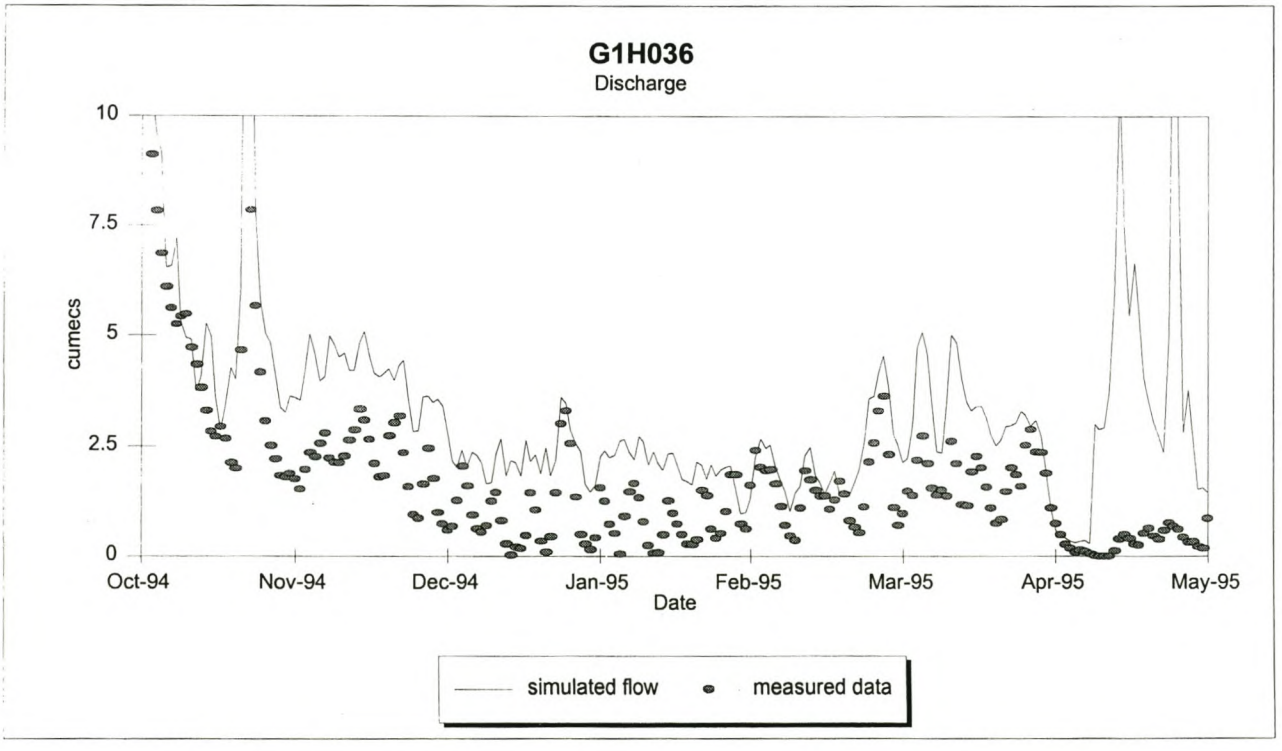

Figure 7.15: Discharge at G1H013 for high flows (verification simulation)

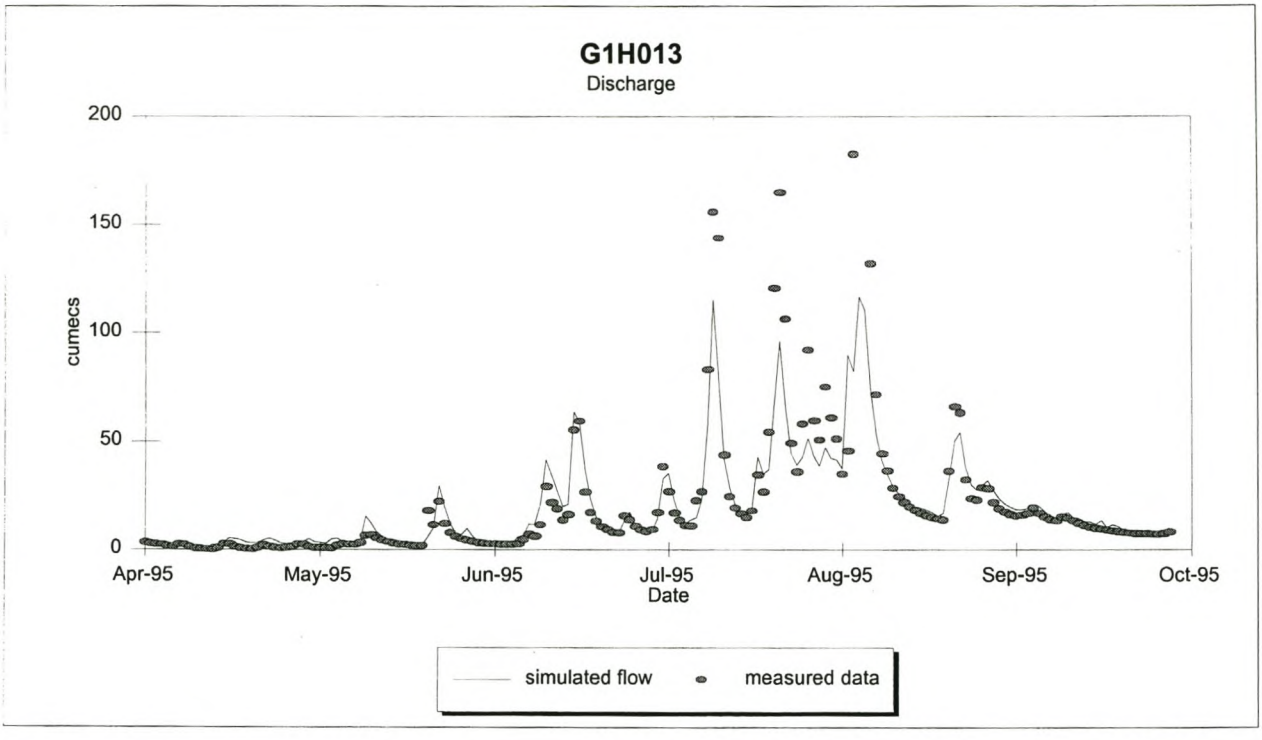

Figure 7.16: Discharge at G1H013 for low flows (verification simulation)

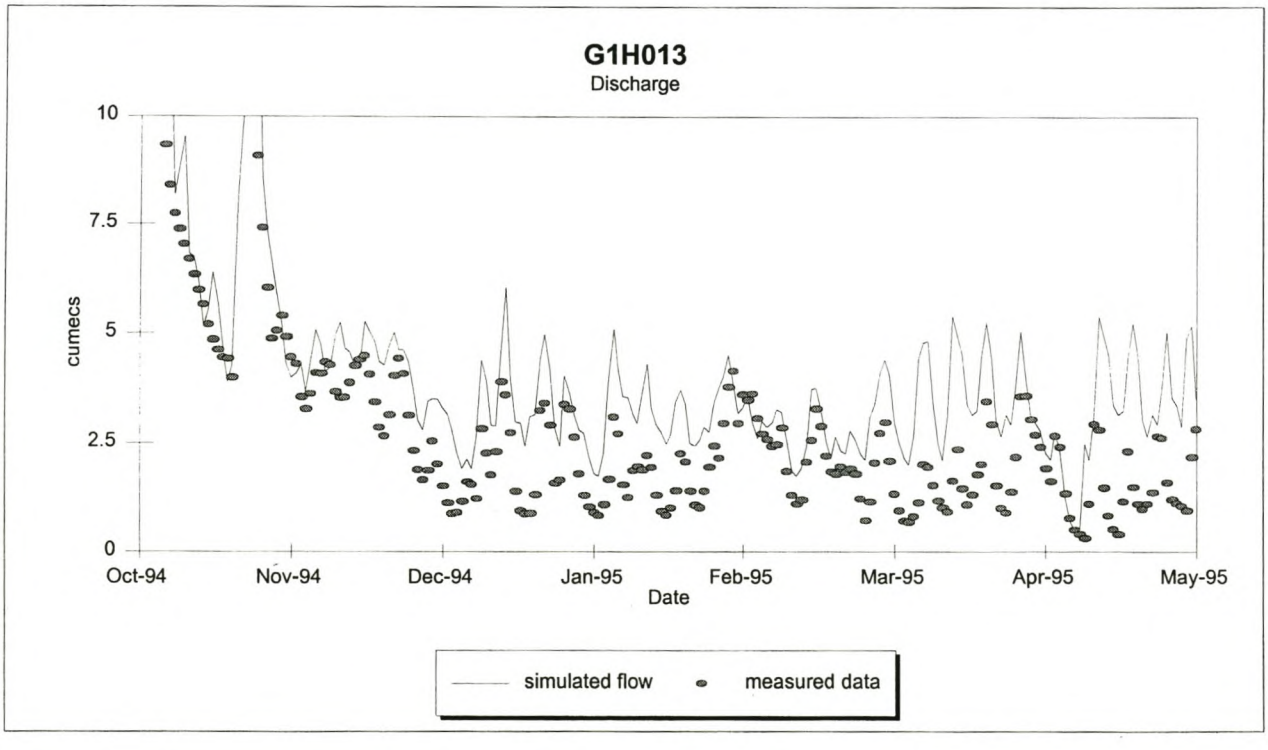

Figure 7.17: Discharge at G1R003 for high flows (verification simulation)

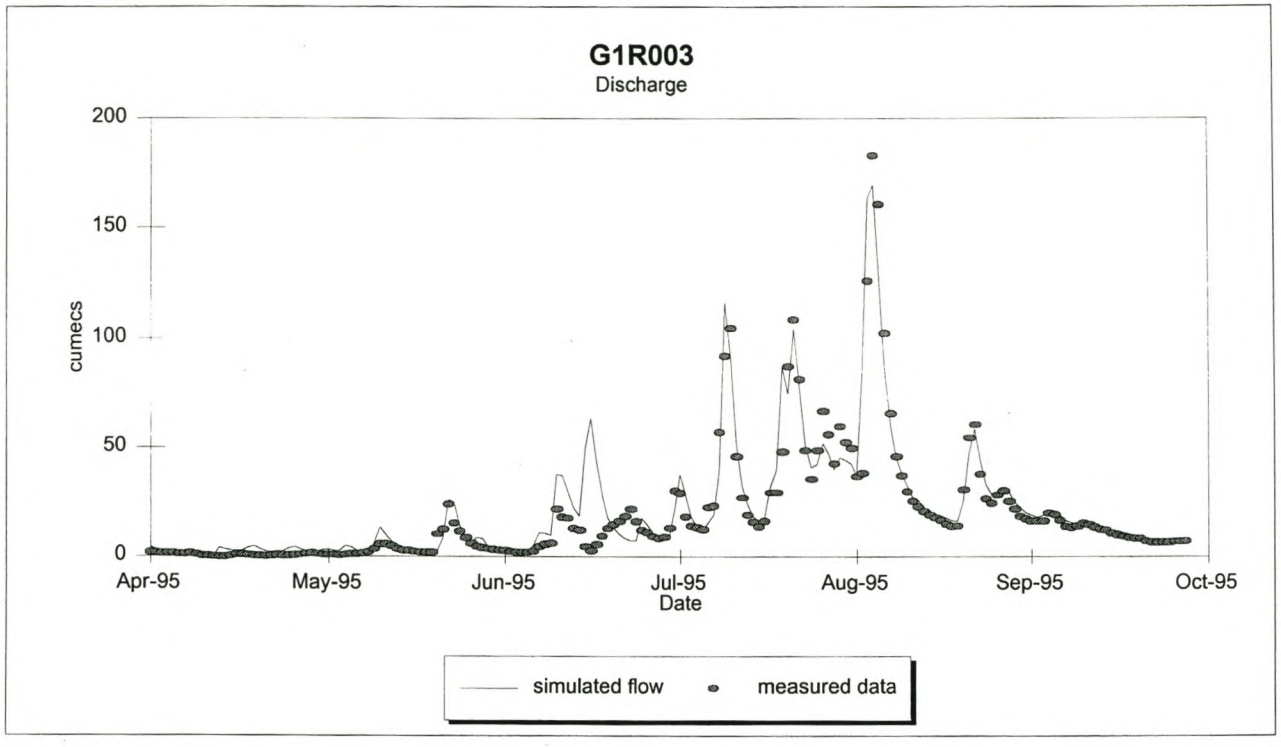

Figure 7.18: Discharge at G1R003 for low flows (verification simulation)

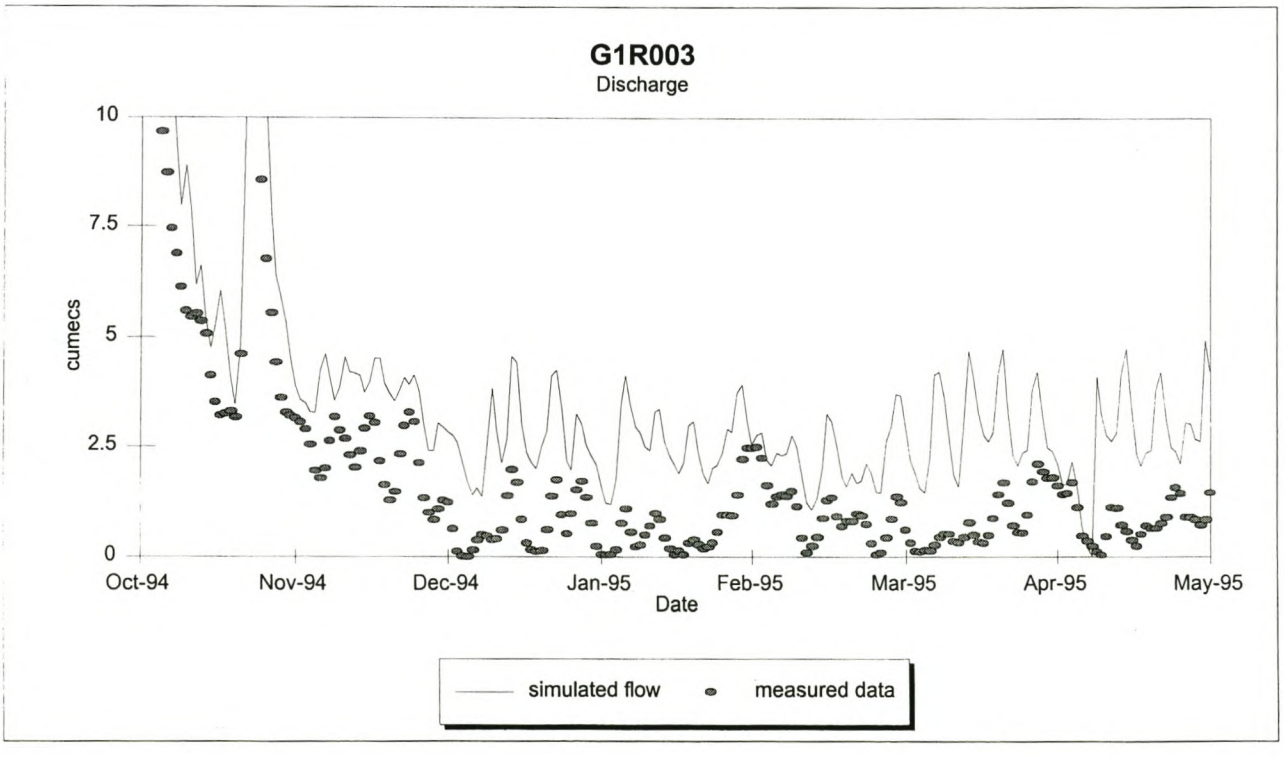

CHAPTER 8

WATER QUALITY MODEL SENSITIVITY, CALIBRATION AND VERIFICATION

8.1 INTRODUCTION

The focus of this chapter is on the sensitivity of the water quality parameters used in the various water quality processes and the calibration and verification of the water quality simulation. The accuracy of the water quality parameters is largely dependent on the accuracy of the flow simulation; therefore, the errors of the flow simulation have to be borne in mind when analysing the result of the water quality simulation. The sensitivity analysis of the water quality parameters determines the adjustments of these parameters in order to obtain a satisfactory fit that compares reasonably well with the observed data.

8.2 MODEL CALIBRATION AND SENSITIVITY PROCEDURE

Following a similar calibration procedure to that of the flow calibration (refer to section 7.3), the following steps were taken in the calibration of the water quality processes:

- Determination of a reliable calibration period with respect to water quality data, bearing in mind the objectives and decision on an optimum calibration period for the flow simulation
- Determining accuracy of boundary conditions
- Introducing water quality of ungauged tributaries
- Calibrating water quality by adjusting the parameters
- Introducing point sources .

8.3 DETERMINATION OF RELIABLE CALIBRATION PROCEDURE

The calibration period was based on the years after the change of preservation of water quality samples that took place in 1989 (refer to section 4.6.1). The period October 1993 to Sept 1994 is optimal for the flow calibration, as it occurs after the critical year.

8.4 BOUNDARY AND INITIAL CONDITIONS

The only known measure of error that can express the accuracy of the boundary conditions, is the error calculated in the infilling method (refer to section 6.3.1). These errors are summarized in Table 8.1.

Table 8.1: Accuracy of water quality boundary conditions

Water Quality Variable	G1H004
TDS	-2.8% error in mean concentration $R^2 = 0.93$ for load
Phosphates	-5.5% error in mean concentration $R^2 = 0.92$ for load
Temperature	Summer mean error -0.19 %, Winter mean error -3.5 % $R^2 = 0.75$
Oxygen	The accuracy of oxygen could not be analysed as no data is available. The oxygen is however dependent on the temperature data and thus as a rough estimate the same measure of error exists for the oxygen as for the temperature.

As water flows out of the system at Misverstand (G1R003), DUFLOW calculates the corresponding outflowing quality for the specific outflowing volume. Therefore, the downstream water quality boundary accuracy is dependent on the accuracy of the downstream flow boundary.

An error in the initial values does not have an effect on the calculations, as any errors occurring due to inaccuracies of the initial values are soon cancelled after few time steps. Enough time has been given in the simulation run for the flow to stabilise before any results are written to a file.

8.5 ADDITION OF UNGAUGED WATER QUALITY SUBCATCHMENTS

The water quality load contributions from areas that were ungauged had to be estimated. The same ungauged areas are applied for estimating the ungauged water quality loads as was used for ungauged flows (Table 7.3 and Figure 7.1). It has been assumed that the ungauged runoff has similar water quality characteristics as the neighbouring gauged tributaries. As a moving regression is suitable to describe the water quality-flow relationship, the same *'infilling'* method, as has been described in section 6.3.1, has been used to approximate the daily water quality of ungauged runoff. The ungauged runoff that has been calculated according to Table 7.3 has been matched with the water quality grab samples of a gauged tributary that is surmised to have similar characteristics. A time series was generated via the moving regression infilling method. Table 8.2 shows the gauged and ungauged areas that have been linked, and has to be read in conjunction with Table 7.2 and Figure 7.1. The summary of the statistics of the infilled values can be read in Tables 8.3 and 8.4.

Figure 8.1 compares the infilled water quality concentration of areas 1 and 2 with infilled concentration of gauging station G1H020, while Figure 8.2 compares areas 4 and 5 with the original infilled concentration time series of G1H039. From the Figures 8.1 and 8.2 one can see that the infilling method does follow the characteristics of the water quality concentration of the corresponding 'linked' gauged area. Most of the ungauged areas experience higher runoff than the gauged areas, primarily due to area size, and this is reflected in the negative "error" in the TDS infilling. Areas 1 and 2 receive less runoff than G1H020 and therefore a positive error in mean concentration is calculated. Interestingly, the infilled phosphate values show all negative errors in mean to the original grab sample.

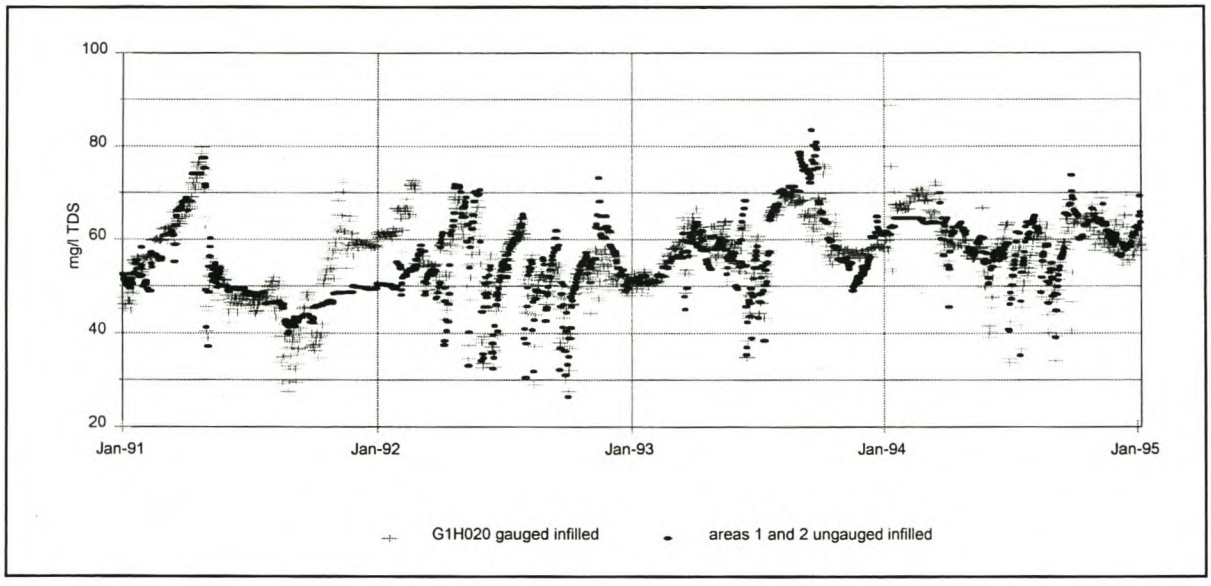

Figure 8.1: Comparison of infilled water quality concentration of areas 1 and 2 with infilled concentration of gauging station G1H020

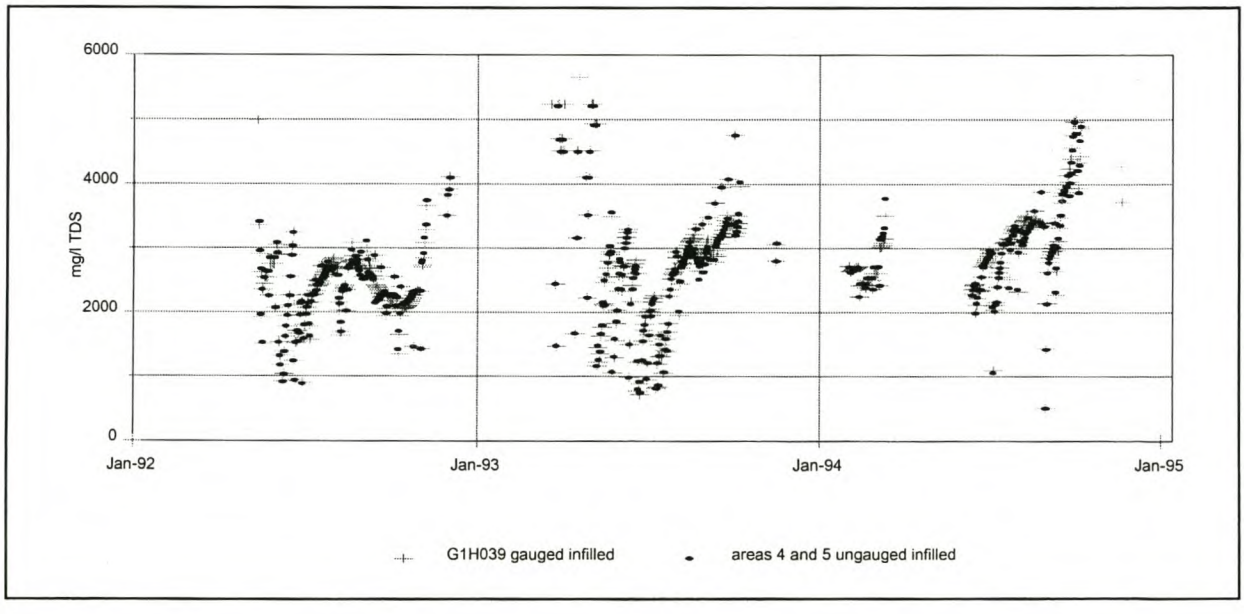

Figure 8.2: Comparison of infilled water quality concentration of areas 4 and 5 with infilled concentration of gauging station G1H039

Table 8.2: Correction of ungauged concentration

Ungauged Catchment Runoff of Area Number:	**Infilled with water quality grab samples of station:**	**Comment**
1 and 2	G1H020	The water quality samples of the upstream gauged areas (A,B,C,D) are of better quality, due to the fresh water in the mountains, than the water quality of runoff from the areas 1 and 2. It has therefore been assumed that the water quality concentration of areas 1 and 2 would rather follow a similar pattern to the concentration data that has been sampled at G1H020.
3	G1H041 (E)	It has been assumed that the water quality from area 3 would be similar to the water quality that has been sampled at G1H041, as both subcatchments drain Table Mountain Sandstone soil, which is of better quality than the water quality of the runoff from the Malmesbury Shales.
4 and 5	G1H039 (F)	As subcatchments 4 and 5 experience similar rainfall-runoff pattern than subcatchment F and also drain Malmesbury Shales, which produces high salinities, it has been assumed that the corrected runoff from subcatchments 4 and 5 could be linked to the water quality samples of G1H039.
6	G1H043 (G)	Subcatchment 6 has been linked with subcatchment G, because of similar rainfall-runoff and also similar soils (Malmesbury Shales).
8	G1H008 (I)	It has been assumed that the water quality from area 8 will be similar to the water quality that has been sampled at G1H008, as both subcatchments drain Table Mountain sandstone soil. The rainfall experienced in subcatchment 8 is however less than subcatchment H, and portions of the flow is diverted to Voëlvlei Dam.
7 and 9	G1H034 (J)	The water quality sampled at G1H034 has been assumed to be similar characteristics to the water quality that can be expected at subcatchments 7 and 9.

Table 8.3: Statistic of ungauged TDS Values

Subcatchment No	No of Samples	Mean Conc (infilled) (mg/l)	Mean Conc (Grab Samples) (mg/l)	% error in mean	Std. Dev (infilled)	Std. Dev (grab samples)	R^2
1 and 2	319	60.4	60.2	3	9.7	12.1	0.97
3	234	159.7	174	-8	51	88	0.78
4 and 5	130	2636	2712	-3	710	897	0.81
6	110	4693	4718	-0.5	1293	1356	0.77
8	300	113	117	-4	29.4	40.4	0.72
7 and 9	315	6304	6253	8	2214	2297	0.91

Table 8.4: Statistic of ungauged PO_4 Values

Subcatchment No	No of Samples	Mean Conc (infilled) (mg/l)	Mean Conc (Grab Samples) (mg/l)	% error in mean	Std. Dev (infilled)	Std. Dev (grab samples)	R^2
1 and 2	326	0.024	0.028	-14	0.013	0.05	0.75
3	231	0.02	0.024	-15	0.01	0.02	0.57
4 and 5	128	0.29	0.33	-10	0.15	0.21	0.71
6	110	0.03	0.036	-17	0.01	0.02	0.60
8	294	0.016	0.017	-7	0.01	0.01	0.75
7 and 9	317	0.15	0.176	-17	0.15	0.18	0.74

8.6 SENSITIVITY OF WATER QUALITY PARAMETERS

8.6.1 Dispersion

The calibration of the transport dispersion was attempted by adjusting the dispersion for the conservative constituent, TDS. TDS is only dependant on the dispersion and therefore is a good indicator of the influence of the dispersion parameter. As can be seen from the Figure 8.1, dispersion has a minimal effect on the simulated results.

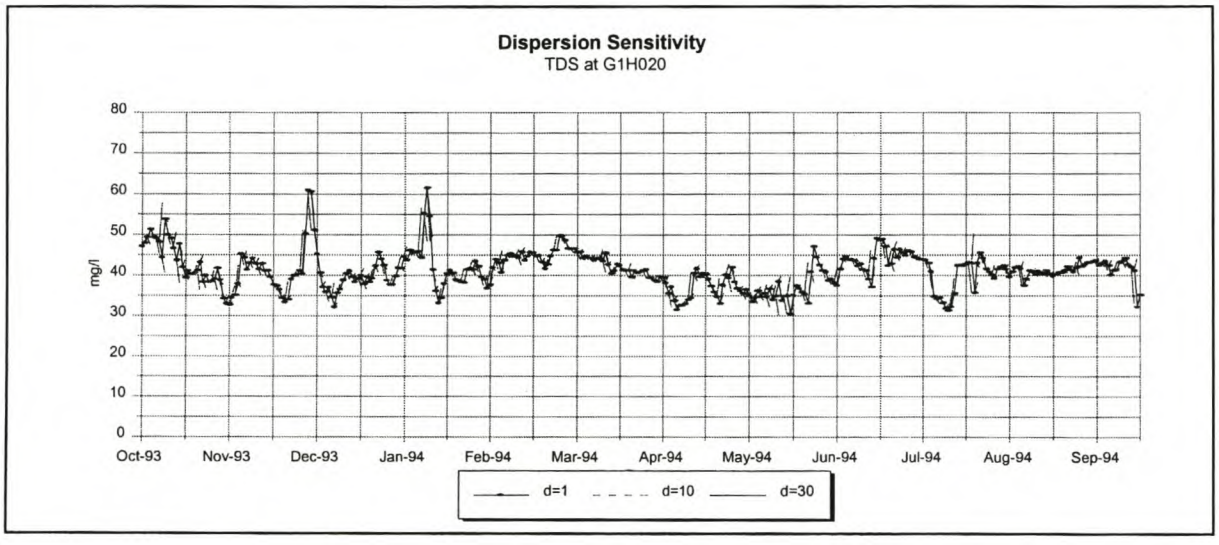

Figure 8.3: Dispersion Sensitivity

DUFLOW has an additional option known as '*decouple*'. If this option is chosen, dispersion is only considered in a downstream direction. Decoupling only takes place at nodes with a discharge.. The DUFLOW manual suggests using the decouple option to prevent flattening of steep concentration gradients at nodes where a discharge is located (STOWA, 1998). A simulation run was completed with dispersion set at 30 m^2/s for both options. The non-decouple option shows a difference of -0.062 % in both mean and variance. The non-decouple option however indicates slightly more unstable calculations just before the discharge points (tributaries entering the system), as can be seen in Figure 8.4.

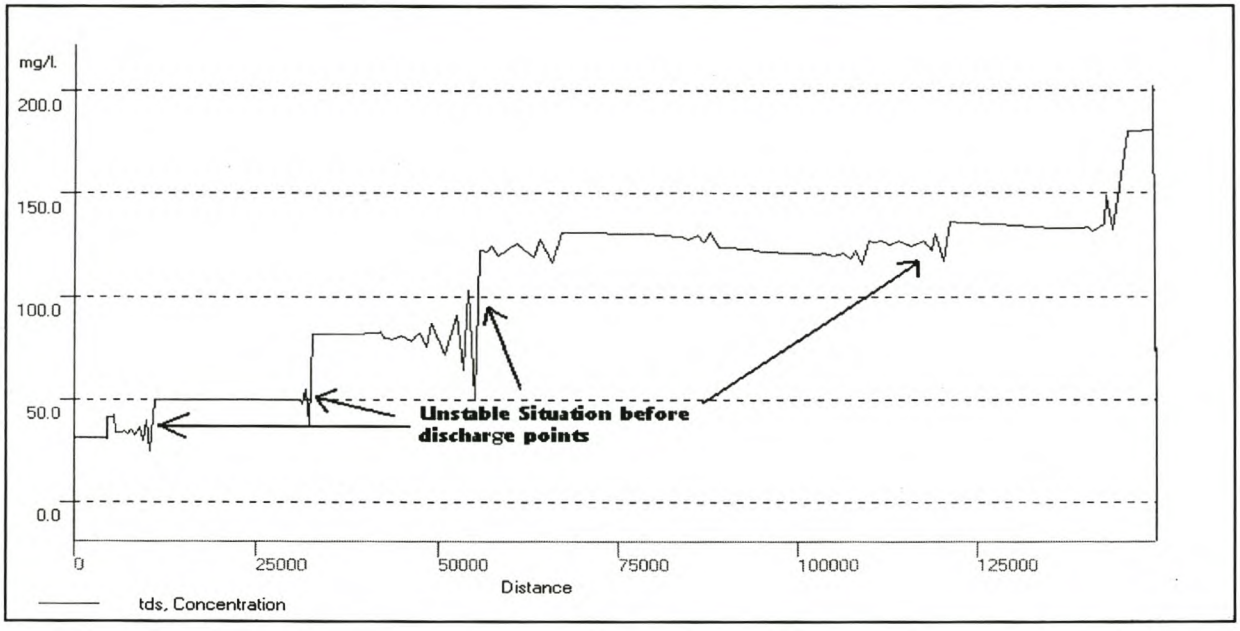

Figure 8.4: Concentration using non-decouple dispersion

8.6.2 Phosphorous

Sensitivity analyses have been performed for the parameters that affect the phosphorous concentration (refer to section 5.4.5.2), which are θ_{min} and k_{min}. The sensitivity runs show that these parameters have insignificant influence on the concentration, and therefore the phosphorous concentration is only dependant on the transport calculations.

8.6.3 Temperature

The parameters that can be changed for calibration purposes occur in atmospheric longwave radiation and water longwave back radiation.

Parameters:

Recalling the equation from section 5.4.5.1, the parameters that have an influence on the atmospheric longwave radiation are A, a constant, and R_L, the cloud cover. The Stefan Boltzmann constant cannot

be varied. The term describing the back radiation of the water surface contains the parameter ϵ (emissivity of a body), as it is represented by Stefan Boltzmann's law.

Figures 8.5 to 8.8 summarize the results for the summer temperatures of the different sensitivity runs completed for the parameters A and R_L. The summer temperatures are more sensitive to changes in the parameters (due to the low flow water depth, refer to equation 5.39). It was decided after the sensitivity runs that a R_L value of 0.03 and an A value of 0.55 seemed to depict an acceptable maximum summer temperature when compared with the maximum summer temperatures of the observed data. The average values calculated are however all lower than the measured data when using these parameters. The reasonable overall averages and visual comparisons of the trends however allowed acceptance of these parameters.

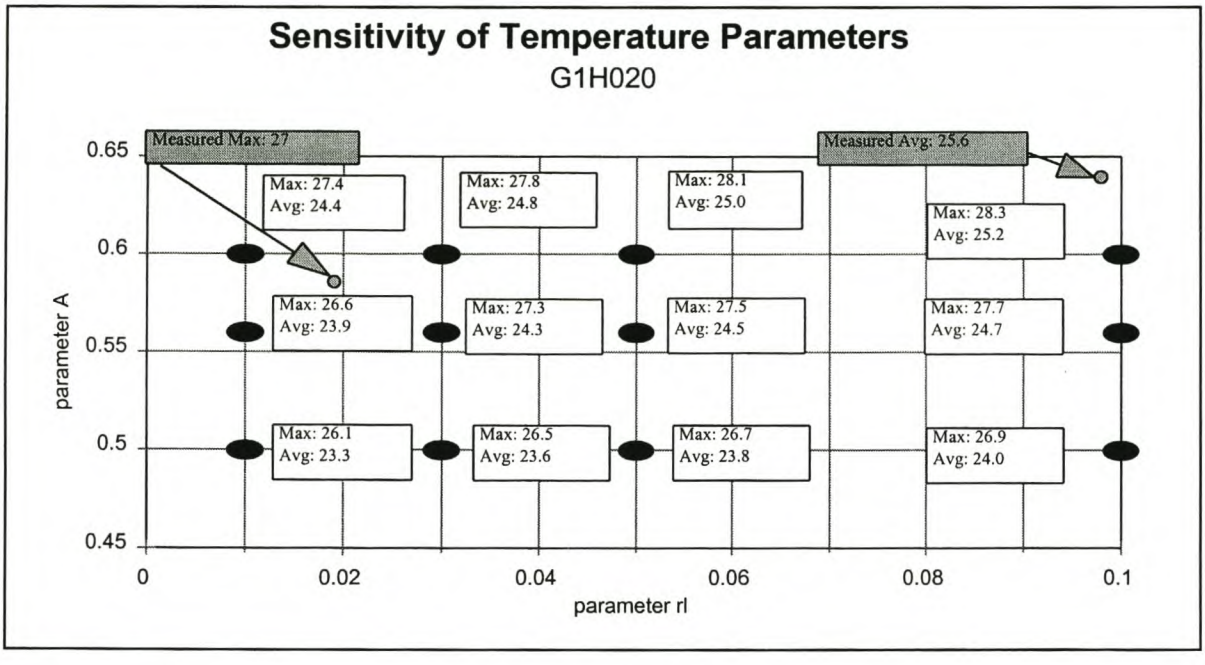

Figure 8.5: Sensitivity of temperature parameters at G1H020

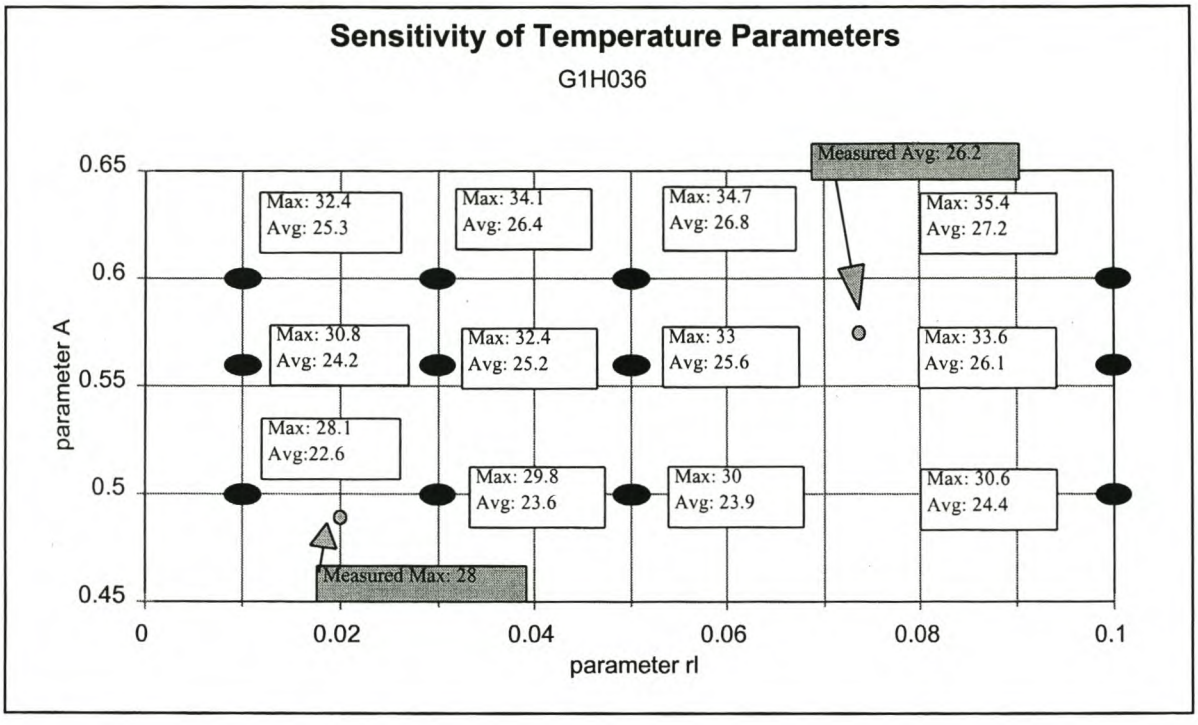

Figure 8.6: Sensitivity of temperature parameters at G1H036

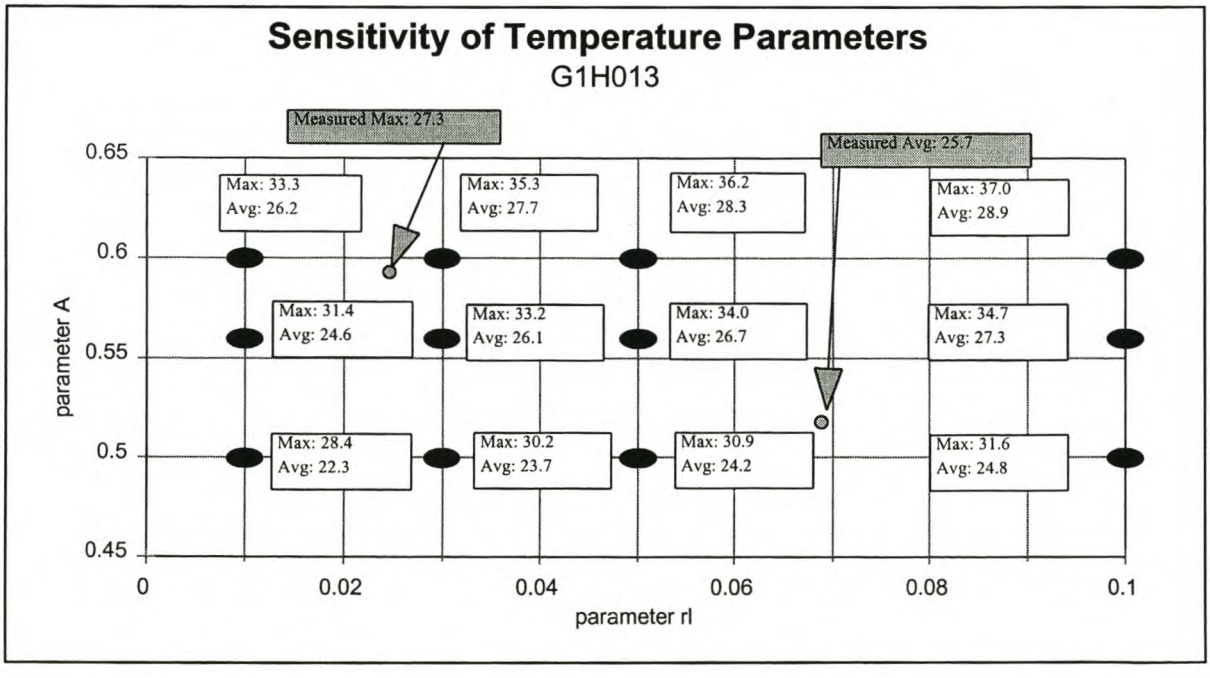

Figure 8.7: Sensitivity of temperature parameters at G1H013

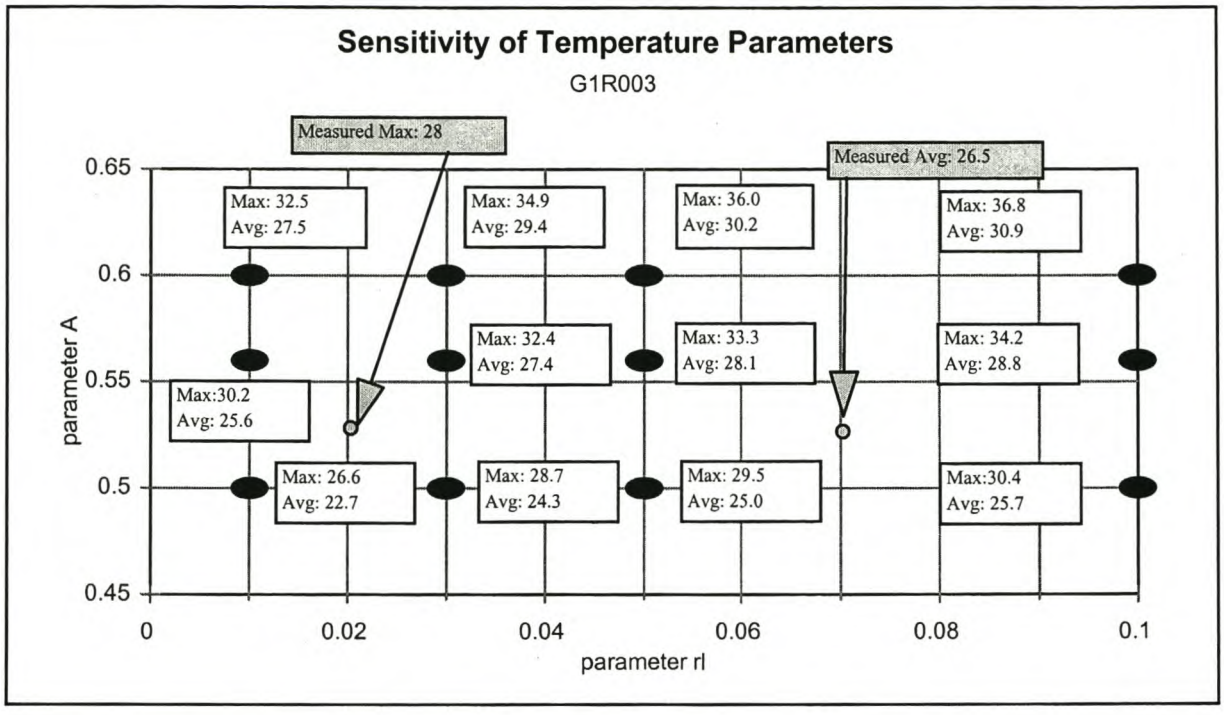

Figure 8.8: Sensitivity of temperature parameters at G1R003

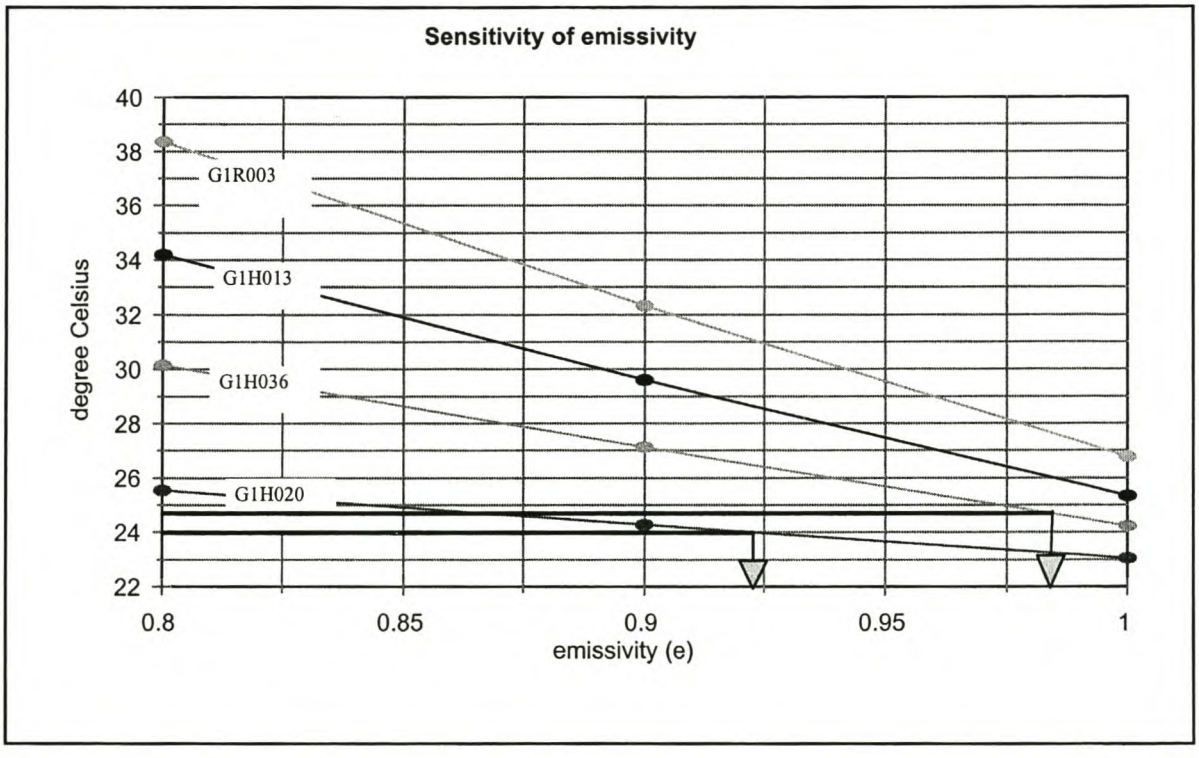

Figure 8.9: Sensitivity of temperature parameter ϵ

Figure 8.9 shows the sensitivity of the emissivity parameter ϵ on temperature. The figure shows the summer temperature averages, that were calculated from three runs of emissivity factors of 0.8, 0.9 and 1 for all the stations in the main stem river. For G1H020 an emissivity of 0.92 would simulate an average of 24°C as was measured (refer also to Table 8.12). An emissivity factor of 0.98 would simulate an average of 24.6°C for G1H036, while for G1H013 and G1R003 a emissivity factor of 1 would simulate their average temperature measured (refer to Table 8.12). The average emissivity of all four ϵ factors simulated is 0.975; this value was used for the Berg River model simulation runs. This value is close to the default value of 0.97.

External variables:

The atmospheric longwave radiation and the back radiation are both influenced by the air temperature, while conduction and evaporation terms are affected by the wind and the evaporation respectively. For a river, the evaporation and conduction will have less effect on the water temperature when compared to the addition of heat through the atmosphere.

Depth:

All the terms are dependent on the depth of the water (refer to equation 5.39). It is evident from the equations that the influence of the water depth on the temperature is much stronger than the influence of the various calibration parameters. Figures 8.10 illustrates an example of how the temperature term is influenced by the depth of the water. Below a depth of 0.5m the temperature term increases exponentially. Therefore, for a water depth below 0.5 m the temperature equations predict the water body to become exponentially warmer as the water depth decreases. This will occur in the summer months when there is low water depth and the solar radiation and air temperature are at their maximum and contribute therefore additional heat.

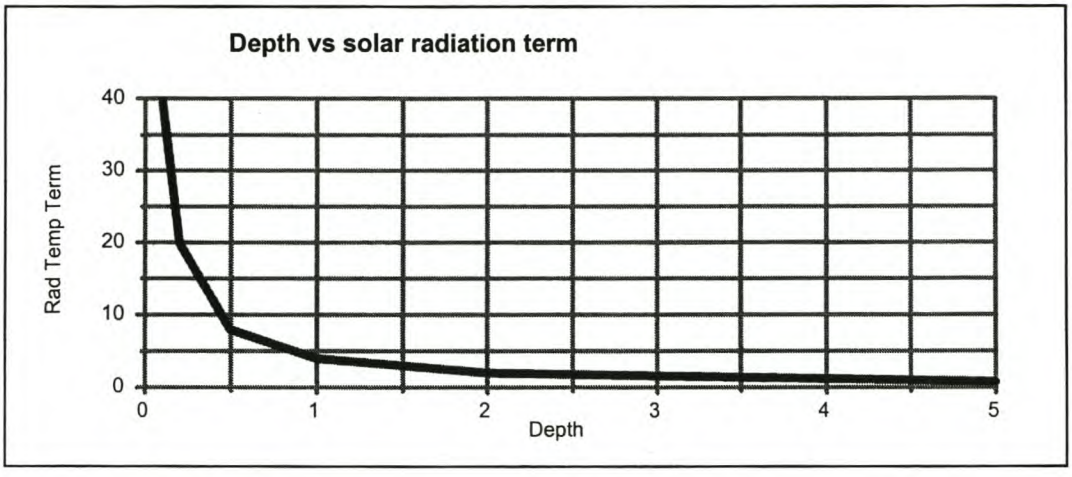

Figure 8.10: Depth influence on solar radiation

8.6.4 Oxygen

As only the water quality variables TDS, PO_4 and Temperature are modelled additional to the oxygen, the effect of the essential influences on the oxygen concentration is not modelled. These are the influences of plant growth and therefore photosynthetic oxygen production; and the oxidation of carbonaceous and nitrogenous waste material, respiration of plants and oxygen demand of the sediments. In this model only two variables influences the modelling of oxygen: k_{re}, and θ_{re} (refer to equation 5.44) and the effect of temperature on the reaeration. The effect of temperature is seen as an external variable and although the sensitivity of the oxygen to the temperature can be assessed, it cannot be altered in the calibration process.

Figure 8.11 presents the influence of θ_{re} on the oxygen values for the different gauging stations. As no data is available for the oxygen concentration, estimating the correct value for this parameter is therefore difficult. The default value of θ_{re} in DUFLOW is 1.024, which has been accepted for the Berg River.

The parameter k_{re} is calculated according to equations 5.47 and 5.48. The parameter k_{re} is dependent on the k_{mas} parameter and the k_{rmin} parameter. The minimum oxygen transfer coefficient (k_{rmin}) is defined by the user, and the DUFLOW default value of 0.1 m/d has been applied. The k_{rmin} parameter has however never been used, as the calculated mass transfer coefficient (k_{mas} in equation 5.47) has always been larger than the minimum oxygen transfer coefficient.

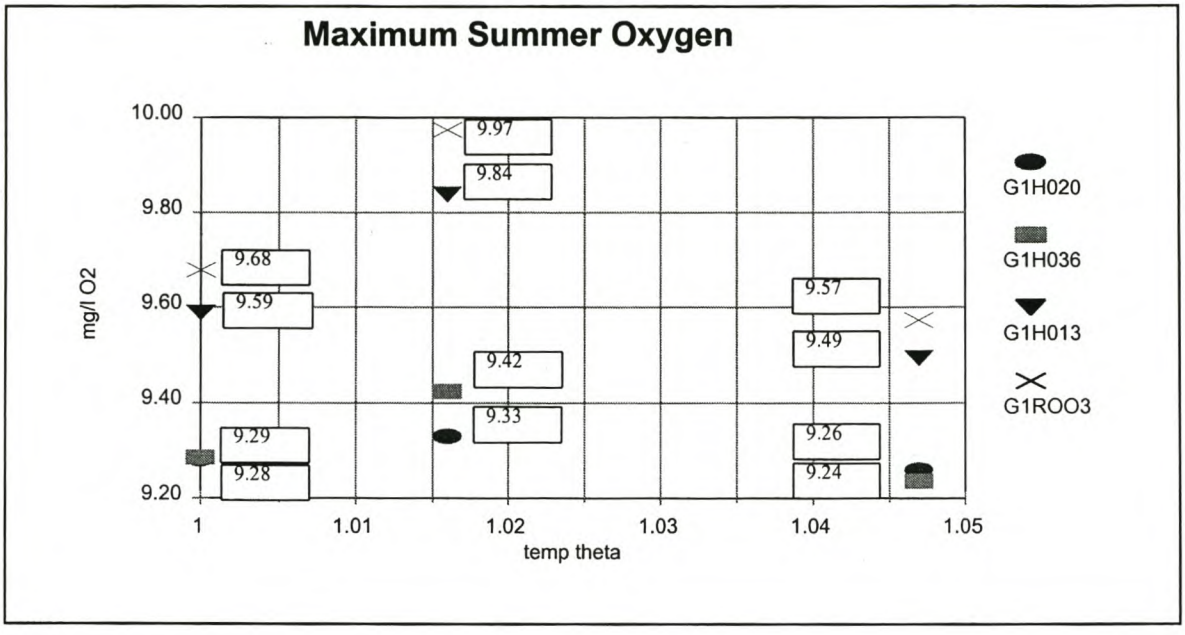

Figure 8.11: Influence of $\theta_{\rho e}$ on summer oxygen values

8.7 SENSITIVITY OF GRAB SAMPLES COMPARED TO INFILLED SAMPLES

Referring back to section 6.3.1, the water quality data was 'infilled' by means of a moving regression. In order to investigate the sensitivity of incorporating the actual grab samples back into the infilled time series, a sensitivity run has been completed with grab samples included in the infilled time series and the results were compared to the results of the simulation runs using only 'infilled' concentration values.

It can be seen from Figures 8.12 and 8.13 that incorporating grab samples in the infilled series does not show significant difference when compared to the runs that were completed with only 'infilled' values.

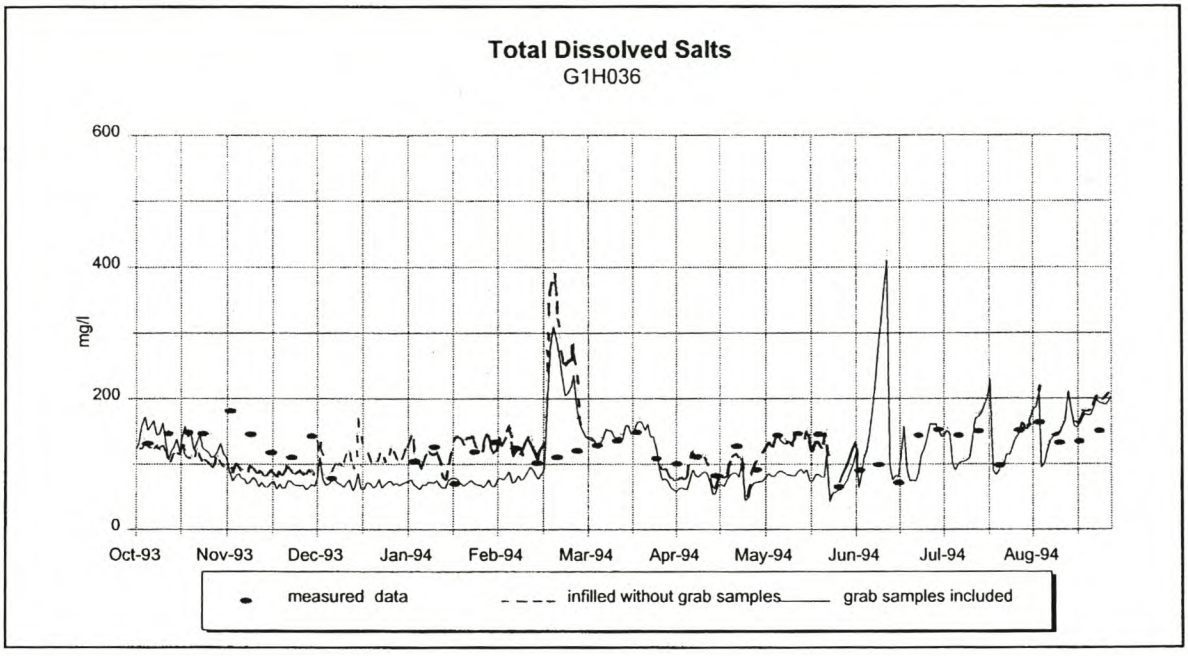

Figure 8.12: Comparison of TDS simulation at G1H036

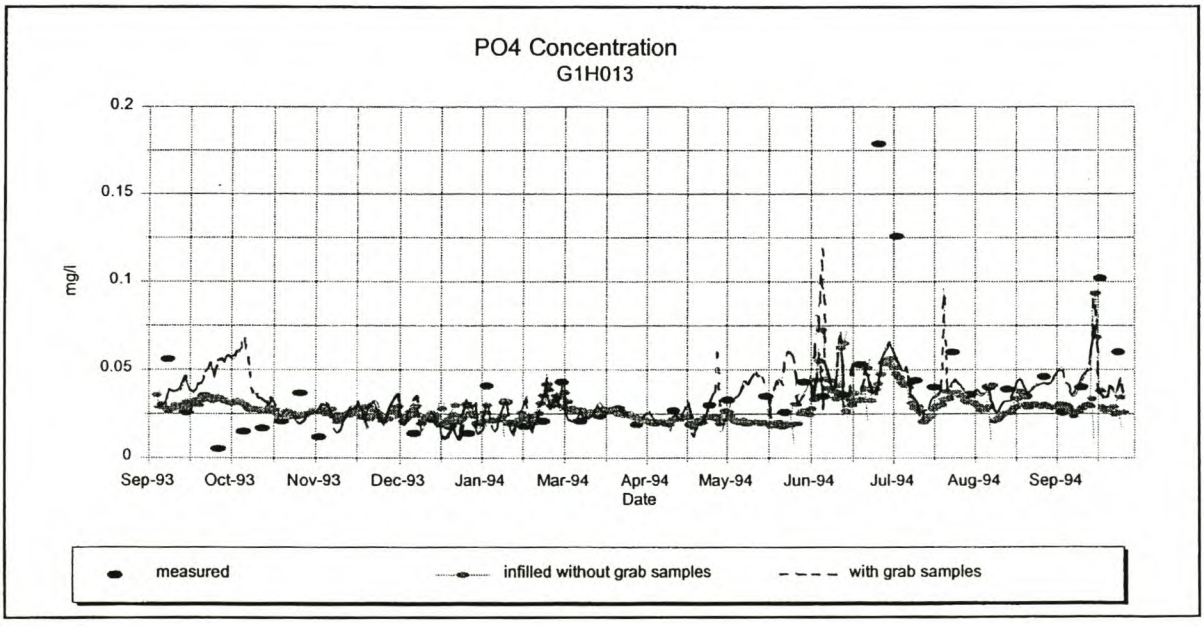

Figure 8.13: Comparison of PO_4 simulation at G1H013

8.8 POINT SOURCES

The Water Quality Situation Analysis (DWAF, 1993) identifies the major point sources in the Berg River catchment. Much of the industrial activity in the Berg River catchment is associated with the agricultural sector, and therefore many of the effluent producers are also associated with this sector (DWAF, 1993). For the DUFLOW model only point sources that have been issued with a permit have been considered. This data was available from the Polmon database from DWAF as monthly measurements. Unfortunately, effluent data was only available for the major sewage treatment plants and only a few point sources that irrigate their effluent. There are however a number of piggeries and wineries in the Berg River catchment that also produce effluents, which are high in oxygen demand and organic loading. The Berg River Situation Analysis (DWAF, 1993) has identified the following point sources:

- 1 Trout Farm
- 2 Fruit and Vegetable processing plants
- 22 Wineries
- 10 Piggeries
- 21 Sewage Treatment Works
- 1 chicken abattoir
- 5 industrial sources

From these only 12 are authorised to discharge into the Berg River or nearby tributaries, which are Franschhoek STW, Bienne Donne STW, Pniel STW, Wemmershoek STW, PPC cement factory at Riebeeck Wes, Paarl STW, Moorreesburg STW, Piketberg STW, Porterville STW and Tulbach STW and PPC de Hoek STW. Many of the point sources do not have quality requirements as they all irrigate their effluent. Effluent quality is not specified on their permits. The majority of the point sources identified have not been issued with permits. Lack of data makes it difficult to evaluate the volume of effluent that gets irrigated, but it has been estimated in the Berg River Situation Analysis (DWAF, 1993) that between G1H004 and G1H020 about 40% of the total annual effluent produced in this reach is irrigated, 21% between G1H020 and G1H036 and about 25% between G1H036 and G1H013.

The point sources that do have permits, and measured water quality and flow volume, have been included in the model. It has been assumed for the point sources (where flow and quality data is available) which do not discharge directly into the Berg River and irrigate their effluent or discharge far up in a tributary that about 25 % of the effluent flow reaches the Berg River. Only one authorized point source, Paarl sewage treatment works, discharges effluent directly into the Berg River.

Table 8.5: Point sources identified in the Berg River Catchment

NAME	PERMIT	MANNER OF DISPOSAL	STANDARD (DWAF, 1993)	COMMENT
Franschhoek Municipality STW	yes	irrigation of sportsfield, discharge into river	General Standard, for Residual Chloride the Special Standard	assumed 25% of flow reaches Berg River main stem
Pniel STW	yes	discharge into Dwars River	General Standard	assumed 25% of flow reaches Berg River main stem
Bien Donne Winery	no	effluent to wineyard, discharge into stormwater drain	none specified	Samples have been taken during study period, have been analysed in Chapter 4
La Motte STW	no	evaporation ponds and seepage	none specified	No data available
Victor Vester STW	no	irrigation, in winter discharge of effluent into the Berg River	none specified	No data available
Wemmershoek Forestry Station STW	no	discharge into Wemmers River	none specified	
King Western Leathers Tannery	yes	evaporation	none specified	no quality standard specified
Paarl Municipality	yes	discharge to Berg River	General Standard, PO4-P less than 4 mg/l 90% of the time	
Stellenbosch Farmers Winery	yes	discharge of effluent to Berg River	none specified	no water quality data available
Wellington municipality STW	yes	irrigation, evaporation	General standard	assumed 25% of flow reaches Berg River main stem
Morreesburg municipality STW	yes	discharge to Sand river	General standard	COD data assumed 25% reaches Berg River main stem, phosphate and TDS data measured at G1H034 readings
Piketburg municipality STW	yes	irrigation, winter balance to stream	General standard	COD data assumed 0.25% reaches Berg River main stem, phosphate and TDS data measured at G1H035 readings
Porterville Municipality STW	yes	discharge to Jakkalskloof river	General standard	COD data assumed 0.25% reaches Berg River main stem, phosphate and TDS data measured at G1H035 readings
Tulbach Municipality STW	yes	discharge to Klip river	General standard	discharge into Voëlvleidam

The variables that have been tested by DWAF are COD, EC, SS and pH. Only Franschhoek STW had occasional phosphate readings, which were of an average of 5.3 mg/l P as PO_4. The variables that are of interest to us are the COD and TDS values. Tables 8.6 and 8.7 summarize the various loads that have been measured.

It can be seen from Tables 8.6 and 8.7 that Paarl municipality discharges about 65% COD and 70 % of TDS of the overall point source totals. It is clear, that for a water quality simulation model, if ever used for management and control purposes, a more extensive database is needed to evaluate the impact of point sources and non-point sources more exactly.

Table 8.6: COD Loads (tons/month)for 1993/1994

	Franschhoek STW	**Pniel STW**	**Paarl STW**	**Wellington STW**	**Moorresburg STW**
October	0.44	0.48	17.4	16.28	1.2
November	0.5	0.7	11.4	13.9	0.73
December	0.52	1.18	13.8	9	1.52
January	0.5	1.05	20.4	16	0.89
February	0.911	0.5	27.2	12.4	0.96
March	1	0.97	85.2	20	1.16
April	1.66	1.15	26	6.9	0.96
May	0.78	0.55	43.6	7	0.83
June	0.66	1.21	34	19.3	0.85
July	0.46	0.96	20.7	9.6	1.09
August	0.41	0.5	11.3	5.1	1.09
September	0.36	0.3	14	9.7	1.06
TOTAL (tons)	**8.2**	**9.55**	**325**	**145.2**	**12.34**

Table 8.7: TDS Loads (tons/month)for 1993/1994

	Franschhoek STW	**Pniel STW**	**Paarl STW**	**Wellington STW**	**Moorresburg STW**
October	0.058	0.28	4.4	1.69	0.06
November	0.059	0.26	4.1	1.6	0.58
December	0.079	0.21	4.6	1.45	0.57
January	0.096	0.23	4.6	1.31	0.55
February	0.08	0.15	4.9	1.33	0.49
March	0.1	0.18	6.1	0.84	0.47
April	0.092	0.24	5.9	1	0.42
May	0.087	0.24	5.8	0.78	0.45
June	0.1	0.39	7.1	1.95	0.49
July	0.065	0.31	4.2	1.35	0.46
August	0.06	0.14	3.3	1.1	0.49
September	0.057	0	4	1.46	0.59
TOTAL (tons)	**0.933**	**2.63**	**58.9**	**15.86**	**5.62**

8.9 RESULTS OF WATER QUALITY MODEL CALIBRATION

8.9.1 TDS

The simulated values were compared with the measured data and *'infilled values'* for low flows (October to March) and high flows (April to May) and overall. The contribution to the salt load in the Berg River from the point sources with a permit seems to be insignificant when compared to the total salt load contributed by the tributaries. Paarl sewage treatment works adds a yearly load of 145.2 tons, while the total load measured at G1H020 already consists of 15798 tons of TDS in the year. Of concern is, however, all the non-point sources and point sources that are not controlled, which have an additional impact on the overall TDS load.

Irrigation return flows, which are high in salts and nutrients, have not been included in the model, due to insufficient knowledge of the volumes and concentrations. The irrigation return flows have a significant impact on the TDS and phosphate concentrations, particular in the summer months, and the absence of these concentrations should be borne in mind when analysing the results.

- *TDS Concentration results:*

  (Table 8.11, Figures 8.26-8.29)
  The coefficient of determination is low for the concentration analysis (Table 8.11), between 0.3 and 0.67 for the high flow period and only between 0.03 and 0.47 for the low flows.

  High TDS Concentration is discharged into the river in the reach between G1H020 and G1H036. This can be seen from Figures 8.26 and 8.27, and also from Table 8.11, where the % error increases from -31% to 14%. This is the result of additional TDS concentration from subcatchments 4 and 5, that have been infilled by using grab samples of G1H039. Figure 8.14 shows the TDS concentration of G1H039 and also of G1H041, which also discharges into the river in this reach (refer to Figure 7.1). Subcatchments 4 and 5 follow the same pattern as the TDS concentration of G1H039. The high concentration peaks shown in February and also in the winter months at G1H036 and the stations downstream are also a result of the high TDS discharging into the river from subcatchments 4 and 5. Unfortunately, the accuracy of the gauging station G1H039 was rated 0 (Table 7.1), but it was the only estimate of gauged TDS loads (refer to section 7.6 and 8.5). The

actual effect of incoming TDS concentration from G1H039 is little, due to low flows. As subcatchments 4 and 5 have however a higher runoff, the loads discharging into the river do have an impact on the concentration. It can therefore be concluded that the TDS concentration of subcatchments 4 and 5 is considerably less than was assumed.

Low TDS concentration is discharged into the river during the summer months. The concentration shows high undersimulation at all stations (Figures 8.26 to 8.29), especially at G1R003, while the phosphate simulation shows hardly any undersimulation during the summer months (Figures 8.38-8.41). The undersimulated TDS concentration could therefore be due to a missing TDS point source.

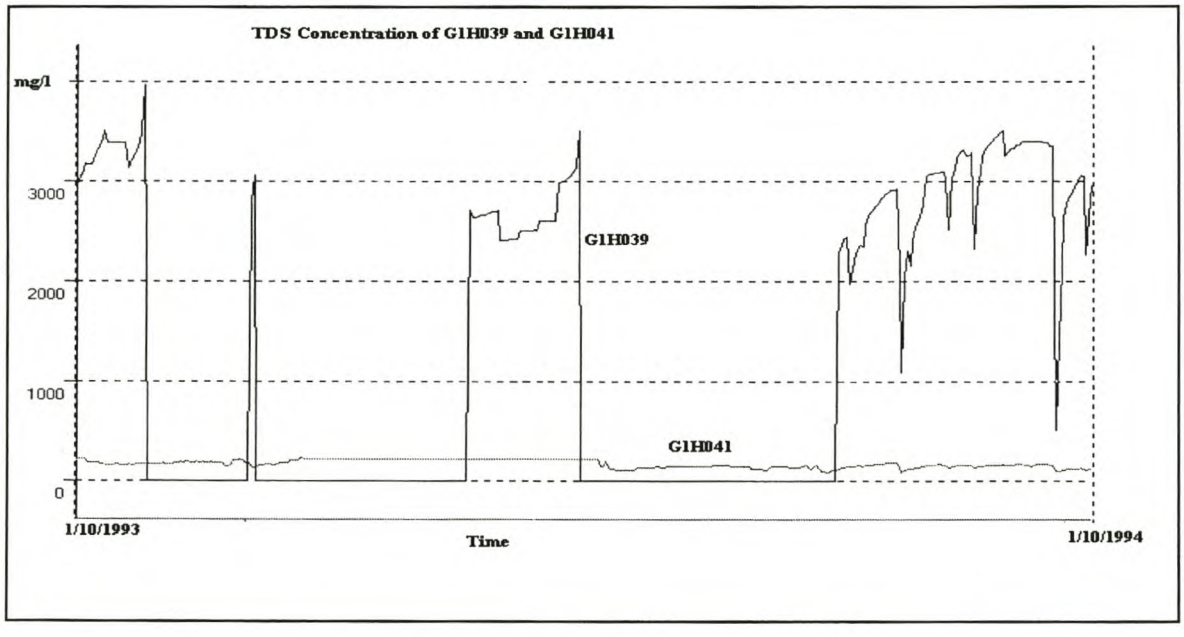

Figure 8.14: TDS Concentration of G1H039 and G1H041

- *TDS Loads Results:*

Low Flow :

(Table 8.10, Figures 8.18-8.21)

The coefficient of determination for the loads is higher than for the concentration (Table 8.8), this

is because the load is dependent on the flow simulated. For the low flow period the load follows the trend of the measured data less accurately than the high flow (refer to Figures 8.18 to 8.25). Referring to Table 7.6, it can be seen that the discharge in the low flow period is oversimulated by 54% at G1H036, and this explains the 68% error in the TDS loads at G1H036, as this could be the result of the flow oversimulated for the periods March and April. The other stations also show similar errors in the load simulation when compared to the flow simulation (Tables 8.10 and 7.6). Interestingly, the TDS load shows however a smaller error in the loads for the low flow period than the flow simulated (88% error in the flow and only 35% error in the TDS load simulation), which could be the result of addition of ungauged TDS loads of the ungauged areas 7 and 9 (Figure 7.1). These areas contribute minimal runoff to the main stem, but significant TDS loads (as these areas drain the Malmesbury shales, which produce high salinity concentration). Referring to Figures 8.18 to 8.21, one can see that the short lived peaks introduced by releases from Voëlvlei Dam are clearly defined in the load simulation at G1H013 and G1R003.

High Flow:

(Table 8.10, Figures 8.22-8.25)

The overall TDS loads for the high flow months are oversimulated at all stations, except at G1H020. The TDS peak shows a difference of - 50000 g/s at station G1R003 (Figure 8.25),-30000 g/s at G1H013 (Figure 8.24) and a oversimulation of 25000 g/s at G1H036 (Figure 8.23). The error introduced therefore occurs mainly in the reach from G1H036 to G1H013, and could be the result of additional non-point salinity runoff.

8.9.2 Phosphate as PO_4

The phosphate modelling is influenced by advection only (the biological and chemical processes have been omitted due to lack of data on other dependent variables). This has to be borne in mind when analysing the results, as phosphate concentration is in reality not only influenced by advection, although it is often the most influential.

Irrigation return flows, which are high in salts and nutrients, have not been included in the model, due

to insufficient knowledge of the volumes and concentrations. The irrigation return flows have a significant impact on the TDS and phosphate concentrations, particular in the summer months.

- *PO_4 Concentration results:*

(Table 8.13, Figures 8.38-8.41)

The coefficient of determination is low for the concentration analysis (Table 8.13), between 0 and 0.68 for the high flow period and only between 0.15 and 0.57 for the low flows. Station G1H036 shows a 0% coefficient of determination and referring to Figure 8.38, it can clearly be seen that the concentration is greatly undersimulated between March and June, the error in the simulation decreases from -1% to -32% (Table 8.13) from G1H020 to G1H036. This undersimulation is not evident at the downstream stations (Figures 8.39 and 8.41). The measured phosphate concentration has decreased from 0.04 mg/l to 0.024 mg/l (low flow) and from 0.08 mg/l to 0.05 mg/l (high flow) from station G1H020 to G1H036. The errors in concentration mean are also the highest for station G1H036 (-32% at low flow and -55% for high flow). From the verification runs it can also be seen that although the values are undersimulated at G1H036, the measured phosphate values decrease at the downstream stations and the % error between the measured and the simulated phosphate is less. This error could be due to a missing point source in the reach of G1H020 and G1H036, as the flow is not undersimulated during these months (refer to Figure 7.4); the TDS concentration is undersimulated in these months, but not to such a high degree as for the phosphate simulation.

The simulated mean phosphate concentration does not differ between G1H013 and G1R003 for low and high flows. The measured phosphate mean concentration does however decrease from G1H013 to G1R003 for the high flows; this could be due to missing ungauged flows in this reach. One can see from Figures 8.39 to 8.41 that small phosphate concentration peaks are simulated in June and end September at all three stations: G1H036, G1H013 and G1R003. Figure 8.15 shows the phosphate concentrations of the gauged tributaries discharging into the Berg River main stem. As one can see from Figure 8.15, the small peaks simulated in the winter months are mainly a result of phosphate inflow from the subcatchments 4 and 5 that have been estimated with grab samples of G1H039.

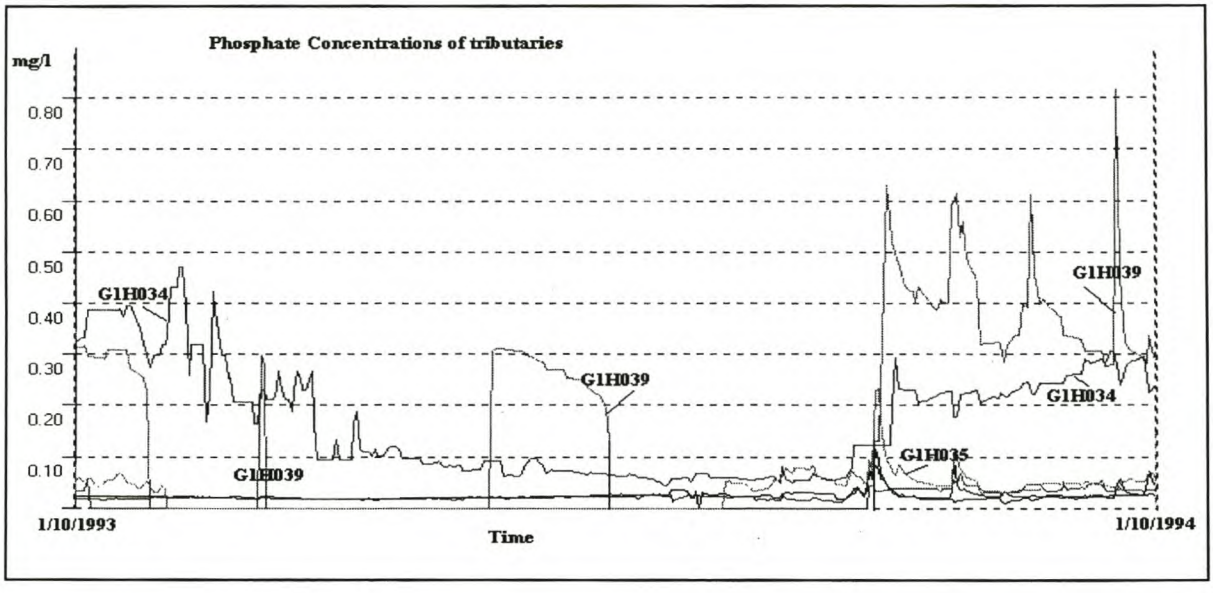

Figure 8.15: Phosphate Concentrations of Tributaries

- *PO_4 Loads Results:*

Low Flow :

(Table 8.12, Figures 8.30-8.33)

The coefficient of determination for the loads is higher than for the concentration (Table 8.10 and 8.11), this is because the load is dependent on the flow simulated. For the low flow period the load follows the trend of the measured data less accurately than the high flow. As for the TDS loads, the phosphate loads are oversimulated in the months March/April, due to the flow oversimulated in these months. At all stations the phosphate loads are oversimulated, especially at G1R003 where the simulated values show a 103% oversimulation. This oversimulation is mainly due to 88% oversimulation of flow at G1R003 (Table 7.6). The other stations also show similar errors in the load simulation when compared to the flow simulation (Tables 8.12 and 7.6). Referring to the figures, one can see that the short lived peaks introduced by releases from Voëlvlei Dam are clearly defined in the load simulation at G1H013 and G1R003, this explains also the improvement of the coefficient of determination downstream of G1H036.

High Flow:

(Table 8.12, Figures 8.34-8.37)

The phosphate peak in the summer was measured to be approximately 60 g/s at G1H013 and 40 g/s at G1R003. For all stations the phosphate peak is undersimulated. This could be the result of additional non-point runoff occurring during a flood. The high flow phosphate loads show high coefficient of determinations (0.95 to 0.98). At G1H020 the total load in the summer period is already undersimulated by 42% . The model adds phosphate loads from the tributaries and ungauged subcatchments in the reach from G1H013 to G1R003, where in reality the phosphate mass has reduced from 48.2 tons to 25.6 tons.

8.9.3 Temperature

(Figures 8.42 to 8.45 and Table 8.14)

It can be perceived from the results, that the temperature model predicts the winter months better than the summer months. This could be the result of the algorithm, as the temperature increases exponentially when the water depth decreases (equation 5.39 and Figure 8.10). The water depth is simulated very low (0.2-0.6m) in the summer months. The model follows the seasonal trend quite accurately (R^2 between 0.8 and 0.98). At station G1R003 the temperature is oversimulated for the summer months and undersimulated for the winter months. The occasional outliers in the simulation are due to outliers in the radiation and evaporation rates (refer to Figures 6.6 and 6.7).

8.9.4 Oxygen

(Table 8.15, Figures 8.46-8.49)

The calibration of the oxygen model concentrated on the temperature simulation, as oxygen is dependent on the values of temperature in the river. Many factors affect the concentration of oxygen, such as plant photosynthesis and point sources. The error of the simulated data is also very dependent on the accuracy of the meteorological influences on the oxygen. There are outliers simulated for the May and June months, and this is due to occasional peaks from the radiation data and minor instabilities in the simulation calculation, due to higher velocities in the winter months.

8.10 WATER QUALITY MODEL VERIFICATION

Unfortunately, for the station G1H036 the flow measurements are incomplete from the 3rd of July onwards. It therefore should be noted that the statistical comparison for the high flows are not included for this station. The simulated values were compared with the measured data and *'infilled values'* for low flows (October to March) and high flows (April to May) and overall, as well as to the errors that were experienced in the calibration simulation.

8.10.1 TDS

In the year October 1994 to October 1995, several peaks are experienced during the high flow months instead of one defined peak, as was the case for the calibration year. The maximum peak occurs mid-July and reaches only a value of approximately 40000 g/s at G1H013 and G1R003, compared to the maximum peak of 120000 g/s (at G1R003) for the calibration year (refer to Figure 8.25 and 8.57). The measured data for the low flow period nevertheless has more or less the same pattern as for the calibration period.

- *TDS Concentration results:*

  (Table 8.17, Figures 8.53 - 8.56)
  The coefficient of determination is low for the concentration analysis, between 0.04 and 0.58 for the high flow period and between 0.23 and 0.30 for the low flows. Although the concentration shows high oversimulation in March and April for the calibrated TDS simulation (Figures 8.26 to 8.29), this is not evident in the verification simulation. The concentration is oversimulated downstream from G1H036 for the high flow period in the calibration year, while the verified run shows undersimulated concentration at all stations. G1H020 shows similar errors to the calibration simulation, while for G1H013 and G1R003 the yearly errors are higher than the errors of the calibration run. This could be the result of different point sources and non-point sources that have occurred in this year.

  The simulation of the concentration during the winter months shows an erratic pattern, which is the result of high inflowing TDS from G1H043 (Figure 8.16). For the calibration year, subcatchments

4 and 5 (due to pattern of G1H039) contributed most of the salts in the winter months. As one can see from Figure 8.16 high TDS concentration is discharged from G1H034; the flow however is an average of 0.006 m^3/s for G1H034 during these months and therefore the load contribution to the river is minimal.

Similar to the calibration results, there exists undersimulation in the summer months at all stations. At G1R003 the simulated and measured TDS values are about 125 mg/l different (Figure 8.61). This could be the result of the same missing point sources or also due to unknown abstractions.

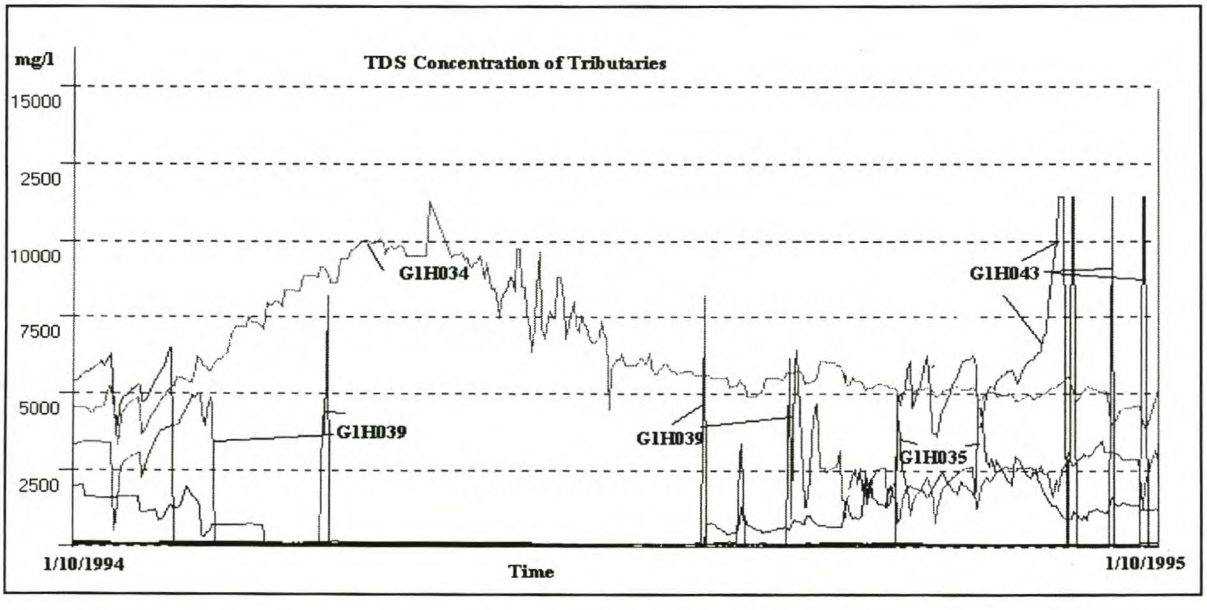

Figure 8.16: TDS Concentration of tributaries for the verification year

- *TDS Loads Results:*

Low Flow :

(Table 8.16, Figures 8.50 - 8.53)

As for the calibrated run, the coefficient of determination for the loads is higher than for the concentration, this is because the load is dependent on the flow simulated. One can see from the

figures that the short lived peaks introduced by releases from Voëlvlei Dam are clearly defined in the load simulation at G1H013 and G1R003, but that the model is unable to simulate these loads to near zero load, as was measured. This is because the model gets unstable for zero water depths, and for modelling purposes a minimum water depth has been provided for in the coding. Interestingly, just as for the concentration, the loads are undersimulated for all stations for the verification run and oversimulated downstream from G1H020 for the calibration run. This could be the result of the definite oversimulation of loads in March/April for the calibration values, which does not occur in the verification run. The verification values show a higher coefficient of determination than the calibration values (compare Tables 8.10 and 8.16).

High Flow:

(Table 8.16, Figures 8.54 - 8.57)

It can be seen from Figures 8.56 and 8.57 that the infilled salt loads stay consistent for the main peak in mid-July downstream from G1H013. In the model, however, salt loads are added from the ungauged subcatchments and the tributaries, which can be seen by the increased simulated values for this peak. In the calibrated year the infilled TDS values do however increase in the peak (Figures 8.23 and 8.24), and this could mean that in reality most of the salts have already been discharged into the river by the previous flow peaks in the verification period, whereas in the calibration period only one major peak occurs. The overall TDS mass for the high flow months is undersimulated at all stations, except at G1R003.

8.10.2 Phosphate as PO_4

In the year October 1994 to October 1995, several peaks are experienced during the high flow months instead of one defined peak, as was the case for the calibration year. The maximum peak occurs mid-July and reaches only a value of approximately 15 g/s at G1H013 and G1R003, compared to the maximum peak of 40 g/s (at G1R003) for the calibration year (refer to Figure 8.37 and 8.69). The measured data for the low flow period nevertheless has more or less the same pattern and the same mass as for the calibration period.

- *PO_4 Concentration results:*

(Table 8.19, Figures 8.70-8.73)

The coefficient of determination is low for the concentration analysis; the verified model shows however a better correlation to the measured data than the values for the verification simulation (Tables 8.19 and 8.13). Both the verification values and the calibrated values show a high oversimulation at G1H036 (Figures 8.71 and 8.39), this error therefore could be the result of an unknown point or non-point source in the reach between G1H020 and G1H036, and is not only the result of a sudden high concentration measurement. The concentration is undersimulated most of the time at all stations (except at G1R003). This is also the case for the calibration year, except that G1R003 shows a 6% undersimulation for the low flow for the calibrated values and a 3% oversimulation for the verified values (Table 8.19 and 8.13).The simulation of the concentration during the winter months shows an erratic pattern, which is a result of the phosphate concentration discharging from G1H039 (refer to Figure 8.17).

- *PO_4 Loads Results:*

Low Flow :

(Table 8.18, Figures 8.57-8.60)

At all stations the phosphate loads are oversimulated, especially at G1R003 where the simulated values show a 159% oversimulation. The calibrated values show a oversimulation of 103% (Table 8.12), and it can therefore be concluded that the flows (88% oversimulation, Table 7.6) and the loads are over-corrected in the reach from G1H013 and G1R003. The other stations also show similar errors in the load simulation when compared to the flow simulation (Tables 8.18 and 7.6), and it is evident that the mass errors are dependent on the errors of the flow simulation. Referring to the figures, one can see that the short lived peaks introduced by releases from Voëlvlei Dam are clearly defined in the load simulation at G1H013 and G1R003, just as for the calibrated values and the coefficients of determinations, as well as the errors, are similar.

High Flow:

(Table 8.18, Figures 8.66-8.69)

The phosphate peak in the summer was measured to be approximately 19 g/s at G1H013 and 15 g/s at G1R003. At all stations the phosphate peak is undersimulated, except for G1R003 where the phosphate peak is oversimulated as additional loads are introduced between reach G1H013 and G1R003 (compare also to Figures 8.34 and 8.37). This could be the result of additional non-point runoff occurring during a flood. The high flow phosphate loads show high coefficients of determination (0.92). The errors are less at G1H013, with only -18% undersimulated compared to -55% undersimulation for calibrated values.

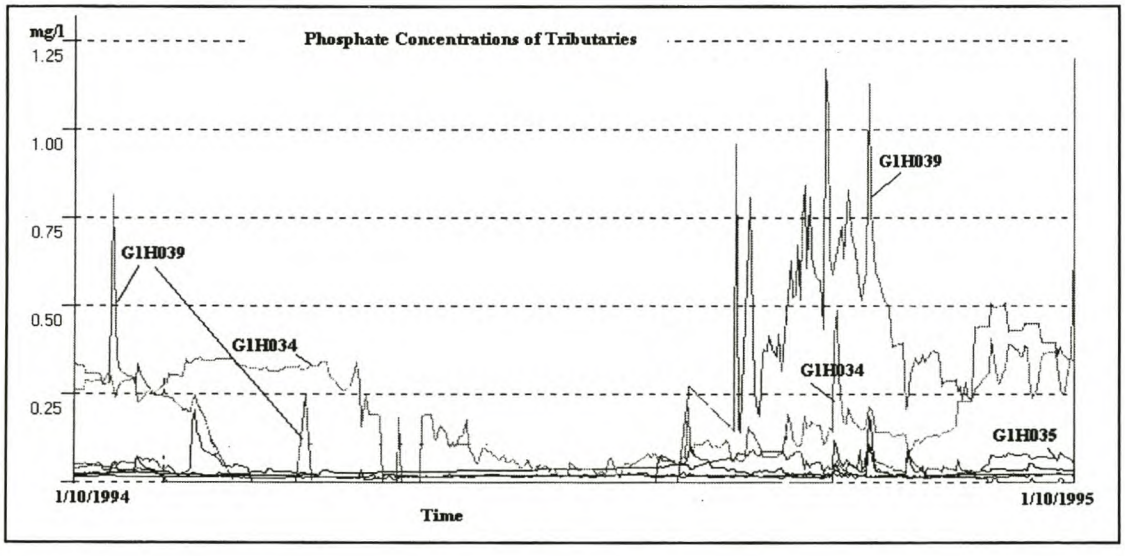

Figure 8.17: Phosphate Concentration of tributaries for verification year

8.10.3 Temperature

(Table 8.20, Figures 8.74-8.77)

The temperatures are simulated higher for the summer period for the verification run than for the calibrated model. The verification results show higher temperature values than the actual measured temperature, while the calibrated simulation results produced lower temperature values. The overall

errors are less for the verified model than for the calibrated model, except for the reach from G1H013 to G1R003, where the error in the low flow period has increased to about 18%. The standard deviations have all increased (refer to Table 8.20).

From Figure 8.77 it can be seen that the summer temperatures are oversimulated at G1R003, and this could indicate that the parameters, that were acceptable for the calibration year, might not be acceptable for the verification year.

8.10.4 Oxygen

(Table 8.21, Figures 8.78-8.81)

The verification run showed small variation to the calibrated run. Table 8.21 summarizes the results and the percentage difference from the measured data. The percentage errors should be compared with the errors obtained from the calibration simulation (Table 8.15). Both runs are influenced by the saturation oxygen concentration, as little information is available on the oxygen in the Berg River. Only the flow and the meteorological data influence the oxygen concentration in this study. The low flow period shows a 1% oversimulation, while the high flow shows a 1% undersimulation. The standard deviations do not differ significantly. From the slight differences between the calibrated and the verified oxygen simulations it can be perceived that the parameters applied in the oxygen simulation are acceptable for another time period. The outliers seen in Figures 8.78 to 8.81 are due to undersimulation of temperature in the winter months.

8.11 WATER QUALITY SIMULATION WITHOUT UNGAUGED RUNOFF

The addition of ungauged runoff and loads was based on the conclusion that a considerable volume of flow and therefore also loads are missing in the mass balance (refer to Table 7.4). To assess whether the method (of adding ungauged loads and runoff) applied was successful, a simulation run without ungauged subcatchments was completed. The results, compared to the actual measured data, were compared to the simulation results of section 8.9.

8.11.1 TDS

- *TDS Concentration Results:*

  (Table 8.23, Figures 8.90 - 8.93)

  Comparing Figures 8.90 to 8.93 to Figures 8.26 to 8.29, it can be seen (as already mentioned in section 8.9.1) that subcatchments 4 and 5 overcorrect the concentration in March and April. The peaks simulated in the winter months, which have also been added by subcatchments 4 and 5, are also missing. The addition of the ungauged flow improved the concentration for September, October and November; but it had little improvement in the summer months. This can be seen especially at G1R003 (Figures 8.93 and 8.29), where considerable concentration is still missing. The concentration at G1H036 has been overcorrected the most, as the % error in concentration shifted from -32% to 14% for the low flow and -36% to 44% in the high flow. The overall concentration at high flow is always undersimulated without the addition of ungauged concentration, and oversimulated with ungauged runoff (except at G1H020).

- *TDS Loads Results:*

  Low Flow :

  (Table 8.22, Figures 8.82 - 8.85)

  With the low flow load results it can be seen again that the estimation of the ungauged TDS has been overcorrected in March and April with the addition of subcatchments 4 and 5. The TDS loads have improved considerably, when including the ungauged loads, for the months October and November (Figures 8.82 to 8.85 and 8.18 to 8.21). The short-lived peaks occurring from releases of Voëlvlei Dam, are already slightly oversimulated without any additional loads. The loads simulated in the three months December, January and February show little change.

  High Flow :

  (Table 8.22, Figures 8.86 - 8.89)

  Referring to Figure 8.86 and 8.87 the peak simulated in high flow has improved with the addition of ungauged TDS loads for G1H020 and G1H036. A TDS load peak of 2090 g/s has been simulated

with addition of ungauged loads at G1H036, while 888 g/s has been simulated without the addition of ungauged loads. The measured peak was 2529 g/s , thus the % error improved from -65% to -17%. Interestingly, the peak measured at G1H013 and G1R003 is already higher simulated with only gauged loads (G1R003 is 79% and G1H013 26% higher), than the measured peak. This could be due to unknown abstractions of winter floods.

It can be concluded that the addition of ungauged subcatchments does improve the TDS concentrations and loads for the months of October and November, and in the winter months. Little change has been found during the months December, January and February. Subcatchments 4 and 5 however overcorrect the TDS concentrations and loads, especially in the months March and April. This can also be seen in Table 8.8 which shows that a 57% improvement in errors occurred for the TDS concentration in the second reach (G1H020 to G1H036). The estimated TDS loads for subcatchments 4 and 5 seem incorrect (also refer to Figures 8.16). The TDS loads have been estimated with grab samples of station G1H039. Unfortunately, the station has a accuracy rating of 0 (refer to Table 7.1), but due to no additional choice of tributary, these grab samples were the only estimate.

Table 8.8: Absolute % error difference between the simulation without ungauged loads and the simulation with ungauged loads for TDS

Yearly % error difference	G1H020	G1H036	G1H013	G1R003
TDS Loads	28	96	64	68
TDS Concentration	7	57	38	26

8.11.2 Phosphate as PO_4

- *PO_4 Concentration results:*

(Table 8.25, Figures 8.102-8.105)

Comparing the errors in concentrations between the simulation with ungauged phosphate loads and the simulation run without ungauged phosphate loads (Table 8.13 and Table 8.25), one can see that the % error has improved for all the stations for low and high flow, when including the ungauged phosphates. The % error has improved about 10% for the low flow and about 20% for the concentrations at high flow. One can see in Figures 102 to 105 and Figures 8.38 to 8.41, that the addition of ungauged phosphates does correct the concentration peaks especially in the winter months.

- *PO_4 Loads Results:*

Low Flow :

(Table 8.24, Figures 8.94-8.97)

One can see from Figures 8.94 to 8.97 that the PO_4 loads have improved in the months October and November (as also the TDS loads). There is little change in the low flow loads, except for the small peaks occurring in November and December at station G1H036 (compare Figure 8.95 to 8.31), that are improved. The overall % error is less for stations G1H020 and G1H036, but have been over-corrected for stations G1H013 and G1R003. This is because, without any ungauged phosphate loads, the loads are already oversimulated at these stations.

High Flow :

(Table 8.24, Figures 8.98-8.101)

One can see from Figures 8.98 to 8.101 that the PO_4 load peaks are very undersimulated for all stations, if additional loads from the ungauged subcatchments are missing. The % error in the simulation run without the ungauged phosphates shows about 80% undersimulation. This error has been improved to about 40% undersimulation when the ungauged loads are added to the model.

It can be concluded that the addition of ungauged phosphate loads has proved to be successful for the high flows, as the error has been halved in the high flows. This proves that a considerable percentage of phosphate load is discharged into the river in a flood. Table 8.9 shows the % error improvements from the run without ungauged loads and the simulation run with ungauged loads for the overall yearly values.

Table 8.9: Absolute % error difference between the simulation without ungauged loads and the simulation with ungauged loads for phosphates

Yearly % error difference	G1H020	G1H036	G1H013	G1R003
PO_4 Loads	38	41	28	52
PO_4 Concentration	14	17	21	28

8.11 REFERENCES

DWAF, 1993. G Quibell. *Water Quality in the Berg River: A Situation Analysis*. Department of Water Affairs and Forestry.

Görgens, A.H.M., 1983. *Conceptual Modelling of the Rainfall-Runoff Process in Semi-Arid Catchments*. Hydrological Research Unit, Rhodes University, Report No. 1/83, Grahamstown, South Africa.

Grijsen, J.G. 1986. *River Flow Simulation* in River Flow Modelling and Forecasting (edited by D.A. Kraijenhoff and J.R. Moll). Pg 241-272.

Kraijenhoff, D.A. and J.R. Moll (eds.), 1986. *River Flow Modelling and Forecasting*. D. Reidel Publishing Company.

Table 8.10: Results of TDS Loads after calibration

	Total Load measured (tons)	Total Load simulated (tons)	% diff in total load	mean measured (g/s)	mean simulated (g/s)	Coeff of determination (R^2)	Coeff of efficiency
Low flow period							
G1H020	2577	2077	-19.4	164	132	0.84	0.13
G1H036	3204	5401	68	204	343	0.38	-2
G1H013	6078	6751	11	386	429	0.51	-0.16
G1R003	5598	7595	35	356	483	0.75	0.2
High flow period							
G1H020	13220	12729	-3.7	836	805	0.99	0.97
G1H036	39214	54475	39	2480	3445	0.89	0.74
G1H013	82042	99558	21.3	5189	6296	0.93	0.82
G1R003	81497	133148	63	5154	8421	0.94	-0.06
Yearly							
G1H020	15798	14806	-6.3	501	469	0.98	0.97
G1H036	42419	58760	41	1345	1898	0.9	0.78
G1H013	88120	106309	20.6	2794	3371	0.94	0.85
G1R003	87097	140744	61	2761	4462	0.95	0.15

Table 8.11: Results of TDS Concentration after calibration

	mean measured (mg/l)	mean simulated (mg/l)	% error in mean	Coeff of determination (R^2)
Low flow period				
G1H020	62.6	43	-31	0.24
G1H036	120	136	13.8	0.47
G1H013	141	123	-12.3	0.03
G1R003	219	162	-26	0.10
High flow period				
G1H020	56.5	41	-27	0.30
G1H036	123	176.6	44	0.50
G1H013	158	196	23	0.67
G1R003	210	224	6.7	0.57
Yearly				
G1H020	59.5	42	-29	0.08
G1H036	121	156	29	0.48
G1H013	149	159	6.8	0.56
G1R003	215	193	-10	0.30

Table 8.11: Results of PO_4 Loads after calibration

	Total Load measured (tons)	Total Load simulated (tons)	% diff in total load	mean measured (g/s)	mean simulated (g/s)	Coeff of determination (R^2)	Coeff of efficiency
Low flow period							
G1H020	1.02	1.07	4.7	0.065	0.068	0.39	0.15
G1H036	1.2	1.2	0.6	0.076	0.077	0.75	0.48
G1H013	1	1.4	38	0.06	0.09	0.76	0.3
G1R003	0.6	1.2	103	0.04	0.08	0.98	0.92
High flow period							
G1H020	13.9	7.9	-42	0.9	0.5	0.95	0.63
G1H036	28.6	15.9	-44	1.8	1.0	0.96	0.66
G1H013	48.2	21.2	-56	3.0	1.3	0.96	0.51
G1R003	25.6	24	-6.5	1.6	1.5	0.98	0.91
Yearly							
G1H020	14.9	9	-39	0.47	0.28	0.95	0.67
G1H036	29.8	17.2	-42	0.95	0.54	0.96	0.69
G1H013	49.3	22.6	-54	1.56	0.71	0.96	0.57
G1R003	26.2	25.2	-4	0.83	0.80	0.98	0.92

Table 8.13: Results of PO_4 Concentration after calibration

	mean measured	mean simulated	% error in mean	Coeff of determination (R^2)
Low flow period				
G1H020	0.02	0.025	-0.8	0.3
G1H036	0.04	0.026	-32	0.15
G1H013	0.024	0.023	-3.4	0.20
G1R003	0.024	0.023	-5.9	0.57
High flow period				
G1H020	0.023	0.023	-32	0.68
G1H036	0.08	0.04	-55	0
G1H013	0.05	0.034	-33	0.32
G1R003	0.03	0.034	-9.8	0.25
Yearly				
G1H020	0.03	0.023	-20	0.49
G1H036	0.06	0.031	-48	0.25
G1H013	0.04	0.028	-24	0.42
G1R003	0.027	0.028	2.9	0.36

Table 8.14: Results of Temperature after calibration

	mean measured	mean simulated	% error in mean	Std Dev measured	Std Dev simulated	Coeff of determination (R^2)
Low flow period						
G1H020	24	23	-4.4	2.5	3	0.92
G1H036	24.6	24	-2.9	2.75	2.73	0.81
G1H013	24.2	24.5	1.5	2.52	3.57	0.85
G1R003	25	24.7	-1.6	2.5	3.5	0.85
High flow period						
G1H020	14	13	-7	2.56	2.54	0.92
G1H036	13.6	12.8	-5.9	2.9	2.75	0.81
G1H013	14.1	12.5	-11	2.8	2.9	0.8
G1R003	15.3	12.5	-18	2.77	2.87	0.83
Yearly						
G1H020	19	17.98	-5.4	5.62	5.7	0.98
G1H036	19.1	18.3	-3.9	6.2	6.5	0.95
G1H013	19.1	18.5	-3.1	5.73	6.9	0.96
G1R003	20.15	18.5	-8	5.56	6.9	0.96

Table 8.15: Results of Oxygen after calibration

	mean saturation oxygen	mean simulated	% error in mean	Std Dev sat. Oxygen	Std Dev simulated	Coeff of determination (R^2)
Low flow period						
G1H020	8.65	8.73	0.9	0.45	0.44	0.98
G1H036	8.55	8.61	0.7	0.52	0.5	0.97
G1H013	8.4	8.5	0.6	0.52	0.53	0.98
G1R003	8.3	8.9	7.6	0.51	0.42	0.9
High flow period						
G1H020	10.5	10.3	-1.8	0.62	0.59	0.93
G1H036	10.7	10.6	-0.6	0.72	0.86	0.7
G1H013	10.8	10.7	-0.2	0.79	0.76	0.88
G1R003	10.8	10.8	0	0.83	0.82	0.85
Yearly						
G1H020	9.6	9.55	-0.6	0.95	0.96	0.98
G1H036	9.62	9.61	-0.06	1.23	1.22	0.93
G1H013	9.6	9.62	0.15	1.35	1.31	0.98
G1R003	9.55	9.8	3.3	1.42	4.14	0.94

Table 8.16: Results of TDS Loads after Verification

	Total Load measured (tons)	Total Load simulated (tons)	% diff in total load	mean measured (g/s)	mean simulated (g/s)	Coeff of determination (R^2)	Coeff of efficiency
Low flow period							
G1H020	2683	2669	-0.5	171	170	0.81	0.41
G1H036	3738	4007	-7.2	238	255	0.90	0.80
G1H013	7008	6137	-12	446	390	0.93	0.84
G1R003	6811	6795	-0.2	433	432	0.92	0.75
High flow period							
G1H020	14132	6767	-52	894	428	0.93	0.41
G1H036	N/A						
G1H013	59589	51082	-14	3769	3231	0.92	0.76
G1R003	61961	70959	14.5	3919	4488	0.91	0.80
Yearly							
G1H020	16815	12030	-28	533	381	0.95	0.73
G1H036	N/A						
G1H013	66597	57218	-14	2112	1814	0.92	0.82
G1R003	68772	77756	13	2181	2465	0.92	0.85

NOTE : *For station G1H036 the flow measurements are incomplete from the 3rd of July to end September, and the statistical comparisons have for this reason not been included.*

Table 8.17: Results of TDS Concentration after Verification

	mean measured (mg/l)	mean simulated (mg/l)	% error in mean	Coeff of determination (R^2)
Low flow period				
G1H020	52.3	47	-21	0.23
G1H036	124	96	-27	0.22
G1H013	137	99	-27	0.30
G1R003	191	111	-41	0.11
High flow period				
G1H020	65	47	-27	0.04
G1H036	N/A			
G1H013	148	139	-7	0.58
G1R003	166	147	-12	0.47
Yearly				
G1H020	62	47	-24	0.04
G1H036	N/A			
G1H013	143	119	-17	0.42
G1R003	179	129	-27	0.22

NOTE : *For station G1H036 the flow measurements are incomplete from the 3rd of July to end September, and the statistical comparisons have for this reason not been included.*

Table 8.18: Results of PO_4 Load after Verification

	Total Load measured (tons)	Total Load simulated (tons)	% diff in total load	mean measured (g/s)	mean simulated (g/s)	Coeff of determination (R^2)	Coeff of efficiency
Low flow period							
G1H020	1.0	1.1	5	0.06	0.06	0.25	-0.24
G1H036	2.0	1.1	-46	0.13	0.07	0.85	0.39
G1H013	1.4	1.5	11	0.09	0.098	0.86	0.58
G1R003	0.6	1.5	159	0.04	0.10	0.93	-4.2
High flow period							
G1H020	6.0	5.3	-11	0.38	0.34	0.43	0.15
G1H036	N/A						
G1H013	18.3	15.1	-18	1.2	0.95	0.93	0.80
G1R003	14.8	17.9	21	0.94	1.14	0.92	0.79
Yearly							
G1H020	7.0	6.3	-9	0.22	0.20	0.5	0.33
G1H036	N/A						
G1H013	19.7	16.6	-16	0.62	0.53	0.94	0.84
G1R003	15.4	19.5	26.5	0.49	0.62	0.93	0.86

NOTE : *For station G1H036 the flow measurements are incomplete from the 3rd of July to end September, and the statistical comparisons have for this reason not been included.*

Table 8.19: Results of PO_4 Concentration after Verification

	mean measured (mg/l)	mean simulated (mg/l)	% error in mean	Coeff of determination (R^2)
Low flow period				
G1H020	0.020	0.017	-15	0.18
G1H036	0.062	0.019	-69	0.30
G1H013	0.020	0.019	-15	0.31
G1R003	0.020	0.021	3.4	0.26
High flow period				
G1H020	0.033	0.029	-8.8	0.14
G1H036	N/A			
G1H013	0.043	0.036	-15	0.15
G1R003	0.032	0.038	16	0.72
Yearly				
G1H020	0.026	0.024	-11	0.44
G1H036	N/A			
G1H013	0.031	0.028	-10	0.43
G1R003	0.026	0.029	12	0.72

NOTE : *For station G1H036 the flow measurements are incomplete from the 3rd of July to end September, and the statistical comparisons have for this reason not been included.*

Table 8.20: Results of Temperature after Verification

	mean measured	mean simulated	% error in mean	Std Dev measured	Std Dev simulated	Coeff of determination (R^2)
Low flow period						
G1H020	24	23.1	-3.5	2.6	3.0	0.94
G1H036	24.7	24.3	-1.5	2.8	3.6	0.84
G1H013	24.2	25.7	5.9	2.6	4.2	0.75
G1R003	25.1	27.1	8.3	2.5	4.4	0.72
High flow period						
G1H020	14.1	13.3	-5.4	2.7	2.8	0.94
G1H036	13.6	13.4	-1.8	2.9	3.1	0.85
G1H013	14	13.2	-5.7	2.8	3.9	0.78
G1R003	15.2	13.1	-13	2.8	3.4	0.83
Yearly						
G1H020	19	18.2	-4.2	5.6	5.7	0.98
G1H036	19.1	18.8	-1.6	6.2	6.4	0.96
G1H013	19.1	19.4	1.6	5.8	7.5	0.93
G1R003	20.1	20.1	0	5.6	8.6	0.94

Table 8.21: Results of Oxygen after Verification

	mean saturation oxygen	mean simulated	% error in mean	Std Dev sat. Oxygen	Std Dev simulated	Coeff of Determination (R^2)
Low flow period						
G1H020	8.54	8.66	1.4	0.51	0.51	0.96
G1H036	8.3	8.36	1	0.55	0.57	0.93
G1H013	8.2	8.23	1.4	0.52	0.53	0.94
G1R003	8.3	8.2	1	0.51	0.52	0.93
High flow period						
G1H020	10.5	10.34	-1.5	0.68	0.7	0.89
G1H036	10.45	10.4	-0.4	0.79	0.82	0.79
G1H013	10.54	10.47	-0.75	0.94	0.96	0.76
G1R003	10.8	10.6	-1.8	0.95	1.1	0.75
Yearly						
G1H020	9.53	9.51	-0.2	1.15	1.04	0.97
G1H036	9.37	9.39	0.2	1.3	1.25	0.95
G1H013	9.35	9.36	0.14	1.43	1.37	0.94
G1R003	9.55	9.40	-1.5	1.4	1.8	0.92

Table 8.22: Results of TDS Loads of simulation run without ungauged TDS

	Total Load measured (tons)	Total Load simulated (tons)	% diff in total load	mean measured (g/s)	mean simulated (g/s)	Coeff of Determination (R^2)	Coeff of efficiency
Low flow period							
G1H020	2577	1923	-25	164	122	0.74	-0.19
G1H036	3204	2743	-14	204	174	0.55	0.25
G1H013	6078	3950	-35	386	251	0.59	0.06
G1R003	5598	4389	-22	356	279	0.79	0.51
High flow period							
G1H020	13220	8555	-35	836	541	0.98	0.85
G1H036	39214	16254	-58	2480	1028	0.97	0.47
G1H013	82042	46597	-43	5189	2947	0.85	0.68
G1R003	81497	76346	-6	5154	4828	0.90	0.41
Yearly							
G1H020	15798	10479	-34	501	332	0.98	0.87
G1H036	42419	18997	-55	1345	602	0.98	0.57
G1H013	88120	50471	-43	2794	1603	0.86	0.73
G1R003	87097	80735	-7	2761	2560	0.90	0.53

Table 8.23: Results of TDS Concentration of simulation run without ungauged TDS

	mean measured (mg/l)	mean simulated (mg/l)	% error in mean	Coeff of determination (R^2)
Low flow period				
G1H020	62.6	40.5	-35	0.1
G1H036	120	81	-32	0.49
G1H013	141	85	-40	0.27
G1R003	219	113	-51	0.21
High flow period				
G1H020	56.5	36	-36	0.38
G1H036	123	92	-25	0.44
G1H013	158	121	-23	0.34
G1R003	210	169	-19	0.28
Yearly				
G1H020	59.5	38	-36	0.07
G1H036	121	87	-28	0.44
G1H013	149	103	-31	0.37
G1R003	215	141	-36	0.12

Table 8.24: Results of PO_4 Loads of simulation run without ungauged PO_4

	Total Load measured (tons)	Total Load simulated (tons)	% diff in total load	mean measured (g/s)	mean simulated (g/s)	Coeff of determination (R^2)	Coeff of efficiency
Low flow period							
G1H020	1.02	1.02	-0.8	0.065	0.064	0.31	0.09
G1H036	1.2	0.79	-34	0.076	0.05	0.60	0.10
G1H013	1	0.96	-4.6	0.06	0.06	0.50	0.24
G1R003	0.6	0.81	35	0.04	0.05	0.61	0.26
High flow period							
G1H020	13.9	2.38	-83	0.9	0.15	0.95	0.06
G1H036	28.6	4.26	-85	1.8	0.26	0.95	0.08
G1H013	48.2	8.11	-83	3.0	0.51	0.95	0.18
G1R003	25.6	10.9	-58	1.6	0.69	0.94	0.61
Yearly							
G1H020	14.9	3.4	-77	0.47	0.11	0.95	0.19
G1H036	29.8	5.0	-83	0.95	0.16	0.96	0.20
G1H013	49.3	9.1	-82	1.56	0.29	0.96	0.22
G1R003	26.2	11.7	-56	0.83	0.37	0.94	0.63

Table 8.25: Results of PO_4 Concentrations of simulation run without ungauged PO_4

	mean measured	mean simulated	% error in mean	Coeff of determination (R^2)
Low flow period				
G1H020	0.02	0.023	-3.4	0.22
G1H036	0.04	0.022	-44	0.11
G1H013	0.024	0.019	-17	0.09
G1R003	0.024	0.020	-18	0.51
High flow period				
G1H020	0.023	0.016	-55	0.76
G1H036	0.08	0.021	-74	0.25
G1H013	0.05	0.021	-58	0.46
G1R003	0.03	0.021	-31	0.39
Yearly				
G1H020	0.03	0.019	-34	0.57
G1H036	0.06	0.022	-65	0.13
G1H013	0.04	0.020	-45	0.44
G1R003	0.027	0.025	-25	0.41

Figure 8.18: TDS Loads at G1H020 for low flows (Calibration)

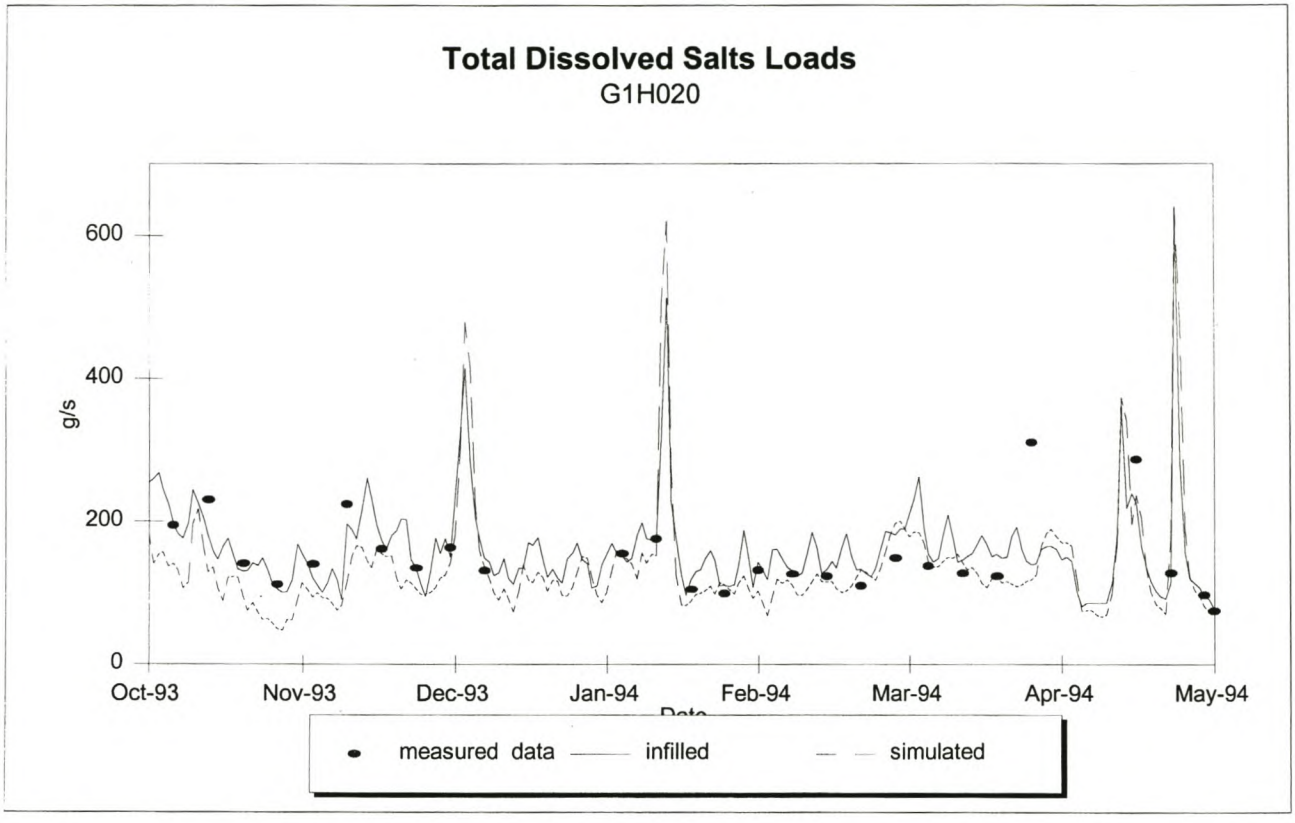

Figure 8.19: TDS Loads at G1H036 for low flows (Calibration)

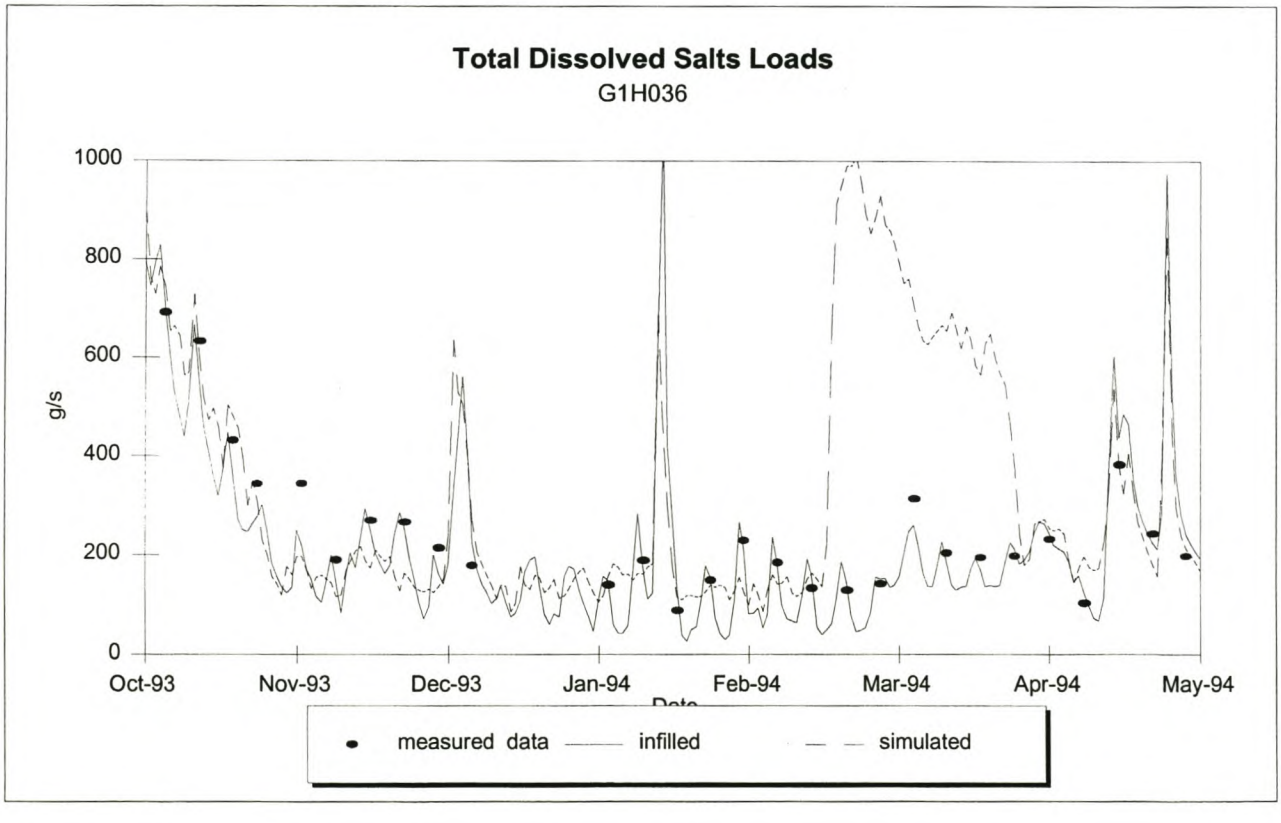

Figure 8.20: TDS Loads at G1H013 for low flows (Calibration)

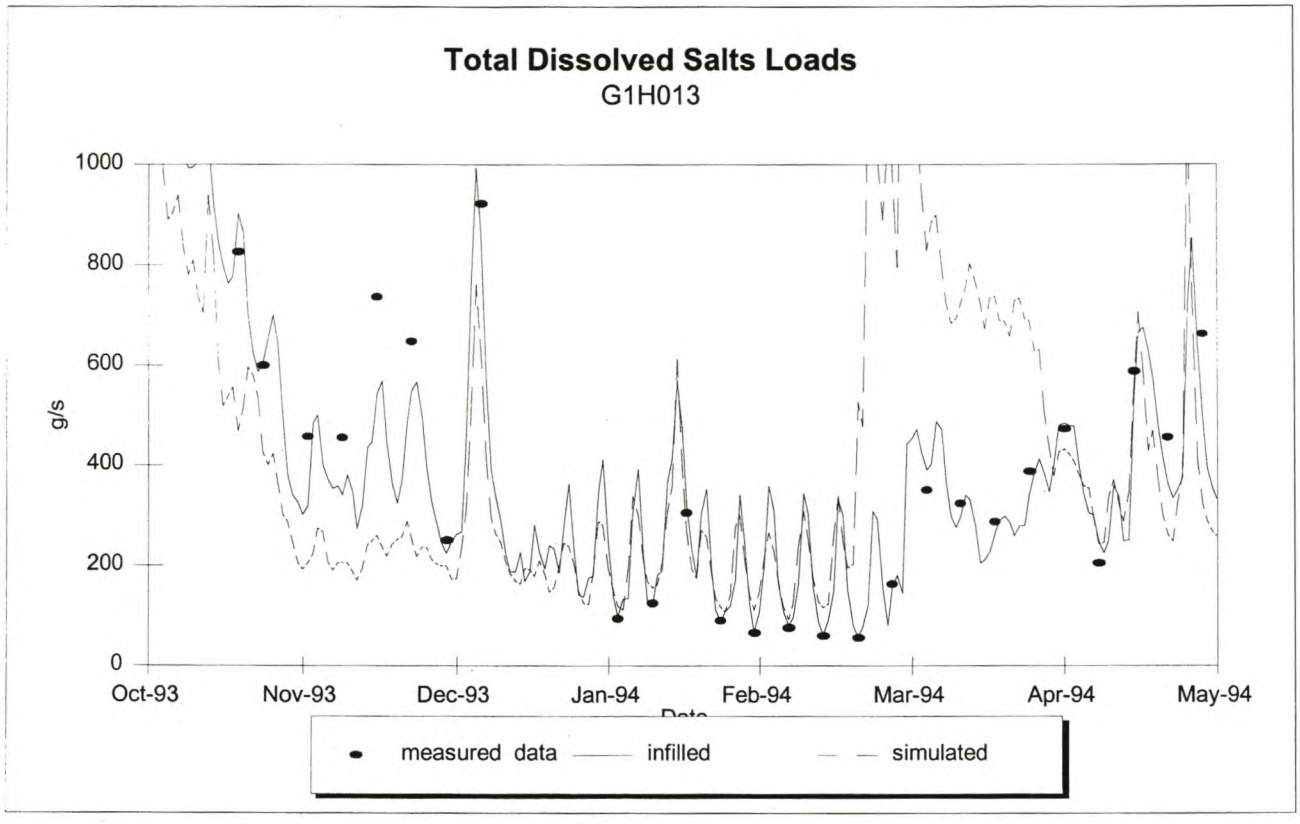

Figure 8.21: TDS Loads at G1R003 for low flows (Calibration)

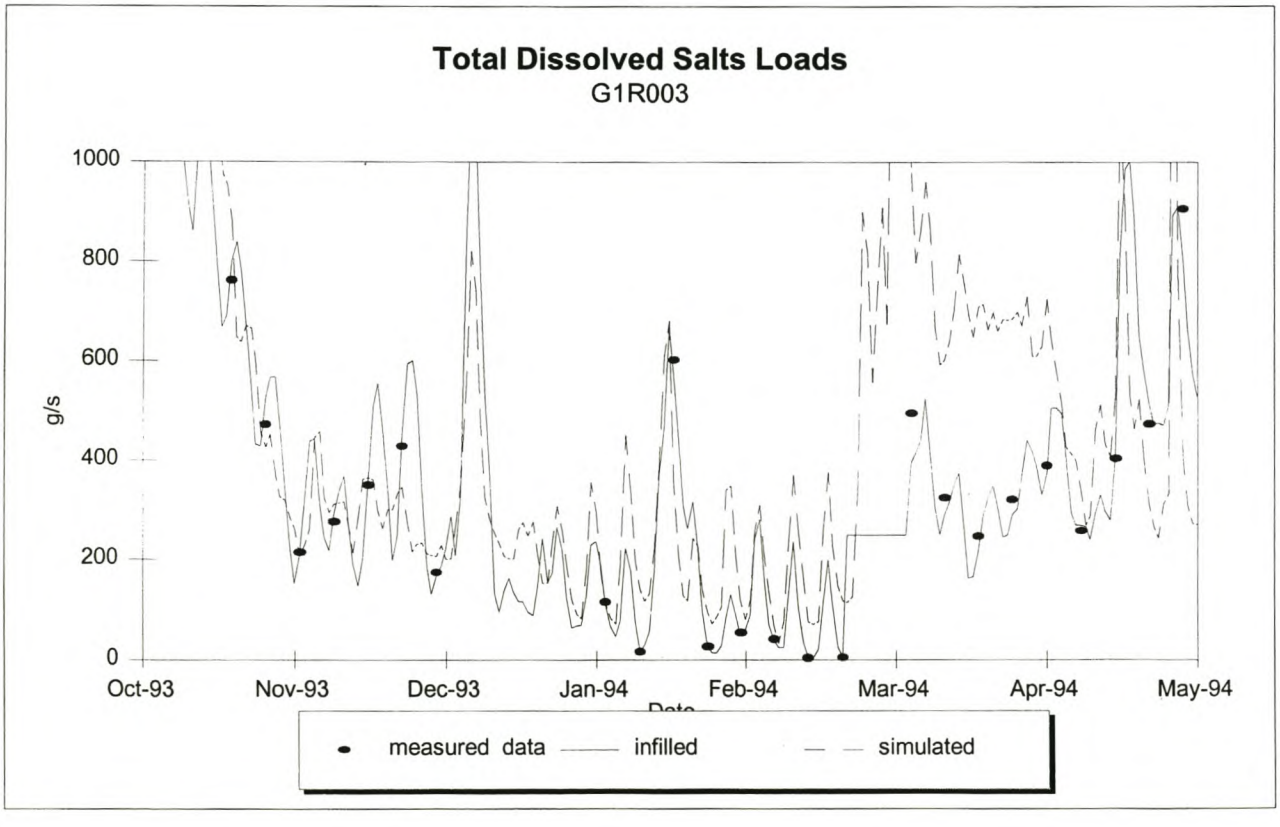

Figure 8.22: TDS Loads at G1H020 for high flows (Calibration)

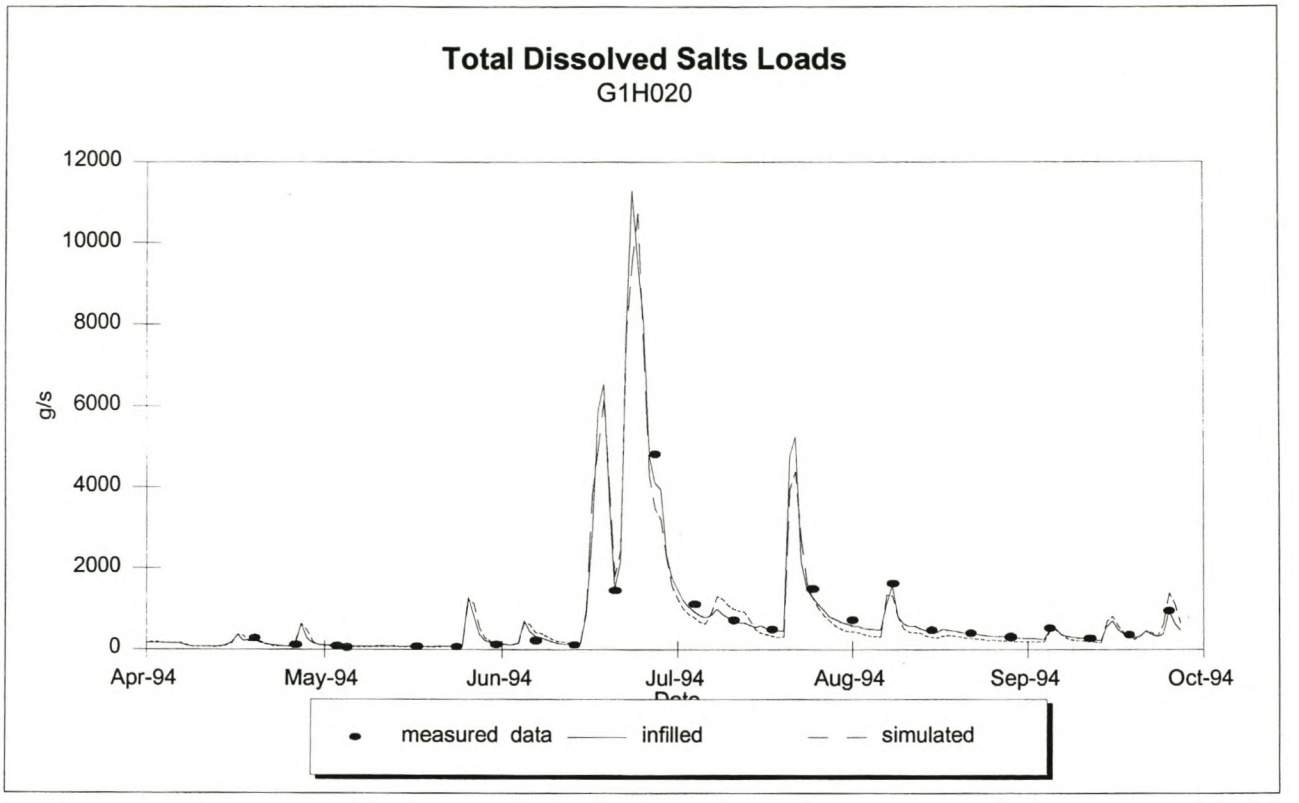

Figure 8.23: TDS Loads at G1H036 for high flows (Calibration)

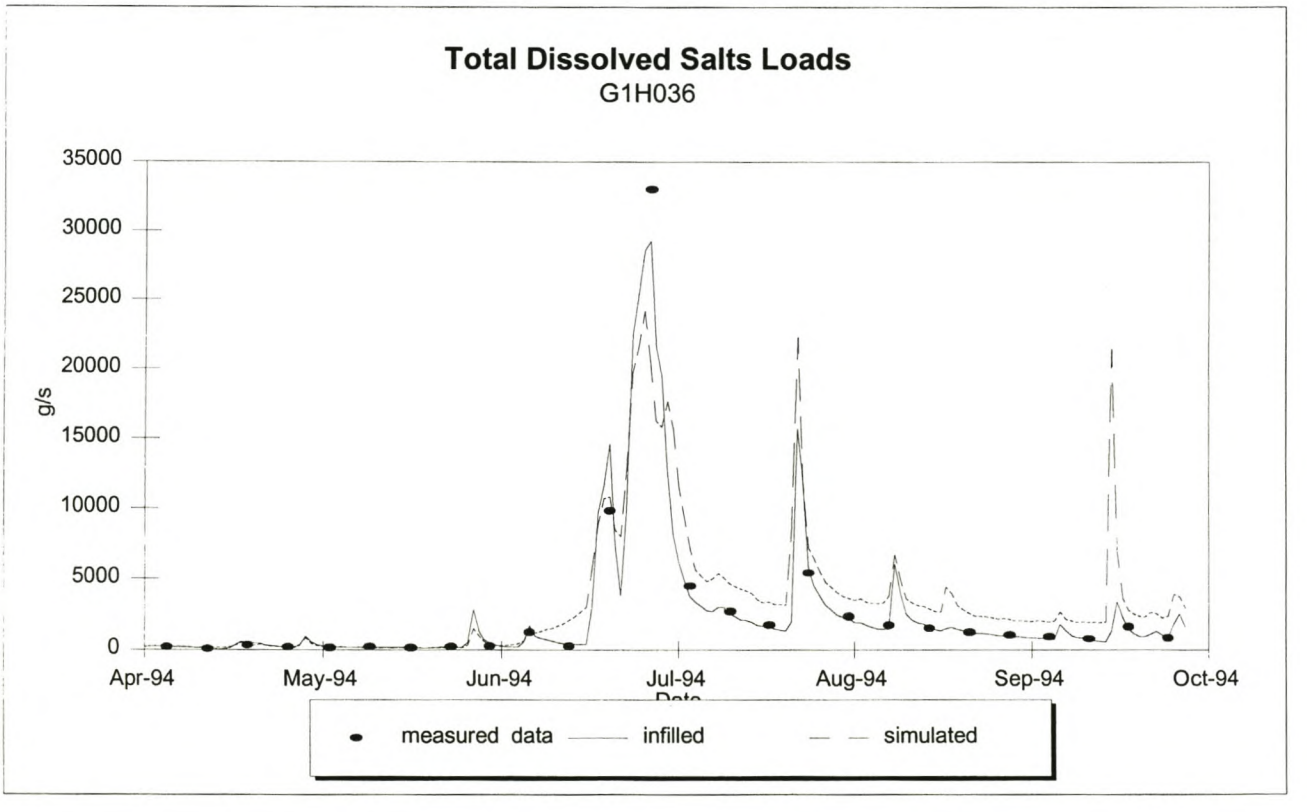

Figure 8.24: TDS Loads at G1H013 for high flows (Calibration)

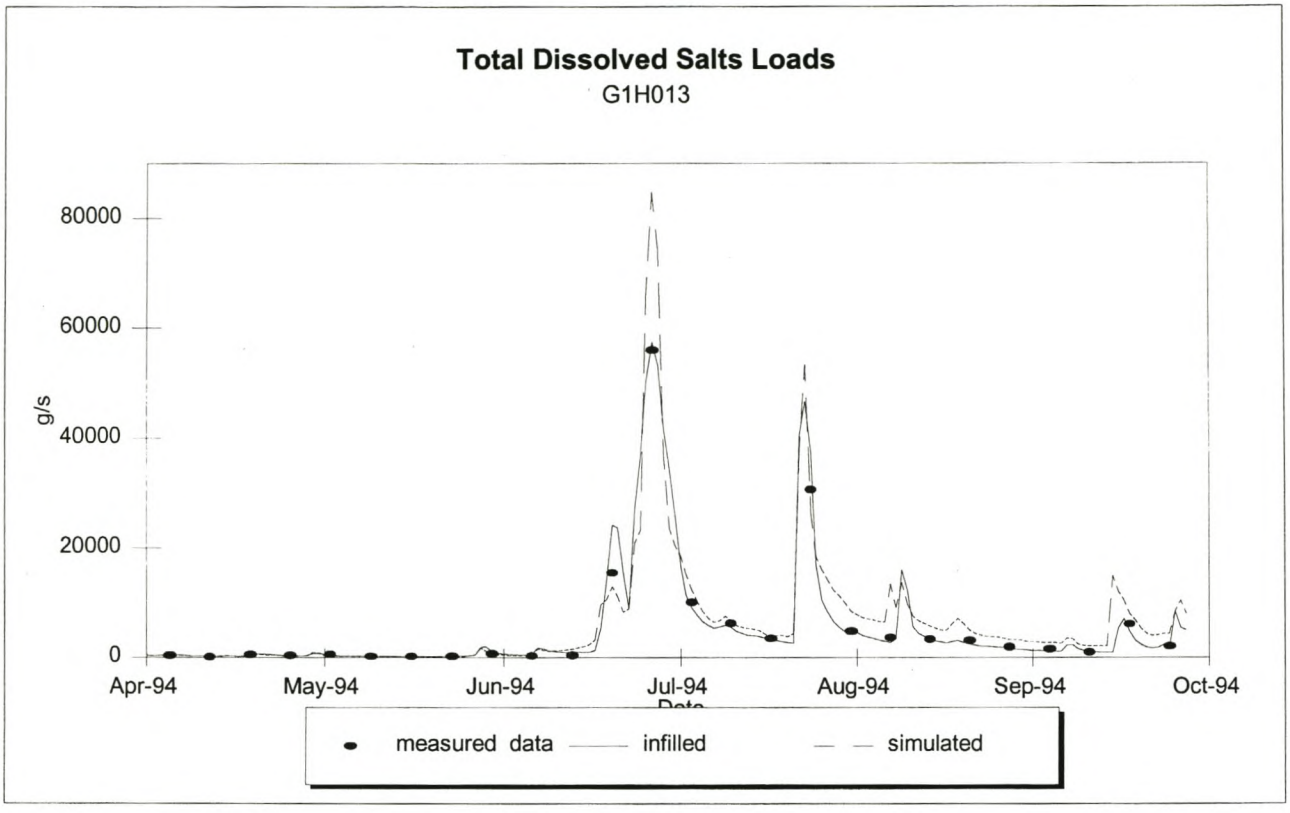

Figure 8.25: TDS Loads at G1R003 for high flows (Calibration)

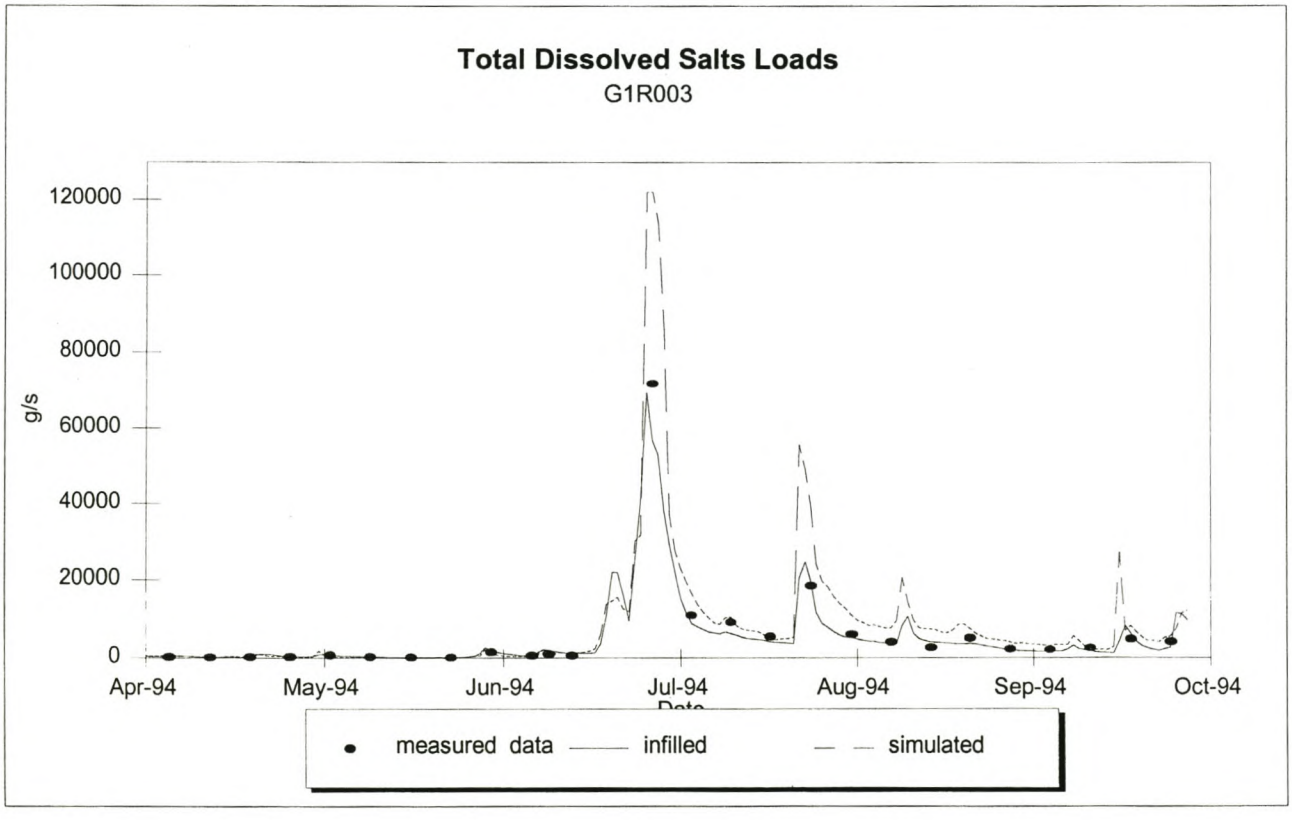

Figure 8.26: TDS Concentration at G1H020 (Calibration)

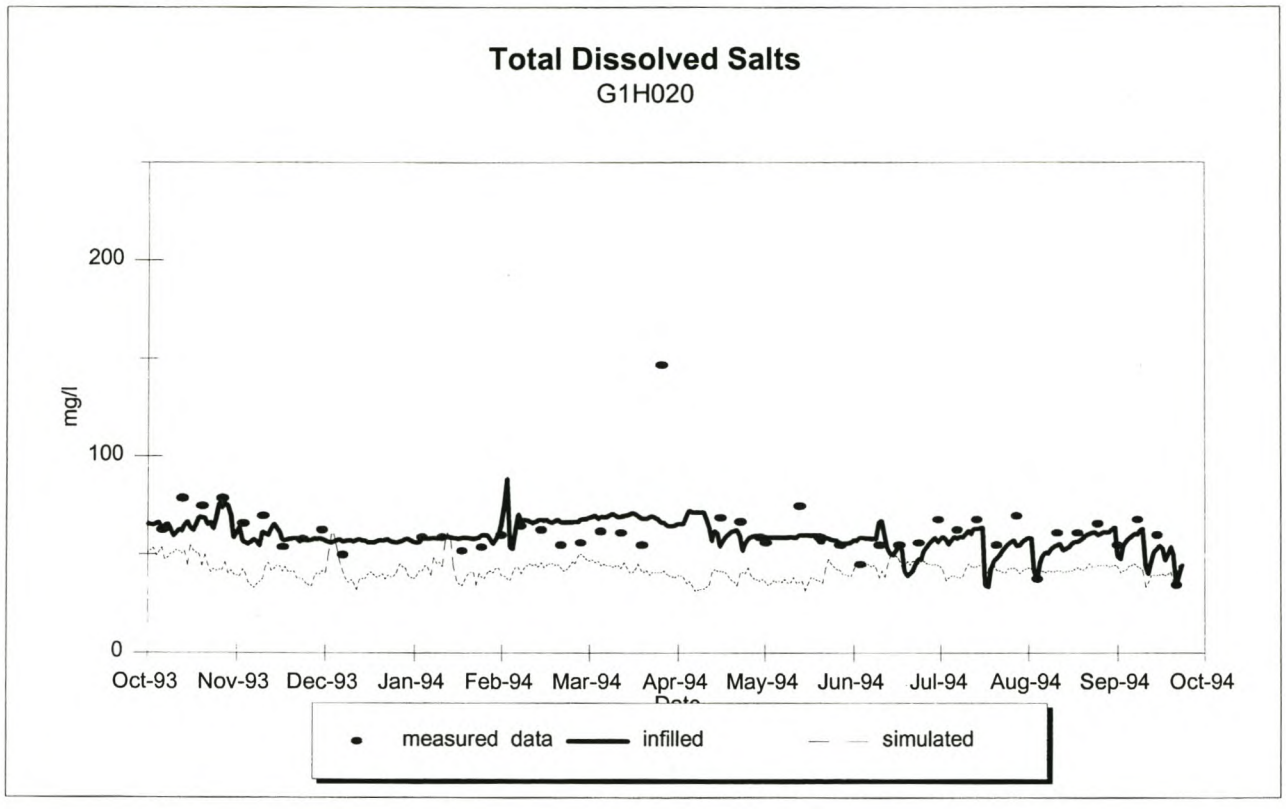

Figure 8.27: TDS Concentration at G1H036 (Calibration)

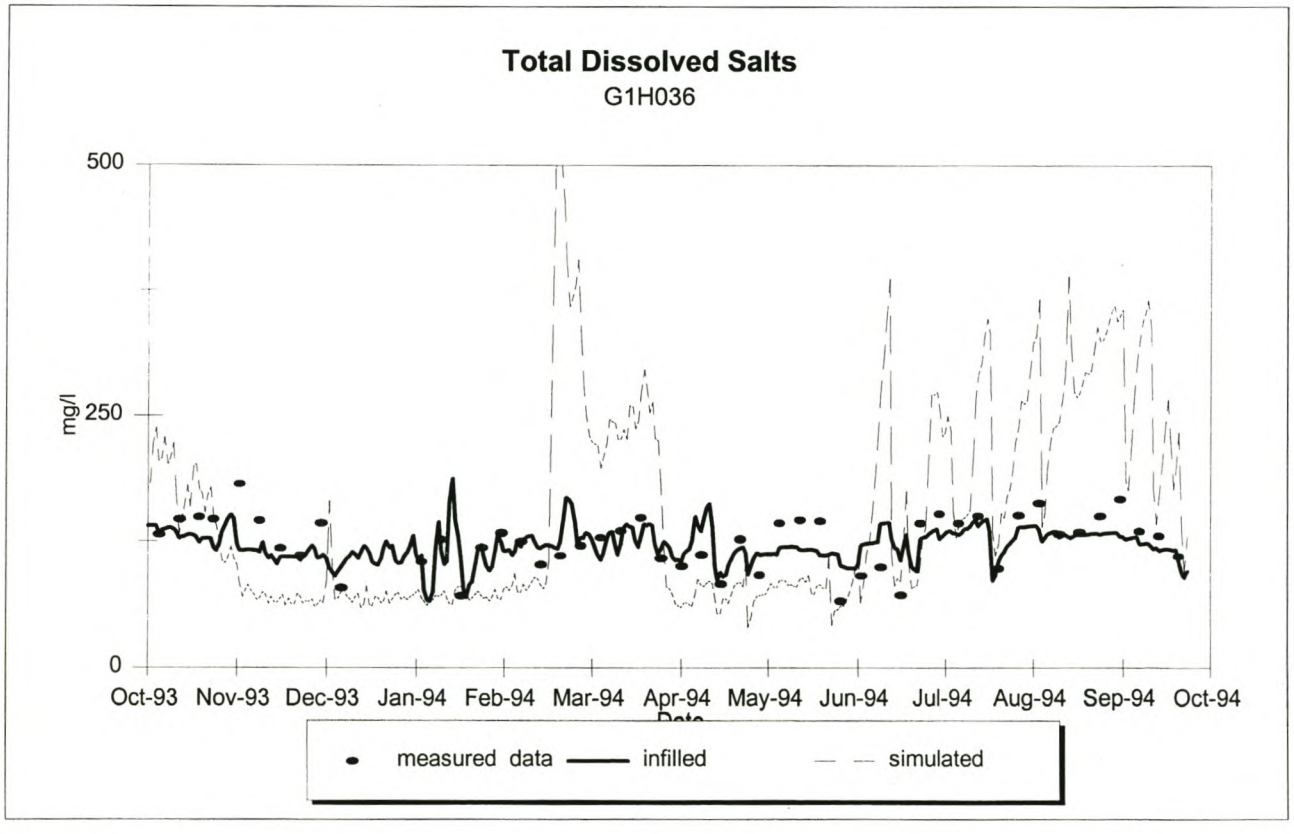

Figure 8.28: TDS Concentration at G1H013 (Calibration)

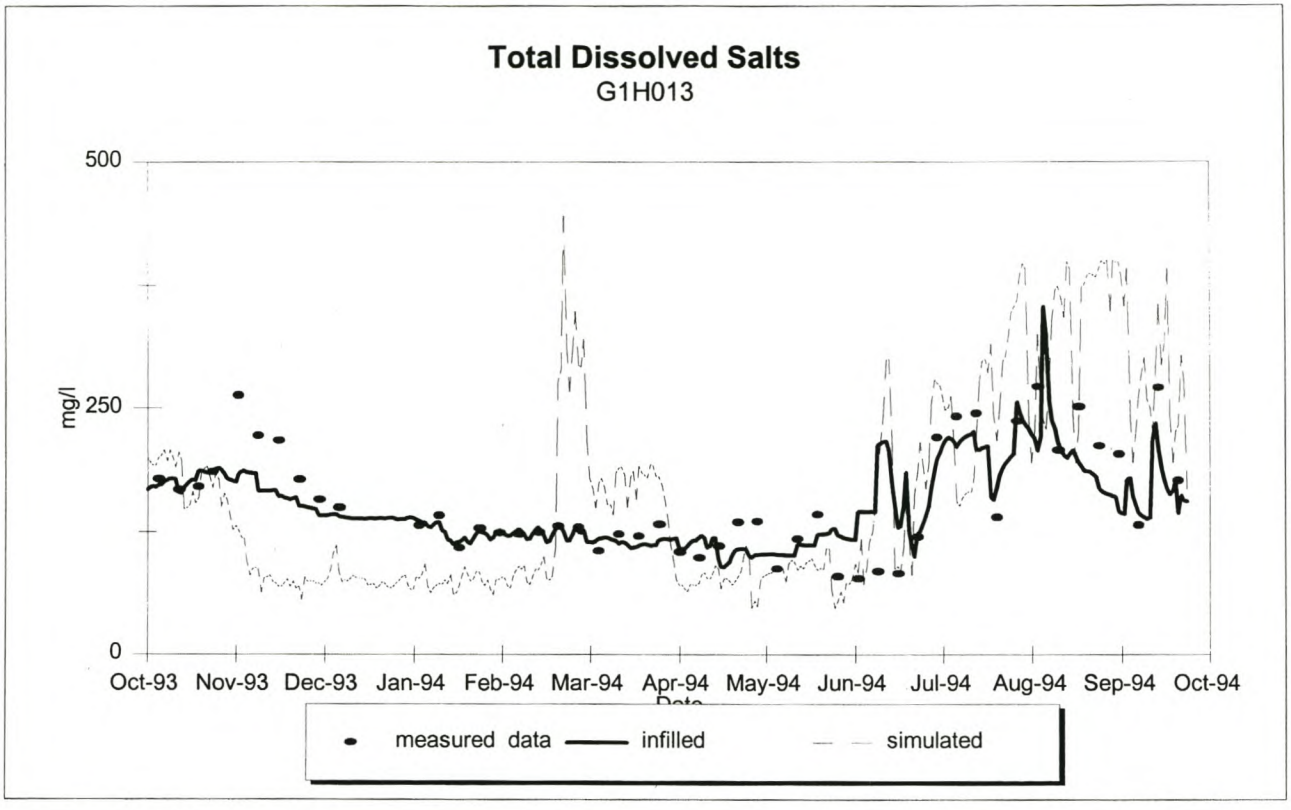

Figure 8.29: TDS Concentration at G1R003 (Calibration)

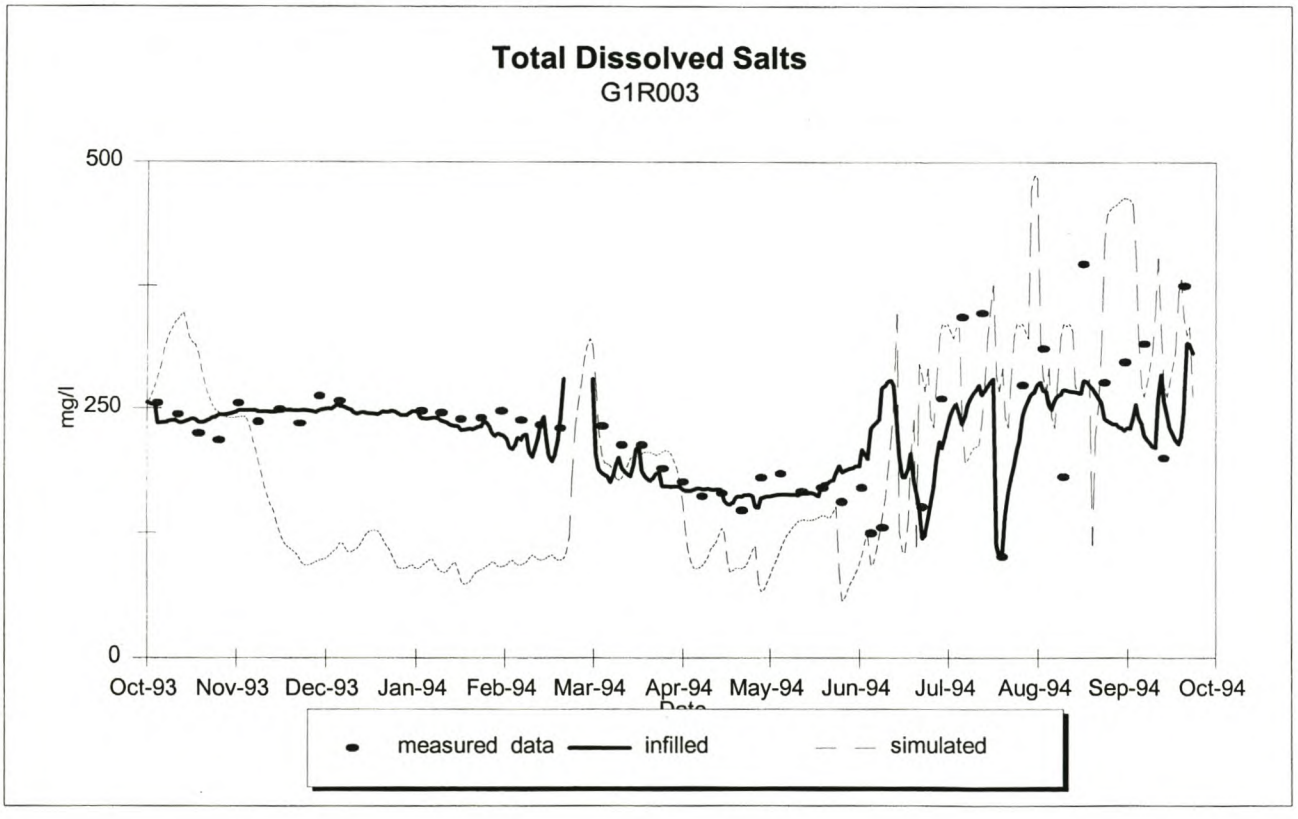

Figure 8.30: Phosphate Loads at G1H020 for low flows (Calibration)

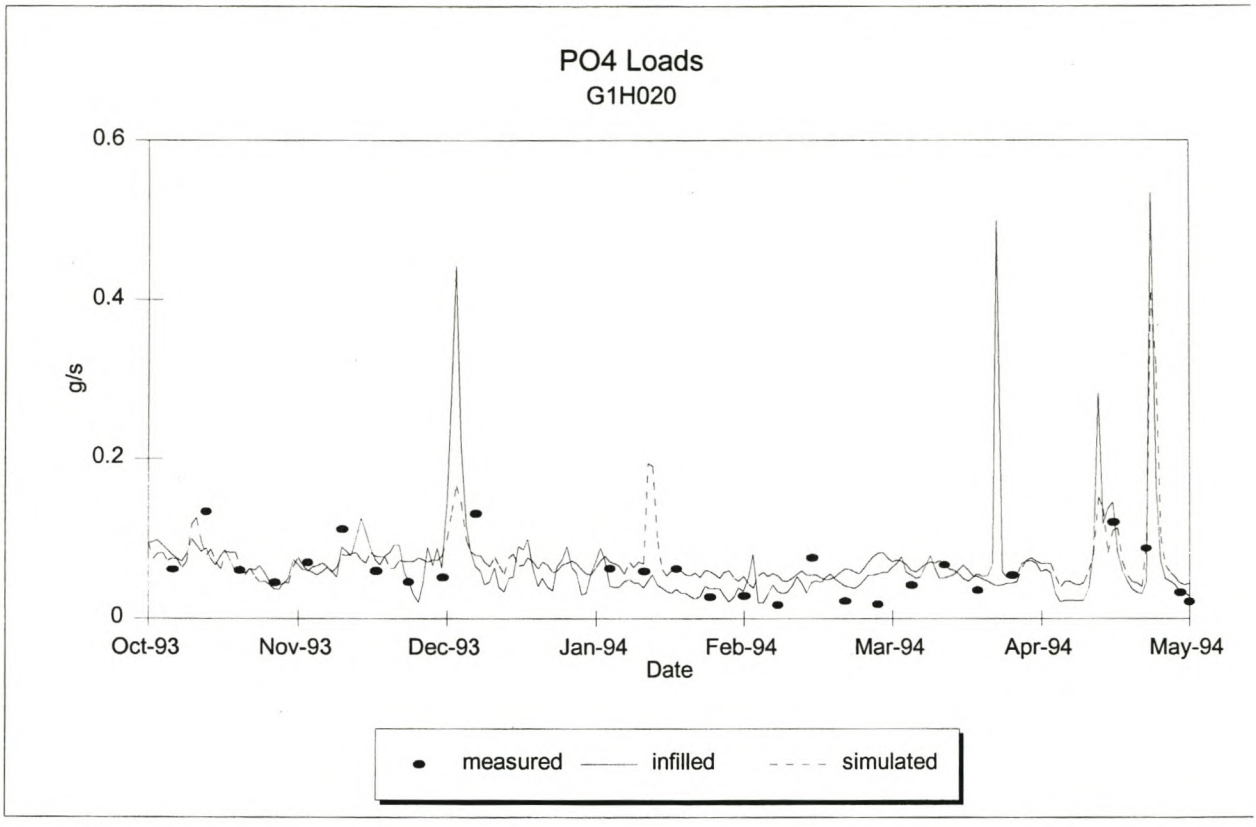

Figure 8.31: Phosphate Loads at G1H036 for low flows (Calibration)

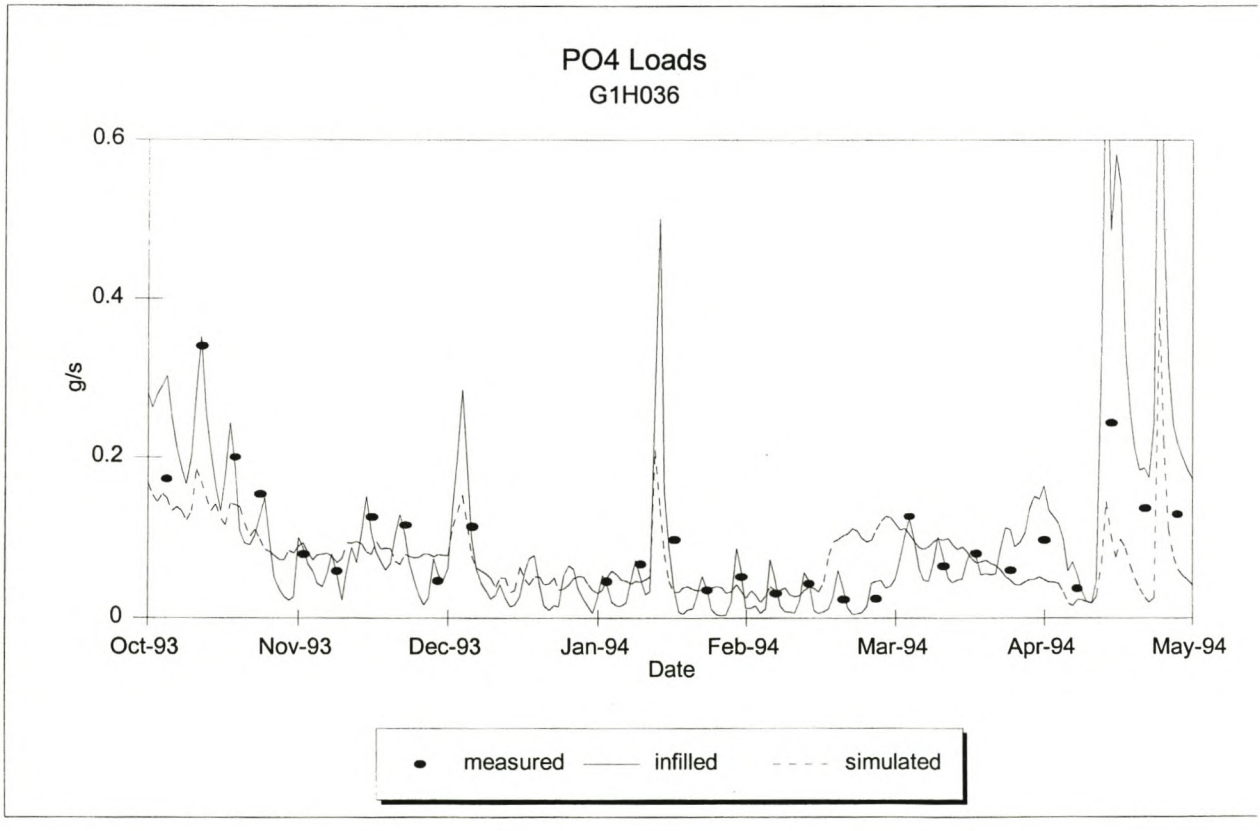

Figure 8.32: Phosphate Loads at G1H013 for low flows (Calibration)

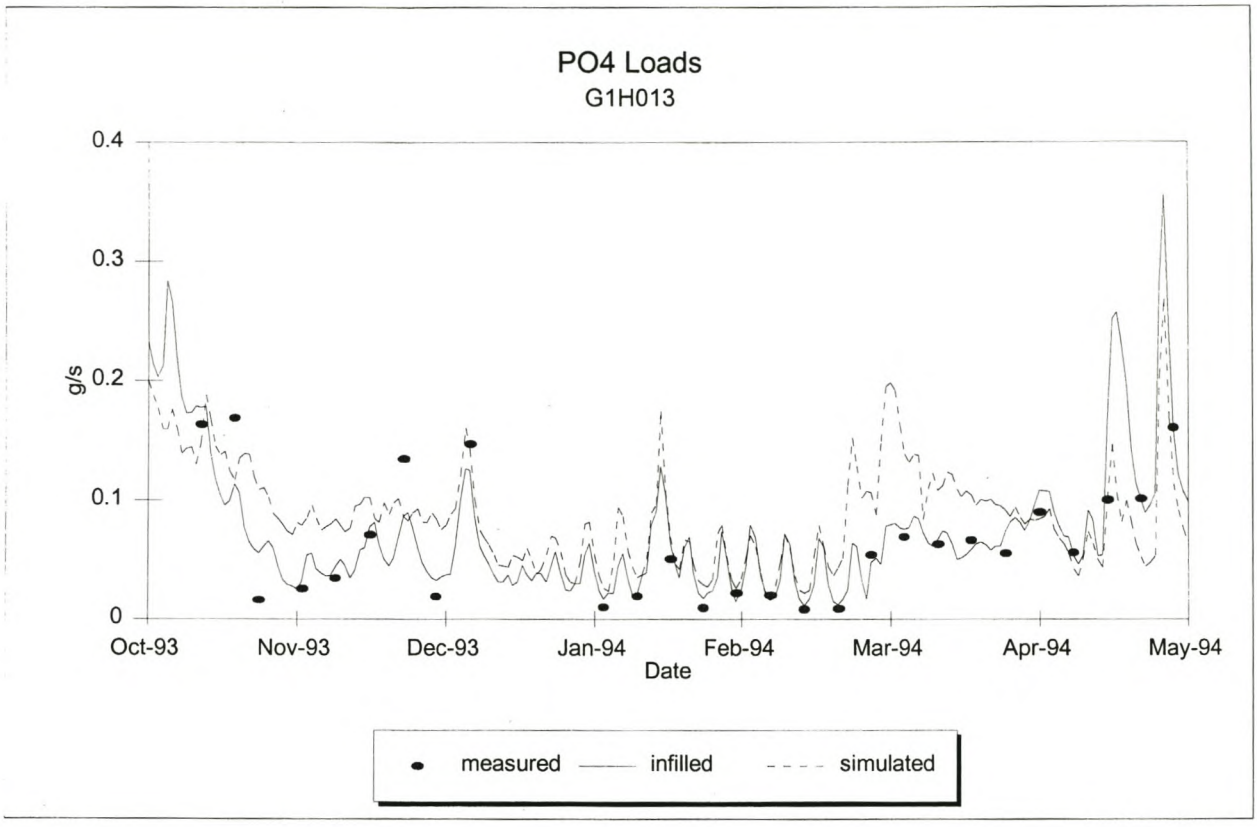

Figure 8.33: Phosphate Loads at G1R003 for low flows (Calibration)

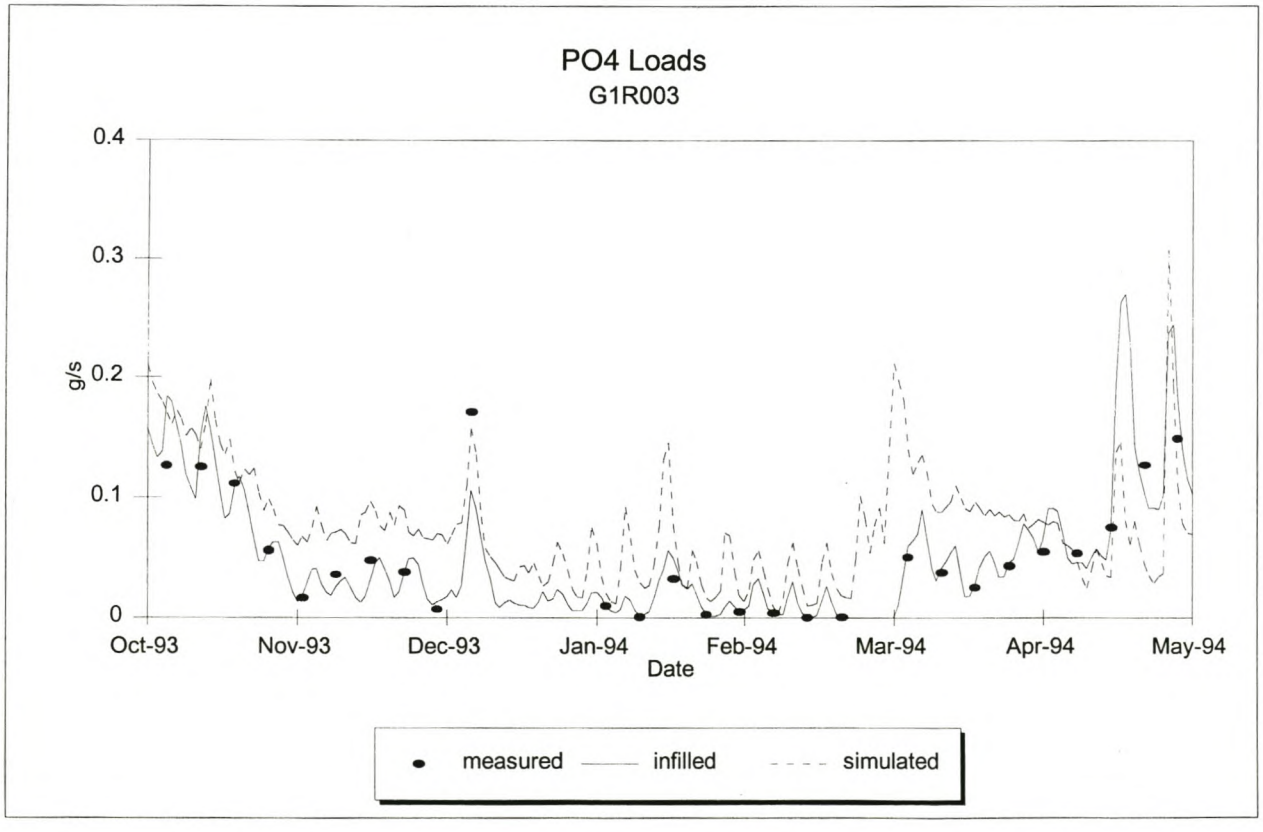

Figure 8.34: Phosphate Loads at G1H020 for high flows (Calibration)

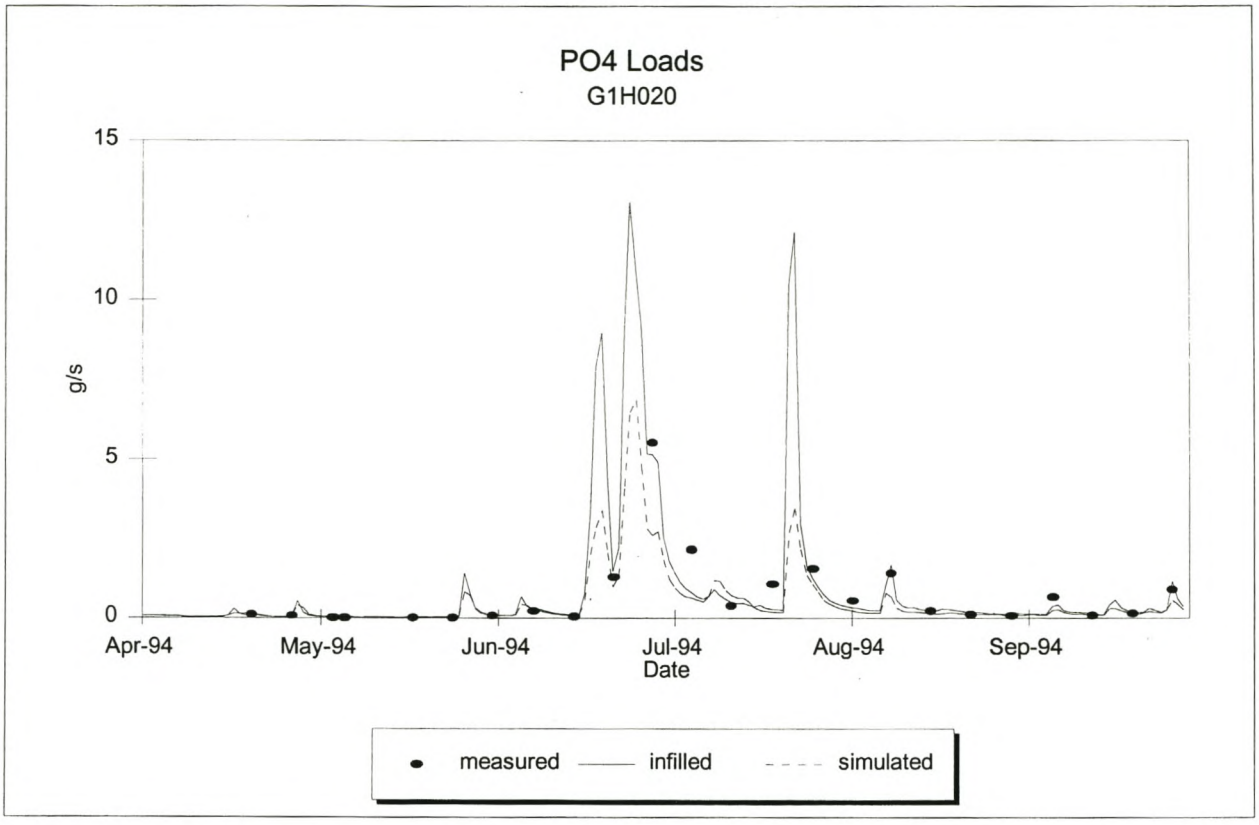

Figure 8.35: Phosphate Loads at G1H036 for high flows (Calibration)

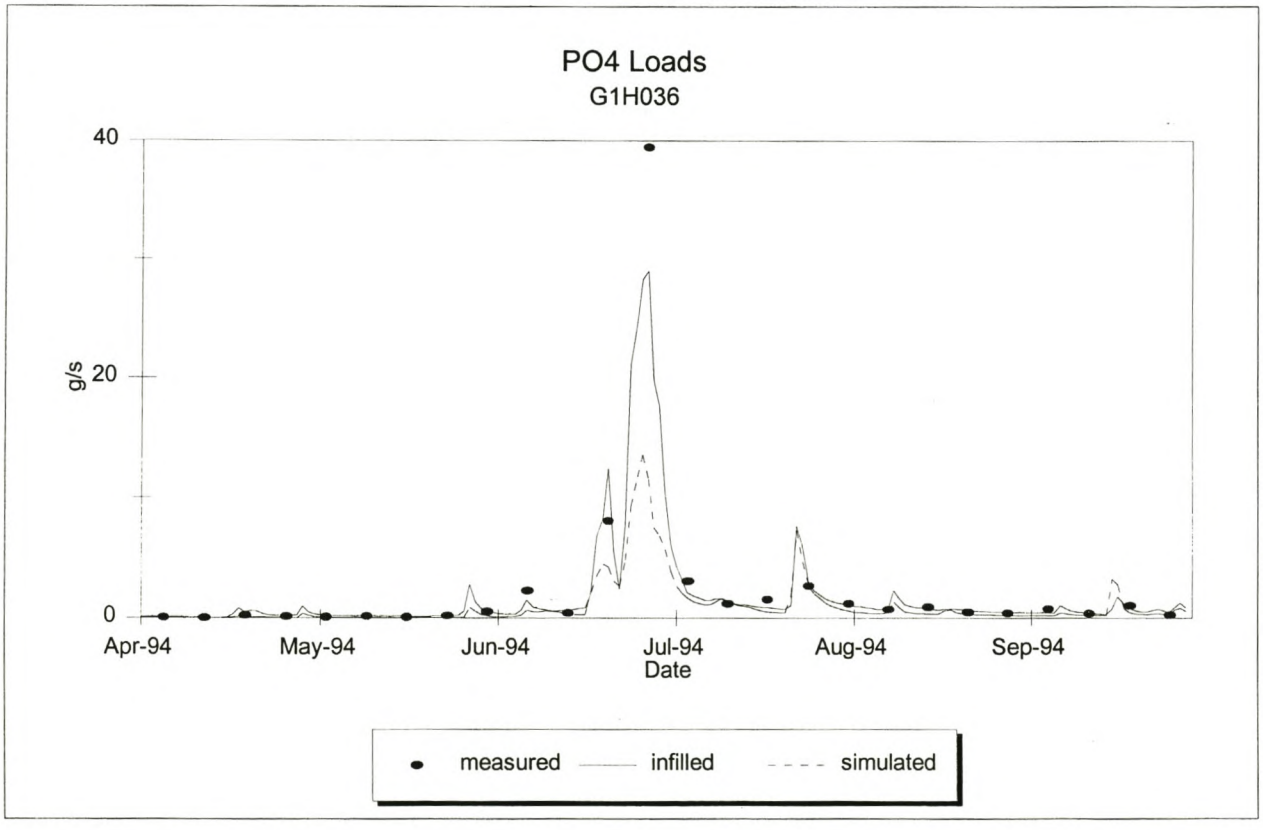

Figure 8.36: Phosphate Loads at G1H013 for high flows (Calibration)

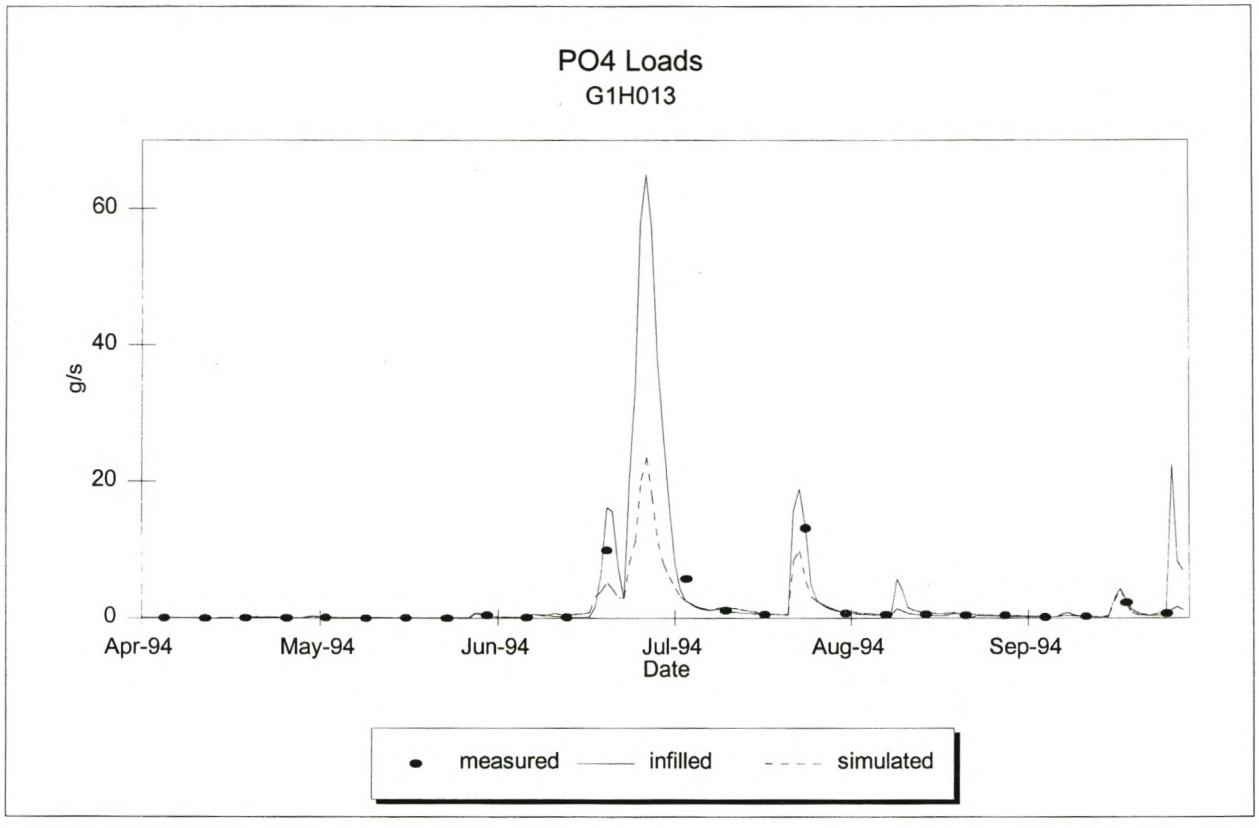

Figure 8.37: Phosphate Loads at G1R003 for high flows (Calibration)

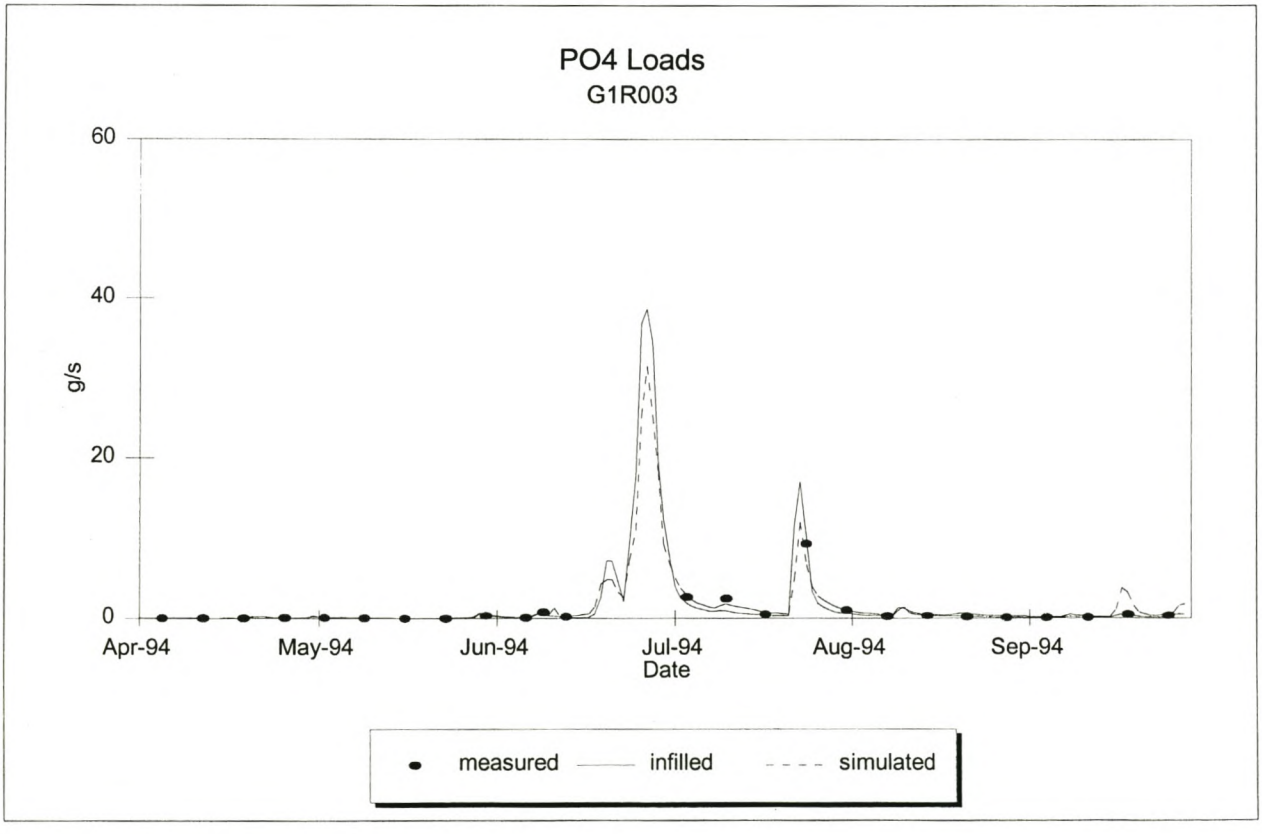

Figure 8.38: Phosphate Concentration at G1H020 (Calibration)

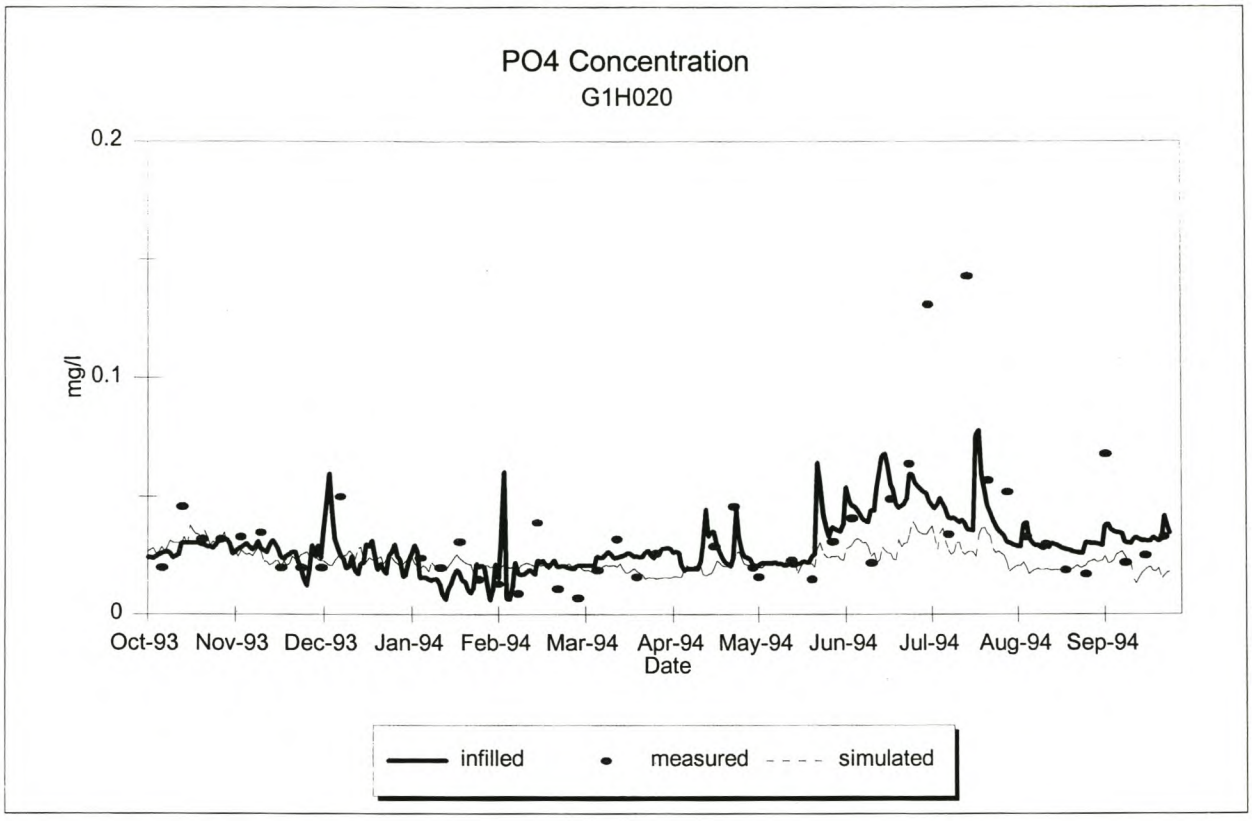

Figure 8.39: Phosphate Concentration at G1H036 (Calibration)

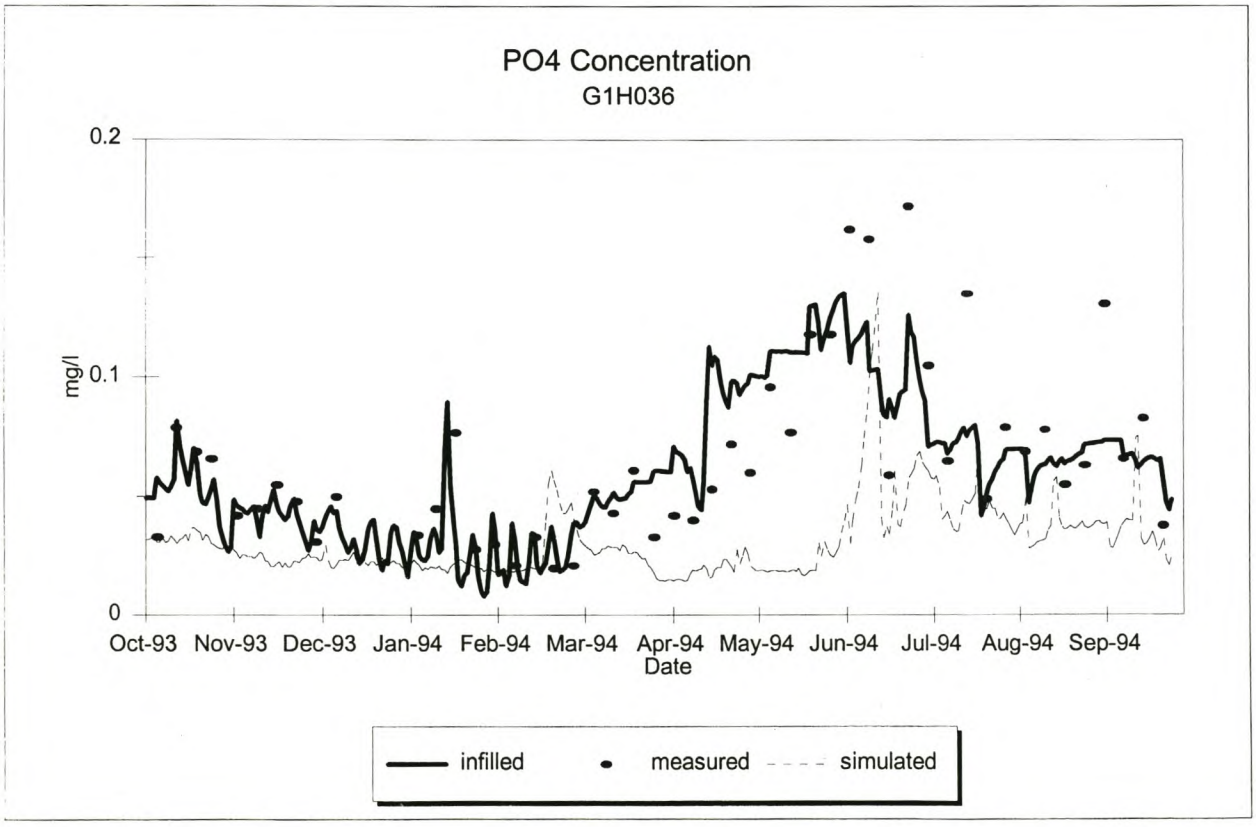

Figure 8.40: Phosphate Concentration at G1H013 (Calibration)

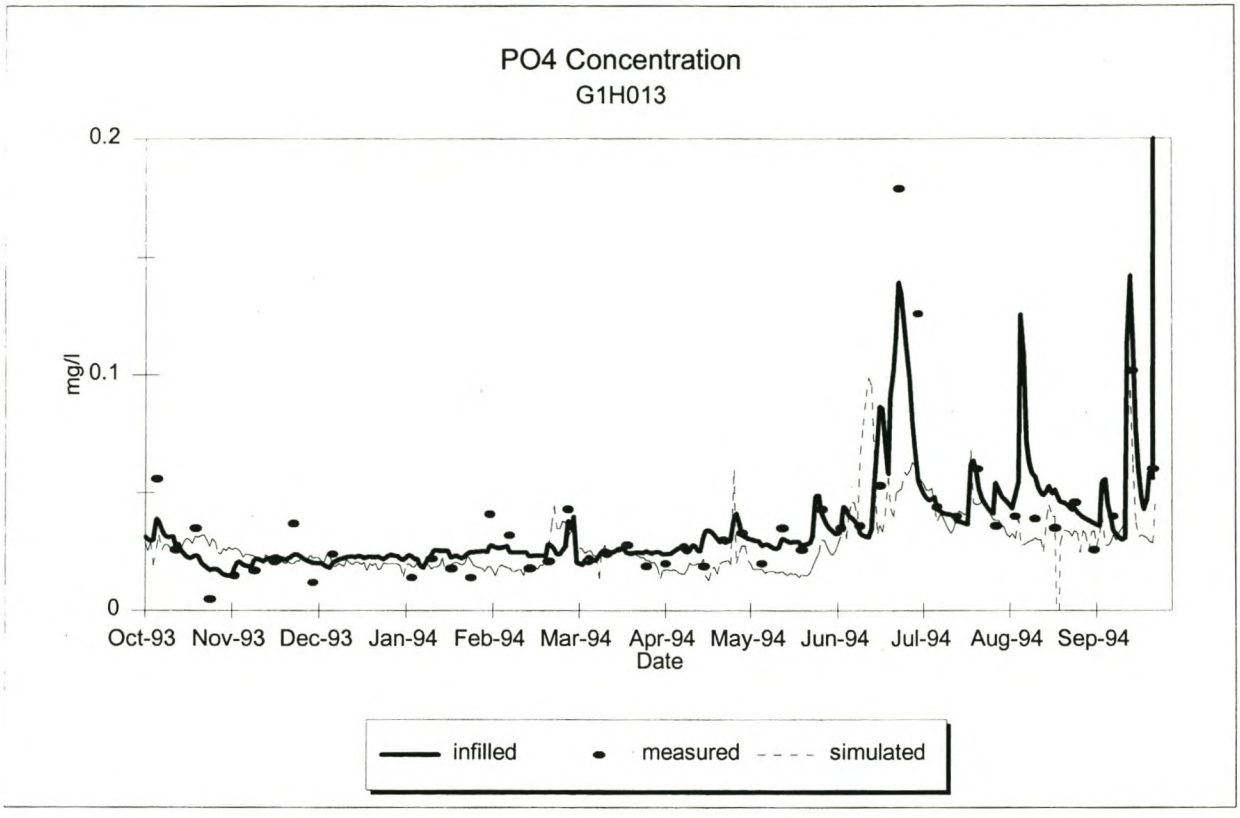

Figure 8.41: Phosphate Concentration at G1R003 (Calibration)

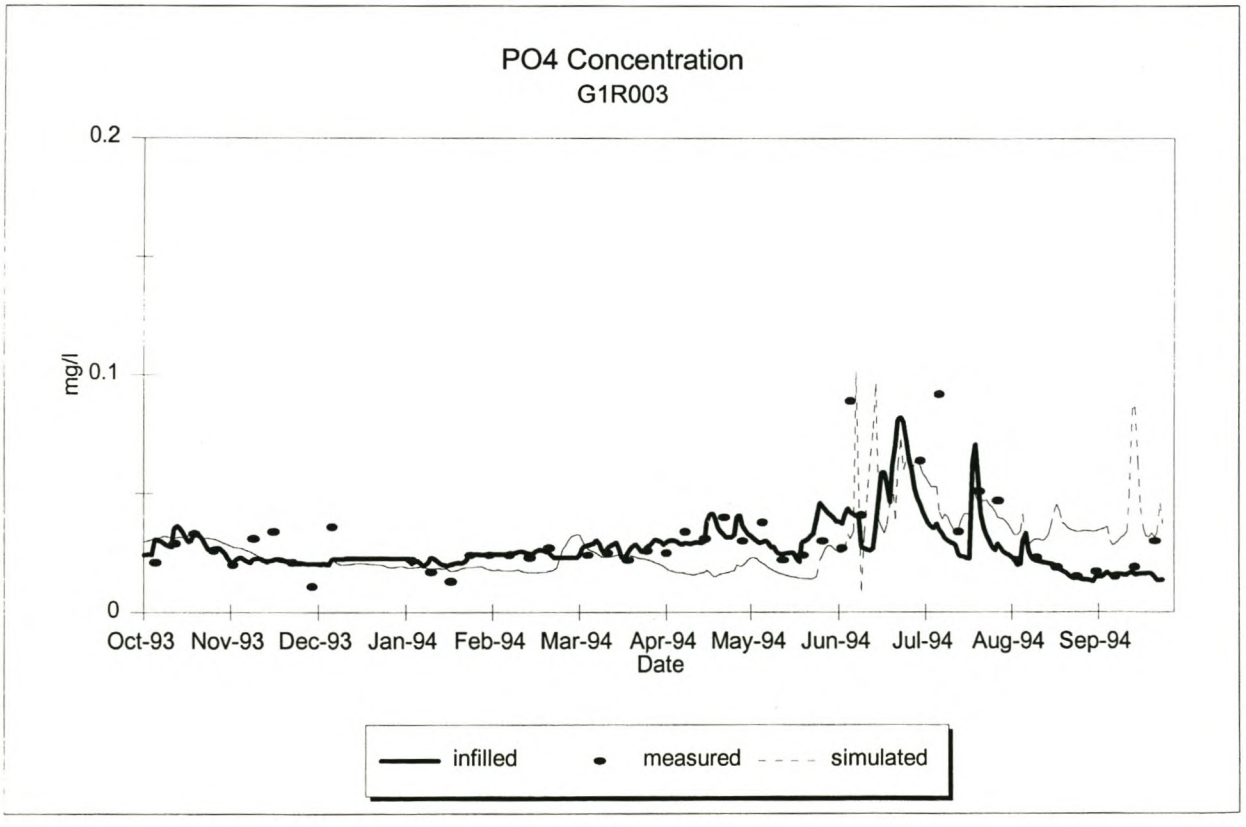

Figure 8.42: Temperature at G1H020 (Calibration)

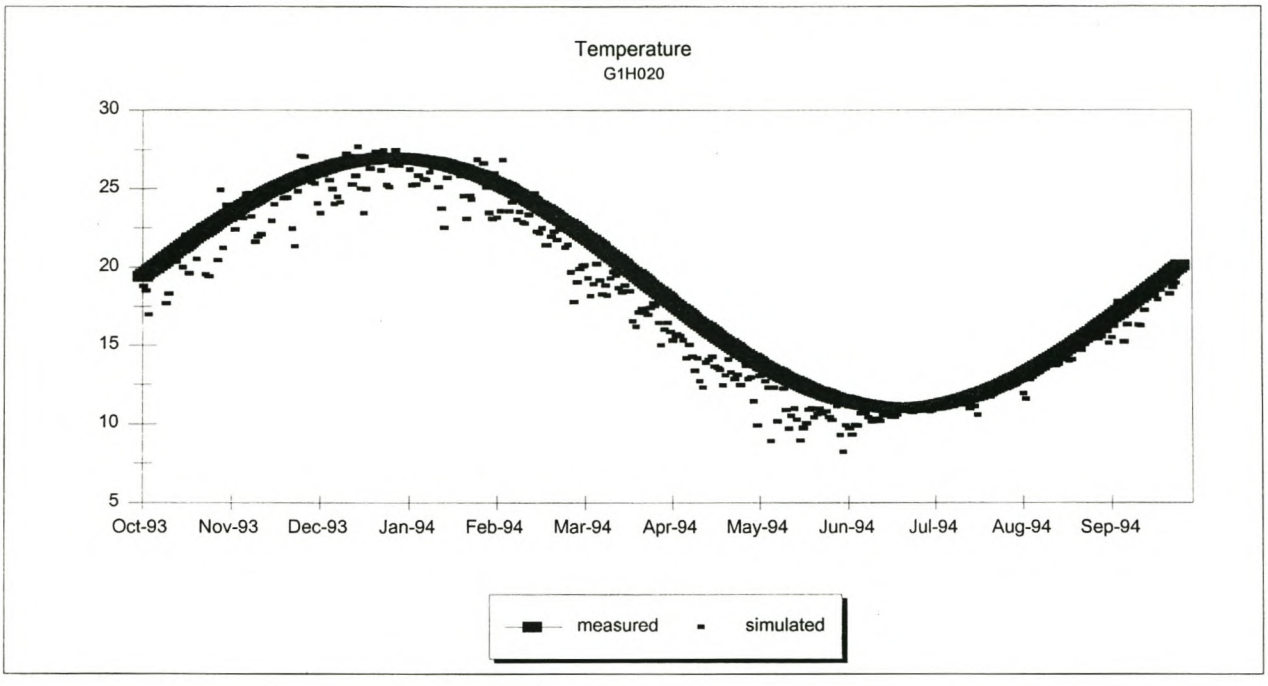

Figure 8.43: Temperature at G1H036 (Calibration)

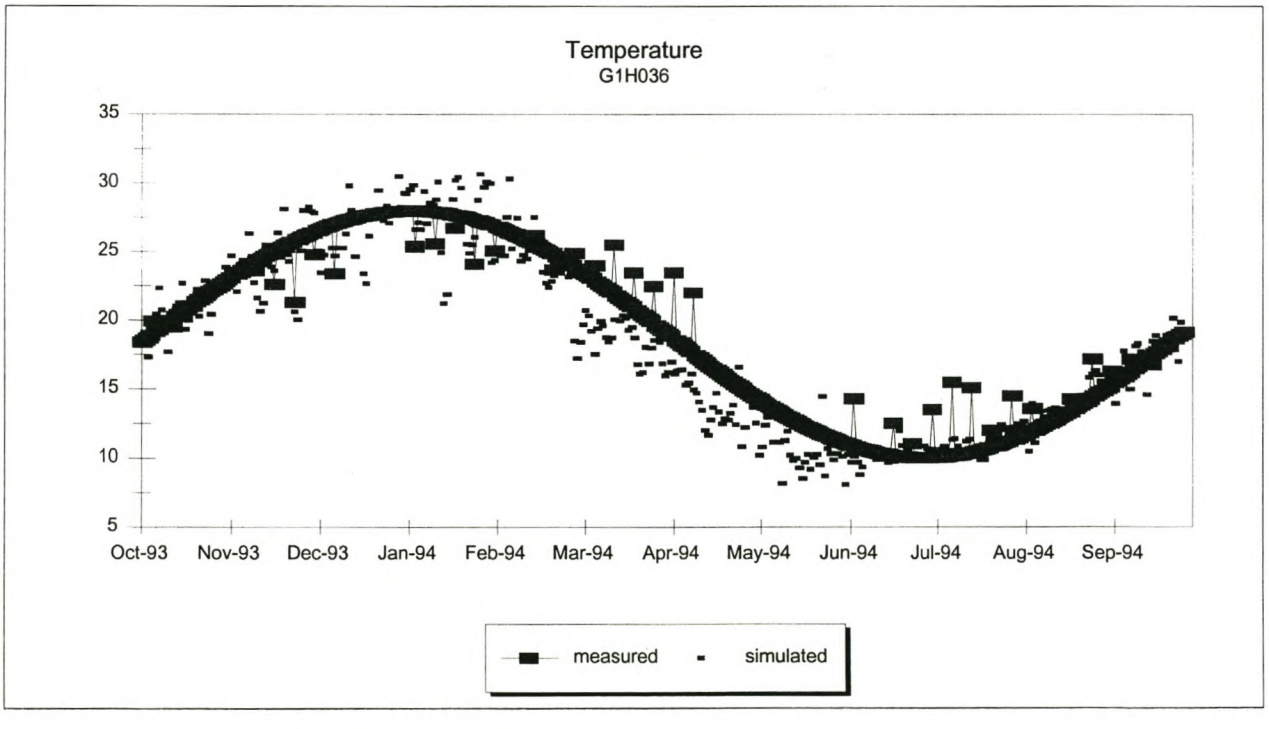

Figure 8.44: Temperature at G1H013 (Calibration)

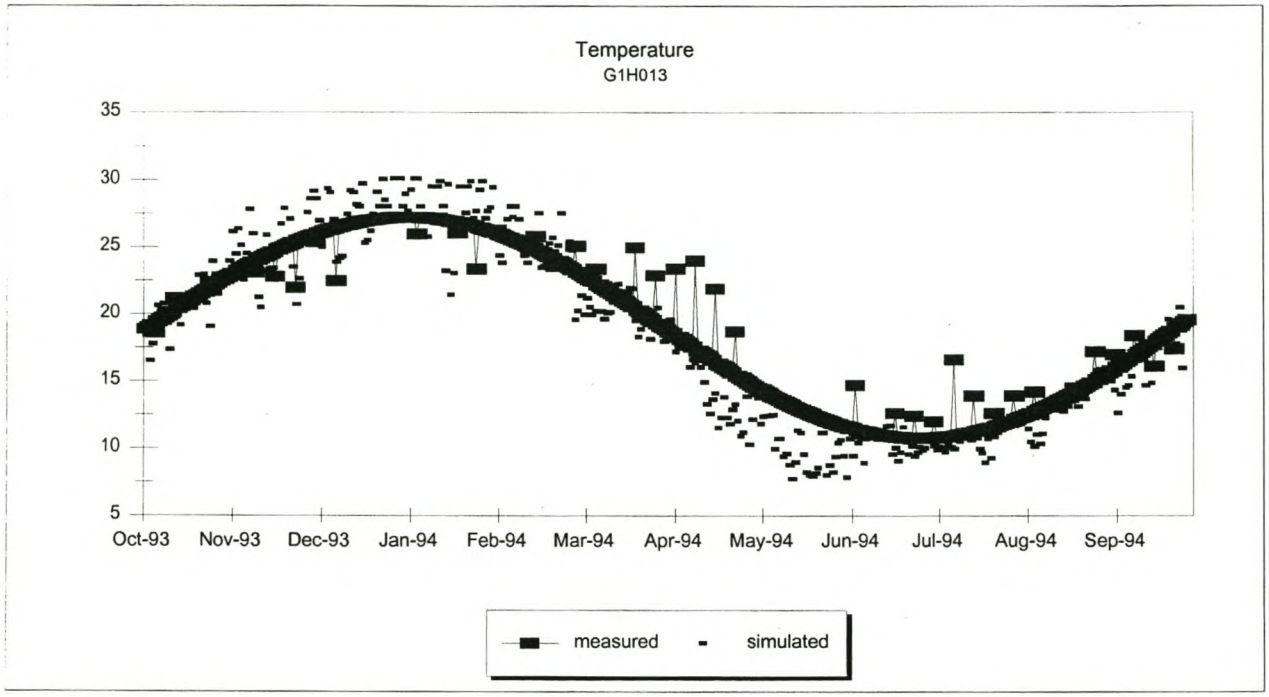

Figure 8.45: Temperature at G1R003 (Calibration)

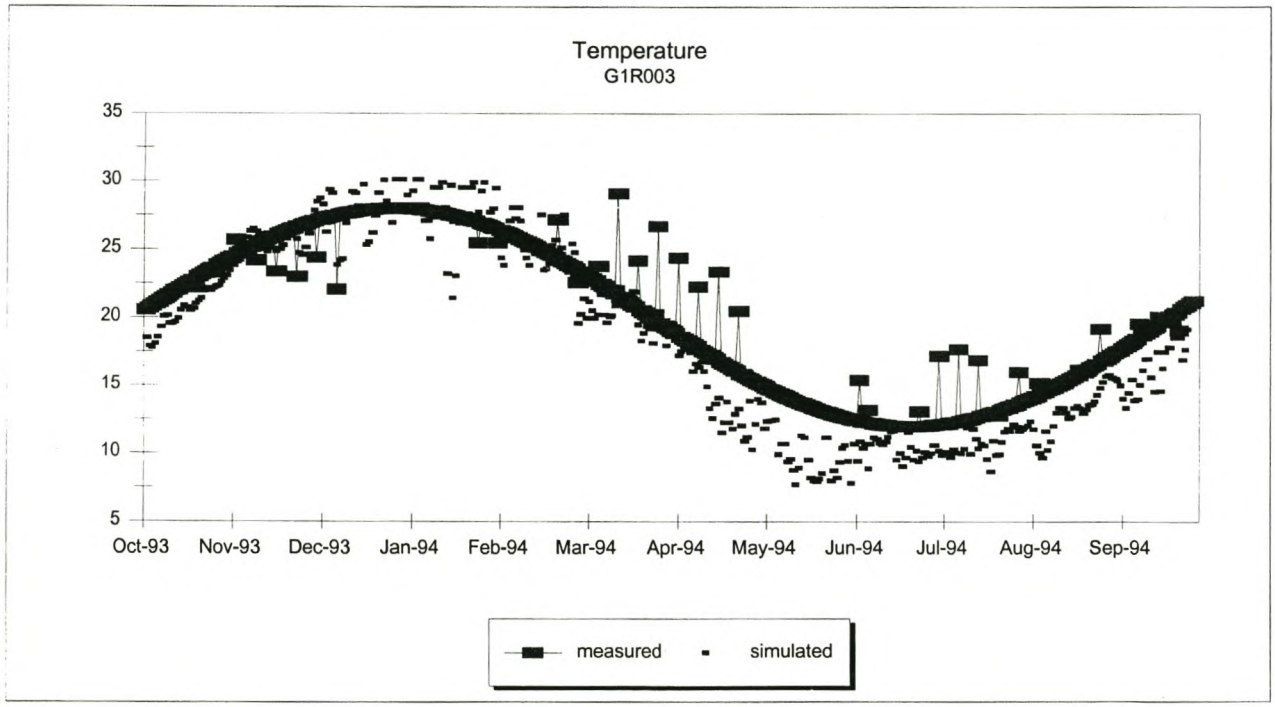

Figure 8.46: Oxygen at G1H020 (Calibration)

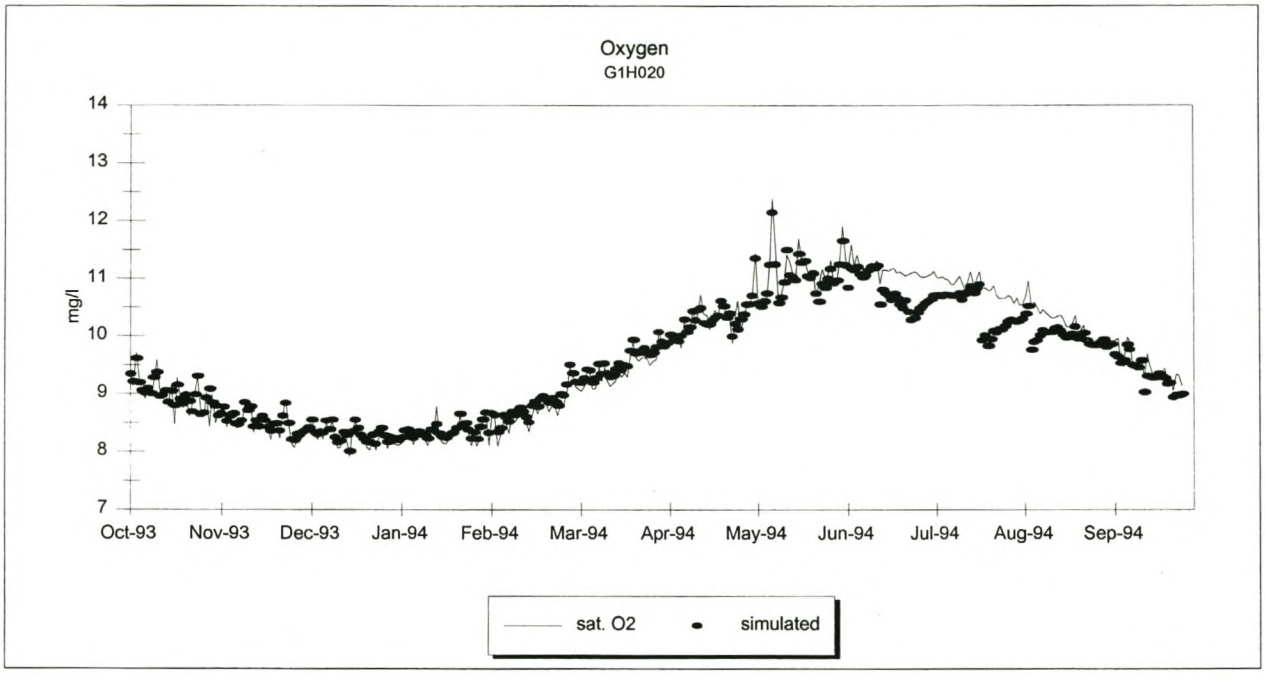

Figure 8.47: Oxygen at G1H036 (Calibration)

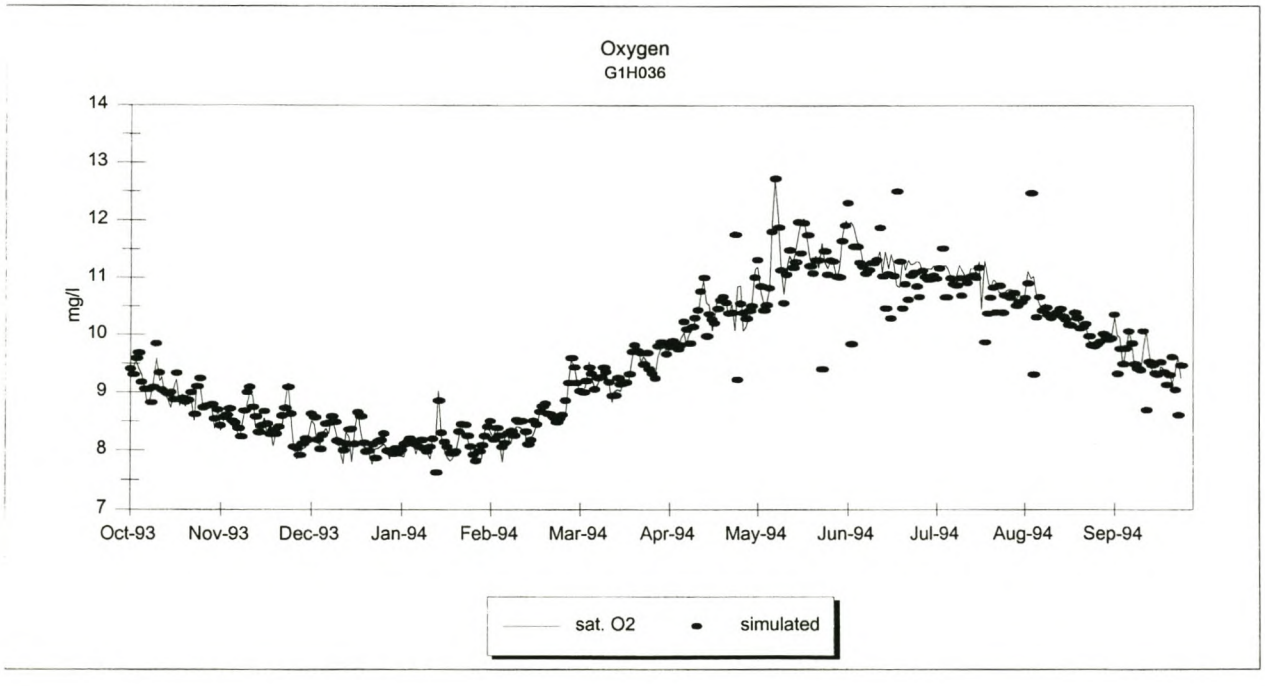

Figure 8.48: Oxygen at G1H013 (Calibration)

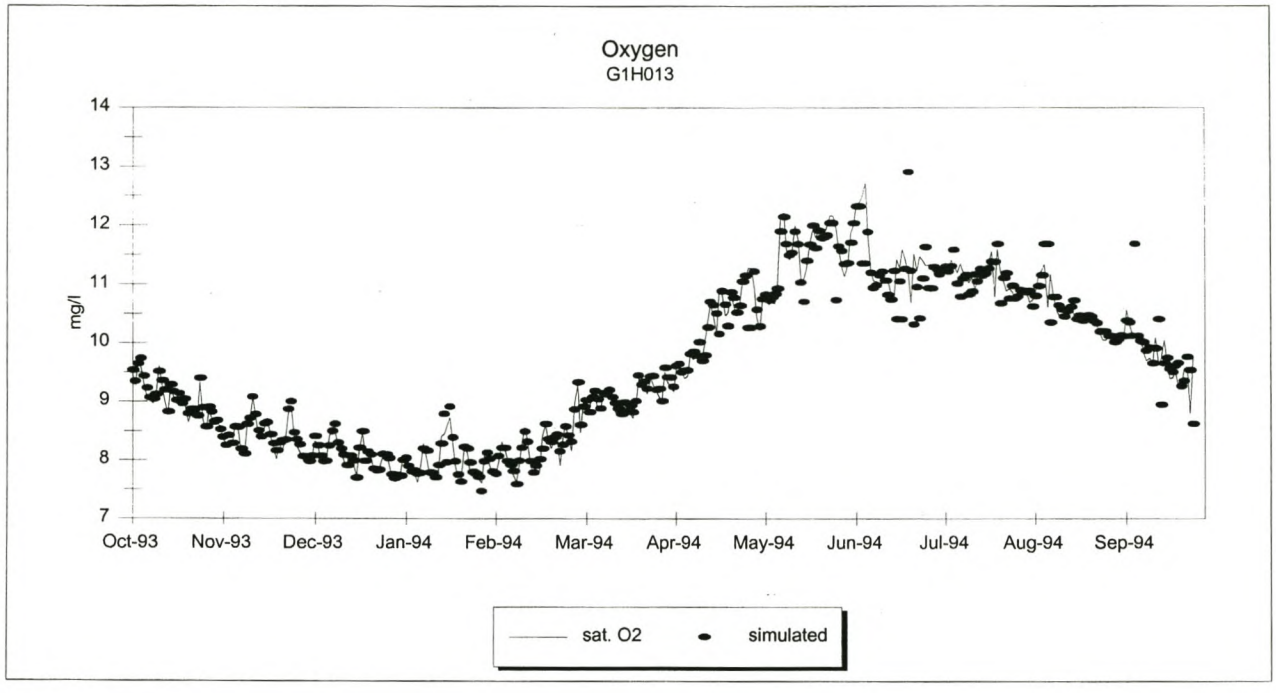

Figure 8.49: Oxygen at G1R003 (Calibration)

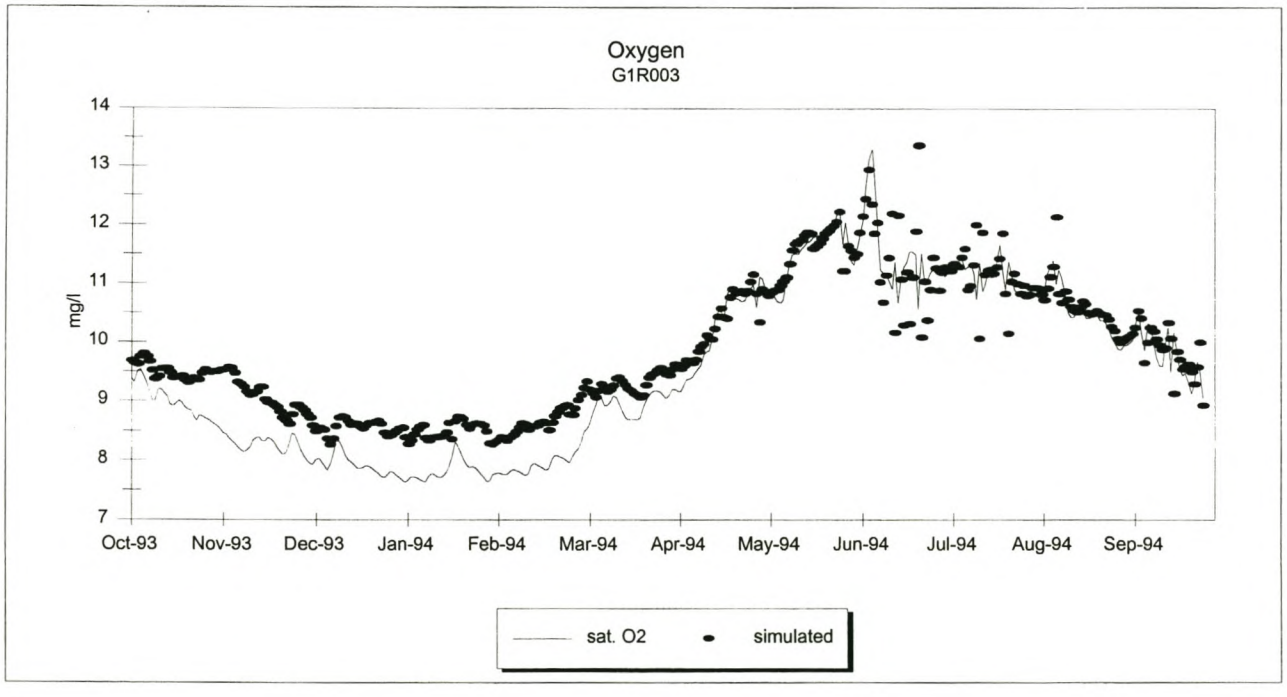

Figure 8.50: TDS Loads at G1H020 for low flows (Verification)

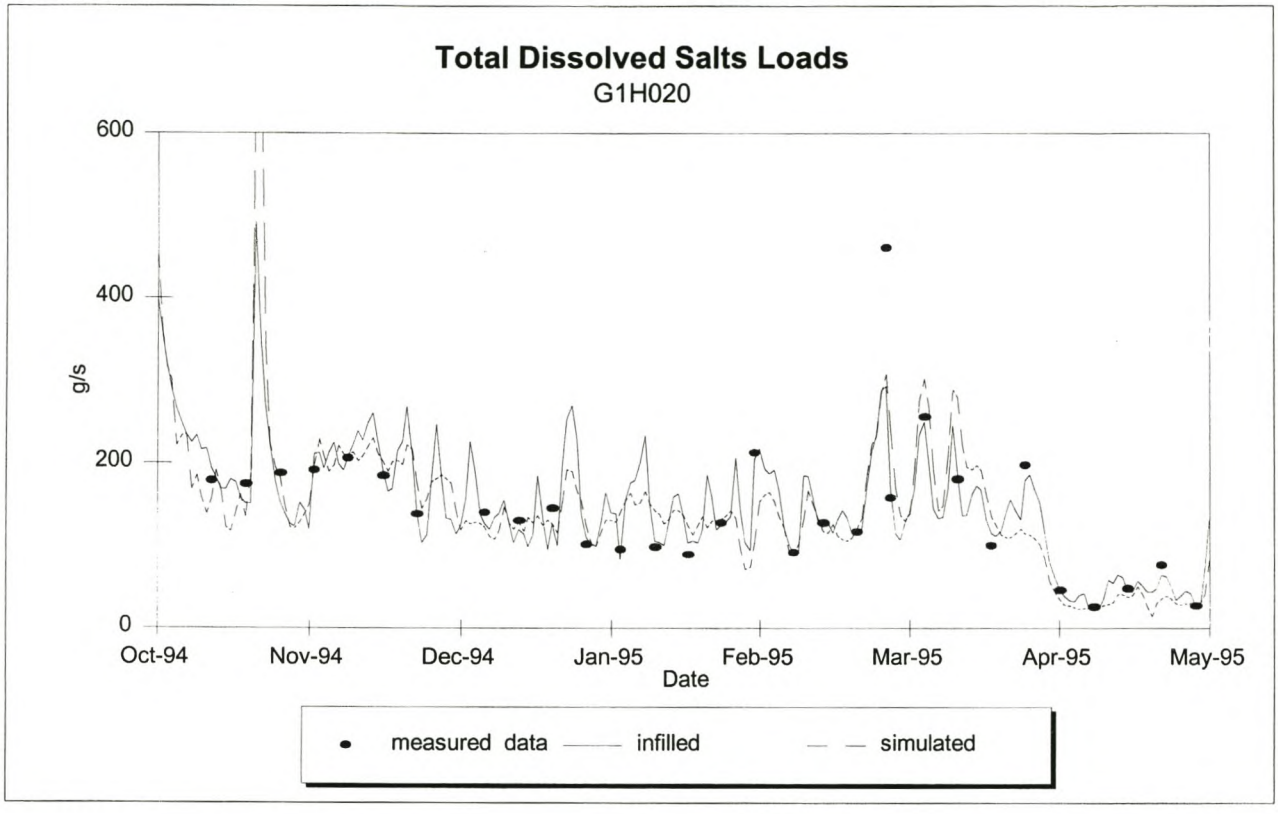

Figure 8.51: TDS Loads at G1H036 for low flows (Verification)

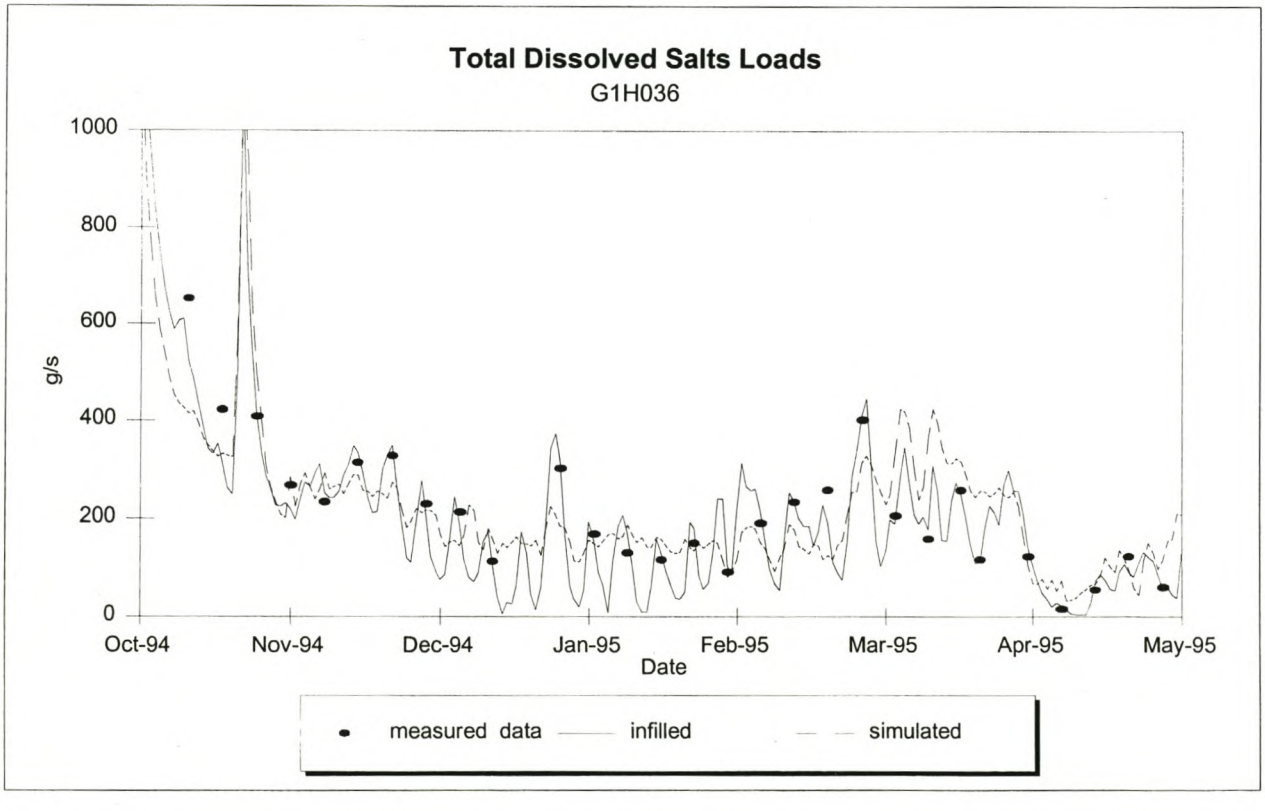

Figure 8.52: TDS Loads at G1H013 for low flows (Verification)

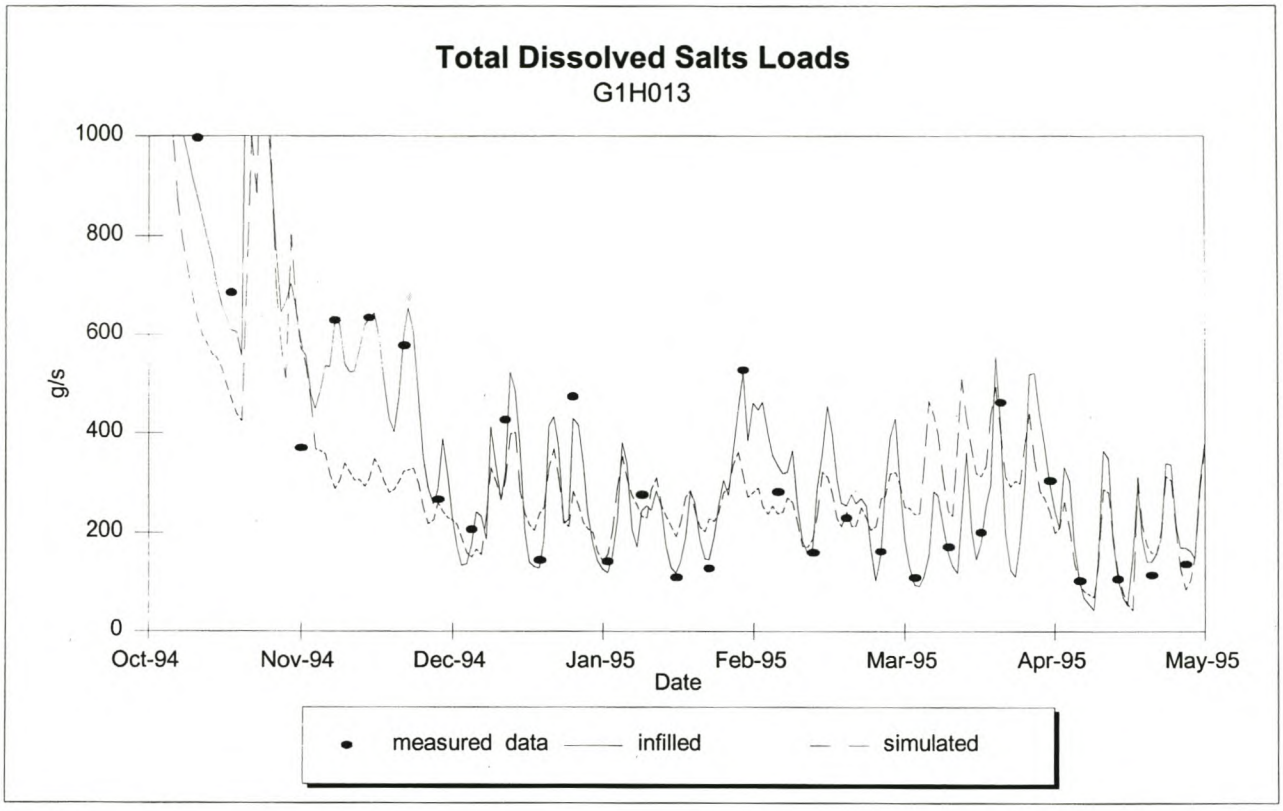

Figure 8.53: TDS Loads at G1R003 for low flows (Verification)

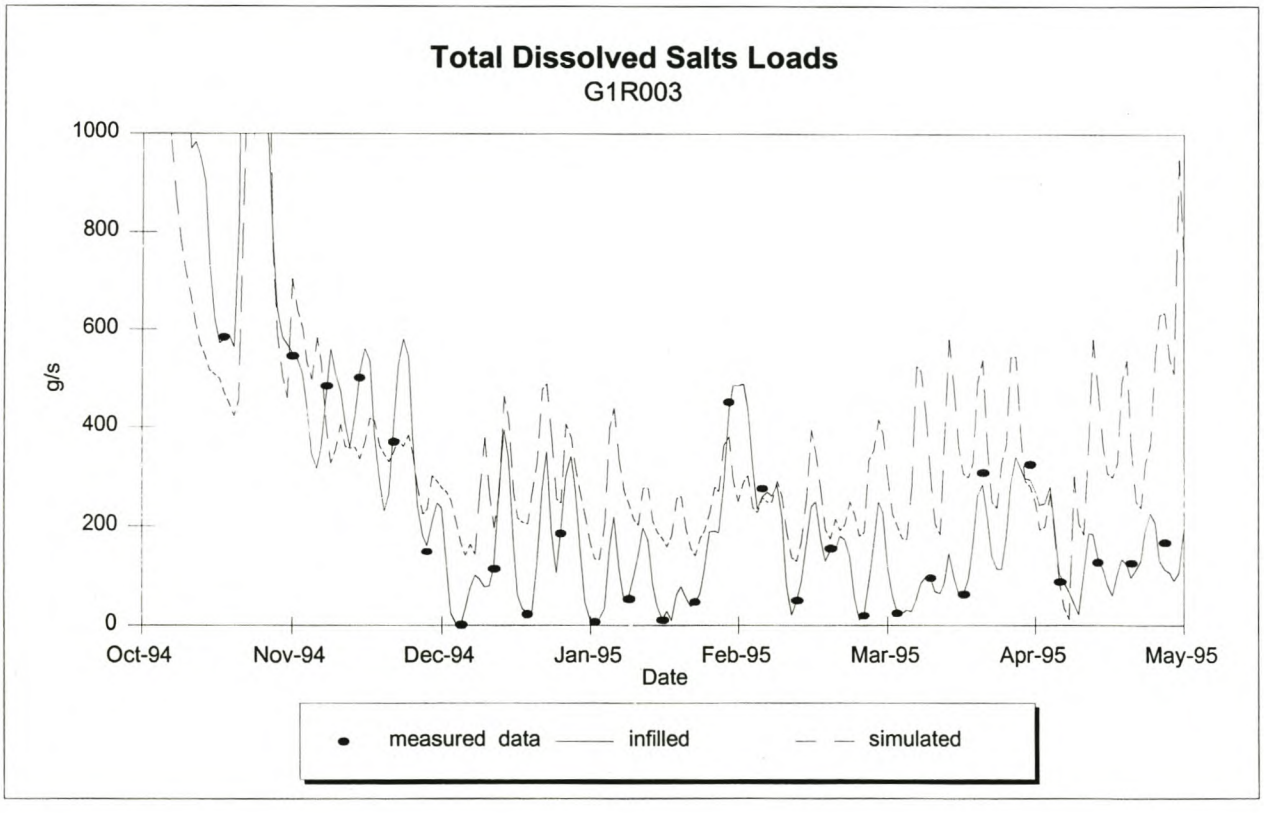

Figure 8.54: TDS Loads at G1H020 for high flows (Verification)

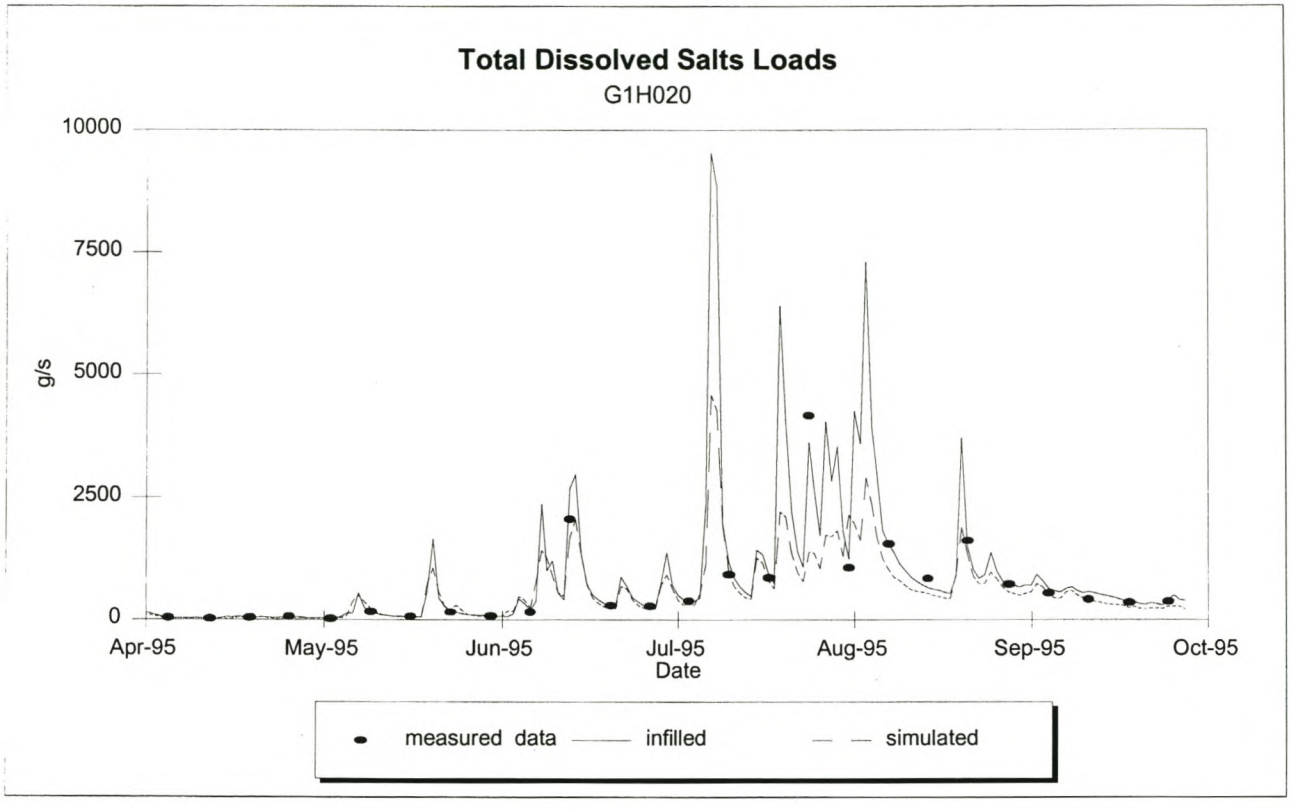

Figure 8.55: TDS Loads at G1H036 for high flows (Verification)

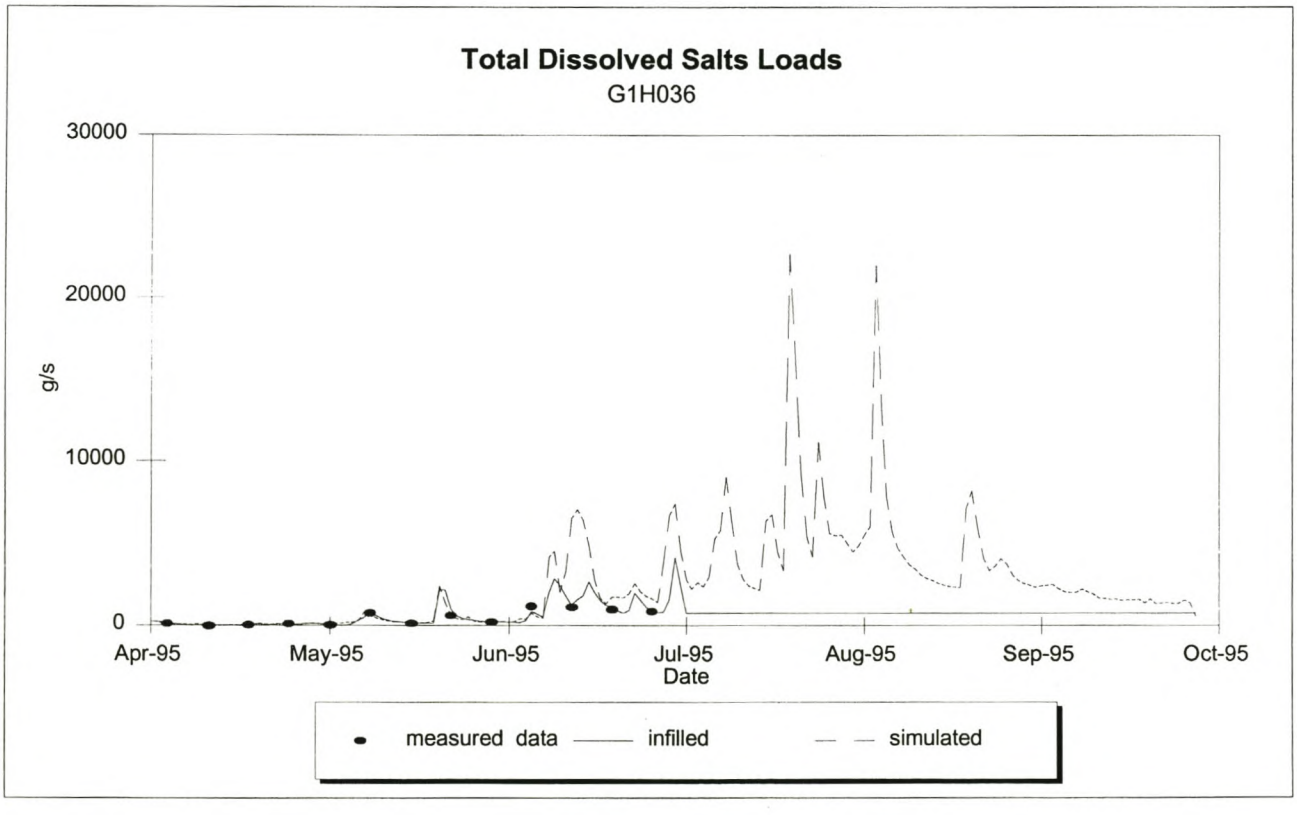

Figure 8.56: TDS Loads at G1H013 for high flows (Verification)

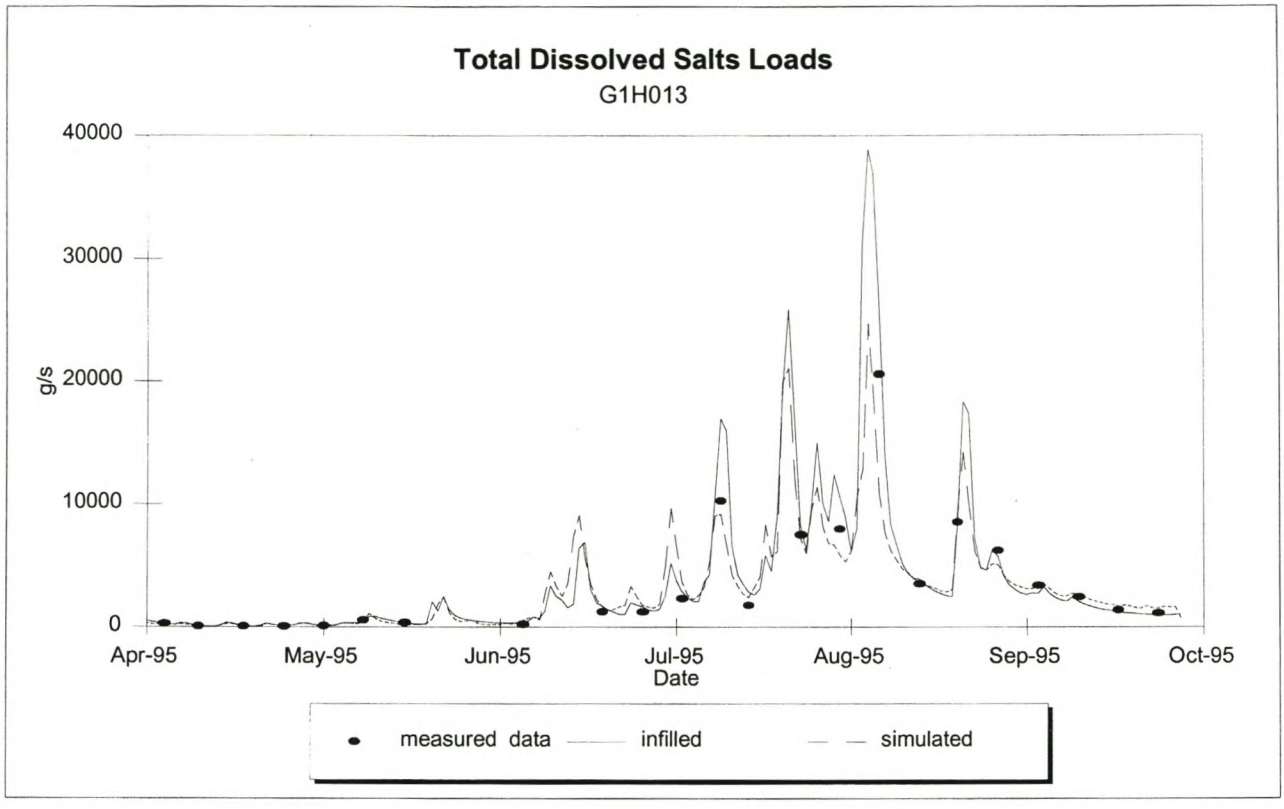

Figure 8.57: TDS Loads at G1R003 for high flows (Verification)

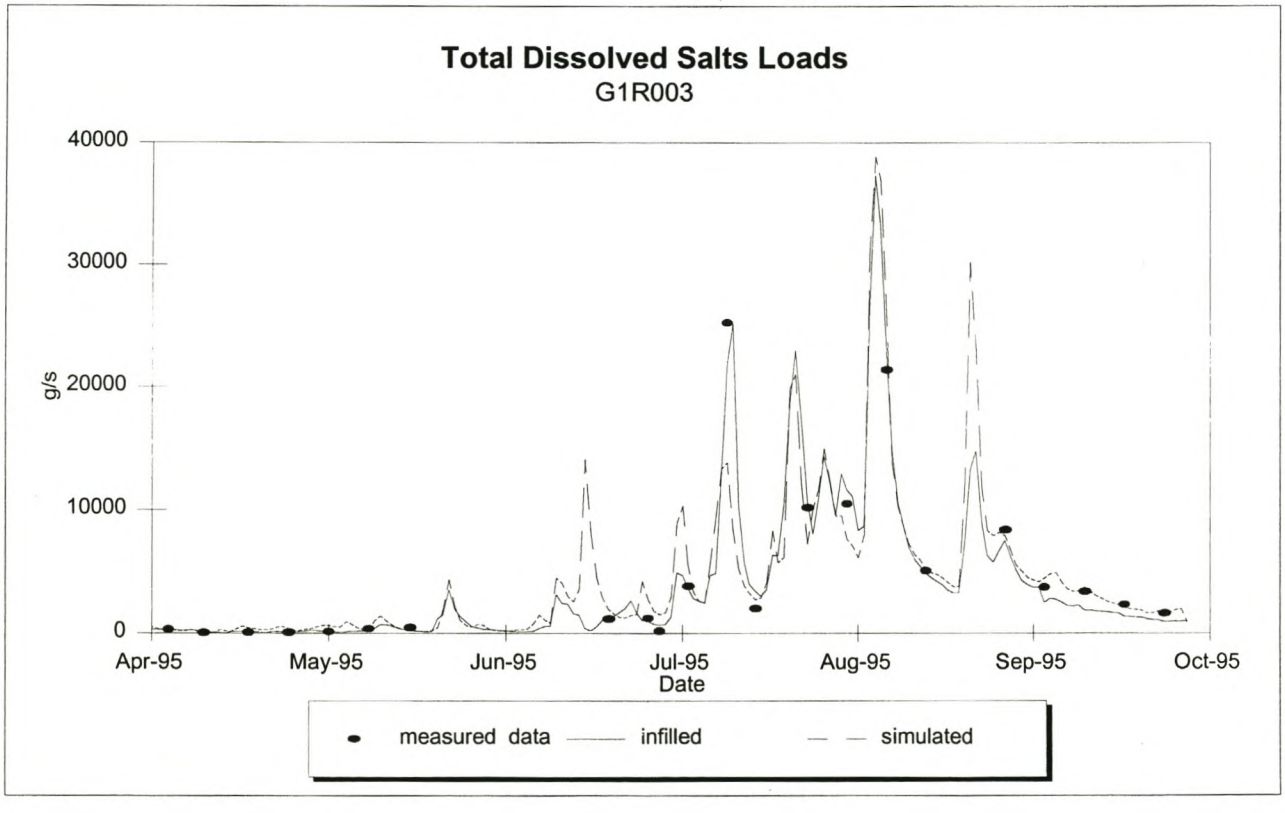

Figure 8.58: TDS Concentration at G1H020 (Verification)

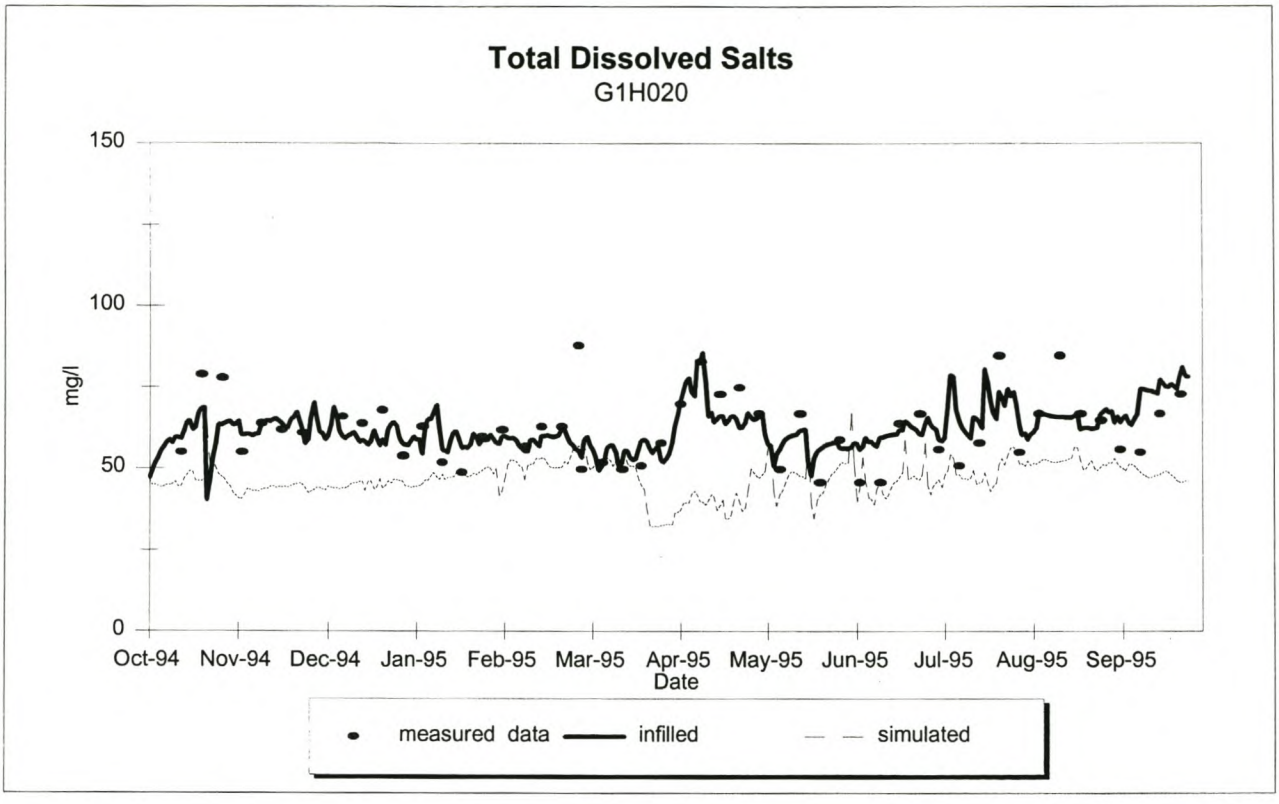

Figure 8.59: TDS Concentration at G1H036 (Verification)

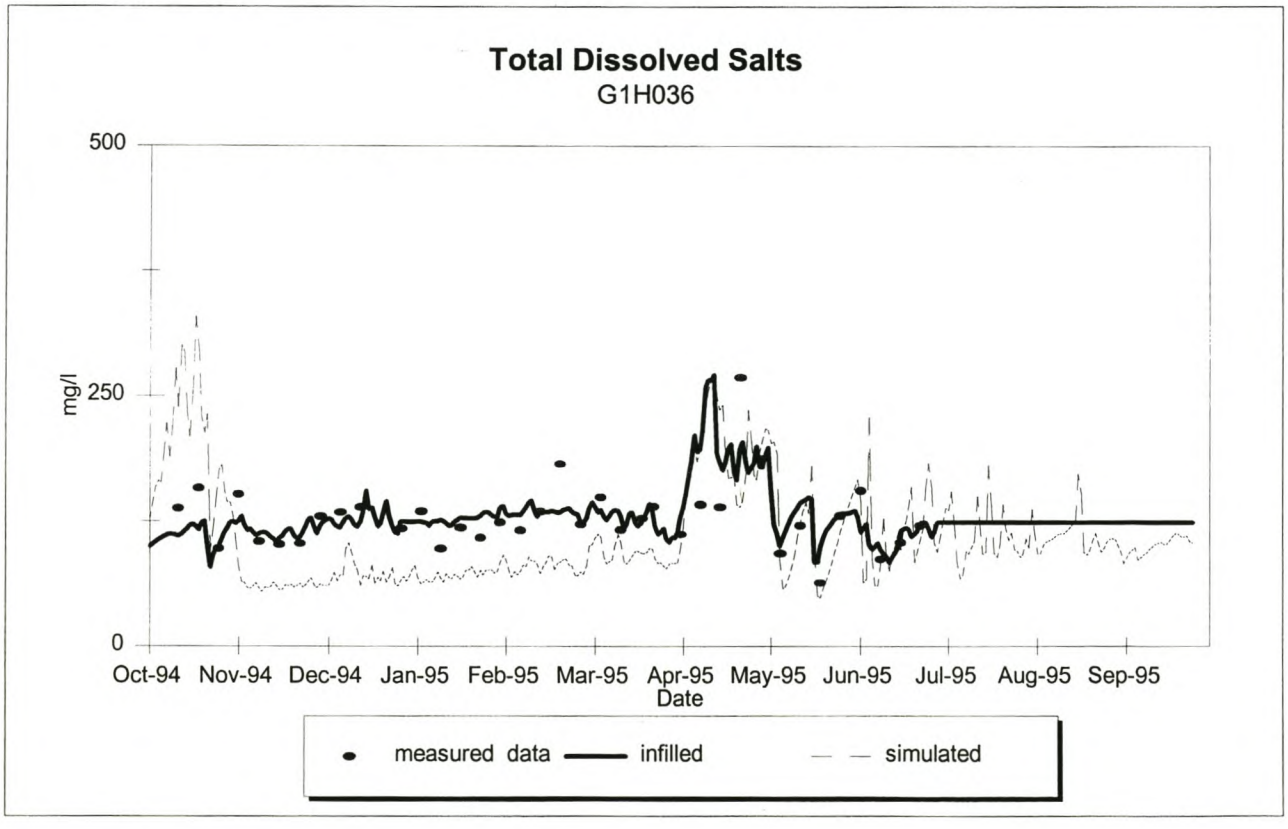

Figure 8.60: TDS Concentration at G1H013 (Verification)

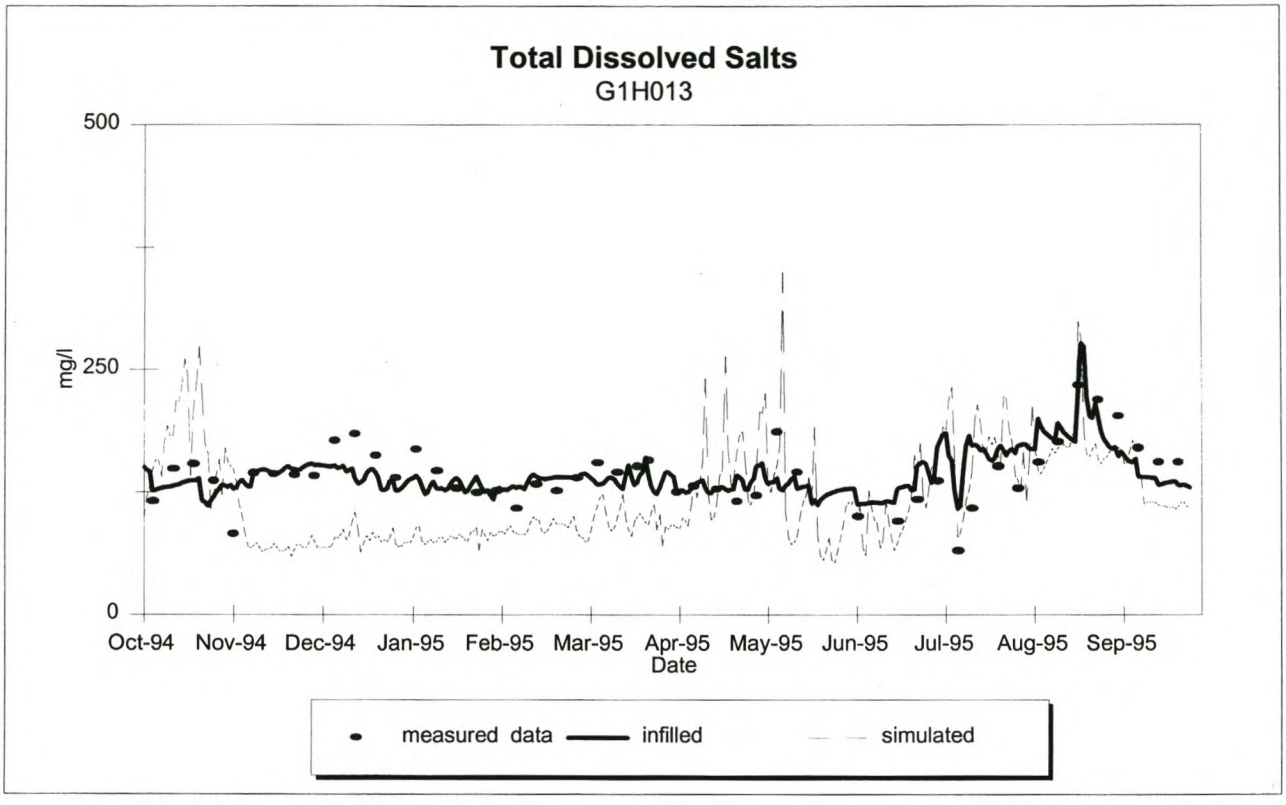

Figure 8.61: TDS Concentration at G1R003 (Verification)

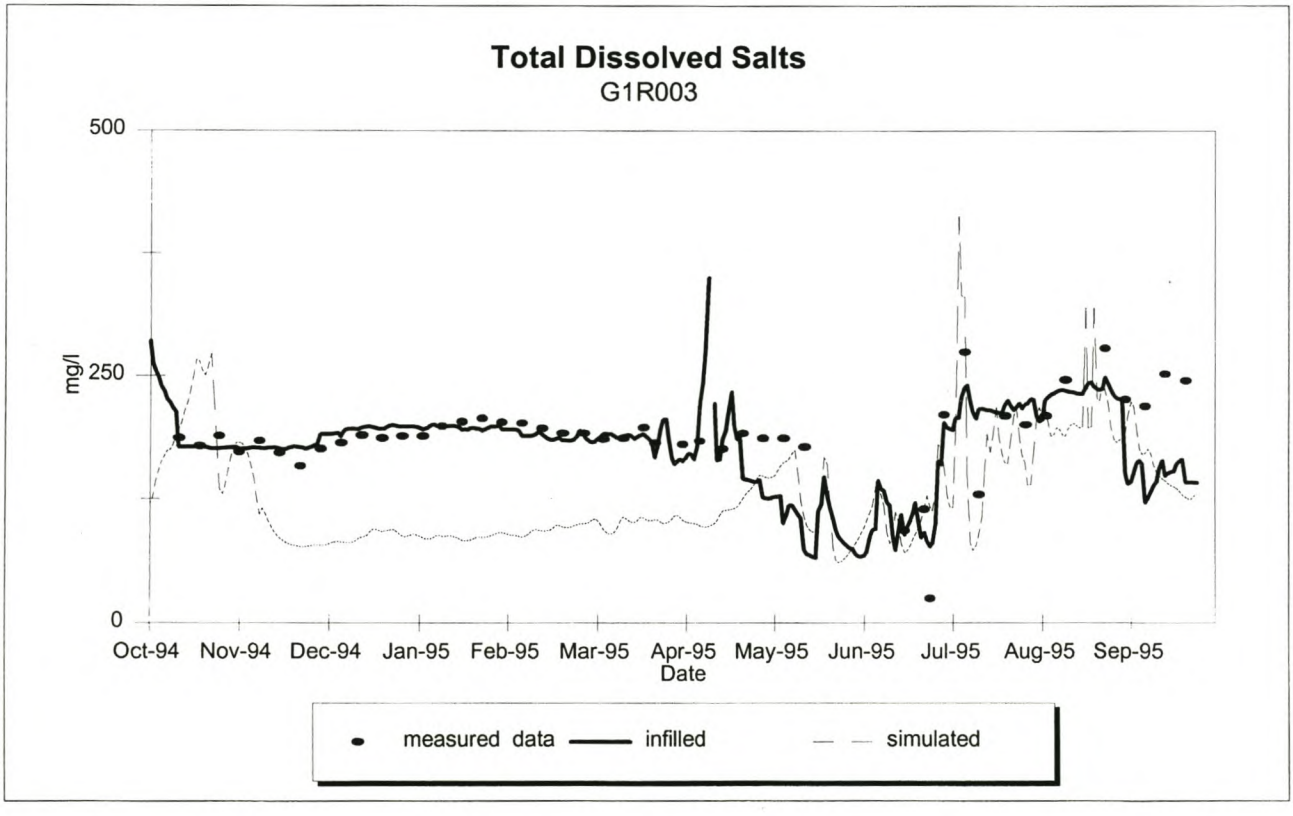

Figure 8.62: Phosphate Loads at G1H020 for low flows(Verification)

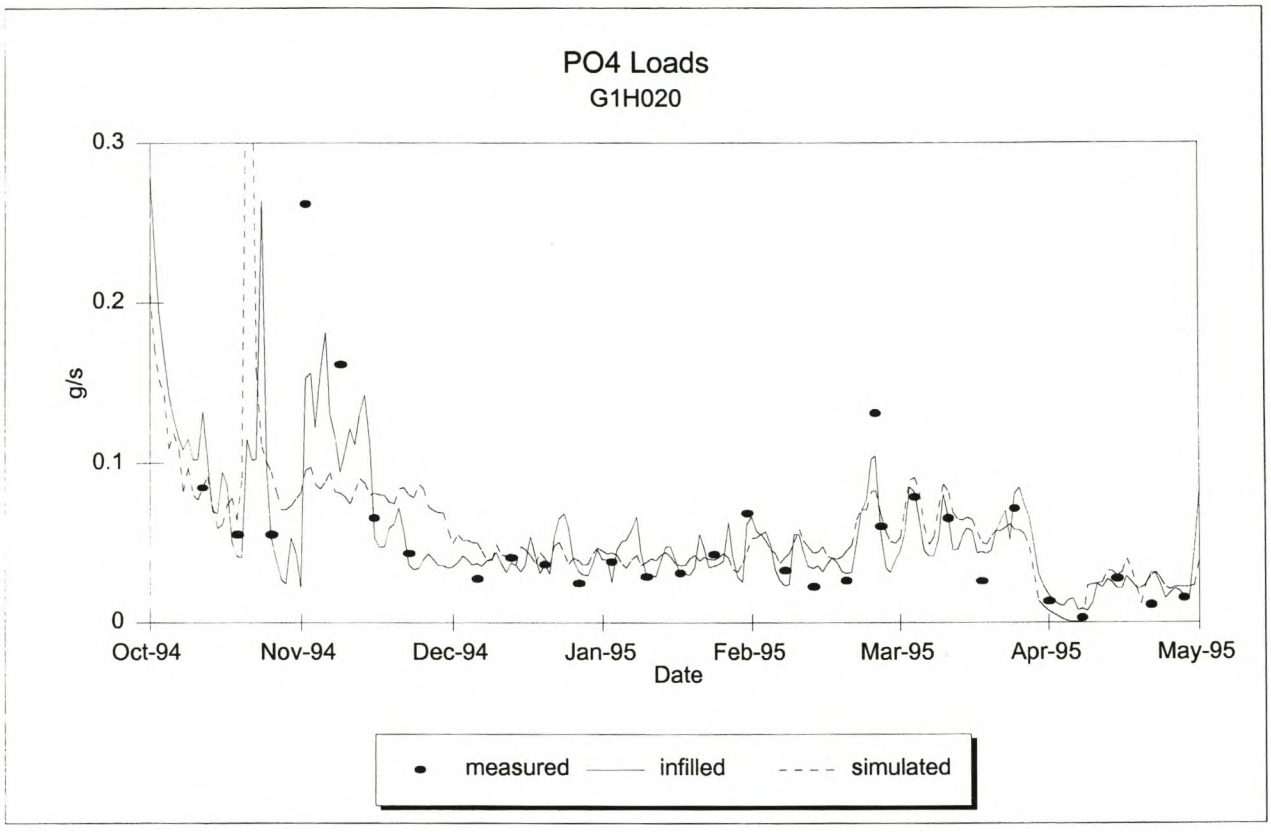

Figure 8.63: Phosphate Loads at G1H036 for low flows (Verification)

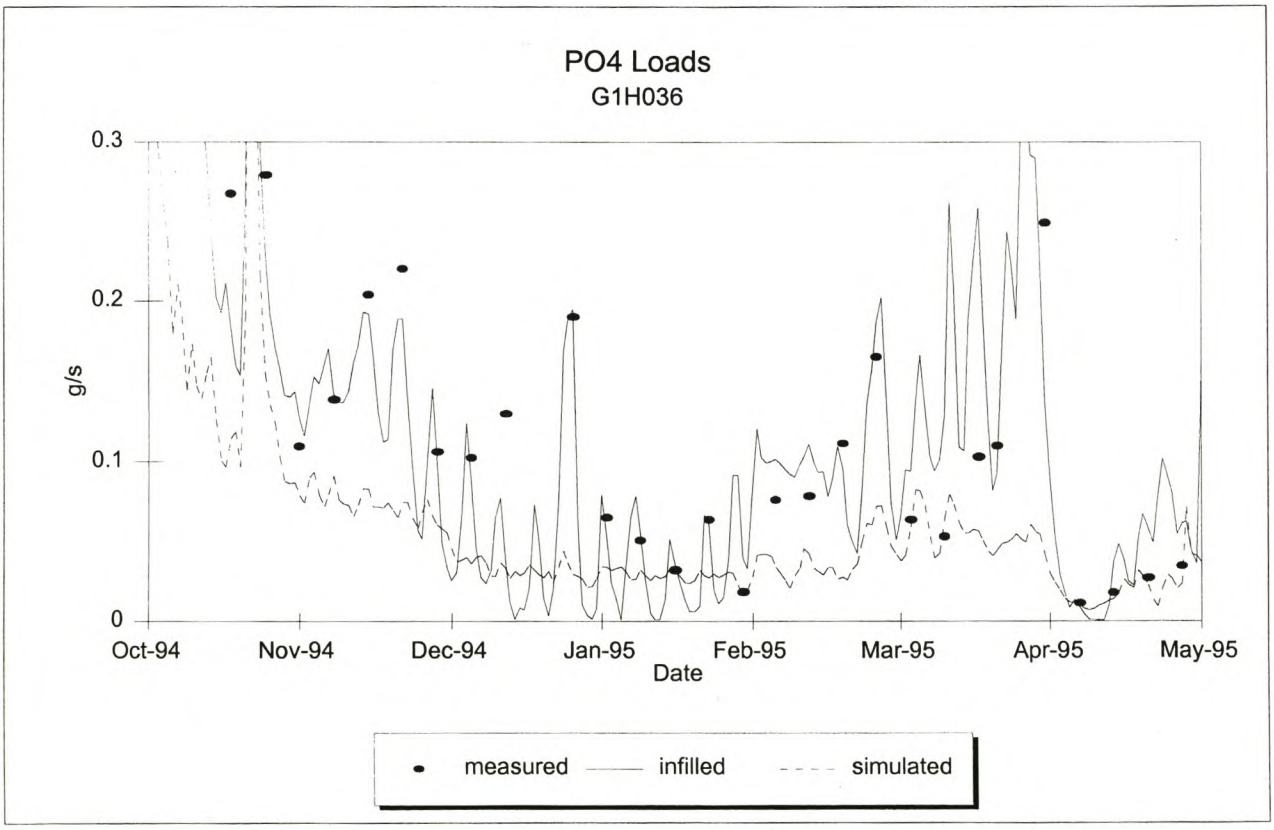

Figure 8.64: Phosphate Loads at G1H013 for low flows (Verification)

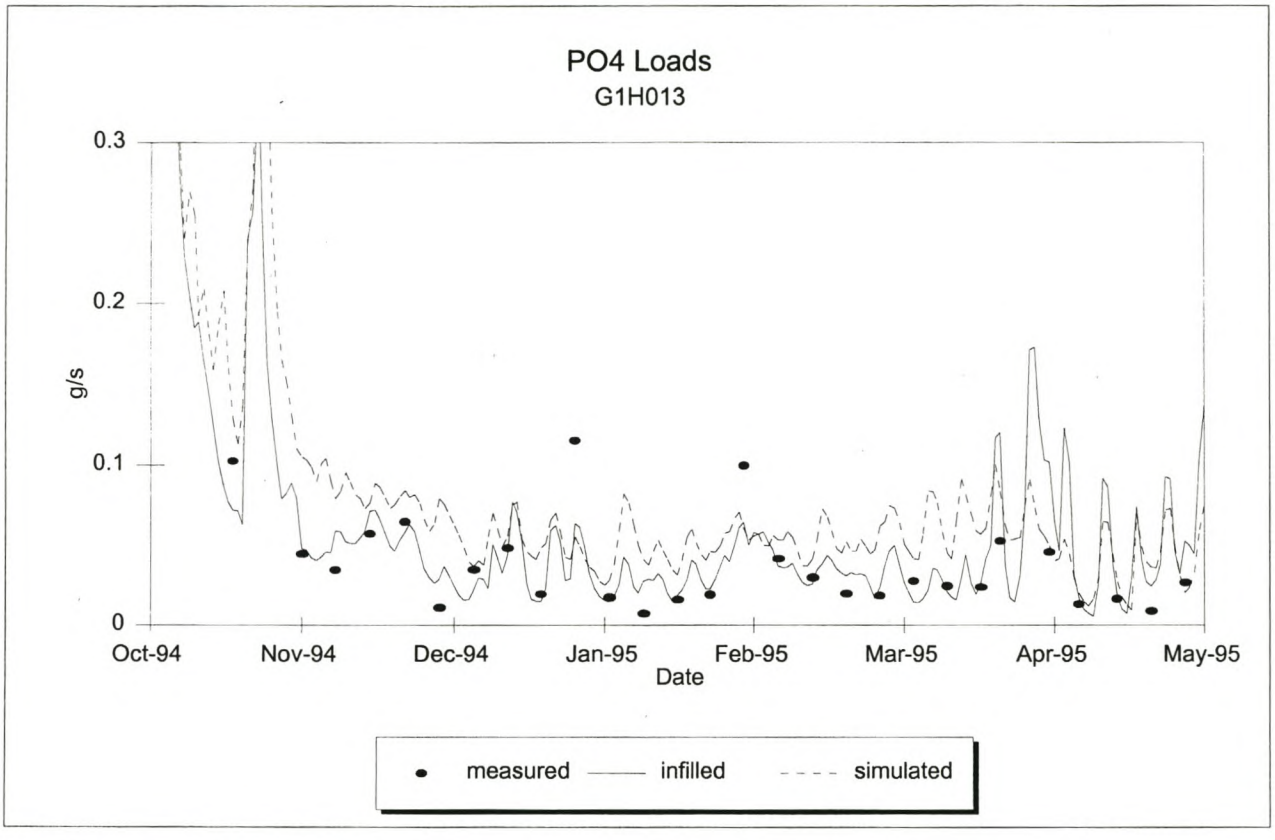

Figure 8.65: Phosphate Loads at G1R003 for low flows (Verification)

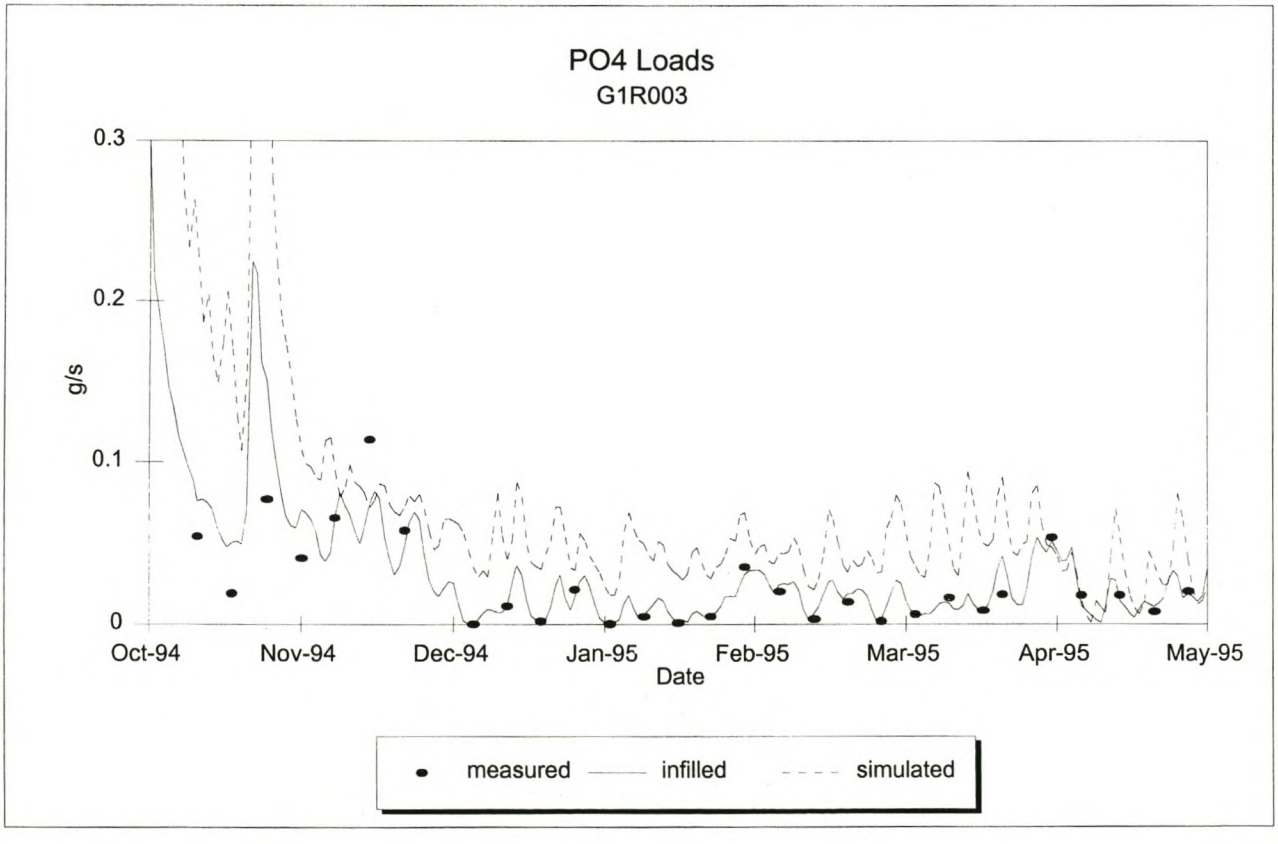

Figure 8.66: Phosphate Loads at G1H020 for high flows (Verification)

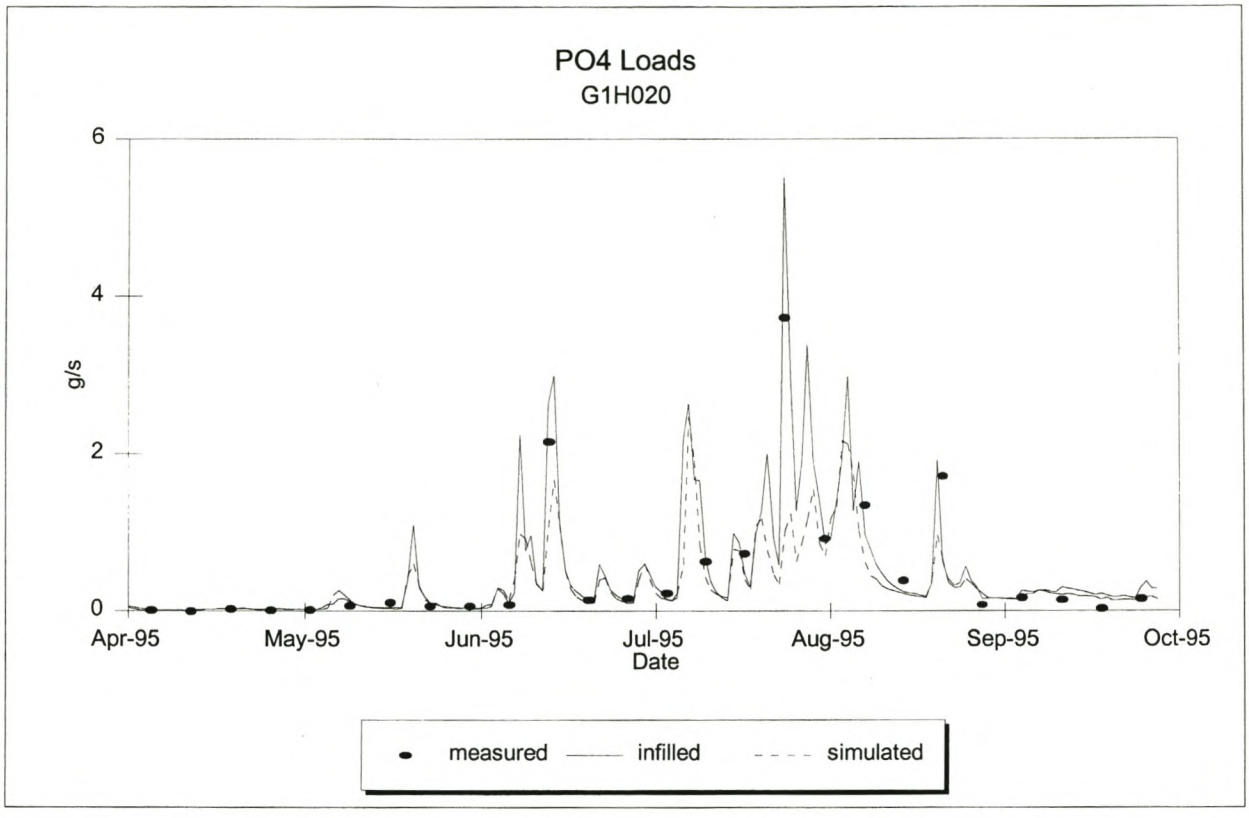

Figure 8.67: Phosphate Loads at G1H036 for high flows (Verification)

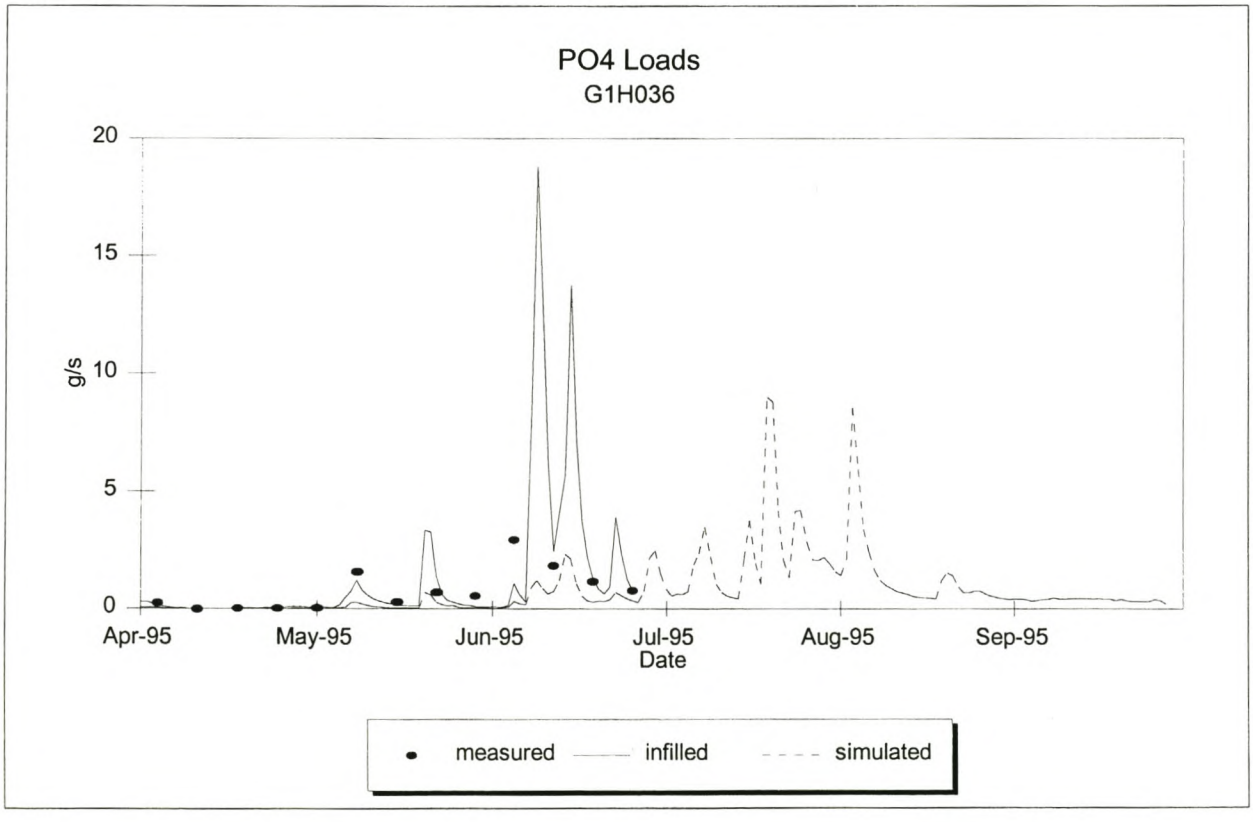

Figure 8.68: Phosphate Loads at G1H013 for high flows (Verification)

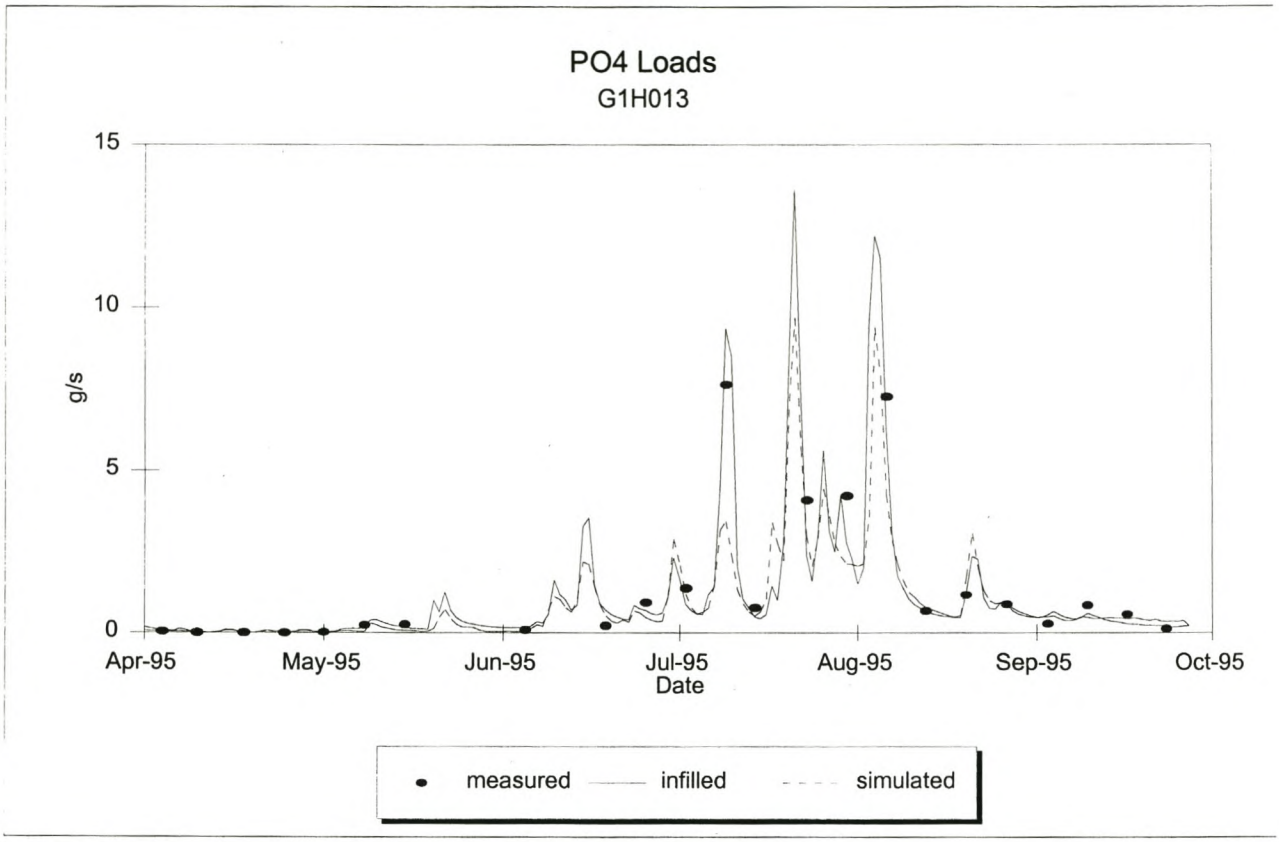

Figure 8.69: Phosphate Loads at G1R003 for high flows (Verification)

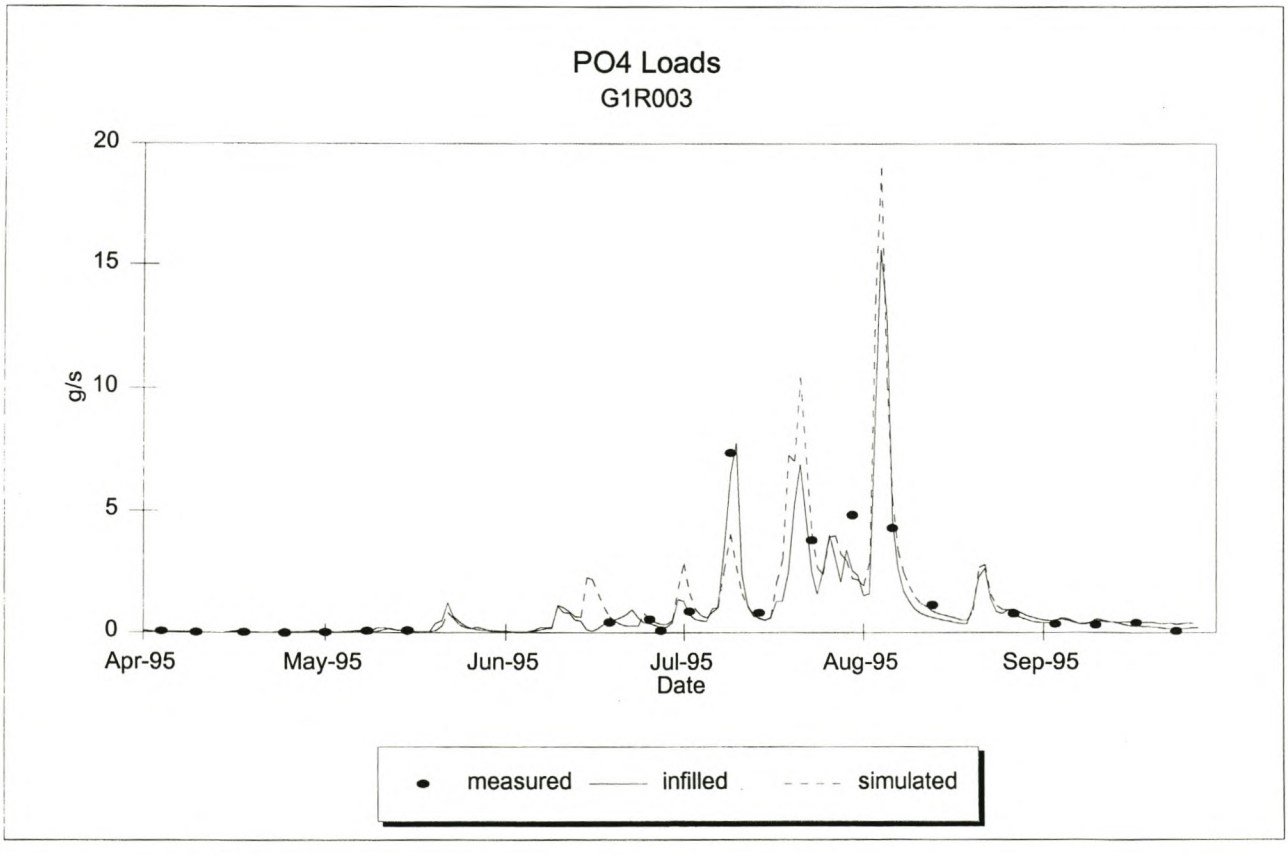

Figure 8.70: Phosphate Concentration at G1H020 (Verification)

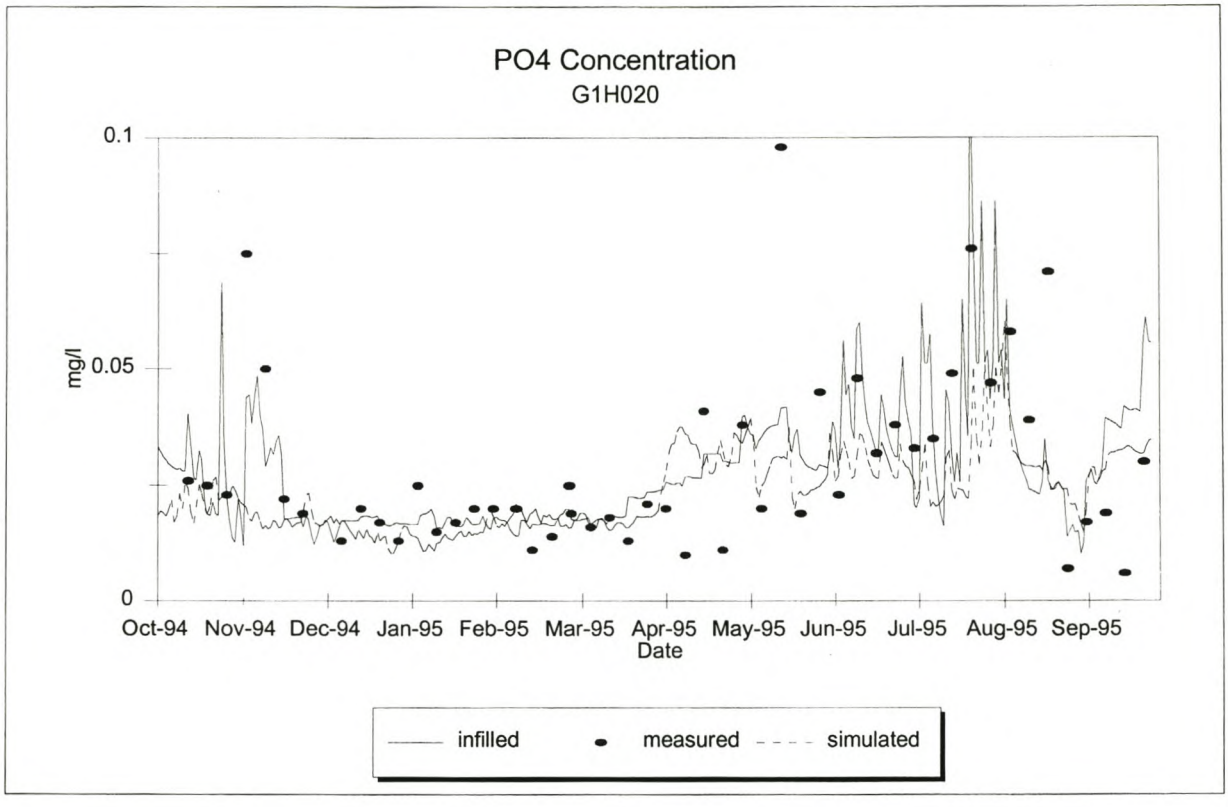

Figure 8.71: Phosphate Concentration at G1H036 (Verification)

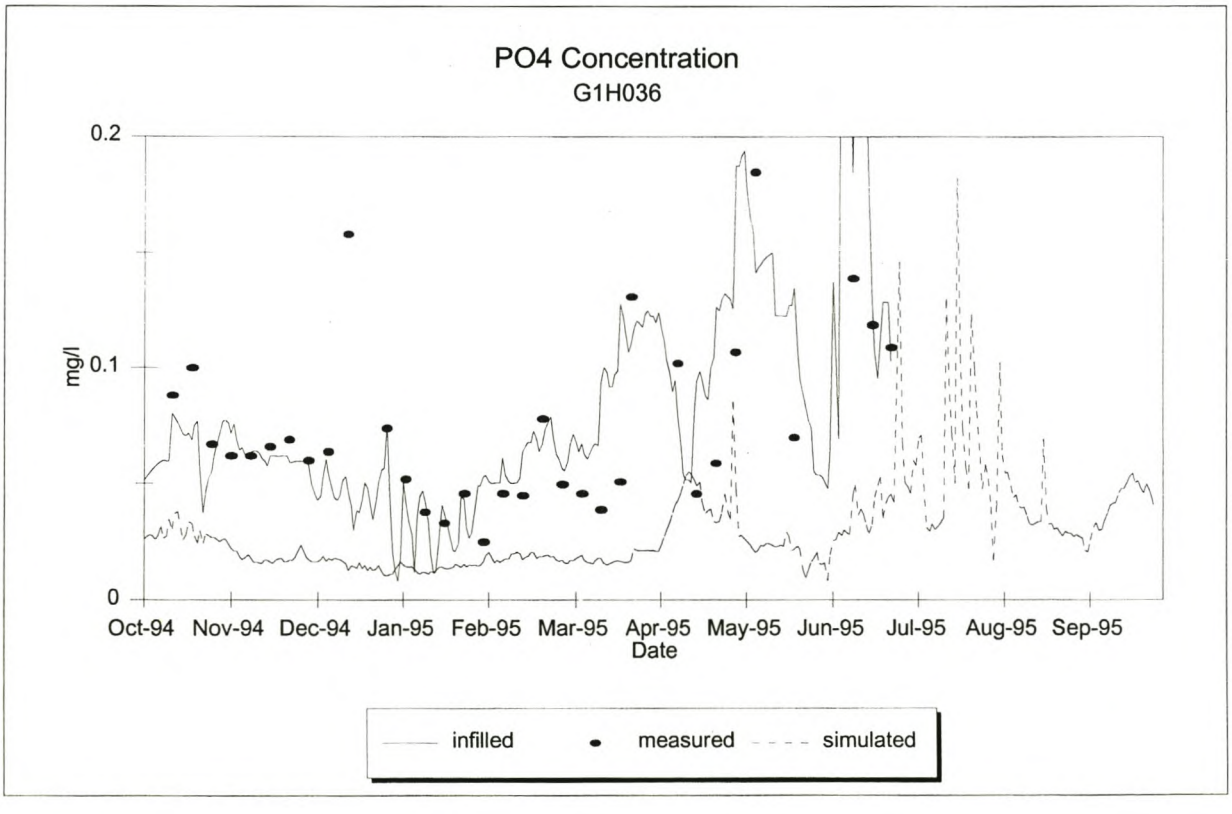

Figure 8.72: Phosphate Concentration at G1H013 (Verification)

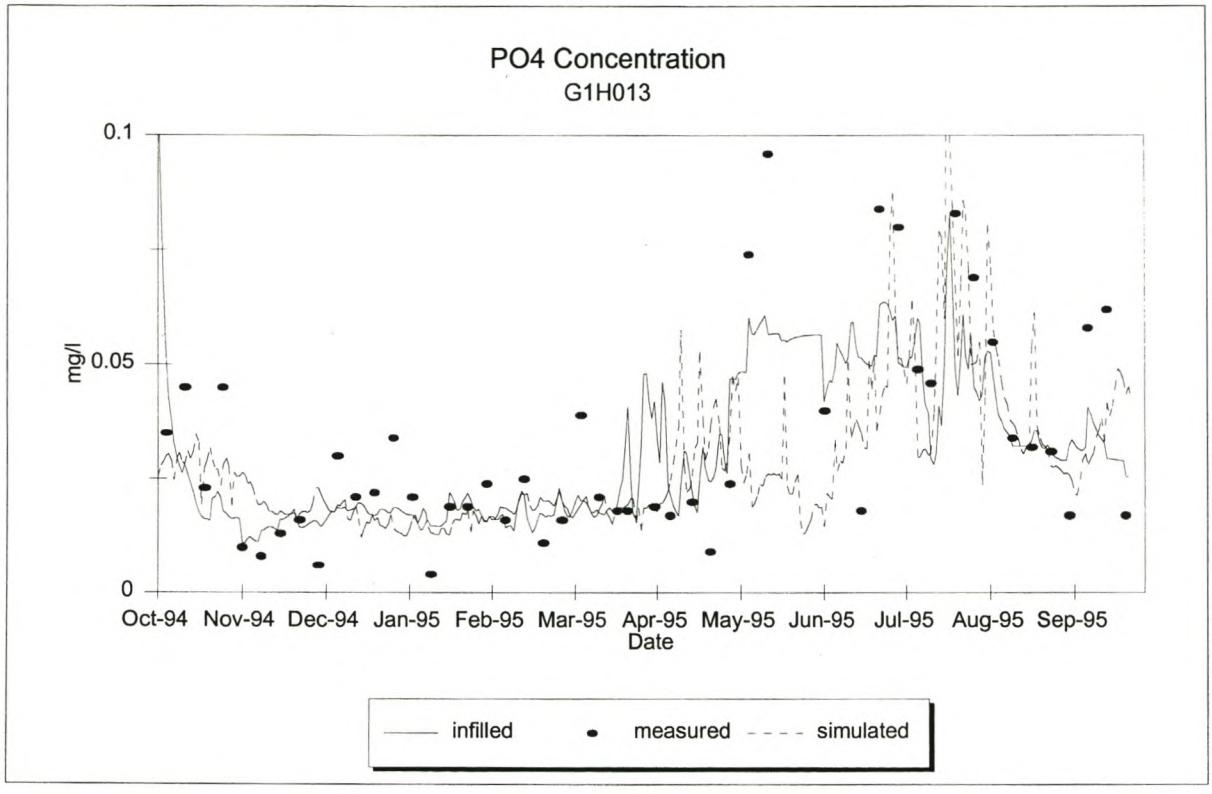

Figure 8.73: Phosphate Concentration at G1R003 (Verification)

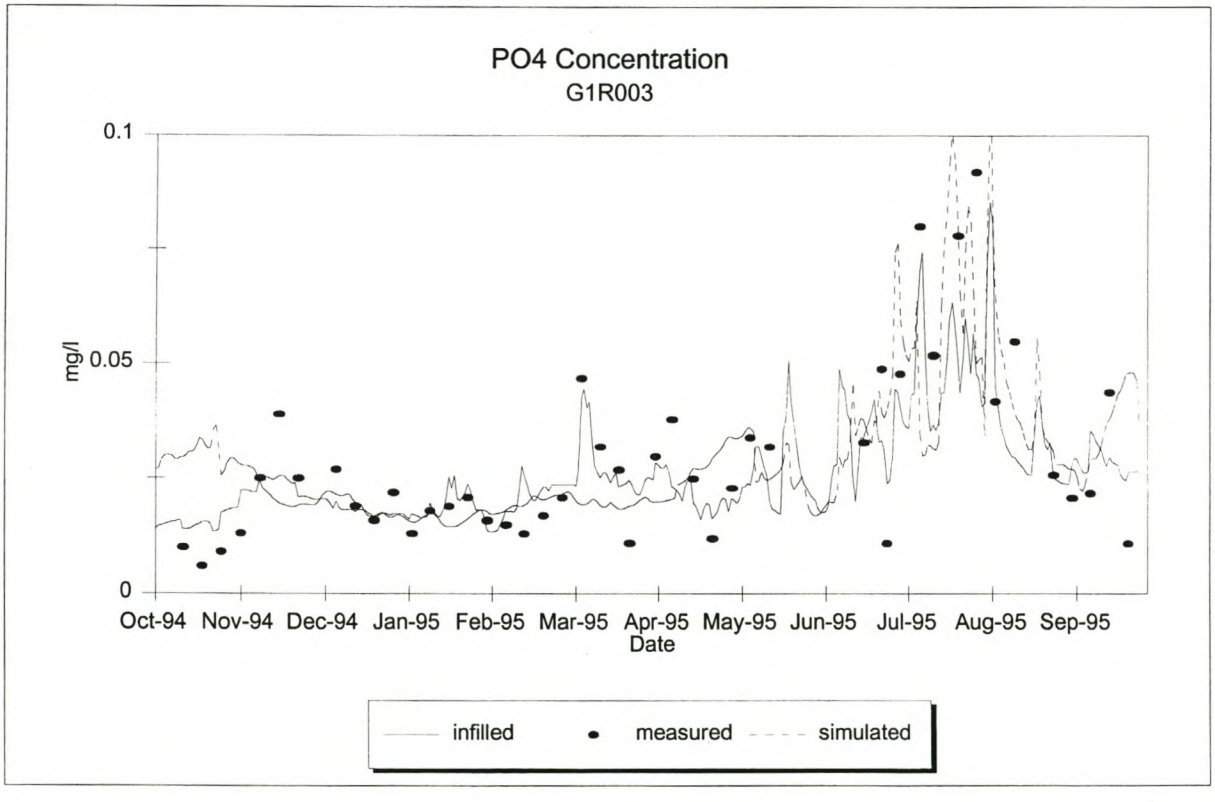

Figure 8.74: Temperature at G1H020 (Verification)

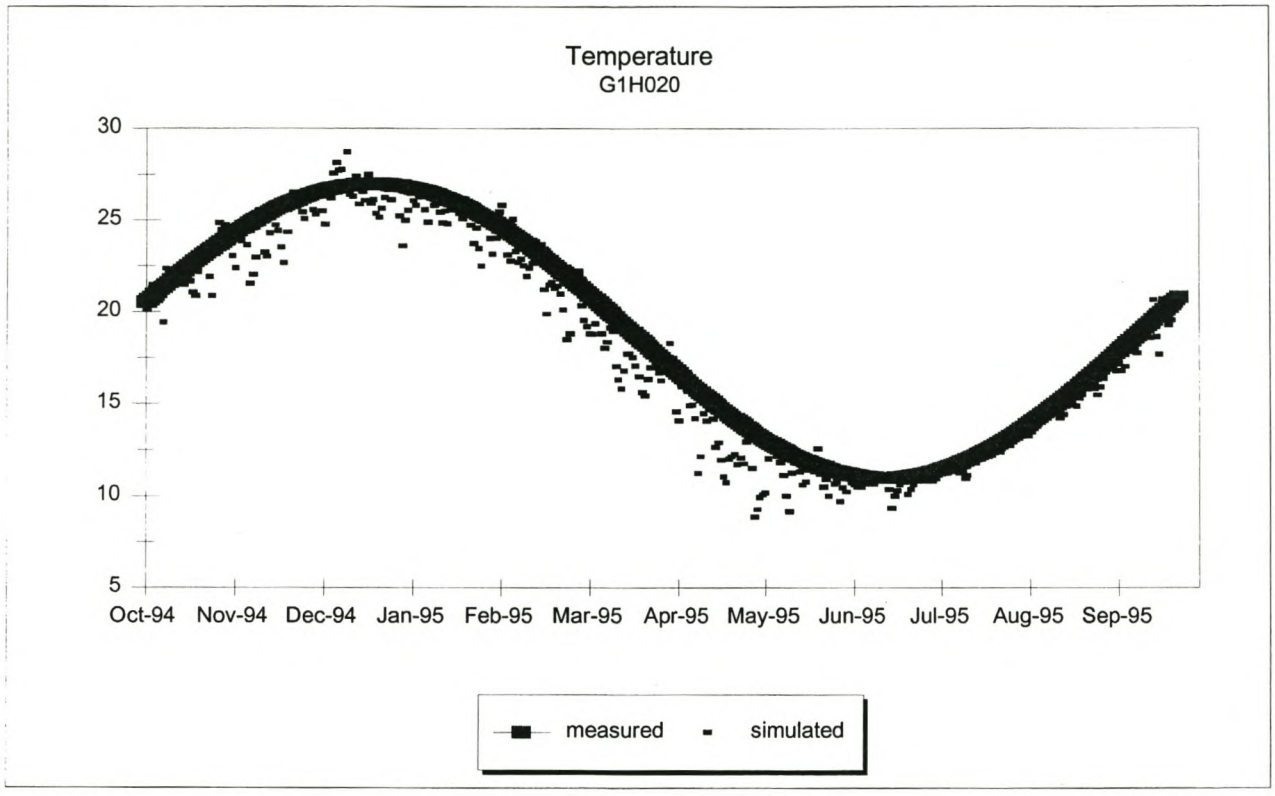

Figure 8.75: Temperature at G1H036 (Verification)

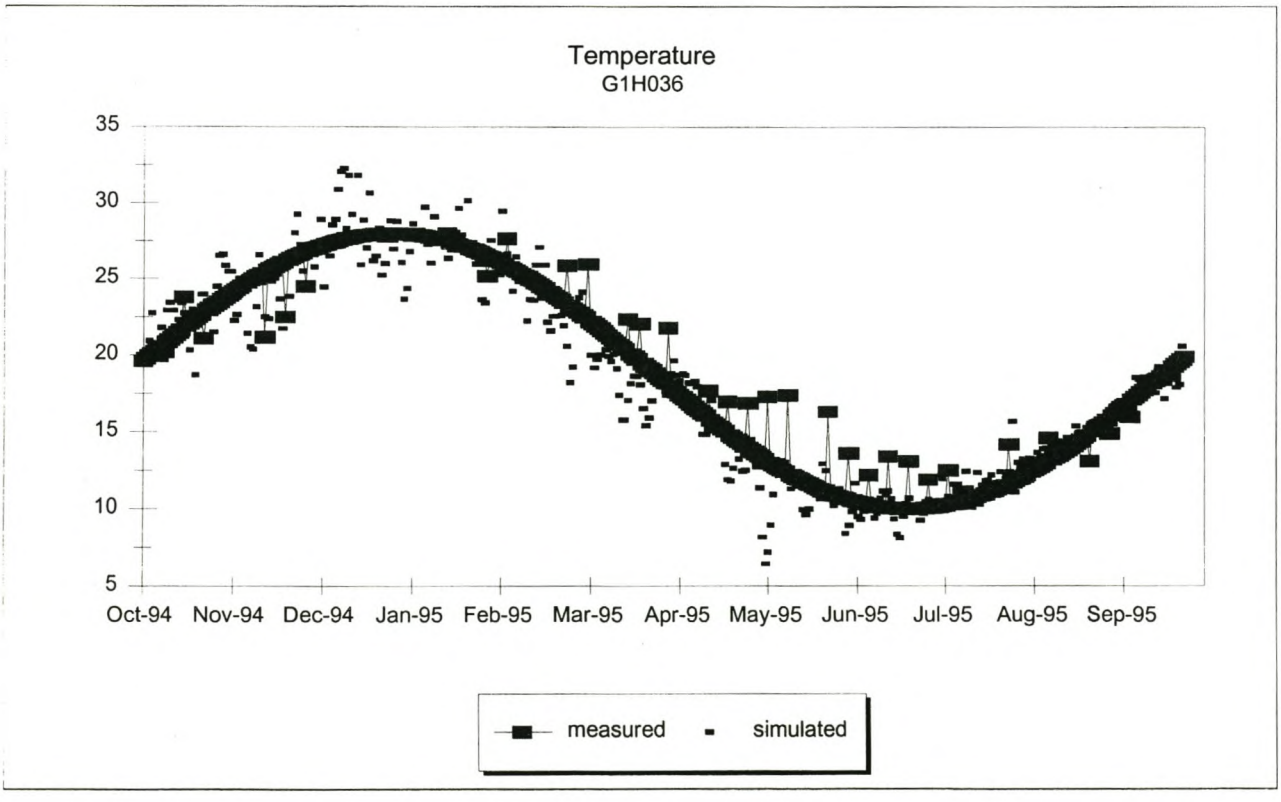

Figure 8.76: Temperature at G1H013 (Verification)

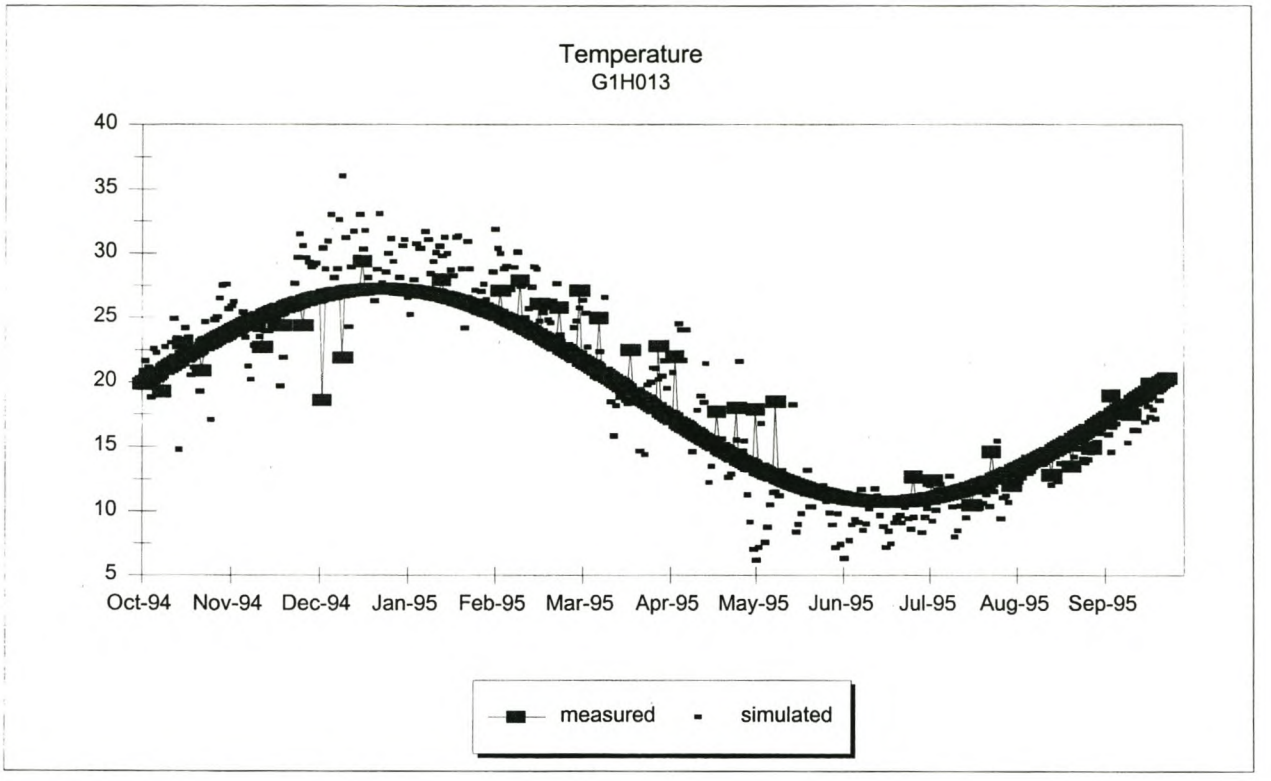

Figure 8.77: Temperature at G1R003 (Verification)

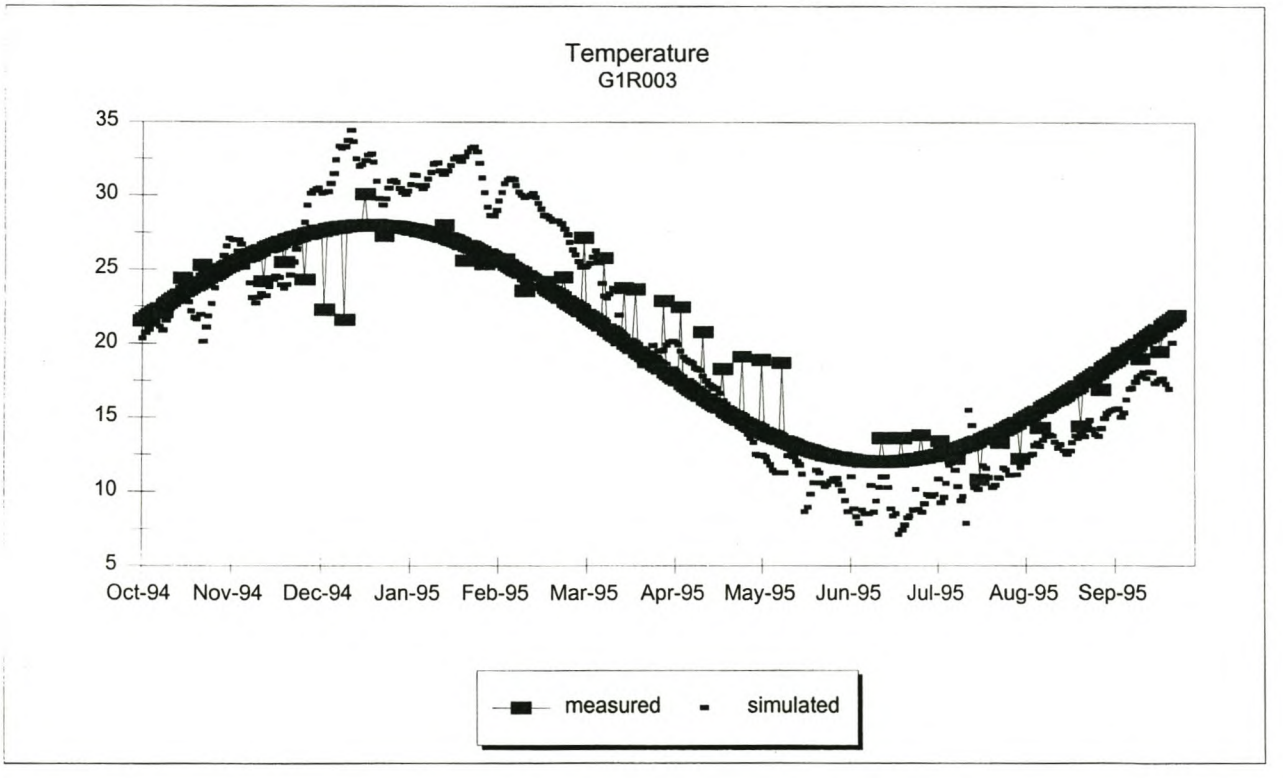

Figure 8.78: Oxygen at G1H020 (Verification)

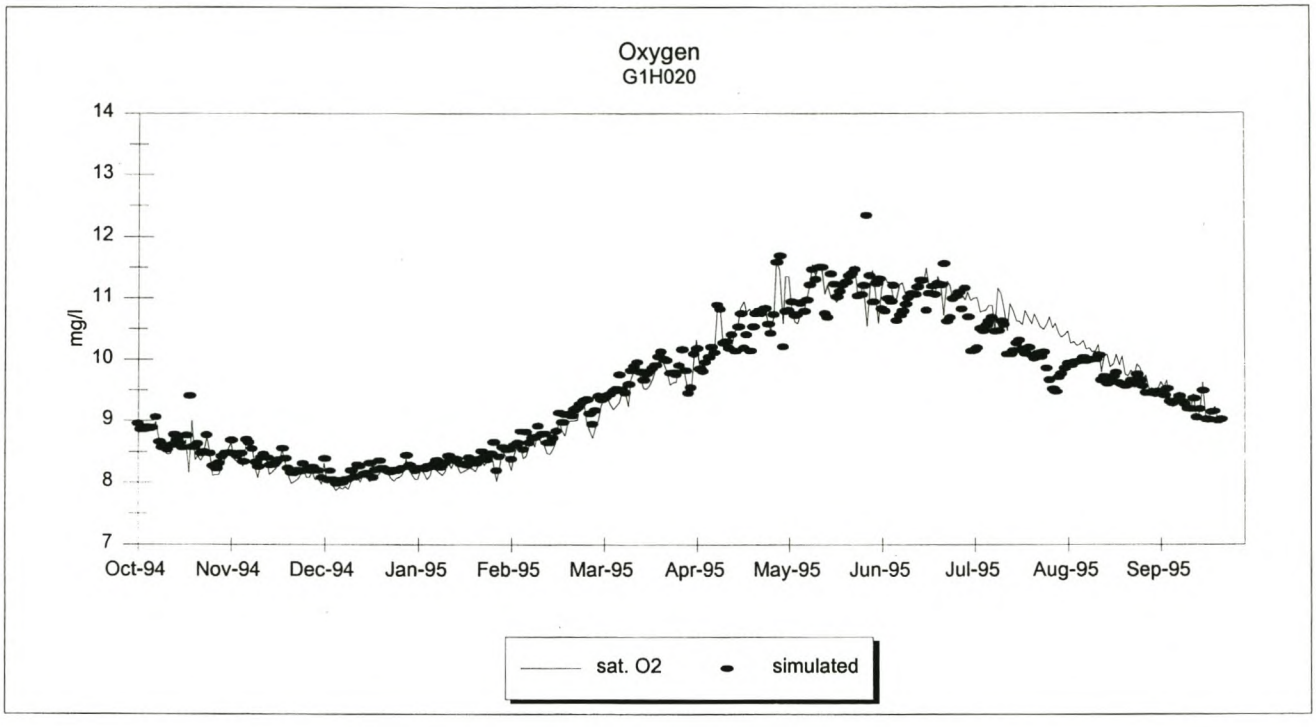

Figure 8.79: Oxygen at G1H036 (Verification)

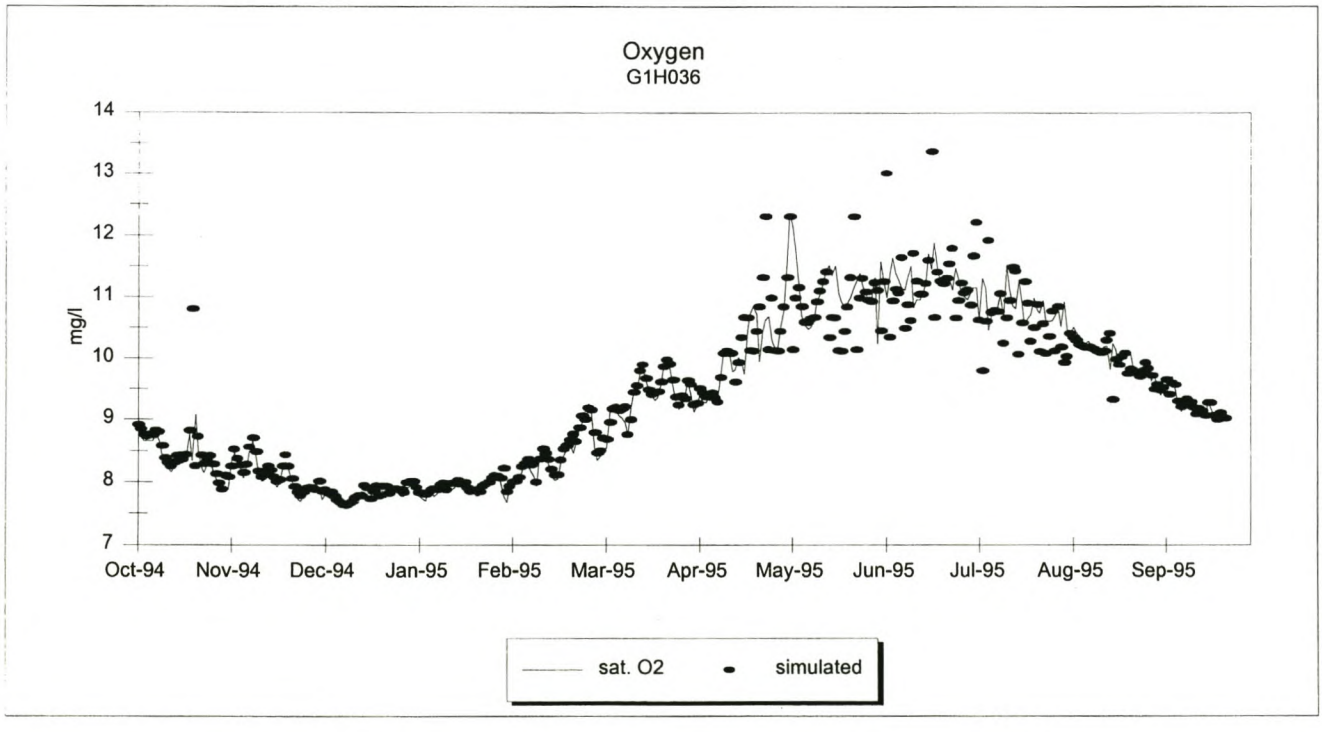

Figure 8.80: Oxygen at G1H013 (Verification)

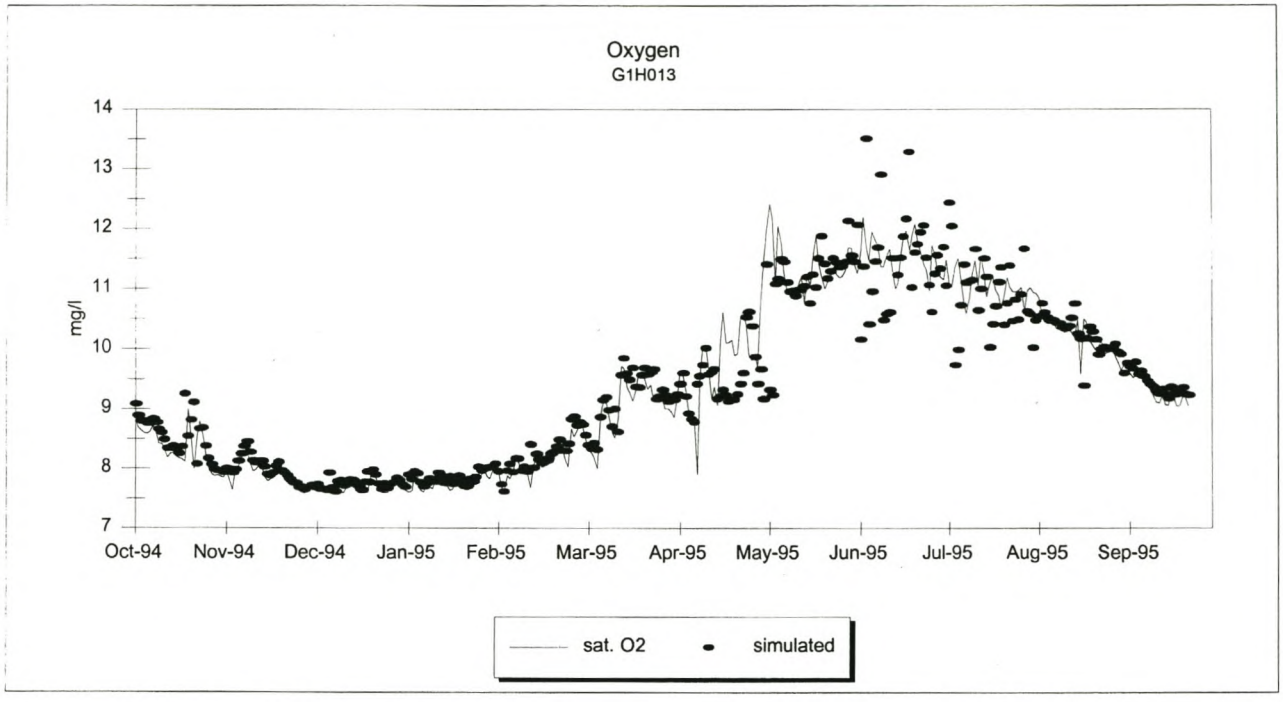

Figure 8.81: Oxygen at G1R003 (Verification)

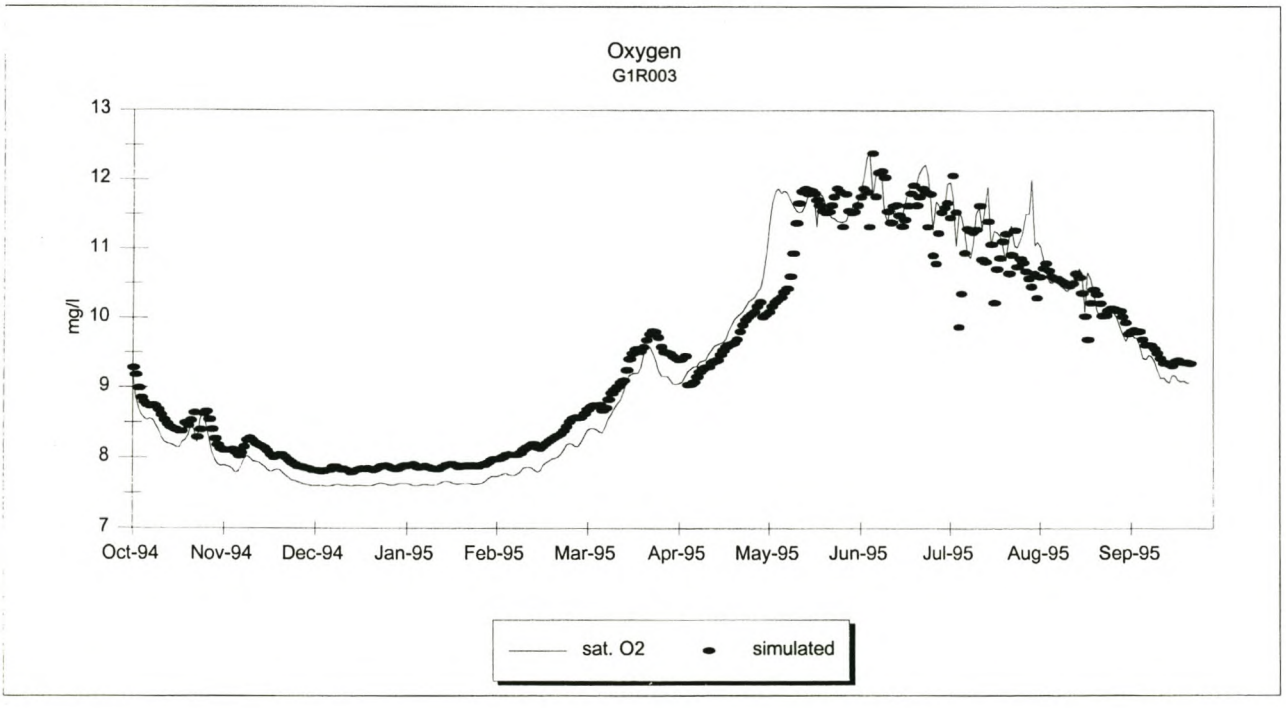

Figure 8.82: TDS Loads at G1H020 for low flows (Simulation without ungauged loads)

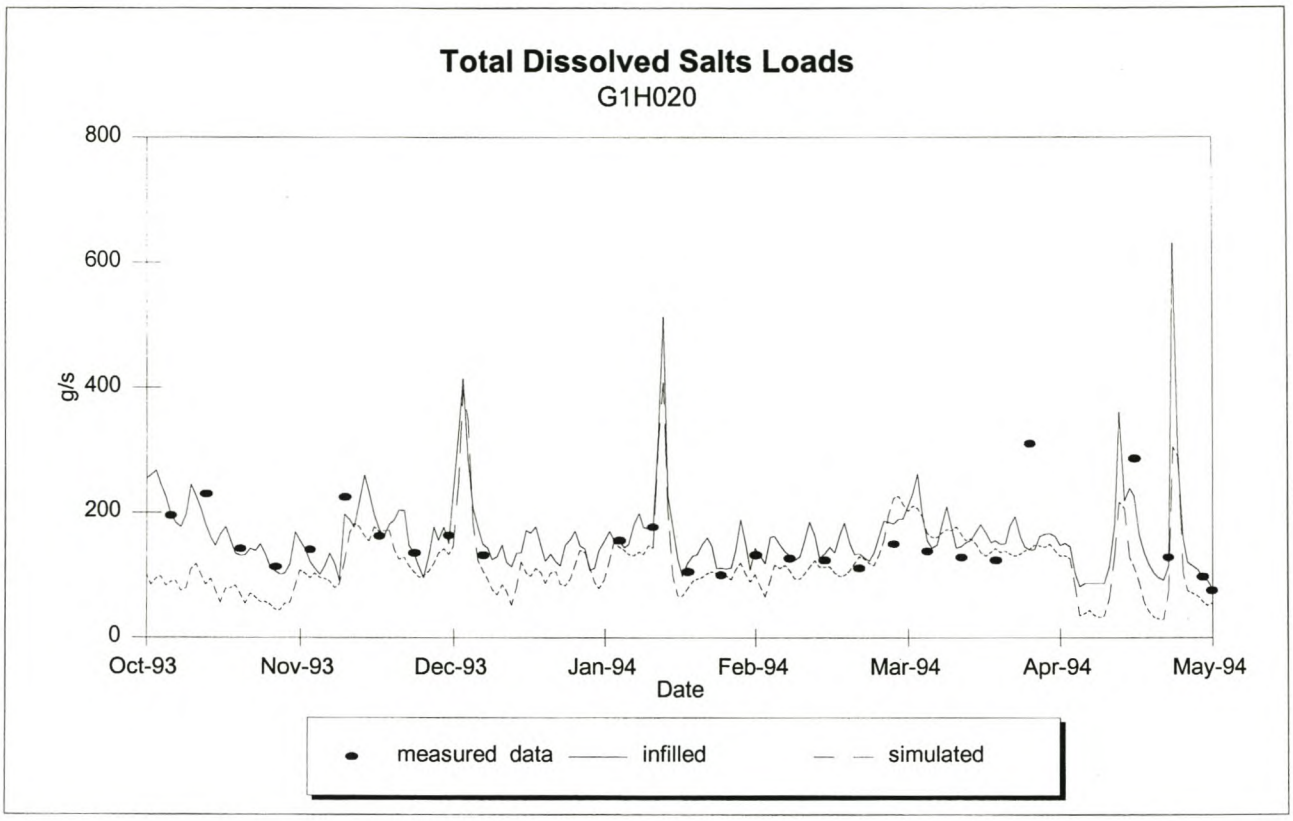

Figure 8.83: TDS Loads at G1H036 for low flows (Simulation without ungauged loads)

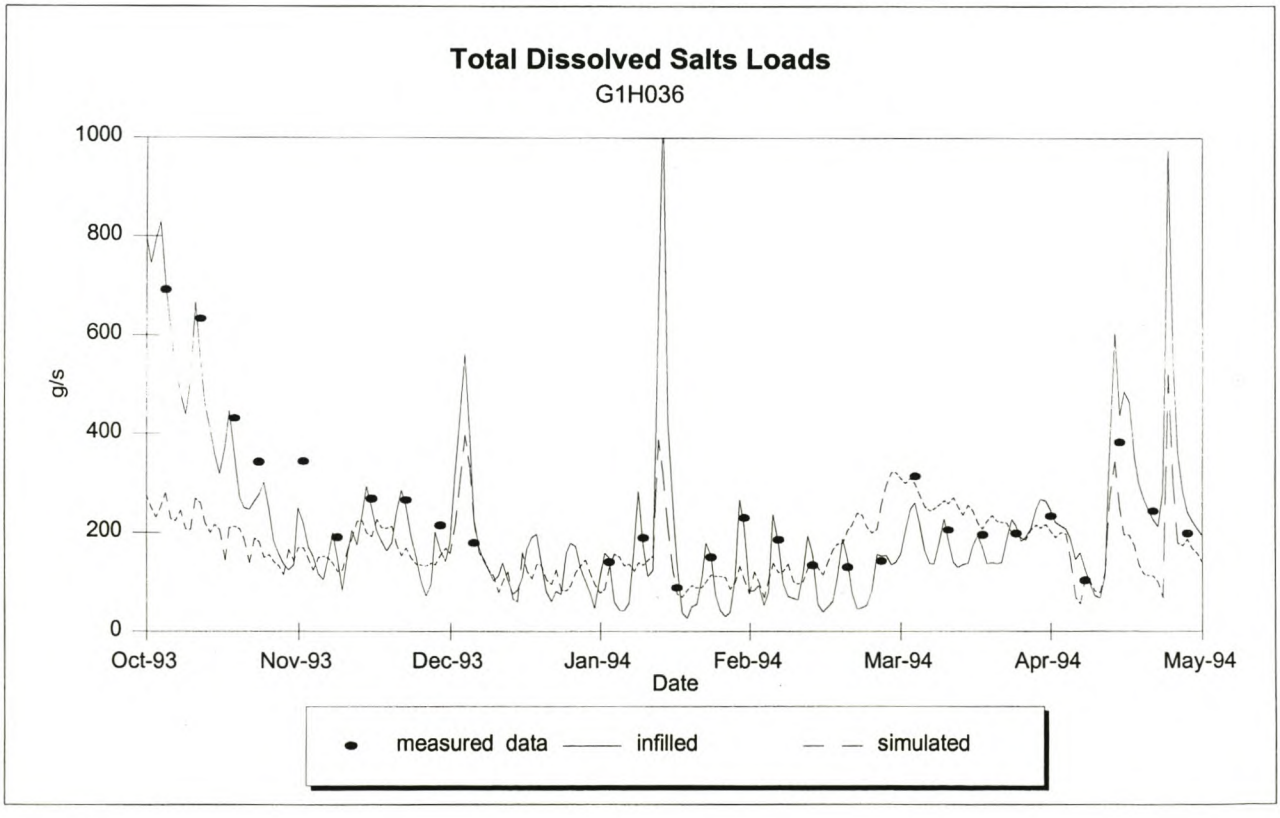

Figure 8.84: TDS Loads at G1H013 for low flows (Simulation without ungauged loads)

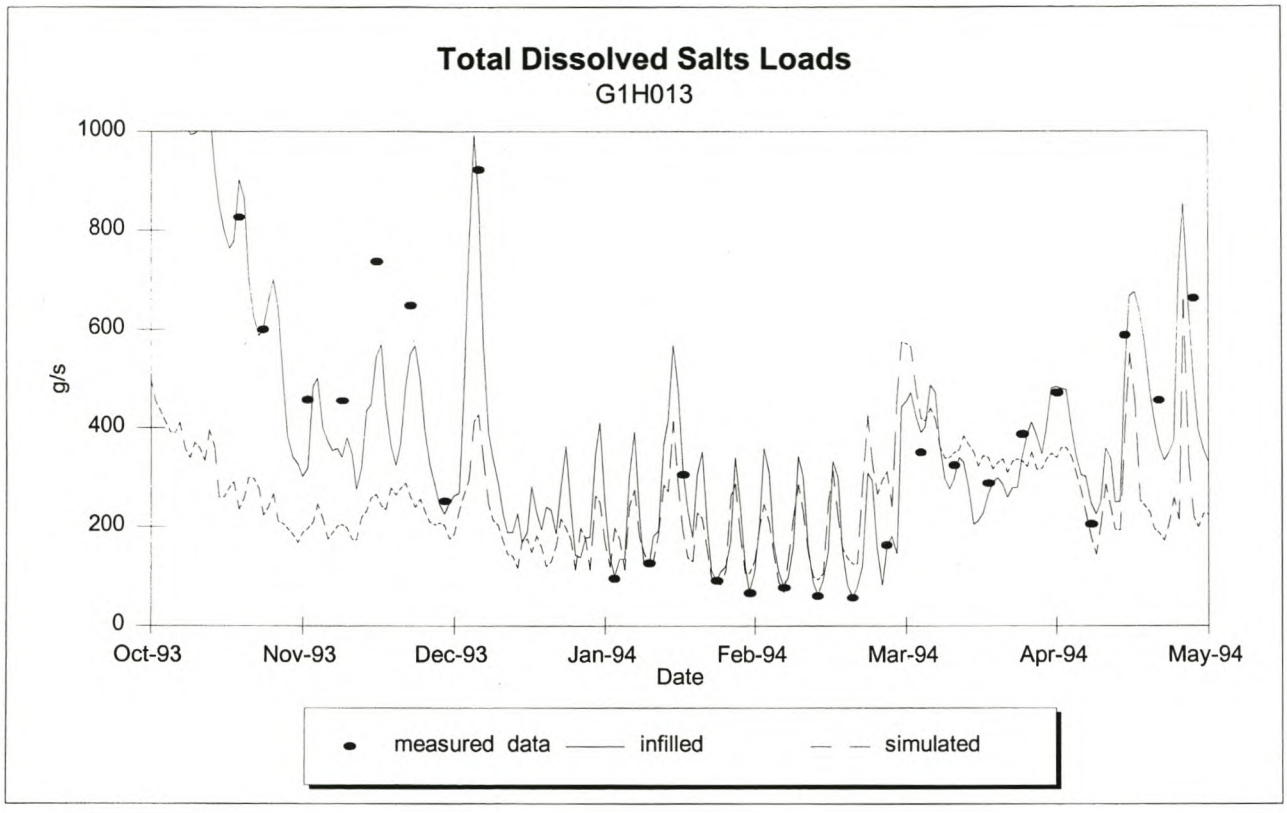

Figure 8.85: TDS Loads at G1R003 for low flows (Simulation without ungauged loadsn)

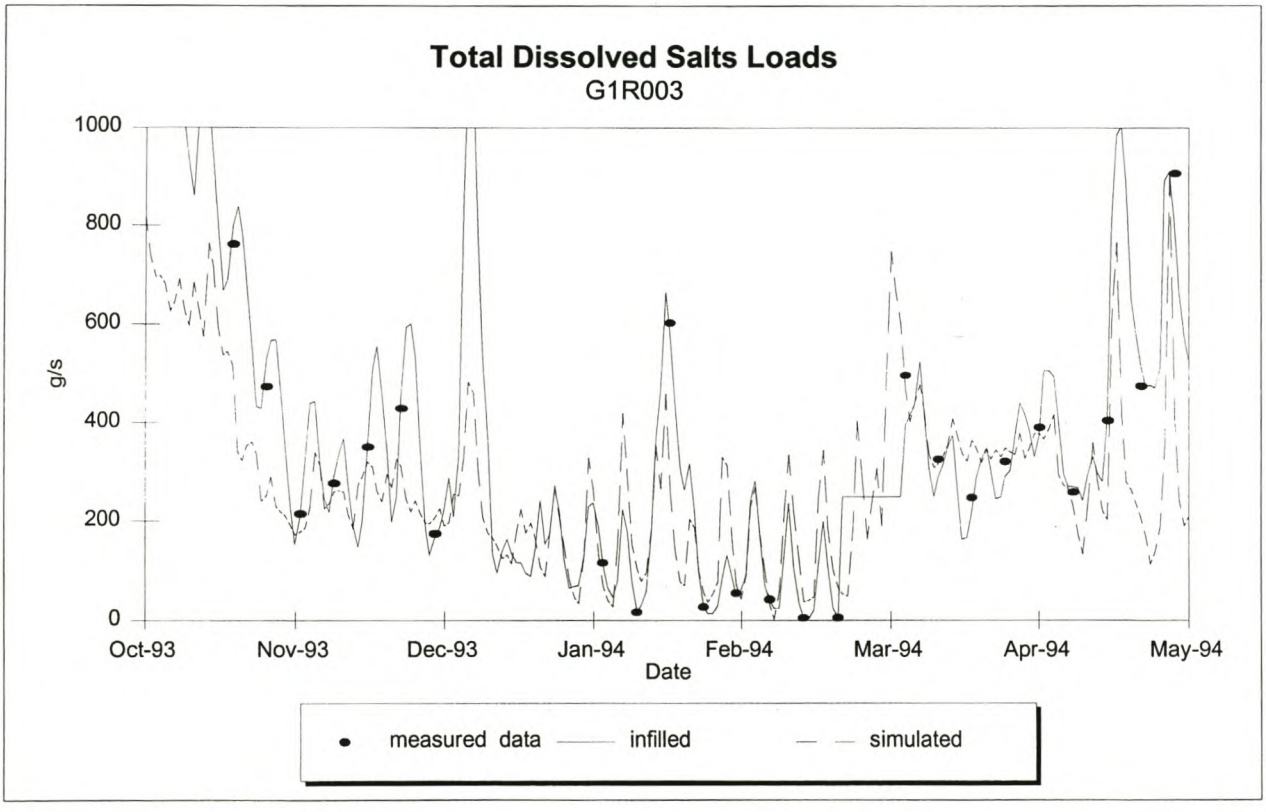

Figure 8.86: TDS Loads at G1H020 for high flows (Simulation without ungauged loads)

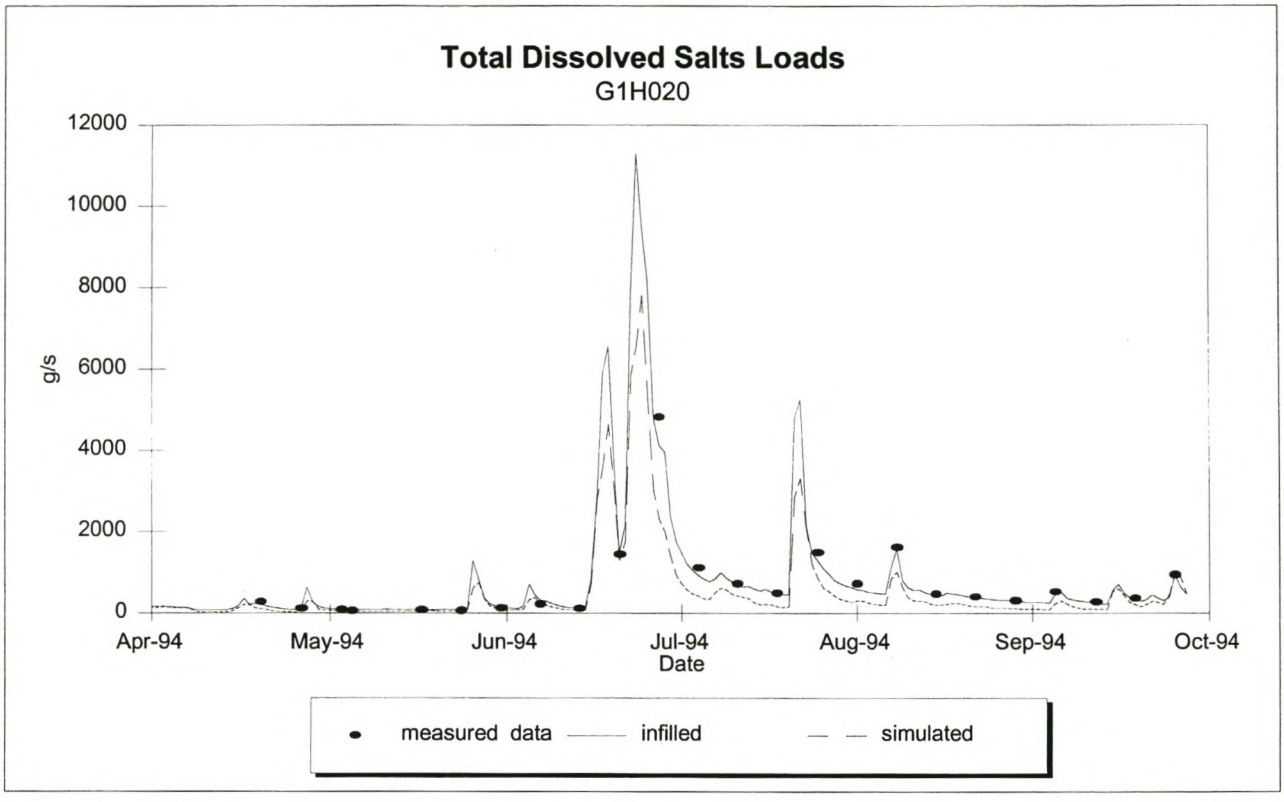

Figure 8.87: TDS Loads at G1H036 for high flows (Simulation without ungauged loads)

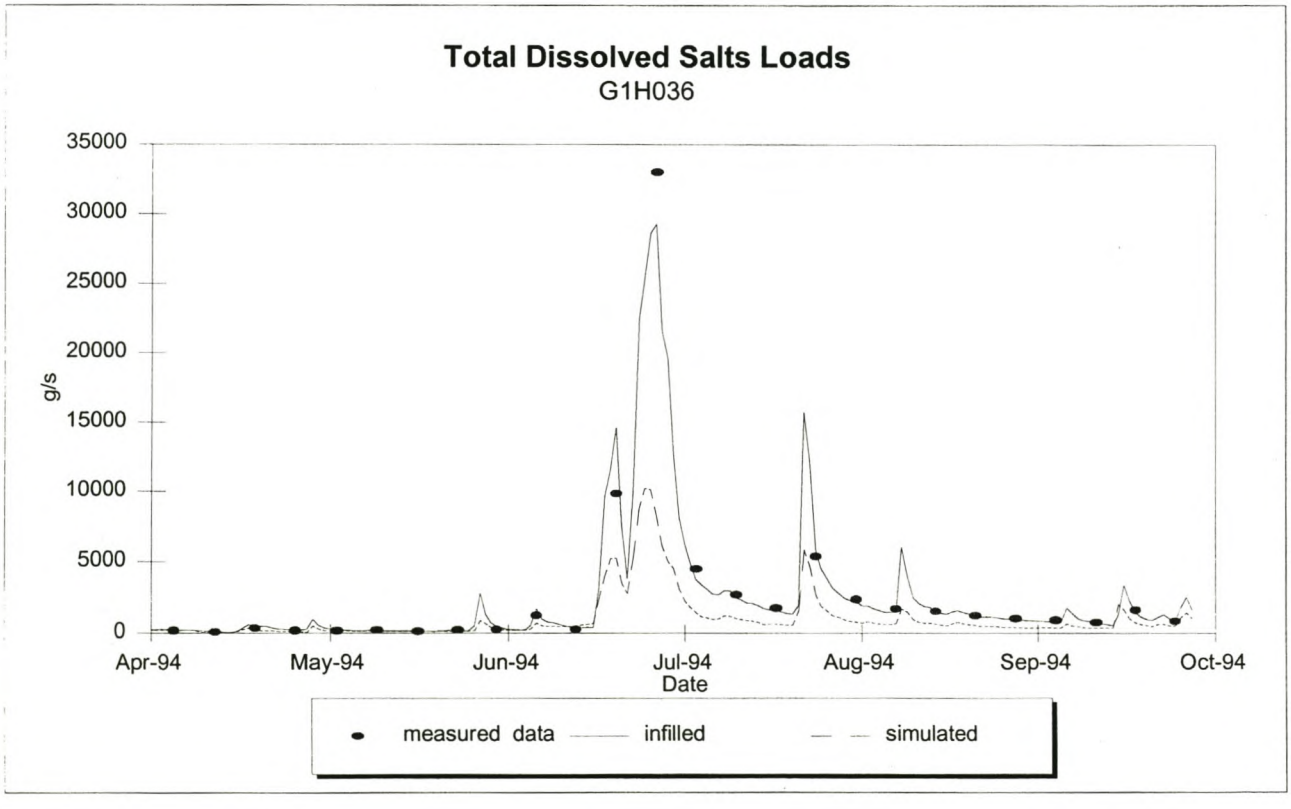

Figure 8.88: TDS Loads at G1H013 for high flows (Simulation without ungauged loads)

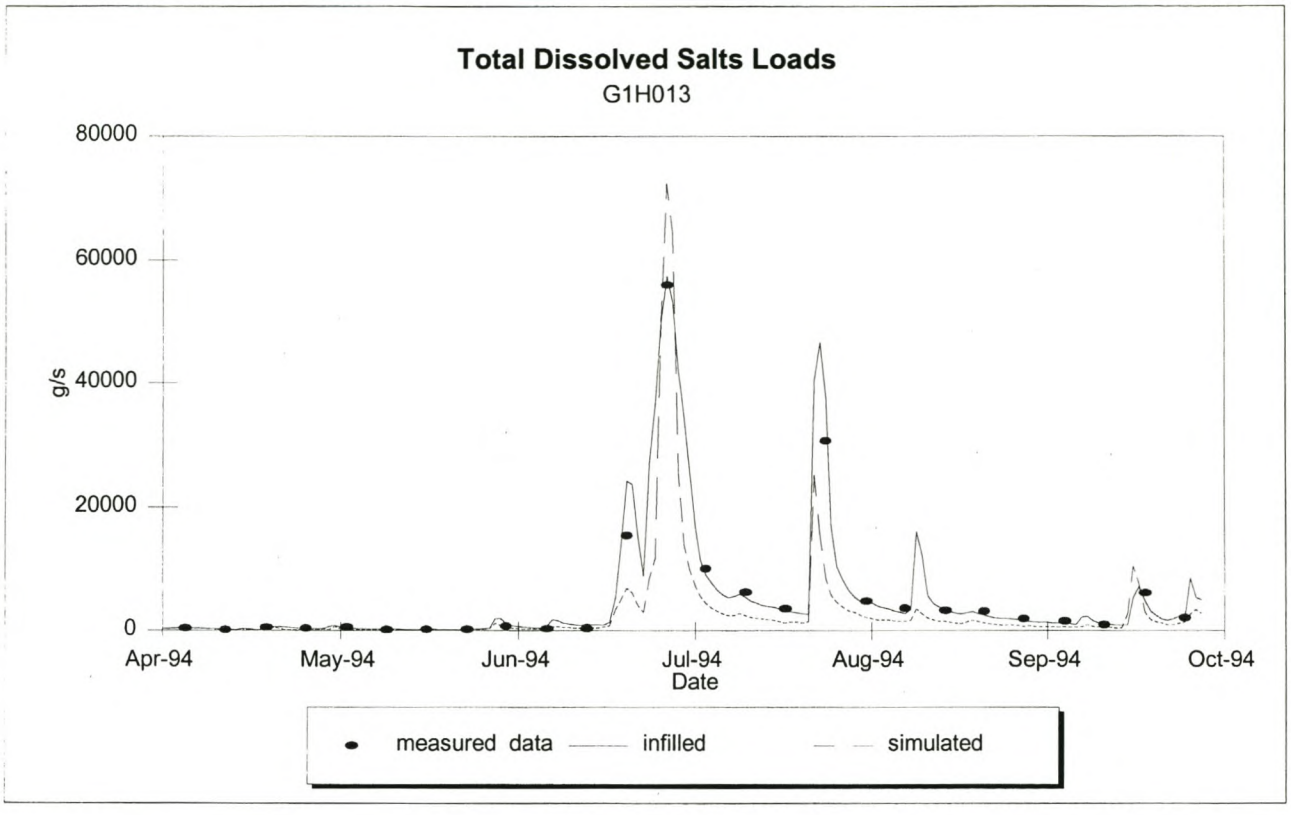

Figure 8.89: TDS Loads at G1R003 for high flows (Simulation without ungauged loads)

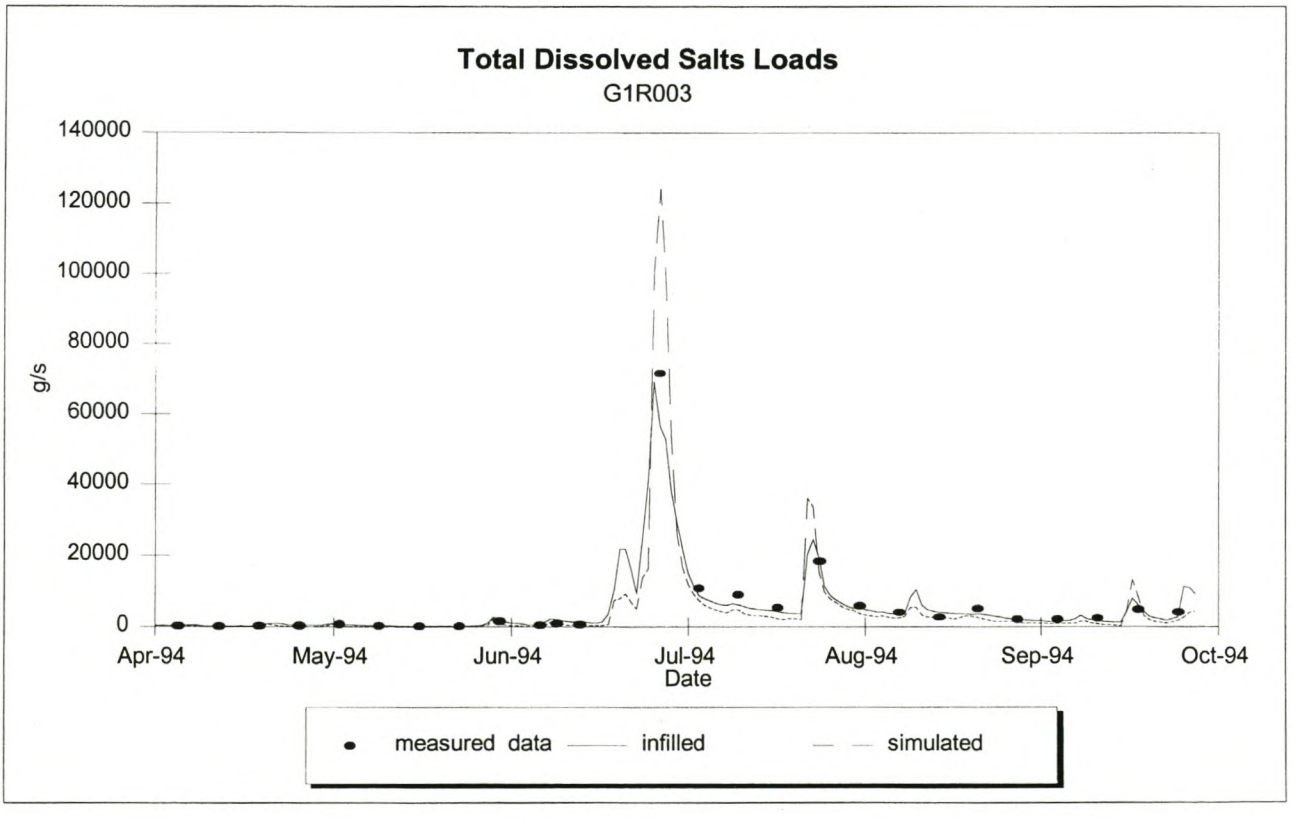

Figure 8.90: TDS Concentration at G1H020 (Simulation without ungauged loads)

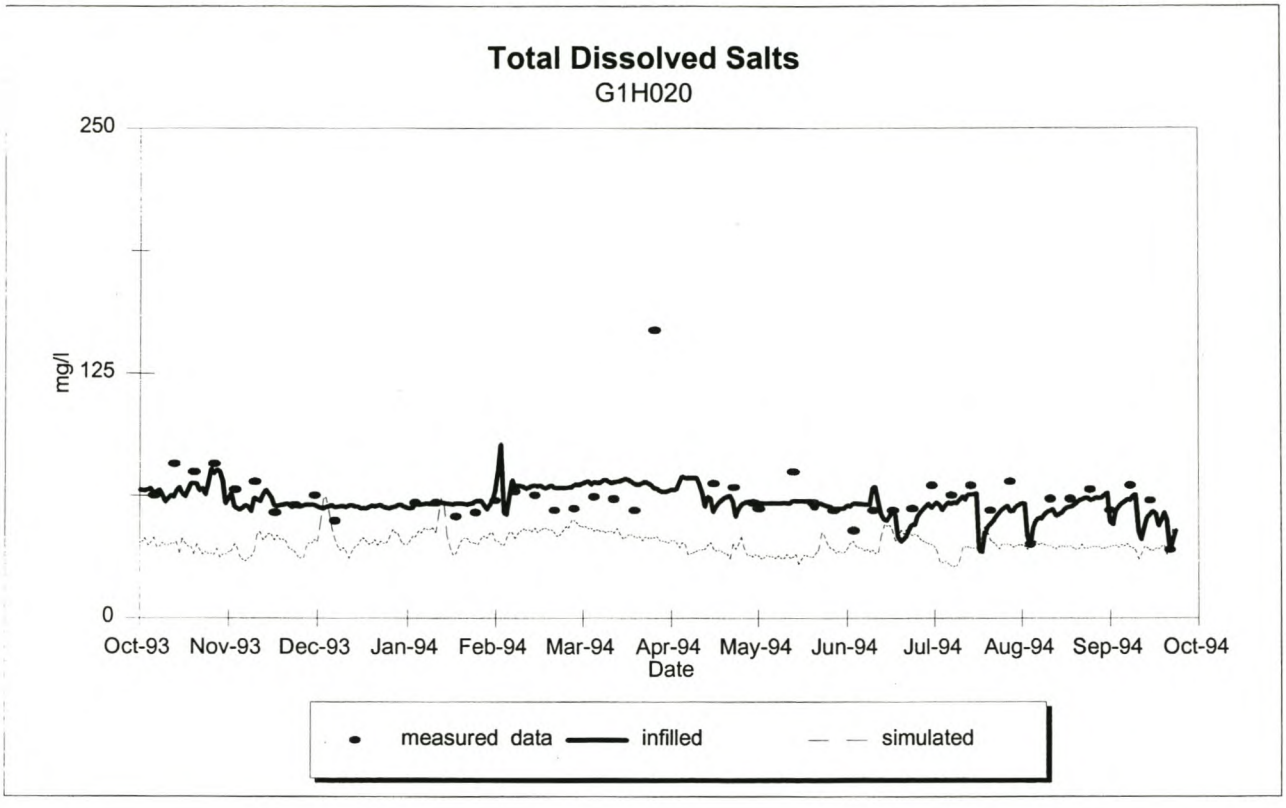

Figure 8.91: TDS Concentration at G1H036 (Simulation without ungauged loads)

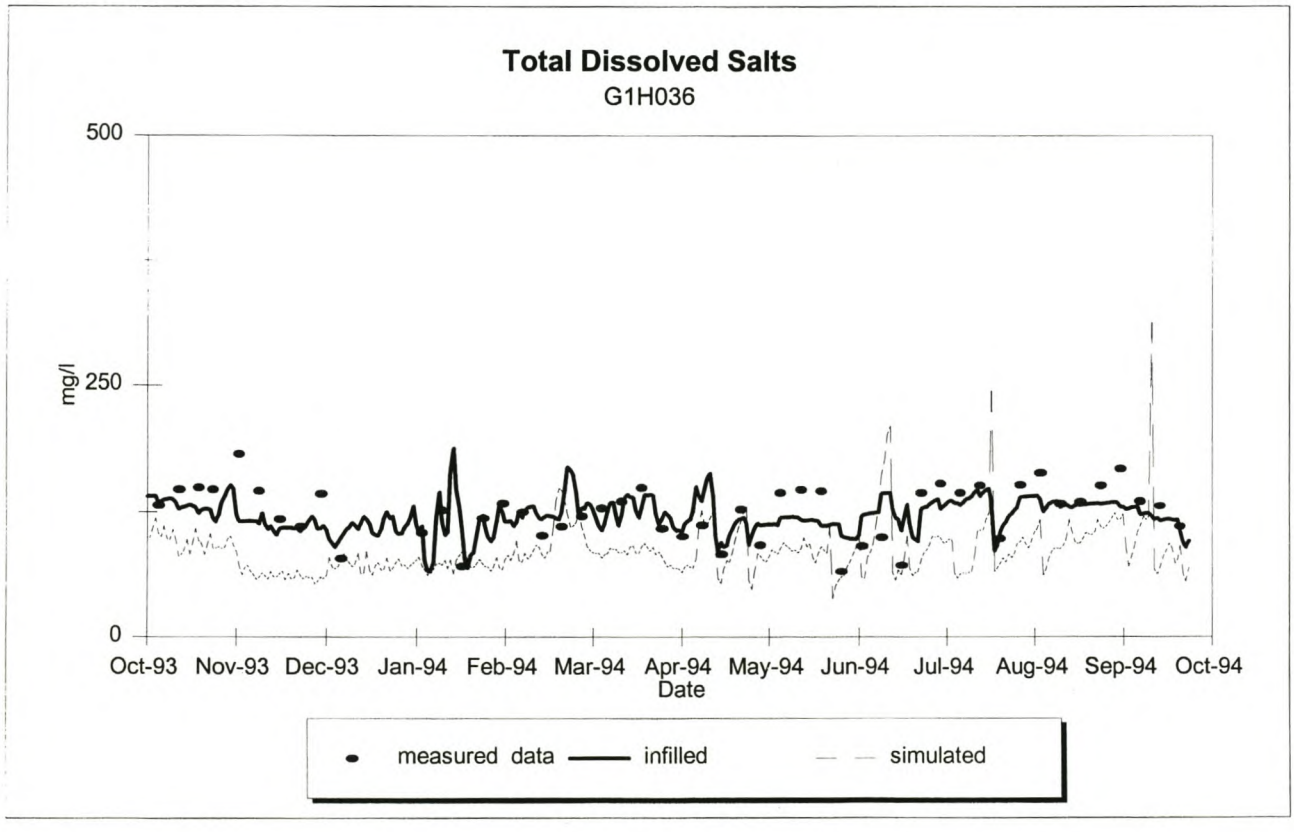

Figure 8.92: TDS Concentration at G1H013 (Simulation without ungauged loads)

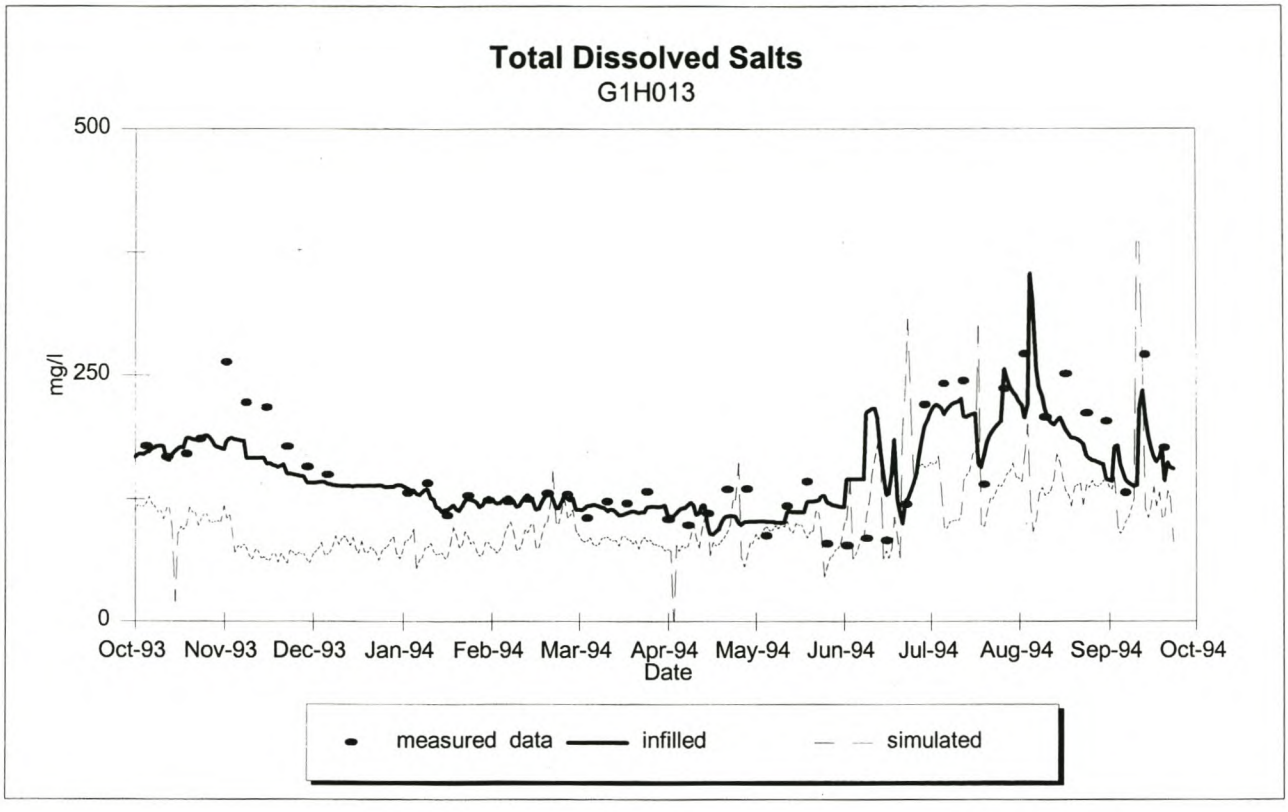

Figure 8.93: TDS Concentration at G1R003 (Simulation without ungauged loads)

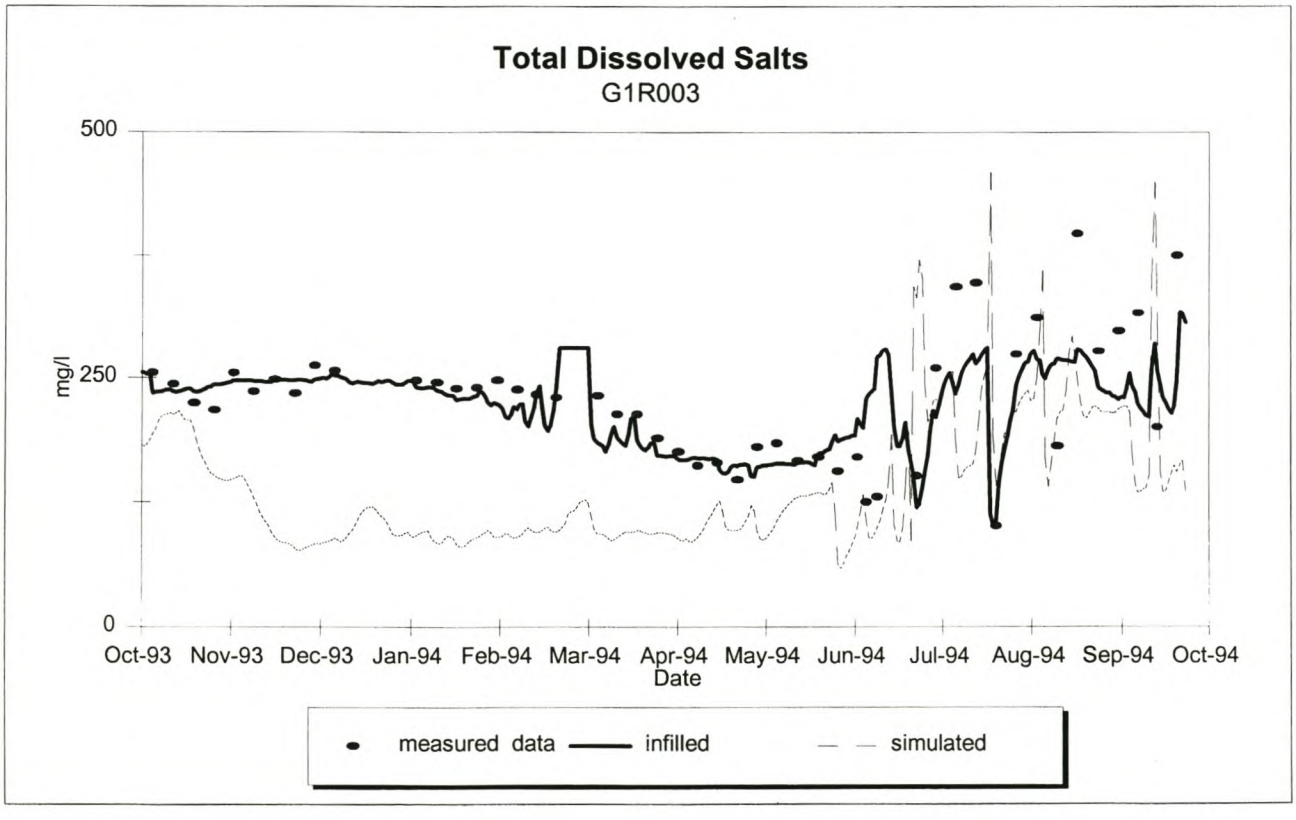

Figure 8.94: Phosphate Loads at G1H020 for low flows(Simulation without ungauged loads)

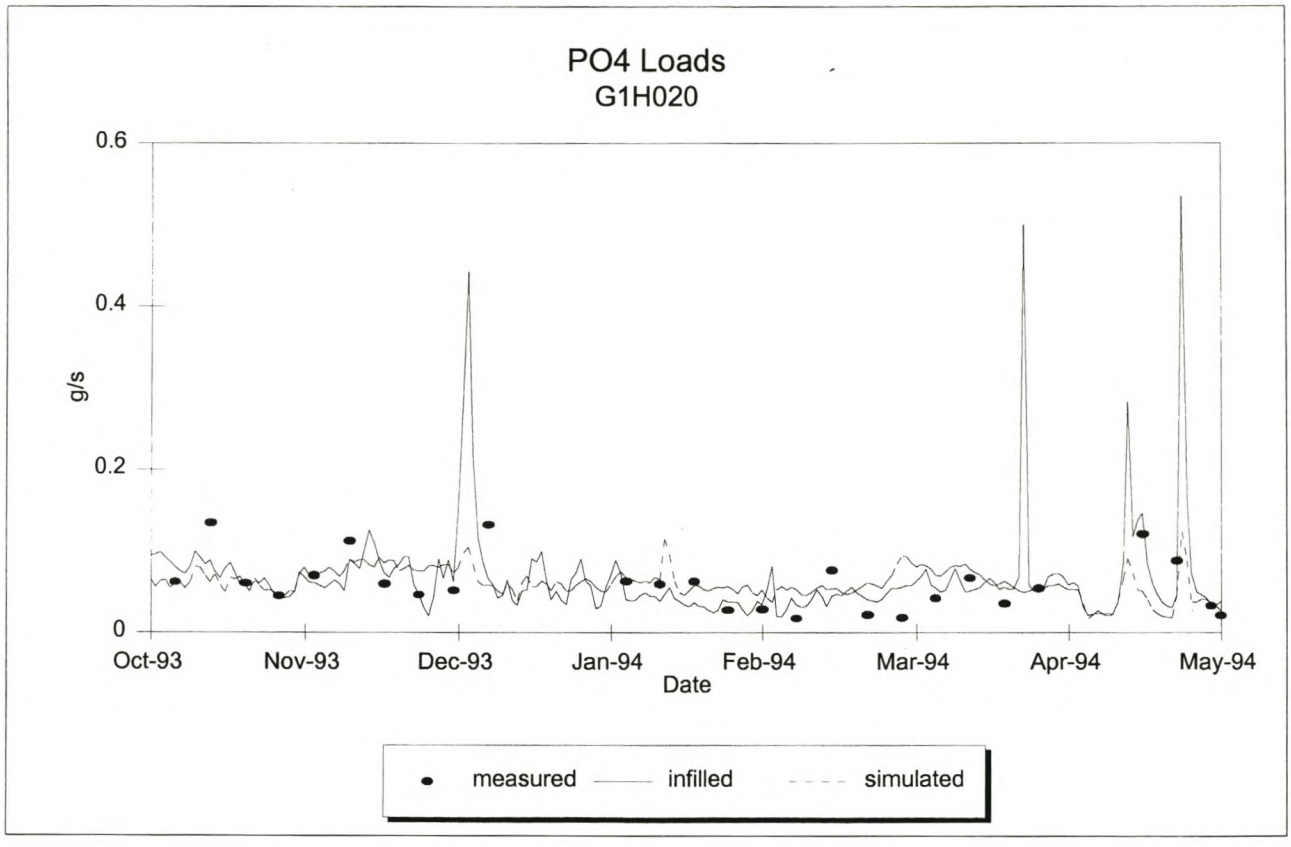

Figure 8.95: Phosphate Loads at G1H036 for low flows (Simulation without ungauged loads)

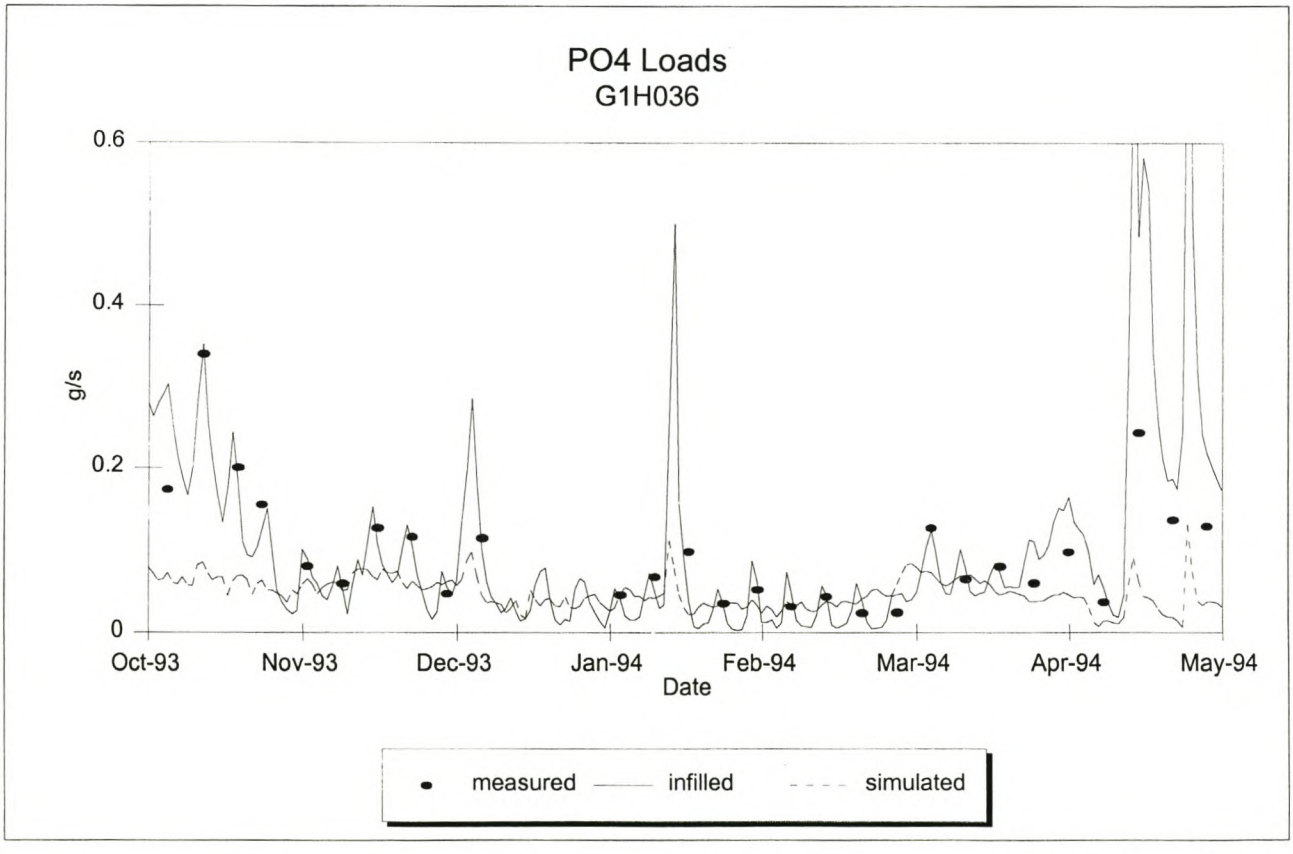

Figure 8.96: Phosphate Loads at G1H013 for low flows (without ungauged loads)

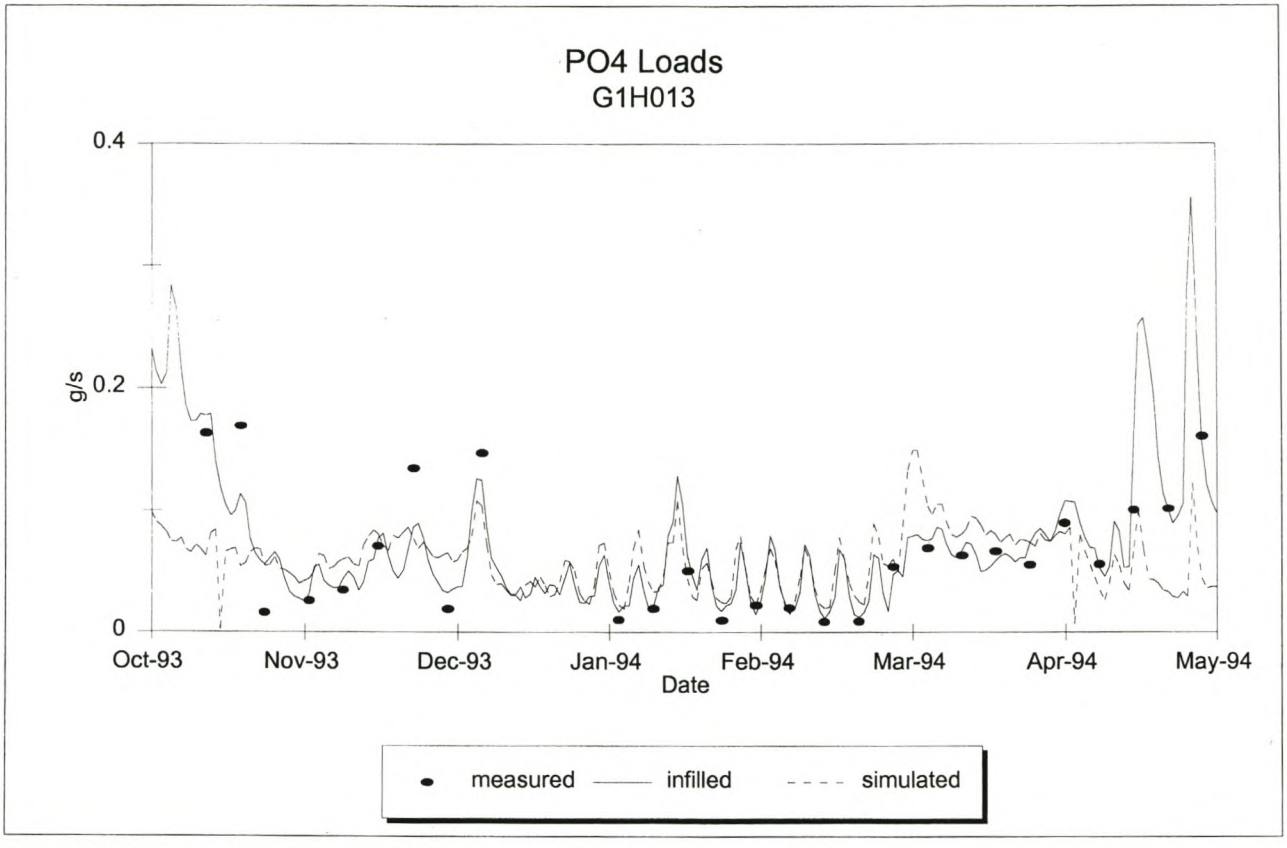

Figure 8.97: Phosphate Loads at G1R003 for low flows (without ungauged loads)

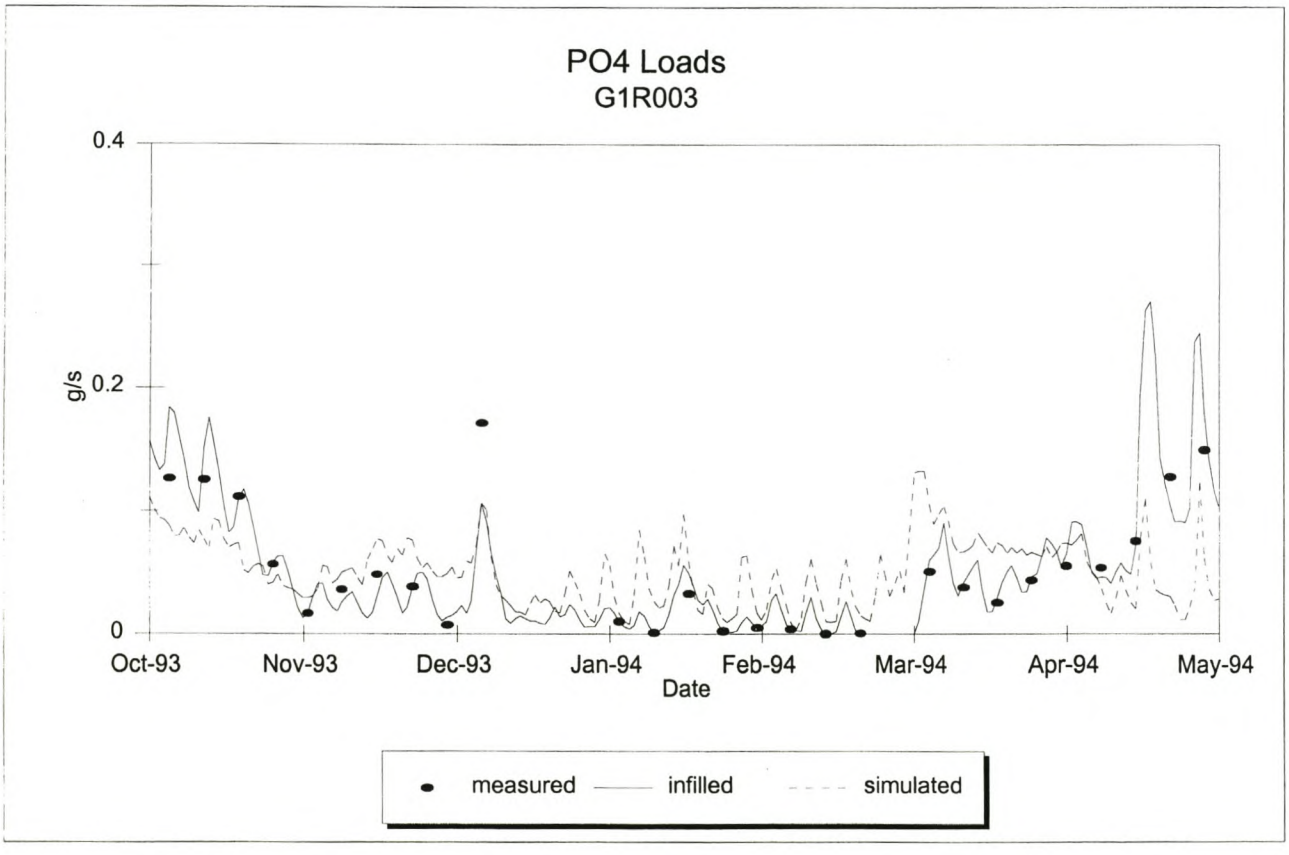

Figure 8.98: Phosphate Loads at G1H020 for high flows (Simulation without ungauged loads)

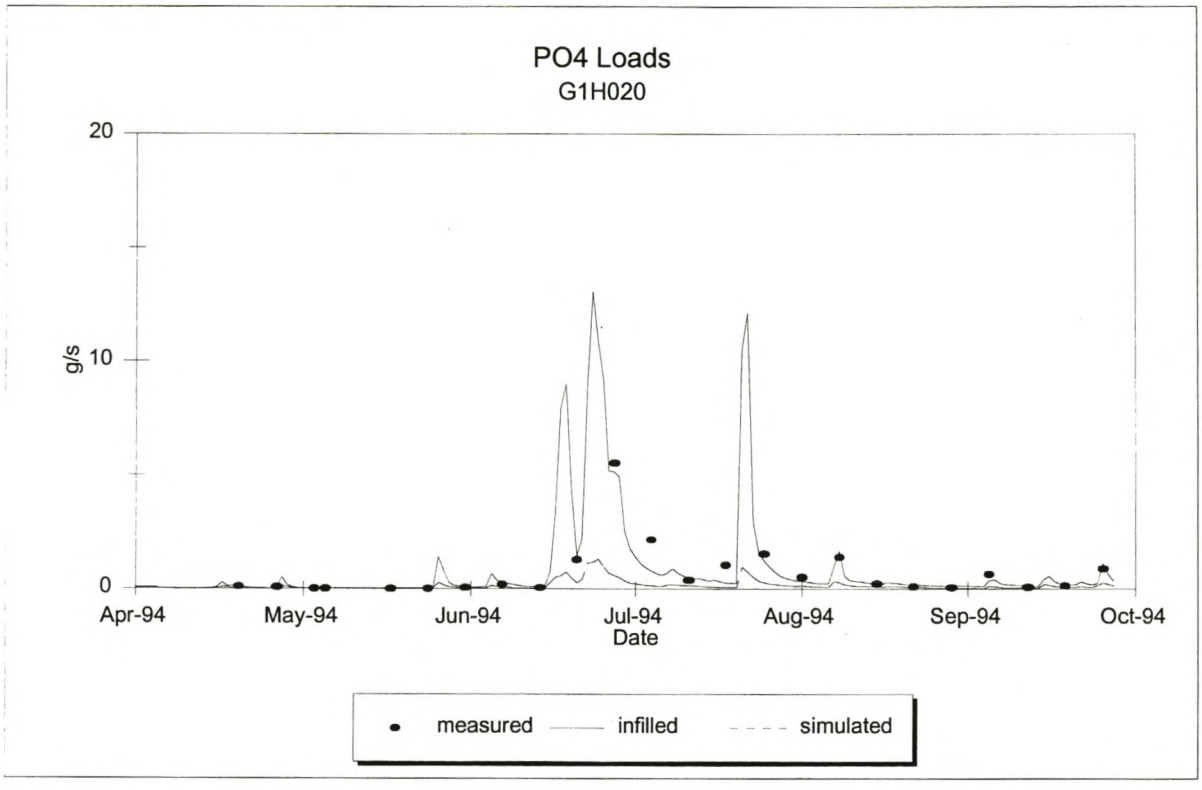

Figure 8.99: Phosphate Loads at G1H036 for high flows (Simulation without ungauged loads)

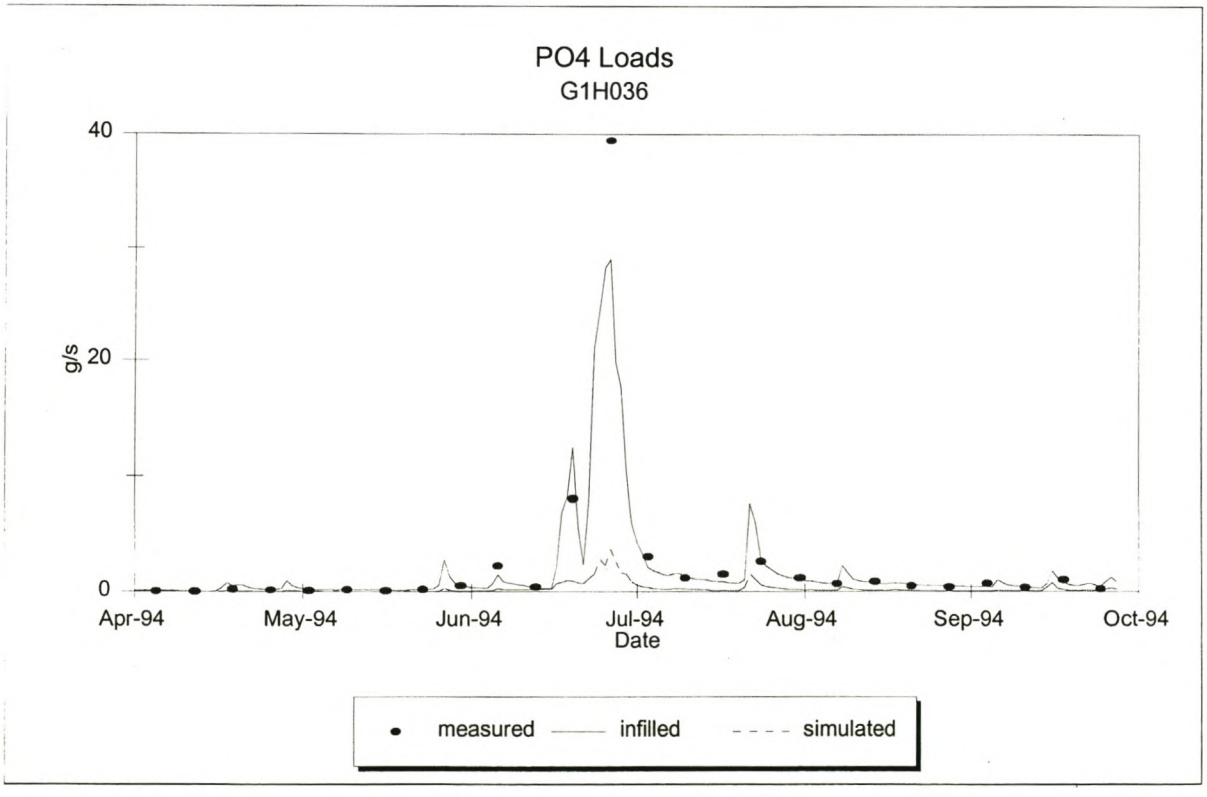

Figure 8.100: Phosphate Loads at G1H013 for high flows (Simulation without ungauged loads)

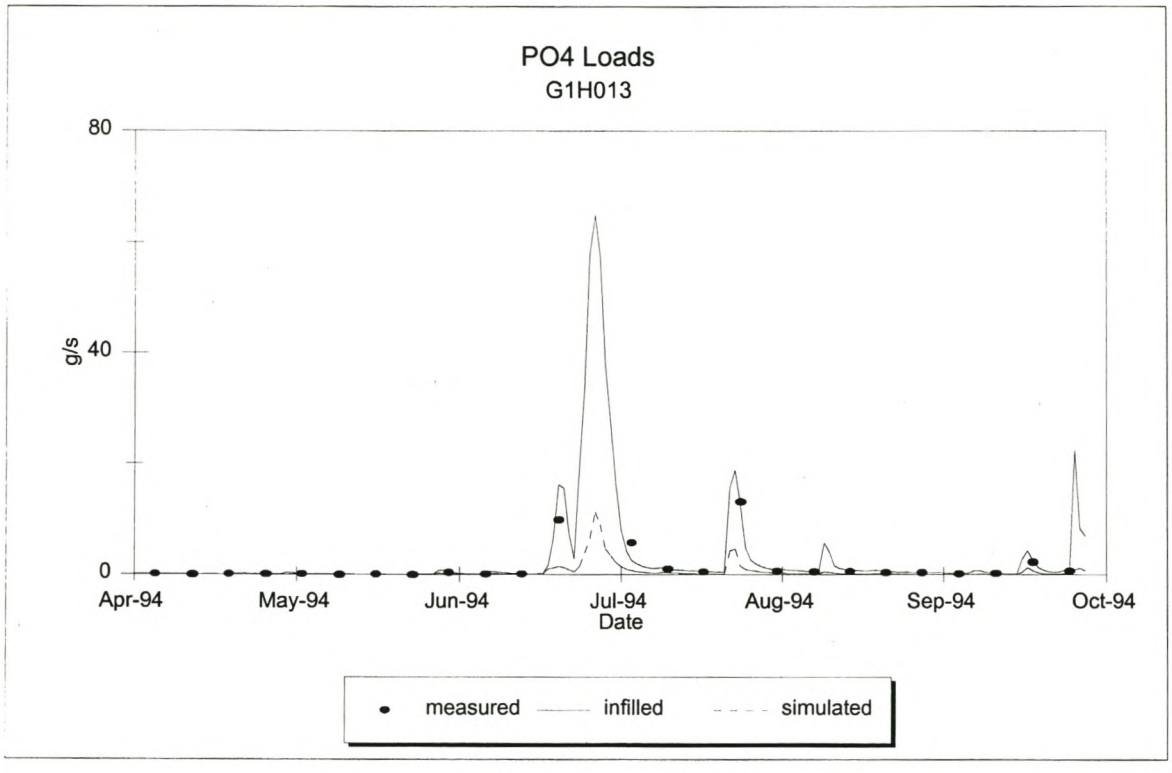

Figure 8.101: Phosphate Loads at G1R003 for high flows (Simulation without ungauged loads)

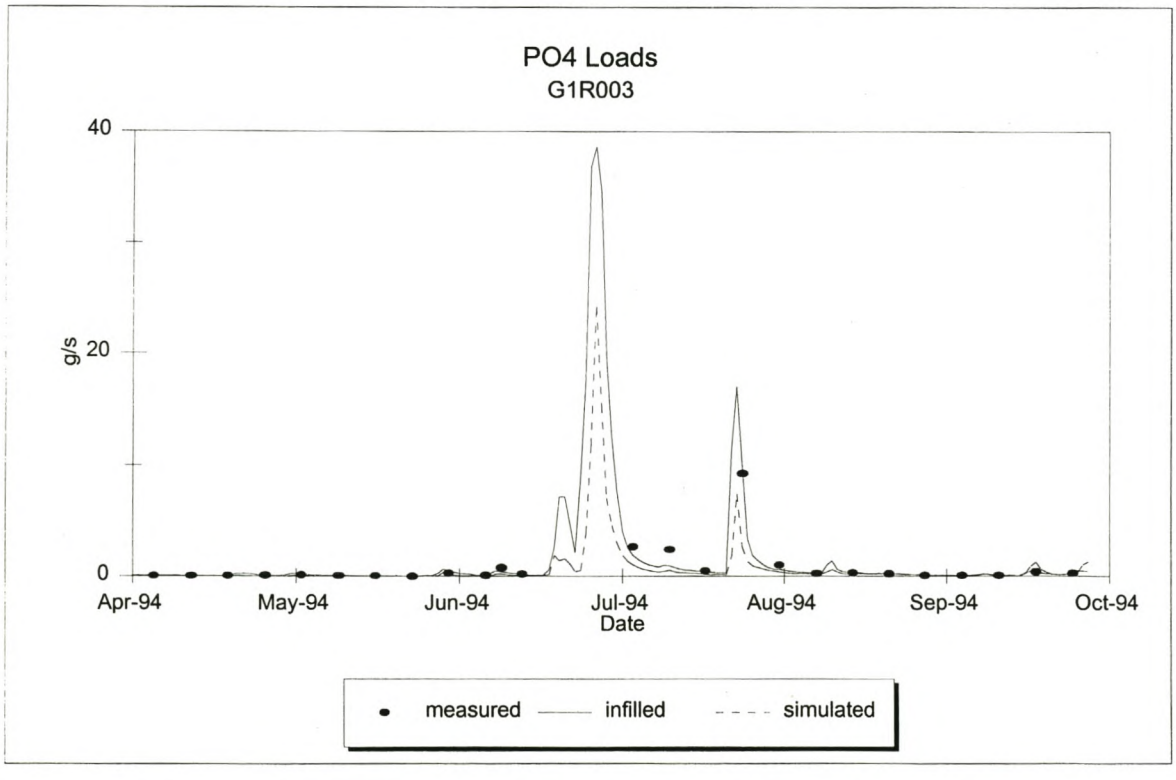

Figure 8.102: Phosphate Concentration at G1H020 (Simulation without ungauged loads)

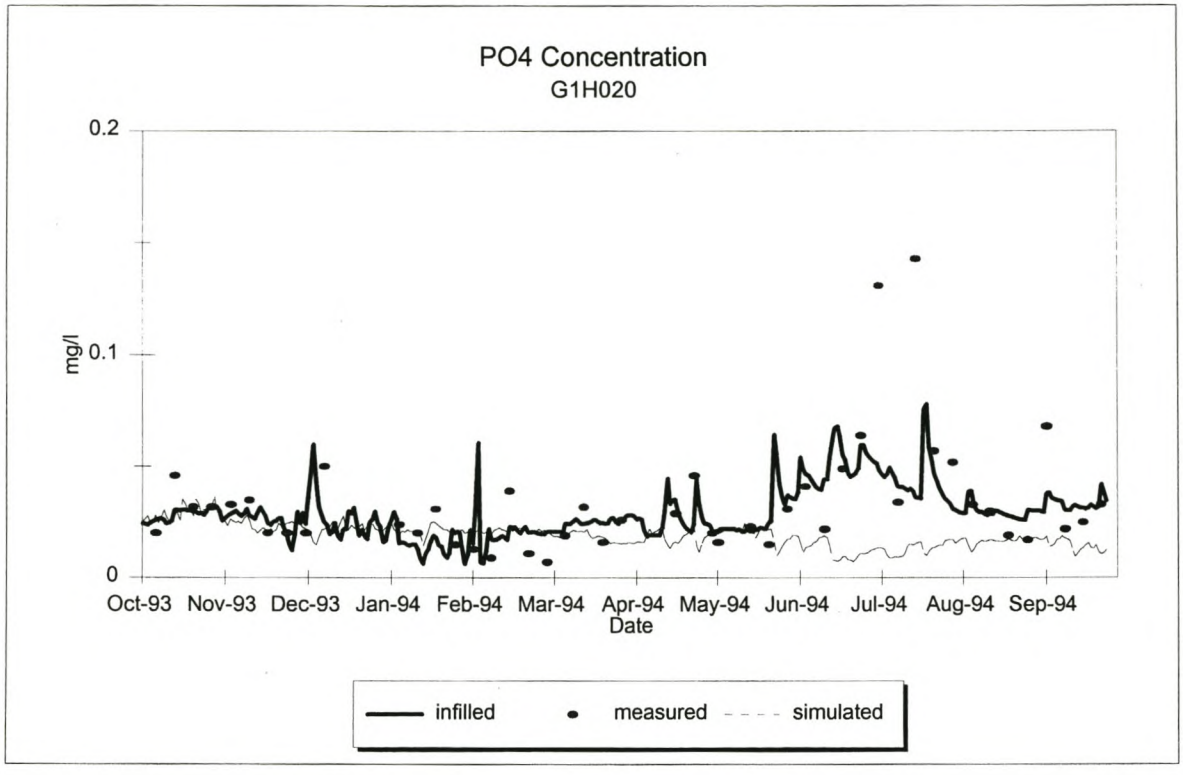

Figure 8.103: Phosphate Concentration at G1H036 (Simulation without ungauged loads)

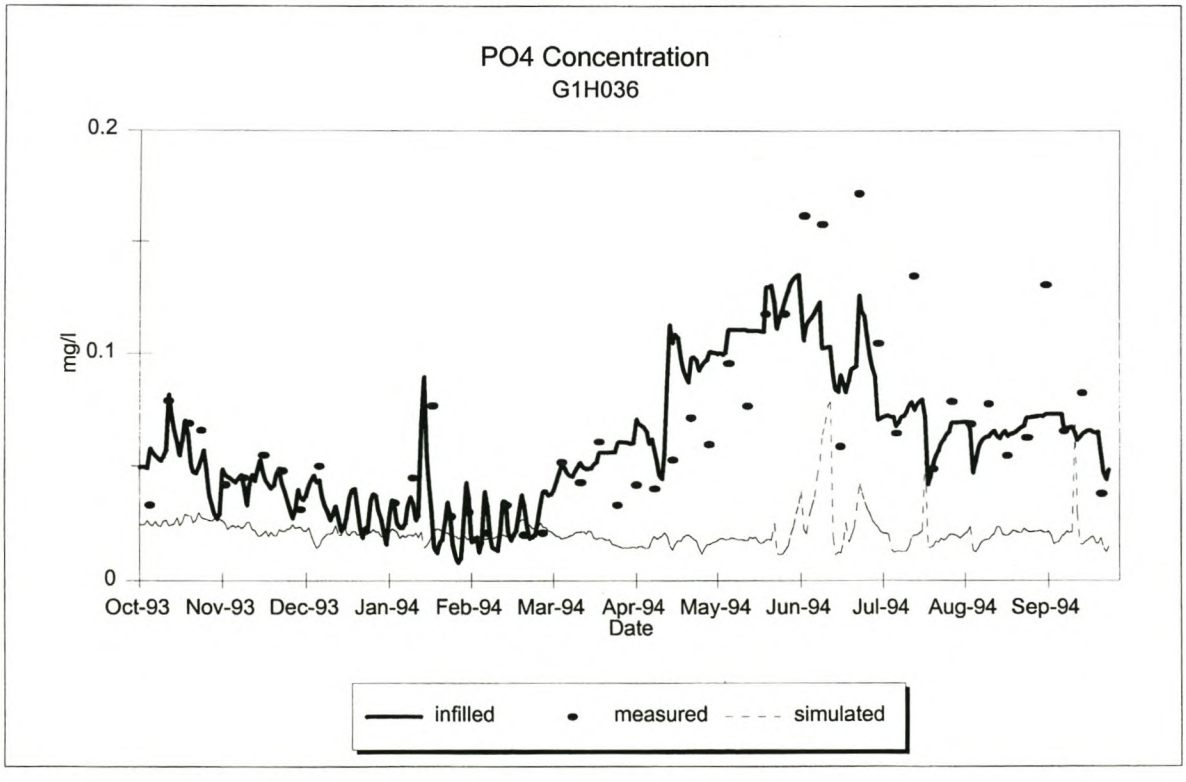

Figure 8.104: Phosphate Concentration at G1H013 (Simulation without ungauged loads)

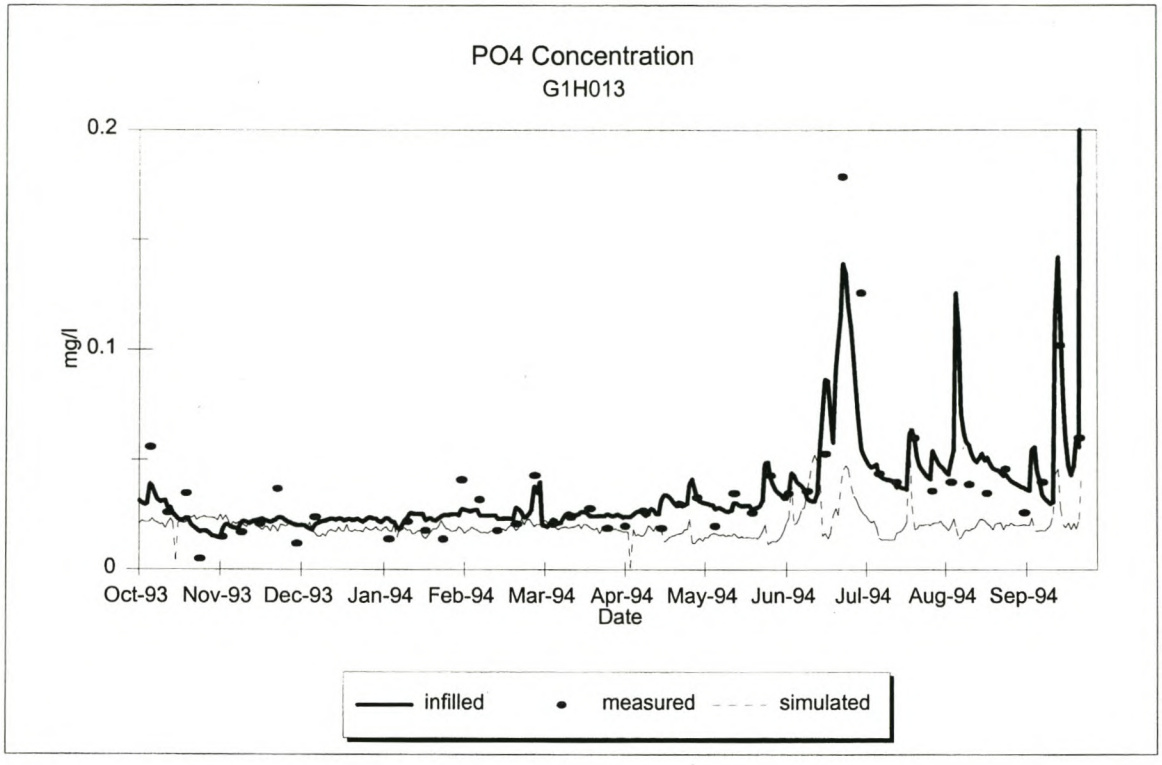

Figure 8.105: Phosphate Concentration at G1R003 (Simulation without ungauged loads)

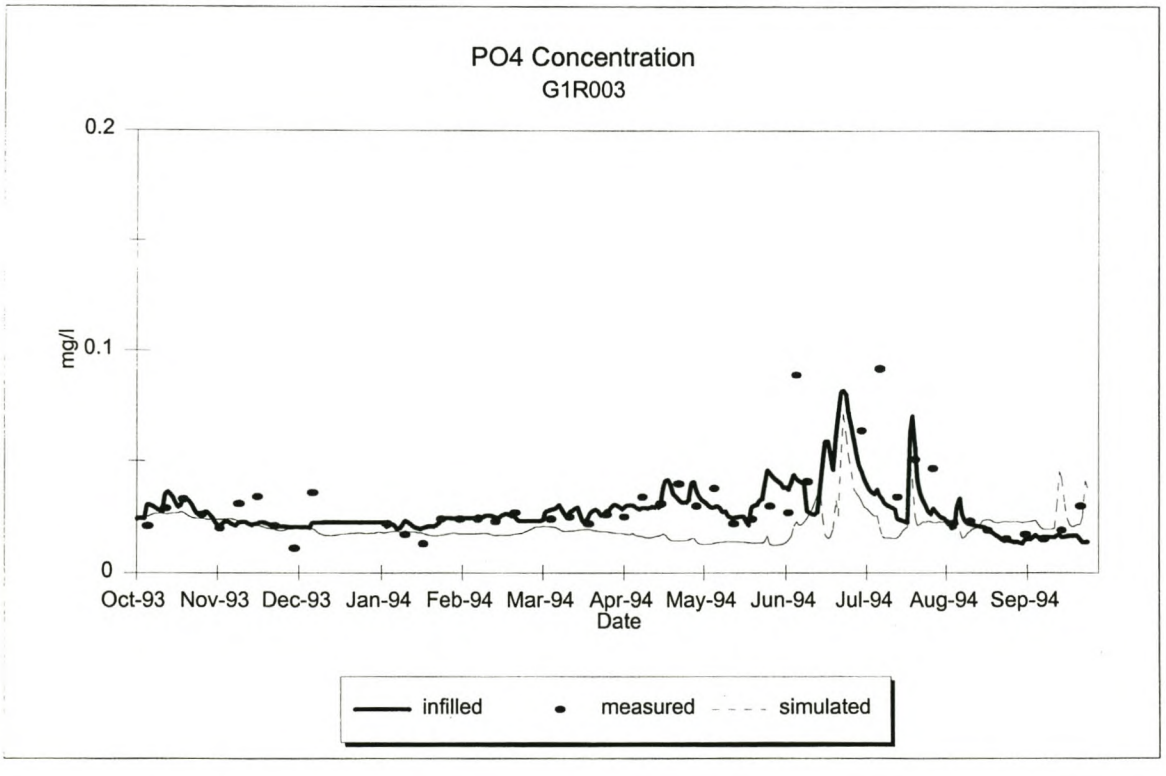

CHAPTER 9

SCENARIO ANALYSIS

9.1 INTRODUCTION

A simulation model allows a user to understand the behaviour of a system as a whole, or any of its parts, in space and time. It is thus of interest to users to utilise this model for different scenarios that can illustrate the potential outcome of certain '*what if*' situations. In Figure 9.1 one can see how a model can be used after verification, by implementing various water quality control actions and examining how the water system reacts to different scenarios and what the model's capability is to predict the outcome of these various scenarios.

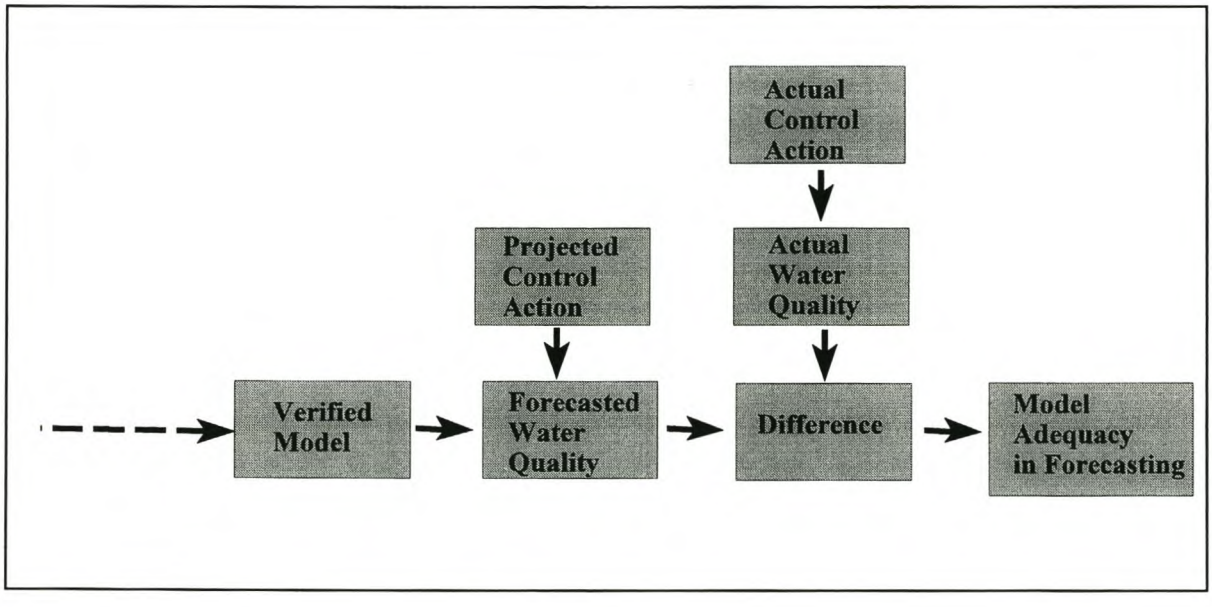

Figure 9.1: Postaudit of models

(after Thomann and Mueller, 1987; pg. 8)

In this chapter different scenarios are examined, in order to determine the model's ability to predict the outcome of different situations that would be important in a water quality control programme. The scenarios that are studied have been divided into three categories:

- Short term scenarios, such as a pollution spill discharging into the river
- Long term alteration of flow and water quality by linking the river simulation model to releases from a reservoir model
- Long term control management of concentrations and loads

These scenarios and the ability of the model to predict the outcome, will be discussed in this chapter.

9.2 OPERATIONAL SHORT TERM SCENARIO

The magnitude of a sudden spill of an effluent can be examined in a short term scenario. The questions that are normally of interest to the river system manager if a sudden spill occurs, are:

- What is the time of travel of the effluent?
- At which rate does the effluent attenuate?

It has been decided to divide the short term scenario into two different scenarios that could occur:

- *spill without option of release of fresh water:*
  If no option of fresh water release is available, the question will be what degree of impact the spill will have on the river and how far, as well as how long, the increased water quality constituent concentration will travel downstream.

- *spill with option of releasing fresh water downstream*
  If fresh water can be released, the question will be what volume and duration of water releases from an upstream source would then be required.

DUFLOW model was linked to a WQIS (Tukker, 2000), in which the user is prompted to enter the following:

- Location of an effluent spill
- Peak value of concentration of a spill, either for COD, TDS or PO_4
- Start and end dates of an effluent spill
- The spill hydrograph shape (Figure 9.2)
- If the user decides to increase the release water, the user is prompted to enter the discharge value and whether the discharge is from Skuifraam (the proposed future dam upstream in the Berg River, refer to section 3.4.5), or from the Voëlvlei Dam (if an effluent spill occurred downstream of the release point of Voëlvlei, refer to section 3.4.1 on details of Voëlvlei Dam).

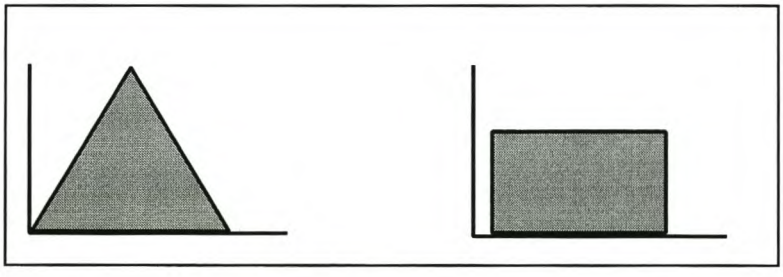

Figure 9.2: Effluent Spill Hydrograph Shapes

A DUFLOW simulation run is then performed and the impacts of the spill can be assessed graphically; either as a longitudinal section in a time step (refer to Figures 9.7 to 9.12), or at a specific cross-section over a time period (refer to Figures 9.5 and 9.6).

To demonstrate the short term scenario analysis, two runs have been completed: one without releases from Skuifraam Dam and one run with releases.

Simulation without any releases:

The month February was chosen as a good indication of a 'worst case' scenario, as the flow in the river

was very low. The spill occurred over a 4 day period, from the 15th February to the 19th February. The average discharge in the river was between 3 and 4 m^3/s. A phosphate spill of triangular effluent shape (refer to Figure 9.2) and a peak concentration of 10 mg/l has been inserted at Wemmers River; the discharge in Wemmers River at the time of the peak (17th February) was 0.2 m^3/s.

Simulation with upstream releases:

For the second simulation run, the same effluent spill incident as for the above mentioned simulation was used, but a release discharge of 20 m^3/s was included additionally in the model. The discharge was released on the 16th February, a day after the occurrence of the effluent spill, and was of trapezoidal shape. By using the simulation model and inserting different volumes of releases, the user can assess on a trial and error approach the volume of water needed to decrease the concentration to an acceptable water quality limit.

Figure 9.3 shows the phosphate concentration over time at selected points downstream from Wemmers River without the release, while Figure 9.4 shows the phosphate concentrations experienced in the river if the release is included in the simulation run. As one can see from Figure 9.3 the concentration between Wemmers River and G1H020 is about 1 mg/l and attenuates to 0.4 mg/l at G1H013, while for the simulation run with the releases included the river experiences a phosphate concentration of 0.6 mg/l between Wemmers River and G1H020 and 0.2 mg/l at G1H013 (refer to Figure 9.4).

The results can also be viewed in space, therefore the user can assess the impact of the spill for a certain time period over the whole river. Figures 9.7, 9.8 and 9.9 illustrate the phosphate concentration for 16 February (one day after the beginning of the spill), the 18th and the 26th February respectively, for the simulation run without any releases. Figures 9.10, 9.11 and 9.12 show the impact the phosphate has on the river with releases discharging from Skuifraam Dam. One can see that with releases from upstream, the concentration in the river is diluted at a faster rate.

The severity of the impact of an effluent spill can therefore be visualized and understood for different scenarios.

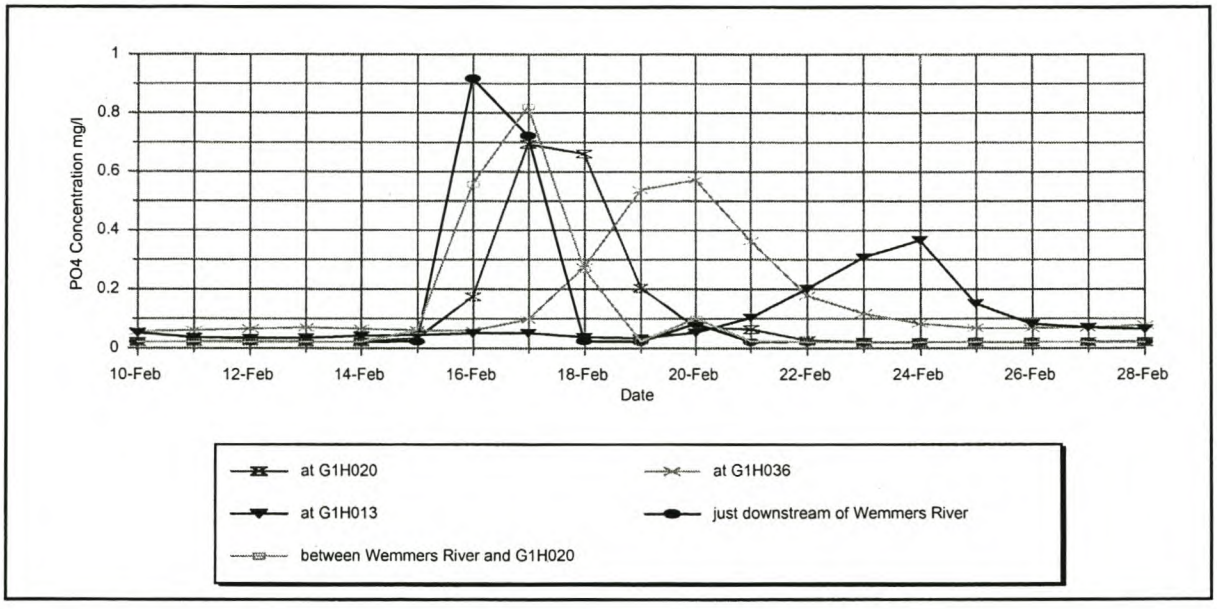

Figure 9.3: Results of Phosphate Spill without release shown in time

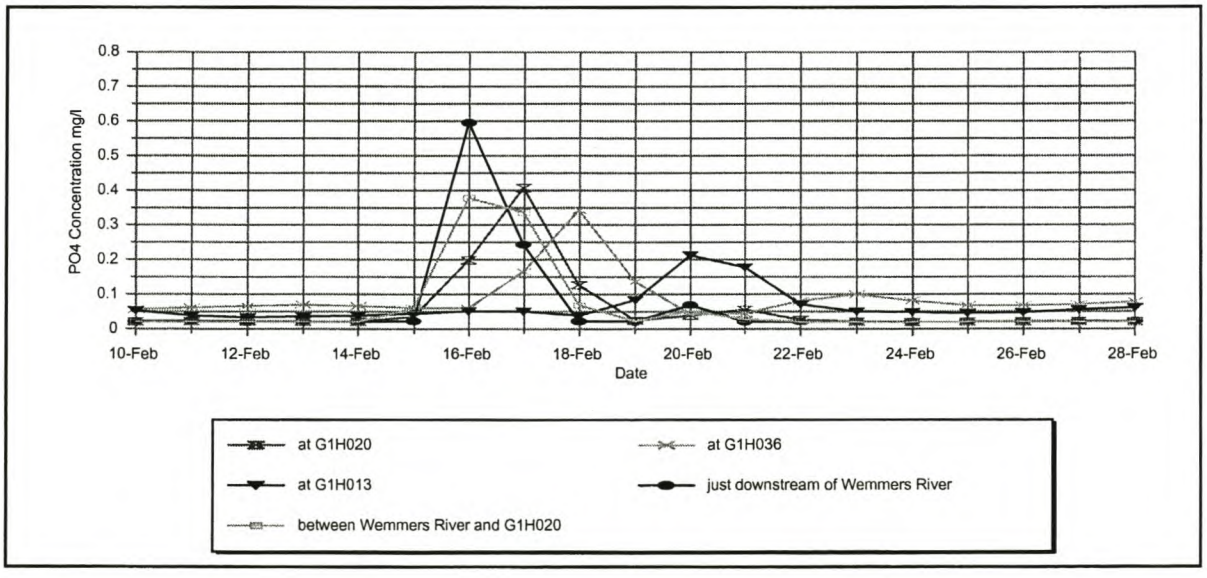

Figure 9.4: Results of Phosphate Spill with release shown in time

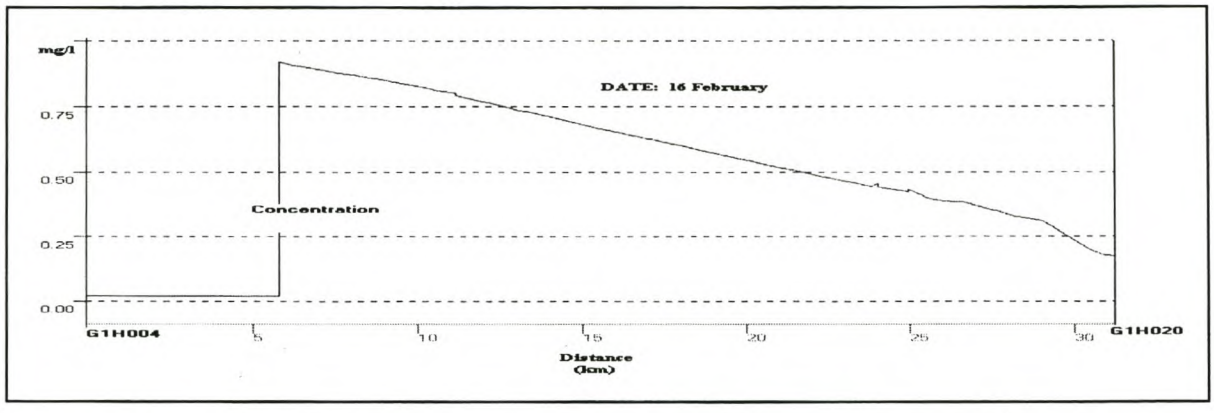

Figure 9.5: Results of Phosphate Spill shown in space without release for 16 February

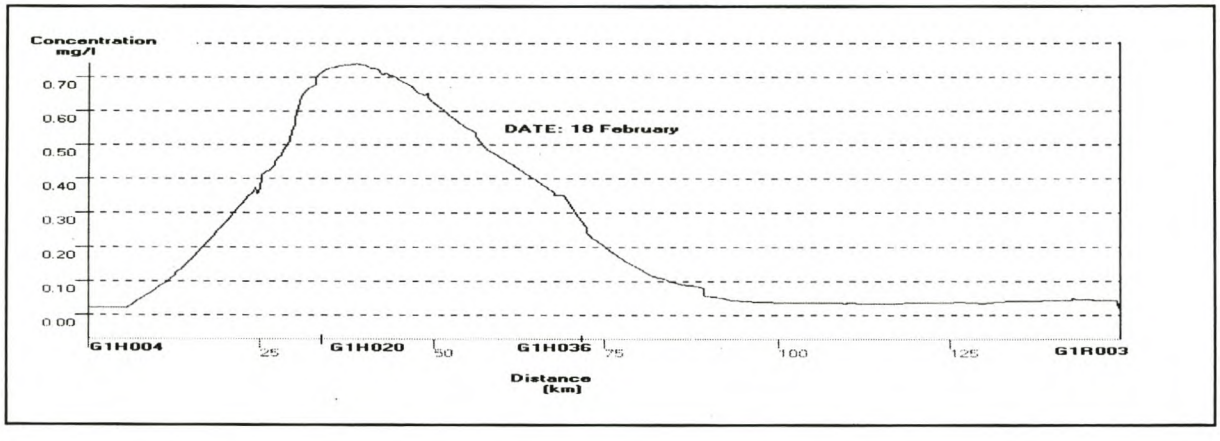

Figure 9.6: Results of Phosphate Spill shown in space without release for 18 February

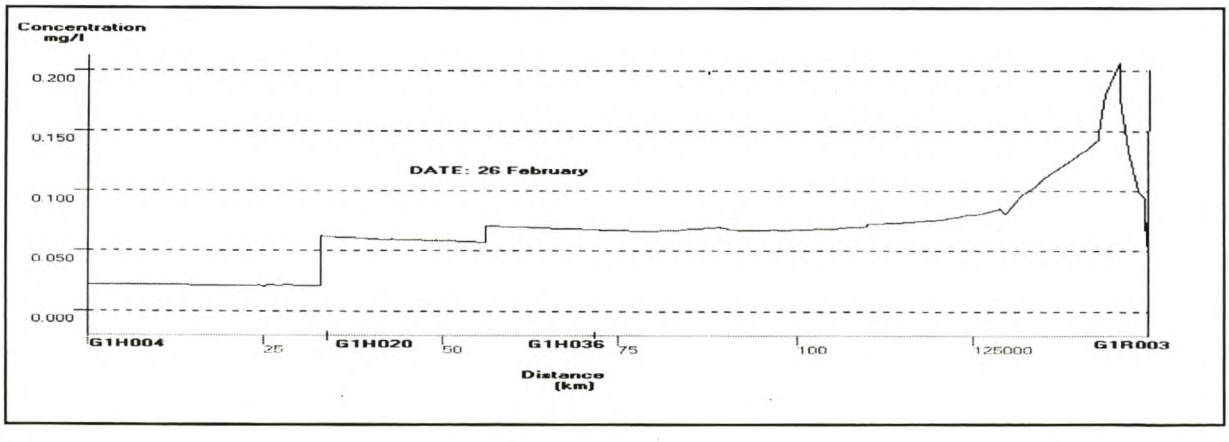

Figure 9.7: Results of Phosphate Spill shown in space without release for 26 February

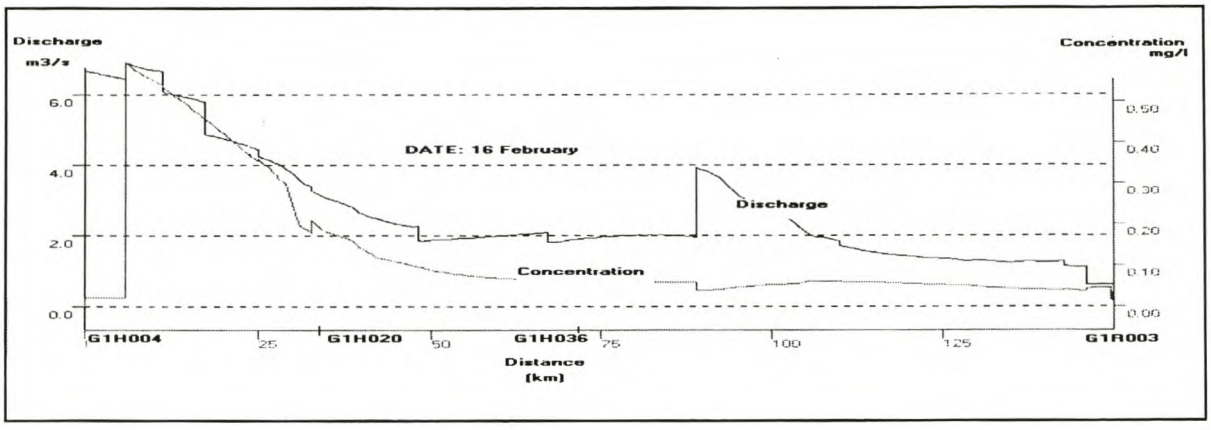

Figure 9.8: Results of Phosphate Spill shown in space with release for 16 February

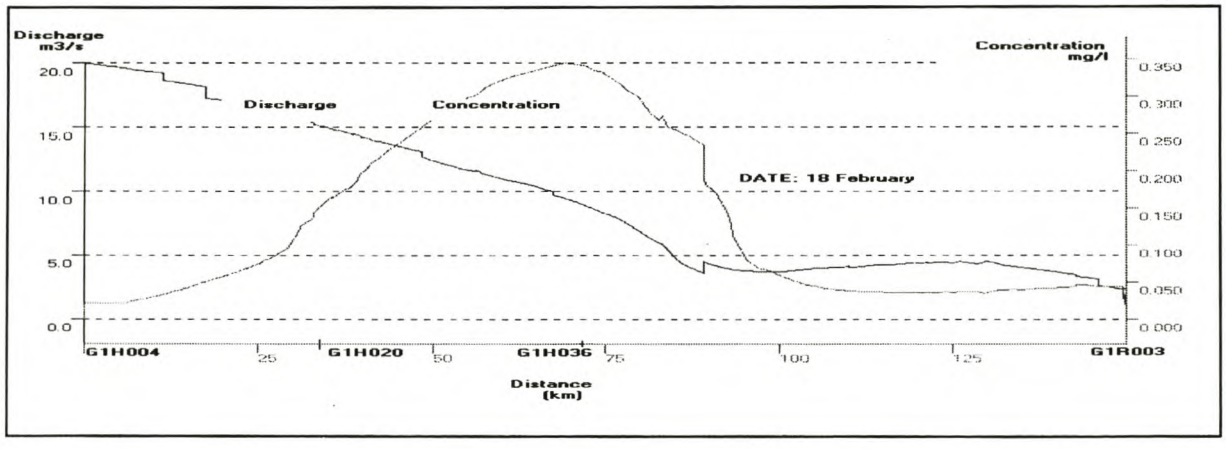

Figure 9.9: Results of Phosphate Spill shown in space with release for 18 February

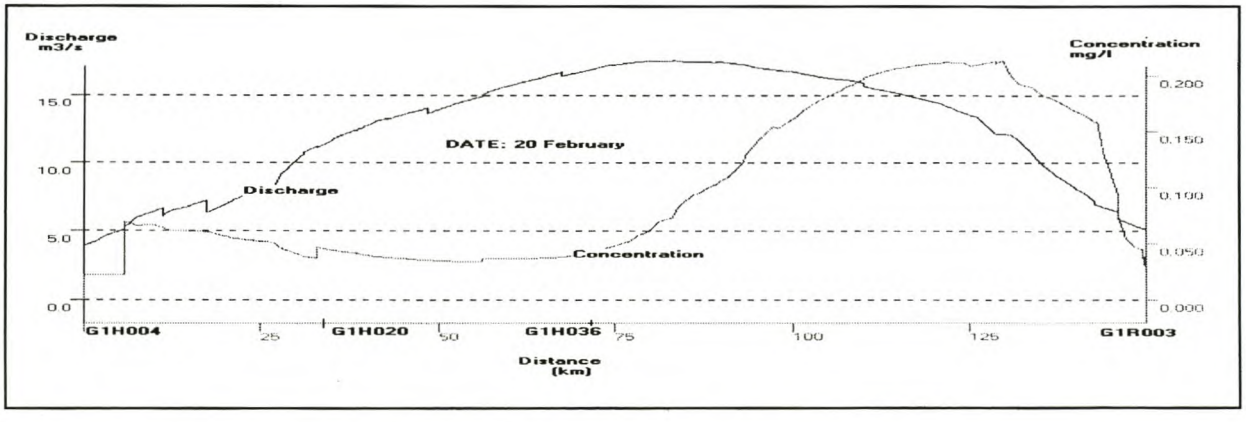

Figure 9.10: Results of Phosphate Spill shown in space with release for 20 February

9.3 LINKAGE TO RESERVOIR MODEL

The simulation model can be applied to a scenario where the upstream boundary conditions are varied according to the water quality and the flow releases that would occur if a reservoir would be constructed in the upstream reaches of the river. The impact of the construction of a dam on the river can therefore be investigated. The reservoir model, using CE-QUAL, has been developed for a concurrent study (Tukker, 2000), representing the water quality situation that would occur if Skuifraam Dam were built. The inflows used in the CE-QUAL reservoir model are the corresponding flows (G1H004), that were used originally as inflows into the river model. The water quality readings at G1H004 and the meteorological conditions at the site were used to drive the reservoir model, these are identical to the data that has been used for the historical river model. Therefore, all conditions for the reservoir model are the same as in the river model, except that the flow and water quality is now first routed through a reservoir before simulated. The simulated water quality release and spill time-series of the dam has been used as the inflowing boundary water quality in the river model. The variables modelled are: TDS, Phosphate as PO_4, temperature and oxygen.

9.3.1 Flow

The environmental and agricultural releases calculated for the Berg River for a large-scale water resources planning study (Ninham Shand, 1999) have been used as the upper boundary flow pattern. Figure 9.11 shows the comparison between the historical flow hydrograph and the release pattern developed for the reservoir.

It can be seen that the flood peak experienced in the winter months would be stored in the dam, until the full supply level and thereafter spill will occur. The maximum flow that would be experienced downstream in the river is 49 m^3/s compared with the 79.9 m^3/s of the historical data (refer to Table 9.1). The total water volume does however not change significantly, as the releases are more consistent and additional water is made available in the summer months. The flow in March and April do not deviate in mean, while the summer months experience higher flow than historically, and the winter slightly lower flow.

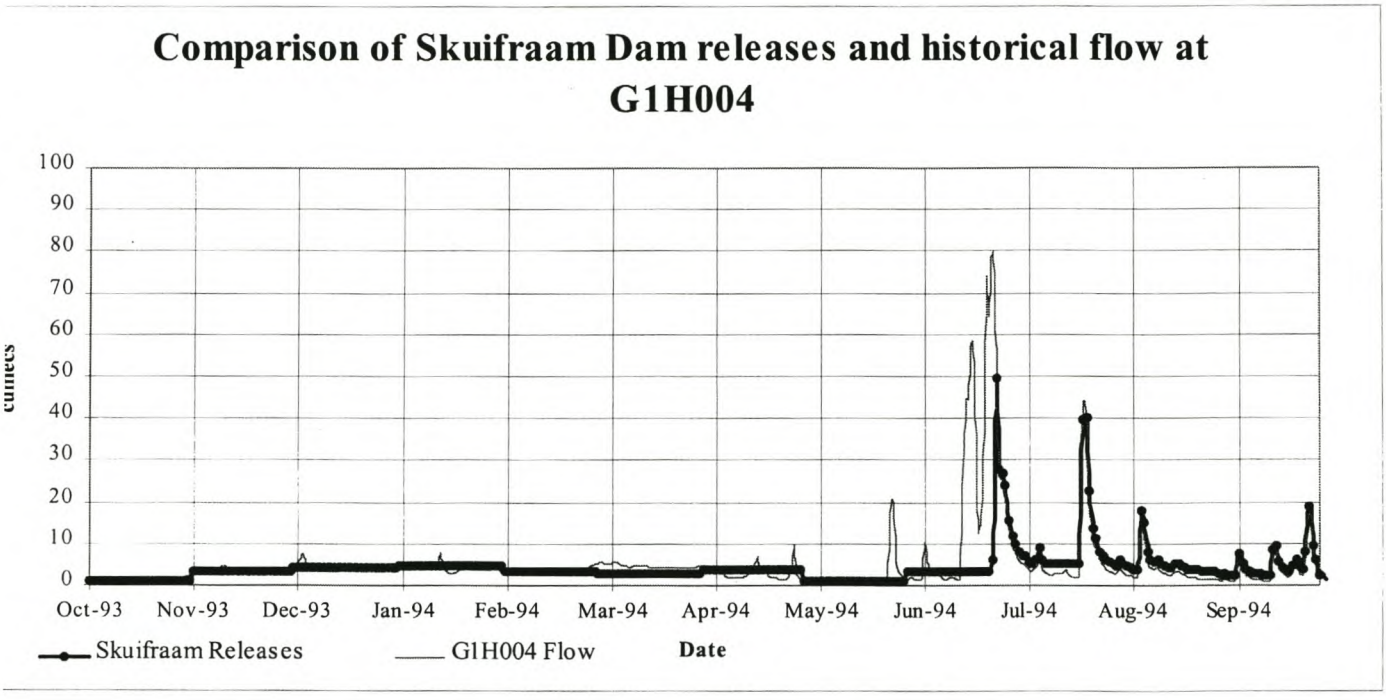

Figure 9.11: Comparison of historical inflow hydrograph and releases of Skuifraam Dam

Table 9.1: Comparison of flows at G1H004 and dam release/spill pattern

	Skuifraam Dam	**Historical Data**
Total (Mm^3)		
Summer	51.5	55.9
Winter	180.9	222.9
Yearly	232.4	278.9
Mean (m^3/s)		
Summer	3.3	3.6
Winter	3.8	4.7
Yearly	3.7	4.4
Maximum	49.7	79.7
Minimum	0.8	0.4

9.3.2 TDS

It can be noticed from Figure 9.12 that the historical data measured at G1H004 possesses more erratic TDS concentrations than the TDS releases of the dam. The consistency is a result of the controlled releases of volumes of water from the dam, smoothed by mixing, while without the dam, the TDS concentration changes with the nature of the historical flow. A slight increase in TDS concentration from 40 mg/l to 48 mg/l is experienced in mid-June. The overall incoming TDS load into the Berg River from upstream does not vary significantly; although the river will experience a slight increase in TDS for all months. The TDS concentration measured at the upper reaches of the Berg River are minimal when compared with the concentrations that are found in the lower reaches.

Table 9.2: Comparison of released TDS from Skuifraam Dam and historical TDS at G1H004

	Skuifraam Dam	**Historical Data**
Total (tons)		
Summer	752.3	666.4
Winter	777.6	619.2
	1529.9	1285.9
Mean (mg/l)		
Summer	43.5	38.5
Winter	44.7	35.6
Yearly	44.1	37
Maximum	48.9	79.8
Minimum	26.6	23.5

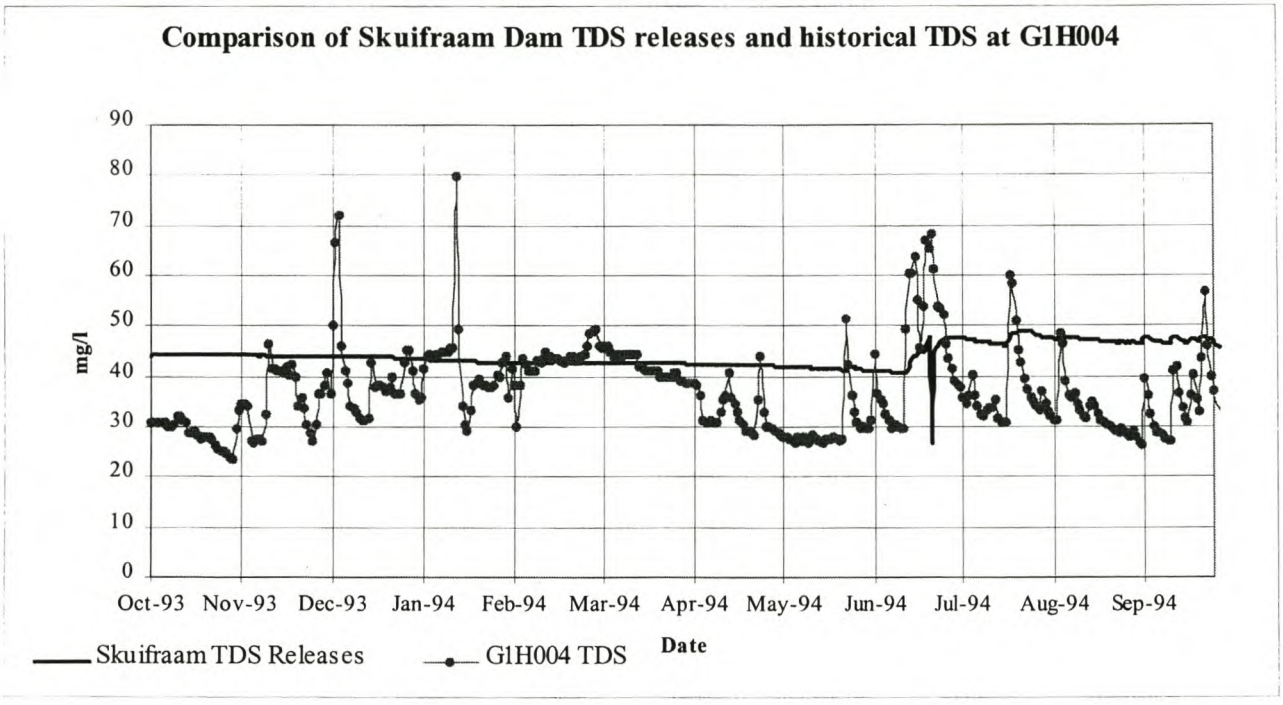

Figure 9.12: Comparison of historical TDS at G1H004 and TDS releases of Skuifraam Dam at G1H004

Results:

The results of the simulation are shown in Table 9.3 for the concentrations and Table 9.4 for the TDS loads. As can be determined from Table 9.3 the mean of the TDS concentration does not show much difference for all the stations. The total load has decreased in the summer months and increased in the winter months (refer to Table 9.4).

It can therefore be concluded that the construction of the dam for this particular year would have had ineffectual impact on the TDS in the river, as the higher salinities experienced in the river are due to the high salinity discharged from the lower tributaries. A WCSA study (DWAF, 1993) on the salinity experienced in the river after construction of Skuifraam Dam, also calculated that the effect of the dam on TDS concentration would be small.

Table 9.3: TDS Concentration after simulation of dam releases

	mean (simulation with historical data) mg/l	mean (simulation with dam concentration) mg/l	% diff in mean
Low flow period			
G1H020	43	45	5
G1H036	136	141	3.4
G1H013	123	118	-4
G1R003	162	148	-8
High flow period			
G1H020	41	45	9.7
G1H036	177	178	0.6
G1H013	196	177	-9.7
G1R003	224	217	-7
Yearly			
G1H020	42	44	4.7
G1H036	156	159	2
G1H013	159	147	-7.5
G1R003	193	184	-4.7

Table 9.4: TDS Loads after simulation using dam spills and releases as the upstream boundary

	mean historical data (g/s)	mean dam loads (g/s)	Total Load historical data (tons)	Total Load dam releases (tons)	% difference
Low flow period					
G1H020	132	196	2077	3077	48
G1H036	343	403	5401	6333	17
G1H013	429	485	6751	7624	13
G1R003	483	521	7595	8196	7.9
High flow period					
G1H020	805	625	12729	9896	-22
G1H036	3445	3016	54475	47694	-12
G1H013	6296	5035	99558	79615	-20
G1R003	8421	7550	133148	119376	-10
Yearly					
G1H020	469	411	14806	12973	-12
G1H036	1898	1713	58760	54027	-9.7
G1H013	3371	2766	106309	87240	-18
G1R003	4462	4045	140744	127572	-9

9.3.3 Phosphate as PO_4

Comparing the phosphates of the historical data measured at G1H004 and the phosphates that would be released from Skuifraam Dam at G1H004, one can conclude that the phosphate values will increase after construction of the dam. The phosphate values show a 200% increase in the summer months. This could be due to eutrophication. Algae growth is significant at this time, as the temperature and radiation are at a maximum (refer to section 5.4.5.2 for description of phosphate sinks and sources). In the months July to September the phosphate values are also slightly higher for the dam releases than for the actual grab samples taken in the river without dam (refer to Table 9.5 and Figure 9.13). This could also be due to algae growth in the dam, which will be more significant in a reservoir as in a river.

Table 9.5: Comparison of Phosphate as PO_4 released from Skuifraam Dam and historical data at G1H004

	Skuifraam Dam	**Historical Data at G1H004**
Total (tons)		
Summer	1.2	0.4
Winter	0.7	0.3
Yearly	1.9	0.8
Mean (mg/l)		
Summer	0.07	0.03
Winter	0.04	0.02
Yearly	0.05	0.02
Maximum	0.09	0.05
Minimum	0.01	0.005

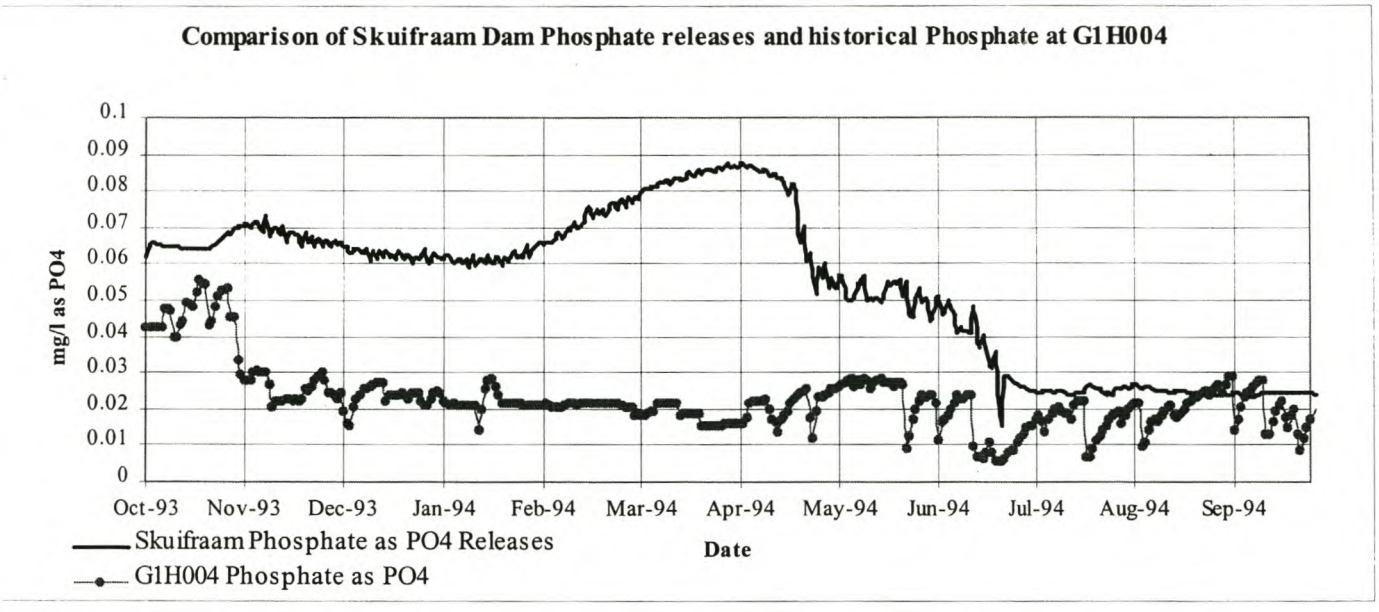

Figure 9.13: Comparison of historical Phosphate as PO4 and releases from Skuifraam Dam

Results:

Table 9.6 summarizes the simulated concentration, while Table 9.7 shows the loads that will be experienced when the dam is constructed.

Higher phosphate loads are experienced in the dam for the summer months. This increase has an impact on the river, as can be seen from the simulation results. The results are higher for all months and at all stations, with the summer concentration showing an increase of about 76% at G1H020. The loads are also more significant and a 230% increase in the loads is experienced in the river reach from Skuifraam Dam and G1H020 during the summer months. The loads simulated in the winter months show only 12% difference. The increase in phosphate values perceived could have a vital impact on the already high phosphate values measured in the river.

Table 9.6: Phosphate Concentration after simulation using dam spills and releases as the upstream boundary

	mean (simulation with historical data) mg/l	**mean (simulation with dam concentration) mg/l**	**% diff in mean**
Low flow period			
G1H020	0.025	0.044	76
G1H036	0.026	0.049	88
G1H013	0.023	0.041	78
G1R003	0.023	0.042	83
High flow period			
G1H020	0.023	0.027	17
G1H036	0.040	0.042	5
G1H013	0.034	0.040	17
G1R003	0.034	0.040	17
Yearly			
G1H020	0.023	0.036	56
G1H036	0.031	0.046	48
G1H013	0.028	0.040	43
G1R003	0.028	0.041	46

Table 9.7: Phosphate Loads after simulation using dam spills and releases as the upstream boundary

	mean historical data (g/s)	mean dam loads (g/s)	Total Load historical data (tons)	Total Load dam releases (tons)	% difference
Low flow period					
G1H020	0.068	0.21	1.0	3.3	230
G1H036	0.077	0.19	1.2	3.0	150
G1H013	0.090	0.19	1.4	3.0	114
G1R003	0.080	0.18	1.2	2.8	133
High flow period					
G1H020	0.5	0.51	7.9	8.1	2.5
G1H036	1.0	1.12	15.9	17.8	12
G1H013	1.3	1.45	21.2	23.0	8.5
G1R003	1.5	1.65	24.0	26.1	8.8
Yearly					
G1H020	0.28	0.36	9.0	11.4	26
G1H036	0.54	0.65	17.2	20.8	21
G1H013	0.71	0.82	22.6	26	15
G1R003	0.80	0.92	25.2	28.9	14.7

9.3.4 Temperature

The temperatures of the dam simulation outflows and G1H004 vary significantly. The maximum temperature is of equal value, but it is experienced in April, while for the historical data the maximum temperature is experienced in December and January (refer to Figure 9.14 and Table 9.8). The temperature of the dam releases do not drop as low as the historical data, as the temperature in the dam will not change as significantly with the meteorological conditions as the river, due to the smoothing effect of the storage in the dam. In December a difference of -10 °Celsius is simulated. The upper layer of the dam will experience these summer increases at nearly the same time as the river, while the lower layers of the dam (where it was assumed that the water release takes place) stay cold due to stratification. These differences could have a significant ecological impact in the river. Additional research should be undertaken to investigate the impact these changes would have on the river ecology.

Table 9.8: Comparison of temperature released from Skuifraam Dam and historical temperature at G1H004

	Skuifraam Dam Outflows	**Historical Data at G1H004**
Mean (°C)		
Summer	15.2	22
Winter	19.7	13.1
Yearly	17.5	17.5
Maximum (°C)	24.6	25
Minimum (°C)	13	10

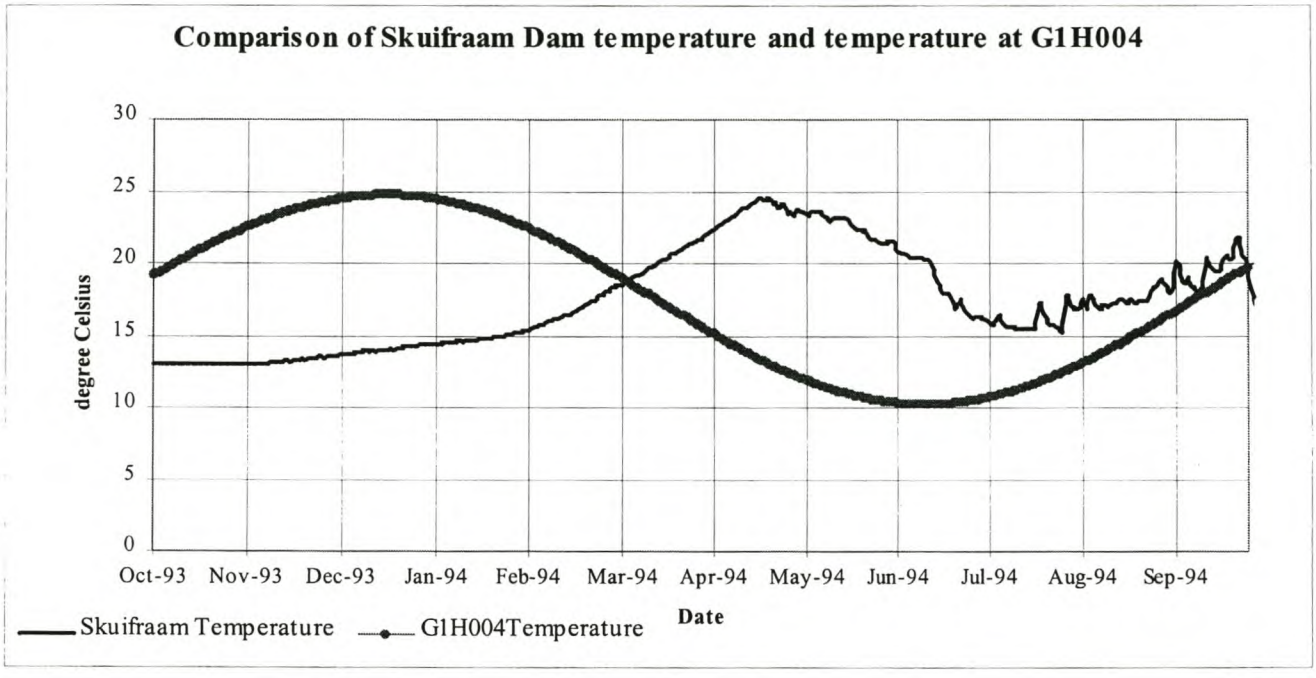

Figure 9.14: Comparison of historical temperature and temperature releases of Skuifraam Dam

Results:

The results of the simulation (refer to Table 9.9) show that the temperature experienced in the river will be lower for the summer months and higher in the winter months. The effect the released temperature of the dam will have on the river, will be felt particularly in the reach from the dam (G1H004) to G1H020. The effect the delay of the maximum temperature has on the overall statistics is averaged out when calculating the temperature values over 6 months. The mean temperature is lower in the summer months, while in the winter months the temperatures all show higher values. This can also be seen when comparing the released temperature of Skuifraam Dam to the temperatures in the river prior to a dam (Figure 9.14) The maximum temperature in the river does not vary in value, but in time, as was seen in Figure 9.14, this delay in maximum temperature could have a significant effect on the ecology of the river and further studies should take place on the degree of impact this delay will have.

Table 9.9: Temperature after simulation using dam spills and releases as the upstream boundary

	mean historical data (°C)	mean dam (°C)	% diff. in mean	Standard deviation historical data	Standard deviation dam	% diff. in standard deviation
Low flow period						
G1H020	23	20.1	-13	3.0	3.1	3
G1H036	24	20.7	-14	2.7	2.8	4
G1H013	24.5	22	-10	3.6	3.1	-14
G1R003	24.7	22.8	-7	3.5	3.1	-11
High flow period						
G1H020	13	15.1	16	2.5	3.4	36
G1H036	12.8	14.1	10	2.7	3.3	22
G1H013	12.5	12.7	2	2.9	3.3	14
G1R003	12.5	12.3	-2	2.9	3.4	14
Yearly						
G1H020	18	17.6	-2	5.7	4.1	-28
G1H036	18.3	17.4	-5	6.5	4.5	-30
G1H013	18.5	17.3	-6	6.9	5.7	-17
G1R003	18.5	17.5	-5	6.9	6.2	-10

9.3.5 Oxygen

The oxygen discharged from the dam is much lower than the oxygen values estimated at G1H004. This difference is because the oxygen calculated for the river simulation is the actual saturation oxygen, as no real data was available to include into the model. The oxygen of the dam is less than the saturation oxygen, because of the dynamics that influence and depletes the oxygen concentration in the dam (refer to section 5.4.5.3 for more description on oxygen processes in a water body) and because the releases are made from the lower layers of the dam. A minimum of 1.3 mg/l is calculated for the dam oxygen, while the saturation oxygen only decreases to a minimum of 8.4 mg/l. Higher oxygen is released in the winter months, when the spill occurs and oxygen from the upper layers of the dam is released into the river (refer to Figure 9.15)

Table 9.10: Comparison of oxygen released from Skuifraam Dam and oxygen at G1H004

	Skuifraam Dam	**Historical calculated Saturation Values**
Mean (mg/l)		
Summer	0.3	8.8
Winter	5.3	10.5
Yearly	2.8	9.7
Maximum (mg/l)	8.6	11.2
Minimum (mg/l)	0	8.4

Results:

Referring to Table 9.10, there is a insignificant difference in oxygen mean for low and high flow period. The yearly values show that there is 0% difference, while the low flow period indicates slightly higher values, with 3% difference the maximum at G1H020, and the high flow period shows slightly lower values, with -5% the maximum difference experienced at G1H020. The minimal differences perceived

from the simulations might be due to high saturation oxygen discharging into the river from the tributaries and also that reaeration of the depleted oxygen takes place shortly after the upstream releases. Therefore, the oxygen level in the river increases to saturation oxygen before reaching the gauging stations. The results indicate that although the oxygen concentration is low in the top reaches of the river, the river has the ability to reaerate and depending on the quality of the water from the tributaries, the oxygen in the river could recover at a fast rate. There is however need for additional research on the severity of the impact of low oxygen discharging into the river.

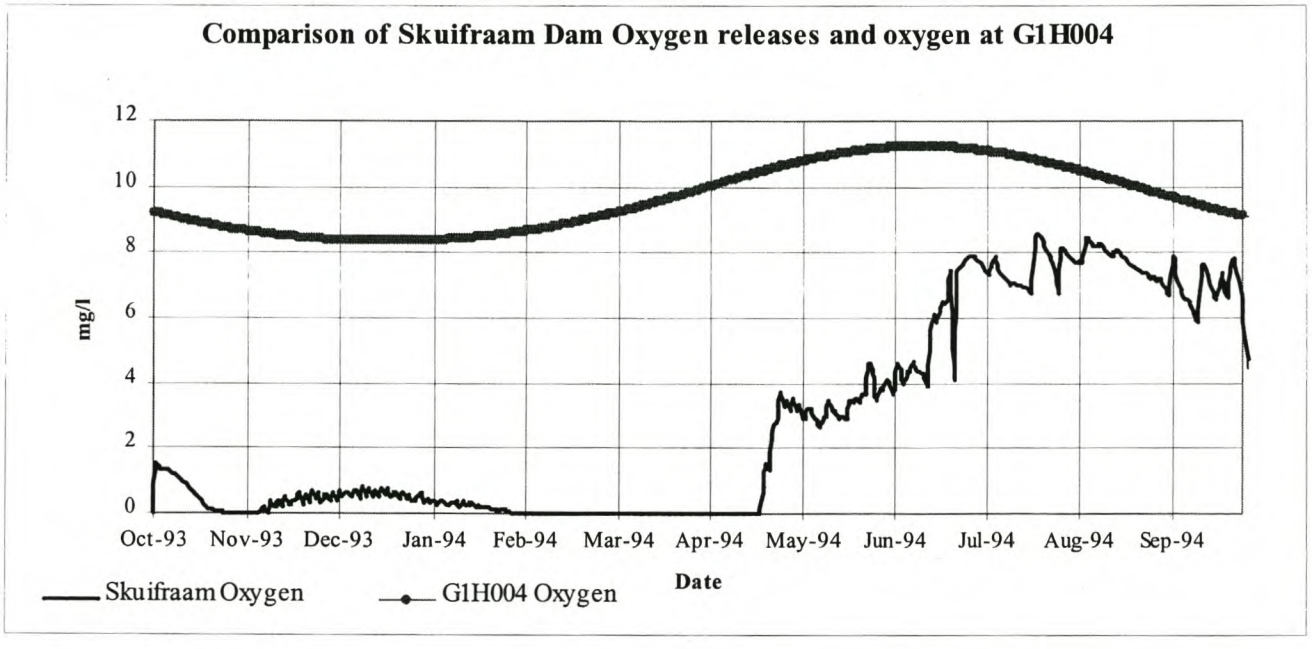

Figure 9.15: Comparison of historical oxygen and releases of Skuifraam Dam

Table 9.11: Oxygen after simulation using dam spills and releases as inflow

	mean historical data (°C)	mean dam spills and releases (°C)	% diff. in mean	Standard deviation historical data	Standard deviation dam spill and releases	% diff. in standard deviation
Low flow period						
G1H020	8.7	9.0	3	0.44	0.45	2
G1H036	8.6	9.1	6	0.50	0.47	-6
G1H013	8.5	8.8	3.5	0.53	0.50	-6
G1R003	8.9	9.2	3	0.42	0.41	-3
High flow period						
G1H020	10.3	9.8	-5	0.60	0.69	15
G1H036	10.6	10.2	-4	0.86	0.76	-12
G1H013	10.7	10.5	-2	0.76	0.96	26
G1R003	10.8	10.6	-2	0.82	0.74	-10
Yearly						
G1H020	9.6	9.4	-2	0.9	0.66	-26
G1H036	9.6	9.6	0	1.2	0.85	-29
G1H013	9.7	9.7	0	1.3	1.12	-14
G1R003	9.8	9.9	-1	1.4	0.95	-32

9.4 LONG TERM CONTROL

A central problem of water quality management is the assignment of allowable discharges to a waterbody so that a given water quality standard downstream of a particular effluent point is met. For instance, the deteriorating water quality in the Berg River is a result of the return flow from the agricultural land (i.e. non-point sources) and from the sewage treatment plants (i.e. point sources). Thus, the question can be asked: how should the load allocation between these two be divided?

DUFLOW cannot model non-point sources. Therefore, to investigate the aforementioned management question, the non-point sources were modelled as "point sources". The user can insert water quality limits upstream at a selected discharge point and downstream at the point of interest to the user. The user is also prompted, as for the short term scenario, for a concentration and a discharge that will be discharged at the selected location. The user can then by a trial and error approach identify the magnitude of loads that may be discharged at the specific location without violating the specific quality limitations. The point loads may also be altered and compared with the non-point discharges.

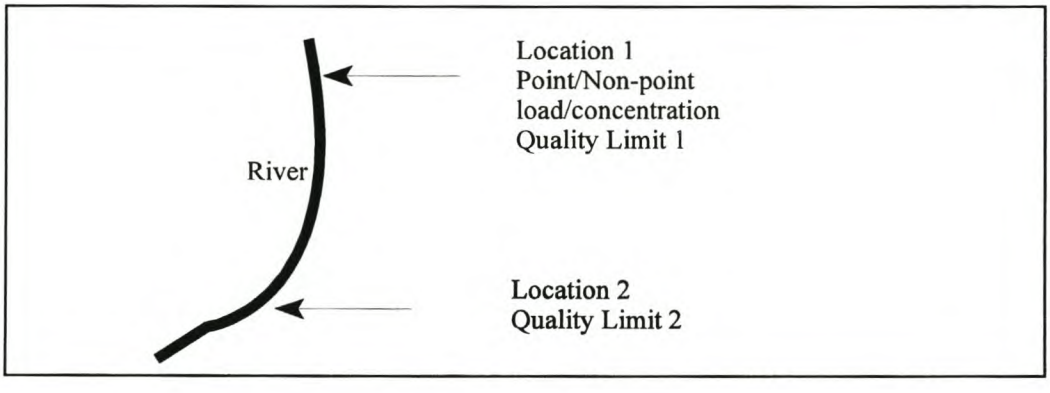

Figure 9.16: Schematisation of long term control scenario

This scenario is similar to the short term scenario, except that the user has additional control by assessing which mass a water quality load discharge into the river upstream may have without violating a particular water quality limit at a downstream source.

9.5 DISCUSSION

From the above discussions it is evident that DUFLOW does have the capability to assist in scenario analyses. It seemed reasonably easy to add releases and spills, the model remained computationally stable during the scenario simulation runs.

A limitation of DUFLOW is that no non-point sources can be modelled and this would have allowed for additional load allocation scenario analyses. The incorporation of a catchment model to the WQIS and DUFLOW would therefore be of advantage for the overall understanding and management of the river system. The DUFLOW modelling package does contain an additional precipitation runoff module (RAM) which has been developed by STOWA in order to improve the applicability of surface water models. RAM has however not been applied to many studies yet, and has not been tested for South African conditions. It is therefore recommended to use models that have been used and tested extensively for South African conditions. Examples of modelling systems used in South Africa are:

- *ACRU hydrological and water quality modelling system:*
  A sediment-nutrient version of the well-known ACRU modelling system has been configured and used for the Mgeni Catchment (Kienzle et. al., 1997)
- *IMPAQ*
  IMPAQ has been developed by Ninham Shand and has been applied to the Eastern Cape Catchment (DWAF, 1995)
- *HSPF*
  (Bricknell et.al., 1993)

Matji (2000) compares the results of phosphorous runoff applied to various catchments with different runoff conditions for different catchment models, such as above mentioned models. The linkage of one of these runoff models would therefore improve the applicability of operational scenario analyses.

9.6 REFERENCES

Bricknell, B.R., Imhoff, J.C., Kittle, J.L., Donigan, A.S., Johanson, 1993. *Hydrological Simulation Fortran Program: Users Manual*. Release 10, EPA, Report 600/R-93/174, Athens, GA.

DWAF, 1993. *Hydro-salinity modelling of the Berg River Basin.* Report by Ninham Shand Inc. in association with BKS Inc. for the Department of Water Affairs. DWAF report no. PG000/00/3392.

DWAF, 1995. *Amatole Water Resources System Analysis, Vol. 2: Main Report.* Report by Ninham Shand Inc. for the Department of Water Affairs. DWAF report no. PR000/00/0295.

Kienzle, S.W., Lorents, S.A. and Schulze, R.E., 1997. Hydrology and Water Quality of the Mgeni Catchment. Water Research Commission, Pretoria, Report TT87/97.

Matji, M., 2000. *Comparative Modelling of Phosphorous Production in Rural Catchments*. Unpublished Master Thesis. University of Stellenbosch.

Ninham Shand, 1999. *Operating Rules for the Skuifraam Schemes*. Correspondence to Department of Water Affairs and Forestry.

Tukker, J., 2000. *Interactive Water Quality Information System for River Management.* Unpublished Master Thesis. University of Stellenbosch.

CHAPTER 10

CONCLUSIONS AND RECOMMENDATIONS

10.1 INTRODUCTION

As water quality is becoming an increasingly important issue, the development of a water quality simulation model is useful for controlling and managing the existing and future water resource systems. Since the early days of the development of computer models, as described in section 2.2, models have become an essential "tool" to simulate solutions to different types of problems in water resources. The objective of this study was to assess the applicability of an existing European model for a winter-rainfall river in South Africa, under conditions very different to those applicable in its country of origin. Following selection criteria that have been declared important by management-orientated user groups (section 2.6), it was decided to apply the hydrodynamic water-quality model DUFLOW, and evaluate its adaptability for representing the Berg River with all its complexities.

The Berg River seemed to be a suitable river to model, as it contains all challenges, for hydraulic modelling (fairly steep slopes, abstractions, diversions of flow, hydraulic structures) and also water quality (non-point and point sources, etc.). The water quality in the Berg River is of great concern, especially in the lower reaches of the Berg River catchment, where the salinities are excessive and high nutrients are also becoming an issue of importance. In Chapter 4 it has been observed, that the phosphorous concentrations have increased considerably over the last ten years. In the vicinity of Paarl/Wellington the sandstone formations give way to Malmesbury shale downstream that leach high salt loads into the main stream, to the tributary flows and through irrigation return flows. With the proposed construction of Skuifraam Dam (refer to section 3.4.5), fresh water from the upper Berg River would be captured. Concerns have been raised that the salinity might increase due to reduction of fresh water. It is therefore important that the model represents the water quality responses in the river realistically, as it can then be used to assist in developing management strategies.

The limitations and the capabilities of DUFLOW are discussed in the first section of this chapter. Recommendations are made on basis of the conclusions drawn and are presented in the second section.

10.2 CONCLUSIONS

10.2.1 Flow Calculations

The finite difference approach DUFLOW uses to calculate the St Venant equations of continuity and momentum is advanced and therefore allows the user to model complex systems. The finite difference approach allows varied space steps, which proved to be advantageous; especially in the upper Berg, where steep slopes required very small space steps for stable calculations. The lower Berg River could then be modelled in larger space steps in order to save running time and superfluous cross-sections.

Structures that were included are weirs at the specific gauging stations and bridges that are found along the main stem of the Berg River. Information was available for most of the structures, and where difficulties were experienced with computational stability, the roughness coefficient was adjusted. The trigger function used in DUFLOW for structure control allows modelling of multiple notches at a weir, such as is found at South African rivers, to cover varying flow levels.

10.2.2 Water Quality Calculations

An advantage of DUFLOW is the open structure it uses for the water quality module. This allows the user to either change the water quality algorithms according to the degree of complexity required or add additional water quality processes that need to be simulated. In future use of the configured model, water quality processes can be added or deleted. Thus, the model is very flexible. In this study, TDS, COD and Temperature algorithms were added to the EUTROF1 module, as these are variables of concern specifically in the Berg River catchment. The Phosphate algorithm had to be simplified, as most of the processes could not be modelled due to lack of data. The results of the Temperature algorithms proved to be satisfactory.

Two-weekly water quality samples were available. As the model has been configured on a daily time step, the samples had to be 'patched' (infilled) in order to include the variables as time series. DUFLOW has an option of entering the time series at irregular time steps, but DUFLOW linearly interpolates the values for the missing flows, which is not quite correct for the distribution of the water quality variables as they are also dependent on the flow value. A moving regression method was used to infill the TDS

and soluble phosphate values, while a simple harmonic function was used for the temperature infilling.

Schematisation points were added at every location were a tributary discharges into the main stem or a point source has been identified. A considerable number of point sources have not been included, due to lack of information. It would a pre-requisite, if the simulation model will be used as an operational tool, that all additional sources of water quality discharge into the river are identified and included in the model.

A limitation of DUFLOW is that it does not allow incoming loads to be input in a diffuse fashion along the length of the modelling reaches. It is therefore difficult to distinguish between non-point and point sources if the model is used as a scenario tool, because the non-point sources have to be treated as point sources.

10.2.3 Results

The accuracy of the results is mainly determined by the accuracy and availability of the input data. Errors in the water quality simulation are dependent on various factors, such as: accuracy of the 'infilling' method, availability of grab samples in the river, accuracy of the flow simulation etc. The flow simulation is also dependent on various factors. The errors that are introduced at the beginning of the flow calculations (i.e. in the first reach) are carried all the way downstream to the end boundary.

The addition of estimated runoff from ungauged subcatchments for the calibration of the flow module proved to be problematic as considerable volume of water is still missing during peak flows for most of the stations. This could be due to underestimation of the flood at the various gauging stations and thus also underestimation for the ungauged runoff. The accuracy of the simulation of the water quality loads is dependent on the errors resulting from the flow simulation.

For additional accuracy of the flow calculations, further research needs to be done on the water losses in the Berg River, i.e. abstractions, irrigation losses and losses due to alien vegetation. The method that has been applied to calculate the evaporation losses are simplistic and other methods could be used to estimate the evaporation losses to obtain better accuracy.

10.2.4 Learning curve

The learning curve time to use the model efficiently is greatly reduced by the user friendly interfaces that DUFLOW uses. This is a major advantage, as it can be operated easily for configuration and scenario analyses by the users. A background on the hydraulics and water quality processes is however needed to fully understand the system.

10.2.5 Limitations

i. Although the finite difference approach to calculate the St. Venants equations proved to be advantageous due to the stability and the choice of unequal time and space steps, a limitation of this approach is however that it is very data intensive compared to other much simpler flow calculation methods.

ii. The different network objects (i.e. weirs, abstraction points, etc.) can only be altered in the network window itself. For adjustments to the objects it would have been easier to change the specific descriptions in an additional textfile or database, especially if numerous objects are configured.

iii. The results are written in a textfile, which take up considerable space (about 50 Mb for the quality files). For use in other systems, such as the WQIS (Tukker, 2000) a database format would have been more suitable for updating and presenting.

iv. Like many European or American models, DUFLOW is not able to simulate evaporation losses from the water body. Such losses can be quite significant in South Africa, and are therefore of importance. These losses had to be treated as abstraction flows at schematisation points.

v. Non-point sources are not modelled as diffuse inflows by DUFLOW. These are however extremely important when considering the nutrient mass balance. From the water quality results it was evident that the agricultural runoff is significant in a flood (all loads are undersimulated).

vi. Water Quality calculations became unstable when negative water depths were experienced for the different runs. Negative water depths are a physical impossibility, but are sometimes simulated in the low flow period, due to inaccuracies between the calculated water level and the configured cross-sections reference level. Although the process calculations were able to be coded to overcome this problem, the transport mathematical formulations were fixed, and the negative water depths affected the calculations. Much effort went into altering the time and space

steps until a stable flow calculation was achieved.

10.2.6 Scenario Analysis

The text files produced by DUFLOW are easily altered for different scenario runs. DUFLOW is capable of simulating different scenarios that are of interest to the user. Three scenarios were looked at: a short term effluent spill scenario, a linkage to a hydrodynamic reservoir model and thirdly an operational long term management scenario. Although simulation time was long due to small calculation time steps (a calculation time step of 10 minutes proved to be stable) and the result file is large in terms of computer space, DUFLOW is capable of simulating various changes and predicting different scenarios.

10.3 RECOMMENDATIONS

Although the information for the Berg River Catchment is probably more extensive than for many other catchments in South Africa, there is still considerable need for additional research and data if a realistic representation of the river is desired. This is especially important when the model is not only used as an analysing "tool" for historical data, but also used to examine management scenarios. Research into the following areas may produce results that would strengthen the model's capability to represent the Berg River Catchment:

10.3.1 Non-point and point sources

There is considerable need to improve the monitoring system for the point and non-point sources along the Berg River catchment. This would ensure that a database would be available of different sources that contribute to nutrient and salt loads in the river. Although DWAF already monitors point sources that have been issued with a water quality permit, there are numerous sources that contribute to the deteriorating water quality in the Berg River. As most of the phosphorous in the river is due to runoff from agricultural land (Bath, 1989), it would be of benefit to link the hydrodynamic river model to a catchment model to estimate water quality loads from ungauged areas, rather than the methods we were forced to use in this study.

10.3.2 Expansion of data information on variables of interest in the Berg River

Oxygen is of interest in the river for ecological reasons, therefore it would be important to explore the oxygen mass balance in the Berg River, by taking grab samples over a longer period and incorporating COD discharges of the point sources into the river. Different algorithms relating to oxygen should be studied and adopted according to the specific river.

The scenario analysis showed that the summer temperature in the river would change considerably (10 degree Celsius change) if Skuifraam Dam were to be built in the upper reaches. This is obviously of concern and there is need to investigate the ecological impact of these temperature changes in the river.

Although earlier studies have been conducted on the phosphorous transport in the Berg River (Bath, 1989), the DUFLOW model has been activated in only the advection equation to analyse the phosphate concentration, as insufficient data is available on other dependent variables. By including data on the suspended solids and therefore the mobilisation of particulates into the river, as well as production of algae, improved results on the simulation and a better understanding on the phosphorous concentration in the river can be expected.

10.3.3 Linkage to other models

As mentioned above, it would be beneficial for management support, if DUFLOW were to be linked to other models as this would also ensure that DUFLOW could be used in other applications. In another study (Tukker, 2000) a user-friendly interface environment was developed and implemented as a water-quality information system (WQIS) that provides analytical, spatial and graphical information based on the requirements of a wide spectrum of users and which integrates simulation models (river and reservoir) into the WQIS. It would be important to broaden this study and integrate a catchment model into the WQIS, as well as further develop the DUFLOW model to support scenario analysis to support decision making.

10.4 REFERENCES

Bath, A.J., 1989. *Phosphate transport in the Berg River, Western Cape.* Technical report of the Department of Water Affairs and Forestry, Pretoria. TR 143.

Tukker, J., 2000. *Interactive Water Quality Information System for River Management.* Unpublished Master Thesis. University of Stellenbosch.